Astrocyte: Neuron Interactions in the Juvenile Form of Batten Disease

Parviainen, Lotta Elisabet

Awarding institution:
King's College London

Title: Astrocyte: Neuron Interactions in the Juvenile Form of Batten Disease

Author: Lotta Parviainen

Astrocyte: Neuron Interactions in the Juvenile Form of Batten Disease

Thesis submitted for the degree of
Doctor of Philosophy
at King's College London
2013

Lotta Parviainen

Department of Neuroscience
Institute of Psychiatry, King's College London
Denmark Hill

Abstract

The neuronal ceroid lipofuscinosis (NCLs, Batten Disease) are inherited, fatal neurodegenerative disorders of childhood. In all forms of NCL, astrocyte activation occurs early in the disease and precedes neuronal loss. However, in the most common juvenile form (JNCL), which is caused by a mutation in the *Cln3* gene, this astrocyte response appears to be compromised. Since astrocytes are crucial for the functioning and survival of neurons, and emerging evidence highlights the pivotal role that reactive astrocytosis plays in the pathogenesis of CNS diseases, any deficits in the biology of these cells could significantly impact neuronal health. In order to study the functioning of JNCL astrocytes, these cells were isolated from a well-characterised mouse model of the disease, *Cln3* deficient mice (*Cln3*$^{-/-}$ mice), and their basic biology characterised. These studies revealed that *Cln3*$^{-/-}$ astrocytes have a disrupted actin and intermediate filament cytoskeleton. Possibly due to these defects, *Cln3*$^{-/-}$ astrocytes have an attenuated ability to response to an activation stimulus, just as observed *in vivo,* and to divide and migrate. They also display pronounced defects in their ability to take-up glutamate and to secrete a range of proteins, including cytokines, neuroprotective factors and the anti-oxidant glutathione, that become even more evident upon stimulation. Additionally, their impaired calcium signalling suggests that communication might be altered in these cells. Most importantly, using a co-culture system, these *Cln3*$^{-/-}$ glia were shown to negatively impact the health of both *Cln3*$^{-/-}$ and wild-type neurons, with the mutant neurons being the most severely affected, probably because of their own compromised biology. This includes a reduction in neurite complexity and displacement of the axon initial segment (AIS), which modulates neuronal excitability and the initiation of axon potentials. Thus, these data show, for the first time, that JNCL astrocytes are functionally compromised and might play an active role in the neurodegeneration observed in JNCL. Further, this information raises the possibility that, in future, astrocytes should be considered as targets for therapeutic interventions.

Acknowledgements

First and foremost, I would like to express my deepest appreciation to my first supervisor Dr. Brenda Williams for her incredible supervisory skills throughout my PhD-study years! I want to thank Brenda for her support in both scientific and non-scientific matters and for her positivity no matter what we were faced with, which I will cherish for years to come. I would also like to extend my appreciation to my second supervisor Professor Jon Cooper, whose passionate attitude towards science has been an inspiration. Thank you both!

None of this work would have not been possible without the help of many people working in the James Black Centre. I would especially like to thank Dr. Sybille Dihanich for all the help and support over the years. Without Sybille's help I would probably still be trying to figure out how to grow glia cells. Dr. Andrew Wong's deep insight into everything going on in the lab, as well as cake making, has helped me to cross many hurdles along the way. There are many other people working in both William's and Cooper's groups I want to express my gratitude to: Dr Greg Anderson, Dr Colin Campbell, Dr Thomas Kühl, Dr Sarah Pressey, and Helen Brooks. Also special thanks to Dr Dafe Uwanogho, Dr Graham Cocks, Dr Matthew Hill, Leo Perfect and Dr Doris Stangl for exchange of bits and pieces in emergencies. Finally, Dr Federica Buonocore – thanks for being there and sharing some fabulous PhD-times with me.

A big portion of my work has been made possible by collaborations with many scientists, whose contribution and expertise I value highly. First of all, Dr. Hannah Mitchison provided the *Cln3*$^{-/-}$ mice used in this study and by doing so made all this work possible. Dr. Rosella Abeti helped me with the calcium imaging studies. Dr. Simon Pope and Professor Simon Heales guided me through the wonders of glutathione measurements. Dr. Matthew Grubb and the members of his research group were instrumental in conducting all the experiments related to the axonal initial segment. Finally, the cell mobility assay was performed in collaboration with Dr. Giovanna Lalli and her PhD student Martina Sonego.

There are so many other people who have been there in one way or another. First of all my family; parents, grandmother, sister, brother in-law, and the most gorgeous nephew in the whole world, thank you all for believing and for simply being there for me. Your support means the world to me. Then friends, I have the most amazing bunch of friends whose friendship I deeply value. Thanks for the wonderful distraction and being so coolly mad:). Kris, there are no words to describe how much I appreciate all the zillion ways you have helped me. Thank you for sticking with me throughout this. I owe you big time.

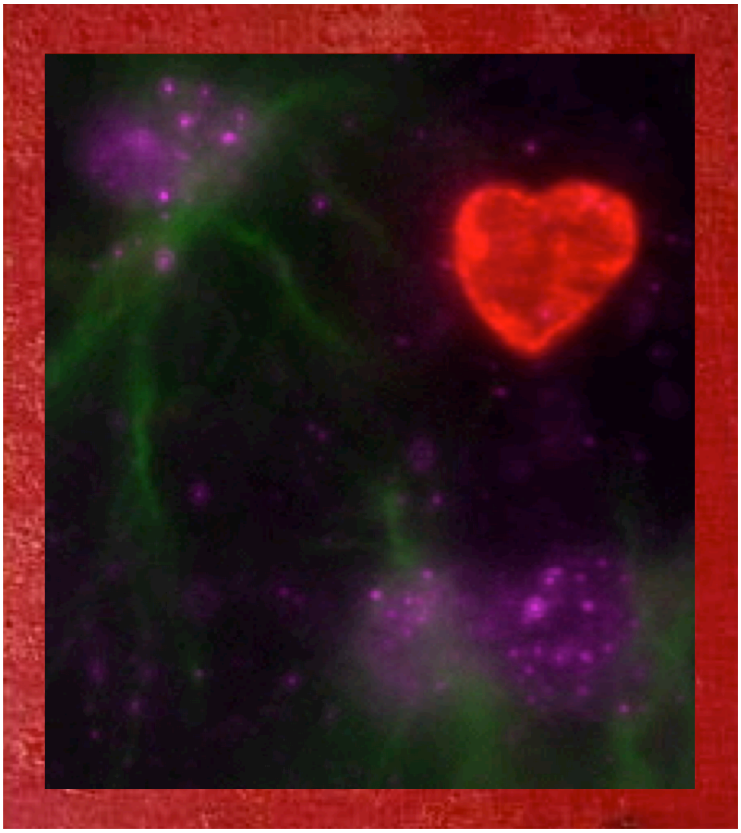

Scientific illustration to show my gratitude and say cheers guys!

Table of Contents

List of Figures

List of Tables

Abbreviations

AA	Arachidonic acid
AAV	Adenoassociated virus
Ach	Acetylcholine
ADHD	Attention deficit hyperactivity
ADT	Adenosine diphosphate
AIS	Axonal initial segment
ALS	Amyotrophic lateral sclerosis
AMPA	2-amino-3-(5-methyl-3-oxo-1,2-oxazol-4-yl) propanoic acid
AnkG	Ankyrin G
ANLS	Astrocyte-neuron lactate shuttle hypothesis
AP	Adapter protein
ApN	Aminopeptidase N
Ara-C	Arabinofuranosyl Cytidine
Aß	Amyloid β
ATP	Adenosine triphosphate
BBB	Blood-brain barrier
BCA	Bicinchoninic acid assay
BDNF	Brain-derived growth factor
BLOC-1	Biogenesis of lysosome-related organelles complex-1
BMP	Bis(monoacetylglyceryl)phosphate
BMT	Bone marrow transplant
BrdU	5'-bromo-2'-deoxyuridine
BSA	Bovine serum album
CAM	Cell adhesion molecules
Cath D	Cathepsin D
CCE	Capacitative Ca2+ entry
CD68	Cluster of differentiation 68
CICR	Calcium-induced calcium release from the ER
CNS	Central nervous system
CNTF	Ciliary neurotrophic factor
CRP	C-reactive protein
CSD	Cortical spreading depression
CSPG	Chondroitin sulfate proteoglycans
Cx43	Connexin 43
CXCT4	Chemokine receptor
CysGly	Cysteinylglycine
DAB	3,3'-Diaminobenzidine
DAG	Diacylglycerol
DAPI	4'-6-Diamidino-2-phenylindole
DCFH-DA	Dichlorodihydrofluorescein diacetate
DHR	Dihydrorhodamine
DIV	Days in vitro
DM	Dissociation medium

DMEM	Dilbecco's Modified Eagles Medium
DRE	Downstream regulatory element
DUSP2	Dual specificity protein phosphatase 2
EAAT3	Excitatory amino acid transporter 3
ECM	Extracellular matrix (6th chapter)
EDTA	Ethylenediaminetetraacetic acid
EE	Early endosome
EEA1	Early endosome antigen 1
EGF	Epidermal growth factor
EPMR	Epilepsy with mental retardation
ER	Endoplasmic reticulum
ERK	Extracellular signal-regulated kinase
ETC	Electron transport chain
FBS	Foetal bovine serum
FGF	Fibroblast growth factor
FGF2	Fibroblast growth factor-2
FL-LDL	Fluorescent low-density lipoprotein
FRAP	Fluorescence recovery after photobleaching
GABA	γ-aminobutyric acid
GAD65	glutamic acid decarboxylase
GAP43	Growth associated protein 43
GCP-2	Glutamate carboxypeptidase-2
GEF	Guanine nucleotide exchange factor
GFAP	Glial fibrillary acidic protein
GGA	γ-ear containing, ADP ribosylation factor-finding protein
GLUT	Glucose transporter
GM-CSF	Granulocyte macrophage colony-stimulating factor
GPCR	G-protein coupled receptor
GPI	Glycosyl-phosphatidylinositol
GPN	Glycyl-L-phenylalanine-beta-naphthylamide
GR	Glutathione reductase
GSH	Reduced form of glutathione
GSSG	Oxidized form of glutathione
GST	Glutathione S-transferase
GTP	Guanosine triphosphate
HBSS	Hanks' balanced salt solution
HPLC	High performance liquid chromatography
ICAM-1	Intercellular adhesion molecule-1
IF	Intermediate filament
IFNγ	Interferon γ
IL	Interleukin
IMS	Industrial methylated spirit
INCL	Infantile neuronal ceroid lipofuscinosis
iNOS	Inducible NOS
INT	Tetrazolium salt
IP-10	Interferon γ induced protein 10

IP_3	Inositol 1,4,5-triphosphate
IP_3R	IP_3 Receptor
iPS	Induced pluripotent stem cell
IRF-2	Interferon regulatory transcription factor-2
JAK	Janus kinase
JNCL	Juvenile neuronal ceroid lipofuscinosis
JNK	c-Jun N-terminal kinase
KC/GRO-α	Growth-regulated α protein
kDa	kilodaltons
KSPG	Keratin sulfate proteoglycans
LAMP	Lysosome-associated membrane proteins
LC3	Microtubule-associated protein I light chain 3
LE	Late-endosome
LGNd	Dorsal lateral geniculate nucleus
LGP	Lysosomal membrane glycoprotein
LIF	Leukemia inhibitory factor
LIMP	Lysosomal membrane protein
LINCL	Late infantile neuronal ceroid lipofuscinosis
LPS	Lipopolysaccharide
LRO	Lysosome-related organelles
LSD	Lysosomal storage disorder
LTP	Long-term potentiation
M-CSF	Macrophage colony-stimulating factor
MALDI-TOF	Matrix-assisted laser desorption/ionization-time of flight
MAP	Microtubular associated proteins
MAPK	Mitogen-activated protein kinase
MCP	Monocyte chemotactic protein 1
MCT	Monocarboxylate transporter
MDC	Macrophage-derived chemokine
MHC	Histocompatibility complex
MIP	Macrophage inflammatory protein
MMP	Matrix metalloproteinase
MnSOD	Manganese superoxide dismutase
MPO	Myeloperoxidase
MPP+	1-methyl-4-phenylpyridinium
MPR	Mannose 6-phosphate receptor
MPS	Mucopolysaccharidosis
MPSIIIB	Mucopolysaccharidosis type IIIB
MPTP	Mitochondrial permeability transition pore
Mrp1	Multidrug resistance-associated protein 1
MVB	Multivesicular body
Myosin-IIB	Non-muscle myosin heavy chain IIB
NAA	N-acetylaspartate
NAAG	N-acetylaspartylglutamate
NADPH	Nicotinamide adenosine dinucleotide phosphatase
NCL	Neuronal ceroid lipofuscinosis

NCX	Sodium-calcium exchangers
NDS	Normal donkey serum
NeuN	Neuronal specific nuclear protein
NF-κB	Nuclear factor-κB
NGF	Nerve growth factor
NGS	Normal goat serum
NMDA	N-Methyl-D-aspartic acid
NO	Nitric oxide
NOS	Nitric oxide synthase
NPC1	Niemann-Pick C1 protein
NSF	N-ethylmaleimide-sensitive factor
NT	Neurotrophin
O4	Oligodendrocyte marker 4
OPA	Orthophosphoric acid
P/S	Penicillin/streptomycin
p75(NTR)	p75 neurotrophin receptor
PBS	Phosphate buffered saline
PDGF	Platelet-derived growth factor
PDL	Poly-D-lysine
PFA	Paraformaldehyde
PGE	prostaglandins
PGn-PA	Plasminogen-plasminogen activator
PI3K/Akt	Phosphatidylinositol 3-kinase/Protein Kinase B
PIP2	Phosphatidylinositol 4,5-bisphosphate
PKA	Protein kinase A
PLC	Phospholipase C
PMCA	Plasma membrane Ca^{2+} ATPases
PPF	Paired pulse facilitation
PPT1	Palmitoyl protein thioesterase 1
ProSAP1	Proline-rich synapse-associated protein 1
PVDF	Polyvinylidene difluoride
RANTES	Regulated and normal T cell expressed and secreted
RILP	Rab7-interacting lysosomal protein
ROS	Reactive oxygen species
S1BF	Somatosensory barrel field cortex
SAP	Serum amyloid P-component
SBDS	Shwachman-Bodian-Diamon syndrome protein
SCF	Stem cell factor
SCMAS	Subunit C of the mitochondrial ATP-synthase
SDF-1	Stromal cell-derived factor-1
SDS-PAGE	Sodium dodecyl sulfate polyacrylamide gel electrophoresis
SERCA	Sarco (endo) plasmic reticulum calcium ATPase
SGOT	Serum Glutamic oxaloacetic transaminase
SNAP25	Synaptosomal-associated protein 25
SNARE	Soluble NSF attachment protein receptor
SOC	Store-operated channels

SOCE	Store operating calcium entry
STAT	Signal transducer and activator of transcription
STIM1	Ca^{2+} sensor stromal interacting molecule 1
TBS	Tris buffered saline
TCA	Tricarboxylic acid
TCEP	Tris-2-carboxyethyl phosphine
TGF-β	Transforming growth factor-β
TGN	Trans-Golgi-network
TIP	Microtubular plus-end tracking protein 3
TIRF	Total internal reflection fluorescence
TLR4	Toll-like receptor 4
TNF-α	Tumor necrosis factor-α
TPO	Thrombopoietin
TPP1	Tripeptidyl peptidase 1
Trk	Tyrosine-kinase receptor
TRP-1	Tyrosinase-related protein 1
VAMP1	Vesicle-associated membrane protein 1
VCAM-1	Vascular cell adhesion protein-1
VDAC	Voltage-dependent anion channels
VEGF	Vascular endothelial growth factor
VGCC	Voltage-gated calcium channels
VIP	Vasoactive intestinal peptide
vWF	Von Willebrand factor
WT	Wild type
Y2H	Yeast two hybrid
γGT	γ-glutamyl transpeptidase
6-OHDA	6-hydroxydopamine

Chapter 1
Introduction

The neuronal ceroid lipofuscinoses (NCLs) are a subgroup of lysosomal storage disorders that form the most common group of childhood neurorogenerative diseases. They are inherited, with only one exception, in an autosomal recessive manner and are all fatal (Goebel, 1995; Haltia, 2006; Haltia and Goebel, 2012). Most of the NCLs share clinical characteristics, including epileptic seizures, mental and motor deterioration, that ultimately lead to the premature death of the affected individuals (Cooper, 2003; Jalanko and Braulke, 2009; Mole et al., 2011; Haltia and Goebel, 2012). The different forms of NCLs also share common pathological features including the accumulation of autofluorescent storage material and progressive, yet, selective neuronal loss that is preceded by glial activation (Bible et al., 2004; Pontikis et al., 2004; Tyynelä et al., 2004; Pontikis et al., 2005; Jalanko and Braulke, 2009; Weimer et al., 2009; Mole et al., 2011; Kuronen et al., 2012; Schmiedt et al., 2012). Despite much research the exact neuropathological mechanisms underlying these devastating brain disorders remains elusive.

The research described in this thesis, uses a tissue culture approach, to investigate the hypothesis that astrocytes play a key role in the pathology of the most common form of NCL, the juvenile form (JNCL). This hypothesis stemmed from observations that, in JNCL, as in all forms of NCL, glial activation precedes neuronal loss, but in mouse models of JNCL, and in the human disease, this glial activation appears to be attenuated (Pontikis et al., 2004; Tyynelä et al., 2004; Pontikis et al., 2005).

In this introduction I will discuss what is known about lysosomal storage disorders including the NCLs, and JNCL in particular. I will give an overview of the cellular dysfunctions associated with these diseases and include evidence detailing why astrocytes could be important players in this field.

1.1 Lysosomal storage disorders

The discovery of the lysosome by Christian de Duve manifested the birth of a new era in the field of cell biology (Duve, 1975). Ten years later, the first

lysosomal disorder, Pompe disease, was identified (HERS, 1963). Subsequently, many similar conditions caused by inborn errors in metabolism and resulting in the build up of lipids within cells have been identified. These were collectively referred to as 'inborn lysosomal diseases' (HERS, 1965; Vellodi, 2005). Currently lysosomal storage disorders (LSDs) forms a group of at least 70 distinct genetic diseases (Futerman and van Meer, 2004; Cox and Cachón-González, 2012). Each of these diseases result either from a defect in the activity of a particular lysosomal protein, or from non-lysosomal proteins whose functions are related to lysosomal biogenesis (Futerman and van Meer, 2004; Ballabio and Gieselmann, 2009; Walkley, 2009; Bellettato and Scarpa, 2010; Vitner et al., 2010; Schultz et al., 2011). These defects cause the accumulation of unwanted substrates that should have been metabolized by the cell. Individually, LSDs are rare, but collectively they show a prevalence of about 1 in 5000-7500 live births (Meikle et al., 1999; Futerman and van Meer, 2004). A variety of pathogenic cascades have been implicated in different forms of LSDs, some are common to many LSDs, whereas others are impaired only in a subset of LSDs (Kiselyov et al., 2007; Vitner et al., 2010; Schultz et al., 2011) but, as stated above, all involve the lysosome.

The lysosome

Lysosomes are cellular organelles that degrade other worn-out cellular organelles, proteins, lipids, carbohydrates, and possibly also viruses and bacteria (Duve, 1975; Kornfeld and Mellman, 1989; Dell'Angelica et al., 2000; Eskelinen et al., 2003; Bonifacino, 2004; Luzio et al., 2007). By controlling the degradation of components they receive via endocytosis, autophagy or the biosynthetic pathway, lysosomes are one of the most important organelles in the regulation of cellular homeostasis (Sachse et al., 2002; Eskelinen et al., 2003; Eskelinen, 2005; Luzio et al., 2007). Lysosomes are membrane-bound, thus, allowing the acid-dependent digestive enzymes within them to work at the required optimum pH, 4.5-5.0, which is maintained by the vacuolar H^+-adenosine triphosphate (ATP)ase (Mullins and Bonifacino, 2001; Nishi and Forgac, 2002). Ultimately, degraded products are re-used by the cell after being transported across the

lysosomal membrane and released into the cytosol. Lysosomal enzymes may also be released into the cytosol, where they may be involved in apoptotic pathways, or into the extracellular space to digest extracellular material (Eskelinen et al., 2003; Luzio et al., 2007; Schröder et al., 2007; Braulke and Bonifacino, 2009; Lübke et al., 2009; Schröder et al., 2010).

The metabolic activities of lysosomes are complemented by lysosome-related organelles (LROs), such as major histocompatibility complex (MHC) class II compartments, lytic granules, melanosomes and platelet-dense granules (Dell'Angelica et al., 2000). LROs share many functional properties with lysosomes, but they differ from them by containing cell-type specific proteins, such as tyrosinase-related protein 1 (TRP-1) in melanosomes, that is involved in synthesis of melanin; and P-selectin in platelet-dense granules, that is thought to function as a receptor for adhesive proteins and mediate platelet aggregation (Jackson, 1988; Israels et al., 1992; McNicol and Israels, 1999; Dell'Angelica et al., 2000; Dell'Angelica, 2004). LROs also require additional cellular machinery for their biosynthesis (Dell'Angelica et al., 2000; Bonifacino, 2004; Dell'Angelica, 2004). For instance, the multi-subunit protein complex, biogenesis of lysosome-related organelles complex-1 (BLOC-1), is pivotal for the biogenesis of melanosomes and platelet dense granules (Dell'Angelica, 2004; Lee et al., 2012).

Lysosomes, however, are not just the cells ‘waste disposal and recycling unit’ but together with LROs are involved in multiple cellular processes (see Figure 1.1) including plasma membrane repair, pathogen defense via phagocytosis and MHC class II antigen presenting and phagocytosis, apoptotic cell death, cell signaling, cholestetol and cytosolic Ca^{2+} homeostasis and autophagy (Luzio et al., 2007; Saftig and Klumperman, 2009; Schröder et al., 2010; Lloyd-Evans and Platt, 2011). Thus, any defect in lysosome function can be devastating due to their impact on multiple, crucial cellular functions (Futerman and van Meer, 2004; Cox and Cachón-González, 2012). This is manifested by the rapidly growing number of human disorders that exhibit primary or secondary defects in the lysosomal system (Vellodi, 2005; Parkinson-Lawrence et al., 2010).

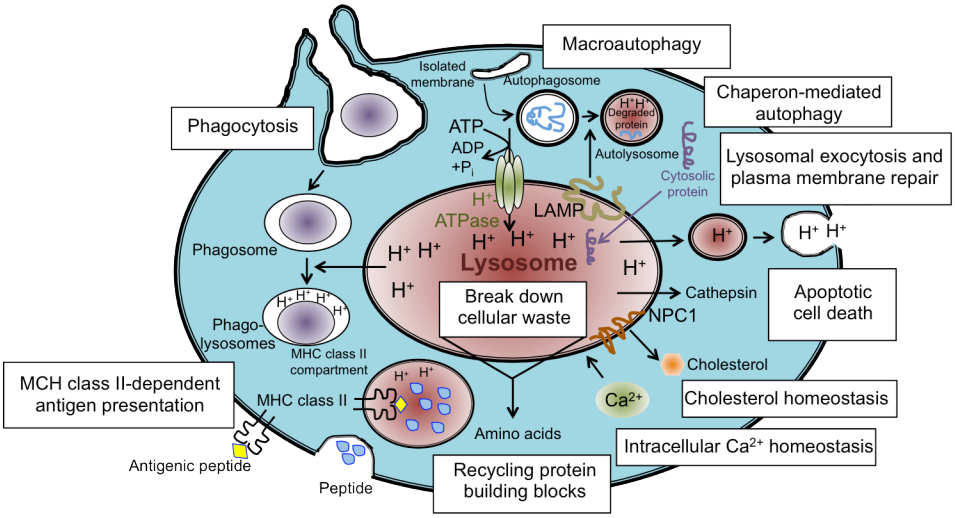

Figure 1.1 Lysosomal functions. Lysosomes are acidic organelles, whose pH is maintained by the proton transportation activity of H^+-ATPase, and are involved in a range of crucial cellular functions. The main role of lysosome is to degrade cellular waste internalized by endocytosis, and intracellular components via autophagy, subsequently they participate in recycling proteins for re-use by the cell. Both the process of macroautophagy, which depends on the fusion of lysosomes with autophagosomes to create autolysosomes controlling turnover of cytoplasmic components, and chaperon-mediated autophagy (direct lysosomal transport of cytosolic proteins) are regulated by lysosome-associated membrane proteins (LAMPs). Another lysosomal membrane protein called Niemann-Pick C1 protein (NPC1) controls the lysosomal cholesterol efflux, important in regulation of cellular cholesterol homeostasis. Lysosomes play a role in apoptotic cell death via release of cathepsins. Lysosomes are also pivotal for cellular pathogenic defense by regulating the maturation of phagosomes to phagolysosomes in phagocytosis, and by being involved in major histocompatibility complex (MHC) class II-dependent antigen presentation. Finally, lysosome exocytosis and plasma membrane repair activities may link lysosomes with autoimmunity, pathogen entry and neurite growth. Lysosomes are also important in intracellular Ca^{2+}-homeostasis by functioning as intracellular Ca^{2+} stores.

Lysosomal proteins

Proteins essential for the function of lysosomes can be classified as either soluble lysosomal hydrolases, also known as acid hydrolases, and integral lysosomal membrane proteins. Each of the 50 known acid hydrolases, including proteinases, peptidases, lipases, nucleases, glycosidases and sulphatases, act on specific substrates and collectively define the catabolic activity of the lysosome (Schröder et al., 2010). Some of these proteases are expressed only in specific tissues, but most of them are expressed ubiquitously (Brix and Jordans, 2005). Soluble lysosomal proteins are synthesized as inactive precursors, and their transportation to, and subsequent activation within, lysosomes is highly regulated (Braulke and Bonifacino, 2009). Lysosomal proteins are heavily glycosylated and oligosaccharide modifications are used for their correct targeting to lysosomes. Indeed, the best understood pathway for transport of

lysosomal enzymes is mediated by mannose 6-phoshate moieties that are attached to lysosomal proteins in the Golgi (Braulke and Bonifacino, 2009; Saftig and Klumperman, 2009). This modification is recognized by different mannose 6-phosphate receptors (MPRs) in the Trans-Golgi-network (TGN), and this ligand-receptor complex then binds clathrin-associated adaptor proteins (APs) and/or Golgi-localized, γ-ear containing, ADP ribosylation factor-finding proteins (GGAs) (Kornfeld and Mellman, 1989; Bonifacino and Traub, 2003; Braulke and Bonifacino, 2009) for transport in clathrin-coated vesicles to the early endosomes (EEs). Due to the acidic pH of endosomes the lysosomal enzymes become dissociated from MPRs and these released enzymes remain in the lumen during EEs maturation to late endosomes (LEs). When LEs fuse with lysosomes activation of the enzymes is initiated, while MPRs are returned back to the TGN by recycling endosomes to carry out further rounds of hydrolase sorting (Braulke and Bonifacino, 2009; Saftig and Klumperman, 2009). Alternative lysosomal targeting systems, including sortilin based lysosomal targeting of cathepsin D, cathepsin H and acid sphingomyelinase, also exist (Lefrancois et al., 2003; Canuel et al., 2008). Cathepsins constitute the main class of lysosomal proteases, and they can be divided into three subgroups, cysteine, aspartyl or serine cathepsins, according to the amino acid at their active site (Conus and Simon, 2008). Overall, having specific delivery systems for lysosomal proteins protects the cells from the potentially harmful effects of prematurely activated lysosomal enzymes.

The mammalian lysosome contains multiple lysosomal membrane proteins, of which at least 120 have been identified (Schröder et al., 2007; Callahan et al., 2009; Lübke et al., 2009; Schröder et al., 2010). Two of the main functions of lysosomal membrane proteins are to assure the acidification of the lysosomal lumen by a proton pump action, and to prevent the release of hydrolases into the cytoplasm in order to protect the cell from unwanted degradation of cytosolic proteins/organelles (Eskelinen et al., 2003). Other functions include facilitation of protein import from the cytosol into the lumen of lysosomes, membrane fusion between lysosomal vacuoles and/or fusion of lysosomes with other membrane organelles, such as endosomes, phagosomes and the plasma

membrane, and transport of degradation products to the cytoplasm (Fukuda, 1991; Eskelinen et al., 2003; Eskelinen, 2006). The main lysosomal membrane proteins are, lysosome-associated membrane proteins (LAMPs), lysosomal membrane glycoproteins (LGPs) and lysosomal integral membrane proteins (LIMPs), some of which can be expressed in a cell-type specific or tissue-specific manner (Eskelinen et al., 2003; Schröder et al., 2007; 2010). These proteins also form a protective polysaccharide-based glycocalyx coat on the inner side of the lysosomal membrane that protects it from digestion by lysosomal enzymes (Eskelinen et al., 2003). It has been estimated that LAMPs and LIMPs are closely packed and comprise more than 50% of the total membrane protein of late endosomes and lysosomes (Marsh et al., 1987). Type 1 lysosomal membrane proteins, which include lysosomal associated membrane protein 1- and 2 (LAMP-1 and LAMP-2), are the major protein components of the lysosomal membrane. Thus, LAMP proteins are routinely used as lysosomal markers (Kornfeld and Mellman, 1989). Mutations in the LAMP-2 gene cause a lysosomal glycogen storage disease, called Danon disease, in humans, and disruption of both LAMPs is associated with an increased accumulation of autophagic vacuoles and unesterified cholesterol (Eskelinen, 2006). Very little is known about the mechanisms for the transport of lysosomal membrane proteins to lysosomes, but this is thought to be regulated by phosphorylation and lipid modification based signal recognition (Braulke and Bonifacino, 2009). For example, many of the lysosomal membrane proteins have been shown to use clathrin/AP/GGA-dependent mechanisms for transportation towards endo/lysosomes when exiting from the TGN either directly, or indirectly via the cell surface, if a constitutive secretory pathway is followed (Eskelinen et al., 2003; Braulke and Bonifacino, 2009; Saftig and Klumperman, 2009). The targeting of some lysosomal membrane proteins occurs independently of the clathrin/AP/GGA-system, and some of them contain a number of distinct sorting motifs. Thus, under different cellular conditions the targeting of lysosomal membrane proteins may vary depending on which distinct trafficking pathways are being used (Saftig and Klumperman, 2009).

Common features of LSDs

Intact lysosomal activity is pivotal for cellular survival and functioning, as described above. Thus, when lysosomal function is altered, neuronal dysfunction and neurodegeneration can follow (Kopra et al., 2004; Walkley, 2007; Wasser et al., 2007; Sann et al., 2009; Walkley, 2009; Walkley et al., 2010). Since the mid-1960s, starting from Gaucher disease, the genetic and biochemical abnormalities present in many LSDs have been elucidated (Futerman and van Meer, 2004; Walkley, 2009; Bellettato and Scarpa, 2010; Schultz et al., 2011; Cox and Cachón-González, 2012). Nearly all LSDs are autosomal recessively inherited monogenic disorders, except for two that are x-linked, Fabry disease and mucopolysaccharidosis (MPS) type II (Hunter syndrome) (Desnick et al., 1989) (Hopwood et al., 1993), and an adult form of autosomal dominant NCL (Parry disease) (Nijssen et al., 2003), caused by mutations in DNAJC5/CLN4 (Anderson et al., 2012).

The storage material that accumulates in different LSDs is heterogeneous with several types of accumulating macromolecules having been identified, including lipids, amino acids, glycoproteins, mucopolysaccharides, sphingolipids, oligosaccharides and sulfatides (Futerman and van Meer, 2004; Ballabio and Gieselmann, 2009; Schultz et al., 2011; Cox and Cachón-González, 2012). Such accumulating intracellular material has been used as a general basis for classifying the LSDs. Since there are obvious limitations with this type of classification system, LSDs have also been grouped according to the characteristics of the defective protein in question (Futerman and van Meer, 2004; Bellettato and Scarpa, 2010; Schultz et al., 2011; Cox and Cachón-González, 2012). The vast majority of LSDs are caused by mutations in genes encoding soluble lysosomal enzymes, resulting in loss of the protein product, an attenuation in catalytic activity, or a disruption of correct folding and glycosylation in the Golgi/endoplasmic reticulum (ER) complex. Alternatively, LSDs can be caused by mutations in non-enzymatic lysosomal proteins that are either soluble or integral membrane proteins (Ruivo et al., 2009; Walkley, 2009; Filocamo and Morrone, 2011). Broadly, these mutated, non-enzymatic lysosomal

proteins are involved in other crucial steps in lysosome biology, such as trafficking, activation/stabilization or post-translational modifications of lysosomal enzymes, or in the transportation of a range of molecules across the lysosomal membrane (Futerman and van Meer, 2004; Ruivo et al., 2009; Saftig and Klumperman, 2009; Filocamo and Morrone, 2011). Even if the genetic defects underlying most of the LSDs have been identified, the primary cause of many of these diseases is still not fully understood. It is possible that a range of pathological mechanisms, such as altered lipid metabolism and autophagosytosis, abnormalities in Ca^{2+} homeostasis and mitochondrial functions arise as result of genetic defects in LSDs, and these mechanisms may be similar across these diseases (Ballabio and Gieselmann, 2009; Walkley, 2009; Bellettato and Scarpa, 2010; Lloyd-Evans and Platt, 2011; Cox and Cachón-González, 2012). Thus, clear-cut genotype-phenotype correlations have not been established in many of these diseases (Walkley, 2009). The progression of LSDs may also be influenced by environmental factors and other modifying genes (Futerman and van Meer, 2004; Walkley, 2009). This raises the important question of how mutations in a single gene, required primarily for lysosomal activities, might lead to such a diverse array of secondary cellular pathogenic events and clinical manifestations?

Many LSDs are clinically non-symptomatic at birth, moreover, children with LSDs typically meet early developmental milestones. This is followed by a phase of developmental delay, indicating that lysosomal dysfunction itself does not alter the complex events that take place during early brain development (Schultz et al., 2011). With more than half of LSDs affecting the brain, as the disease progresses, these children suffer from a wide range of clinical manifestations including mental retardation, dementia, blindness and/or deafness, motor system dysfunction, seizures, sleep and cognitive disturbances (Wraith, 2004; Walkley, 2009; Mole et al., 2011; Cox and Cachón-González, 2012). Very often LSDs result in the devastating disability and premature death of the affected individual. Typically, it is believed that the complex pathogenic processes observed are initiated by lysosomal dysfunction resulting in accumulation of

storage material leading to deficits in other cellular compartments, and eventually dysfunction of the whole cell ending in cell death. Other players such as glial activation have also been suggested to contribute to these events in many LSDs (Walkley, 2009; Bellettato and Scarpa, 2010; Cooper, 2010). Indeed, one common neuropathic feature of LSDs is a neuroinflammatory response mediated by the brain's immune defense system, mainly microglia and astrocytes (Cooper, 2003; 2010; Pressey et al., 2010; Macauley et al., 2011; Di Malta et al., 2012a). Suppressing the glial response in some of these disorders, such as in Sandhoff disease and Niemann-Pick Type C disease, have resulted in improved motor performance, attenuated disease progression or increased life-span, demonstrating the importance of glial cells in these diseases (Wu and Proia, 2004; Zhang et al., 2008; Smith et al., 2009). Many of the common pathological manifestations of LSDs, including the NCLs, have also been shown to occur in other neurodegenerative disorders such as Parkinson disease and Alzheimer disease (Zhang et al., 2009a; Bellettato and Scarpa, 2010; Wong and Cuervo, 2010). Thus, it has been proposed that despite differences in the primary cause of such neurodegenerative disorders, many of them share common pathological processes. Hence, gaining a better understanding of these common mechanisms in one disease may be applicable to a broad range of other neurological disorders, and may increase the applicability of any therapeutic intervention based on inhibiting such mechanisms.

1.2 Neuronal ceroid lipofuscinosis

The term neuronal ceroid lipofuscinosis (NCLs) was first used by Zeman and Dyken in 1969 to describe a group of inherited lysosomal storage disorders that were clinically characterized by progressive decay of visual, motor, and mental functions (Zeman and Dyken, 1969). Prior to this the NCLs were classified for many decades among the so called 'amaurotic family idiocies' due to their clinical resemblance to Tay-Sachs disease (Haltia, 2006; Haltia and Goebel, 2012). The dramatic differences observed between the appearances of infantile (Tay-Sachs), late infantile (Jansky-Bielschowsky) and juvenile (Spielmeyer-Sjögren)

forms of NCL, made it clear that the NCLs are a biochemically heterogeneous group of diseases (Zeman and Dyken, 1969; Haltia, 2003). Based on recent advances, especially in molecular genetic studies, at least 13 different NCL disease-causing genes have been cloned and are listed in Table 1.1 (Goebel, 1995; Mole et al., 2011). Most NCLs (also called Batten disease) are autosomal recessive disorders and collectively form the most common fatal autosomal-recessive neurodegenerative disease of children, with incidences ranging from 0.6 in 100,000 to 13.6 in 100,000 live births (Santavuori, 1988; Goebel, 1995; Augestad and Flanders, 2006; Moore et al., 2008; Mole et al., 2011). Like other storage disorders the NCLs have been named after the predominant storage material that accumulates within cells, which is similar to ceroid and lipofuscin, (Goebel, 1995; Haltia, 2003; Seehafer and Pearce, 2006; Mole et al., 2011). They are also grouped by their age of onset (infantile, late infantile, juvenile) and gene defect (Mole et al., 2011) (see Table 1.1). Perhaps, more simplistically, these different forms can be grouped into those that have defects in genes encoding a soluble lysosomal proteins: CLN1 (PPT1) in infantile (INCL), CLN2 (TPP1) in late infantile (LINCL), CLN5 in Finnish variant LINCL, cathepsin D or CTSD (CLN10) in congenital-NCL and cathepsin F (CLN4/ DNAJC5) in adult onset NCL, and those that have defects in genes that encode transmembrane proteins: CLN3 in juvenile (JNCL), CLN6 in variant LINCL, CLN7 in variant LINCL or Turkish variant LINCL, CLN8 in epilepsy with mental retardation (EPMR) or LINCL variant 3 (Mole et al., 2011; Kousi et al., 2012), an updated database: *http://www.ucl.ac.uk/ncl/mutation.shtml*). The main cellular location of many of these transmembrane NCL-proteins, whose primary functions are still unknown, is either endosomal or lysosomal (Kyttälä et al., 2004; Siintola et al., 2006; Getty and Pearce, 2011). Additionally, a common feature of some NCLs caused by mutations in either soluble or transmembrane forms, such as PPT1, CLN8 and CLN3, is their additional vesicular localization in the cell periphery, thus, these proteins have been proposed to play particular roles in excitatory cells, especially at neuronal synapses (Isosomppi et al., 1999; Heinonen et al., 2000; Lehtovirta et al., 2001; Ahtiainen et al., 2003; Lonka et al., 2004; Getty and Pearce, 2011). However, despite the vast depth of knowledge about the genetic basis of NCLs, it

is currently still unknown how mutations in these genes that encode proteins that function primarily in the endosomal/lysosomal system, lead to such devastating effects in the brain.

NCLs				
Disease Type	Gene Defect	Protein and Function	Mouse Model	Other Animal Model
Congenital (CNCL)	CLN10	Lysosomal hydrolase; Cathepsin D Protein degradation, additional functions	*CtsD*$^{-/-}$ (Saftig et al., 1995)	Dog, Sheep, Drosophila (Tyynelä et al., 2000; Myllykangas et al., 2005; Awano et al., 2006b)
Infantile (INCL)	CLN1	Lysosomal hydrolase; palmitoylprotein Thioesterase 1	*Ppt1*$^{-/-}$, *Ppt1*$^{\Delta ex4}$ (Gupta et al., 2001), (Jalanko et al., 2005)	Dog, Drosophila (Hickey et al., 2006; Sanders et al., 2010)
Late infantile (LINCL)	CLN2	Lysosomal hydrolase; Tripeptidyl peptidase I	*Tpp1*$^{-/-}$ (Sleat et al., 2004)	Dog, Zebrafish (Awano et al., 2006a, Mahmood et al., 2013)
Juvenile (JNCL)	CLN3	Transmembrane protein; Various suggested functions (Getty and Pearce, 2011)	*Cln3*$^{-/-}$, *Cln3*$^{\Delta ex7/8}$, *Cln3*$^{lacZ/lacZ}$ (Katz et al., 1999; Mitchison et al., 1999; Cotman et al., 2002; Eliason et al., 2007)	
Adult (ANCL/Kufs)	CLN4	Gene remains unidentified		
Variant forms: vLINCL	CLN5	Soluble lysosomal protein; Unknown function	*Cln5*$^{-/-}$ (Kopra et al., 2004)	Dog, Sheep, Cow (Melville et al., 2005; Houweling et al., 2006; Frugier et al., 2008)
vLINCL	CLN6	Transmembrane protein in ER; Protein degradation and neuron maturation	*Cln6*$^{nclf/nclf}$ (Bronson et al., 1998)	Sheep (Jolly et al., 1980; Frugier et al., 2008)
vLINCL	CLN7/ MFSD8	Transmembrane protein; Belongs to large major facilitator superfamily (MFS), endolysosomal transporter		
vLINCL (Northern Epilepsy)	CLN8	Transmembrane protein in ER; Lipid metabolism and trafficking	*Cln8*$^{mnd/mnd}$ (Ranta et al., 1999)	Dog (Katz et al., 2005)
Adult NCL (Kufs type B)	CLN13/ CTSF	Cathepsin F; Cysteine protease	*Cat F*$^{-/-}$ (Tang et al., 2006)	
Adult NCL (also cause dementia)	CLN11/ GRN	Progranulin; Glycoprotein	*GRN*$^{-/-}$ (Ahmed et al., 2010)	
Type of JNCL (also cause Kufor-Rakeb syndrome)	CLN12/ ATP13A2	P-type ATPase; Transportation of ions and substrates across membranes		
Type of INCL (also cause progressive myoclonal epilepsy-3)	CLN14/ KCTD7	Potassium channel tetramerization domain containing protein 7		

Table 1.1 NCL classification. This table contains information about all 13 known forms of NCL showing the age of onset, gene defects, affected proteins (red) and their known functions (blue), existing mouse models, and other animal models (Mole et al., 2011).

Although, as mentioned above, the predominant storage material in NCL is ceroid and lipofuscin, its composition is heterogeneous and differs between different forms of NCLs (Seehafer and Pearce, 2006). Generally, it is a combination of oxidized proteins, proteolipids, and very small amounts of metal

ions (Brunk and Terman, 2002; Terman and Brunk, 2004). Post-mitotic cells accumulate lipofuscin over time, and this is often considered as a hallmark of aging where the accumulation rate of lipofuscin inversely correlates with longevity (Terman and Brunk, 2004). The main protein component of the storage material that accumulates in JNCL and in all the different late-infantile variants is the subunit C of the mitochondrial ATP-synthase (SCMAS), while in the infantile, and congenital form it is the sphingolipid activating proteins, saposins A and D, that accumulate (Palmer et al., 1992; Tyynelä et al., 1993; Haltia, 2003; Seehafer and Pearce, 2006; Siintola et al., 2006).

Regardless of their genetic heterogeneity, the different forms of NCLs share several common pathological features (Cooper et al., 2006; Haltia, 2006; Cooper, 2010; Haltia and Goebel, 2012). These include an early glial response (Cooper, 2003; Bible et al., 2004; Mitchison et al., 2004; Pontikis et al., 2004; Oswald et al., 2005; Pontikis et al., 2005; Haber et al., 2006; Haltia, 2006; Kay et al., 2006; Kuronen et al., 2012; Schmiedt et al., 2012), synaptic abnormalities (Virmani et al., 2005; Kim et al., 2008; Partanen et al., 2008; Kielar et al., 2009), and selective loss of particular types of neurons (Mitchison et al., 2004; Oswald et al., 2005; Cooper et al., 2006; Haltia, 2006; Mole et al., 2011; Haltia and Goebel, 2012). Indeed, one unifying feature of NCL pathogenesis is glial activation (both astrocytosis and microgliosis), which differs between forms of NCLs in its timing and level of activation. For instance, in CLN6 sheep (a naturally occurring model of variant LINCL) the activation of astrocytes, microglia and perivascular macrophages is already apparent prenatally, hence, glial activation precedes neuronal loss by several months (Oswald et al., 2005; Kay et al., 2006). In *Ppt1*$^{-/-}$ mice (model of INCL), an early activation of astrocytes takes place before neuronal loss, then subsequently activation of microglia is observed (Kielar et al., 2007). Early glia activation, which occurs long before neuronal loss, has also been reported in different mouse models of JNCL (Pontikis et al., 2004; 2005). However, unlike in other forms of NCL, glia activation in JNCL appears to be attenuated, since astrocytes fail to become fully hypertrophied and up-regulate GFAP and microglia fail to transform fully into macrophages (described in more

detail below) (Pontikis et al., 2004; Tyynelä et al., 2004; Pontikis et al., 2005). Indeed, *Cln3* deficient microglia, have been shown to display specific biological deficits *in vitro* further suggesting that microglial biology is altered in JNCL (S. Dihanich, unpublished data). Thus, the main aim of this thesis was to investigate the potential implications of Cln3 deficiency on the biology of astrocytes, and how glia may impact neuronal survival and function in this disease.

JNCL

Worldwide, JNCL is the most common form of NCL, and it is caused by mutations in the *CLN3* gene (International Batten Disease Consortium, 1995). To date, 57 disease causing mutations have been reported in *CLN3* (NCL gene mutation database: *http://www.ucl.ac.uk/ncl*), with the most common mutation being a 1.02-kb deletion (c.462-677del, g.6060-7025del) of exons 7 and 8 that can be found in 85-90% of all JNCL alleles in homozygous form (International Batten Disease Consortium, 1995, Munroe et al., 1997, Kousi et al., 2012). This deletion mutation results in a frameshift and a truncated protein. The remaining JNCL patients are compound heterozygous for the 1.02-kb deletion with another mutation such as a small insertion, deletion, missense, nonsense, splice site, or intron changes (Mole et al., 2011). The incidence of JNCL differs in different countries, with the highest incidence of 7 per 100,000 live births being observed in Scandinavia (Santavuori, 1988; Uvebrant and Hagberg, 1997).

JNCL pathogenesis

In JNCL the first symptom, which is typically the onset of progressive visual failure, is observed between 4 to 7 years of age and leads eventually to blindness within 2 to 10 years (Boustany et al., 1988; Järvelä et al., 1997; Haltia, 2003; Goebel and Wisniewski, 2004; Krohne et al., 2010; Mole et al., 2011). By 8 - 9 years of age, progressive deterioration of short-term memory and other cognitive functions begins. Spontaneous epileptic seizures commonly appear between 7 and 18 years of age, and worsen as the disease progresses (Järvelä et al., 1997; Lamminranta et al., 2001). By their mid-teens motor skill deficits

develop in affected individuals, and progress to complete immobility. Generally, neuroimaging based studies have revealed progressive brain atrophy, mainly in the cerebral hemispheres, after the age of 10-12 years (Raininko et al., 1990; Autti et al., 1996), and the extent of cerebellar atrophy has been shown to correlate positively with impairments in motor function (Raininko et al., 1990; Nardocci et al., 1995; Autti et al., 1996). Additionally, JNCL patients experience a range of behavioral and psychiatric problems including aggressiveness, hallucinations, sleep problems and depression (Santavuori et al., 1993; Järvelä et al., 1997; Bäckman et al., 2005; Adams et al., 2006). JNCL eventually leads to premature death by the age of thirty or forty, with the mean age being 24 years (Järvelä et al., 1997; Wisniewski et al., 1998).

Post mortem examination of brain tissue samples derived from JNCL patients have revealed that a mild to moderate loss of neurons is evident in all parts of the JNCL brain, resulting in cerebral and cerebellar atrophy (Autti et al., 1997; Haltia et al., 2001; Tyynelä et al., 2004). Selective neuronal depletion occurs in cerebral cortical layers II and V, as well as in the corpus striatum and amygdala with severe loss of granule cells (Braak and Goebel, 1978; 1979; Braak and Braak, 1993). Neurodegeneration also takes place in different hippocampal areas (Tyynelä et al., 2004). Indeed, selective loss of hippocampal and cortical γ-aminobutyric acid (GABA)ergic interneurons is the most prominent feature of JNCL pathogenesis (Braak and Goebel, 1978; 1979; Tyynelä et al., 2004). Generally, neuronal loss seems to take place in brain regions where reactive astrocytosis and microglia activation are also apparent (Haltia et al., 2001; Tyynelä et al., 2004; Mole et al., 2011). The whole retina is often almost completely destroyed and replaced by scar tissue, which is composed of Müeller glia cells as well as other astrocytes (Bozorg et al., 2009; Mole et al., 2011). The accumulation of storage material can be found within various neural cell types (Palmer et al., 1992; Haltia, 2003; Mole et al., 2011), but is not believed to be the cause of neuronal loss, suggesting that additional mechanisms facilitate neurodegeneration in JNCL (Autti et al., 1997; Tyynelä et al., 2004; Jalanko and Braulke, 2009; Mole et al., 2011). Another specific feature of JNCL patients is

their autoimmune response demonstrated by the occurrence of circulating autoantibodies against glutamic acid decarboxylase (GAD65) and other unidentified antigens in the brain (Chattopadhyay et al., 2004; Lim et al., 2006; Castaneda et al., 2008).

Lessons learned from different mouse models of JNCL

To date different gene targeting strategies have been applied to generate four different mouse models for JNCL, *Cln3*$^{\Delta ex1-6}$ *(Cln3*$^{-/-}$*)* knock-out mice*, the* model used for studies described in this thesis (Mitchison et al., 1999), *Cln3*$^{\Delta ex7-8}$ *knock-out* mouse (Katz et al., 1999), the *Cln3*$^{\Delta ex7/8}$ knock-in mouse (Cotman et al., 2002) and *Cln3*^{lacZ} β-galactosidase reporter mice (Eliason et al., 2007). The *Cln3*$^{-/-}$ model represents a null-allele model (Mitchison et al., 1999), and the two other models represent replications of the most common disease-causing 1.02kb CLN3 deletion (Katz et al., 1999; Cotman et al., 2002).

All of these mouse models exist on the same strain background and have phenotypes that resemble those in human JNCL patients, making them all acceptable models of this disease. For instance, accumulation of storage material, glial response accompanied by neurodegeneration and variable neurological defects associated with onset and disease progression have been reported in these different models (Katz et al., 1999; Mitchison et al., 1999; Chattopadhyay et al., 2002; Cotman et al., 2002; Kovács et al., 2006; Eliason et al., 2007; Katz et al., 2008; Osório et al., 2009; Weimer et al., 2009). For example, severe loss of Purkinje cells accompanied by activated cerebellar Bergmann glia (type of astrocyte) in the cerebellum of *Cln3*$^{-/-}$ mice has been shown to precede deficits in motor coordination and balance, providing a link between glial mediated neuronal loss and decline in motor skills in JNCL (Kovács et al., 2006; Weimer et al., 2009). Variable visual defects have been reported in these models (Seigel et al., 2002; Sappington et al., 2003; Weimer et al., 2006; Katz et al., 2008; Osório et al., 2009). Decreased optic nerve axon density and myelination, together with impaired fast axonal transport of amino acids and altered action potentials have been reported in *Cln3*$^{-/-}$ mice, and propose that visual defects in

JNCL are caused by pathological events taking place outside the retina, perhaps in the thalamic nuclei that receive retinal input (Sappington et al., 2003; Weimer et al., 2006). However, impaired retinal function has been shown in the *Cln3*$^{\Delta ex7/8}$ knock-in mouse model (Cotman et al., 2002). Autoantibodies and loss of GABAergic interneurons, two typical pathological features observed in JNCL patients, have also been reported in *Cln3*$^{-/-}$ mice (Mitchison et al., 1999; Chattopadhyay et al., 2002; Pontikis et al., 2004; Castaneda et al., 2008).

An important observation in two of the most-studied models (*Cln3*$^{-/-}$ and *Cln3*$^{\Delta ex7/8}$ knock-in mouse) was that glial activation occurs early in disease progression and takes place in specific brain regions prior to any neuronal loss (Pontikis et al., 2004; 2005; Weimer et al., 2009). Detailed studies in *Cln3*$^{-/-}$ mice revealed up-regulation of markers of astrocytosis and microglia activation in presymptomatic *Cln3*$^{-/-}$ mice (5 months of age), prior to loss of GABAergic interneurons in the hippocampus and neocortex (evident at 14 months of age) (Pontikis et al., 2004). Furthermore, in the cerebellum of *Cln3*$^{-/-}$ mice, activated Bergmann glial cells could be found bordering regions where Purkinje cells were nearly completely lost (Weimer et al., 2009). Additionally, neuritogenesis was found to be defective in the surviving Purkinje cells, with these cells exhibiting dendritic mis-orientation and altered dendritic spine density (Weimer et al., 2009). This activation of glia and loss of Purkinje cells, in addition to altered Purkinje cell dendritic spine morphology occurs before deficits in motor coordination and balance become apparent (Kovács et al., 2006). Thus, it appears that early glial activation precedes selective neuronal loss leading eventually to the typical clinical manifestations observed in JNCL.

The topology and intracellular localization of CLN3

CLN3 encodes a 438-amino acid protein with a predicted molecular weight of 43 kilodaltons (kDa), expressed throughout the whole body including muscle, brain and lungs (Margraf et al., 1999; Stein et al., 2010; Ding et al., 2011). Overall, the mRNA levels for CLN3 in the central nervous system (CNS) are relatively low, with

the highest expression being observed in the gastrointestinal tract and in secretory/glandular tissue around birth (The International Batten Disease Consortium 1995; Pane et al., 1999; Chattopadhyay and Pearce, 2000). CLN3 has no identified homologous proteins, or functional domains, however, CLN3 does display some similarity with fatty acid desaturases and with the equilibrative nucleoside transporter family SLC29 (Baldwin et al., 2004; Narayan et al., 2006b). Despite the lack of homology with other proteins, CLN3 is highly conserved across species, highlighting the fundamental role this protein must play (Taschner et al., 1997; Muzaffar and Pearce, 2008). The membrane topology of the human CLN3 has been extensively studied (Mitchison et al., 1997; Ezaki et al., 2003; Mao et al., 2003; Kyttälä et al., 2004; Nugent et al., 2008), and according to current consensus, CLN3 contains multiple membrane spanning domains (predicted 4-10) with its carboxy terminus facing the cytoplasmic side (Ezaki et al., 2003; Kyttälä et al., 2004; Nugent et al., 2008). The positioning of the N-terminus is still under debate, but based on *in vivo* data this is also thought to be cytoplasmic making CLN3, most likely, a type III transmembrane protein (Ezaki et al., 2003; Kyttälä et al., 2004; 2005). However, uncertainty will remain until the crystal structure of CLN3 is available. Additionally, several predicted posttranslational modifications, such as glycosylation, prenylation, myristoylation and phosphorylation may alter the topological organization of CLN3 (Pullarkat and Morris, 1997; Järvelä et al., 1998; Golabek et al., 1999; Kaczmarski et al., 1999; Ezaki et al., 2003; Mao et al., 2003; Storch et al., 2007; Nugent et al., 2008). For example, CLN3 has been shown to undergo prenylation, which refers to the addition of hydrophobic molecules to a protein, leading to facilitation of CLN3's membrane interactions and trafficking along the endo/lysosomal compartments (Pullarkat and Morris, 1997; Kaczmarski et al., 1999; Storch et al., 2007). Overall, such posttranslational modifications appear to be tissue - and cell type-specific, since mass spectrometric analysis has indicated that the glycosylation of CLN3 varies in different tissues (Ezaki et al., 2003), perhaps suggesting differential roles for CLN3 in different cell-types and tissues.

Due to its low expression levels and the highly hydrophobic nature of CLN3 producing antibodies against this protein has been highly challenging. Hence, determining the precise localization of this protein in different cell types has been problematic, and this has hindered progress towards discovering the precise function of CLN3 (Phillips et al., 2005; Getty and Pearce, 2011). Localization studies have been conducted using a wide range of techniques and by using different CLN3 antibodies, epitope tags and expression constructs. To date, many studies propose that the primary location of CLN3 in mammalian cells is LEs/lysosomes (Fossale et al., 2004; Storch et al., 2004; Phillips et al., 2005; Storch et al., 2007; Tuxworth et al., 2009; Getty and Pearce, 2011; Tuxworth et al., 2011) and that transport to these compartments may be facilitated by interactions between CLN3 and the adaptor proteins AP-1 and AP-3 (Kyttälä et al., 2005). In addition, CLN3 has been proposed to localize to numerous other intracellular compartments including the ER, EEs, recycling endosomes, Golgi, nucleus, lipid rafts, cytoplasm, mitochondria, neuronal processes, synaptosomes and the plasma membrane (proposed cellular localization, functions, and interaction partners of CLN3 are summarized in Figure 1.2) (Katz et al., 1997; Järvelä et al., 1999; Kremmidiotis et al., 1999; Margraf et al., 1999; Luiro et al., 2001; Phillips et al., 2005; Getty and Pearce, 2011). Whether CLN3 is expressed or is actively functioning in any other cellular compartments, except in LEs/lysosomes, is still unknown. Interestingly, in neurons, in addition to being located in LEs/lysosomes CLN3 has also been localized to neuronal processes and synaptosomes; particularly in EEs, presynaptic vesicles, and in vesicles that remain to be identified (Järvelä et al., 1999; Haskell et al., 2000; Luiro et al., 2001; Fossale et al., 2004; Kyttälä et al., 2004; Storch et al., 2004). This distribution would suggest a neuron-specific role for CLN3 relating to synaptic functioning/transmission. However, it is plausible that some of the proposed localizations of CLN3 may be false positives caused by lack of good CLN3 antibodies, mislocalization in over-expression studies and interference with the normal targeting of CLN3 in studies were terminal epitope tags are applied (Phillips et al., 2005). Currently, there is no information available on the specific localization of CLN3 in glial cells.

The proposed functions of CLN3

A crucial step in understanding the molecular basis of JNCL is to identify the precise function of CLN3. To data, the exact function of the highly hydrophobic CLN3 protein remains unresolved despite a decade of intensive research into the primary cause of JNCL. This is because, as stated above, the hydrophobic nature of this protein has hindered the development of sufficiently specific monoclonal or polyclonal antibodies against native CLN3, making the validation of cellular topology, localization and identification of interaction partners by co-immunoprecipitation and colocalization challenging in mammalian cells. However, using a range of animal/yeast models various functions have been attributed to CLN3, including autophagy, intracellular trafficking, regulation of lysosomal pH and size, processing of lysosomal proteins, arginine metabolism, mitochondrial function, apoptotic pathway regulation, lipid metabolism and oxidative homeostasis (summarized in Figure 1.2) (Getty and Pearce, 2011; Mole et al., 2011). Indeed, the primary function of CLN3 may have a knock on effect on several pathways, or CLN3 may have several primary functions each affecting a different pathway and some of these may be cell-type specific. The potential functions of CLN3 and their roles in JNCL pathogenesis are described below. Additionally, these functions may be linked with pathways mediated by numerous interaction partners of CLN3 (described below).

Autophagy. The intralysosomal accumulation of mitochondrial ATP synthase subunit C upon CLN3 deficiency potentially links the functional role of CLN3 with autophagy, since autophagy is essential for mitochondrial turnover (Rubinsztein et al., 2005). Indeed, CLN3 has been linked with autophagosomal membranes, and the buildup of subunit c protein has been found in autophagic vacuoles and lysosomes by means of immunoblotting (Fossale et al., 2004; Cao et al., 2006). Moreover, in *Cln3*$^{\Delta ex7/8}$ mice, CLN3 deficiency has been shown to impair the maturation of autophagosomes based on their ultrastructural morphology, leading to activation of autophagy based on an increased LC3-II/LC3-I ratio (autophagy marker, microtubule-associated protein I light chain 3; LC3). Studies on cerebellar neuronal cell cultures derived from *Cln3*$^{\Delta ex7/8}$ mice suggest that this

protein may also be involved in the trafficking of autophagic vacuoles to the perinuclear region where the fusion with LEs/lysosomes takes place (Cao et al., 2006). The suggested link between CLN3 and autophagy is supported by experiments where restoring autophagy in cerebellar *Cln3*$^{\Delta ex7/8}$ *cells* using lithium, or an inositol monophosphatase (IMPase) inhibitor called L690,330 (Sarkar et al., 2005), resulted in protection of these cells from cell death induced by amino acid deprivation (Chang et al., 2011). Thus, defects in autophagy particularly in CLN3 neurons may increase their susceptibility to cell death and be a key element in neuronal pathogenesis in JNCL.

Intracellular trafficking. In addition to disrupted autophagy, CLN3 deficiency has been linked with a number of disrupted intracellular trafficking processes. For instance, *Cln3*-silenced HeLa cells displayed an impaired exit of mannose 6-phosphate receptor from the TGN (Metcalf et al., 2008). Further, an altered localization of LEs/lysosomes together with impaired endocytosis has been reported in cerebellar neuronal *Cln3*$^{\Delta ex7/8}$ precursor cells (Fossale et al., 2004; Cao et al., 2011). Finally, fast axonal transport of amino acids in the optic nerves of *Cln3*$^{-/-}$ mice is attenuated (Weimer et al., 2006). This may lead to impaired communication between the retina and projection nuclei within the thalamus, resulting in a reduced number of neurons within the dorsal lateral geniculate nucleus (LGNd) in *Cln3*$^{-/-}$ mice (Weimer et al., 2006). Hence, a lack of axonal transport may provide a mechanistic explanation for the visual deficits in JNCL. Overall, it appears that CLN3 may be required for intracellular trafficking of both cellular organelles and small molecules.

Lysosome related functions. In the budding yeast, *S. cerevisiae*, deletion of BTN1 (homologue of Cln3) results in a reduced vacuolar pH (Croopnick et al., 1998; Pearce and Sherman, 1998; Pearce et al., 1999a), while in the fission yeast *S. pombe* an increased lysosomal pH is observed (Gachet et al., 2005). Despite these contrasting results, these experiments suggest that the btn1 protein is involved in vacuolar pH maintenance (Pearce and Sherman, 1998; Pearce et al., 1999a; 1999b; Gachet et al., 2005). Furthermore, elevated lysosomal pH is

evident in fibroblasts derived from JNCL patients (Holopainen et al., 2001). The size of lysosomes has also been shown to be affected by alterations in CLN3 expression (Golabek et al., 2000; Holopainen et al., 2001; Kitzmüller et al., 2008) and a number of reports, using mouse models, human cell lines and *post mortem* tissue, have revealed changes in both the activity and processing of lysosomal proteins, such as cathepsins (mutated in congenital NCL) and TPP1 (mutated in late infantile NCL) with CLN3 deficiency (Prasad and Pullarkat, 1996; Sleat et al., 1998; Junaid and Pullarkat, 1999; Mitchison et al., 1999; Golabek et al., 2000; Fossale et al., 2004; Eliason et al., 2007; Metcalf et al., 2008). Lysosomal import of arginine was demonstrated to be attenuated in JNCL patient lymphoblasts (Ramirez-Montealegre and Pearce, 2005), moreover, alterations in mitochondrial arginine metabolism, as well as in plasma membrane arginine uptake, in *Cln3*$^{-/-}$ mice link CLN3 functioning with the regulation of cellular arginine metabolism (Chan et al., 2009). For instance, altered arginine levels may cause the observed changes in the activities of the urea cycle enzymes associated with the citrulline-nitric oxide (NO) recycling pathway and alterations in regulation of nitric oxide synthase (NOS) in *Cln3*$^{-/-}$ mice (Chan et al., 2009). Overall, these studies highlight the range of lysosomal functions attributed to CLN3, which may act to catalyze the neuropathological events observed in JNCL. For example, alterations in NO signaling have the potential to alter a range of physiological processes such as apoptosis, synaptic function and immune response (Garthwaite and Boulton, 1995; Szabó, 1996; Prast and Philippu, 2001; Holán et al., 2002; Bronte and Zanovello, 2005; Guix et al., 2005).

Proteolipid modifications. It has been speculated, based on sequence analysis and gas chromatography/mass spectrometry desaturase assays, that CLN3 may be a novel palmitoyl-protein Δ9-desaturase, which converts membrane-associated palmitoylated proteins to their respective palmitoleated products, (Narayan et al., 2006b; 2008). Thus, CLN3 may potentially be involved in proteolipid modifications. Furthermore, metabolic labeling of fibroblasts derived from JNCL-patients revealed that CLN3 may be involved in phospholipid bis(monoacetylglyceryl)phosphate (BMP) synthesis (Hobert and Dawson, 2007)

contributing to the determination of membrane properties of intracellular organelles. For instance, negatively charged BMP may participate in the degradation of lipids and membranes at the interface of the inner membranes of lysosomes by facilitating the adhesion of the positively charged soluble lysosomal proteins (Gallala and Sandhoff, 2011). Thus, mutated human CLN3 could participate in lysosomal pathogenesis via altering membrane lipid metabolism.

Oxidative homeostasis. Increased protein oxidation, possibly arising from significant alterations in the levels of pro-and antioxidant molecules, such as decreased levels of glutathione (major antioxidant in the brain), have been observed in the CNS of both *Cln3*$^{-/-}$ and *Cln3*$^{\Delta ex7/8}$ mice (Benedict et al., 2007; Weimer et al., 2007; Herrmann et al., 2008). Additionally, oxidative stress induced cell death was observed to be accelerated in cerebellar precursor cells derived from *Cln3*$^{\Delta ex7/8}$ mice (Fossale et al., 2004), and Drosophila lacking functional CLN3 were shown to be hypersensitive to oxidative stress, while responding normally to other kinds of physiological stresses (Tuxworth et al., 2011). Taken together, CLN3 appears to be required for managing the cellular response to oxidative stress, possibly via affecting antioxidant production and this may contribute to neuronal degeneration in JNCL.

Neuronal activity altering functions. Increasing evidence links CLN3 with neuronal cell communication. Autoantibodies detected against GAD65, an enzyme that converts the excitatory neurotransmitter glutamate to the inhibitory neurotransmitter GABA, could result in the decreased activity of this enzyme in the *Cln3*$^{-/-}$ mouse brain (Chattopadhyay et al., 2002; Pears et al., 2005). This may be one the reasons behind diminished GABA production and elevated presynaptic levels of glutamate in these brains, which in turn may be linked to the preferential loss of GABAergic neurons observed in both JNCL patients and *Cln3*$^{-/-}$ mice (Braak and Goebel, 1978; 1979; Mitchison et al., 1999; Chattopadhyay et al., 2002; Pontikis et al., 2004; Tyynelä et al., 2004). In addition, cerebellar granule cells derived from *Cln3*$^{-/-}$ and *Cln3*$^{\Delta ex7/8}$ mice exhibit

particular vulnerability to 2-amino-3-(5-methyl-3-oxo-1,2-oxazol-4-yl) propanoic acid (AMPA) and/or N-Methyl-D-aspartic acid (NMDA)-type glutamate receptor-mediated excitotoxic insults (Kovács et al., 2006; Kovács and Pearce, 2008; Finn et al., 2011). Indeed, selective inhibition of AMPA receptors in *Cln3*$^{-/-}$ mice was shown to lead to improvements in the motor function (Kovács and Pearce, 2008; Kovács et al., 2011). Furthermore, the receptor binding sites of cholinergic and glutamergic receptors were shown to be reduced in *Cln3*$^{\Delta ex7/8}$ mice (Herrmann et al., 2008), and the reduced expression of dopamine transporters and receptors in JNCL patients in various brain regions provides additional evidence for disrupted neuronal communication (Ruottinen et al., 1997; Aberg et al., 2000; Rinne et al., 2002). Finally, early abnormalities in dopamine catabolism, causing neuronal loss in the substantia nigra, has also been demonstrated to precede the development of motor deficits in *Cln3*$^{-/-}$ mice (Weimer et al., 2007). Therefore, several lines of evidence propose that CLN3 is an essential part of the complex regulatory processes involved in neuronal activity and information processing. However, the mechanisms behind this, and how they may relate to the clinical manifestations of JNCL remain elusive.

In conclusion, CLN3 has been proposed to have multiple functions, which most likely display cellular specificity. However, the primary function of this protein remains unknown, given that the lack of specific antibodies has made conducting experiments to determining the localization, trafficking and overall function of CLN3 difficult. Broadly, it appears that CLN3 may play a role in the trafficking of subcellular organelles and maintenance of cellular homeostasis. Research has also provided some evidence that CLN3 may have multiple interaction partners, which may mediate the observed participation of this protein in the numerous biological processes described.

Protein interaction partners of CLN3

By applying different techniques, such as a yeast-2-hybrid (Y2H) screen, mammalian two-hybrid and GST-pull down assays, many protein interaction partners of CLN3 have been proposed, which in turn have highlighted the

potential involvement of this protein in a range of cellular functions (Phillips et al., 2005; Getty and Pearce, 2011; Mole et al., 2011; Uusi-Rauva et al., 2012). For instance, CLN3 appears to interact with the cytoskeletal protein **β-fodrin** (β-II-spectrin chain) and the associated multifunctional **Na^+-K^+-ATPase complex** (Uusi-Rauva et al., 2008). Via β-fodrin, CLN3 might also be indirectly connected to actin and centractin (ARP1), creating not only a link between CLN3 and the cytoskeleton, but also with dynein, myosin and maybe other motor proteins involved in intracellular transport (Beck and Nelson, 1996; De Matteis and Morrow, 2000; Bennett and Baines, 2001). It has been demonstrated that β-fodrin architecture was altered in both JNCL patient fibroblasts and *Cln3*$^{-/-}$ mouse brain sections (Uusi-Rauva et al., 2008). However, abnormal β-fodrin cytoarchitecture did not lead to an altered ion pumping activity of the associated Na^+-K^+-ATPase complex in *Cln3*$^{-/-}$ primary embryonic (*E16.5*) cortical neuronal cultures. Instead, endocytosis, and thus the plasma membrane-associated expression of this ATPase, explored by means of TIRF-microcopy, was significantly altered. Thus, CLN3 could be involved in the formation of a multiprotein complex with β-fodrin and Na^+-K^+-ATPase at the plasma membrane (Nelson and Hammerton, 1989; Uusi-Rauva et al., 2008; Kizhatil et al., 2009). The activity of this Na^+-K^+-ATPase is responsible for maintaining the relatively high concentrations of intracellular potassium, but low concentrations of sodium ions, found in resting neurons (resting potential), and for returning neurons back to baseline after depolarization (Rakowski et al., 1989; Wright, 2004). Additionally, the different functional subunits (α, β and the auxiliary FXYD protein subunits) of this Na^+-K^+-ATPase also carry out a range of activities (Geering, 2005; 2008). For example, the chaperone function of the β-subunit is involved in the formation of tight junctions, cell polarity, cell-cell adhesion and in inhibition of cell motility, potentially linking CLN3 with a number of secondary functions (Geering, 2008). Furthermore, abnormal formation of β-fodrin containing complexes may have neuron specific implications, since at the synapse β-fodrin interacts with synapsin-1, a protein involved in synaptic transmission/neurotransmission regulation (Zimmer et al., 2000).

CLN3 has also been proposed to interact with **Hook1**, which is a microtubule binding proteins associated with the regulation of endocytosis (Krämer and Phistry, 1996; 1999; Luiro et al., 2004). Indeed, by analysing the trafficking of fluorescent low-density lipoprotein (BODIPY FL-LDL) and biotinylated transferrin, receptor-mediated endocytosis and recycling were demonstrated to be defective in JNCL patient fibroblasts, possibly due to the lack of correct CLN3-Hook1 interactions. Furthermore, via HooK1, CLN3 may have an indirect connection with the endocytic guanosine triphosphate (GTP)ases Rab7, Rab9 and Rab11 reinforcing its role in endocytic membrane trafficking (Tuvim et al., 2001; Luiro et al., 2004; Heasman and Ridley, 2008). Indeed, recently, CLN3 was proposed to interact directly with active GTP-bound **Rab7** and with Rab7-interacting lysosomal protein (**RILP**), which is a dynein motor protein (Jordens et al., 2001; Uusi-Rauva et al., 2012). Abnormalities in these connections were shown to affect the movement and intracellular localization of late endosomes and lysosomes, proposing a regulatory role for CLN3 in these cellular transport mechanisms. Hook1 is also known to interact with Ankyrin G, which is a scaffolding protein associated with the spectrin-actin cytoskeleton and targeting of proteins, such as voltage-gated sodium channels and cell adhesion proteins, to the peripheral membrane (Zhou et al., 1998; De Matteis and Morrow, 2000; Jenkins and Bennett, 2001; Garrido et al., 2003; Weimer et al., 2005; Pan et al., 2006; Kizhatil et al., 2009). However, no defects were discovered in the interactions between Hook1 and Ankyrin G, or their localization in tissue derived from *Cln3*$^{-/-}$ mice (Weimer et al., 2005). It was speculated, however, that nearly a threefold increase in the expression of Hook1, caused by a lack of CLN3, may lead to alterations in the functioning and positioning of membrane associated proteins via altered Hook1-Ankyrin G interactions.

The C-terminus of CLN3 has been shown to form a connection with the Ca^{2+}-binding protein **calsenilin** (Chang et al., 2007), which exerts its functions both in the cytosol and in the nucleus (Buxbaum et al., 1998; Carrión et al., 1999; Burgoyne et al., 2004). For instance, calsenilin has been shown to enhance Ca^{2+} induced apoptosis, regulate A-type currents influencing neuronal excitability via

binding to voltage-gated potassium channels, be involved in trafficking of Golgi glycosyltransferases and it may even function as a transcription repressor by interacting with downstream regulatory element (DRE) sites in DNA (Carrión et al., 1999; An et al., 2000; Jo et al., 2001; Lilliehook et al., 2002; Quintero et al., 2008). *In vitro* binding and immunoprecipitation assays revealed that when intracellular Ca^{2+} concentrations are high, the CLN3-calsenilin connection is disrupted leading to a reduction in cell death induced by high Ca^{2+} (Chang et al., 2007). Hence, CLN3 deficiency may expose cells to Ca^{2+}- induced cell death suggesting that CLN3 may have anti-apoptotic abilities via regulation of calsenilin mediated cell death pathways.

Recently, it was proposed from a yeast-2-hybrid screen, and confirmed by co-immunoprecipitation studies, that the C-terminal segment of CLN3 connects with cytoskeleton associated non-muscle myosin heavy chain IIB (**myosin-IIB**), (Getty et al., 2011). Myosin-IIB is an actin-binding protein, predominantly expressed in the brain, that is involved in actin-cross linking and has actin contractile properties making it central for determining cell polarity, adhesion, division, growth and motility (Simons et al., 1991; Rochlin et al., 1995; Tullio et al., 2001; Lo et al., 2004; Ryu et al., 2006; Vicente-Manzanares et al., 2007; 2009). Indeed, primary mouse embryonic fibroblasts derived from *Cln3*$^{-/-}$ mice exhibited significant migration defects in a scratch assay (Getty et al., 2011). The migration of these *Cln3*$^{-/-}$ cells was not impaired by blebbistatin, which is an inhibitor of myosin II ATPase, as it was in WT cells, proposing that migration of *Cln3*$^{-/-}$ cells was already compromised due to dysregulated myosin-IIB function (Getty et al., 2011). Additionally, the morphology of *Cln3*$^{-/-}$ fibroblasts was altered, they had elongated, narrow cell bodies and a disrupted myosin-IIB intracellular distribution (Getty et al., 2011). In neuronal cells myosin-IIB is pivotal for axonal outgrowth and dendritic tree formation by controlling growth cone motility (Bridgman et al., 2001; Tullio et al., 2001; Ryu et al., 2006). Additionally, myosin-IIB participates in synaptic transmission by altering vesicle trafficking in presynaptic nerve terminals (Takagishi et al., 2005). Thus, CLN3 via its interaction with myosin-IIB may be linked to various neuronal cell specific activities, and

more generally to determination of cellular morphology.

CLN3 has been shown to bind to Shwachman-Bodian-Diamon syndrome protein (**SBDS**) in *S. cerevisiae* (yeast homologues: Btn1 and Sdo1, respectively), and this interaction was also confirmed by co-immunoprecipitation of CLN3 and SBDS from NIH-3T3 cells (Vitiello et al., 2010). SBDS protein is mutated in Shwachman-Bodian-Diamon syndrome, which is an autosomal recessive disorder associated with defects in immunity, skeletal and hematological malfunctions, exocrine pancreatic deficiency and cardiac disorders (Boocock et al., 2003; Burroughs et al., 2009). SBDS is a highly conserved protein whose proposed functions are many fold, including regulation of apoptosis, mitosis, inhibition of genomic instability, ribosomal functions via connection with 60S and other ribosomal proteins, regulation of DNA and ER stress responses (Ganapathi et al., 2007; Hesling et al., 2007; Menne et al., 2007; Austin et al., 2008; Ball et al., 2009; Watanabe et al., 2009). Deletion of the Btn1 protein in yeast developed modifications in vacuolar pH and vATPase-dependent transportation of H^+ and ATP hydrolysis, while deletion of Sdo1 lead to a decrease in both of these properties (Vitiello et al., 2010). Hence, both of these proteins appear to function within the same pathway. It was proposed that Sdo1 (SBDS) acts as a regulatory element of Btn1 (CLN3), and thus provides a mechanism underlying the abnormal vacuole/lysosome biology in JNCL. However, this hypothesis remains untested in mammalian cells.

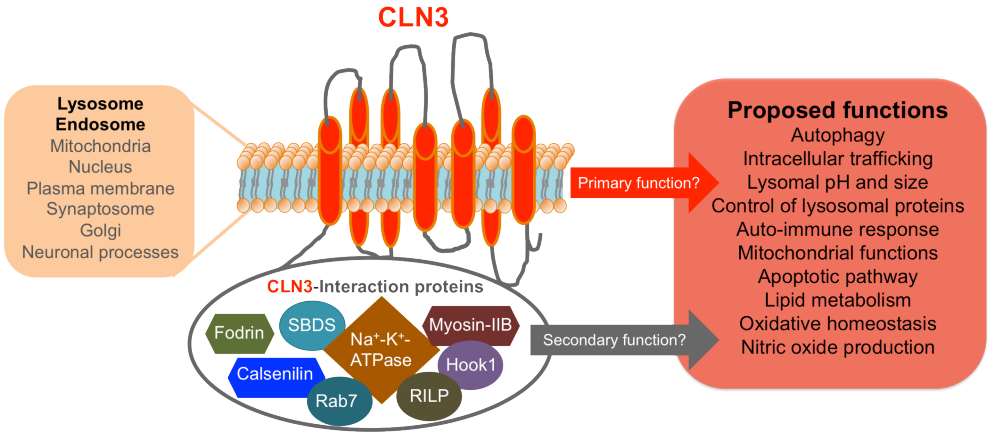

Figure 1.2. The properties of CLN3. This image summarizes the proposed cellular localizations of the transmembrane protein CLN3. The primary location of CLN3 is thought to be endo/lysosomal, but many other locations have also been suggested. CLN3 has many proposed interaction partners, and most likely CLN3 interacts with these proteins in a dynamic and cell-type dependent fashion.

The research described above highlights that CLN3 is a multifunctional protein, required for many aspects of a cell's biology, including protein trafficking, lysosomal functioning, transmission of signals required for cell-cell communication, organization of the cell's structural framework and regulation of apoptotic pathways (summarized in Figure 1.2). Possibly many of these functions can be related to activities of the numerous potential interaction partners of CLN3, as described above. Whether CLN3 interacts with same proteins in all cell types, and whether it has cell type specific functions remain elusive. Particularly interesting from the JNCL point of view are the proposed neuron-specific functions of CLN3, whose alterations may directly lead to the clinical and pathological manifestations typical of JNCL (Järvelä et al., 1999; Haskell et al., 2000; Luiro et al., 2001; Chattopadhyay et al., 2002; Kyttälä et al., 2004; Pears et al., 2005; Kovács et al., 2006; Storch et al., 2007; Finn et al., 2011; Kovács et al., 2011). However, as stated, glial activation has been shown to precede neuronal loss, and the appearance of the first clinical symptoms in different JNCL mouse models (Mitchison et al., 1999; Cotman et al., 2002; Pontikis et al., 2004; 2005; Kovács and Pearce, 2008; Weimer et al., 2009). Given the importance of glial cells for the proper functioning of neurons in both the healthy and diseased CNS

(Verkhratsky and Butt, 2007; Barres, 2008; Allen and Barres, 2009; Sofroniew and Vinters, 2010; Verkhratsky and Parpura, 2010), any abnormalities in glial functioning may significantly disrupt this relationship. In JNCL, as previously stated, the glia response appears attenuated (Pontikis et al., 2004; Tyynelä et al., 2004; Pontikis et al., 2005) and our recent *in vitro* studies have confirmed that *Cln3*$^{-/-}$ microglia have an impaired ability to respond to an activation stimulus, both in terms of changing their morphology and in secreting a specific sub-set of proteins (S. Dihanich, unpublished data). This has provided the first direct evidence for a functional role of CLN3 in glia cells. The research described in this thesis extends these studies to astrocytes, to determine how CLN3 deficiency impacts their function (Chapters 3 and 4), and the impact that these cells together with *Cln3*$^{-/-}$ microglia may have on neuronal health (Chapter 6).

In the next sections, the importance of glial-neuronal interactions is discussed together with the problems that can arise when this communication breaks down.

1.3 Cells of the central nervous system

The adult CNS is composed of neurons and glia (astrocytes, oligodendrocytes and microglia (Kandel et al., 2012) and although the CNS contains many different type of neurons, these are far outnumbered by the glia (HAWKINS and OLSZEWSKI, 1957; Pfrieger and Barres, 1995; Barres, 2008; Purves, 2011). The cellular interactions between neurons and glia are extremely complex and essential for the proper functioning of the CNS. Among the most important functions of glial cells are to provide structural and homeostatic support for neurons, insulate neurons electrically, guide neuronal differentiation, and clear cell debris (Verkhratsky and Butt, 2007; Allen and Barres, 2009; Kettenmann et al., 2011). In addition to being pivotal in the healthy CNS, glia also help defend the brain against infection and disease (Pekny and Nilsson, 2005; Sofroniew and Vinters, 2010; Zhang et al., 2010; Liu et al., 2011; Singh et al., 2011).

Neurons

Neurons are highly specialized cells that send and receive information, allowing communication within the brain, and between the brain and the body (Purves, 2011; Kandel et al., 2012). They communicate with one another by means of action potentials (rapid reversals of voltage across the plasma membrane of axons) (Barnett and Larkman, 2007; Debanne et al., 2011; Purves, 2011; Sasaki et al., 2011; Kandel et al., 2012). The action potential travels along the axon to the synapse, where the electrical signal is converted into a chemical signal (neurotransmitters) that is propagated to the dendritic spines of the postsynaptic neuron (Llinás et al., 1985; Llinás, 1988; Wang et al., 2009a). Neurons frequently have multiple dendrites that form complex branched networks that are specialized to receive presynaptic inputs (Jan and Jan, 2001; Häusser, 2007; Conde and Cáceres, 2009).

The initiation of the action potential takes place in a specialized region located at the start of an axon, called the axonal initial segment (AIS), that is composed of multiple proteins, including a high number of Na^+ channels required for membrane depolarization (Ogawa and Rasband, 2008; Grubb and Burrone, 2010a; Buffington and Rasband, 2011; Grubb et al., 2011). The arrival of an action potential at the synapse results in the influx of Ca^{2+} and the fusion and release of synaptic vesicles containing neurotrasmitters with the plasma membrane (Sudhof, 2004; Lodish et al., 2007; Purves, 2011). The released neurotransmitters then interact with receptors expressed by post-synaptic neurons (Sudhof, 2004). The membrane fusion of synaptic vesicles requires the interaction of specific proteins called soluble N-ethylmaleimide-sensitive factor (NSF) attachment protein receptor (SNARE)-complex proteins (Söllner et al., 1993a; 1993b; Kavalali, 2002; Ungar and Hughson, 2003; Ramakrishnan et al., 2012). These include, vesicle-associated membrane protein 1 (VAMP1) and/or 2, also called synaptobrevins, on synaptic vesicles that interact with syntaxin and synaptosomal-associated protein 25 (SNAP25) on the presynaptic plasma membrane enabling SNARE-mediated vesicle fusion and exocytosis of neuroactive factors (Rizo et al., 2006; Ramakrishnan et al., 2012). The synaptic

vesicle proteins synaptophysin 1 and 2 are also involved in the regulation of SNARE-complex formation via interaction with VAMPs (Washbourne et al., 1995; Becher et al., 1999). Furthermore, the post-synaptic neuronal membranes, and thus synaptic transmission, may be altered by other molecules and metal ions, such as zinc, which may be present in the synaptic cleft (Huang, 1997). Neuronal cells are also capable of altering the expression of neurotransmitter receptors at synaptic membranes, which modifies their response to pre-synaptic stimuli (Beattie et al., 2000; Man et al., 2000; Carroll et al., 2001; Shi et al., 2001). Additionally, increasing evidence demonstrates that glia, particularly astrocytes, are pivotal regulators of neuronal activity via active participation in the regulation of synaptic transmission and plasticity, suggesting that brain function results from the coordinated activity of neuron-glia networks, and not exclusively from neuronal networks (Volterra and Meldolesi, 2005; Allen and Barres, 2009; Perea et al., 2009; Araque and Navarrete, 2010; Perea and Araque, 2010; Santello et al., 2012; Verkhratsky et al., 2012a).

Astrocytes

Active research on astrocytes over the last three decades has significantly increased our knowledge of their function. Originally described as a connective tissue that binds nervous elements together (Rudolf Virchow, 1858), astrocytes are now recognized as not only being pivotal for providing metabolic and trophic support for neural networks, but also as active participants in synaptic transmission, CNS synaptogenesis, brain energy metabolism and blood-brain barrier (BBB) maintenance (Ridet et al., 1997; Volterra and Meldolesi, 2005; Abbott et al., 2006; Verkhratsky and Butt, 2007; Allen and Barres, 2009; Kimelberg, 2010; Parpura and Zorec, 2010; Sofroniew and Vinters, 2010; Verkhratsky and Parpura, 2010). These cells also use Ca^{2+}-based signaling as a form of communication (basic astrocyte functions are summarized in Figure 1.3) (Allen and Barres, 2009; Verkhratsky and Parpura, 2010; Nag, 2011). Astrocytes have been shown to be critical participants in numerous disorders that affect the CNS, including all forms of NCLs (Bible et al., 2004; Pontikis et al., 2004; Tyynelä

et al., 2004; Pekny and Nilsson, 2005; Sofroniew and Vinters, 2010; Macauley et al., 2011; Kuronen et al., 2012; Schmiedt et al., 2012).

Astrocytes are divided into two main subtypes, protoplasmic and fibrous, based on their morphological appearance. Protoplasmic astrocytes are located throughout the gray matter and have several stem branches, which give rise to numerous, very complex, finely branching processes (Verkhratsky and Butt, 2007; Theodosis et al., 2008; Matyash and Kettenmann, 2010). Fibrous astrocytes are located throughout the white matter and extend long fiber-like processes (Peters et al., 1991; Verkhratsky and Butt, 2007). However, as well as these two main astrocyte classes, that are both composed of heterogeneous groups of astrocytes, there are also Bergmann glial cells in the cerebellum; interlaminar and polarized astrocytes of the deep cortical layers in the primate brain; Müller glial cells of the retina; perivascular and marginal astrocytes; tanycytes located at the ventricular walls of the hypothalamus and spinal cord; velate astrocytes of the cerebellum where each one forms a sheath surrounding a granule neuron; and pituicytes in the neurohypophysis (Oberheim et al., 2006; Verkhratsky and Butt, 2007; Oberheim et al., 2009; Kimelberg, 2010; Kimelberg and Nedergaard, 2010; Matyash and Kettenmann, 2010; Zhang and Barres, 2010; Oberheim et al., 2012). Thus, overall, astrocytes comprise a heterogeneous population of cells, and it is believed that their different morphologies reflect their functional diversity (Zhang and Barres, 2010; Molofsky et al., 2012). It is also important to note that human astrocytes are considerably more complex morphologically than their rodent counterparts (Oberheim et al., 2009).

Both protoplasmic and fibrous astrocytes connect with blood vessels via their endfeet processes, and connect with one another via gap junctions comprising connexins 43 (Cx43) and 30 (Cx30) protein subunits, which enable diffusion of small molecules between connected astrocytes (Freeman, 2010; Matyash and Kettenmann, 2010; Sofroniew and Vinters, 2010; Zhang and Barres, 2010). The close connection with blood vessels enables astrocytes to control CNS blood flow, as a response to neuronal activity, in a coordinated manner via release of

vasoactive molecules including prostaglandins (PGE), nitric oxide and arachidonic acid (AA) (Gordon et al., 2007; Iadecola and Nedergaard, 2007). Protoplasmic astrocytes also form close connections with synapses where they control transmitter and ion homeostasis, and therefore regulate synaptic transmission. The processes of fibrous astrocytes connect with axons at nodes of Ranvier, the unmyelinated sites of action potential propagation, providing a location for direct signaling between axons and astrocytes (Butt et al., 1994; 1999; Freeman et al., 2010; Matyash et al., 2010; Sofroniew and Vinters, 2010; Zhang et al., 2010). Under physiological conditions protoplasmic astrocytes have non-overlapping domains, which may become disrupted under severe pathological conditions leading to long-term reorganization of tissue architecture with consequences that remain poorly understood (Bushong et al., 2002; Ogata and Kosaka, 2002; Wilhelmsson et al., 2006; Halassa et al., 2007; Verkhratsky and Butt, 2007; Sofroniew and Vinters, 2010; Sun and Jakobs, 2011).

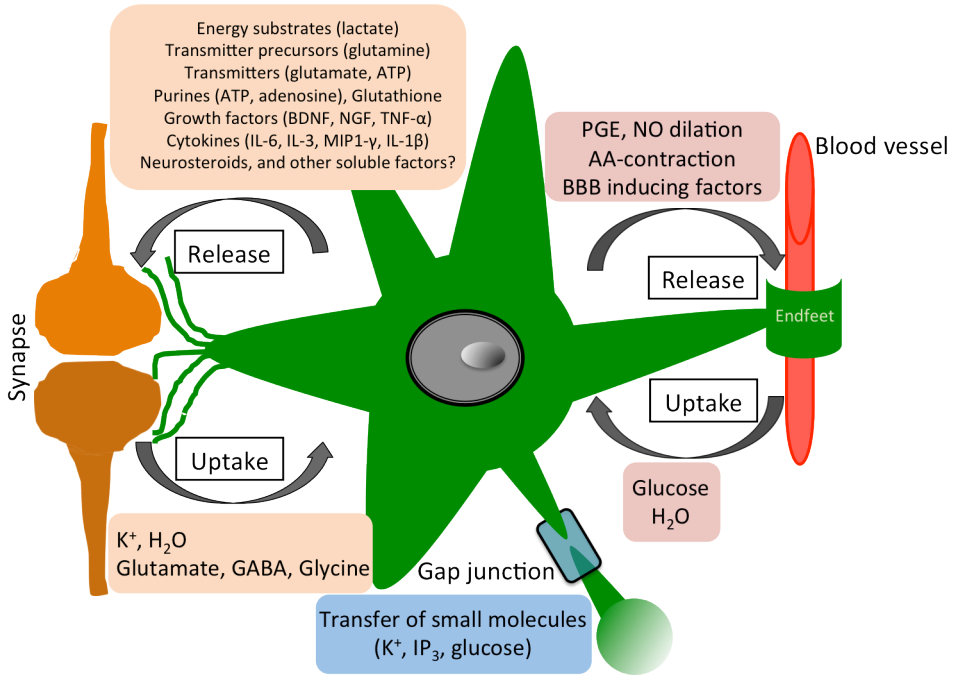

Figure 1.3. Functions of astrocytes in the healthy CNS. Schematic representation that summarizes the functions of astrocytes in the healthy CNS. Astrocytes are in close connection with blood vessels via endfeet, and with synapses via their highly complex processes. Astrocytes are connected to one another via gap junctions that allow diffusion of soluble factors (examples given in brackets). Arachidonic acid (AA) released by astrocytes causes contraction of blood vessels, while prostaglandin (PGE) induce nitric oxide (NO) mediated dilation of the vessels. In contrast, astrocytes can take up glucose and H_2O from the blood. Astrocytes can regulate synaptic activity via release and uptake of numerous neuro- and glial-active factors (examples given in brackets).

During development astrocytes are generated after neurons (Verkhratsky and Butt, 2007), despite this, astrocytes are important for the maturation and survival of neurons within both the grey and white matter. During the development of the white matter, impaired gap junction-mediated astrocyte communication has been shown to result in dysmyelination (Lutz et al., 2009). Additionally, in the gray matter, for example, astrocytes guide the migration of neuroblasts and developing axons by establishing molecular boundaries via the expression of astrocyte-derived extracellular matrix molecules, such as tenascin-C, and different proteoglycans, such as chondroitin sulfate proteoglycans (CSPG) and keratin sulfate proteoglycans (KSPG) (Powell et al., 1997a; 1997b; Powell and Geller, 1999). Furthermore, astrocyte-derived molecules like thrombospondins have been shown to be pivotal for the development and functioning of synapses (Ullian et al., 2001; 2004a; Christopherson et al., 2005; Barres, 2008). In addition to enhancing synaptic formation, astrocytes play an equally important role in developmental synaptic pruning by producing complement C1q expression inducing factors at synapses, which triggers microglia based removal of that synapse (Stevens et al., 2007; Barres, 2008; Stephan et al., 2012).

Ca^{2+} signaling in astrocytes

As stated above, astrocytes play an active role in brain function and information processing, both during development and in the postnatal brain. A large number of these functions are regulated by the astrocyte's intracellular Ca^{2+} signaling system. It was first reported about 20 years ago that individually cultured astrocytes display intracellular Ca^{2+} elevations in response to neurotransmitters (Cornell-Bell et al., 1990a). Indeed, astrocytes express receptors for a whole range of neurotransmitters, and their strategic location in close proximity to synapses provides a perfect opportunity for astrocytes to monitor and regulate neuronal activity (Haydon, 2001; Fellin et al., 2006b; Theodosis et al., 2008; Halassa and Haydon, 2010). Astrocytes also display transient, spontaneous increases in intracellular Ca^{2+}, independent of any external stimulus, that can spread into adjacent astrocytes as a synchronous intercellular Ca^{2+} wave

(Cornell-Bell et al., 1990a; Hirase et al., 2004; Fiacco and McCarthy, 2006; Scemes and Giaume, 2006; Kuga et al., 2011). Additionally, neurons and glia can communicate via Ca^{2+} since neuronal activity can directly induce glial Ca^{2+} waves (Dani et al., 1992), and glial Ca^{2+} waves can directly cause calcium transients and activation of neurons (Nedergaard, 1994; Parpura et al., 1994; Hassinger et al., 1995; Newman and Zahs, 1998).

Many studies on astrocytes *in vitro*, *in situ* and *in vivo* have identified the expression of numerous metabotropic and ionotropic receptors that, upon activation via binding of neurotransmitters, such as ATP and glutamate, trigger Ca^{2+} release from the ER (basic Ca^{2+}-signaling mechanisms are presented in Figure 1.4) (Finkbeiner, 1993; Porter and McCarthy, 1995; Kirischuk et al., 1996; Porter and McCarthy, 1996; Hamilton et al., 2008; Verkhratsky et al., 2009). This occurs through activation of the phospholipase C (PLC)/inositol 1,4,5-triphosphate (IP_3) pathway (Franke et al., 2012; Illes et al., 2012). Upon activation of metabotropic G-protein coupled receptors (GPCR), PLC hydrolyzes the membrane lipid phosphatidylinositol 4,5-bisphosphate (PIP2) to generate diacylglycerol (DAG) and IP_3, resulting in IP_3-receptor (IP3-R) activation and Ca^{2+} release from the ER (Scemes, 2000; Parri and Crunelli, 2003; Fiacco and McCarthy, 2006; Scemes and Giaume, 2006). Cells have many mechanisms to clear cytosolic Ca^{2+}, either by pumping it out from the cell via plasma membrane Ca^{2+} ATPases (PMCA), or sodium-calcium exchangers (NCX), which can operate in both directions, or by storing it in intracellular Ca^{2+}-stores such as the ER, as illustrated in Figure 1.4 (Koch et al., 1986; Jaiswal, 2001; Carafoli, 2002; Guerini et al., 2005; Petersen et al., 2005; Case et al., 2007; Verkhratsky et al., 2012a). Efficient Ca^{2+}-clearance mechanisms are essential since excess Ca^{2+} may cause aggregation of proteins, nuclei acids and lipids, which may be detrimental for the cell (Carafoli, 2002; Petersen et al., 2005). As mentioned above, one of the major roles of the ER is to function as a dynamic Ca^{2+} store making the ER an integral part of the astrocyte's Ca^{2+} homeostatic machinery. Ca^{2+} pumps, such as the sarco (endo) plasmic reticulum calcium ATPase (SERCA), play an important part in ER based Ca^{2+} clearance activities, by transporting Ca^{2+} into the ER lumen

against it's concentration gradient (Gunteski-Hamblin et al., 1988; Vangheluwe et al., 2005). Additionally, mitochondria and lysosomes can also participate in intracellular Ca^{2+} clearance and storage (Duchen, 2000; Michelangeli et al., 2005; Lloyd-Evans and Platt, 2011). Finally, influx of Ca^{2+} from the extracellular space can also occur via store-operated channels (SOC), which respond to fluctuations in intracellular levels of Ca^{2+} and depletion of intracellular Ca^{2+} stores (Verkhratsky et al., 1998; Lo et al., 2002; Parpura et al., 2011; Verkhratsky et al., 2012a). Recently, the Ca^{2+} sensor stromal interacting molecule 1 (STIM1) and Calcium release-activated calcium channel protein 1 have been shown to mediate the store-operated Ca^{2+} entry (SOCE) pathways in astrocytes (Moreno et al., 2012).

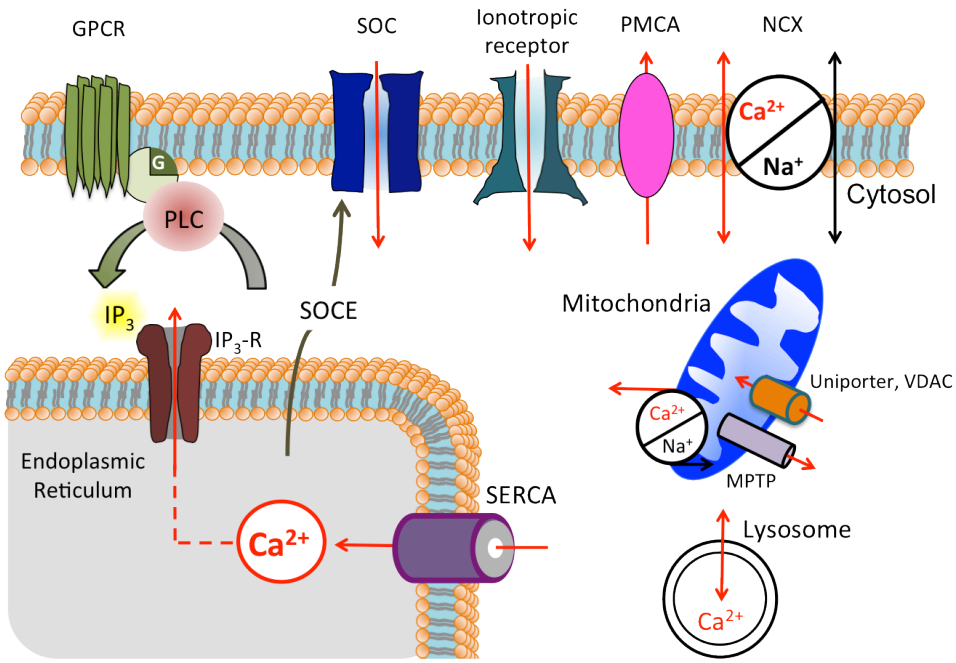

Figure 1.4. Basic calcium signaling mechanisms in astrocytes. Several mechanisms are involved in intracellular Ca^{2+} accumulation. This could be caused by the entry of Ca^{2+} from the extracellular space through ionotropic or metabotropic receptors (GPCR), store-operated channels (SOC) or via plasma membrane Na^{+}/Ca^{2+} exchangers (NCX). Intracellular Ca^{2+}-stores (endoplasmic reticulum (ER), mitochondria or lysosomes), may also function as an additional source for cytosolic Ca^{2+}, which can be released from the ER via IP3-receptors (IP3-R) activated by GPCR and phospholipase C (PLC) based production of IP3. The sarco (endo) plasmic reticulum calcium ATPase (SERCA) functions to refill the ER Ca^{2+}-stores. Mitochondrial Ca^{2+} uptake takes place via voltage-dependent anion channels (VDAC), or mitochondrial NCX, whereas mitochondrial Ca^{2+} release occurs via transient opening of the mitochondrial permeability transition pore (MPTP). Lysosomes are also involved in the regulation of intracellular Ca^{2+}-homeostasis. Cytosolic Ca^{2+} can be cleared to the extracellular space by plasma membrane Ca^{2+} ATPases (PMCA). Cytosolic Ca^{2+} influx or efflux may also occur via plasma membrane NCX, depending on the intracellular Na^{+} concentration.

The mechanisms behind spontaneous Ca^{2+} oscillations in astrocytes, particularly those that occur in absence of any stimulus, are not fully understood. The observed increase in Ca^{2+} concentrations during these oscillations is thought to be generated by release from the ER Ca^{2+} store via IP3-R activation and influx from an extracellular source possibly through voltage-gated calcium channels (VGCCs) (Duffy and MacVicar, 1994; Jalonen et al., 1997; Parri et al., 2001; Nett et al., 2002; Parri and Crunelli, 2003; Wang et al., 2006; Parpura et al., 2011; Verkhratsky et al., 2012a). Importantly, these spontaneous Ca^{2+} oscillations have been shown to induce NMDA receptor mediated neuronal excitability *in situ* via

glutamate release from astrocytes (Parri et al., 2001; Parri and Crunelli, 2003). NMDA receptors are essential for a range of neuronal functions including neuronal differentiation, synaptogenesis and migration (Komuro and Rakic, 1993; 1998). Thus, spontaneous astrocytic Ca^{2+} oscillations may be related to a wide range of neuronal activities.

The propagation of Ca^{2+} waves within astrocyte networks involves two possible mechanisms: 1) gap junction-mediated diffusion of molecules, such as IP_3, that induce Ca^{2+} release from intracellular Ca^{2+} stores in neighboring cells (Boitano et al., 1992; Giaume and Venance, 1998; Scemes and Giaume, 2006), 2) released chemical transmitters, such as ATP, that bind to receptors on neighboring astrocytes to induce intracellular signaling cascades leading to Ca^{2+} release from intracellular stores (Guthrie et al., 1999; Cotrina et al., 2000; Kozlov et al., 2006). This propagation of Ca^{2+} signals may facilitate efficient communication within astrocyte networks, referred to as the astrocyte 'syncytium', that forms intimate associations across many synapses, potentially enabling the synchronization of neuronal activity via secretion of neuroactive factors (gliotransmission), and creating a powerful buffering capacity within these networks (Aguado et al., 2002; Kuga et al., 2011; Parpura et al., 2012).

Astrocytic Ca^{2+} elevations may also result in the release of gliotransmitters such as ATP (Coco et al., 2003; Pascual et al., 2005), glutamate (Parpura et al., 1994; Fellin et al., 2004; Parpura et al., 2011) and D-serine (Schell et al., 1995; Mothet et al., 2005; Henneberger et al., 2010). These gliotransmitters form the molecular basis for glial-glial and glial-neuronal communication (Cornell-Bell et al., 1990a; Araque et al., 1999; 2001; Fellin et al., 2006b; Zorec et al., 2012). For instance, release of D-serine from astrocytes can control NMDA-receptor dependent plasticity in a whole network of excitatory synapses located within an astrocyte syncytium, and thus facilitate long-term potentiation (LTP) and memory formation (Henneberger et al., 2010). Additionally, glutamate released by astrocytes may regulate synaptic transmission and neuronal excitability (Bezzi et al., 1998; Pasti et al., 2001), and ATP, which becomes metabolized to

adenosine, may cause activity-dependent heterosynaptic depression at excitatory synapses (Grover and Teyler, 1993; Pascual et al., 2005; Serrano et al., 2006). This release of gliotransmitters from astrocytes may occur via release through unpaired connexons (hemichannels), ionotropic purinergic receptors, transporters such as exchange via the cystine-glutamate antiporter or organic anion transporters, or via Ca^{2+} dependent exocytosis (Szatkowski et al., 1990; Parpura et al., 1994; Cotrina et al., 1998; Warr et al., 1999; Iglesias et al., 2009; Verkhratsky and Parpura, 2010; Parpura et al., 2011; Verkhratsky et al., 2012a).

Astrocytes as regulators of CNS homeostasis

One of the most fundamental functions of astrocytes is to regulate CNS homeostasis (see Figure 1.5) (Verkhratsky and Butt, 2007; Allen and Barres, 2009; Sofroniew and Vinters, 2010). This encompasses many different activities, including **cellular homeostasis** by controlling neurogenesis; **defensive homeostasis** by functioning as part of the adaptive/defensive immune response in the CNS; **morphological homeostasis** by controlling migratory pathways for neural cells during development and synaptogenesis/pruning; **molecular homeostasis** by controlling levels of neurotransmitters and hormones in the extracellular space; **metabolic homeostasis** by controlling and storing (glycogen) and providing energy substrates (lactate) for neurons; and **organ homeostasis** by regulating the BBB (Verkhratsky and Butt, 2007; Sofroniew and Vinters, 2010; Verkhratsky et al., 2012a). Moreover, astrocytes are also important for the maintenance of **fluid, ion and pH homeostasis**. For instance, astrocytes can maintain the extracellular pH and ion levels within physiological limits because they express bicarbonate transporters, proton ATPases, Na^+/H^+ exchangers, monocarboxylic transporters and transporters of K^+ (Simard and Nedergaard, 2004; Obara et al., 2008). Their expression of transporters for neurotransmitters, such as glutamate, glycine and GABA, enable astrocytes to control the levels of these neurotransmitters at synaptic sites, and thus dictate synaptic activity (Adams et al., 1995; Conti et al., 2004; Sattler and Rothstein, 2006; Seifert et al., 2006; Goubard et al., 2011). Upon being taken into astrocytes, these

neurotransmitters are converted by specific enzymes into their precursors, for example, glutamine synthetase will convert glutamate to glutamine, which can the be returned to the synapse, taken up by neurons and converted back into an active neurotransmitter (Westergaard et al., 1995). Lastly, astrocytes connected via gap junctions within functional networks may synchronize their ability to scavenge potentially detrimental molecules such as glutamate and potassium, thus, protecting neurons from their harmful effects (Seifert et al., 2006; de Lanerolle et al., 2010).

Astrocytes are positioned perfectly to take up glucose from blood vessels by employing their endfeet (Morgello et al., 1995; Simard et al., 2003; McKenna, 2012). Under physiological conditions the main energy substrate in the CNS is glucose, which is taken up by astrocytes or neuronal cells via glucose transporters (GLUT1 in astrocytes, GLUT3 in neuronal cells). Glucose can then be utilized by the tricarboxylic acid (TCA) cycle in mitochondria to satisfy neuronal energy demands, while some glucose in converted to lactate or glycogen (Pellerin et al., 2007). It has been discovered that astrocytes store energy in form of glycogen, which they can convert into lactate to help neurons to sustain glutamatergic neurotransmission during times when synaptic activity is high (called ANLS: astrocyte-neuron lactate shuttle hypothesis, presented in Figure 1.5) (Pellerin, 2003; Occhipinti et al., 2009; Pellerin and Magistretti, 2012). It is believed that glutamate released into the synaptic space upon neuronal activity is co-transported with Na^+ into astrocytes by glutamate transporters (GLAST and GLT-1 in rodent astrocytes). This activates the astrocytic Na^+/K^+ ATPase, which functions to clear the accumulating intra-astrocytic Na^+ and allow entry of extracellular K^+ in an ATP dependent manner. Additionally, glutamine synthetase, the enzyme that converts glutamate to glutamine so that it can be returned to neurons for conversion back to glutamate, requires ATP. Thus, to meet the energy demands arising from Na^+/K^+ ATPase and glutamine synthetase activity, astrocytic glycolysis, which primarily utilizes blood-derived glucose, is activated to produce pyruvate (ATP production) and lactate. This lactate is then transported to neurons by monocarboxylate transporters (MCT1, or 4 in

astrocytes and MCT2 in neurons) and used to fuel the neuronal energy demands. Thus, shuttling lactate is an essential element in energy coupling between astrocytes and neurons. Indeed, it has been shown that correct functioning of MCTs is required for long-term memory formation and for the maintenance of LTP (Pellerin et al., 2005; Pierre and Pellerin, 2005; Isaac et al., 2007; Maekawa et al., 2009; Pierre et al., 2009). Consequently, disrupting the expression of MCTs in astrocytes causes amnesia, which can be rescued by L-lactate supplementation, re-enforcing the importance of correct astrocyte-neuron lactate transport for memory formation (Suzuki et al., 2011).

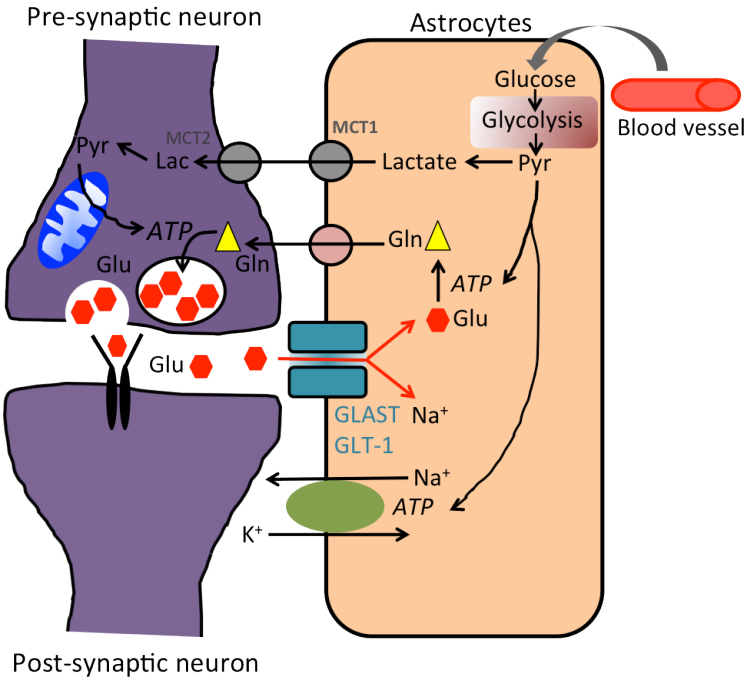

Figure 1.5. Lactate shuttling mediates metabolic coupling between neurons and astrocytes. Glutamate released in the synaptic cleft during glutamatergic neurotransmission is co-transported with Na^+ to astrocytes via glutamate transporters (GLAST, GLT-1). The resulting increase in intra-astrocytic Na^+ concentration activates the glia-specific Na^+/K^+ ATPase that functions to clear Na^+ and to allow the influx of K^+ in an ATP dependent fashion. Glutamine synthetase produces glutamine (Gln) from glutamate (Glu), also in an ATP dependent manner. Glutamine diffuses from astrocytes into the extracellular space and into neurons where it is used to resynthesize glutamate. Both the ATPase pump activation and the glutamine synthesis activate astroglial glycolysis, which utilizes blood-derived glucose to produce the required energy substrate pyruvate (Pyr) and subsequently lactate. Lactate is released into the extracellular space via the astrocytic monocarboxylate transporter (MCT1), where it gets taken up by neurons via MCT2 and preferentially converted to pyruvate and used as the major fuel for neuronal activity.

Astrocytes also play a critical role in protecting neurons from oxidative stress via the synthesis and secretion of the antioxidant, glutathione (GSH; reduced form) composed of cysteine (Cys), glycine (Gly) and glutamate (Glu) (Heales et al., 1996; Dringen, 2000; Chen et al., 2001; Dringen et al., 2001; Gegg et al., 2005; Frade et al., 2008). System X_c^- mediates the uptake of cystine into astrocytes (particularly under high intra-astrocytic concentrations of Glu), where it gets rapidly reduced to cysteine, which is a rate-limiting precursor in the synthesis GSH (Bridges et al., 2012). GSH production is especially important in the CNS, where metabolic activity resulting in the production of free radicals is high, and endogenous levels of other antioxidants are fairly low (Dringen, 2000). Both immunofluorescence and histochemical studies on brain material have shown that neurons contain low levels of GSH, while glial cells display a much greater GSH content (Slivka et al., 1987; Philbert et al., 1991; Pearce et al., 1997). The release of GSH by astrocytes via multidrug resistance-associated protein 1 (Mrp1) is well established (presented in Figure 1.6) (Yudkoff et al., 1990; Juurlink et al., 1996; Sagara et al., 1996; Dringen et al., 1999b; Hirrlinger et al., 2002; Minich et al., 2006) (Hirrlinger et al., 2002; Minich et al., 2006). Once in the extracellular space GSH is cleaved by the astrocyte-associated ectoenzyme γ-glutamyl transpeptidase (γGT) to produce cysteinylglycine (CysGly) (Dringen et al., 1997). The astrocyte-derived CysGly is then further cleaved by the neuron-associated ectoenzyme aminopeptidase N (ApN) to produce L-cysteine, which is taken up by neurons via excitatory amino acid carried 1 (EAAC1) (Aoyama et al., 2008). This mechanism provides neurons with sufficient L-cysteine, which is the liming substrate for neuronal GSH production (Aoyama et al., 2006). Indeed, it has been shown that intracellular GSH levels in neurons are higher in neurons co-cultured with astrocytes than in pure neuronal cultures (Dringen et al., 1999b; Gegg et al., 2005). Importantly, oxidative stress resulting possibly from the lack of antioxidant production has been suggested to contribute towards neuronal loss in JNCL (Fossale et al., 2004; Benedict et al., 2007; Tuxworth et al., 2011). Indeed, reduced glutathione levels observed in the *Cln3*$^{-/-}$ mouse brain would suggest that astrocytic glutathione production or secretion may be disrupted in this disease (Benedict et al., 2007).

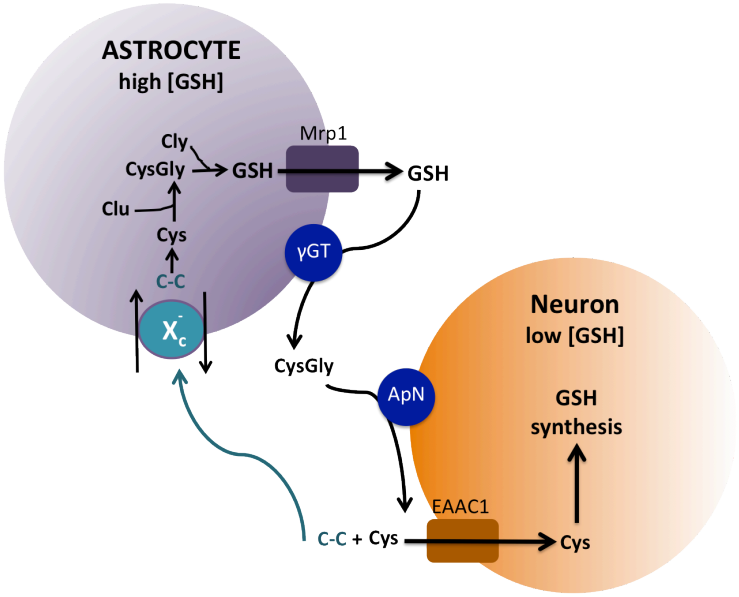

Figure 1.6. Astrocytes provide the substrates for neuronal glutathione production. In astrocytes, cystine (C-C) transported by system x_c^- (X)-transporter into the cells is reduced into cysteine (Cys), which together with glutamate (Glu) is used for astrocytic glutathione (reduced form GSH) synthesis. GSH is released by astrocytes via multidrug resistance protein 1 (Mrp1). GSH is then cleaved by the astrocyte-associated enzyme γ-glutamyl transpeptidase (γGT) and the neuron-associated enzyme aminopeptidase (ApN) to produce cysteine, which gets taken up by neurons via excitatory amino acid carrier 1 (EAAC1). Cysteine, which is the rate limiting substrate for neuronal GSH production, is then used for neuronal GSH synthesis. Alternatively, Cys can become oxidixed, thus, supplying C-C to support system x_c^- activity.

Basic cytoskeletal organization in astrocytes

The cytoskeleton of any cell, not only astrocytes, is the most integral cellular component for its existence and proper functioning. The cytoskeleton of an astrocyte is composed of three main types of polymers, actin filaments, microtubules, and a group of polymers collectively termed intermediate filaments, that are crucial for controlling cell-shape and many cellular mechanisms such as proliferation, migration, uptake and release of soluble factors (Etienne-Manneville, 2004; Pekny and Pekna, 2004; Potokar et al., 2007; Wade, 2007; Dominguez and Holmes, 2011; Middeldorp and Hol, 2011). These different components of the cytoskeleton are all organized into functional networks that together arrange and support the structure of intracellular compartments and keep the shape of the cell intact, but that can also dynamically restructure their network in response to external and internal

stimuli. The key differences between the main cytoskeletal polymers are their mechanical rigidity, their polarity, the dynamics of their reorganization, and the type of molecular motors they form functional partners with (reviewed in Fletcher and Mullins, 2010).

Microtubules are composed of α- and β-tubulin heterodimers, have complex dynamics of assembly and disassembly, and out of three main polymers they are the stiffest (Desai and Mitchison, 1997; Amos and Schlieper, 2005). These α- and β-tubulin dimers polymerize end to end into protofilaments, which ultimately form the building blocks for the hollow microtubule structure (Mandelkow and Mandelkow, 1994). Altogether thirteen (this number may vary) protofilaments bind together laterally to form a single microtubule and this basic structure can subsequently be extended further by the addition of more protofilaments (Amos and Schlieper, 2005). Microtubules have a distinct polarity, which defines some of their biological activities. Tubulin polymerizes in a specific manner, an α-subunit from one tubulin dimer contacts a β-subunit of the next tubulin dimer to form a protofilament with one end exposing only α-subunits (- end), and the other end only β-subunits (+ end). Since the protofilaments bundle parallel with each other, in a fully formed microtubule there is one (–) end with only exposed α-subunits, and one (+) end with only exposed β-subunits (Desai and Mitchison, 1997).

Microtubules are extremely dynamic structures, since they are constantly assembled and disassembled at the (+) end in a GTP-GDP dependent manner (Weisenberg and Deery, 1976; Weisenberg et al., 1976; Mitchison and Kirschner, 1984; van der Vaart et al., 2009). Microtubules can form nearly linear tracks that span the length of the whole cell, making them essential for the development and maintenance of cell shape (Brangwynne et al., 2006; Efremov et al., 2011). Furthermore, microtubules are involved in the intracellular transport of vesicles, mitochondria and other cellular components, cell signaling, cell division and mitosis (Potokar et al., 2007; 2008; Garnham and Roll-Mecak, 2012). Many factors facilitate such functional diversity: the binding of various regulatory

proteins, including microtubular associated proteins (MAPs) (Couchie et al., 1985; Itoh and Hotani, 2004); the expression of different tubulin isotypes with different functions (Sullivan, 1988; Nielsen et al., 2001; Miller et al., 2010); and post-translational modification of tubulin (Garnham and Roll-Mecak, 2012). In addition to the movement of microtubules generated by their own dynamic instability, motor proteins can move along α- and β-fibers (Mallik and Gross, 2004). The most common microtubule motor proteins are dynein, which moves towards the (-) end, and kinesin, which moves towards the (+) end. The main function of these motors is to allow transport of cargo between different intracellular compartments and locations (Goldstein and Yang, 2000; Karcher et al., 2002; Mallik et al., 2004; Gennerich and Vale, 2009; Akhmanova and Hammer, 2010; Hirokawa, 2011).

Actin forms the thinnest filaments of the cytoskeleton (6nm in diameter) and exists in two states within the cell, as monomers (G-actin) or as two-stranded helical filaments (F-actin) that are formed from the assembly of the G-actin monomers (Guasch et al., 2003; Pollard and Cooper, 2009; Efremov et al., 2011). In a similar fashion to microtubules, actin filaments are polarized (Cramer, 1999). These filaments grow faster at one end and assembly and disassembly is regulated by binding and dissociation of ADP/ATP, which is controlled by many actin-binding proteins (cross-linking proteins, motor proteins, branching proteins and polymerization proteins) (Remedios et al., 2003). For instance, interactions between actin filaments and myosin motor proteins are important in cellular mobility and protein trafficking (Stachelek et al., 2001; Vicente-Manzanares et al., 2007; 2009). The actin cytoskeleton also plays a fundamental role in phagocytosis, adhesion, and the uptake and released of soluble factors (Zigmond, 1996; Potokar et al., 2007). For instance, disrupting the actin cytoskeleton by using agents such as cytochalasin D alters various fundamental functions of astrocytes including glutamate clearance, hormone modulation of cell growth, many aspects of calcium signaling and Cl^- conductance (Cotrina et al., 1998; Lascola et al., 1998; Duan et al., 1999; Sergeeva et al., 2000). Generally the dynamic organization of the actin cytoskeleton is regulated by small Rho

GTPases (Hall, 1998; Bishop and Hall, 2000).

Intermediate filaments (IF) are generally considered to be the least rigid of all the cytoskeletal polymers, and they have the ability to crosslink with each other, as well with actin filaments and microtubules (Stewart, 1993; Fuchs and Weber, 1994; Wiche, 1998; Wiche and Winter, 2011). IFs are not polarized, and as such the directional movement of molecular motors is not supported by IFs (Zackroff and Goldman, 1979; Ananthakrishnan and Ehrlicher, 2007). IFs are dynamic components of the cytoskeleton that are encoded by approximately 70 genes in eukaryotic cells (Hesse et al., 2001; Zimek et al., 2003). Structurally, all IFs proteins are predicted to have the same secondary structure; a non-alpha-helical N-terminal head, a C-terminal tail domain, and a central alpha-helical domain, termed the rod (Fuchs and Weber, 1994). IFs can also form homo- or heteropolymers with each other resulting in the formation of a variety of possible IF protein networks (Steinert et al., 1999). The IF network forms a crucial part of the astrocyte cytoskeleton, and is composed from GFAP, vimentin, nestin and synemin (Pekny and Pekna, 2004). GFAP is the main IF in mature astrocytes and it is also required during astrocyte development (Middeldorp and Hol, 2011), while both vimentin and nestin are expressed abundantly by immature astrocytes (Pekny and Pekna, 2004). However, nestin requires vimentin as a polymerization partner because nestin cannot form IFs on its own or with GFAP (Eliasson et al., 1999). The functional importance of each astrocyte-expressed IFs under physiological conditions is not well understood (Pekny and Pekna, 2004; Sofroniew and Vinters, 2010). When faced with pathological situations, astrocytes up-regulate the expression of GFAP, vimentin and nestin and change their morphology (Mucke and Eddleston, 1993; Pekny et al., 1999; Pekny and Pekna, 2004). In order to study the individual roles of each IF in astrocytes, studies in mice deficient in either GFAP (*GFAP*$^{-/-}$) (Gomi et al., 1995; Liedtke et al., 1996; McCall et al., 1996; Pekny and Nilsson, 2005), Vimentin (*Vim*$^{-/-}$) (Colucci-Guyon et al., 1994), or both IFs (*GFAP*$^{-/-}$*Vim*$^{-/-}$) (Eliasson et al., 1999; Macauley et al., 2011) have been generated. These studies demonstrated that IF up-regulation is responsible for both positive and negative outcomes in the diseased

CNS. For instance, *GFAP*$^{-/-}$*Vim*$^{-/-}$*Ppt1*$^{-/-}$ mice were used to study the role of IFs in reactive astrocytosis in INCL (Macauley et al., 2011). Upon attenuated astrocyte activation, due to the lack of intermediate filament expression in the *GFAP*$^{-/-}$*Vim*$^{-/-}$*Ppt1*$^{-/-}$ mice, the disease appeared earlier and progressed more rapidly than in *Ppt1*$^{-/-}$ mice. Thus, in INCL, astrocyte activation appears to help protect against neurodegeneration (Macauley et al., 2011). The process of astrocyte activation is reviewed in more detailed below.

Recently it has been proposed that IFs, together with actin filaments and microtubules, are involved in vesicle delivery and transport in astrocytes (Potokar et al., 2007; 2008; Kreft et al., 2009; Potokar et al., 2010). Investigating the mobility of fluorescently labeled vesicles in cultured astrocytes with depolymerized IFs, or in astrocytes derived from *GFAP*$^{-/-}$*Vim*$^{-/-}$ mice, revealed that IFs are crucial for determining the directional mobility of exocytotic vesicles (Potokar et al., 2007). In addition, astrocyte IFs have also been shown to reduce stimulation-dependent mobility of whole subcellular compartments such as endosomes and lysosomes, and also to regulate the mobility of recycling vesicles (vesicles that fuse to and are then retrieved from the plasma membrane) in cultured astrocytes (Potokar et al., 2010). Furthermore, interferon γ (IFNγ) induced activation has been shown to increase membrane MHC class II expression in astrocytes (Hirsch et al., 1983; Shrikant and Benveniste, 1996). For this to occur, the MHC II complex needs to be delivered to the cell surface by being transported in membrane-bound vesicles. Live cell imaging of cultured astrocytes revealed faster movement of such vesicles in IFNγ treated WT astrocytes compared to the IF-deficient astrocytes derived from *GFAP*$^{-/-}$*Vim*$^{-/-}$ mice (Vardjan et al., 2012). Thus, IFs appear to facilitate the delivery of membrane-associated protein complexes in activated astrocytes. Generally, the upregulation of IFs under pathological conditions may alter the function of astrocytes by influencing vesicle trafficking, which may subsequently impact exocytosis and endocytosis and alter cell-cell communication, based on diffusion of soluble factors between astrocytes and other neural cells. Any abnormalities in the dynamic organization of IF networks may significantly alter such functions.

1.4 Astrocytes in disease

Reactive astrocytosis, the process of astrocyte activation, takes place in response to virtually all forms of acute and chronic CNS injury or disease and can be both harmful and beneficial (summarized in Figure 1.7) (Ridet et al., 1997; Sofroniew, 2009; Sofroniew and Vinters, 2010; Colangelo et al., 2012; Parpura et al., 2012). For instance, scar-forming reactive astrocytes that inhibit axonal regeneration are often seen as detrimental to clinical outcome (Fawcett and Asher, 1999; Sofroniew, 2009), yet, reactive astrocytes can be beneficial in several ways including: 1) uptake of excess and potentially excitotoxic glutamate (Swanson et al., 2004; Kim et al., 2011; Coulter and Eid, 2012); 2) stabilization of the extracellular fluid and ion balance (Simard and Nedergaard, 2004; Obara et al., 2008; Zador et al., 2009); and 3) protection from oxidative stress via glutathione production (Heales et al., 1996; Dringen, 2000; Chen et al., 2001; Dringen et al., 2001; Gegg et al., 2005; Frade et al., 2008; Vargas et al., 2008). Indeed, via enhanced soluble factor secretion, activated astrocytes not only alter neuronal biology, but also impact the interplay between themselves and other glial cells (Liberto et al., 2004; Lucas et al., 2006; Bélanger and Magistretti, 2009; Sofroniew, 2009; Lehnardt, 2010; Liu et al., 2011; Singh et al., 2011). Finally, the gap junction mediated coupling within the astrocyte syncytium may also be altered upon reactive astrocytosis (Kielian, 2008).

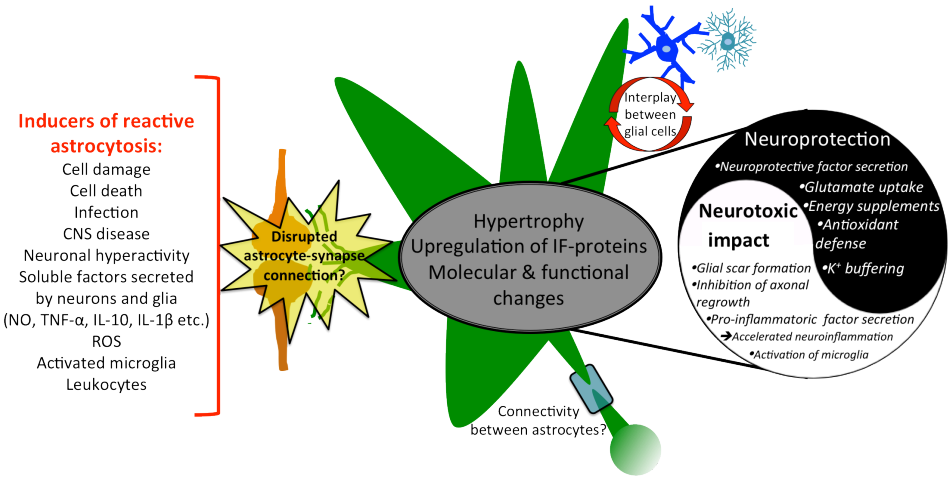

Figure 1.7. Reactive astrocytosis. A number of cellular and molecular triggers may lead to activation of astrocytes (reactive astrocytosis). Upon activation several molecular and functional changes occur. Such changes may have a neuroprotective or neurotoxic impact that may result in disrupted connection between astrocytes and neuronal synapses. Astrocyte connectivity via gap junctions and the interplay between astrocytes and other glial cells may also be altered upon astrocyte activation.

The changes that astrocytes undergo upon activation differ greatly depending on the nature and severity of the insult, but include alterations in molecular expression, progressive cellular hypertrophy and, in severe cases, proliferation, disruption of individual astrocytic domains and scar formation (Pekny and Nilsson, 2005; Sofroniew, 2009; Sofroniew and Vinters, 2010). According to current understanding, astrocytes (mainly post-mitotic in the healthy, mature CNS), may become proliferative only under very severe circumstances, such as in severe focal lesions, infections or areas suffering from chronic neurodegeneration (Lindholm et al., 1992; Norton et al., 1992; Satoh et al., 1996; Bush et al., 1999; Horner et al., 2000; Colodner et al., 2005; Sofroniew and Vinters, 2010). One hypothesis behind the proliferation of activated astrocytes is that such cells revert to a immature state, making them capable of proliferating in similar fashion to immature, stem-cell like astrocytes (Cahoy et al., 2008; Zamanian et al., 2012).

Generally, upregulation of GFAP, is the best-known hallmark of reactive astrocytosis (Pekny and Pekna, 2004; Pekny and Nilsson, 2005), but up-regulation of vimentin and re-expression of nestin are also established hallmarks of this process (Pekny and Pekna, 2004; Pekny and Nilsson, 2005). Thus, it appears that

IF proteins may play a particular role in astrocytes activation. This has been confirmed in a number of mouse models with different types of genetic depletion of astrocyte IF proteins (Pekny, 2001; Pekny and Pekna, 2004; Pekny and Nilsson, 2005). *GFAP*$^{-/-}$ mice developed normally, but displayed enhanced neuronal LTP compared to control mice, suggesting that GFAP is an important factor in astrocyte-neuronal interactions (McCall et al., 1996). Upon ischemia, however, the LTP and also paired pulse facilitation (PPF) seen in *GFAP*$^{-/-}$ mice was significantly depressed, which was accompanied by a marked increase in the loss of CA1 and CA3 hippocampal pyramidal neurons compared to control mice (Tanaka et al., 2002). Similarly, ablating scar-forming, reactive astrocytes in models of traumatic brain injury (Myer et al., 2006), autoimmune encephalomyelitis (Voskuhl et al., 2009), spinal cord injury (Faulkner et al., 2004), ischemia (Li et al., 2008) and in INCL (Macauley et al., 2011) resulted in more dramatic tissue damage, increased neurodegeneration and accelerated neuroinflammation. Thus, in some cases the IF protein mediated activation of astrocytes appears to play a protective role against pathogenic disease progression. However, in some cases the lack of IFs makes astrocytes act as protective and beneficial players to halt the progression of the pathogenic events. For instance, the *GFAP*$^{-/-}$*Vim*$^{-/-}$ astrocytes in an entorhinal cortex lesion mouse model (CNS trauma model) showed a profoundly reduced hypertrophy of astrocyte processes, when compared to reactive astrocytes in WT mice, and this was accompanied by significant synaptic regeneration in the hippocampus, suggesting that reactive astrocytes act as inhibitors of neuroregeneration in this type of CNS insult (Wilhelmsson et al., 2004). Indeed, other studies suggest that several aspects of CNS regeneration are improved in absence of astrocytic IFs (Larsson et al., 2004; Cho et al., 2005; Widestrand et al., 2007). For example, adult hippocampal neurogenesis has been demonstrated to be increased in *GFAP*$^{-/-}$*Vim*$^{-/-}$ mice compared to WT mice, thus, modulating astrocyte IF related reactivity may regulate adult neurogenesis (Larsson et al., 2004). Attenuation of post-traumatic reactive astrocytosis in an optic nerve injury model has been shown to aid axon regeneration, again suggesting that long lasting reactive astrocytosis has a negative impact on neuronal regeneration (Cho et al., 2005).

Overall, the specific role of reactive astrocytosis in progression of pathological events seems to be disease type specific. In an effort to explore the underlying mechanisms of reactive astrocytosis in CNS disorders, the presence of factors mediating inflammatory responses, such as presence of inflammatory cells ($CD45^+$ leukocytes, $CD68^+$ macrophages, $CD3^+$ T-cells) and expression levels of soluble inflammatory factors (pro- and anti-inflammatory cytokines, chemokines e.g), have been investigated (Christopherson et al., 2005; Garwood et al., 2011; Macauley et al., 2011; Parpura et al., 2012; Vardjan et al., 2012; Zamanian et al., 2012).

An immune response can occur in the brain as a result of virtually any CNS insult or disease such as different forms of NCLs (Allan and Rothwell, 2003; Saha et al., 2008; Frank-Cannon et al., 2009; Macauley et al., 2011; Mole et al., 2011). The process of neuroinflammation, like astrocytosis, may have a beneficial or detrimental impact on disease progression (Allan and Rothwell, 2003; Lucas et al., 2006; Frank-Cannon et al., 2009). Microglial cells are generally accepted as the main immune cells of the brain (Lehnardt, 2010; Kettenmann et al., 2011), however, astrocytes function as essential regulators of this inflammatory response. Numerous studies have revealed that activated astrocytes can release a wide selection of potent mediators of neuroinflammation, including chemokines, cytokines and growth factors, that may exert either neuroprotective or harmful effects on neuronal survival and function in the injured brain (Ridet et al., 1997; John et al., 2003; Farina et al., 2007; Ricci et al., 2009; Ransohoff and Brown, 2012).

Understanding the precise role of astrocytes in neuroinflammation has been challenging due the fact that astrocyte are able to secrete an extensive range of soluble factors in response to many different stimuli, including Interferon-γ (IFNγ), interleukin-6 (IL-6), interleukin-10 (IL-10) and tumor necrosis factor-α (TNF-α) (Ridet et al., 1997; Farina et al., 2007; Ransohoff and Brown, 2012). Moreover, various cytokine receptors are expressed upon astrocytes, and as such cytokine signaling can occur both in an autocrine and paracrine fashion

(John et al., 2003). Another issue that has made establishing the exact roles of individual secreted proteins challenging is that many of them interact with each other either antagonistically or synergistically (John et al., 2003; Trendelenburg and Dirnagl, 2005). Thus, it is likely that many cytokines, for example, may simultaneously mediate both neuroprotective and harmful effects. For instance, some research has shown that IL-1β can exacerbate the outcome of neuronal injury both *in vivo* and *in vitro* (Relton and Rothwell, 1992; Hailer et al., 2005). In contrast, other studies have shown IL-1β can exhibit neuroprotective properties, such as aiding remyelination, blood-brain barrier repair, neurotrophic factor production and protection against ischemia induced neurodegeneration, possibly via enhancing production of various growth factors such as ciliary neurotrophic factor (CNTF), nerve growth factor (NGF) and platelet-derived growth factor (PDGF) (Gadient et al., 1990; Strijbos and Rothwell, 1995; DeKosky et al., 1996; Ohtsuki et al., 1996; Silberstein et al., 1996; Herx et al., 2000; Herx and Yong, 2001; Juric and Carman-Krzan, 2001). In addition to secreting IL-1β, astrocytes express the IL-1-receptor and can thus respond to IL-1β themselves by secreting neuroprotective factors such as NGF, CNTF and fibroblast growth factor-2 (FGF-2) (Juric and Carman-Krzan, 2001; John et al., 2003; Liberto et al., 2004). Thus, via protein secretion astrocytes are able to regulate their own biology and importantly alter the survival and functioning of neuronal cells, as well as other glial cells.

Communication between astrocytes and microglia

Reactive gliosis is a very complex phenomenon involving interactions between different glial cells and neurons, leading eventually to neuronal survival or death, axonal regeneration or withdrawal (Fok-Seang et al., 1998; Allan and Rothwell, 2001; Liberto et al., 2004; Ricci et al., 2009; Sofroniew and Vinters, 2010; Liu et al., 2011). Generally activation of microglia and astrocytes correlates closely with disease progression and severity (Pontikis et al., 2004; Teismann and Schulz, 2004; Pontikis et al., 2005; Block et al., 2007; Weimer et al., 2009; Garwood et al., 2011; Liu et al., 2011). In many cases, microglial activation precedes astrocyte

activation, and the former may accelerate the latter (Saura, 2007; Liu et al., 2011; Pascual et al., 2012). Indeed, microglial cells are considered to be the first line of defense, and under physiological conditions, microglia are ramified and apply their motile processes to control and police the pathogenic modifications occurring in their local microenvironment within the CNS (Nimmerjahn et al., 2005; Kettenmann et al., 2011; Pascual et al., 2012; Kettenmann et al., 2013). Once the microenvironment changes microglia become activated very rapidly and undergo a pronounced morphological transformation, proliferate and increase secretion of various soluble factors (Aloisi, 2001; Raivich et al., 2002; Davalos et al., 2005; Kingwell, 2012). This may lead to astrocyte activation, which may also be a microglia-independent phenomenon (Liu et al., 2011; Tian et al., 2012). Activated astrocytes, on the other hand, not only facilitate the activation and recruitment of more distant microglia, but may also inhibit some actions of these activated microglia (Hailer et al., 2001; Liu:2011gy Min et al., 2006; Tian et al., 2012). For instance, the propagation of astrocyte calcium waves has been proposed to be involved in astrocyte-mediated facilitation of microglial activation. This suggestion is based on the demonstration that ATP released from astrocytes upon calcium wave propagation can activate surrounding microglia by inducing their rapid proliferation, promoting secretion of cytokines and microglial migration towards injury site (Hide et al., 2000; Verderio and Matteoli, 2001; Schipke et al., 2002; Bianco et al., 2005; Davalos et al., 2005; Haynes et al., 2006). The inhibitory influences of activated astrocytes upon microglia activation are manifold (Liu et al., 2011). These include the ability of transforming growth factor-β (TGF-β), which is mainly produced by astrocytes (Ramírez et al., 2005), to deactivate microglia by downregulating the expression of molecules associated with antigen presentation and production of pro-inflammatory cytokines, NO and oxygen free radicals (Herrera-Molina and Bernhardi, 2005).

Astrocytes and microglial cells communicate with each other via the proteins they secrete (Krieglstein et al., 1995; Vincent et al., 1997). For instance, TGF-1β secreted by activated astrocytes has been reported to have neuroprotective properties, which may be due to its inhibitory effect on microglia, making them

revert to an anti-inflammatory phenotype (Prehn et al., 1993; Henrich-Noack et al., 1996; Ruocco et al., 1999; Schilling et al., 2001; Paglinawan et al., 2003). Additionally, activation of the chemokine receptor (CXCT4) in activated microglia may result in TNF-α release that in turn can cause the Ca^{2+}- dependent release of glutamate from astrocytes (Bezzi et al., 2001). This microglial- and TNF-α-dependent potentiation of astrocyte glutamate release may lead to excitotoxity and the subsequent apoptotic death of surrounding neurons. In summary, the proteins released by astrocytes have significant consequences on neuronal function and survival, and upon microglial activation. These consequences depend on various factors, such as type, duration and severity of the insult (Lucas et al., 2006). *In vitro* systems where astrocytes and microglial cells are co-cultured together with neurons provide a useful tool to explore such connectivity between these different glial cell types and to determine how this may influence neurons. This approach will be used in this thesis to determine the impact of *Cln3* deficient glial cells on neuronal health (Chapter 6).

A previous *in vitro* study revealed that CLN3 deficiency causes a whole range of biological alterations in microglia (S. Dihanich, unpublished data). *Cln3*$^{-/-}$ microglia displayed a compromised morphology under both unstimulated (increased number of morphologically activated *Cln3*$^{-/-}$ microglia) and stimulated conditions (impaired morphological transformation in *Cln3*$^{-/-}$ microglia), as has also been observed *in vivo* (Pontikis et al., 2004; 2005). Furthermore, activated *Cln3*$^{-/-}$ microglia displayed specific protein secretion deficits, releasing significantly less of the chemokines: macrophage inflammatory protein-1γ (MIP-1γ), MIP-1, regulated and normal T cell expressed and secreted (RANTES), a matrix metalloproteinase: matrix metalloproteinase-1 (MMP-1) and a glycoprotein: Von Willebrand factor (vWF). This deficiency in chemokine secretion by activated *Cln3*$^{-/-}$ microglia is particularly interesting in terms of the interplay between microglia and astrocytes in JNCL disease. Chemokines are involved in immune cell recruitment and phagocytosis (Ransohoff, 2009; Rostène et al., 2011). As such, *Cln3*$^{-/-}$ microglia may have a reduced capacity to attract immune cells, such as astrocytes, potentially explaining the attenuated astrocyte

response evident in *Cln3*$^{-/-}$ mice. For instance, stimulation of astrocytes with RANTES has been shown to induce chemokine synthesis (monocyte chemoattractant protein-1 (MCP-1), MIP-2, RANTES etc.), and up-regulate intercellular adhesion molecule-1 (ICAM-1) (Luo et al., 2002). Astrocytic expression of ICAM-1 has potential implications in the regulation of the immune system, since ICAM-1 has been shown to be required for optimal stimulation of naïve T-cells (Siu et al., 1989; Van Seventer et al., 1990; Kuhlman et al., 1991). Thus, diminished secretion of RANTES by *Cln3*$^{-/-}$ microglia may plausibly lead to down-regulation of ICAM-1 in astrocytes, which would result in impaired T-cell adhesion and/or activation causing impaired immune-response in *Cln3*$^{-/-}$ mice.

In summary, astrocytes contribute to both physiological and pathophysiological mechanisms within the brain. The intimate structural-functional relationship between astrocytes and neurons is required for correct synaptic transmission and, thus, for many higher brain functions (Fellin et al., 2006b; Perea et al., 2009; Araque and Navarrete, 2010; Perea and Araque, 2010; Santello et al., 2012). Neuron-mediated, or otherwise evoked, and/or spontaneous fluctuations in astrocyte intracellular Na^+ or Ca^{2+} concentrations can lead to increased lactate production and the secretion of various gliotransmitters via Ca^{2+}-dependent exocytosis (Pellerin and Magistretti, 1994; Pellerin, 2003; Pellerin et al., 2007; Parpura and Zorec, 2010; Santello et al., 2012; Zorec et al., 2012; Verkhratsky et al., 2012a). Such release and uptake of a complex range of soluble factors forms the basis for communication within the astrocyte syncytium, and also for bidirectional neuron-glial communication. Furthermore, reactive astrocytosis manifests itself in virtually all CNS pathologies (Ridet et al., 1997; Sofroniew and Vinters, 2010; Singh et al., 2011). The complex changes that take place within reactive astrocytes may have both beneficial and detrimental consequences depending on the disease context (Sofroniew, 2009; Sofroniew and Vinters, 2010). Dysfunction of either astrocytes themselves, or the process of reactive astrocytosis, as has been observed *in vivo* in *Cln3*$^{-/-}$ mice (Pontikis et al., 2004; 2005), may significantly alter the course of disease progression making them as integral component of pathogenesis (Pekny and Pekna, 2004; Pekny and Nilsson,

2005; Zhang et al., 2008; Macauley et al., 2011; Di Malta et al., 2012a). As such, investigating how Cln3 deficiency impairs astrocyte biology may provide important clues on their contribution to the pathogenesis of JNCL.

1.5 Aims of this thesis

An early glial response precedes neuronal loss in all forms of NCL. However, in the Juvenile form this glial response is apparently attenuated, with astrocytes failing to become hypertrophied and exhibiting a reduced upregulation of the intermediate filament protein, GFAP, and microglia failing to fully transform into brain macrophages. This may have a significant impact on the pathogenesis of JNCL, since proper glial function is crucial for the maintenance of correct CNS homeostasis that is essential for normal neuronal function and survival. Initial studies on the biology of *Cln3*$^{-/-}$ microglia, using a tissue culture approach have revealed that not only do these cells fail to fully transform upon stimulation, but that their protein secretion profile is altered in a way that may influence their interactions with astrocytes.

The main aim of this PhD thesis was to extend these studies to astrocytes, to investigate how the loss of CLN3 function impacts the biology of these cells, and whether the compromised biology of glial cells contributes to the pathogenesis of JNCL. Additionally, in order to be able to assess neuron glial interaction more effectively, the impact of CLN3 deficiency on some aspects of the neuronal cell biology was also characterized.

This study has four specific aims:

1) To compare the response of *Cln3*$^{-/-}$ and wild type (WT) astrocytes to activation stimuli
2) To investigate whether *Cln3*$^{-/-}$ astrocytes differ functionally from WT astrocytes.
3) To explore how CLN3 deficiency affects neuronal cell biology
4) To investigate whether *Cln3*$^{-/-}$ glia influence neuronal health

These studies revealed that the function of astrocytes is dramatically altered by loss of CLN3 and, most importantly, that *Cln3*$^{-/-}$ glia have a negative impact on the health of both JNCL and WT neurons. In contrast healthy glia were found to ameliorate the defects observed in *Cln3*$^{-/-}$ neuron*s.* These findings provide novel information about the role that glial cells may play in the pathogenesis of JNCL and point to astrocytes as novel targets for future therapeutic approaches.

Chapter 2
Materials and Methods

2.1 Animals

Homozygous *Cln3*$^{ex1-6}$ mice (*Cln3*$^{-/-}$ mice) on a C57BL/6J background were used as a model of JNCL (Mitchison et al., 1999) and homozygous *Tpp1* deficient mice on a C57BL/6J background backcrossed with NODSCID mice were used as a model of LINCL (Sleat et al., 2004). Wild type (WT) mice on the same strain background were used as controls. All animal housekeeping and procedures were carried out according to the UK Scientific Procedures (Animals) Act (1986), under the authority of Project License 70/6567.

2.2 Histology

Mouse tissue for histological analysis

Sections from *Cln3*$^{-/-}$ and *Tpp1*$^{-/-}$ mouse brains were used to study glial activation. Control tissue was generated from WT mice. Mice were deeply anaesthetised with sodium pentobarbitone (1g/kg), then injected into the left ventricle with 100µl heparin (5,000 units/ml) before being transcardially perfused with phosphate buffered saline (PBS) followed by a freshly prepared and filtered solution of 4% paraformaldehyde (PFA) in PBS. The brains were then removed carefully and post-fixed overnight at 4°C in 4% PFA, before being cryoprotected in 30% sucrose in Tris buffered saline plus 0.05% sodium azide (TBS-A) at 4°C. Brains were bisected along the midline, the cerebella were removed and one hemisphere of each brain was cut into sequential 40µm coronal sections using a Microm freezing microtome. The sections were collected and stored in cryoprotectant solution (TBS-A + 30% ethylene glycol + 15% sucrose). To carry out subsequent quantitative analyses, a 1 in 6 series of sections were selected as previously described (Bible et al., 2004; Pontikis et al., 2004; 2005; Kielar et al., 2007).

Human tissue

To investigate glial activation in the human NCL brain, paraffin-embedded tissue blocks prepared from the primary visual cortical region of human LINCL and JNCL *post mortem* tissue (n=2 in both cases) were obtained from the Human Brain and

Spinal Fluid Resource Centre, Los Angeles and the MRC London Neurodegenerative Diseases Brain Bank, Institute of Psychiatry, King's College London. These specimens were obtained from routine autopsies of NCL patients with informed written consent from their families. Following autopsy, tissue was fixed immediately by using 4% neutral buffered formaldehyde, processed and embedded in paraffin wax blocks. Study protocols for the use of human material were approved by the Ethical Research Committees of the Institute of Psychiatry (approval numbers 223/00, 181/02).

7μm thick sections were cut from paraffin wax using a Leitz 1400 base sledge microtome. The cut sections were transferred to 20% IMS (Industrial Methylated Spirit, Sigma) to aid flattening, and then floated into a water bath containing deionised water at 45°C. Flattened sections were mounted on clean Superfrost Plus slides (VWR) and placed overnight on a hotplate at 45°C to allow them to adhere properly to the glass. To aid the adhering, these sections were placed overnight in an oven at 37°C before staining.

2.3 Primary cell cultures

Mixed glial cultures

These cultures were generated from post-natal day 1-4 (P1-P4) *Cln3*$^{-/-}$ or WT mouse cerebral cortices. Tissue was dissected out in cold Hanks' Balanced Salt Solution (HBSS, GIBCO Life Technologies) then incubated in trypsin-ethylenediaminetetraacetic acid (EDTA) (0.5mg/ml, Sigma; 1ml per 4 cortices) for 10 minutes at 37°C followed by the addition of an equal volume of trypsin inhibitor (0.5mg/ml, Sigma). The trypsinised tissue was dissociated by passing 10-15 times through a 5ml pipette followed by three times through a 21G, and then 23G, syringe using a 1ml hypodermic needle. After washing twice in HBSS (by centrifugation at 900rpm for 5 minutes) cells were re-suspended in Dilbecco's Modified Eagles Medium (DMEM, Gibco), supplemented with 10% foetal bovine serum (FBS, Biosera) and penicillin/streptomycin (50 U/ml / 50μg/ml, P/S, Sigma)

and plated onto dried poly-D-lysine (PDL, 25μg/ml, Sigma) coated T75 (Corning Costar) flasks at a density of 2-3 cortices per flask in 10ml of culture medium. Cultures were then incubated at 37°C in a humidified incubator (5% CO_2). The next day half of the culture medium was replaced with fresh medium, and thereafter half of the medium in each flask was replaced with fresh medium every 2-3 days. Once these cultures researched confluence (12-14 days) they were composed of a base layer of non-dividing astrocytes and an upper layer of dividing microglia and a few oligodendrocytes. At this point cultures were either maintained as mixed glial cultures for minimum of three weeks, to allow the maturation and growth of all glial cells, and used in co-culture experiments described below (cultures derived from P2-P4 WT and *Cln3*$^{-/-}$ mice) or they were used to generate pure astrocyte cultures (cultures derived from P1-P2 WT and *Cln3*$^{-/-}$ mice).

Cortical astrocyte cell cultures

These cultures were generated from mixed glial cultures using a modification of the shaking method reported by McCarthy and de Vellis, as previously described (McCarthy and de Vellis, 1980; Williams et al., 1995). Flasks containing the mixed glial cultures were shaken at 180rpm on a Stuart® Shaker (Barloworld Scientific) for 10-12 hours at 37°C in a humidified incubator (5% CO_2) to detach microglia cells and oligodendrocytes. These floating cells were then removed with the medium leaving behind a monolayer consisting mainly of astrocytes. This monolayer was then cultured in growth medium (same as used for mixed glial cultures), supplemented with Ara-C (Arabinofuranosyl Cytidine, $2x10^{-5}$ mol/l) for 7 days *in vitro* (DIV) to remove any remaining dividing cells. Using this procedure we were able to generate astrocyte cultures that were >99% pure (see below).

Once the mixed glia or astrocytes cultures were ready to be used for experiments, they were treated with trypsin-EDTA (0.5mg/ml, 5ml/T75 cell culture flask) for 5-10 minutes at 37°C, followed by the addition of an equal volume of trypsin inhibitor (0.5mg/ml). Detached cells were then collected by centrifugation at 900rpm for 5 minutes, resuspended in HBSS and then

centrifuged once more, before being diluted in growth medium for plating. When these cells were used for immunofluorescence staining or for protein secretion analysis they were plated on PDL coated coverslips (13mm diameter, VWR) at a density of 20,000-30,000 cells/coverslip placed in wells of 24-well plates (Corning Costar). For intracellular Ca^{2+}-measurements astrocytes were plated on PDL-coated coverslips (25mm diameter, VWR) at density of 50,000 (low density), 75,000 (normal density) or 100,000 (high density) cells/coverslips. For Western blot analysis, glutamate clearance and all glutathione measurements, astrocytes were plated at a density of 100,000 cells/6-well plate (Corning Costar, PDL-coated). When lactate secretion and cell migration were examined astrocytes were plated at a density of 50,000 cells/24-well plate (Corning Costar and Essen Image Lock 24-well plate, respectively, both were PDL-coated).

Neuronal cultures

WT or *Cln3*$^{-/-}$ mouse cerebral cortices from P0 mice were dissected out in cold dissociation medium (DM: Ca^{2+}/Mg^{2+} free HBSS from Gibco supplemented with 33.4mM glucose, 10mM Kynurenic acid, 100mM $MgCl_2$ and 1M Hepes (pH 7.4), all chemicals used were obtained from Sigma). This tissue was dissociated by incubation in 5ml of papain solution (50 U/ml made in 90 µg/µl cysteine-HCL, pH 7.4) at 37 °C for 10 minutes (repeated twice), then washed three times with DM before addition of 3ml of trypsin inhibitor (100mg trypsin inhibitor plus 100mg of bovine serum album (BSA) in 10ml of DM, pH 7.4) for 3 minutes at 37 °C, to stop protease activity. The trypsin inhibitor treatment was repeated twice more. Subsequently, cells were washed three times with DM and then suspended in 3ml of growth medium (Neurobasal medium (Gibco) supplemented with 10ml B27 (x50, Gibco), 50 U/ml/50µg/ml P/S, 2mM l-glutamine). The cell suspension was then pipetted 10-15 times using a 200ul pipette until fully dissociated and the cells pelleted (900rpm for 5 minutes) and re-suspended in growth medium. Cells were then plated at a concentration of 250,000-300,000 cells/coverslip on PDL (50µg/ml) coated 13mm glass coverslips (VWR) placed in 24- well plates (Corning Costar) and incubated at 37°C in a humidified incubator (5% CO_2). For

Western blot analysis, neuronal cells were plated at a density of 1,000,000 cells/6-well plate (Corning Costar, PDL-coated). Every two days, half of the growth medium was replaced with fresh growth medium and to prevent glial growth cultures were grown in Ara-C (2.5µM, added at 2 DIV) containing growth medium. The composition of these cultures was assessed by immunofluorescence staining after 7 DIV. The vast majority of the cells in these cultures were neurons, with small numbers of astrocytes, microglia and very few oligodendrocytes. Using this procedure we were able to generate neuronal cultures that were >94% pure (see below).

Neuron-glia co-cultures

Co-cultures were composed of neurons that had been cultured for 7 DIV prior to being combined with 3-4 week old mixed glial cultures. To generate these co-cultures, approximately 50,000 mixed WT or *Cln3*$^{-/-}$ glial cells were plated on top of WT or *Cln3*$^{-/-}$ neuronal cultures. The following day, the neuronal cell culture medium was replaced with fresh medium to remove any floating, unbound glial cells from the wells. After 2 or 7 DIV, supernatants were collected for cytotoxicity assays and cultures were fixed for immunofluorescence staining, as described below.

2.4 Analysis of cell division *in vitro*

Once activated, astrocytes may re-enter the cell-cycle (Ridet et al., 1997; Sofroniew and Vinters, 2010). To investigate whether *Cln3*$^{-/-}$ astrocytes differ from their WT counterparts in their ability to proliferate in response to activation, the incorporation of 5'-bromo-2'-deoxyuridine (BrdU) was used, to detect cells in S-phase of the cell cycle, in combination with immunostaining for Ki67 to detect all cells capable of proliferating. BrdU (10μM, Sigma) was added directly to medium bathing lipopolysaccharide (LPS)/IFNγ activated or untreated astrocytes. 6 hour after addition of BrdU, cells were fixed in 4% paraformaldehyde in PBS for 15 minutes and then stored in PBS until analysed for BrdU and Ki67 expression.

2.5 Immunostaining protocols

Immunofluorescence staining *in vitro*

For immunofluorescence analysis cultures grown on coverslips were fixed with 4% PFA for 10-20 minutes at room temperature, and then permeabilised with 0.1% Triton X-100 (Sigma) for 5-15 minutes (except when otherwise stated). Following three washes in phosphate buffered saline (PBS) cells were incubated with the appropriate primary antibody (Table 2.1) diluted in either 10% normal goat serum (NGS) or normal donkey serum (NDS) in PBS, or 3% BSA (depending on the host species that the secondary antibody was raised in) for 1 hour at room temperature or overnight at 4^{o}C. Where antibody classes permitted, cells were incubated with various primary antibodies simultaneously. Coverslips were then washed three times in PBS and incubated for 30 minutes to 1 hour at room temperature with the appropriate secondary antibodies (Table 2.2) in the presence of 10% NGS or NDS, or 3% BSA. Where appropriate, nuclei were counterstained with DAPI (4'-6-Diamidino-2-phenylindole, 0.5-1μg/ml, 1:2000, Sigma). Coverslips were mounted using either Fluoromout G or Prolong gold (both Southern Biotech). In all experiments, to ensure that the observed staining was specific, controls were included in which primary antibodies were omitted and/or incorrect secondary antibodies were used.

Immunofluorescence staining for BrdU

Fixed cells were treated with 95% methanol for 30 minutes at room temperature. After rinsing with PBS, cells were permeabilized with 1M HCl for 10 minutes on ice, followed by 2M HCl for 10 minutes at room temperature. To neutralize the acid, 0.1M sodium borate (Sigma) was added for 12 minutes at room temperature. After a 1 hour block in 15% NGS, astrocytes were incubated with the anti-BrdU and Ki67 antibodies overnight at 4°C. The following day, the standard protocol for immunofluorescence staining (see above) was followed. To calculate the percentage of Ki67, BrdU and BrdU/Ki67 expressing cells per coverslip, an average of the values from the 5 fields from a total of three coverslips per experiment was used.

Immunohistochemistry for mouse tissue

Sections for immunohistochemistry were prepared as described above. Endogenous peroxidase activity was reduced in 1% H_20_2 in TBS for 40 minutes at room temperature. Next, sections were rinsed in TBS before unspecific antibody binding was blocked in 15% normal serum in TBS-T (TBS + 0.3% Triton-X) for 30 minutes at room temperature. Sections were then incubated with the appropriate primary antibody (see Table 2.1 for details) diluted in 10% NS in TBS-T at 4°C overnight. Sections were then rinsed with TBS prior to incubation with the appropriate biotinylated secondary antibody diluted in 10% NS in TBS-T for 2 hours (see Table 2.2 for details). Sections were then rinsed further with TBS before addition of the avidin-biotinperoxidase complex (Vectastain Elite ABC kit, Vector Laboratories) diluted at 1:1.000 in TBS, for 2 hours. The visualization was carried out by a standard DAB reaction (0.05% 3,3'-diaminobenzidine tetrahydrochloride HCl; Sigma) for 5-15 minutes depending on the primary antibody used. This reaction was stopped by rinsing the sections with cold TBS. The sections were then mounted onto chrome-gelatine coated slides, dried overnight at room temperature, cleared and dehydrated in 100% industrial methylated spirit (IMS) and 100% xylene before the sections were covered by placing a coverslip onto them with DPX (VWR).

Immunohistochemical staining of paraffin sections

A series of adjacent 7μm paraffin sections from JNCL and LINCL cases were immunohistochemically stained for the astrocyte marker GFAP and the microglial marker CD68 to study the extent of glial activation in human tissue. To reveal the relationship between neuronal morphology and glial activation, these sections were also counterstained with hematoxylin. Firstly, sections were dewaxed in xylene and endogenous peroxidase activity was quenched by treating sections with 1% H_2O_2 in methanol for 30 minutes. Sections were then washed under a running tap and antigen retrieval performed by boiling sections in 0.01M Citrate buffer at pH 6.0 for 20 minutes, before rinsing in deionised water followed by TBS. The sections were then outlined with a grease pen (PAP-pen, Dako) and blocked in 15% normal Swine serum (Dako) in TBS-T for 30 minutes. Sections were then incubated with the anti-GFAP and anti-CD68 antibodies diluted with 10% normal swine serum in TBS-T overnight. The following day, sections were rinsed in TBS and then incubated for 30 minutes in the appropriate biotinylated secondary antibodies diluted 1:200 in TBS-T plus 10% normal swine serum. Subsequently, sections were rinsed three times in TBS for 5 minutes and incubated in avidin-biotin peroxidase complex diluted 1:1000 in TBS (Vectastain Elite ABC kit; Vector Laboratories) for 30 minutes at room temperature. After rinsing in TBS the sections were incubated in 0.05% 3,3'-diaminobenzidine tetrahydrochloride HCl (DAB, Sigma) and 0.001% H_20_2 in TBS for 5 to 10 minutes to visualize immunoreactivity. This reaction was stopped by adding ice-cold TBS to the sections. Sections were then counterstained in 0.7% Harris's haematoxylin (Sigma) for 10-30 seconds followed by differentiation in 0.5% HCl containing 70% IMS for 5-10 seconds. The stain was then allowed to develop by leaving sections in running tap water, before dehydration in graded concentrations of IMS, clearing in xylene, and then coverslipped with DPX [p-xylene-bis(pyridinium bromine)] (VWR).

Primary antibodies	Cells labeled/function	Antibody type	Concentration	Manufacturer
GFAP	Astrocytes	Rabbit polyclonal	1:1000 (IHC, ICC) 1:5000 (IHC-P) 1:10,000 (WB)	Dako
		Mouse IgG1	1:200	Chemicon
CD68	Microglia	Rat	1:150 (IHC, ICC)	Serotec
O4	Oligodendrocytes	Mouse IgM	1:100	Covance
Ki-67	Diving cells	Rabbit polyclonal	1:200	Novocastra
BrdU	Dividing cells	Rat	1:5000	Serotec
MAP2	Neurons	Mouse IgG2a	1:1000	Abcam
MAP2	Neurons	Rabbit polyclonal	1:1000	Abcam
AnkG	Ankyrin G (axonal initial segment)	Mouse IgG2a	1:200	NeuroMab
$PanNa_v$	Na^+-channel	Mouse IgM	1:100	Sigma
Phalloidin	F-actin	N/A	1:300	Invitrogen
Nestin	Intermediate filament	Mouse IgG1	1:1000 (ICC, WB)	Chemicon
Vimentin	Intermediate filament	Rabbit	1:500 (ICC) 1:1000 (WB)	Abcam
β-actin	Cytoskeleton	Rabbit	1:500 (ICC) 1:10,000 (WB)	Biolegends
α-tubulin	Cytoskeleton	Mouse IgG1	1:1000	Sigma
β-tubulin	Cytoskeleton	Rabbit polyclonal	1:1000	Sigma
P-STAT-1	Phosphorylated-STAT-1 (JAK-STAT)	Rabbit polyclonal	1:50	Cell Signaling
P-P65	Phosphorylated-P65 subunit (Nf-Kβ)	Rabbit polyclonal	1:100	Cell Signaling
Calretinin	Immature granule cells	Rabbit polyclonal	1:5000	Swant
Calbindin	GABA-ergic interneurons	Rabbit polyclonal	1:20000	Swant
Parvalbumin	GABA-ergic interneurons	Rabbit	1:10000	Swant
NeuN	Mature neurons	Mouse IgG1	1:100	Chemicon
Synaptophysin	Pre-synaptic marker	Mouse IgM	1:200 (ICC) 1:5000 (WB)	Stressgen
SNAP25	SNARE-complex	Mouse IgG1	1:200 (ICC) 1:5000 (WB)	Chemicon
VAMP2	SNARE-complex	Mouse IgG1	1:200 (ICC) 1:10,000 (WB)	Synaptic Systems
LAMP1	Lysosomal membrane protein	Mouse IgG2a	1:500	Developmental Studies of Hybridoma Bank
Cath D	Lysosomal hydrolase	Rabbit polyclonal	1:200	Santa Cruz Biotechnology
EEA1	Early endosomes	Mouse IgG1	1:200 (ICC) 1:10,000 (WB)	BD Bioscience
Rab 7	Small GTPase	Rabbit polyclonal	1:500	Sigma
Cx43	Connexin 43 (gap junctions)	Rabbit polyclonal	1:500	Invitrogen
TNF-α	Cytokine	Rabbit Polyclonal	1:1000	Abcam
MIP-1γ	Cytokine	Mouse Ab	1:1000	Cell Sciences

Table 2.1. Details of primary antibodies used. Abbreviations: glial fibrillary acidic protein (GFAP), cluster of differentiation 68 (CD68), oligodendrocyte marker 4 (O4), 5'-bromo-2'-deoxyuridine (BrdU), microtubular associated proteins (MAP2), ankyrin G (AnkG), voltage-gated sodium channel (PanNav), neuronal specific nuclear protein (NeuN), synaptosome-associated protein 25 (SNAP25), vesicle-associated membrane protein 2 (VAMP2), lysosome-associated membrane proteins 1 (LAMP1), cathepsin D (Cath D), early endosome antigen 1 (EEA1), connexin 43 (Cx43), tumor necrosis factor-α (TNF-α), macrophage inflammatory protein-1γ (MIP-1γ), immunohistochemistry (IHC), immunocytochemistry (ICC), Western blotting (WB).

Secondary antibodies	Fluorochrome	Concentration	Manufacturer
Goat anti rabbit IgG	Alexa 488, 546, 633	1:500, 1:1000	Invitrogen
Goat anti mouse IgG, IgM, IgG1, IgG2A	Alexa 488, 546, 633	1:500, 1:1000	Invitrogen
Goat anti rat	Alexa 546	1:500, 1:1000	Invitrogen
Goat anti rabbit IgG (H+L)	Alexa 790, 680	1:5000,1:10000	Invitrogen
Goat anti mouse IgG (H+L)	Alexa 790, 680	1:5000, 1:10000	Invitrogen
Biotinylated goat anti rabbit IgG (H+L)	N/A	1:1000	Vector

Table 2.2. Details of secondary antibodies used.

2.6 *In vitro* studies on astrocyte, neuronal and co-cultures based on immunostaining

Analysis of culture composition

The purity of the astrocyte or neuronal cultures, and the composition of mixed glial cultures were assessed using an array of cell-type specific markers. Glial GFAP was used to identify astrocytes, oligodendrocyte marker 4 (O4) to identify oligodendrocytes, cluster of differentiation (CD68) to identify microglial cells and MAP2 and/or neuronal specific nuclear protein (NeuN) to identify neurons.

Cytoskeletal staining

To compare the cytoskeletal organization of WT and *Cln3*$^{-/-}$ astrocytes, the expression of actin, microtubules and intermediate filaments was investigated. 24 hour after plating cells were fixed differently according to the cytoskeletal polymer under investigation. GFAP immunoreactivity was used to visualize the intermediate filament organization of astrocytes; Phalloidin was used to visualize F-actin filaments; and primary antibodies against β- and α-microtubules were used to visualize microtubular organization. In order to visualize the F-actin filaments with phalloidin, cells were washed once with a 1:1 mixture of buffer (20mM Pipes (pH 6.1), 276 mM KCl, 6mM $MgCl_2$, 4mM EDTA and 640mM sucrose) and MilliQ H_2O, then fixed for 10 minutes at room temperature in phalloidin (1:300, Invitrogen, AlexaFluor 546) diluted in an EM-Grade PFA (Polysciences Inc.) solution (50% buffer described above, 25% EM-Grade PFA,

and 25% MilliQ H_2O). After this step, cells were washed once with buffer solution and twice with PBS. DAPI (1:2000 diluted in PBS) was added for 5 minutes prior to mounting in Prolong gold mounting solution (Invitrogen). For visualization of microtubular structures cultures were washed twice with cold TBS, then fixed and permeabilized with ice-cold methanol for 5 minutes, followed by incubation in ice-cold methanol/acetone for 5 minutes. Cultures were then washed three times in TBS before a blocking step was carried out (2% BSA in TBS-T for 10 minutes in room temperature) followed by incubation with anti-β- and α-microtubules antibodies diluted in 2% BSA /TBS-T for 30 minutes at room temperature. After washing the cultures three times in TBS-T, the cells were incubated with the relevant secondary antibodies diluted in 2% BSA in TBS-T for 1 hour at room temperature.

Localization of the AIS

The axon initial segment (AIS) and its localization along the axon is considered to be a reflection of neurons information-processing capabilities, since these cells have been shown to dynamically re-locate their AIS in a activity-dependent manner enabling them to fine-tune their own excitability (Grubb and Burrone, 2010b). To obtain information about the position of the AIS along the axons of WT and *Cln3*$^{-/-}$ neurons, 5 or 7 day old neuronal cultures were exposed to depolarization by increasing the KCl content of the culture medium from 5mM to 15mM for 48 hour. The NaCl content of the medium bathing control cultures was also increased to 15mM to provide isotonic control conditions for this experiment. It is known that AIS re-localization is dependent on the activity of L-type calcium channels (Grubb and Burrone, 2010b). Thus, to investigate the mechanism behind re-localization of the AIS in WT and *Cln3*$^{-/-}$ neurons, 1µM nifedipine (Sigma) was added to the medium in certain experiments. The location for the AIS was determined using an anti-ankyrin G (AnkG) antibody, anti-PanNa_v (voltage gated sodium channel marker) was used to identify the localization of all different isoforms of potassium channels crucial for initiation of action potentials, and MAP2 was used to visualize neuronal cell bodies and processes. Additionally, a cocktail of anti-calbindin, -calretinin, and -parvalbumin

antibodies was used to identify inhibitory neurons present in these cultures.

Immunofluorescence staining was carried out as described above except for the fixation step. For AnkG labeling, cultures were fixed with 4% PFA (TAAB Laboratories, in 3% sucrose, 60mM PIPES, 25mM HEPES, 5mM EGTA, 1mM MgCl2, pH 7.4), for 20 minutes at room temperature, and then incubated with the antibody for 1 hour at room temperature. For staining with the $PanNa_v$ antibody, a 1% PFA fixation was used for 20 minutes at room temperature followed by a 3 hour incubation with the antibody.

All image acquisition and analysis was done blind to experimental group, as previously described (Grubb and Burrone, 2010b). Neurons with a detectable AIS, that clearly originated from the soma of one particular cell, were imaged using a x40 oil immersion objective on a Zeiss laser scanning confocal microscope coupled to Zeiss imaging software, using 488nm and 543nm lasers, along with the appropriate excitation and emission filters. Acquired image stacks were converted into single maximum intensity *z*-axis projections, which were saved as 16bit TIFF files and analyzed with custom-written functions in Matlab (Mathworks). To measure the position of the AIS along the axon, a line profile was drawn starting at the soma and moving along the axon past the detected AnkG staining. Averaged profiles were then smoothed using a 40-point (approximately 5µm) sliding mean, and normalized between 1 (maximum smoothed fluorescence, location of the AIS max position) and 0 (minimum smoothed fluorescence). The AIS start (most proximal) and end (most distal) positions were acquired where the normalized and smoothed profile dropped to 0.33. The position with the peak fluorescence value was considered as the position of maximum value of each profile, representing the area within the AIS with the highest amount of AnkG expression. In each experiment a minimum of 40 cells were analyzed from two different coverslips.

Neurite complexity measurements

Axonal and dendritic processes are one of the defining characteristics of neurons, and are a critical determinant of neuronal connectivity (Pfenninger, 2009; Meldolesi, 2011; Purves, 2011). To compare the ability of WT and *Cln3*$^{-/-}$ P0 cortical neurons to extend these processes, neurite complexity was analyzed, with 'neurite' being used as a collective term for dendrites and axons that are formed by neurons in culture. To do this, the number of primary, secondary, and tertiary neurites was counted, the total length of all primary neurites was measured, as well as the length of the longest primary neurite (which presumably represents the axon). Additionally, the soma sizes of these neurons were determined. To visualize neuronal morphology cultures were stained with MAP2, as described above, and images taken, using the x40 objective on a Zeiss AxioImager Z1 fluorescence microscope, of 40 cells per genotype per experiment in a way that the whole neuron was imaged. All these quantitative measures of neurite complexity and soma size were carried out manually from 40 cells per genotype in each experiment (repeated three times) using the ImageJ program with set µm/pixel calibration. Similar measurements of neurite complexity and soma size were also obtained from neurons co-cultured with glial cells.

Distribution of SNARE-complex proteins

The interactions among the synaptic vesicle proteins VAMP2, SNAP25 and syntaxin1 (so called SNARE proteins) are crucial for the fusion of synaptic vesicles with presynaptic terminals allowing the release of neurotansmitters (review in Kavalali, 2002). Through interactions with VAMP2, synaptophysin has also been proposed to be involved in this fundamental process (Washbourne et al., 1995; Schubert et al., 2011). In addition, endosomes may play an important role in the transport of these proteins to the synapse. Since synaptic pathology has been reported in the NCLs (Kim et al., 2008; Partanen et al., 2008; Kielar et al., 2009), the expression patterns of these SNARE complex proteins, and the distribution of endosomes, was compared in *Cln3*$^{-/-}$ and WT cortical neuron cultures. MAP2 was used to identify neurons in combination with antibodies against SNAP25, VAMP2, synaptophysin and early endosome antigen 1 (EEA1). In all cultures

nuclei were visualized using DAPI.

The number of SNAP25, VAMP2, synaptophysin expressing puncta and EEA1 expressing early endosomes were quantified along the neurites of WT and *Cln3*$^{-/-}$ cortical neurons in order to study their transport along neuronal processes. These measurements were carried out in two regions along each neurite: 0-25µm and 25µm-50µm from the start of the neurite. Identical image acquisition parameters were applied within each experiment, and subsequent quantification was carried out using ImageJ. Specific threshold values were determined and applied within each experimental set of images to distinguish SNAP25, VAMP2, synaptophysin and EEA1 immunopositive puncta from background. An average of the values from the 10-20 cells counted per experiment was used to provide the percentage area of puncta immunoreactive for each protein in the regions of the neurite under investigation. In co-culture experiments the distribution of SNAP25 and synaptophysin (neuron specific SNARE-proteins) were explored only qualitatively. In addition, Western blotting was used to measure the total intracellular expression of each of these proteins in both neuronal cultures and in co-cultures, as described below.

Analysis of cell death in co-cultures

Live/dead analyses

To reveal the identity of the cells undergoing cell death in co-cultures, a live/dead fixable cellular marker conjugated to a red fluorochrome (Invitrogen) was used in combination with cell-type specific markers (GFAP, CD68 and MAP2 to identify astrocytes, microglia and neurons, respectively). On the day of analyses (after 9 or 14 days in culture), the Live/Dead dye (1µl/well) was added to the culture medium and incubated for 30 minutes at 37°C to allow damaged/dying cells to take up this amine-reactive fluorescent dye. Cultures were then washed three times with PBS prior to fixing and staining with relevant antibodies.

Cytotoxicity

Overall cytotoxicity in co-cultures was evaluated by measuring lactate dehydrogenase (LDH) release using a Cytotox 96 assay kit (Promega) according to manufacturer's instructions. This assay is based on the enzymatic conversion of a tetrazolium salt (INT) into a red formazan product, at a level that is directly proportional to amount of LDH present in the sample. This product is measured at 492nm by using a plate reader (Wallac 1420 Victor3 plate reader, Perkin-Elmer, Waltham). After collection of half of the medium from each culture to measure the %LDH released into the medium, the remaining cells were lysed in 0.1% Triton X-100 for 30 minutes. The LDH content of these latter samples was used as a measure of total LDH content (100% LDH). LDH release from cells was calculated as a percentage of total LDH (%LDH) in each sample, and presented as average of %LDH±SEM.

Pharmacological activation of astrocytes

To compare the ability of WT or *Cln3*$^{-/-}$ astrocytes to respond to activation, primary astrocytes cultures were exposed to LPS (Sigma) plus IFNγ (Thermo Scientific) (Bolaños et al., 1994). These compounds were added directly to the culture medium to give a final concentration of 1μg/ml LPS and 100 U/ml of IFNγ. WT and *Cln3*$^{-/-}$ astrocytes were exposed to this activating stimulus for a range of times, as indicated in the specific experiments described below. In all cases, untreated cultures that did not receive any stimulation were used as controls. Following stimulation cell responses were compared by (1) immunofluorescence staining to study cell morphology and protein localization; (2) Western blotting to quantify protein expression; (3) HPLC to analysis the synthesis and secretion of glutathione; (4) assessing migration using a scratch assay; and (5) collection of cell medium from cultures for analysis of secreted soluble factors.

Activation of specific signaling cascades by LPS and IFNγ

To assess the ability of LPS and IFNγ to transduce a signal in astrocytes the nuclear translocation of appropriate downstream signaling components were investigated. Upon binding to its receptor, toll-like receptor 4 (TLR4), LPS initiates

a downstream signaling cascade that ultimately leads to the nuclear translocalization of the phosphorylated forms of the nuclear factor-κβ (NF-κB) subunits P65 and P50, resulting in the expression of NF-κB regulated genes (Wang and Baldwin, 1998; Chow et al., 1999). Upon binding to its receptor, IFNγ-R, IFNγ on the other hand, activates the Janus kinase (JAK)-signal transducer and activator of transcription (STAT) signaling pathway leading to the nuclear translocalization of phosphorylated form of STAT1 and the inhibition or activation of the transcription of genes regulated by this factor (Horvath, 2004). Therefore, the ability of LPS to activate P-P65 and IFNγ to activate P-STAT1 in stimulated and non-stimulated WT and *Cln3* deficient astrocyte cultures was analyzed. GFAP was used to identify astrocytes and phospo-specific primary antibodies were used to identify the NF-κB subunit P65 (P-P65) and STAT1 (P-STAT1). The standard immunofluorescence staining protocol described above was followed except when labeling with anti-P-STAT1 where, a 10 minutes incubation in methanol at room temperature was used to permeabilise cells, and blocking was carried out with 15% NGS for 1 hour. The percentage of cells expressing either P-P65 or P-STAT1 in their nuclei was quantified, as described below.

Assessment of morphological changes following activation

To visualize the morphological changes that WT and *Cln3*$^{-/-}$ astrocytes underwent upon activation with LPS/IFNγ, cultures were stained with GFAP and the observed changes in cell soma size measured using ImageJ. Images of 5 random fields of cells, whose processes were not overlapping, were taken from two different coverslips per genotype, per experiment. The soma size of these cells was then measured by manually drawing around the body of each cell and allowing ImageJ to calculate the enclosed area by using the µm/pixel-information provided. The average cell body size of *Cln3*$^{-/-}$ astrocytes was normalized to the corresponding values from WT astrocytes.

Cell counts

Where data analysis included cell counts from immunostained cultures, five random fields were counted per culture, and averaged to determine the percentage of cells expressing each marker within the total population. All counts were averaged from at least three coverslips per condition, and were obtained from at least three different experiments (unless otherwise stated), and the standard error of the mean calculated (SEM).

2.7 Western blotting

This technique was use to assess changes in levels of proteins in WT and *Cln3*$^{-/-}$ astrocytes known to accompany astrocyte activation, such as GFAP, nestin and vimentin. In all experiments activation with LPS/IFNγ was carried out for 24 or 48 hour and untreated samples were used as controls.

Preparation of cell-lysates

After activation, cultures were washed twice with ice-cold PBS then 150µl of ice-cold lysis buffer (50mM Tris-HCL, pH 7.5, 150nM NaCl, 1mM EDTA, 1% Triton X-100, protease inhibitor cocktail set III (1:1000) and phosphatase inhibitor cocktail set II (1:100) (Calbiochem)) was added and the cells scraped into the buffer. This lysate was then incubated on ice for 10 minutes and spun at 14000rpm for 5 minutes. Before storage at -80°C, 40µl of 4×sample buffer (150mM Tris-HCL, pH 6.8, 12% SDS, 30% glycerol, a few grains of bromophenol blue and 5% β-mercaptoethanol) was added. On the day the gel was run, samples were thawed and boiled for 5 minutes at 95 °C, then spun briefly at 14000rpm. To allow equal loading of the samples, a BCA protein assay kit (Thermo Scientific) was used to quantify the total amount of protein in each sample according to manufacturer's instructions.

Electrophoresis, transfer of proteins and sample quantification

Samples (20µg/sample) were run on a 12% NuPAGE® Bis-Tris, sodium dodecyl sulfate polyacrylamide gel electrophoresis (SDS-PAGE) gel for approximately 2

hours at 120V. The gels were then incubated for 5-10 minutes in transfer buffer (25mM Tris-HCL, 192mM Glycine, 0.01% SDS and 20% methanol), before proteins were transferred to Immuno-Blot polyvinylidene difluoride (PVDF) membranes (Bio-Rad laboratories, Hercules, CA) that had been incubated in methanol for 10 minutes, followed by 5-10 minutes in transfer buffer (25mM Tris-HCL, 192mM Glycine, 0.01% SDS and 20% methanol). The Transfer was carried out at 30V for 1.5 hour. Membranes were then blocked for 1h in 5% non-fat dry milk in TBS containing 0.1% Tween-20 (TBS-T) to prevent the non-specific binding of antibodies, and incubated with primary antibodies, diluted in 3% BSA containing 0.1% Tween-20, overnight at 4°C. Membranes were then washed three times in TBS-T and incubated with the relevant fluorescently labeled secondary antibodies, diluted in 5% non-fat dry milk in TBS-T for 1 hour, at room temperature before being washed three times in TBS-T. After washing, immunoreactive bands were visualized using an Odyssey Infrared Imaging System (Li-COR Biosciences). Quantification of protein levels was performed from three biological replicates using a gel quantification program provided in ImageJ. The arbitrary fluorescent values that represent the relative amount of protein obtained from *Cln3*$^{-/-}$ cell samples were normalized to corresponding WT cell samples.

Western blotting analysis was also used to quantify the expression levels of SNARE-complex and EEA1-proteins expressed by neurons that had been grown alone or in co-cultures with glial cells. In these experiments, neuronal cultures were lysed after 7 DIV, and co-cultures were lysed after 14 DIV, following the same protocol as described above, except here, the arbitrary fluorescent values for each protein in each sample were normalized to β-actin values. Three biological replicates were quantified in each case.

2.8 Protein secretion profiling assay

Protein secretion is one of the fundamental properties of astrocytes, which they use to communicate with and control the biology of other cells in the

surrounding tissue (Majumder et al., 1996; Ridet et al., 1997; Liberto et al., 2004; Bélanger and Magistretti, 2009; McKimmie and Graham, 2010; Allaman et al., 2011). The quantitative analysis of the levels of proteins secreted by *Cln3*$^{-/-}$ and WT astrocytes grown under basal conditions, and at various time points (6 hour, 24 hour and 72 hour) after activation with LPS/IFNγ, was carried out by Myriad RBM (Austin, TX, USA) (RodentMAP version 2.0 cytokine analysis).

All supernatant samples were collected and stored at -80°C until sent for analysis. Before shipping, samples were allowed to thaw at room temperature, mixed well by vortexing then centrifuged at 13000 x g (5 minutes) to remove any cell debris. Simultaneous analysis of 59 different proteins from each of the samples, was carried out by Myriad RBM (quantified proteins listed in Chapter 4, Table 4.1) using an automated quantification system described briefly below. Sample were added into the capture microsphere multiplexes of the RodentMAP (multi-analyte profiling) version 2.0 using robotics, thoroughly mixed and incubated for 1 hour at room temperature. Multiplexed cocktails of biotinylated reporter antibodies for each multiplex were then added, mixed and incubated for a further hour at room temperature. The reaction was then developed using a Streptavidin-phycoerythrin solution by incubation for 1 hour at room temperature. Results were processed using a Luminex 100 instrument and the data analyzed using patented data analysis software developed by Myriad RBM. Appropriate control samples were run with each multiplex to ensure accurate assay performance. The expression levels of 59 different proteins were quantified from three different biological samples for each treatment per genotype. These values were normalized to the relative number of cells in the culture from which the medium was collected, as determined by counting DAPI stained nuclei in five random fields from each fixed culture subsequent to cell supernatant collection. The difference in secreted protein levels between WT and *Cln3*$^{-/-}$ astrocytes are presented as % Change in tables 4.1 and 4.2 of Chapter 4. Some selected secreted proteins levels are also presented as a time course of altered secretion levels over time.

2.9 Glutathione measurements

Determination of intracellular reduced glutathione levels using reverse-phase HPLC

The principle underlying this method is the separation of reduced glutathione (GSH) from other components within the samples by using reverse-phase high performance liquid chromatography (HPLC). In this particular method the mobile phase: 15mM orthophosphoric acid (OPA) is forced through a chromatography column contains C_{18} chains under high pressure. Hydrophobic interactions with the C_{18} chains delay the progress of molecules as they are forced to pass through the column. Retention time, which is the time taken for a particular molecule to be eluted from the column, depends upon the molecule's hydrophobicity, and remains identical under the same conditions.

To quantify GSH levels in our samples, an electrochemical method of detection was used (Riederer et al., 1989). Eluent from the column was passed into an electrical cell (model 5010) that forms part of the Coulochem II electrochemical detector (ESA, Analytical Aylesbury, UK), which includes two electrodes in series set to constant voltage optimized for the proteins being measured. The voltage at the upstream electrode (E1) is set below that which the protein of interest will oxidize in order to remove the more readily oxidized proteins within the sample. The downstream electrode (E2) is set to a voltage, which is the optimal oxidizing voltage for the molecule of interest. The retention time is used to identify the molecules, and the peak height at this time corresponds to the current they induce at E2. Thus, peak height is directly proportional to the concentration of the molecule of interest. Figure 2.1 illustrates typical chromatograms obtained from the reverse-phase HPLC GSH runs in this study.

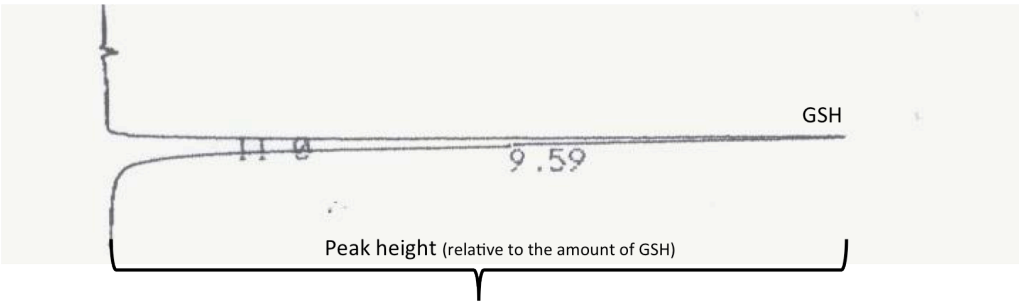

Figure 2.1. A typical GSH-chromatogram from reverse-phase HPLC. This figure illustrates a typical chromatogram from a reverse-phase HPLC run designed to quantify the amount of reduced form of glutathione (GSH). The peak height is directly proportional to the concentration of GSH.

The correct voltage at E2 for the molecule of interest was initially determined by using a voltammogram, where a standard concentration of the protein of interest is run through the column at a range of different voltages, and the peak height is plotted against voltage. The optimal voltage is chosen based on which of the voltages provides the maximal, or near maximal, peak height while maintaining the background current low and producing a clean, narrow peak on the chromatograph.

Preparation of astrocyte samples for GSH measurement

To perform intracellular glutathione (GSH) measurements, some cultures were stimulated with LPS (1μg/ml) plus IFNγ (100U/ml) for 24 hour or 48 hour while others received no stimulation and were used as controls. Cells were washed twice in 1ml HBSS (minus phenol red), removed from wells with 1ml trypsin-EDTA (0.5 mg/ml, minus phenol red), then centrifuged at 500 x g for 5 minutes at 4°C. Cell pellets were resuspended in 300μl of isolation medium (320mM sucrose, 10mM Tris, 1mM EDTA, pH 7.4) and frozen in liquid nitrogen before being stored at -80°C. The GSH levels obtained were normalized to the total amount of protein in each sample, which was determined using a Lowry protein assay (Thermo Scientific) according to the manufacturer's instructions.

Measurement of intracellular levels of glutathione

Intracellular GSH levels were determined electrochemically, and separation by reverse-phase HPLC, as described above (Riederer et al., 1989; Gegg et al., 2005).

To do this, samples were thawed and GSH was extracted by the addition of an equal volume of 15mM OPA, followed by thorough vortexing. Unwanted proteins in the sample were pelleted by centrifugation at 10,000 g for 5 minutes (Eppendorf 5415R). The supernatant was then injected into the HPLC using a Jasco autosampler (model AS-2055 Plus; Jasco, Essex, UK) with an injection volume of 50µl. Subsequently, the sample was passed through a 3mm x 10mm guard column, and into a 4.6mm x 250mm analytical column packed with 5µM octadecasilyl-silica (HPLC Technology Co Ltd, purchased from Chromacol Ltd, Hertfordshire, UK). Both of these columns were kept in a block heater set at 30°C (model 7970; Jones Chromatography, Mid Glamorgan, UK). The mobile phase was pumped through the HPLC-system at 0.5ml.min^{-1} by using a Jasco PU-1580 pump (Jasco, Essex, UK). Normally in this type of setup the pressure of the column was in the range of 50 – 70 kg.cm^{-2}, and the retention time for the GSH was around 9.5-14 minutes. The electrode potentials were set at E1=100 mV and E2=450 mV, and the total run time/sample was 20 minutes. A Chromjet integrator (model SP4400; ThermoFinnigan, Thermo Fisher Scientific, Hemel Hempstead, UK), which is connected to the E2 electrode, recorded the generated current generating chromatograms in real-time. Standards of 5µM GSH in 15mM OPA were run at the beginning and end of each the experiment. Peak heights of these standards were used to calculate the appropriate GSH concentration in each sample, which were corrected for sample dilution, normalized for intracellular protein content, and shown as nmol/mg protein. Three replicates were used in each experiment, and these experiments were repeated four separate times.

Measurement of intracellular levels of oxidized and total glutathione

In addition to the GSH, the oxidized form (GSSG) may also exist in cells. In order to calculate the total levels of glutathione in the samples, from which GSSG levels can be calculated, cells were prepared for HPLC as described above. However, subsequent to cell suspension in isolation medium, samples were split in half. One half of each sample was used for GSH measurements as described above, and the remaining half was treated with glutathione reductase (GR) in the

presence of reduced nicotinamide adenosine dinucleotide phosphatase (NADPH) to convert the GSSG to GSH (Stewart et al., 2002). To do this, samples were incubated at 37°C for 10 minutes with an equal volume of isolation medium (320mM sucrose, 10mM Tris, 1mM EDTA, pH 7.4) containing 500uM NADPH and 2 units of GR, snap-frozen in liquid nitrogen and stored at -80°C until used to determine GSH levels by HPLC, as described above. The difference between total glutathione concentration and GSH concentration was used to calculate the concentration of GSSG. These measurements were carried out from three different samples, and repeated once.

Determination of glutathione levels in the culture medium

Glutathione levels in the culture medium were measured using the GSH-Glo glutathione assay kit (Promega) that consists of a two-step reaction system allowing the quantification of reduced glutathione levels based on a luminescent signal (Figure 2.2). In the first step, glutathione S-transferase (GST) produces luciferin from luciferin-NT, which is a luciferin byproduct that is only formed in the presence of reduced glutathione (GSH). In the second reaction, stabilized luciferase from *Photinus pyralis* induces the release of light by luciferin. The light signal generated is proportional to the amount of GSH present in the sample.

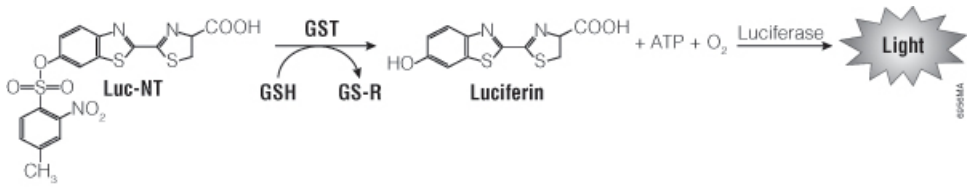

Figure 2.2. Schematic illustration of the GSH-Glo glutathione assay. The GSH-Glo glutathione assay is performed in two steps. In the first step, samples are treated with a luciferin-NT substrate and glutathione S-transferase. Glutathione present in the sample drives the formation of luciferin. In the second step, Luciferin Detection Reagent is added to produce light. The amount of light detected is directly proportional to the amount of GSH in the reaction. Image was obtained from Promega webpage (*http://www.promega.com/products/pm/gsh-glo-glutathione-assay/).*

This experiment was carried out according to the manufacturer's instructions. Briefly, prior to the start of the experiment, the medium was changed to serum-free, phenol red-free medium (otherwise identical to the routinely used

astrocyte cell culture medium). At the end of an incubation period of 8 hour, half of the medium was removed to be used for GSH measurements, and centrifuged at 5031 g for 2 minutes to pellet any cell debris. To make sure the obtained results were not due to unspecific release of GSH, the other half of the medium was used to measure the amount of LDH released into in the medium, which was compared to total amount of LDH per sample (100% LDH) obtained by lysing the cells in the culture with Triton X-100 (final concentration 0.1%). The LDH measurements were carried out as described above (cytotoxicity assay).

In some experiments, the importance of the actin cytoskeleton to glutathione secretion was examined by using an inhibitor of actin polymerization called Cytochalasin D (1µM). This inhibitor was added to the WT astrocytes 30 minutes prior to the start of the 8 hour measurement period, otherwise the extracellular GSH measurements were carried out as described below.

In order to measure the total amount of glutathione, 50µl of each of the sample was treated with tris-2-carboxyethyl phosphine (TCEP), which is a strong reducing agent that converts the oxidized form of glutathione into measurable GSH, for 10 minutes at room temperature. For the GSH measurements, 50µl of sample was combined with 50µl of GSH-Glo reagent, which contained luciferin-NT and glutathione S-transferase in 50mM tricine buffer (pH 7.9), in a well of a 96-well plate (Corning). The samples were then mixed briefly and incubated at room temperature for 30 minutes. 100µl of the luciferin detection reagent, which was reconstituted with luciferin detection buffer according to the manufacturer's instructions, was then added to each of the sample-containing wells and their luminesence recorded using a plate reader (Wallac 1420 Victor3 plate reader, Perkin-Elmer, Waltham). GSH concentrations in each sample were then calculated using a standard curve, which was run alongside the samples in each experiment.

2.10 Cell mobility assay

In order to investigate whether the ability of the *Cln3*$^{-/-}$ astrocytes to migrate was compromised, a scratch wound assay was performed. Once astrocytes cultures were confluent (24 – 72 hours after plating) a scratch was made using the Essen Wound-maker, generating a cell-free region that was approximately 800µm – 900µm wide. Cultures were then washed three times with PBS, to remove any cell debris from the scratched area, before the addition of growth medium containing Ara-C (to inhibit cell proliferation), to which LPS/IFNγ was or was not added. Cultures were then placed in the IncuCyte live cell imaging system (Essen) and the wound width measured every 1 hour for 24 hour. The rate of migration was obtained by measuring the width of the existing wound over time. Three samples per condition were analyzed in each experiment and this experiment was repeated four times.

2.11 Intracellular calcium measurements

Fluctuations in the levels of intracellular Ca^{2+} ($[Ca^{2+}]_i$) were investigated to determine the ability of WT and *Cln3*$^{-/-}$ astrocytes to generate spontaneous Ca^{2+}-oscillations and calcium waves, to response to ATP-treatment and to study Ca^{2+}-release from the ER following thapsigargin (SERCA-pump inhibitor)-treatment.

To measure intracellular Ca^{2+}-levels, cells were loaded with 5µM fura-2 AM (Invitrogen), together with 0.005% Pluronic acid (Sigma) diluted in astrocyte growth medium, for 30 minutes at room temperature. Cells were then washed three times with HBSS (-phenol red, $+Ca^{2+}/Mg^{2+}$), and recording medium added. The composition of this medium varied in each experiment (see below for details). Measurements were obtained using a Nikon epifluorescence inverted microscope equipped with a 20 X fluorite objective (Tokyo, Japan). In this system, a Xenon arc lamp creates excitation light, which is selected using 10nm bandpass filters, centered at 340nm and 380nm, that are kept in a computer-controlled filter wheel, both with emission at >515nm (Cairn Research, Faversham, UK). A CCD camera (Orca ER; Hamamatsu, Welwyn Garden City, UK) was used to collect the emitted light, which passes through a long-pass filter. All

imaging data was collected at 5 seconds intervals, digitized and subsequently analyzed using Kinetic Imaging software (Wirral, UK). The traces obtained are presented as ratios of excitation at 340nm and 380nm and were acquired from at least two coverslips (approximately 50 cells/field), and from two separate cell preparations. The concentration of free intracellular Ca^{2+} is proportional to the ratio of fluorescence at 340/380. This relationship is described by the Grynkiewicz equation (Grynkiewicz et al., 1985):

$$[Ca^{2+}]_I\ (nM) = K_d \text{ X } [(R-R_{min})/R_{max}-R)] \text{ X Sfb},$$

where Kd (for Ca^{2+} binding to fura-2 at 37°C) = 225nM, R=340/380 ration, R_{max} =340/380 ration under Ca^{2+}-saturating conditions, R_{min} =340/380 ratio under Ca^{2+}-free conditions, and Sfb=ratio of baseline fluorescence (380nm) under Ca^{2+}-free and Ca^{2+}-bound conditions. HBSS buffer (-phenol red, $+Ca^{2+}/Mg^{2+}$) was used as the recording medium in all spontaneous Ca^{2+} oscillation studies. When the response of WT and *Cln3*$^{-/-}$ astrocytes to ATP (100µM) treatment was under investigation, $[Ca^{2+}]_i$ measurements were carried out in a special recording buffer: a HEPES-buffered salt solution (156mM NaCl, 3mM KCl, 2mM $MgSO_4$, 1.25mM KH_2PO_4, 2mM $CaCl_2$, 10mM glucose, and 10mM HEPES, pH 7.35). When the effect of thapsigargin (1µM) on ER-Ca^{2+} release was explored, the recording medium used was HBSS buffer (-phenol red, $-Ca^{2+}/Mg^{2+}$) to avoid any extracellular Ca^{2+}. Subsequently, in order to allow the store operating calcium entry (SOCE) to take place after ER-Ca^{2+} depletion was complete, Ca^{2+} (100µM) made in HBSS buffer (-phenol red, $-Ca^{2+}/Mg^{2+}$) was added to cells.

2.12 Lactate secretion assay

In the CNS energy is transferred from astrocytes to neurons in the form of lactate (Pellerin et al., 1998). To compare the ability of WT and *Cln3*$^{-/-}$ astrocytes cultures to secrete lactate, culture medium was replaced, 24 hour after cells were plated, with 500µl of serum-free, phenol-red-free DMEM containing glucose (4.5g/l), P/S (50U/ml / 50µg/ml), and l-glutamine (2mM). After a 4 hour incubation, half of

the culture medium was collected and centrifuged at 400 g for 4 minutes, at 4°C, then stored in -80°C until lactate measurements were carried out, while the other half was used to quantify the total amount of protein in each sample using a BCA protein assay kit. Lactate was measured using a fluorometric L-Lactate Assay Kit (Abcam), according to the manufacturer's instructions. In this assay, lactate present in the sample reacts with the provided enzyme mix to generate a product, which interacts with a lactate probe to produce color (570nm). Absorbance was measured using a microplate reader (Wallac 1420 Victor3 plate reader, Perkin-Elmer, Waltham). In each assay, a standard curve was generated using cell-free culture media containing known concentrations of L-lactate, and the concentration of L-lactate in each sample was calculated from this standard curve. The obtained lactate levels were normalized to the total amount of protein in each sample, and presented as mean percentage of lactate (from total amount of protein present in sample)±SEM. Three technical repeats were measured in each experiment, and the experiment was repeated four times.

2.13 Glutamate clearance assay

To evaluate the glutamate clearance capacity of WT and *Cln3*$^{-/-}$ astrocytes, culture medium was replaced with 1.5ml of serum free, phenol red free DMEM supplemented with 2mM glutamate. After incubation for 2 hour at 37°C to allow astrocytes to take up some of the added glutamate, 750µl of medium was removed, and the glutamate concentration determined using a Glutamate Assay kit (Abcam), according to manufacturer's instructions. In this assay the provided glutamate enzyme mix recognizes glutamate present in the sample leading to a colour reaction that can be detected at 450nm and measured using a microplate reader (Wallac 1420 Victor3 plate reader, Perkin-Elmer, Waltham). In order to calculate the concentration of glutamate remaining in each sample, a standard curve was created using cell-free culture media containing known concentrations of glutamate. The amount of glutamate that was taken up by WT and *Cln3*$^{-/-}$ astrocytes was obtained by comparing these values to control samples in which serum-free, phenol-free medium +2mM glutamate was added to wells that did not contain any astrocytes. These numbers were normalized to the amount of

total cell protein in each sample, which was determined using a BCA protein assay kit. Data is presented as the mean percentage ± SEM. Three technical repeats were measured per experiment and this experiment was repeated four times.

2.14 Fluorescence microscopy

Immunofluorescently stained cells were visualized (except in the AIS-localization studies, see above) using a Zeiss AxioImager Z1 fluorescence microscope (Carl Zeiss, Ltd) with a monochrome AxioCamMR3 camera using AxioVision 4.8. Imaging software (Carl Zeiss, Welwyn Garden City).

2.15 Statistics

All quantitative data was collected using Microsoft Excel spreadsheets, and analyzed using Graphpad PRISM. Most frequently, to allow comparisons of groups, one-way ANOVA with Bonferoni correction was used to test for statistical significance. However, when two groups were compared with each other a Student's T-test was used. In the AIS analysis where the impact of high potassium induced depolarization on AIS localization was examined, non-parametric group comparisons were carried out using the Mann-Whitney U-test for two independent samples. A non-parametric, two-way ANOVA on ranked data was used to test the impact of Nifedipine on AIS-localization in non-depolarized and depolarized neurons (effect of drug x treatment interaction). The Kolomogrov-Smirnov test was used to test the difference in frequency distributions between two samples. In general, three technical replicates were used, and experiments were repeated at least three times (unless otherwise stated). Data was presented as mean ± SEM (unless otherwise stated) and changes were considered significant with a p-value of ≤ 0.05. P-values ≤ 0.05 marked with *, P-values ≤ 0.01 marked with **, P-value ≤ 0.001 marked with ***.

Chapter 3
The basic biology of *Cln3*$^{-/-}$ astrocytes

3.1 Introduction

During development astrocytes are crucial players in the regulation of neurogenesis (Song et al., 2002) and in the formation of brain circuits (Müller and Best, 1989). In the adult brain astrocytes not only actively participate in, and dictate, many of the brain's important functions, but also provide a defense against potential pathological insults (see Chapter 1, Sections 1.3 and 1.4). Moreover, astrocytes form intimate connections with neurons, especially at synapses, where astrocytes perform many essential 'housekeeping' roles, including providing metabolic support to neurons, controlling neurotransmitter and ion homeostasis and monitoring and responding to synaptic activity (reviewed in Verkhratsky and Parpura, 2010; Parpura et al., 2012).

Considerable evidence has now accumulated that astrocytes become activated in response to all forms of CNS disease or injury, a phenomenon generally referred to as reactive astrocytosis (Pekny and Nilsson, 2005). This reactive astrocytosis has been shown to influence the progression and outcome of disease, and may be either harmful or beneficial (Ridet et al., 1997; Pekny and Nilsson, 2005; Sofroniew and Vinters, 2010) (see also Chapter 1, section 1.4). The changes that astrocytes undergo upon activation appear to differ with the nature and severity of the insult (Sofroniew, 2009; Sofroniew and Vinters, 2010), but include increased secretion of various cytokines, progressive cellular hypertrophy and, in severe cases, proliferation and eventually glial scar formation. Generally, the upregulation of intermediate filament proteins, in particular GFAP, by reactive astrocytes is considered to be one of the best-known hallmarks of this process (Pekny and Pekna, 2004), together with upregulation of vimentin and re-expression of the stem/progenitor cell marker nestin (Pekny and Nilsson, 2005; Sofroniew and Vinters, 2010).

As mentioned above (see Chapter 1, Section 1.4), intimate interactions between neurons and astrocytes exists in both healthy and diseased brains, yet despite much research the actual role that astrocytes play in the diseased CNS is still poorly understood (Sofroniew and Vinters, 2010; Zamanian et al., 2012). Such

information could be beneficial in understanding disease progression and in the development of novel therapeutic interventions to combat CNS diseases. Indeed, this may be particularly relevant when considering JNCL, the disease I focus upon in this thesis.

In JNCL, as in all the other forms of NCL, activation of both astrocytes and microglial cells has been shown to precede neuronal loss (Mitchison et al., 2004; Pontikis et al., 2004; 2005; Cooper et al., 2006). However, in JNCL this early glial response appears to be impaired, since astrocytes fail to become hypertrophied and microglia fail to transform into phagocytotic brain macrophages (Pontikis et al., 2004; 2005). This impaired activation of glia in JNCL is markedly different to the pronounced glial responses seen in mouse models of all other forms of NCL (Bible et al., 2004; Kielar et al., 2007; Partanen et al., 2008; Kuronen et al., 2012; Schmiedt et al., 2012). Recently, we have shown that cultured *Cln3*$^{-/-}$ microglia have a similarly incomplete morphological response to artificial stimulation, paralleling our *in vivo* observations. In addition, these microglia displayed specific differences in their cytokine expression profile compared to wild type microglia (S. Dihanich, unpublished data), in particular, chemokines involved in directed chemotaxis (MIP-1γ, MIP-2 and Rantes) were significantly downregulated.

In this chapter, I describe *in vitro* experiments designed to systematically characterize the biology of *Cln3*$^{-/-}$ astrocytes using astrocyte cultures established from the cortices of P1-P2 WT and *Cln3*$^{-/-}$ mice. Specifically, I compare the cytoskeletal structure and endo/lysosomal system of WT and *Cln3*$^{-/-}$ astrocytes, in order to build a picture of how mutations in the *Cln3* gene influence the basic properties and structural organization of this cell type. I will then ask whether cultured *Cln3*$^{-/-}$ astrocytes show an impaired morphological response to stimulation as seen *in vivo*.

3.2 Results

Attenuated glial response in *Cln3*$^{-/-}$ mice and in human JNCL

Unlike in other forms of NCLs in which a robust glia activation is observed (Oswald et al., 2005; Kielar et al., 2007; Partanen et al., 2008; Macauley et al., 2009), the morphological response of astrocytes and microglia is attenuated in *Cln3*$^{-/-}$ mice (Pontikis et al., 2004; 2005). Using an increase in GFAP and CD68 expression as a hallmark of astrocyte and microglia activation respectively (Pekny 2004), we investigated whether this attenuated glial response is also evident in *post mortem* tissue from JNCL patients.

We first compared the extent of astrocyte and microglia activation in cortical sections from *Cln3*$^{-/-}$ and *Tpp1*$^{-/-}$ mice, a mouse model for Late Infantile NCL (LINCL), one of the earliest onset and fastest progressing forms of NCL. In the cortex of *Tpp1*$^{-/-}$ mice, astrocytes appeared to be fully activated, displaying intense GFAP immunoreactivity, with many thickened processes and pronounced hypertrophy compared to the GFAP expressing astrocytes in the cortex of age-matched WT mice (Figure 3.1 A a, figure provided by Andrew Wong). In contrast, as described previously in the *Cln3*$^{-/-}$ cortex, (Pontikis et al., 2004; 2005), astrocyte activation appears compromised early in the disease progression (6.5 months, and 12 months), with GFAP expressing astrocytes in *Cln3*$^{-/-}$ mice exhibited only thin cellular processes (Figure 3.1 A a, compare higher magnification images). However, by the end stages of the disease (21 months of age) GFAP expressing astrocytes in *Cln3*$^{-/-}$ mice appear to become fully hypertrophied, as observed in the *Tpp1*$^{-/-}$ mice. Additionally, a gradual increase in the number of CD68 expressing activated microglia was detected in the *Cln3*$^{-/-}$ mouse cortex over the course of the disease, which again is in agreement with previous findings suggesting that the early activation of *Cln3*$^{-/-}$ microglia is attenuated both *in vivo* and *in vitro* (Figure 3.1 A b) (Pontikis et al., 2004; 2005; Kielar et al., 2007, Dihanich, unpublished data). At the end stage of the disease, it appears that the activation of both *Cln3*$^{-/-}$ astrocytes and microglia is attenuated early in the disease process, with these glial cells failing to completely transform.

To examine whether a similar attenuated glial response was also evident in human JNCL, the extent and nature of astrocytosis and microglia activation were compared in JNCL and LINCL *post mortem* cortical tissue (Figure 3.1 B, figure provided by Andrew Wong). Sections from the cortex of both JNCL and LINCL cases were immunostained for either GFAP or CD68 and counterstained with haematoxylin. Numerous intensely stained hypertrophied astrocytes with many thickened processes were observed in the cortex of LINCL cases (Figure 3.1 B). In comparison, markedly fewer and less intensely stained GFAP expressing astrocytes were observed in the cortex of JNCL cases, and these astrocytes appeared smaller with fewer and thinner processes. Similarly, dramatically fewer and less morphologically transformed CD68 positive microglia were evident in JNCL, compared to a high number of CD68 positive morphologically activated microglia and macrophages in LINCL cortical tissue. This impaired morphological response in human JNCL glia correlates with the *in vivo* findings in mice as presented here (Figure 3.1 A) and as previously reported (Pontikis et al., 2004; 2005).

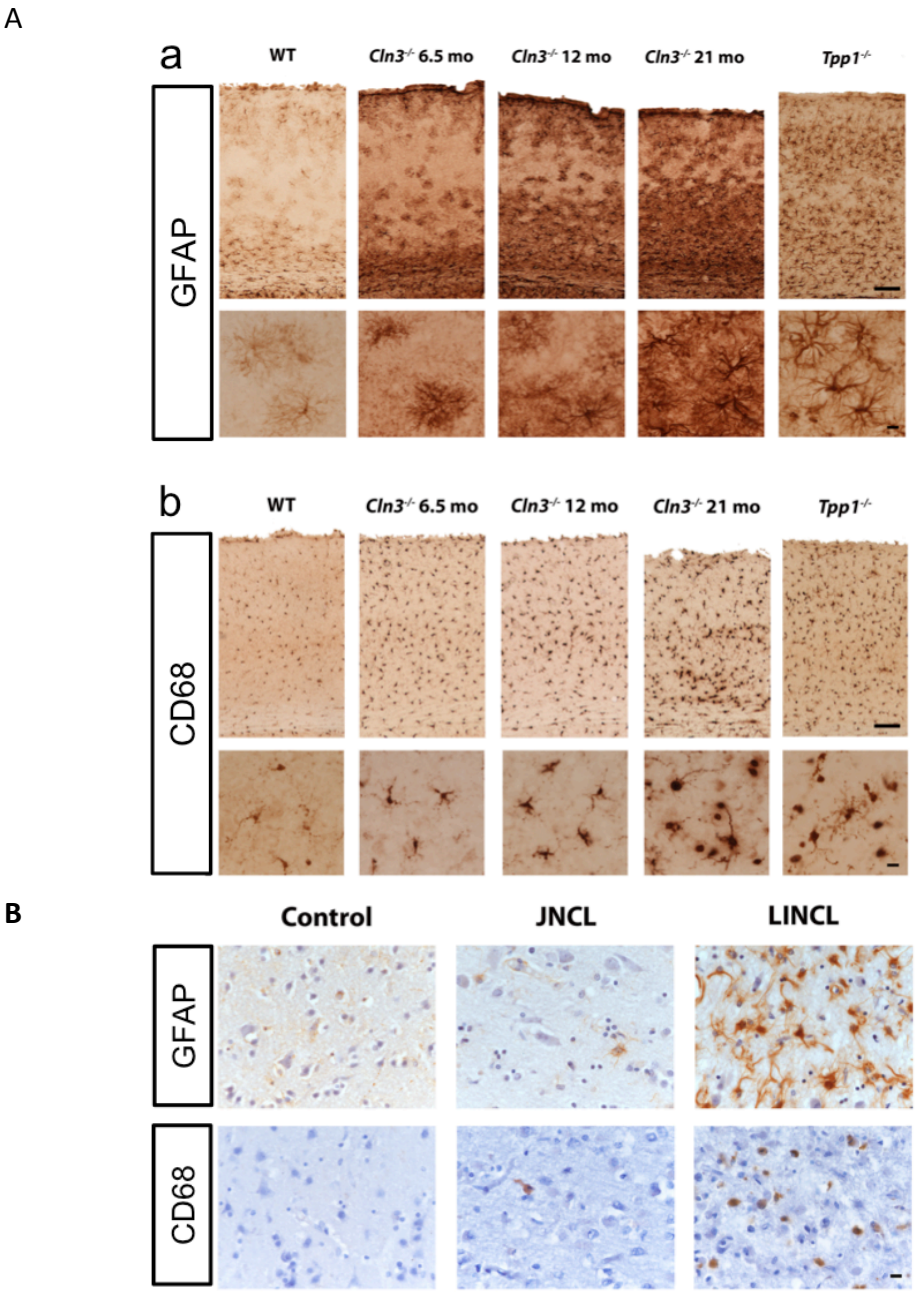

Figure 3.1. Attenuated glia response in *Cln3*$^{-/-}$ mice tissue and in human JNCL. Cortical sections from WT, *Tpp1*$^{-/-}$ and *Cln3*$^{-/-}$ mice or from control, LINCL and JNCL cases were stained with GFAP or CD68 to investigate the level of reactive astrocytosis or microglia activation, respectively. (A) A profound reactive astrocytosis (a) and microglia (b) activation was apparent in *Tpp1*$^{-/-}$ *mouse* sections, as determined by the presence of hypertrophied astrocytes with intense GFAP expression and morphologically transformed microglia; brain macrophages with round, non-process bearing cell bodies, with intense CD68 expression compared to WT mice tissue. This reactive astrocytosis and microglia activation was much less profound in *Cln3*$^{-/-}$ mice section at the early stages of the dsease (6.5, and 12 months). However, at the end stage of the disease (12 months), a complete activation of both astrocytes and microglia can be observed in *Cln3*$^{-/-}$ mice. (B) Reactive astrocytosis was observed in both human INCL and JNCL, but to different extents. In LINCL cases astrocytes were intensely stained, with hypertrophied cell bodies and numerous thickened processes. In JNCL cases GFAP staining was paler and fewer less hypertrophied astrocytes with thinner processes were evident. Also microglia activation was less profound in JNCL cases with only few CD68 positive microglia being evident. Scale bar in (A a, b) is 100µm, and (A a, b higher magnification), and (B) is 10µm.

Generation of pure astrocyte cell cultures

In order to compare the biology of *Cln3*$^{-/-}$ and wild type astrocytes, pure astrocyte cultures were generated from P1-P2 wild type or *Cln3*$^{-/-}$ cortices using a modification of the shaking method described by Mccarthy and de Vellis (1980) (McCarthy and de Vellis, 1980) (see Chapter 2, Section 2.3).

Initially, these cultures were composed of microglia, astrocytes and, occasionally, a few oligiodendrocytes. To isolate the astrocytes these mixed cultures were shaken (180rpm, 10-12 hours) as soon as they became confluent (after approximately 12-14 days). At this stage the astrocytes have formed a monolayer on the base of the culture dish, and have stopped dividing due to contact inhibition. The microglia and oligodendrocytes sit on top of the astrocytes and are easily detached by the shaking. After replacement of the medium the remaining cells, mainly astrocytes, were treated for one week with Ara-C (an anti-mitotic agent) to remove any remaining dividing microglia and oligodendrocytes. The purity of these cultures was then assessed by immunocytochemistry using CD68 to identify microglia, O4 to identify oligodendrocytes, GFAP to identify astrocytes and MAP2 together with NeuN to identify neurons (Figure 3.2 A, 3.2 B, 3.2 C). DAPI was used to identify all nuclei, as an aid to cell counting. Cells were identified as astrocytes if they expressed GFAP and/or if they did not express either CD68, 04, or any neuronal markers, because it is well established that not every astrocyte *in vitro* expresses GFAP (Cahoy et al., 2008).

Neither WT nor *Cln3*$^{-/-}$ astrocyte cultures contained MAP2/NeuN expressing neuronal cells (Figure 3.2 B). Indeed, the primary astrocyte cell cultures generated using this procedure were > 98% pure with 1% - 2% of the population being CD68^{+} microglia, and O4^{+} oligodendrocytes being rare (0.1%) (Figure 3.2 A-D). All the astrocyte cultures used in this study from here onwards have been generated and their purity checked as described here.

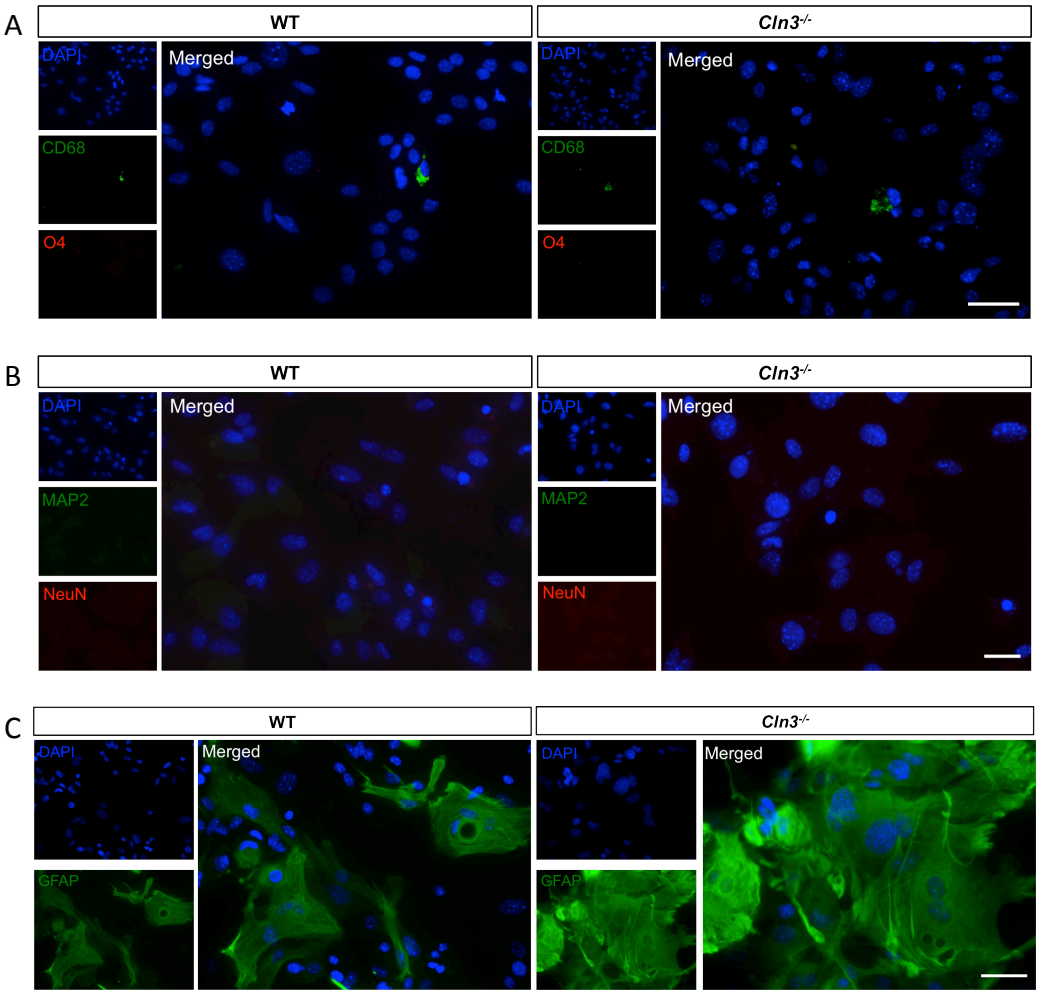

D

Mean percentage of each glial cell type ± SEM			
Sample	**% Astrocyte (GFAP$^+$, CD68$^-$, O4$^-$, MAP2$^-$, NeuN$^-$)**	**% Microglia (CD68$^+$)**	**% Oligodendrocyte (O4$^+$)**
WT	98.80±0.28	1.9±0.17	0.10±0.10
***Cln3*$^{-/-}$**	98.86±0.10	1.05±0.13	0.10±0.03

Figure 3.2. Generation of astrocyte cultures. Primary cortical astrocyte cultures generated from P1-P2 *Cln3*$^{-/-}$ or WT mice were stained with CD68 to identify microglia, O4 to identify oligodendrocytes, MAP2 together with NeuN to identify neurons and GFAP to identify astrocytes. DAPI was used to visualize all nuclei. WT and *Cln3*$^{-/-}$ astrocyte cultures contained few microglia or oligodendrocytes (A) and no neurons (B). The vast majority of cells were GFAP-expressing astrocytes (C). The percentage of each cell type was determined by counting 5 random fields per coverslip and a minimum of three coverslips per experiment. The means ± SEM shown in (D) are from three separate experiments. Scale bar in (A) and (C) is 50µm, and in (B) 20µm.

Cln3$^{-/-}$ and WT primary astrocytes respond similarly to activation *in vitro* with LPS and IFNγ

As described above, glial activation seems to be attenuated in JNCL (see Figure 3.1 (Pontikis et al., 2004; 2005). In order to investigate this response further and in a controlled manner, where *Cln3*$^{-/-}$ and WT astrocytes could be directly compared, we used a combination of the bacterial endotoxin LPS and the cytokine IFNγ to activate primary astrocytes *in vitro*. This is a commonly used activation method for astrocytes, and it has been previously demonstrated that LPS synergizes with IFNγ to produce a maximal transcriptional response in these cells (Chung and Benveniste, 1990; Bolaños et al., 1994; Schindler and Brutsaert, 1999; Gegg et al., 2005; Sheng et al., 2011; Cortés-Vieyra et al., 2012). However, before being able to study the response of *Cln3*$^{-/-}$ astrocytes to activation, we first needed to determine whether these cells retained the ability to response to this stimulus.

Toll-like receptor 4 (TLR4), which is required for LPS mediated activation of downstream signaling pathways, belongs to the IL-1R/TLR superfamily and in general is involved in the host defense against Gram-negative bacteria (O'Neill, 2000). TLR4 has also been shown to be expressed in primary astrocytes in culture (Bowman et al., 2003). Upon binding of LPS to TLR4, the receptor dimerizes and undergoes a conformational change allowing the recruitment of downstream signaling molecules and activation of downstream kinases, including the transcriptional factor NF-κB (Akira and Takeda, 2004). More precisely, NF-κB is activated after nuclear translocation and phosphorylation of the NF-κB subunits p65 and p50 (Gorina et al., 2011) (Figure 3.3 A). Subsequently, the NF-κB activation induces expression of its target genes, such as TNF-α, IL-27, IL-15, MMP-9 and VCAM-1 (Gorina et al., 2011).

IFNγ is a multifunctional cytokine that organizes a diverse array of biological responses (Boehm et al., 1997; Billiau et al., 1998). Indeed, it has been shown that astrocytes express the receptor for INFγ and can thus have a biological respond to this ligand (Rubio and de Felipe, 1991; Wang and Zhou, 2005). Upon

binding, INFY causes a conformational change in its receptor, IFNγ-R, which leads to phosphorylation and activation of Jak2 and Jak1 and recruitment of STAT1. Phosphorylation of Stat1 (P-STAT1) induces its dissociation from the receptor, which allows P-STAT1 to translocate to the nucleus where it binds to an IFNγ-activated site (GAS) element to either activate or suppress the transcription of IFNγ-regulated genes, such as ICAM-1, interferon regulatory transcription factor-2 (IRF-2), TNF-α and IFNβ (Schroder et al., 2004) (Figure 3.4 A).

To ensure that exposure to LPS plus IFNγ resulted in the transduction of an activation signal in both WT and *Cln3*$^{-/-}$ astrocytes, the nuclear localization of the phosphorylated form of NF-κB subunit P65 (P-P65) and STAT-1 (P-STAT1) was compared (see Chapter 2, Section 2.6). LPS/IFNγ stimulation is known to induce a rapid nuclear localization of the downstream activators P-P65 and P-STAT1 (Baeuerle and Henkel, 1994; Haspel et al., 1996; Wang and Baldwin, 1998), so the nuclear localization of these proteins was quantified after growth under basal conditions or after stimulation with LPS/IFNγ (1μg/ml / 100U/ml) for 15 minutes, 30 minutes, 2 hours, 6 hours and 12 hours (Figure 3.3 B and C, and Figure 3.4 B and C). The selected time points allowed the evaluation of both rapid and long-term nuclear expression of these downstream activators. The concentrations of LPS and IFNγ used in this study were selected based on previous studies (Bolaños et al., 1994; Gegg et al., 2005). At the end of the experiment cells were fixed with 4% PFA, and immunostaining carried out for P-P65 and P-STAT1 following the described protocols (see Chapter 2, Section 2.6).

Under basal conditions only a few cells had a nuclear P-P65 signal in WT (0.9±0.5%) and *Cln3*$^{-/-}$(0.9±0.7%) astrocyte cultures, indicating that there was hardly any activation of the NF-κB signaling cascade under these conditions. Upon treating WT and *Cln3*$^{-/-}$ astrocytes with LPS/IFNγ, a proportion of cells exhibit nuclear P-P65 signal (Figure 3.3 B and C). This proportion ranged from 18.9±7.1% (15 minutes) to 51.8±6.1% (2 hours) in WT astrocyte cultures, and from 29.6±8.1% (15 minutes) to 56.4±10.4% (2 hours) in *Cln3*$^{-/-}$ astrocyte cultures. However, there was no significant difference in the percentage of cells

expressing nuclear P-P65 between WT and *Cln3*$^{-/-}$ astrocytes at any of the time points tested (Figure 3.3 C). Thus, both WT and *Cln3*$^{-/-}$ astrocytes can respond to LPS treatment and the NF-κB signaling mechanism appears not to be grossly altered in *Cln3*$^{-/-}$ astrocytes.

A

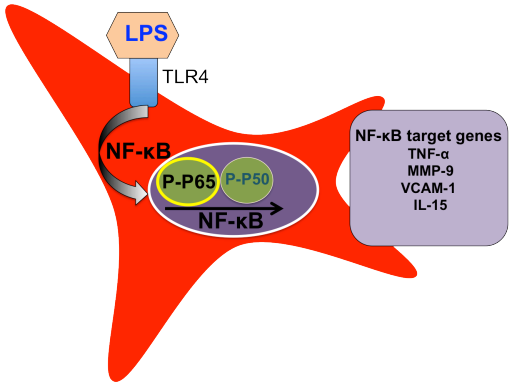

B

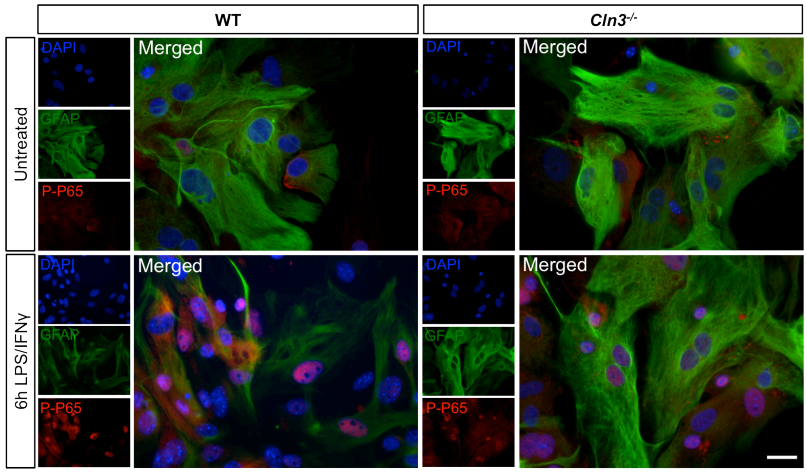

C

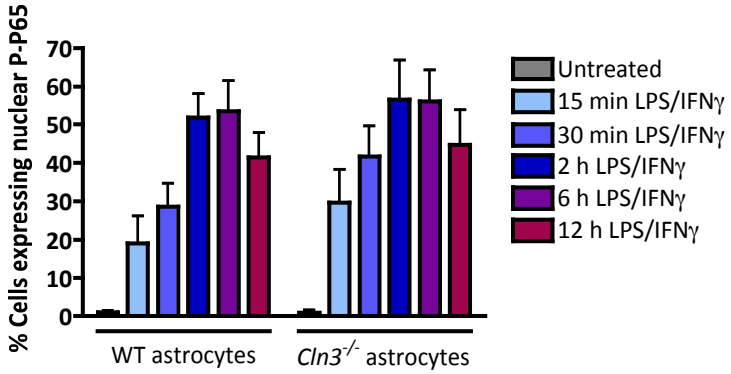

Figure 3.3. LPS induced signaling is not altered in *Cln3*$^{-/-}$ astrocytes. WT and *Cln3*$^{-/-}$ astrocytes were stained with GFAP and phospho specific P65 to identify cells where activation of NF-κB had occurred. DAPI was used to visualize all nuclei. (A) Schematic illustration of the signaling pathway induced by LPS in astrocytes. LPS activates TLR4 leading to NF-κB activation. The NF-κB transcription factor is activated after nuclear translocation of the phosphorylated forms of the Nf-κB subunits P65 and P50, followed by induction of NF-κB target genes, such as TNF-a, IL-15, MMP-9, and VCAM-1. (B) Few WT or *Cln3*$^{-/-}$ astrocytes with nuclear-located P-P65 were observed under basal conditions, while many WT and *Cln3*$^{-/-}$ astrocytes had P-P65 expressed in the nucleus upon exposure to LPS. (C) The percentage of cells expressing P-P65 in the nucleus was determined by counting 5 random fields per coverslip and a minimum of three coverslips per experiment. The means ±SEM shown in (C) are from three separate experiments. Scale bar in (B) is 20µm.

The activation of the JAK-STAT1 pathway in both WT and *Cln3*$^{-/-}$ astrocytes was studied by staining untreated or LPS/INFγ treated cultures with an antibody against P-STAT1 (Figure 3.4 B), and the percentage of cells expressing nuclear P-STAT1 quantified (Figure 3.4 C). There were no cells with a nuclear P-STAT1 signal in untreated WT and *Cln3*$^{-/-}$ cultures (Figure 3.4 C). However, upon treating WT and *Cln3*$^{-/-}$ astrocytes with LPS/IFNγ, a large proportion of cells exhibit a nuclear P-STAT1 signal (Figure 3.4 B and C). This proportion ranged from 86.7±17.4% (15 minutes) to 92.0±16.7% (2 hours) in WT astrocyte cultures, and from 89.1±23.0% (15 minutes) to 88.3±17.0% (2 hours) in *Cln3*$^{-/-}$ astrocyte cultures. Again there was no significant difference in the proportion of cells expressing P-STAT1 between WT and *Cln3*$^{-/-}$ astrocyte cultures. Thus, this JAK-STAT1 signaling cascade is activated upon LPS/INFγ exposure in both WT and *Cln3*$^{-/-}$ astrocytes. Based on these studies we consider that LPS/INFγ can be used to study whether there are any biological differences in the response of WT and *Cln3*$^{-/-}$ astrocytes to activation.

A

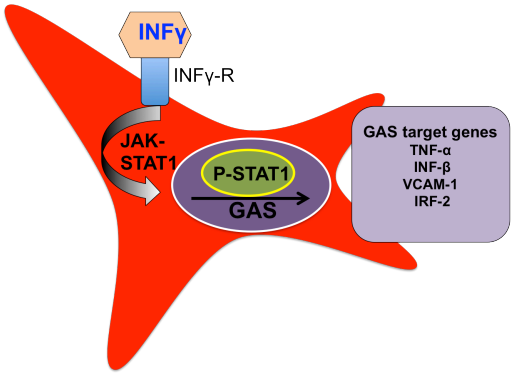

B

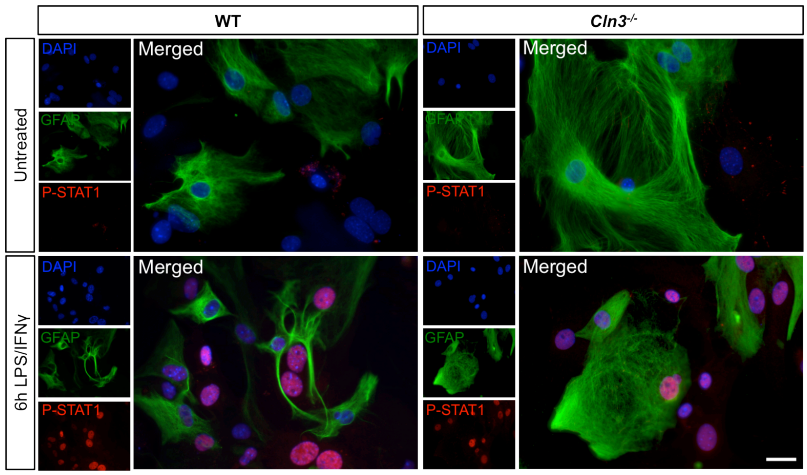

C

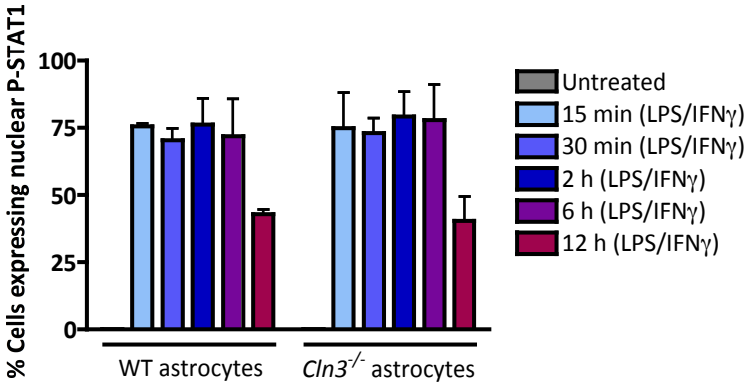

Figure 3.4. INFγ induced signaling is not altered in *Cln3*$^{-/-}$ astrocytes. WT and *Cln3*$^{-/-}$ astrocytes were stained with GFAP and phospho specific STAT1 to identify cells where the JAK-STAT1 pathway had been activated. DAPI was used to visualize all nuclei. (A) Schematic illustration of the signaling pathway induced by INFγ in astrocytes. INFγ activates INF-R causing a conformational change in the IFNγ-R, and activation of the JAK-STAT1 pathway: phosphorylation of STAT1 (P-STAT1) and dissociation of STAT1 from the IFNγ-R allowing it to translocate to the nucleus where it binds to the promoter of IFNγ-regulated activation sites (GAS) to either activate or suppress transcription of IFNγ-regulated genes, such as ICAM-1, IRF-2, TNF-α and IFNβ. (B) No WT and *Cln3*$^{-/-}$ astrocytes with nuclear P-STAT1 were observed under basal conditions, however the vast majority of these astrocytes had a nuclear P-STAT1 signal upon exposure to INFγ. (C) The percentage of cells expressing P-STAT1 in the nucleus was determined by counting 5 random fields per coverslip and a minimum of three coverslips per experiment. There was no difference between WT and *Cln3*$^{-/-}$ in their response to INFγ. The means ±SEM shown in (C) are from three separate experiments. Scale bar in (B) is 20µm.

Expression of intermediate filaments is altered in *Cln3*$^{-/-}$ astrocytes cultured under basal conditions and after activation with LPS/INFγ

Under pathological conditions, astrocytes undergo various changes, including upregulation of genes encoding the IF proteins, GFAP, Vimentin and Nestin (Mucke and Eddleston, 1993). Intriguingly, these changes, particularly in GFAP expression, appear attenuated in both *Cln3*$^{-/-}$ mice and in human JNCL patient tissue, as described previously (Figures 3.1 A and B). To further explore changes in intermediate filament proteins following stimulation in WT and *Cln3*$^{-/-}$ astrocytes, the expression levels of GFAP, nestin and vimentin was quantified from cell lysates derived from untreated and LPS/IFNγ treated (24 hours and 48 hours) astrocyte cultures using Western blotting (see Chapter 2, Section 2.7).

Astrocyte cultures were generated as described before, and then passaged onto 6-well plates. Approximately 24 hours after plating the medium was replaced with fresh medium, to which LPS/IFNγ was added to activate the astrocytes. Control cultures received no LPS/IFNγ. After 24 hours or 48 hours the cells were lysed and the BCA (bicinchoninic acid) protein quantification kit (Thermo Scientific) used to quantify the total amount of protein in each sample prior to loading equal amounts of protein (20µg) per sample onto a 12% SDS-PAGE gel. The expression levels of each intermediate filament protein in samples treated with LPS/IFNγ were normalized to expression levels in untreated samples.

No significant differences were detected in the expression levels of GFAP after 24 hours LPS/IFNγ treatment compared to untreated samples in neither WT (15±20.3% increase) nor in *Cln3*$^{-/-}$ astrocytes (9.2±28.4% decrease) (Figure 3.5 A). GFAP expression was however significantly upregulated (23.8±3.6% increase) in WT astrocytes after 48 hours of LPS/IFNγ treatment compared to controls (Figure 3.5 A). In *Cln3*$^{-/-}$ astrocytes such an upregulation of GFAP did not occur (5.0±17.4% increase in LPS/IFNγ treated versus untreated samples, Figure 3.5 A). Unlike GFAP, Nestin (Figure 3.5 B) and vimentin (Figure 3.5 C) expression were not significantly altered in LPS/IFNγ treated WT or *Cln3*$^{-/-}$ astrocytes after 24 hours or 48 hours when compared to untreated samples.

These results indicate that WT astrocytes respond to activation with LPS/IFNγ by upregulating expression of GFAP, just like astrocytes do *in vivo*, whereas *Cln3*$^{-/-}$ astrocytes appeared to be less capable of such an upregulation. Neither genotype responded to LPS/IFNγ treatment by upregulating vimentin or nestin. Based on these results, the activation process is attenuated in *Cln3*$^{-/-}$ astrocytes *in vitro*, which is in agreement with the *in vivo* and post-mortem findings described above (Figure 3.1). However, since quantification of housekeeping proteins was not conducted in this study, additional work is required to verify these results.

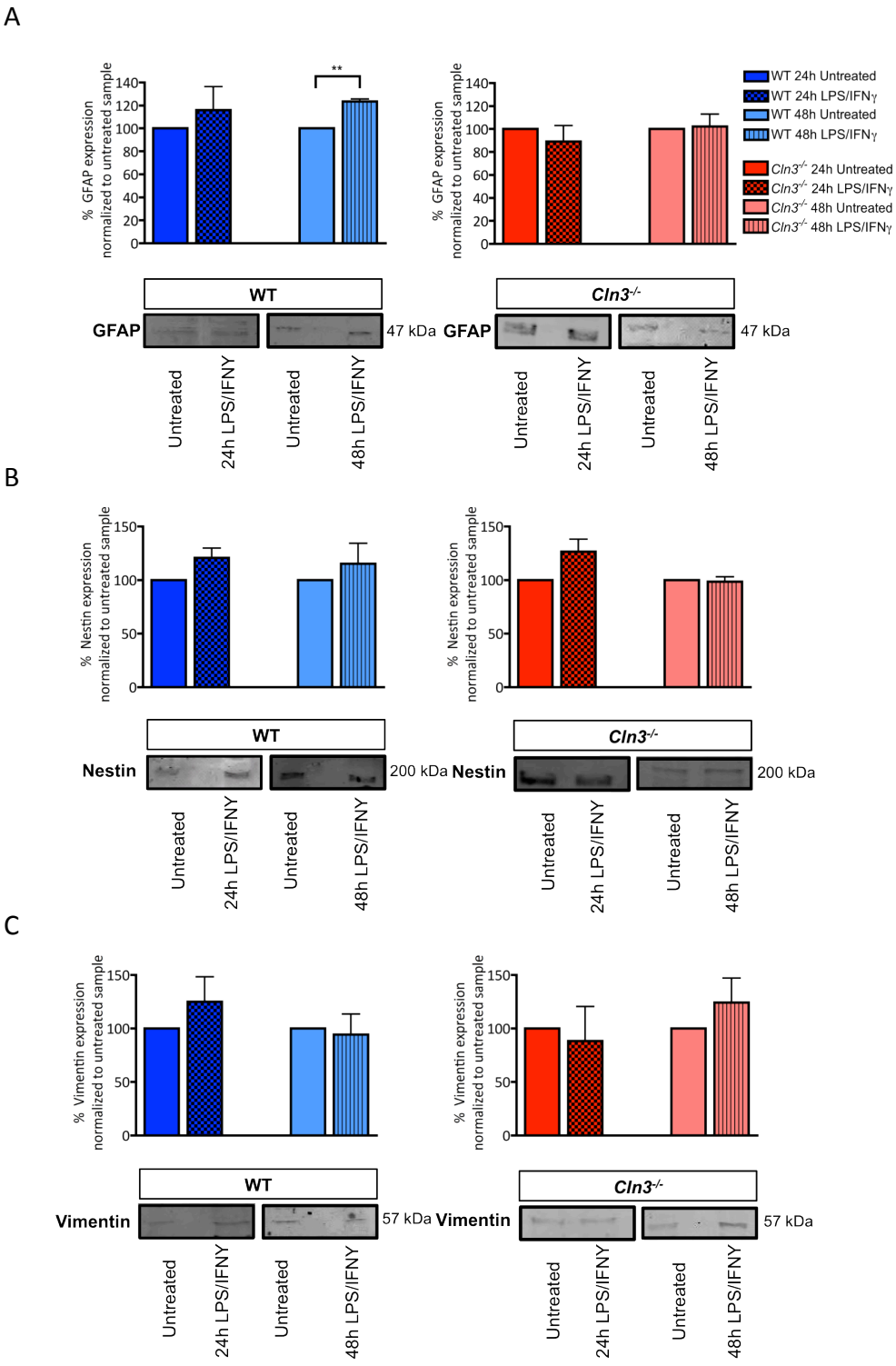

Figure 3.5. Lack of GFAP upregulation in *Cln3*$^{-/-}$ astrocytes. WT and *Cln3*$^{-/-}$ astrocyte were plated onto 6-well plates, some cultures were activated for 24 hours or 48 hours with LPS/IFNγ, others received no treatment. Cultures were lysed and equal amounts of protein (20ug) per sample were loaded onto a 12% SDS-PAGE gel. After Western blotting the expression levels of intermediate filament proteins were quantified and the levels from samples treated with LPS/IFNγ were compared to those from untreated samples. (A) GFAP expression was upregulated in WT but not in *Cln3*$^{-/-}$ LPS/IFNγ treated cultures. (B) Nestin and (c) vimentin expression did not significantly change in WT or *Cln3*$^{-/-}$ astrocytes under any conditions tested. Results are from n=3 experiments.

The levels of intermediate filament expression in WT and *Cln3*$^{-/-}$ astrocytes, under the same experimental conditions as above, were compared to examine whether there was any difference between their expression levels between these two genotypes. Untreated *Cln3*$^{-/-}$ astrocytes expressed more GFAP protein compared to WT astrocytes after 24 hours (50.0±21.4% increase) and this difference reached significance after 48 hours (121.5±54.8% increase) (Figure 3.6 A). Under LPS/IFNγ exposure, GFAP expression levels were higher in *Cln3*$^{-/-}$ astrocytes compared to WT counterparts after 24 hours of treatment (47.1±15.6%) and after 48 hours of treatment (18.7±35.3%), but these differences were not statistically significant (Figure 3.6 A). Interestingly, the level of nestin was significantly lower in untreated *Cln3*$^{-/-}$ astrocytes compared to WT after 24 hours (25.3±1.5% reduction) and after 48 hours (42.6±15.6% reduction). However, there was no clear difference in nestin expression between *Cln3*$^{-/-}$ *and* WT astrocytes in LPS/IFNγ treated samples (Figure 3.6 B). Vimentin expression was slightly higher in untreated *Cln3*$^{-/-}$ astrocytes after 24 hours (36.6±22.5% increase) when compared to WT samples, and slightly reduced after 48 hours (15.0±32.4% decrease), but these differences were not statistically significant. Again, after LPS/IFNγ treatment, vimentin expression levels were very similar in both genotypes (Figure 3.6 C). Thus, the *Cln3*$^{-/-}$ astrocytes have significantly more intracellular GFAP, and significantly less nestin under untreated conditions than do WT astrocytes. This may suggest that *Cln3*$^{-/-}$ astrocytes have a more activated (higher GFAP expression), but less immature (lower nestin expression) phenotype than WT astrocytes under resting conditions.

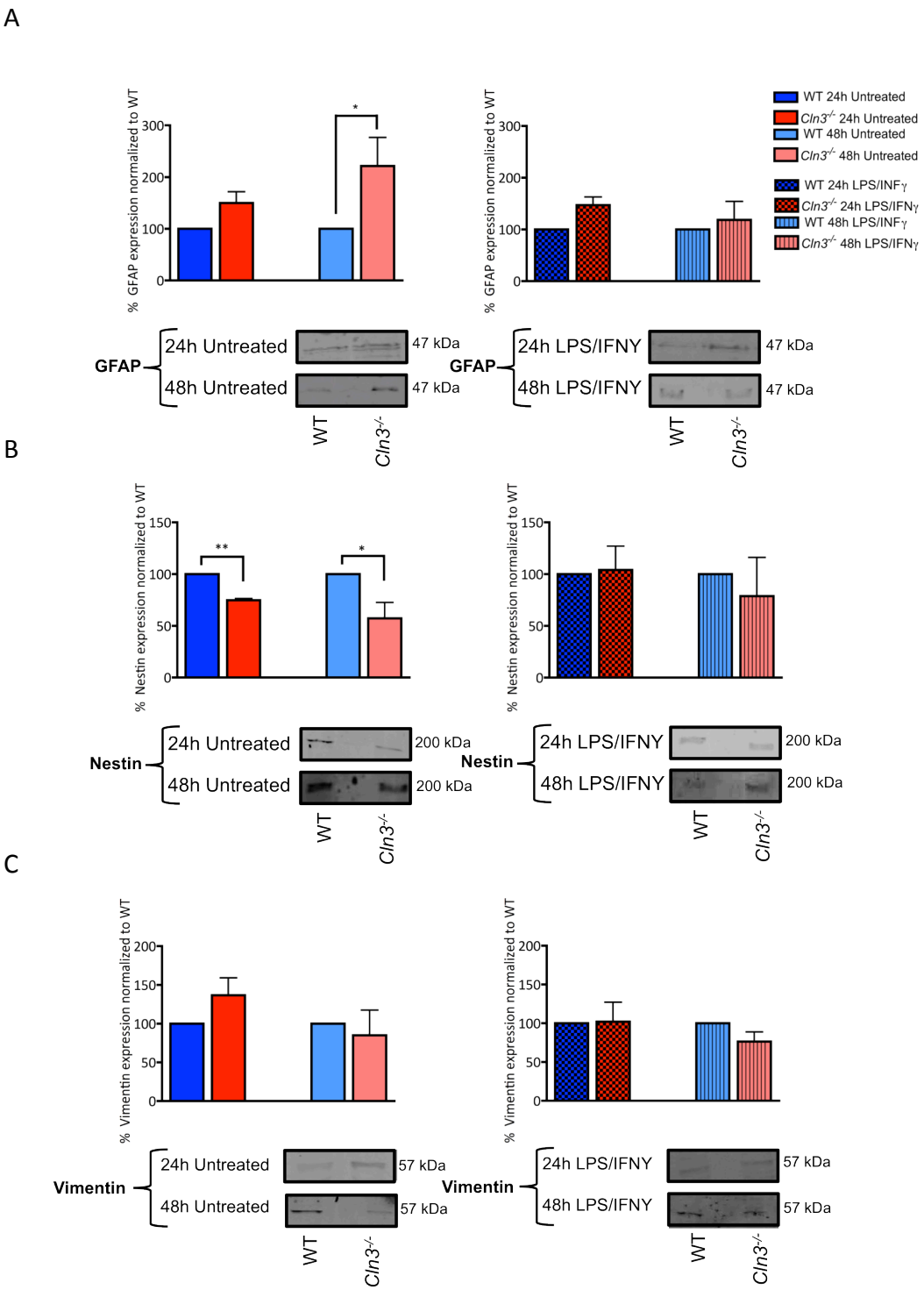

Figure 3.6. *Cln3*$^{-/-}$ astrocytes express more GFAP and less nestin under basal conditions. The expression levels of intermediate filaments were quantified in untreated and LPS/IFNγ treated samples after 24 hours and 48 hours and the levels expressed by WT and *Cln3*$^{-/-}$ astrocyte compared. (A) GFAP expression was upregulated in untreated *Cln3*$^{-/-}$ samples compared to WT. (B) Nestin expression was downregulated in untreated *Cln3*$^{-/-}$ samples compared to WT. (C) Vimentin expression did not significantly differ between untreated or treated WT and *Cln3*$^{-/-}$ astrocytes. Results are from n=3 experiments.

Cln3$^{-/-}$ astrocytes have disrupted intermediate filament and actin cytoskeleton organization, but show normal α- and β- microtubular organization

Cytoskeletal elements, actin microfilaments, microtubules and intermediate filaments, form a dynamic network within astrocytes, that is vital for their function under both physiological and pathological conditions (Cotrina et al., 1998; Pekny and Pekna, 2004; Potokar et al., 2007; Sofroniew and Vinters, 2010) (see Chapter 1, Sections 1.3 and 1.4). Various studies have suggested that CLN3 is either directly or indirectly connected with a number of cytoskeletal elements and that CLN3 deficiency may result in cytoskeleton related dysfunction in these cells. For example, via myosin-IIB interaction, CLN3 may be involved in cell migration via actin-based cytoskeleton re-organization (Getty and Pearce, 2011; Getty et al., 2011; reviewed in Mole et al., 2011).

In order to explore whether the cytoskeleton within *Cln3*$^{-/-}$ astrocytes had been altered, WT and *Cln3*$^{-/-}$ astrocyte cultures were labeled using antibodies that recognize GFAP to identify the major intermediate filament in these cells, and antibodies against α- and β-tubulin to identify microtubules (see Chapter 2, Section 2.6). Phalloidin was used to visualize F-actin filaments (Figure 3.7).

The intermediate filament organization of GFAP expressing *Cln3*$^{-/-}$ astrocytes was highly disrupted, appearing disorganized and lacking a fine fibrous appearance (Figure 3.7, see arrow heads in b). In contrast, the intermediate filament organization looked highly structured in WT astrocytes (Figure 3.7, see arrows in a). In addition, GFAP expressing *Cln3*$^{-/-}$ astrocytes appeared to have a larger cell body than GFAP expressing WT astrocytes (this difference in soma size was evident with all cytoskeletal components – compare a to b, c to d, e to f, and g to h). Quantitative measurements of soma size confirmed this observation (see Figure 3.8). Furthermore, most WT astrocytes displayed a highly ordered and well-defined F-actin filament organization (examples marker with arrows), whereas the F-actin filaments, as seen with GFAP expressing intermediate filaments, appeared less defined and were highly disorganized in *Cln3*$^{-/-}$ astrocytes (Figure 3.7, – compare c to d, examples marked with arrow heads).

Indeed, most *Cln3*$^{-/-}$ astrocytes lacked the presence of F-actin filaments that spanned the cell body, a feature common for WT astrocytes cultured under these untreated, basal conditions (Figure 3.7 – compare c to d). However, the α- and β-microtubular organization of WT and *Cln3*$^{-/-}$ astrocytes appeared similar (Figure 3.7 – compare e to f and g to h, examples marker with arrows). In conclusion, enlarged *Cln3*$^{-/-}$ astrocytes have an abnormally organized actin and intermediate filament cytoskeleton, but have an apparently normal organization of microtubules.

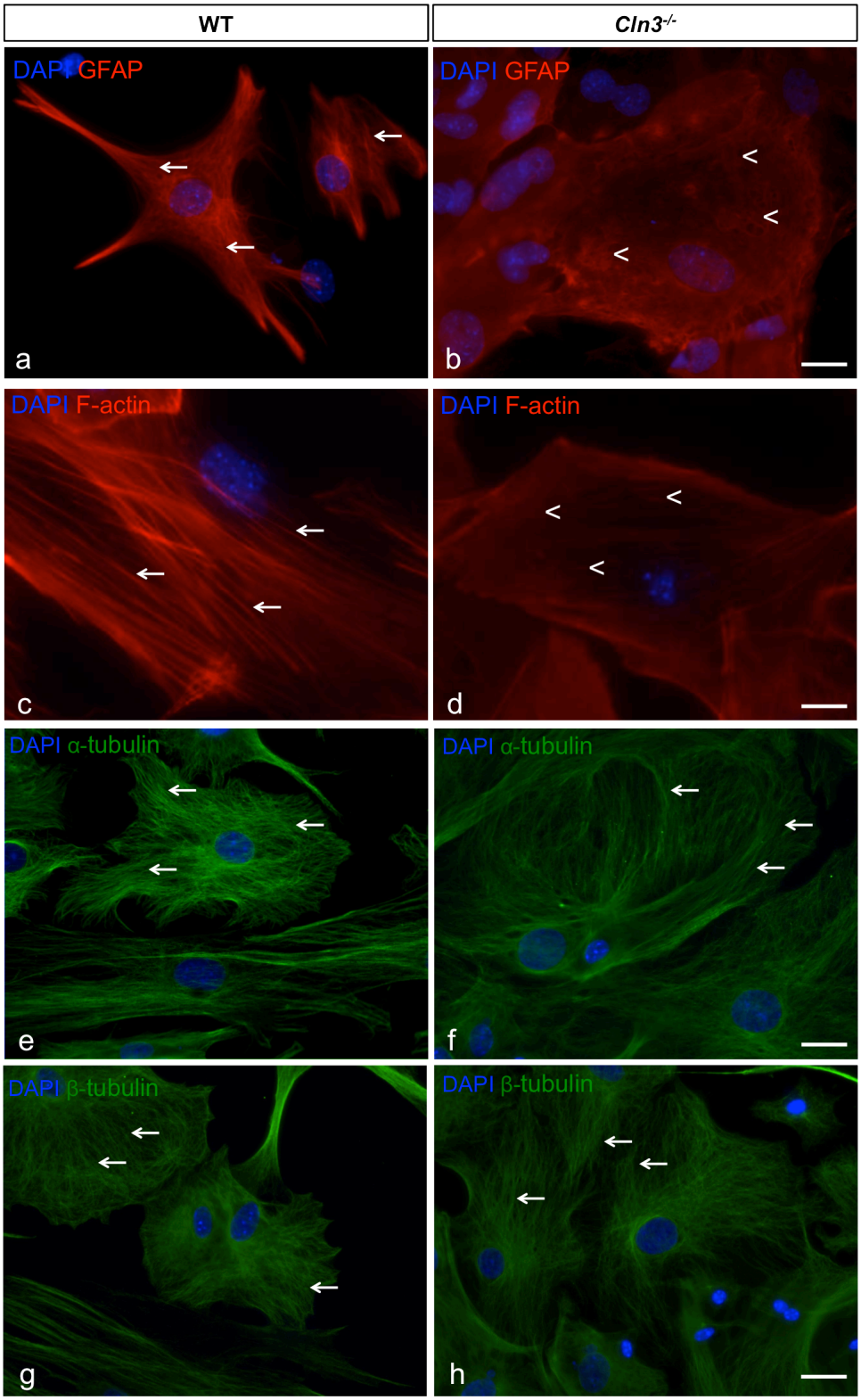

Figure 3.7. *Cln3*$^{-/-}$ astrocytes have a disrupted cytoskeleton. To investigate their cytoskeletal organization and morphology, WT and *Cln3*$^{-/-}$ astrocytes were stained with GFAP to visualize intermediate filaments, phalloidin to visualize F-actin, and α- or β-tubulin to visualize microtubules. DAPI was used to visualize all nuclei. WT astrocytes had a well organized intermediate filament, F-actin and microtubule cytoskeleton (arrows), while *Cln3*$^{-/-}$ astrocytes had a highly disrupted intermediate filament and F-actin cytoskeleton (arrow heads) but their microtubule structure appeared normal (arrow). The cell body size of *Cln3*$^{-/-}$ astrocytes appeared larger that of WT astrocytes. Scale bar is 25µm.

Morphological response to LPS/IFNγ is attenuated in *Cln3*$^{-/-}$ astrocytes

As well as up-regulating cytoskeletal proteins, astrocytes respond to activation by changing morphologically. Upon activation, cultured WT astrocytes change from flat, polygonal cells to smaller, contracted and highly branched cells (Levison et al., 1998). As described above, this process appears attenuated *in vivo* in *Cln3*$^{-/-}$ mice and in JNCL patients (see Figure 3.1). To determine whether this is also the case *in vitro*, the morphology of WT and *Cln3*$^{-/-}$ astrocytes were compared under basal and stimulation conditions (LPS/INFγ treatment for 24 hours or 48 hours, see Chapter 2, Section 2.6). Staining with GFAP was used to reveal the morphology of these cells. As described above, the untreated *Cln3*$^{-/-}$ astrocytes had a strikingly different morphology when compared with WT astrocytes; they appeared to be bigger and flatter with a disorganized cytoskeleton (Figure 3.8 A – compare a to b). Upon stimulation, WT astrocytes had already begun to transform morphologically after 24 hours exposure to LPS/INFγ; changing from broad, non-process-bearing flat cells, to have a shrunken soma and multiple processes (see arrow heads in Figure 3.8 A, image c). These characteristic morphological changes became more apparent with prolonged LPS/LPSγ exposure (Figure 3.8, image e). In contrast, no significant morphological transformation of *Cln3*$^{-/-}$ astrocytes could be detected until 48 hours of exposure to LPS/INFγ, when their soma size decreased and some cells extended more processes (Figure 3.8 A, images d and f). In order to quantify this morphological transformation we decided to compare the soma size of WT and *Cln3*$^{-/-}$ astrocytes under basal conditions and after stimulation. This was carried out using ImageJ by drawing a line around the borders of a GFAP expressing cell soma and allowing the program to measure the enclosed area (Figure 3.8 B). After LPS/IFNγ activation for 24 hours or 48 hours, the cell soma of WT astrocytes reduced in size. This reduction was statistically significant after 24 hours (30.5±3.3% decrease), but did not reach statistical significance after 48 hours, most likely due to smaller body size of untreated WT astrocytes at this timepoint, due to the prolonged period that these cells had been kept in culture (21.1±5.1% decrease). As noted in Figures 3.2 and 3.7 above, and confirmed here, *Cln3*$^{-/-}$ astrocytes have significantly bigger cell bodies that WT astrocytes

under basal conditions (84.3±15.8% increase) (Figure 3.8 C and A – compare a to b). After 24 hours of LPS/IFNγ treatment the soma size of *Cln3*$^{-/-}$ astrocytes remains unchanged (Figure 3.8 C, and A – compare b to d). However, after a 48 hours exposure to LPS/INFγ, *Cln3*$^{-/-}$ astrocytes also start to change their soma size, and there was no significant difference in size when compared to WT astrocyte soma at this time point (Figure 3.8 C, and A – compare e to f).

These results suggested that cultured *Cln3*$^{-/-}$ astrocytes have an attenuated ability to change their morphology upon activation, only undergoing a morphological transformation after a prolonged exposure to stimuli. Moreover, *Cln3*$^{-/-}$ astrocytes also have enlarged cell bodies under basal conditions. The abnormal actin and intermediate cytoskeletal organization in *Cln3*$^{-/-}$ astrocytes (see Figure 3.7) could partly cause their altered morphological appearance and slower morphological transformation.

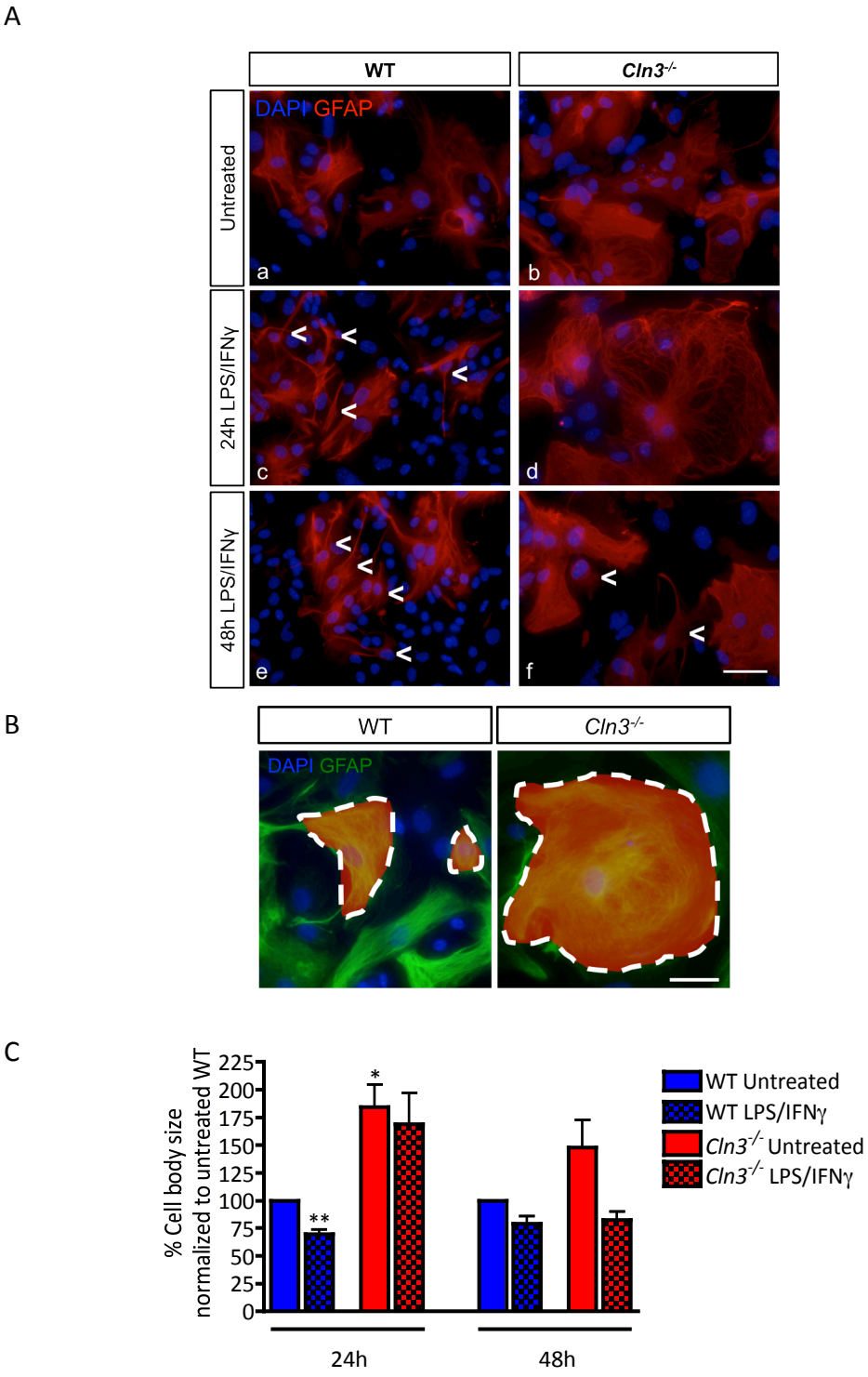

Figure 3.8. Attenuated morphological transformation of *Cln3*$^{-/-}$ astrocytes. WT and *Cln3*$^{-/-}$ astrocyte were treated with LPS/IFNγ for 24 hours or 48 hours. Untreated cells were grown under basal conditions. Following activation, cells were stained with GFAP, to visualize morphological changes and DAPI was used to visualize all nuclei. (A) WT astrocytes changed their morphology dramatically after a 24 hours exposure to LPS/INFγ and these changes become more enhanced over time. In general *Cln3*$^{-/-}$ astrocytes remain morphologically unchanged after 24 hours of stimulation, but showed changes after 48 hours activation. (B) ImageJ was used to quantify the cell some size across all these experimental conditions. (C) Cell soma sizes were determined by quantifying 10 random fields per coverslip and a minimum of two coverslips per experiment. The mean±SEM is from three separate experiments. Scale bar is 50µm.

WT astrocytes proliferate more actively than *Cln3*$^{-/-}$ astrocytes

The issue of astrocyte proliferation in the diseased brain is still highly controversial. In healthy CNS tissue, astrocytes do not actively proliferate, indeed the majority of them appear to be post-mitotic (Bush et al., 1999; Colodner et al., 2005; Horner et al., 2000; Norton et al., 1992). According to our current understanding, there is no astrocyte proliferation under conditions where reactive astrocytosis is moderate, or mild (Sofroniew, 2009; Sofroniew and Vinters, 2010). However, astrocytes may become proliferative in more severe conditions, such as in severe focal lesions, infections or areas suffering from chronic neurodegeneration (Lindholm et al., 1992; Norton et al., 1992; Satoh et al., 1996; Bush et al., 1999; Horner et al., 2000; Colodner et al., 2005; Gadea et al., 2008; Carlén et al., 2009). Therefore, the ability of *Cln3*$^{-/-}$ astrocytes to proliferate *in vitro* was tested under both basal and activated conditions.

To investigate the proliferation of WT and *Cln3*$^{-/-}$ astrocytes, these cells were exposed to LPS/INFγ for 24 hours or 48 hours, and were given a 6 hours pulse of BrdU, that will be incorporated into cells that go though S-phase during this time period (see Chapter 2, Section 2.4). Subsequently cells were fixed and analyzed for BrdU incorporation and the expression of Ki67, which labels cells in any active phase of the cell cycle (G1, S phase and G2, but not in G0) (Figure 3.9 A and B).

Under basal conditions the percentages of dividing astrocytes (%Ki67) in WT cultures were 8.3±5.6% (24 hours) and 18.0±2.3% (48 hours) (Figure 3.9 C). Upon stimulation this percentage increased to 24.7±6.0% (24 hours) and 23.8±6.7% (48 hours). As such, activation for 24 or 48 hours did not significantly increase the number of dividing cells within WT cultures (Figure 3.9 Compare A to B and C). Neither did the percentage of WT astrocytes that went through S phase (labeled with BrdU) during the last 6 hours of culture increase significantly upon LPS/IFNγ treatment (Figure 3.9 Compare A to B and C). Similarly, the percentage of Ki67^{+} or BrdU^{+} cells observed in *Cln3*$^{-/-}$ astrocyte cultures did not change significantly in response to LPS/IFNγ treatment (Figure 3.9 Compare A to B and C). However, the percentage of Ki67^{+} astrocytes in *Cln3*$^{-/-}$ cultures was always less, under basal

conditions and upon LPS/IFNγ treatment, than that seen in WT astrocyte cultures, although this difference was not statistically significant. In contrast, the percentage of astrocytes that went through S phase ($BrdU^+$) in a 6 hours period in *Cln3*$^{-/-}$ cultures was significantly lower under untreated conditions at 24 hours and 48 hours (%BrdU labeled astrocytes was 67.8±7.9% (24h untreated) and 68.5±10.9% (48h untreated) lower in *Cln3*$^{-/-}$ cultures compared with WT astrocytes). The percentage of BrdU labeled cells in *Cln3*$^{-/-}$ astrocyte cultures was also lower compared to WT after stimulation, but these differences were not statistically different. Calculating the labeling index (%BrdU/Ki67, Figure 3.9 C) to determine whether their overall pattern of proliferation is perturbed revealed no significant difference between WT and *Cln3*$^{-/-}$ astrocyte cultures under any condition analyzed (Figure 3.9 C).

Taken together, these data suggest that under resting conditions only very few astrocytes are dividing, and LPS/IFNγ based stimulation does not change this significantly in cultures from either genotype. However, the rate of division of *Cln3*$^{-/-}$ astrocytes appeared to be slower, as indicated by a lower percentage of BrdU expressing cells, particularly under resting conditions.

A

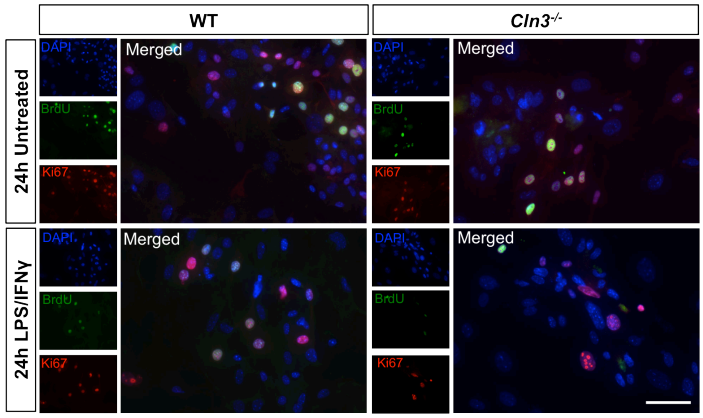

B

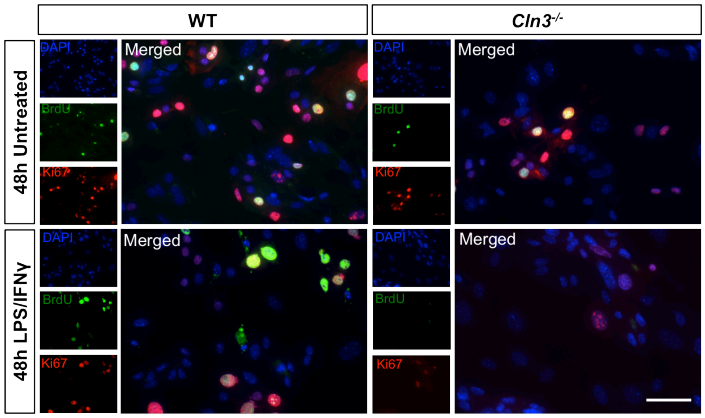

C

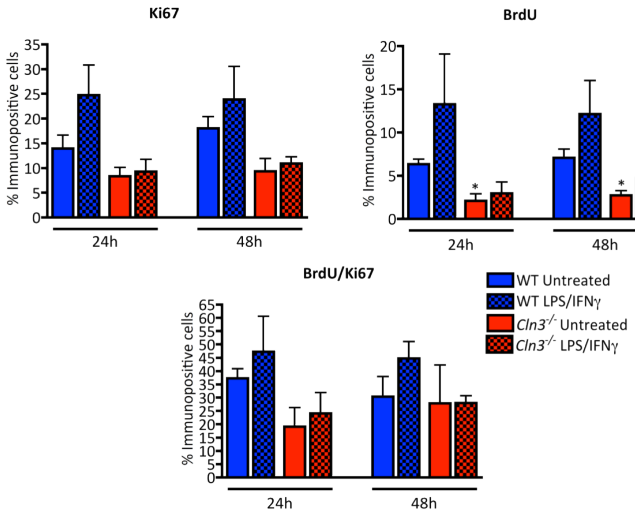

Figure 3.9. Proliferation of *Cln3*$^{-/-}$ astrocytes is attenuated. WT and *Cln3*$^{-/-}$ astrocyte cultures were activated with LPS/IFNγ for 24 hours or 48 hours. Untreated cells were kept under basal conditions. Cultures were treated with BrdU for 6h, then fixed and analyzed for the expression of BrdU and Ki67. DAPI was used to visualize nuclei. (A) Shows a representative field of BrdU and Ki67 positive cells from treated and untreated WT or *Cln3*$^{-/-}$ astrocyte cultures after 24 hours, and 48 hours (B). (C) Percentage of Ki67, BrdU and BrdU/Ki67 expressing cells in treated and untreated WT and *Cln3*$^{-/-}$ astrocyte cultures. Results expressed as mean percentages±SEM were generated by counting 5 random fields per coverslip and three coverslips per experiment. Experiment was repeated four times. Scale bar is 50 µm.

No accumulation of autofluorescent storage material occurs within cultured WT or *Cln3*$^{-/-}$ astrocytes

One of the main pathological features of lysosomal storage disorders is a striking accumulation of autofluorescent storage material mainly within cells in the CNS and less so throughout the rest of body of the affected individual. In JNCL autofluorescent ceroid lipofuscin deposits enriched in subunit c of the mitochondrial ATP synthase complex accumulate within autolysosomes (Palmer et al., 1992). According to recent evidence there is no direct connection between accumulation of storage material and neuron loss in NCLs (Cooper et al., 2006; Griffey et al., 2006). Nevertheless, since such deposits are a hallmark of this disease, we investigated whether such autofluorescent storage material was visible within the cortex of *Cln3*$^{-/-}$ mice as well as cultured *Cln3*$^{-/-}$ astrocytes.

Cortical tissue derived from WT and *Cln3*$^{-/-}$ mice was used to examine accumulation of autofluorescent storage material (Figure 3.10 A, pictures provided by Andrew Wong). Compared to WT cortical tissue a clear increase in autofluorescent storage material could be seen in *Cln3*$^{-/-}$ mouse tissue exposed to a 488nm wavelength. Three different wavelengths, 488nm, 546nm and 633nm, were used to visualize the accumulation of any autofluoresecent storage material within cultured astrocytes. Neither WT nor *Cln3*$^{-/-}$ astrocytes displayed autofluorescence (Figure 3.10 B). This could be due to the relatively short period of time these *Cln3*$^{-/-}$ astrocytes had been grown in culture. However, *Cln3*$^{-/-}$ astrocytes have a highly compromised biology as presented above, and in Chapter 4, supporting the observations that the build-up of this material is not the primary cause for the astrocyte defects observed.

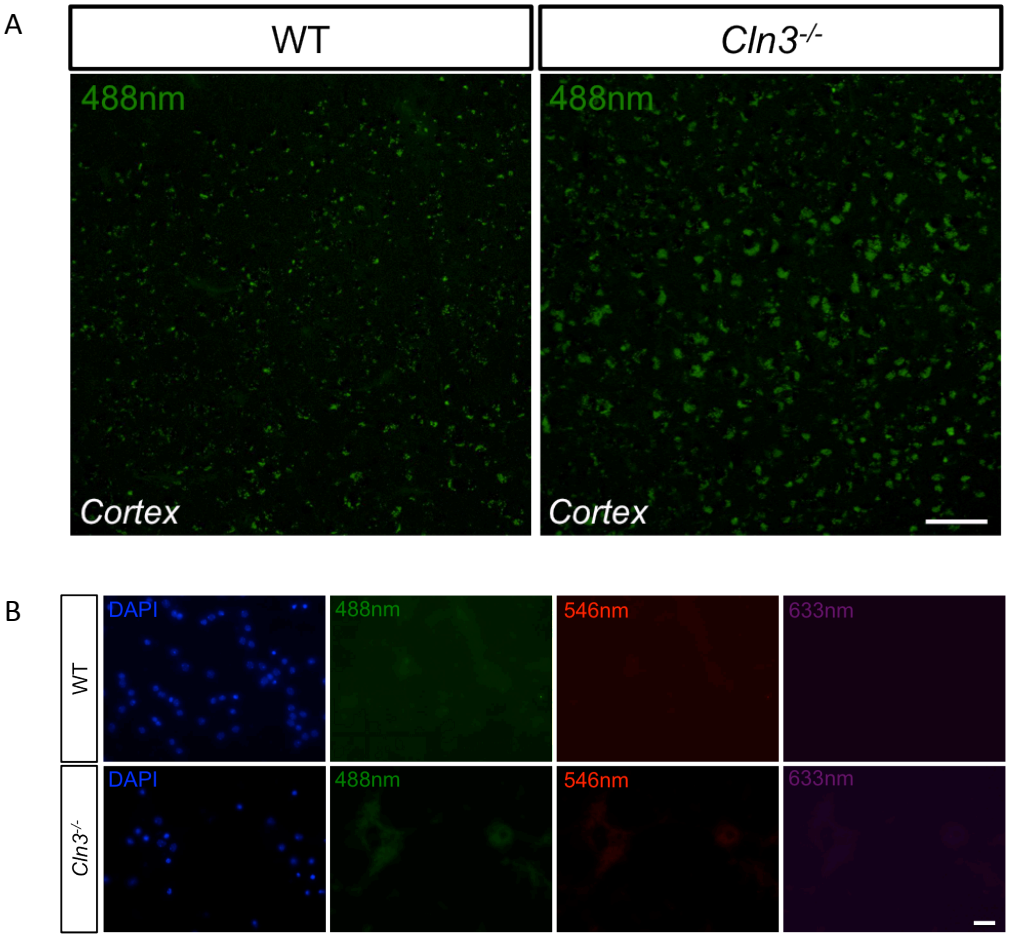

Figure 3.10. No accumulation of autofluorescent storage material within *Cln3*$^{-/-}$ astrocytes. (A) Cortical tissue derived from WT and *Cln3*$^{-/-}$ mice were used to investigate the accumulation of autofluorescent storage material *in vivo* when exposed to one wavelength, 488nm. More autofluorescent material was evident in *Cln3*$^{-/-}$ than in WT cortical tissue. (B) The accumulation of autofluorescent storage material was analysed in primary cortical WT and *Cln3*$^{-/-}$ astrocyte cultures. Cells were exposed to three particular wavelengths, 488nm, 546nm and 633nm, to visualize any autofluorescent material within cells and DAPI was used to visualize all nuclei. Neither WT nor *Cln3*$^{-/-}$ astrocytes showed accumulation of any autofluorescent storage material within their cell bodies. Scale bar in (A) is 50µm and in (B) scale bar in 20µm.

CLN3 is expressed within the endo/lysosomal compartment (Fossale et al., 2004; Kyttälä et al., 2005; Phillips et al., 2005; Uusi-Rauva et al., 2008; 2012), but the functioning of CLN3 within this compartment is not well understood (see Chapter 1, Section 1.2). Thus, our next step using these astrocyte cultures was to look at the organization of the endo/lysosomal system.

Cln3$^{-/-}$ astrocytes have an altered late endo-lysosomal associated protein expression pattern

Lysosomes are very dynamic organelles and their intracellular localization may vary. For example an acidic intracellular pH causes a redistribution of lysosomes from their predominantly perinuclear location into the cytosol, also nutrients have been shown to alter lysosomal positioning in the cell (Korolchuk and Rubinsztein, 2011; Korolchuk et al., 2011). Under normal physiological conditions, lysosomes are maintained in the perinuclear region by mictotubule-associated motors (Jordens et al., 2001). We therefore decided to study whether loss of CLN3 altered late endosomal/lysosomal distribution within astrocytes by studying the expression of cathepsin D and LAMP1. Cathepsin D, which is a lysosomal aspartyl protease, was detected using an antibody that recognizes both the processed cathepsin D isoform present in lysosomes, and the unprocessed precursor forms present in the Trans-Golgi network, and endo-lysosomal pathway. The LAMP1 antibody used is typically considered to detect protein expressed on the lysosomal membrane, or in late endosomes or pre-lysosomes (Reggio et al., 1984; Chen et al., 1985; Lippincott-Schwartz and Fambrough, 1986; Eskelinen et al., 2003). It has been shown that lysosomal membrane proteins (such as LAMP1) can be packaged into vesicles at the TGN that are different from vesicles that transport lysosomal hydrolases (such as cathepsin D), and co-localization of these two proteins can be consider to mark mature lysosomes (Karlsson and Carlsson, 1998).

Immunostaining of WT and *Cln3*$^{-/-}$ astrocytes with cathepsin D or LAMP1 antibodies revealed a punctate, vesicular staining pattern clustered around the nucleus and dispersed within the cytosol (Figure 3.11). However, in *Cln3*$^{-/-}$ astrocytes, less cathepsin D and LAMP1 appeared within the perinuclear region when compared with WT astrocytes (Figure 3.11), suggesting that the distribution or amount of endo/lysosomes is altered in *Cln3*$^{-/-}$ astrocytes. Moreover, there appeared to be more cathepsin D and LAMP1 positive vesicles in WT astrocytes compared to *Cln3*$^{-/-}$ astrocytes, and both cathepsin D and

LAMP1 positive vesicles appeared to be fractionally smaller in the *Cln3*$^{-/-}$ astrocytes. Finally, co-localization of cathepsin D and LAMP1 can be considered to identify mature lysosomes, and it appears that in WT astrocytes more co-localization is observed than in *Cln3*$^{-/-}$ astrocytes (Figure 3.11, compare higher power images between WT and *Cln3*$^{-/-}$ astrocytes). This suggests that endo/lysosomal trafficking and maturation is altered, even if these changes are moderate, in *Cln3*$^{-/-}$ astrocytes.

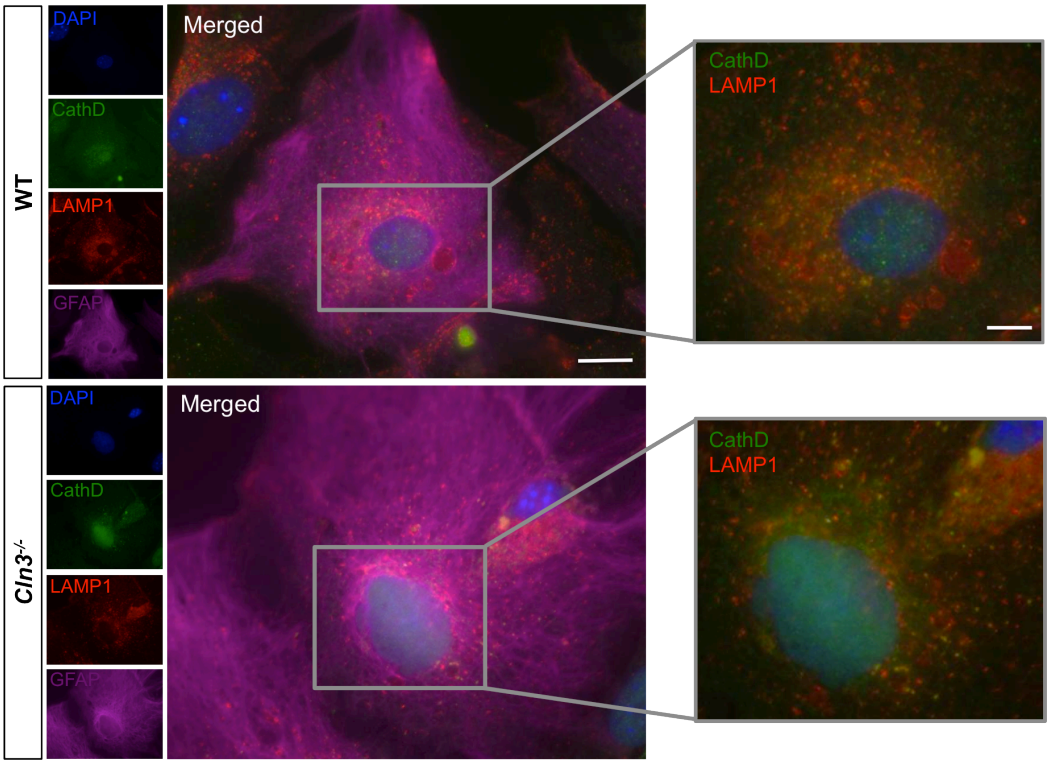

Figure 3.11. CLN3 affects compartmentalization of cathepsin D and LAMP1 endo-lysosomal markers. WT and *Cln3*$^{-/-}$ astrocytes were stained with antibodies against GFAP to visualize astrocytes, cathepsin D (CathD) to visualized both unprocessed and processed forms of this lysosomal hydrolase and LAMP1 to visualize the late endosomes, pre-lysosomes and mature lysosomes. DAPI was used to visualize all nuclei. Both CathD and LAMP1 were localized in dispersed vesicles within the cytosol, as well in the perinuclear area of WT and *Cln3*$^{-/-}$ astrocytes. CathD and LAMP1 positive vesicles dispersed equally in the cytosols of WT and *Cln3*$^{-/-}$ astrocytes. However, they were more numerous in WT than *Cln3*$^{-/-}$ astrocytes, with these vesicles being localized closer to the nucleus in WT astrocytes. Higher magnifications show co-localization of CathD and LAMP1 as an indication of mature lysosomes, with more co-localization apparent in WT astrocytes. Scale bar is 20µm in x40 magnification, and 10µm in higher power images.

The expression and distribution of early endosomes is not influenced by lack of CLN3 protein in astrocytes

CLN3 has frequently been reported to be associated with the early endosomal marker EEA1 especially along neuronal processes, but less so in non-neuronal cells, such as HELA-cells (Kyttälä et al., 2004). Thus, to obtain information about the association of CLN3 with the endosomal system in astrocytes, the effect of its absence on the localization of EEA1-positive early endosomes (EEs) was assessed by immunofluorescence microscopy.

No significant difference was observed in the distribution of EEA1 positive early endosomes between WT and *Cln3*$^{-/-}$ astrocytes (Figure 3.12). In both of these cell types EEs are relatively evenly distributed around the cytosol, with a slight preference to be located around the nucleus. There was also no apparent difference in the intensity and size of the EEs between these two genotypes. However, possibly due to the larger cell body size of *Cln3*$^{-/-}$ astrocytes (see quantification of cell soma size in Figure 3.8) there appeared to be more EEs in *Cln3*$^{-/-}$ astrocytes.

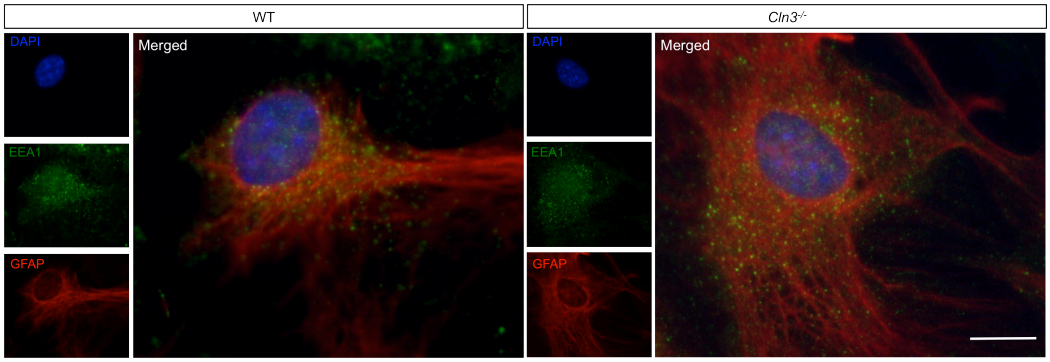

Figure 3.12 Expression and distribution of EEA1 is not altered in *Cln3*$^{-/-}$ astrocytes. WT and *Cln3*$^{-/-}$ astrocyte cultures were stained with GFAP to visualize astrocytes and EEA1 to visualize early endosomes. In both genotypes the EEA1 expressing EEs had a similar intensity, size and distribution. Scale bar is 20µm.

The expression and distribution of Rab7 is influenced by the lack of CLN3 protein in astrocytes

The endocytosis pathway regulates many physiological events in the cell. Rab7 is a late-endosome/lysosome associated small GTPase that plays a pivotal role in

endocytosis. Together with its interaction partners such as RILP, Rab7 contributes to processes such as endosomal sorting, biogenesis of lysosomes and phagocytosis (see Chapter 1, Section 1.2) (Jordens et al., 2001; Zhang et al., 2009b). As early endosomes mature into late endosomes they underdo a so-called Rab-conversion where Rab5 is displaced by Rab7 (Rink et al., 2005). This conversion takes place simultaneously with the dynein-mediated movement of endosomes down microtubules from the periphery of the cell towards the microtubule-organizing center located in the perinuclear region (Driskell et al., 2007; Johansson et al., 2007). Recently, it has been demonstrated that CLN3 interacts with Rab7 in various cellular models (Luiro et al., 2004; Uusi-Rauva et al., 2012). Considering the importance of the correct functioning of the small GTPase Rab7 to the overall endo-lysosomal homeostasis in the cell, the expression pattern of Rab7 was investigated in both WT and *Cln3*$^{-/-}$ astrocytes.

In both genotypes Rab7 expressing late endosomes were localized mainly in the cytosol. Overall there appeared to be more Rab7 expressing late endosomes in WT than in *Cln3*$^{-/-}$ astrocytes. Additionally, these Rab7 expressing LEs tended to be clustered in a band adjacent to the nucleus in WT astrocytes (marked with dashed line, Figure 3.13), but were more randomly expressed within the cytosol of *Cln3*$^{-/-}$ astrocytes. Thus, CLN3 may be involved in the expression and localization of Rab7, highlighting the potential importance of CLN3 in functioning of the endo/lysosomal system.

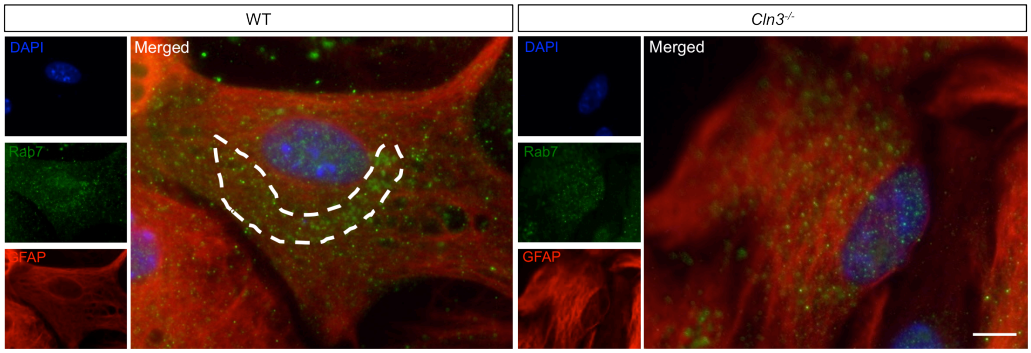

Figure 3.13 Rab7 labeled late endosomes show an altered localization in *Cln3*$^{-/-}$ astrocytes. WT and *Cln3*$^{-/-}$ astrocytes were labeled with GFAP to visualize astrocytes and an antibody that recognizes the small GTPase Rab7, which labels late endosomes (LEs). DAPI was used to label all nuclei. Rab7 was distributed around the cytosol of both WT and *Cln3*$^{-/-}$ astrocytes. In WT astrocytes Rab7 labeled LEs were more numerous and localized in a band of vesicles around the nucleus (marked with dashed line), whereas Rab7 positive LEs were more randomly distributed in *Cln3*$^{-/-}$ astrocytes and were fewer in number. The density and size of these Rab7 LEs appeared very similar in both genotypes. Scale bar is 20µm.

3.3 Discussion

There is an increasing evidence that points towards the involvement of both microglia and astrocytes in the early stages of disease progression in all forms of NCLs. Unusually, mouse models of JNCL display an attenuated microglia and astrocyte response (Pontikis et al., 2004; 2005) (Figure 3.1), which is in marked contrast to the pronounced glial response observed in models of other forms of NCL (Bible et al., 2004; Oswald et al., 2005; Cooper, 2010; Kuronen et al., 2012; Schmiedt et al., 2012). In this chapter we used an *in vitro* approach to investigate the basic structure of JNCL astrocytes and their response to stimulation. *Cln3*$^{-/-}$ astrocytes were found to have abnormal cytoskeletal organization, with disrupted actin and intermediate filaments, accompanied by altered expression levels of intermediate filament proteins. Their cell bodies were significantly larger than wild-type astrocytes and they showed a diminished ability to transform morphologically upon activation, possibly due to severe abnormalities in their cytoskeleton. As might be expected from cells lacking a highly conserved lysosomal protein, the number and localization of late endosomes and lysosomes was altered in *Cln3*$^{-/-}$ astrocytes, with these cells displaying a more dispersed cytosolic localization of both of these compartments, and a reduced number of mature lysosomes.

Implications of a disrupted cytoskeleton on the biology of *Cln3*$^{-/-}$ astrocytes

Emerging evidence indicates that a large number of neurodegenerative diseases are associated with dysfunctional cytoskeletal components, resulting in effects upon vesicle or cellular organelle trafficking, vesicular biogenesis, and synaptic signaling in neurons (McMurray, 2000). In this chapter I show for the first time that *Cln3*$^{-/-}$ astrocytes have cytoskeletal abnormalities (Chapter 3, Figure 3.7).

Some of the proposed interaction partners for CLN3 connect this protein directly with the cytoskeleton (Luiro et al., 2004; Weimer et al., 2005; Uusi-Rauva et al., 2008; Getty et al., 2011). For instance, CLN3 has been reported to form a transient interaction with the Hook1 protein, which is a microtubule-associated protein (Luiro et al., 2004). However, microtubular organization in *Cln3*$^{-/-}$ astrocytes was not altered, suggesting that in astrocytes the link between CLN3-Hook1 is not crucial for the correct organization of the microtubular cytoskeleton. However, Hook1 also indirectly links CLN3 with Ankyrin G, which is an adaptor protein binding to the spectrin-actin cytoskeleton that functions as a scaffold protein between many cytosolic proteins and the peripheral membrane (Luiro et al., 2004). The severely disorganized actin cytoskeleton observed in *Cln3*$^{-/-}$ astrocytes could potentially arise because the ankyrin G/Hook1 interaction with the spectrin/actin cytoskeleton is compromised in these cells leading into incorrect polymerization of actin microfilaments, although this awaits experimental verification. Furthermore, the C-terminal fragment of CLN3 has been shown to interact with nonmuscle myosin-IIB, which is an actin-binding motor protein (Getty et al., 2011), and could further explain the lack of correct polymerization of actin in *Cln3*$^{-/-}$ astrocytes. CLN3-myosin interactions have also been associated with neuronal processes and synapse development and will be discussed in this connect in Chapter 5. Additionally, among other defects, upon myosin-IIB deficiency cell migration is markedly impaired (Lo et al., 2004). Indeed, *Cln3*$^{-/-}$ mouse embryonic fibroblasts show a reduced ability to migrate, which could be due to the loss of correct CLN3-myosin-IIB functional interaction in these cells (Getty et al., 2011). Based on evidence discussed above and detected defects in actin cytoskeleton organization in *Cln3*$^{-/-}$ astrocytes, their

ability to migrate was subsequently investigated by performing a scratch assay (see Chapter 4, Figure 4.12).

The intermediate filament (IF) network, composed of GFAP, nestin and vimentin forms an important component of the cytoskeleton of astrocytes (Eliasson et al., 1999). In this study, IF organization was also found to be highly disorganized in *Cln3*$^{-/-}$ astrocytes. Many emerging roles for IFs in astrocytes have been discovered, yet the principal function of individual IFs remains unresolved (Pekny and Pekna, 2004; Middeldorp and Hol, 2011). Numerous mouse models have been created that either overexpress or lack GFAP and/or Vimentin, whose knock-down together with GFAP is required for total ablation of IFs in astrocytes (Pekny and Pekna, 2004; Middeldorp and Hol, 2011). These studies indicate that IFs are required for migration, neuronal-glial interactions, gliotransmission and formation of the BBB (Pekny and Pekna, 2004; Pekny and Nilsson, 2005). As such, any of these important functions may be compromised in *Cln3*$^{-/-}$ astrocytes due to a disrupted IF cytoskeleton and astrocyte migration in addition to neuronal-glial interactions will be investigated further in Chapters 4. and 6 respectively.

IFs are not normally considered to be required elements for cell motility, unlike actin filaments and microtubules. However, the motility of primary astrocytes derived from *GFAP*$^{-/-}$, *Vim*$^{-/-}$, and *GFAP*$^{-/-}$*Vim*$^{-/-}$ mice was found to be severely compromised, as was their morphology (Lepekhin et al., 2001). Moreover, changes in GFAP expression has also been observed to ability of astrocytes to proliferate (Rutka and Smith, 1993; Toda et al., 1994; Elobeid et al., 2000). This could explain our findings that GFAP is overexpressed by *Cln3*$^{-/-}$ astrocytes under unstimulated conditions (Results Chapter 3, Figure 3.6), and these cells show an attenuated ability to proliferate (Chapter 3, Figure 3.9). Moreover, GFAP has been demonstrated to be involved in mitosis and cytokinesis, further reinforcing the potential link between GFAP expression abnormalities and the attenuated proliferation observed in *Cln3*$^{-/-}$ astrocytes (Inagaki et al., 1994; Pekny et al., 1998; Yasui et al., 1998; Kawajiri et al., 2003).

One of the most pivotal functions of astrocytes is associated with their ability to secrete and respond to different gliotransmitters, such as ATP, glutamate, D-serine, chemokines and cytokines (Volterra and Meldolesi, 2005; Verkhratsky and Butt, 2007; Halassa and Haydon, 2010; Parpura and Zorec, 2010). Various different mechanisms have been proposed to be involved in gliotranmission. The main one being exocytosis, that is dependent on an intracellular Ca^{2+} signaling response (Parpura and Zorec, 2010; Zorec et al., 2012). Overall, this process of exocytosis of gliotransmitters requires packaging of vesicles with the releasable cargo, transport of these cargo containing vesicles along the cytoskeleton to the plasma membrane, where they dock and fuse with the membrane and release their cargo into the extracellular space (Bezzi et al., 2004; Crippa et al., 2006; Halassa and Haydon, 2010). It has been demonstrated *in vitro* that depolymerization of IFs influences the directional mobility of vesicles in astrocytes (Potokar et al., 2007). Importantly, by disrupting the IF network the track length of vesicles was reduced (Stenovec et al., 2007), and the overall mobility of the vesicles was decreased (Potokar et al., 2008) Moreover, the stimulus-accelerated mobility of recycling glutamategic vesicles, stimulus-inhibited mobility of peptidergic vesicles and stimulus-mediated-inhibition of endo/lysosomes mobility was absent in *GFAP*$^{-/-}$*Vim*$^{-/-}$ astrocytes (Potokar et al., 2010). Thus, changes in IF expression that accompany astrocyte activation may result in altered vesicle trafficking and hence astrocyte functioning under pathological conditions (Potokar et al., 2008; 2010; 2011). Thus, keeping in mind that the IF and actin cytoskeleton are both disrupted in *Cln3*$^{-/-}$ astrocytes, we considered that their ability to secrete various proteins may be disrupted, and experiments to test this hypothesis are described in Chapter 4 (see Tables 4.1 and 4.2 and Figure 4.7).

Gene expression microarray studies of the whole brain, cerebellum, retinae and pure hippocampal neuronal cultures all derived from *Cln3*$^{-/-}$ mice revealed a range of differentially expressed genes with particular emphasis on genes involved in neurotransmitter metabolism, immunoresponse, metabolism and, crucially, cytoskeletal organization (Brooks et al., 2003; Elshatory et al., 2003;

Chattopadhyay et al., 2004; Luiro et al., 2006). However, none of these experiments specifically focused on astrocytes or reported alterations in the expression of any astrocyte specific markers. In future it would be informative to carry out such gene expression studies on pure *Cln3*$^{-/-}$ astrocyte cultures.

Observations presented here on the cytoskeletal abnormalities in *Cln3*$^{-/-}$ astrocytes provide novel insights into the possible importance of CLN3 in the organization of the cytoskeleton in this cell type. Indeed, the disordered intermediate filament and actin cytoskeleton, as discussed above, could be the result of the CLN3 protein being required for the correct assembly of these polymers in astrocytes, either by interacting with them directly, or indirectly via proposed interaction partners, such as myosin-IIB and Hook1 (Luiro et al., 2004; Weimer et al., 2005; Getty et al., 2011). Systematic screening of interaction partners for CLN3 specifically in astrocytes would enable the confirmation of proteins involved in this process. However, such studies are difficult to conduct due to the lack of specific antibodies against CLN3 (Phillips et al., 2005). Nevertheless, methods such as glutathione S-transferase (GST) interaction pull-down assays combined with matrix-assisted laser desorption/ionization-time of flight (MALDI-TOF) mass spectrometric analysis could be applied to address this question (Luo et al., 1997; Berggård et al., 2007; Lalonde et al., 2008; Miernyk and Thelen, 2008). Regardless of not knowing the precise mechanisms behind the disrupted actin and intermediate filament cytoskeleton in *Cln3*$^{-/-}$ astrocytes, these abnormalities are bound to have severe functional implications for the overall biology of these cells. For example, agents such as cytochalasin D, which inhibits the actin microfilament polymerization, has significant effects on a range of astrocyte functions, including Ca^{2+} based signaling (Cotrina et al., 1998), glutamate clearance (Duan et al., 1999), and astrocyte migration (Etienne-Manneville and Hall, 2001). The ability of *Cln3*$^{-/-}$ to carry out these particular functions were therefore investigated, see Chapter 4. Taken together these findings support the hypothesis that CLN3 is involved in cytoskeletal organization (Jalanko and Braulke, 2009; Getty and Pearce, 2011) linking CLN3 to a wide range

of cellular activities dependent on dynamic re-arrangement of different cytoskeletal components.

Altered intermediate filament protein expression in *Cln3*$^{-/-}$ astrocytes

When astrocytes undergo major structural changes, as they do during reactive astrocytosis, the demand for cytoarchitectural structural support provided by intermediate filament networks becomes increasingly necessary (Pekny et al., 1995; Pekny and Pekna, 2004). Thus, the disrupted cytoskeletal structure of *Cln3*$^{-/-}$ astrocytes, described above, together with the significant differences detected in their expression levels of intermediate filament proteins, could have a major impact on their ability to change morphologically. Indeed, our data suggest that this is the case for *Cln3* deficient astrocytes *in vitro,* and *in vivo* in both murine and human JNCL (see Chapter 3, Figures 3.1 and 3.5 and 3.6).

Our data revealed that the level of GFAP expression in *Cln3*$^{-/-}$ astrocytes grown under basal conditions was significantly higher than that of WT astrocytes. This would suggest that the properties of *Cln3*$^{-/-}$ astrocytes are already different from the moment of isolation, perhaps due to differences in the molecular cues present in the *Cln3*$^{-/-}$ brains, even at this early developmental stage, leading to the initiation of astrocytosis in these diseased mice. Embryos from different JNCL mice models do not show any overt abnormalities in brain architecture and onset of neurological deficits only become evident starting from 1-4 months of age, depending on the mouse model (Katz et al., 1999; Mitchison et al., 1999; Cotman et al., 2002; Eliason et al., 2007). Accordingly, JNCL patients often have apparently normal development and neurological functions, until they reach the pre-teen years (Mole et al., 2011). It is feasible that CLN3 is important for some aspects of CNS development, and it may be possible that accumulative negative effects arising from CLN3 deficiency start during developmental stages, for instance, resulting in altered intermediate filament expression, as observed in astrocytes isolated from P2 cortex (see Results Chapter, Figure 3.6). Such early changes may represent a primary defect that eventually leads to the neuronal

dysfunction and neurodegeneration associated with JNCL. Certainly, based on *in vivo* data, a glial response precedes neuronal loss in an extremely specific manner in the *Cln3*$^{-/-}$ mouse brain, suggesting that primary pathogenic changes may also be glial-based rather than being purely neuronal in this disease. A mouse in which astrocytes constitutively overexpress GFAP has been engineered (Messing et al., 1998; Duan et al., 1999), and, interestingly, in this model these astrocytes contained highly complex intracellular aggregates of IFs and small stress proteins. These small stress proteins were identified as Rosenthal fibers. Intriguingly the accumulation of these fibers is also the hallmark of Alexander disease, which is an autosomal dominant neurodegenerative disorder (Messing et al., 1998; Quinlan et al., 2007). Thus, the over expression of GFAP in *Cln3*$^{-/-}$ astrocytes may have a detrimental neurotoxic effect.

Activated astrocytes upregulate GFAP, as well as vimentin and nestin, in the diseased brain (Pekny and Pekna, 2004; Pekny and Nilsson, 2005). To activate our cultured astrocytes we used LPS/IFNγ, which led to significantly increased GFAP expression, but only in WT astrocytes (Chapter 3, Figure 3.5). This coincides with our *in vivo* observations that astrocytes in the *Cln3*$^{-/-}$ mouse cortex, and those in JNCL patients, fail to significantly upregulate GFAP to the same extent as seen in other forms of NCL (Chapter 3, Figure 3.1). As such, *Cln3*$^{-/-}$ astrocytes have an intrinsically reduced ability to upregulate GFAP upon activation, despite expressing higher levels of this protein than WT astrocytes under resting conditions. This could again have significant functional implications, since impairment in the glial response to injury/disease has been shown to have detrimental effect on disease progression in other forms of NCL (Macauley et al., 2011).

Based on gene expression prolifing the astrocyte cultures used in this study are suggested to closely resemble immature instead of mature astrocytes (Cahoy et al., 2008; Foo et al., 2011; Zamanian et al., 2012). As such, detectable expression of GFAP together with nestin and vimentin was expected to be present in both WT and *Cln3*$^{-/-}$ astrocyte cultures, even under basal conditions (Chapter 3,

Figures 3.5 and 3.6). However, perhaps due to their immature nature, astrocytes of neither genotype responded to LPS/IFNγ stimulation by upregulating vimentin and nestin expression (Chapter, Figure 3.5). However, the fact that nestin was significantly downregulated in untreated *Cln3*$^{-/-}$ compared to WT astrocytes, suggests that *Cln3*$^{-/-}$ astrocytes derived from postnatal mice are not fully capable of returning to a stem cell like state, or they have taken on a more mature phenotype. This could imply that reactivated astrocytes in *Cln3*$^{-/-}$ mice brain display an attenuated plasticity hindering their ability to proliferate and regenerate, which could have detrimental implications over the course of disease progression in JNCL. In order to examine this issue further it would be interesting to compare the self-renewal and differentiation potential of reactive astrocytes isolated from adult *Cln3*$^{-/-}$ mice with those from WT mice. This could be done by growing these cells *in vitro* and testing their ability to differentiate into different neural cell types, or by using transplanting studies to reveal their developmental potential *in vivo* (Robel et al., 2011).

Importance of accurate morphological dynamics in astrocytes

Protoplasmic astrocytes constitute the most common type of astrocytes in the healthy gray matter. These astrocytes have extremely complex morphology, having a relatively small cell body with many thin primary processes, which extend into the neighboring neuronal networks forming a complex system of very fine branches (Montagnese et al., 1988; Ogata and Kosaka, 2002; Oberheim:2006ea Nedergaard et al., 2003; Theodosis et al., 2008; Allen and Barres, 2009; Lushnikova et al., 2009). Astrocytes employ their processes to ensheath structural elements of neurons, particularly synapses, as well as to connect themselves with the vascular system. The properties of astrocytes are incredibly diverse, as these cells not only function as a structural and nutritional support system for neurons, but are active partners in information processing and regulation of synaptic function, among other things (Verkhratsky and Butt, 2007; Sofroniew and Vinters, 2010; Parpura et al., 2012; Zorec et al., 2012). One property that enables astrocytes to carry out such a wide range of duties is their

ability to transform their morphology dynamically in response to changes in their environment (Theodosis et al., 2008; Allen and Barres, 2009; Nag, 2011; Sun and Jakobs, 2011). These types of structural alterations can be observed not only at the level of their soma and primary processes, but also at the level of their fine, distal processes that enwrap synapses. Indeed, one single astrocyte has been estimated to enwrap around 4-8 neuronal cell bodies and 300-600 neuronal processes (Halassa et al., 2007). This ability of astrocytes to interact with several neurons facilitates their influence upon the local microenvironment (Halassa et al., 2007).

The attenuated morphological transformation in *Cln3*$^{-/-}$ astrocytes, which was observed initially *in vivo* and is replicated here *in vitro* (Chapter 3, Figures 3.1 and 3.8) may alter their functional repertoire. For instance, long-term potentiation has been shown to increase the surface area of the astrocyte process enwrapping a synapse and the number of synapses enwrapped by a single astrocyte (Lushnikova et al., 2009). Astrocytes also show a morphological response to glutamate released from neurons by increasing their number of filapodia (Cornell-Bell et al., 1990b). Importantly, such morphological plasticity of astrocytes may form the mechanistic basis for the correct release of neuroactive molecules such as glutamate, ATP and D-serine from astrocytes in response to synaptic activity (Bezzi et al., 2004; Zhang et al., 2004; Mothet et al., 2005; Pascual et al., 2005), as well as the correct positioning of glutamate transporters that are essential for uptake of excess glutamate from the synaptic cleft (Huang and Bergles, 2004). Lastly, such re-arrangement of astrocyte processes has been suggested to be involved in stabilization of the structure of dendritic spines (Murai et al., 2003; Carmona et al., 2009; Filosa et al., 2009). This is achieved by localized expression of the glycosyl-phosphatidylinositol (GPI) – anchored glyco-protein ephrin-A3 upon the astrocyte processes that envelop the synapse (Murai et al., 2003). Ephrin-A3 subsequently activates the tyrosine kinase receptor EphA4 located on dendritic spines of adjacent neurons, and induces spine retraction. In contrast, the inhibition of such interactions was shown to distort spine shape and organization in hippocampal slices (Murai et al., 2003). This

astrocyte-neuron crosstalk is widely dependent on these dynamic changes in astrocyte structure and may be compromised in *Cln3*$^{-/-}$ astrocytes, since even under basal conditions these cells display morphological differences, having larger and rounder cell bodies than WT astrocytes. This may result in developmental differences between the brains of WT and *Cln3*$^{-/-}$ mouse embryos, since during development and early postnatal stages, such problems in morphological dynamics could directly lead into altered astrocyte-neuron crosstalk. Subsequently, this could gradually result in progressive changes in neuronal function given the importance of astrocyte-neuron crosstalk to synaptic functioning and plasticity (Carmona et al., 2009; Filosa et al., 2009). The direct impact of *Cln3*$^{-/-}$ glial cells on the morphological appearance (soma size and neurite complexity) of both WT and *Cln3*$^{-/-}$ neurons was investigated in these studies using co-culture experiments and these results will be presented in Chapter 6.

Reactive astrocytes undergo dramatic morphological changes in the diseased brain, and they have been shown to develop highly hypertrophied, thick primary processes, which can extend toward the core region of an injury (Wilhelmsson et al., 2004). Given their close relationship with neurons and their ability to secrete neuroactive substances, these hypertrophied astrocytes are considered, in certain circumstances, to be vital for neuronal protection and regeneration as well as for wound healing, whereas in other contexts they have been shown to negatively impact neuronal regeneration and survival (Sofroniew, 2009; Sofroniew and Vinters, 2010; Zamanian et al., 2012). Our data reveal that *Cln3*$^{-/-}$ astrocytes display an attenuated ability to change their morphology upon activation with LPS/IFNγ (see Chapter 3, Figure 3.8). Of direct relevance when considering the cytoskeleton, astrocyte morphology and disease progression, is a recent study revealing the contribution of astrocytes and their intermediate filaments to the pathological progression of INCL (Macauley et al., 2011). It was established that the additional absence of the intermediate filament proteins GFAP and vimentin in *Ppt1*$^{-/-}$ mice (*GFAP*$^{-/-}$*Vimentin*$^{-/-}$*Ppt1*$^{-/-}$), accelerated their disease progression, suggesting that endogenous activation of astrocytes is

protective against subsequent neuronal loss in INCL (Macauley et al., 2011). Unlike in INCL, where a profound astrocytosis is observed, the failure of *Cln3*$^{-/-}$ astrocytes to fully morphologically transform could result in a loss of this protective influence of astrocytes. The generation of mice where only astrocytes carry the Cln3 mutations will help to identify the precise role of these cells in JNCL pathogenesis.

Microtubules, actin and a variety of actin-binding proteins have been shown to be involved in the morphological transformation of astrocytes (Ridet et al., 1997; Small et al., 1999; Derouiche et al., 2002; Burgos et al., 2007). Myosin has also been implicated in this process, since myosin enables cell contraction and formation of extensions via its association with actin (Padmanabhan and Shelanski, 1998). As stated above, CLN3 has been suggested to interact with myosin (Getty et al., 2011). This interaction could provide a potential mechanistic explanation for the lack of morphological transformation in *Cln3*$^{-/-}$ astrocytes that we have observed. In addition, the Rho small GTPases are important regulators of shape, adhesion and cell movements (Chen et al., 2006). As a step towards identifying potential biomarkers and modifier genes, which may affect the clinical progression of JNCL, genetic alterations in JNCL patients were examined (Lebrun et al., 2011). Among such dysregulated genes was the guanine nucleotide exchange factor 1 for small GTPases of the Ras family (RAPGEF1), which activates downstream GTPases like Rho (Lebrun et al., 2011). Thus, altered activation of Rho GTPases by RAPGEF1 could lead to the observed compromised morphological response in *Cln3*$^{-/-}$ astrocytes. Indeed, RAPGEF1 plays a role in a range of signal transduction pathways involved in regulation of growth, differentiation, neuronal migration and radial glia attachment, especially during brain development (Tanaka et al., 1994; Erickson and Cerione, 2004; Richardson et al., 2004; Rossman et al., 2005; Voss et al., 2008). One could directly test the affect of alterations in activity of Rho GTPases on RAPGEF1 in astrocytes by either depleting or overexpressing this Rho activator, or by using pharmacological agents to regulate Rho activity.

Particularly interesting from a clinical perspective is the involvement of astrocytes in epileptogenesis, which is one of the most prominent clinical features of JNCL. Such mechanisms could include the Ca^{2+} dependent release of glutamate by astrocytes that directly excite neighboring neurons, or impaired astrocytic glutamate and K^+ uptake (Tian et al., 2005; de Lanerolle et al., 2010; Seifert and Steinhäuser, 2011; Losi et al., 2012). Either of these events may result in the formation of a hyperexcitable astrocyte-neuron network, which could cause a seizure. It may be that a disrupted cytoskeletal organization that results in a dysfunctional morphological response, could also lead to alterations in both glutamate and K^+ homeostasis in *Cln3*$^{-/-}$ astrocytes and thus contribute towards increased seizure probability. Indeed, excess extracellular glutamate in *Cln3*$^{-/-}$ mice (Chattopadhyay et al., 2002) and moderately altered expression of the glutamate transporters EAAT1 and EAAT2, that are expressed by astrocytes, have been shown in JNCL patient samples (Hachiya et al., 2006). Additionally, we go on to show that glutamate clearance is impaired in *Cln3*$^{-/-}$ astrocytes (Results Chapter 4, Figure 4.11), and that *Cln3*$^{-/-}$ neurons have a distally located AIS possibly due to hyperactivation (see Chapter 5, Figures 5.5-5.10).

In this study immunolabeling with GFAP was used to visualize the morphology of WT and *Cln3*$^{-/-}$ astrocytes, despite the fact that GFAP labeling does not fully represent the complexity of astrocyte morphology (Bushong et al., 2002; Verkhratsky and Butt, 2007; Theodosis et al., 2008; Song et al., 2009; Matyash and Kettenmann, 2010; Sofroniew and Vinters, 2010; Nag, 2011; Sun and Jakobs, 2011). This is because distal astrocytic processes contain extremely small amounts of intermediate filaments, including GFAP, and also not all astrocytes *in vitro* express enough GFAP to enable immunocytochemical visualization. Consequently, GFAP-based labeling of astrocytes may significantly underestimate the branching of their filamentous processes. Other labeling methods such as Golgi staining, filling astrocytes with dyes, or the expression of reporter proteins in astrocytes, have been demonstrated to provide markedly more accurate illustrations of the structural complexity of astrocytes (Bushong et al., 2002; Sun and Jakobs, 2011). Nevertheless, labeling the WT and *Cln3*$^{-/-}$

astrocytes with GFAP provides a good comparison of the morphologies of these two cell types under both basal and activated conditions. However, it would be interesting to extend these studies on morphological differences between *Cln3*$^{-/-}$ and WT astrocytes by using some of the other more complete labeling methods available.

Cell proliferation defects in *Cln3*$^{-/-}$ astrocytes

Our data revealed evidence that *Cln3*$^{-/-}$ astrocytes proliferate less actively than their wildtype counterparts (see Chapter 3, Figure 3.9). Generally, proliferation of astrocytes in the adult brain has remained a controversial issue. Radial glial-based production of astrocytes stops shortly after birth, and in the post-natal brain astrocytes have previously been thought to derive either from progenitors in the SVZ, or from local proliferative astrocytes (Cameron and Rakic, 1991; Levison and Goldman, 1993; Marshall et al., 2003; Kriegstein and Alvarez-Buylla, 2009). Recently it has been reported that existing mature astrocytes within the post-natal cortex act as a major source of new astrocytes (Ge et al., 2012). However, generally in the healthy post-natal brain, astrocyte turnover is very low and the majority of mature astrocytes are post-mitotic and long-lasting cells (Skoff and Knapp, 1991; Norton et al., 1992; Bush et al., 1999; Horner et al., 2000; Colodner et al., 2005). Astrocyte proliferation in different pathological scenarios has also turned out to be a rather controversial issue (Sofroniew and Vinters, 2010), mostly due to lack of appropriate astrocyte-specific markers making it difficult to distinguish all astrocytes regardless of their maturation state. In some pathological conditions where reactivation of astrocytes is relatively mild, proliferation does not occur (Sofroniew, 2009; Sofroniew and Vinters, 2010). However, in extremely severe situations, such as in cases of infection and acute demyelinating lesions, where reactive astrocytosis is very aggressive, actively dividing astrocytes have been reported in human specimens (Colodner et al., 2005; Sofroniew and Vinters, 2010), although the source of these newly dividing astrocytes is not well understood (Bush et al., 1999; Buffo et al., 2008; Gadea et al., 2008; Carlén et al., 2009; Sofroniew, 2009). Nevertheless, the ability to proliferate can be seen as an important part of the

biology of, at least some, astrocytes under both physiological and pathological conditions (Zamanian et al., 2012). Our data revealed that although the number of Ki67 proliferating astrocytes did not differ between WT and *Cln3*$^{-/-}$ astrocytes, the *Cln3*$^{-/-}$ astrocytes divided more slowly, as indicated by the number of BrdU expressing cells being significantly reduced in these cultures (Chapter 3, Figure 3.9). The number of actively proliferating astrocytes (percentage of BrdU^{+} cells) was reduced in *Cln3*$^{-/-}$ astrocyte cultures under both basal and activated conditions (Chapter 3, Figure 3.9). Lack of astrocyte proliferation during early development (potentially associated with lack of CLN3 function) could affect neuronal guidance and process extension (Powell and Geller, 1999; Emsley et al., 2004). Indeed, it has been shown that in the cerebellum of *Cln3*$^{-/-}$ mice, activated Bergmann glia were found within regions displaying dramatic Purkinje cells loss was evident, and remaining Purkinje cells displayed defective migration, neuritogenesis, and maturation (Weimer et al., 2009). This provides some evidence that glial responses can negatively influence neuronal biology in the *Cln3*$^{-/-}$ mouse brain.

The proliferation of astrocytes in JNCL mice has been studied indirectly by quantifying the number of S100β, a calcium binding protein expressed predominantly in astrocytes regardless of their activation status (Boyes et al., 1986), positive astrocytes in *Cln3*$^{\Delta ex7/8}$ mice in brain regions where reactive astrocytosis and subsequent neuronal loss were the most prominent (Pontikis et al., 2005). In this study, no significant change in the number of S100β positive astrocytes was found, either in the primary somatosensory barrel field cortex (S1BF) or hippocampal CA1 of *Cln3*$^{\Delta ex7/8}$ mice, compared with wild-type littermate controls (Pontikis et al., 2005). Similar counts of the number of S100β positive astrocytes were also made in *Ppt1*$^{-/-}$ mice, where significantly more S100β positive astrocytes was observed in both the S1BF and CA1 compared to healthy controls (Parviainen, unpublished data). Based on these data astrocyte numbers do appear to increase in at least some mice models of NCLs, whereas in JNCL such an increase in astrocyte number does not occur. A thorough analysis of glial proliferation in human JNCL brain sections is yet to be undertaken. In fact,

such studies have never been conducted in any form of NCLs. This could plausibly be achieved by identifying proliferating cells with the proliferation marker MIB-1 in association with different glial cell specific markers, such as GFAP for astrocytes and CD68 for microglia. However, studies on lymphoblasts derived from JNCL patients, and on immortalized JNCL lymphoblast cell lines, have reported reduced growth rates in these mutant cell-types compared to normal cells (Persaud-Sawin et al., 2002). This slower growth was not accompanied by a reduced rate of thymidine incorporation into DNA, indicating that cell cycle entry is not altered in these types of CLN3 deficient cells. Alternatively, the reduced BrdU incorporation observed in the present study suggests that *Cln3*$^{-/-}$ astrocytes have a slower cell cycle time. Thus, perhaps, CLN3 deficiency alters both the entry and progression of cell cycle differently in different cell-types.

What could the slower division of *Cln3*$^{-/-}$ astrocytes mean? If indeed, astrocyte division was also slower in *Cln3*$^{-/-}$ mice, this could lead to a smaller astrocyte population and a net reduction in levels of secretion of molecules generated by activated astrocytes. Subsequently, this could have either a negative or positive impact on ongoing neurodegeneration in the *Cln3*$^{-/-}$ mice brain, since these molecules could be involved in regulation of inflammation response, controlling axonal regeneration, neuroprotection or reestablishments of proper neuronal connectivity (Ridet et al., 1997; Dong and Benveniste, 2001; Liberto et al., 2004; Di Giovanni et al., 2005; Byrnes et al., 2007; Bélanger and Magistretti, 2009; Sofroniew and Vinters, 2010; Zamanian et al., 2012). The purpose of activated proliferating astrocytes remain elusive, yet the cell cycle plays a key role in this process (Sherr, 1996; Kato et al., 2003). Cell cycle progression is controlled by two classes of proteins: the cyclins and cyclin-dependent kinases (CDKs) (Vermeulen et al., 2003). Moreover, by inhibiting the cell cycle via manipulating the activity of these cell cycle regulators astrocyte activation can be reduced (Di Giovanni et al., 2005; Wang et al., 2008). This reduction was accompanied by decreased neuronal apoptosis, smaller lesion volume, and reduced glial scar formation in *in vivo* models of MCAO, photothrombotic ischemia and traumatic brain injury (Di Giovanni et al., 2005; Wang et al., 2008). Thus, in JNCL the

disease-associated reduced rate of astrocyte proliferation might also play a positive role in the progression of this disease.

Alterations in endo/lysosomal distribution and maturation in *Cln3*$^{-/-}$ astrocytes

Lysosomes are dynamic cellular organelles, whose positioning in a cell is highly regulated. Indeed, one of the key elements of the overall cell physiology is the correct localization and expression of relevant endo-lysosomal proteins to ensure efficient degradation and recycling of cellular waste (Lippincott-Schwartz and Fambrough, 1986; Theodosis et al., 2008; van Meel and Klumperman, 2008). Early endosome expression and localization was not altered in *Cln3*$^{-/-}$ astrocytes (Chapter 3, Figure 3.12). However, *Cln3*$^{-/-}$ astrocytes showed specific alterations in both the number of late endosomes and lysosomes, and the localization of these compartments within the cell when compared to WT astrocytes. These findings correlate well with the suggested cellular functions, and primary localization of the CLN3 protein, which both point towards endo/lysosomal pathways (Fossale et al., 2004; Kyttälä et al., 2004; 2005; Metcalf et al., 2008; Getty and Pearce, 2011; Uusi-Rauva et al., 2012). The connection between CLN3 deficiency and compromised endo-lysosomal organization has been demonstrated in other models for JNCL (Fossale et al., 2004; Uusi-Rauva et al., 2012). For example, early and late endosomal compartments were found to be more dispersed in *Cln3*$^{\Delta ex7/8}$ cerebellar neurons compared to WT controls (Fossale et al., 2004), as were late endosomes in *Cln3*$^{-/-}$ astrocytes (Chapter 3, Figures 3.11 and 3.13). On the other hand, over-expression of the protracted disease causing late endosome/lysosome localized CLN3E295K mutation (Aberg et al., 2009) in HeLa cells caused perinuclear clustering of late endosomes/lysosomes (Uusi-Rauva et al., 2012). Importantly, analyses of fibroblasts isolated from JNCL patients (compound heterozygous mutation (CLN3E295K/*CLN3*$^{\Delta ex7/8}$) or homozygous mutation (*CLN3*$^{\Delta ex7/8}$/*CLN3*$^{\Delta ex7/8}$)) showed perinuclear clustering of late endosomal compartments (Ogata and Kosaka, 2002; Huang and Bergles, 2004; Luiro et al., 2004; Oberheim et al., 2006; Uusi-Rauva et al., 2012). Such findings supporting perinuclear accumulation of endo/lysosomes upon *CLN3* mutation are in contrast with the findings in this

study that show the opposite effect. This may be a reflection of the different roles CLN3 plays in different cell types, that may be dictated by cell type specific localization of CLN3 (Getty and Pearce, 2011; Mole et al., 2011). Alternatively, it has been suggested that mutations in *Cln3* rather than complete deletion of *Cln3* may impact the cell differently due to a functionally active truncated CLN3 (Kitzmüller et al., 2008; Sarpong et al., 2009). This view, however, has been challenged by evidence showing that truncated CLN3 is not functionally active (Phillips et al., 2005; Getty and Pearce, 2011).

The more dispersed cytosolic localization of Rab7 expressing late endosomes in *Cln3*$^{-/-}$ astrocytes correlates well with recent findings indicating that CLN3 have a direct connection with active GTP-Rab7 and its effector RILP (Uusi-Rauva et al., 2012). The Rab7 protein is required for aggregation and fusion of late endosomes with lysosomes and is important for maintenance of the perinuclear localization of lysosomes (Bucci et al., 2000). Thus, it is feasible that the direct connection between Rab7 and CLN3 is important for the correct transportation and maturation of late endosomal and lysosomal compartments in astrocytes. The reduced number of LAMP1/Cathepsin D expressing mature lysosomes at perinuclear regions in *Cln3*$^{-/-}$ astrocytes (Results Chapter, Figure 3.10), would further suggest that transport from the TGN to late endo/lysosomes is impaired in these cells. Furthermore, one of the potential interaction partners of CLN3 is a protein called Hook1 (Luiro et al., 2004; Weimer et al., 2005), which may connect CLN3 to the microtubular cytoskeleton and members of the Rab GTPases family involved in endocytosis and fusion of late endosomes with lysosomes (Krämer and Phistry, 1996; 1999; Walenta et al., 2001; Richardson et al., 2004; Weimer et al., 2005). Indeed, receptor-mediated endocytosis was found defected in CLN3-deficient JNCL fibroblasts, which may potentially be explained by dysfunctional CLN3-Hook1 interaction (Luiro et al., 2004). Additionally, co-immunoprecipitation studies suggested that Hook1 may interact with endocytic Rab7, 9 and 11, possibly linking CLN3 further with membrane trafficking events (Luiro et al., 2004). Hence, disturbance in the interactions between Hook1-Rab7-CLN3, or Rab7-RILP-CLN3 protein complexes and the cytoskeleton may possibly

provide a mechanistic explanation for the altered localization of endo/lysosonal structures in *Cln3*$^{-/-}$ astrocytes. One could test the assembly of such protein complexes in astrocytes by carrying out binding studies. Furthermore, it would be interesting to explore the dynamic trafficking of endo/lysosomes in live *Cln3*$^{-/-}$ astrocytes by using fluorescently labeled endo/lysosomal markers, such as LysoTracker Red, LAMP-1 and LAMP-2, under different pharmacological manipulations. For example, induced alterations in the intracellular pH, where acidification redistributes lysosomes from their predominantly perinuclear location towards the cell periphery, could be used (Korolchuk and Rubinsztein, 2011). Prior to such studies, one would need to examine the pH in the endo/lysosomal compartments in the *Cln3*$^{-/-}$ astrocytes, since CLN3 (or btn1 protein in yeast) has been linked with regulation of lysosomal pH (Pearce et al., 1999b; Golabek et al., 2000; Kim et al., 2003; Padilla-Lopez and Pearce, 2006). In particular, CLN3 deficiency has been shown to acidify lysosomal compartments in human HEK-293 cells (Golabek et al., 2000), which itself could explain the observed alterations in the distribution of lysosomes in *Cln3*$^{-/-}$ astrocytes. Additionally, measuring endocytosis in these cells would give a direct answer to the question of whether this process is affected in *Cln3*$^{-/-}$ astrocytes.

The normally appearing expression and distribution of the early endosomes in *Cln3*$^{-/-}$ astrocytes suggests that the CLN3 protein is not involved in early endosomal related processing in astrocytes. This finding agrees with previous research showing that early endosomal expression patterns were not effected in HELA cells over-expressing the mutant CLN3E295K (Uusi-Rauva et al., 2012). On the other hand, early endosomal expression has been found to be altered in *Cln3*$^{\Delta ex7/8}$ cerebellar neurons (Fossale et al., 2004). It may well be that CLN3 protein dictates early endosome transportation and expression only in specific cell types, such as in neuronal cells, via still unidentified mechanisms.

Generally, endo/lysosomes are dynamic organelles and their localization within cells is highly regulated and can be altered in response to various treatments. In addition to alterations in intracellular pH, which is one of the best-known

effectors of intracellular lysosomal positioning, the positioning of lysosomes can also be affected by nutrients, where addition of growth factors and amino acids may induce movements of lysosomes toward the plasma membrane, while starvation may lead to increased perinuclear localization (Korolchuk and Rubinsztein, 2011; Korolchuk et al., 2011). However, the physiological relevance of such alterations in lysosomal positioning is not fully understood. One possible explanation for the preferred perinuclear localization of lysosomes could be that this positioning enables efficient fusion of autophagosomes, that are also delivered to perinuclear regions via microtubule-dependent transport, with lysosomes (Korolchuk and Rubinsztein, 2011). Autophagy is a nonselective process involved in recycling of cytoplasmic components, and impaired autophagy has been revealed to be a common feature of neurodegeneration in Parkinson, Huntington, and Alzheimer diseases, and in LSDs (Rubinsztein et al., 2005; Cao et al., 2006; Wong and Cuervo, 2010; Korolchuk et al., 2011; Li et al., 2011). Indeed, CLN3 deficiency has also been linked with disrupted autophagy (Cao et al., 2006; Chang et al., 2011). Interestingly, recently it was shown that lysosomal storage in *Sumf1*$^{-/-}$ astrocytes (derived from a mouse model of multiple sulfatase deficiency, MSD, which is a type of severe LSD) impairs autophagosome maturation, which in turn, has an impact upon the survival of co-cultured cortical neurons (Di Malta et al., 2012b). As such, abnormal autophagy caused by altered lysosomal positioning and maturation in *Cln3*$^{-/-}$ astrocytes may also be an important component of neurodegeneration in JNCL.

Taken together results described in this chapter, and in the literature, indicate that changes in the endo/lysosomal compartments is a common feature in cells carrying a *Cln3* mutation or deletion, although the exact changes observed appear to be cell type specific. One potential common factor in all of these cell types in which altered endo/lysosomal membrane trafficking has been observed could be Rab7, since many abnormalities associated with CLN3 deficiency can be connected with functions related to Rab7. For example, CLN3 deficiency has been shown to affect lysosomal/vacuolar pH and size, processing of lysosomal hydrolases, as well as autophagy (Pearce et al., 1999a; Holopainen et al., 2001;

Fossale et al., 2004; Gachet et al., 2005; Cao et al., 2006), and all of these listed abnormalities have previously been linked with dysfunctional Rab7 (Press et al., 1998; Bucci et al., 2000; Gutierrez et al., 2004; Jäger et al., 2004; Vanlandingham and Ceresa, 2009). One common link between CLN3 and Rab7 is their localization in autophagosomal membranes, and they have both been proposed to be involved in the maturation of autophagic vesicles (Jäger et al., 2004; Cao et al., 2006). Indeed, careful investigation of autophagy pathways in *Cln3*$^{-/-}$ astrocytes should be carried out to investigate this issue. For instance, live cell imaging could be used to monitor trafficking of a fluorescently labeled LC3 (widely used autophagy marker) and labeled endo/lysosomal proteins in these cells (Bampton et al., 2005).

Are primary astrocyte cultures a good tool to study the biology of *Cln3*$^{-/-}$ astrocytes?

Using an *in vitro* system in this study enabled us to address specific questions regarding the function of *Cln3*$^{-/-}$ astrocytes in a controlled environment, without the interference of factors present in an *in vivo* setting. Such *in vitro* investigations of astrocyte biology has not previously been carried out in the field of NCL research, yet this approach has been frequently used to study the biological functions of astrocytes and the process of reactive astrocytosis (Bolaños et al., 1996; Duan et al., 1999; Guthrie et al., 1999; John et al., 1999; Lepekhin et al., 2001; Stewart et al., 2002; Morita et al., 2003; Paradisi et al., 2004; Gegg et al., 2005; Frade et al., 2008; Lange et al., 2012). However, several limitations regarding the use of this purification method have emerged. For instance, it has been speculated that astrocytes isolated using this method may be more similar to radial glia, astrocyte progenitor cells or perhaps even reactive astrocytes, than the mature astrocytes of adult brain (Cahoy et al., 2008; Foo et al., 2011; Lange et al., 2012). Additional causes for concern include the use of serum in the growth medium, since prolonged culturing of cells in serum may cause irreversible alterations in their properties (Jochems et al., 2002; Gstraunthaler, 2003; van der Valk et al., 2004). Indeed, using serum to culture

any primary CNS derived cells, may be considered to be non-physiological, since most proteins present in serum would not be present in the CNS due to their inability to cross the blood-brain barrier (Banks, 1999). Regardless of these limitations, these astrocyte cultures provided an extremely useful tool offering novel insights on how lack of CLN3 could influence the biology of these cells, and allowed direct comparison between them and 'normal' wild-type astrocytes. Important finding made in such cultures can be further explored and confirmed, for example, in organotypic slices or *in vivo*.

Also, these astrocyte cultures were not 100% pure, displaying a purity of > 98%. The very few other cells present in these cultures were mainly microglia cells, and rarely oligodendrocytes. It is crucially important to ensure microglia contamination is as minimal as possible in such cultures for several reasons: microglia and astrocytes differ in their ontogenic origin (monocytic for microglia, and neuroectodermal for astrocytes), astrocytes and microglia cells have different physiological, and functional responses upon activation (Saura, 2007). For instance, microglia may carry out functions that were previously thought to be astrocyte driven, such as LPS induced expression of nitric oxide synthetase-2 (NOS2) and subsequent production of NO in culture conditions (Solà et al., 2002; Saura, 2007). Ideally one would wish to work with 100% pure astrocyte cultures to ensure that any results obtained can be directly attributed to these cells, rather than any cell-contaminants in the culture, or interactions of those contaminating cells with the astrocytes. Given that the presence of the other glial cells was minimal within these astrocyte cultures, the data we have obtained most likely provide an accurate representation of differences between WT and *Cln3*$^{-/-}$ astrocytes. Working with 100% pure cultures might also be problematic. Astrocytes do not exist in isolation in the CNS, instead existing and functioning in close collaboration with other cell types, such as microglia and neurons. As such, any results obtained from pure astrocyte cultures may not be a true reflection of the complex range of astrocyte functions *in vivo*. Perhaps the best answer is to initially examine the basic cellular biology in the simplest

possible setting then move on to testing the gained information in more complex settings; mixed cultures with different cell-types.

Moreover, one could argue whether the use of LPS/IFNγ to activate astrocytes is valid. JNCL disease mechanisms include neuroinflammation (Seehafer et al., 2011), and astrocyte and microglia activation has been implicated to underlie these inflammatory responses in the CNS (Allan and Rothwell, 2003; Schubert and Ferroni, 2003; Zhang et al., 2010; Garwood et al., 2011; Ransohoff and Brown, 2012). Several *in vitro* studies have demonstrated that astrocytes respond to cytokines like IFNγ and to microbial products like LPS, and that in astrocytes IFNγ synergizes with LPS to produce a maximal transcriptional response (Chung and Benveniste, 1990; Bolaños et al., 1994; Schindler and Brutsaert, 1999; Gegg et al., 2005; Sheng et al., 2011; Cortés-Vieyra et al., 2012). Thus, using these agents to mimic astrocyte activation should closely resemble the reactive astrocytosis taking place in the *Cln3*$^{-/-}$ mouse brain. Indeed, this activation method resulted in very similar changes in cultured WT astrocytes to those observed to occur *in vivo* upon reactive astrocytosis; morphological transformation, upregulation of intermediate filaments, and secretion of soluble factors such as chemokines and cytokines (Chapter 4, Tables 4.1 and 4.2, Figure 4.7). Despite these limitations, we are confident that these cultures provide a valid method for comparing the biological differences between *Cln3*$^{-/-}$ and WT astrocytes. Ultimately, the significance of any fundamental findings from this study will need to be confirmed in JNCL animal models, or perhaps in differentiated iPS cells derived from JNCL patients. For example, mouse models where only astrocytes, only microglia, or both microglia and astrocytes carry the *Cln3* deletion, would enable the precise contribution of glial cells to neurodegeneration in JNCL to be determined. Additionally, the role of reactive astrocytosis in JNCL could be studied by depleting intermediate filaments (GFAP and vimentin) required for astrocyte activation in a *Cln3*$^{-/-}$ mouse model (*GFAP*$^{-/-}$*/Vim*$^{-/-}$*/Cln3*$^{-/-}$), much as has already been done in *Ppt1* deficient mice (Macauley et al., 2011). Together, these studies would establish whether

astrocytes are indeed integral players in the neuropathology in JNCL, and whether modulation of astrocyte activation will impact disease progression.

Taken together, we have shown that isolated *Cln3*$^{-/-}$ astrocytes differ from their healthy counterparts. They have an abnormal cytoskeletal organization and enlarged cell body size, together with altered intermediate filament expression. The expression of endosomal/lysosomal proteins and the distribution of these compartments within the cytosol were also observed to be altered. Indeed, it was demonstrated that *Cln3*$^{-/-}$ astrocytes showed an attenuated morphological response to activation and an attenuated ability to proliferate, both of which are dependent on functional cytoskeletal re-organization. Furthermore, such deficits are bound to affect other typical astrocyte functions that also depend upon the cytoskeleton, such as protein secretion and uptake, as well as migration. Thus, our next step was to investigate these possibilities (Chapter 4). Having a better picture of how *Cln3*$^{-/-}$ astrocytes differ from their healthy counterparts will ultimately aid our understanding on the role of astrocytes as a potential mediator of neuropathological events in JNCL.

Chapter 4
Functional differences between WT and *Cln3*$^{-/-}$ astrocytes

4.1 Introduction

It has become increasingly apparent that astrocytes are not just passive bystanders with supportive roles, but perform many vital functions in the healthy CNS, including being active contributors to many higher brain functions such as information processing and the formation of neuronal circuits (Sofroniew and Vinters, 2010). Furthermore, astrocytes are also active players in pathological situations when they may contribute to, or play primary roles in, clinical and pathological mechanisms (Liberto et al., 2004; Seifert et al., 2006; Barres, 2008; De Keyser et al., 2008; Sofroniew, 2009; Takano et al., 2009). Thus, mutations in astrocyte-expressed genes that result in protein dysfunction may impact on many brain functions and on disease progression. We have shown that *Cln3*$^{-/-}$ astrocytes have a disrupted cytoskeleton, probably resulting in their attenuated ability to morphologically transform and to proliferate, as well as alterations in their endo/lysosomal system. These defects could impact on their ability to perform a range of functions that are vital in a healthy brain (see Chapter 3 and discussion therein). Indeed, various reports have suggested that defects in several important cellular functions in which astrocytes are involved, may contribute to the neuropathological events observed in JNCL. These include early deficits in the regulation of oxidative stress (Benedict et al., 2007; Tuxworth et al., 2011); the inability to effectively regulate extracellular glutamate levels, together with an increased vulnerability of glutamate receptors towards excitotoxicty (Chattopadhyay et al., 2002; Pears et al., 2005; Kovács and Pearce, 2008; Finn et al., 2011; Kovács et al., 2011); and an early inflammatory reaction (Lim et al., 2006; 2007; Seehafer et al., 2011). In this chapter we therefore tested the ability of *Cln3*$^{-/-}$ astrocytes to carry out a range of basic functions.

Calcium based signaling forms the basis for astrocyte-astrocyte and astrocyte-neuron intercellular communication in the CNS (Cornell-Bell et al., 1990a; Charles et al., 1991; Haydon, 2001; Zorec et al., 2012). For instance, ER mediated Ca^{2+} release via activation of the PLC pathway is required for gliotransmission - the secretion of molecules such as ATP, glutamate and D-serine by astrocytes that directly regulate the function of both neuronal and glial cells (Zorec et al., 2012)

(see Chapter 1, section 1.3). Thus, basic Ca^{2+} signaling mechanisms including the increase in intracellular Ca^{2+} upon ATP application; ER Ca^{2+} release upon inhibition of the SERCA-calcium pump (to evaluate ER Ca^{2+} content) and subsequent clearance of the cytosolic Ca^{2+}, and spontaneous Ca^{2+} oscillations, were compared in WT and *Cln3*$^{-/-}$ astrocytes. From these experiments it will be possible to determine whether the response to external stimuli (neurotransmitters), the intracellular pathways involved in Ca^{2+} regulation, or intercellular communication via a propagating Ca^{2+} wave have remained intact in *Cln3*$^{-/-}$ astrocytes.

One the most fundamental ways in which astrocytes influence neuronal and glial function in the CNS is via the secretion of soluble factors (Ridet et al., 1997; Bélanger and Magistretti, 2009; Sofroniew and Vinters, 2010). To begin examining whether protein secretion by astrocytes may play a role in inflammation and progression of neurodegeneration in the *Cln3*$^{-/-}$ mouse brain, a protein secretion assay to quantify a number of cytokines, chemokines, growth factors and anti- and pro-inflammatory factors was performed. To gain a better understanding on the contribution of astrocytes to the increased levels of oxidative damage observed in JNCL, the ability of *Cln3*$^{-/-}$ astrocytes to produce and secrete glutathione (the major antioxidant in the brain) was also examined. Finally, to meet the high energy demands of neurons, astrocytes secrete lactate, thus this ability was also tested. In addition to protein secretion, astrocytes also contribute to neuron function and survival by keeping the levels of various neurotransmitters under control with the synaptic cleft (Anderson and Swanson, 2000; Oliet et al., 2001; Sattler and Rothstein, 2006; Seifert et al., 2006; Goubard et al., 2011). Given that glutamate mediated excitotoxity has been suggested to play a role in neurodegeneration in *Cln3*$^{-/-}$ mice (Kovács et al., 2006; Kovács and Pearce, 2008; Finn et al., 2011; Kovács et al., 2011), the ability of *Cln3*$^{-/-}$ astrocytes to take up glutamate was also explored.

It is well established that astrocytes are relatively mobile cells, and reactive astrocytes have been shown to migrate to the site of injury and in some cases

form an isolating glial scar (Silver and Miller, 2004; Borán and García, 2007). Migration defects have been shown previously in *Cln3*$^{-/-}$ embryonic fibroblasts (Getty et al., 2011), suggesting that the CLN3 protein is involved in re-arrangement of the cytoskeleton enabling migration to take place. Hence, potential migration defects were explored in *Cln3*$^{-/-}$ astrocytes by carrying out a scratch assay.

These functional assays will provide essential insights into the biology of *Cln3*$^{-/-}$ astrocytes, and how their functional range is altered compared to healthy cells. Also, these studies may reveal novel aspects of CLN3 function in glial cells. Most importantly, any alterations in the astrocyte-related functions mentioned above could have a significant impact on neuronal function and survival in JNCL. Indeed, as discussed above, many of the problems reported in the JNCL brain could arise by, or be exacerbated by, defects in astrocyte biology. Thus, a better understanding of any defects in astrocyte functioning could provide novel targets for therapies in JNCL.

4.2 Results

Calcium signaling in *Cln3*$^{-/-}$ astrocytes

Calcium is the most widespread signaling molecule used by all types of living cells (Berridge et al., 2000; Carafoli, 2002; Petersen et al., 2005). Numerous cellular mechanisms exist to keep the intracellular calcium ($[Ca^{2+}]_i$) concentration tightly controlled (concentration gradient between intracellular and extracellular compartments is approximately 20,000 times) to ensure efficient Ca^{2+} based signaling and also to remove excess intracellular Ca^{2+} due do its harmful effect on biological pathways (Case et al., 2007). Astrocytes possess a chemical type of excitability, which is based on movements of Ca^{2+} between intracellular compartments and cell membrane Ca^{2+} fluxes (Verkhratsky and Kettenmann, 1996; Araque et al., 2001). This type of astrocyte Ca^{2+} based excitability is thought to form the basis for gliotransmission; a secretion of various transmitters from astrocytes as a response to elevations in $[Ca^{2+}]_i$, which can

signal to adjacent neurons or other glial cells (Zorec et al., 2012). Moreover, Ca^{2+} is exploited by astrocytes as an intercellular signal that enables the formation of functionally connected astrocyte networks (Cornell-Bell et al., 1990a; Dani et al., 1992; Giaume and Venance, 1998; Kuga et al., 2011). Astrocytes have been shown to express numerous metabotropic receptors, that upon activation ultimately trigger production of inositol 1,4,5-triphosphate ($InsP_3$), leading to $InsP_3$-induced calcium release from the ER (Kastritsis et al., 1992; Finkbeiner, 1993; Porter and McCarthy, 1995; Kirischuk et al., 1996; Hamilton et al., 2008). For example, ATP, which acts via P2Y-receptors and the GTP-binding protein G_q, activates phospholipase C and subsequent formation of IP_3. Upon binding to its receptor (IP_3-receptor) located on the ER membrane, IP_3 initiates the opening of this receptor leading to the release of stored Ca^{2+} from the ER into the cytosol resulting in the activation of a number of Ca^{2+} dependent signaling mechanisms (Fam et al., 2000; Hamilton et al., 2008). This type of IP_3-mediated release of Ca^{2+} from internal stores is a mechanism that is used by many classical neurotransmitters including glutamate and acetylcholine (Ach) (Verkhratsky and Kettenmann, 1996; Verkhratsky et al., 1998). It has also been demonstrated that intercellular diffusion of IP_3 via gap junctions and IP_3-induced Ca^{2+} release, together with ATP mediated signaling, represent the main mechanisms governing the propagation of intercellular calcium waves that underlie long-range signaling in astrocyte networks (Guthrie et al., 1999; Kuga et al., 2011). Numerous proteins are located in the ER that regulate the movements of $[Ca^{2+}]_i$ across its membrane, and help to maintain the high Ca^{2+} gradient in the ER. For example, an ATP-dependent pump called smooth ER calcium ATPase (SERCA) located in the ER membrane, is one of the main ways in which this high ER Ca^{2+} gradient is maintained in a cell (Mattson et al., 2000b).

Many studies have illustrated that astrocytes have spontaneous Ca^{2+}-oscillations, which occur independently without any externally applied stimulus, and that such Ca^{2+} signaling may be essential for communication between neurons and astrocytes (Parri et al., 2001; Aguado et al., 2002; Nett et al., 2002). This increase in intracellular Ca^{2+} concentrations during spontaneous Ca^{2+} oscillations is either

initiated by the influx of extracellular Ca^{2+} via voltage-gated channels into the cytosol (Parri et al., 2001; Aguado et al., 2002), or by release from the ER-Ca^{2+} store (Parri and Crunelli, 2003; Wang et al., 2006). These spontaneous intracellular Ca^{2+} signals have particular characteristics, such as large amplitude and long duration. Furthermore, these oscillations may take place asynchronously in the distal processes of astrocytes, or they may propagate variable distances both intracellularly or intercellularly (Parri et al., 2001; Nett et al., 2002; Hirase et al., 2004).

No previous studies have been conducted to investigate the calcium signaling in astrocytes in any of the different forms of NCLs. As such, this study provides novel insights into the basic Ca^{2+}-based signaling properties of these cells.

Cln3$^{-/-}$ astrocytes have smaller and less frequent spontaneous calcium oscillations, and do not form a synchronized calcium wave

To explore the spontaneous calcium oscillations in WT and *Cln3$^{-/-}$* astrocytes, cultures were prepared as described in Chapter 2 (Section 2.3), then cells were plated onto PDL coated 25mm glass coverslips at a density of 50,000 cells/coverslip to study spontaneous calcium oscillations in non-sheet forming (low density) astrocyte cultures; or at density of 100,000 cells/coverslip to study spontaneous calcium oscillations in sheet-forming (high density), astrocyte cultures.

Spontaneous calcium oscillations were analyzed within 48 -72 hours of plating. $[Ca^{2+}]_{I,}$ was measured using the ratiometric and sensitive calcium indicator, Fura-2. Cultures were incubated with Fura-2 AM, which is lipid soluble and thus diffuses across the plasma membrane, in the presence of 0.02% pluronic acid, to aid loading, for a minimum of 20 minutes at 37°C. Subsequently, cultures were washed several times with recording medium (Chapter 2, Section 2.11). The fluorescence measurements were obtained at room temperature using an epifluorescence inverted microcope (Nikon, Japan) equipped with a 20x fluorite objective. In order to record the spontaneous Ca^{2+} oscillations present in WT and

Cln3$^{-/-}$ astrocytes, cultures were left untouched for at least 30 - 45 minutes (first 20 minutes is illustrated in Figures 4.1 and 4.2).

When WT astrocytes were cultured as non-sheet forming cells (low cell density) they began to show spontaneous calcium oscillations approximately 5 minutes after the start of the recordings, as can be seen from an increase in the ratio of excitation at 340nm and 380nm (F 340/380), which directly correlates with increased $[Ca^{2+}]_I$ (Figure 4.1). Once initiated, these $[Ca^{2+}]_I$ oscillations occurred frequently and randomly in WT astrocytes (Figure 4.1, grey bars illustrate the frequency of the oscillations). The amplitude of these spontaneous calcium oscillations was variable ranging from 10% to 120% above baseline (Figure 4.1). The spontaneous $[Ca^{2+}]_I$ oscillations in non-sheet forming *Cln3*$^{-/-}$ astrocytes were much less frequent and had a smaller amplitude than those observed in WT astrocytes (Figure 4.1, compare the frequency and amplitude of the spontaneous $[Ca^{2+}]_I$ oscillations marked with grey between WT and *Cln3*$^{-/-}$ astrocyte cultures). In addition, the initiation of the oscillations was more variable in *Cln3*$^{-/-}$ astrocytes, ranging from a few minutes to around 7 - 8 minutes after recordings were started. As in WT cultures, the amplitudes of these oscillations in non-sheet forming *Cln3*$^{-/-}$ astrocytes were variable, generally ranging from 10% to 50% above baseline, and rarely reaching more than 100% above baseline (Figure 4.1).

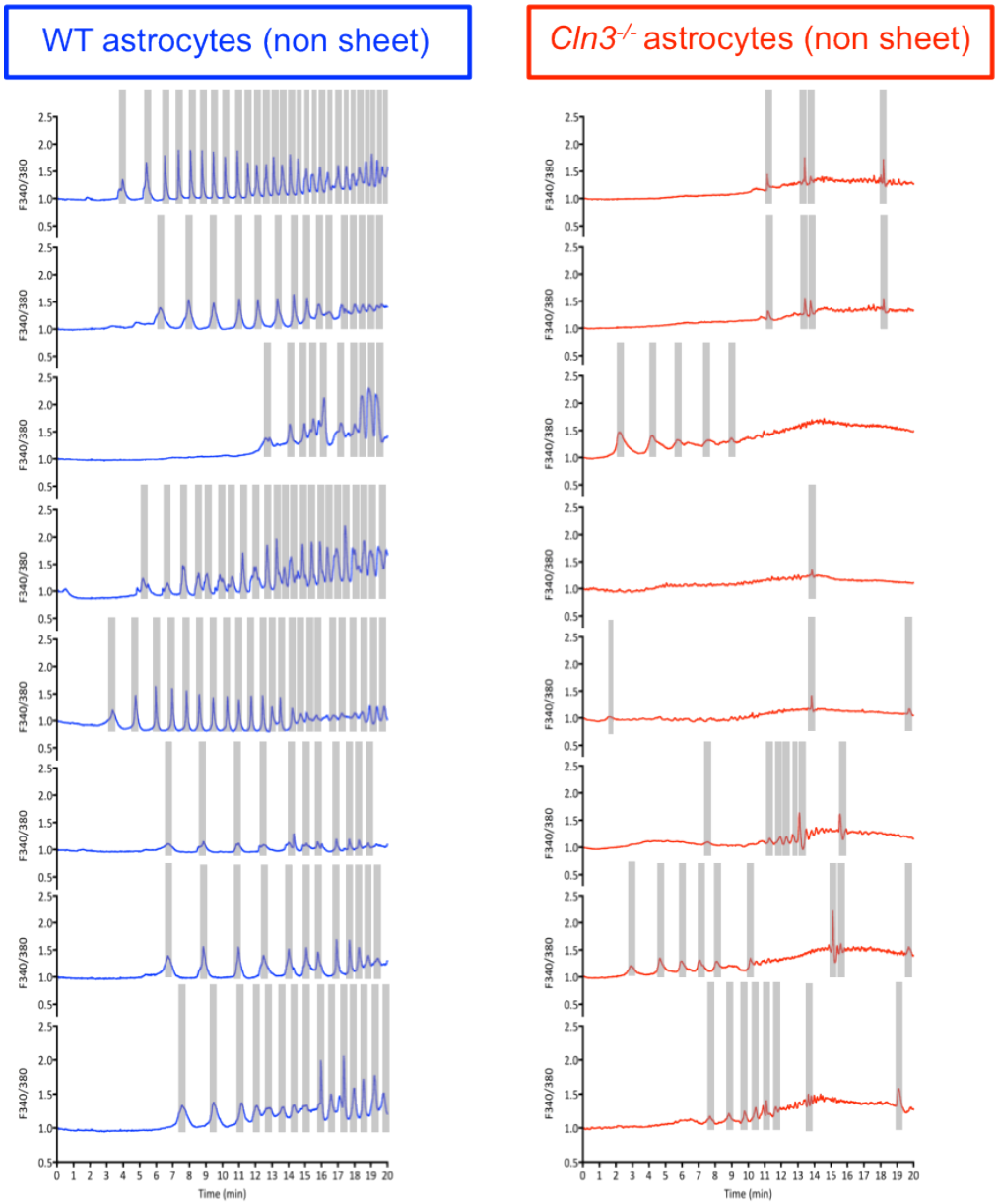

Figure 4.1. *Cln3*$^{-/-}$ astrocytes show specific alterations in spontaneous $[Ca^{2+}]_I$ oscillations. Recordings of Fura-2 fluorescence from WT and *Cln3*$^{-/-}$ astrocytes plated on PDL coated 25mm coverslip at a density of 50,000 cells/coverslip (non-sheet forming, 4.1) or 100,000/cells/coverslip (sheet forming, 4.2). Spontaneous $[Ca^{2+}]_I$ oscillations were measured from undisrupted, non-sheet forming WT and *Cln3*$^{-/-}$ astrocyte cultures under basal conditions over a period of 30-45 minutes, from which the first 20 minutes is shown. The figure illustrates the spontaneously induced changes in $[Ca^{2+}]_I$ in eight randomly selected WT and *Cln3*$^{-/-}$ astrocytes in one experiment. WT astrocytes had frequent, non-synchronized and large spontaneous $[Ca^{2+}]_I$ oscillations marked with grey bars. The *Cln3*$^{-/-}$ astrocytes exhibited less frequent and smaller spontaneous $[Ca^{2+}]_I$ oscillations. Data is presented as 340nm/380nm ratio, which directly correlates with the change in intracellular free Ca^{2+} levels. In total approximately 30-50 cells/experiment were recorded. This experiment was repeated twice.

In confluent, sheet-forming astrocyte cultures waves of $[Ca^{2+}]_I$ may propagate from cell to cell (Cornell-Bell et al., 1990a). This type of $[Ca^{2+}]_I$ wave propagation

between astrocytes may proceed with no obvious discontinuity, and with such a high velocity that it appears that the closely connected cells exhibit a simultaneous $[Ca^{2+}]_I$ elevation, hence the name 'calcium wave'. Also, these intercellular calcium waves are distinguishable from spontaneous oscillations in individual cells due to their larger amplitude and the prolonged plateau phase of the $[Ca^{2+}]_I$ elevation (Cornell-Bell et al., 1990a). The mechanism enabling this type of intercellular calcium signaling between astrocytes is not yet fully understood, but is thought to involve intercellular diffusion of IP_3 via gap junctions and ATP mediated signaling between adjacent astrocytes (Guthrie et al., 1999; Kuga et al., 2011). Indeed, the formation of a propagating calcium wave, which initiated approximately 6min after the start of the recordings, was obvious in high-density, sheet-forming WT astrocyte cultures (Figure 4.2, synchronized calcium wave marked with yellow bar). This synchronized, simultaneous $[Ca^{2+}]_I$ elevation among WT astrocytes had a typically large amplitude (from 150% up to nearly 250% increase above baseline), and a clear plateau phase with prolonged high intracellular calcium levels after the initiation of the wave (Figure 4.2). In sheet-forming *Cln3*$^{-/-}$ astrocyte cultures, however, formation of a synchronized, simultaneous $[Ca^{2+}]_I$ elevation did not occur (Figure 4.2). Instead, the *Cln3*$^{-/-}$ astrocytes showed spontaneous calcium oscillations that did not propagate as a wave. These spontaneous calcium oscillations occurred with a very low frequency, similar to those observed in non-sheet forming *Cln3*$^{-/-}$ astrocyte cultures (compare frequency of spontaneous calcium oscillations marked with grey in *Cln3*$^{-/-}$ astrocyte cultures in Figures 4.1 and 4.2). However, most of these $[Ca^{2+}]_I$ oscillations in sheet-forming *Cln3*$^{-/-}$ astrocyte cultures had a bigger amplitude (ranging from 10% to 100% increase above baseline) than in non-sheet forming *Cln3*$^{-/-}$ astrocyte cultures (compare the amplitude of spontaneous $[Ca^{2+}]_I$ oscillations in Figures 4.1 and 4.2). Overall, these results indicate that *Cln3*$^{-/-}$ astrocytes have less frequent and smaller spontaneous $[Ca^{2+}]_I$ oscillations when compared to WT astrocytes. Moreover, *Cln3*$^{-/-}$ astrocytes do not create a synchronized, propagating calcium wave suggesting that intercellular signaling between *Cln3*$^{-/-}$ astrocytes is compromised.

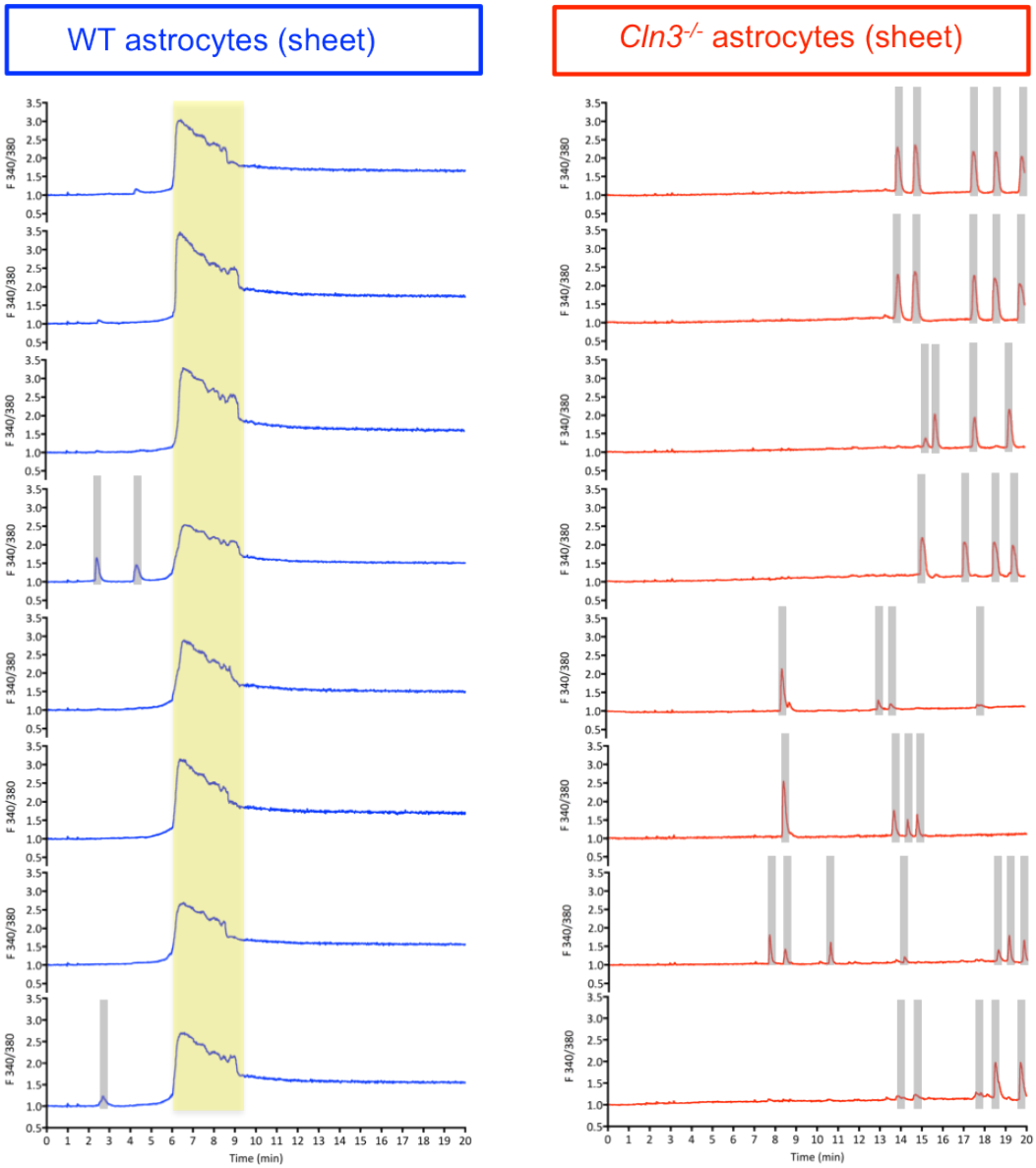

Figure 4.2. *Cln3*$^{-/-}$ astrocytes do not generate a synchronized calcium wave. In sheet-forming WT astrocyte cultures a spontaneously occurring propagating $[Ca^{2+}]_I$ wave was generated, marked with yellow bar, whereas spontaneous Ca^{2+} oscillations are marked with grey bar. This synchronized $[Ca^{2+}]_I$ wave had a large amplitude, and a prolonged plateau persisting for several minutes after initiation. The sheet-forming *Cln3*$^{-/-}$ astrocytes did not exhibit any propagating calcium waves, instead, *Cln3*$^{-/-}$ astrocytes had non-synchronized, spontaneous $[Ca^{2+}]_I$ elevations. In total 40-50 cells/experiment were recorded. This experiment was repeated twice.

One of the essential properties of astrocytes, which enables the intercytoplasmic exchange of ions and small molecules, is that they are highly coupled by gap junctions (Giaume and Venance, 1998). Correct assembly of connexin proteins is required for the formation of gap junctions and, in cultured astrocytes, the major connexin is connexin 43 (Cx43) (Dermietzel et al., 1991; Giaume et al., 1991). Indeed, synchronous $[Ca^{2+}]_I$ waves that comprise hundreds of astrocytes have

been proven to be sensitive to inhibition of gap junctions (Kuga et al., 2011). Given that synchronous $[Ca^{2+}]_I$ wave propagation did not occur in *Cln3*$^{-/-}$ astrocyte cultures, Cx43 expression was compared in WT and *Cln3*$^{-/-}$ astrocyte cultures by means of fluorescence immunocytochemistry (Figure 4.3). For this experiment, WT and *Cln3*$^{-/-}$ astrocytes were plated onto PDL coated 13mm glass coverslips at a density of 20,000 cells/coverslip. Cultures were fixed with 4% PFA in PBS 48h after plating and co-labeled with antibodies against Cx43 and GFAP. Both WT and *Cln3*$^{-/-}$ astrocytes showed punctate Cx43 staining localized relatively evenly around the whole cell body, as visualized with GFAP (Figure 4.3). Thus, no dramatic difference in the localization of Cx43 was observed between WT and *Cln3*$^{-/-}$ astrocytes. However, there appeared to be more Cx43 expression in WT astrocytes particularly at cell-to-cell contact regions (marked with dashed line, Figure 4.3). To confirm this observation quantification of the levels of Cx43 expression in WT and *Cln3*$^{-/-}$ should be carried out. Additionally, the connectivity between gap junctions (formed by connexin proteins) should be examined to determine whether they are functionally intact in *Cln3*$^{-/-}$ astrocytes. However, the observation that *Cln3*$^{-/-}$ astrocytes do express Cx43 in a relatively similar fashion to WT astrocytes suggests that gap junction formation is not overtly disrupted in these cells.

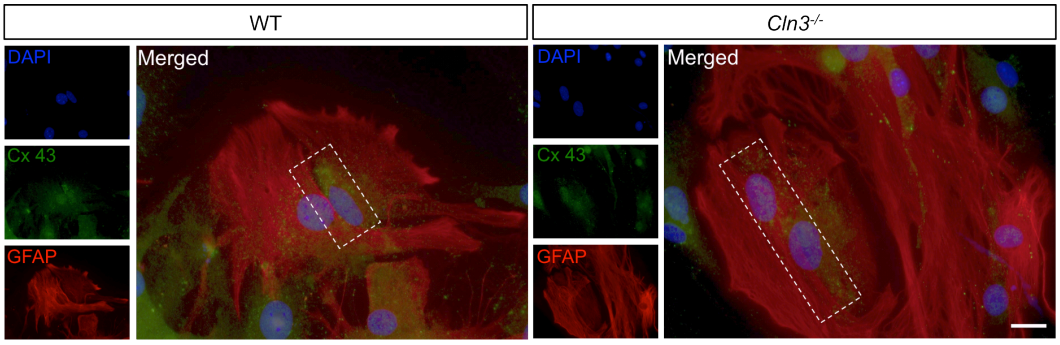

Figure 4.3. Connexin 43 is expressed by both *Cln3*$^{-/-}$ and WT astrocytes. WT and *Cln3*$^{-/-}$ astrocyte cultures were stained with GFAP to visualize the astrocyte cell bodies and with an antibody against connexin 43 (Cx43) and DAPI was used to visualize all nuclei. Both WT and *Cln3*$^{-/-}$ astrocytes expressed Cx43, which was expressed throughout the cytosol of the cells with no apparent difference in the localization. WT astrocytes express slightly more Cx43 than *Cln3*$^{-/-}$ astrocytes at cell-to-cell contact region marked with dashed line. Scale bar is 20µm.

Cln3$^{-/-}$ *astrocytes have a normal response to ATP*

It is well established that extracellular ATP can act as an activity-dependent signaling molecule, which is important for communication between neurons and astrocytes (Fields and Stevens, 2000; North and Verkhratsky, 2006). ATP based signaling is also important for propagation of the calcium wave, and thus communication among astrocytes (Guthrie et al., 1999; Stout et al., 2002). Upon binding to P2Y purinergic receptors, ATP induces PLC activation leading to IP_3-R activation and release of Ca^{2+} from the ER-stores. In order to compare this ATP induced Ca^{2+} release from the ER in WT and *Cln3*$^{-/-}$ astrocytes, cultures were established and the fluorescence based, ratiometric, calcium indicator, Fura-2, used to measure $[Ca^{2+}]_I$ levels, as described above. Subsequent to Fura-2AM loading, cells were washed with recording medium and then the Ca^{2+} recordings were carried out in this same medium (see Chapter 2, Section 2.11). The addition of ATP (100µM) took place approximately 2 minutes after the start of the recordings.

Examples of average Ca^{2+} traces from WT and *Cln3*$^{-/-}$ astrocytes (50 cells in each case/experiment) upon ATP application are presented in Figure 4.4 A. This ATP application induced a substantial, rapid increase in $[Ca^{2+}]_I$ levels in both WT (Δ(Max $[Ca^{2+}]_I$-baseline) is 2.44±0.42) and *Cln3*$^{-/-}$ (Δ(Max $[Ca^{2+}]_I$-baseline) is 2.39±0.28) astrocytes, followed by a sustained (plateau) Ca^{2+} elevation (Figure 4.4 A and B). There was no significant difference in the elevation of $[Ca^{2+}]_I$ induced by ATP between WT and *Cln3*$^{-/-}$ astrocytes (Figure 4.4 B). To explore how these cells return back to baseline following the ATP induced increase in $[Ca^{2+}]_I$ levels, the difference between the Maximum $[Ca^{2+}]_I$ levels and $[Ca^{2+}]_I$ levels 2 minutes after ATP application were calculated (presented as Δ(Max $[Ca^{2+}]_I$-$[Ca^{2+}]_I$ 2 min after ATP addition) (Figure 4.4 C). No significant difference in the ability of WT and *Cln3*$^{-/-}$ astrocytes to return back to baseline was found (Figure 4.4 C, Δ(Max $[Ca^{2+}]_I$-$[Ca^{2+}]_I$ 2min after ATP addition) is 1.68±0.31 for WT astrocytes and 1.61±0.18 for *Cln3*$^{-/-}$ astrocytes). These results suggest that WT and *Cln3*$^{-/-}$ astrocytes have a very similar response to ATP, and that the cellular mechanisms

involved in clearance of cytosolic Ca^{2+} resulting from an ATP activated Ca^{2+} response are not altered in *Cln3*$^{-/-}$ astrocytes.

A

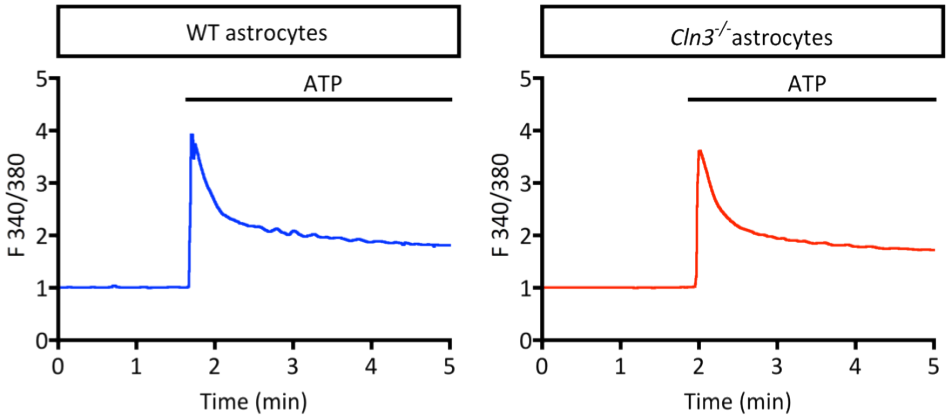

B

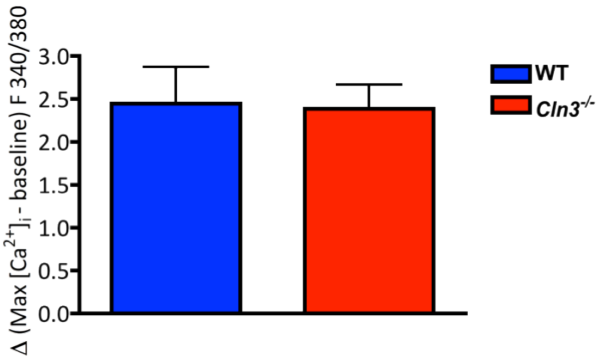

C

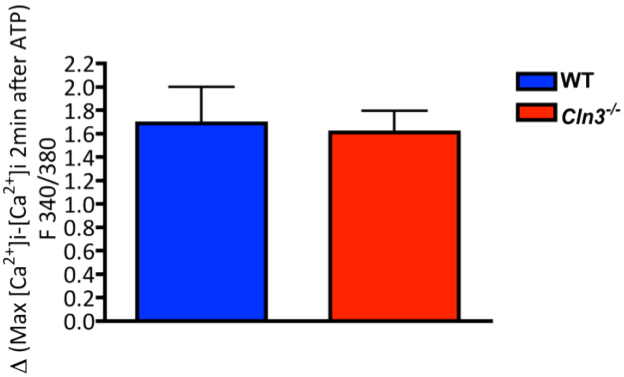

Figure 4.4. WT and *Cln3*$^{-/-}$ astrocytes show a similar response to ATP. Fura-2 was used to measure changes in $[Ca^{2+}]_I$ levels in both WT and *Cln3*$^{-/-}$ astrocytes upon ATP application. (A) Represents examples of typical calcium traces from WT and *Cln3*$^{-/-}$ astrocytes upon ATP application (100µM), which have been marked with a horizontal line. These calcium traces represent the average $[Ca^{2+}]_I$ level (50 cells in both cases/experiment) calculated from the ratio $Fura_{340}/Fura_{380}$, normalized to the first readout. Both WT and *Cln3*$^{-/-}$ astrocytes have a rapid, transient increase in $[Ca^{2+}]_I$ induced by ATP followed by a sustained (plateau) Ca^{2+} elevation. (B) Shows no significant difference in the maximum increase in $[Ca^{2+}]_I$ induced by ATP, presented as Δ(Max $[Ca^{2+}]_I$ – baseline) in WT and *Cln3*$^{-/-}$ astrocytes. (C) Shows no significant difference in the recovery of WT and *Cln3*$^{-/-}$ astrocytes after ATP treatment presented as Δ(Max $[Ca^{2+}]_I$-$[Ca^{2+}]_I$ 2min after ATP addition). In each experiment the intracellular calcium was measured from 30-55 cells and the experiment repeated six times. The mean percentages±SEM are shown in (B) and (C).

Cln3$^{-/-}$ *astrocytes release and clear ER-stored calcium differently to WT astrocytes*

Many Ca^{2+} signaling mechanisms are based on the highly regulated release of Ca^{2+} from intracellular stores, such as the ER. Indeed, the ER has its own inbuilt Ca^{2+} machinery to uptake and release Ca^{2+} appropriately. This machinery includes SERCA - calcium pumps that transport Ca^{2+} into the ER lumen against the concentration gradient (Camello et al., 2002; Beck et al., 2004). Additionally, the ER has Ca^{2+} release channels: IP_3-receptors activated by the second messenger IP_3; and RYRs (ryanodine/caffeine receptors) (Bezprozvanny, 2005; Hamilton, 2005). The Ca^{2+} release from the ER is thought to be crucial for gliotransmission and for intercellular signaling between astrocytes (Kuga et al., 2011; Parpura et al., 2011; Verkhratsky et al., 2012a). Thus, as an intracellular Ca^{2+} store, the ER serves two opposing roles; as a Ca^{2+} buffer by removing Ca^{2+} from the cytosol via activity of SERCA pumps, and as a releaser of Ca^{2+} in response to cell activation, causing an increase in the $[Ca^{2+}]_i$. Upon depletion of the intracellular Ca^{2+} stores, such as when thapsigargin is used to inhibit SERCA pump activity, the Ca^{2+} permeability of the plasma membrane increases. This type of Ca^{2+} influx pathway, associated with a reduced Ca^{2+} content in internal stores, is called either store-operated or capacitative Ca^{2+} entry (SOCE or CCE), and it takes place via store-operated Ca^{2+} channels (SOC) (Putney, 1990; Lo et al., 2002). Physiologically, the SOCE is important for both refilling after depletion of the ER - Ca^{2+} store and for producing the plateau phase of the transient $[Ca^{2+}]_I$ elevations - providing enough intracellular Ca^{2+} to outlast the period of cellular activation (Putney, 2007).

To compare the ER Ca^{2+} content, Ca^{2+} release from the ER and subsequent store-operated Ca^{2+} entry form the extracellular space in WT and *Cln3*$^{-/-}$ astrocytes, thapsigargin, a specific SERCA blocker, was used. WT and *Cln3*$^{-/-}$ astrocyte cultures were loaded with Fura-2AM, as described previously, then cells were washed three times with HBSS (-Ca^{2+}/ Mg^{2+}) to make sure that no Ca^{2+} was present in the medium. The baseline recordings were made in HBSS (-Ca^{2+}/ Mg^{2+}) and thapsigargin (1uM), prepared in HBSS (-Ca^{2+}/ Mg^{2+}), was added after 1

minute to specifically study the increase in $[Ca^{2+}]_I$ due to ER Ca^{2+} depletion. The Ca^{2+} release from the ER was monitored over the next 3 minutes, followed by addition of Ca^{2+} (100µM) to the medium to investigate the process of SOCE in these cells.

Thapsigargin administration induced highly variable responses in WT and *Cln3*$^{-/-}$ astrocytes (compare examples of WT (10 cells) and *Cln3*$^{-/-}$ (10 cells) Ca^{2+} traces, Figure 4.5 A). The WT astrocytes release Ca^{2+} from the ER relatively slowly, with all astrocytes showing a similar increase in $[Ca^{2+}]_i$ levels upon thapsigargin treatment (Figure 4.5 A). In contrast, some of the *Cln3*$^{-/-}$ astrocytes show a large and very rapid increase in $[Ca^{2+}]_i$ levels upon thapsigargin treatment, whereas some show a smaller and slower increase (Figure 4.5 A). The SOCE following Ca^{2+} depletion from the ER and subsequent application of Ca^{2+} (at 4 minutes, marked with blue horizontal line in Figure 4.5 A) was observed to be functional in both WT and *Cln3*$^{-/-}$ astrocytes; seen as a similar transient increase in $[Ca^{2+}]_i$.

In both WT and *Cln3*$^{-/-}$ astrocyte cultures great variability in the changes in $[Ca^{2+}]_i$ levels was observed within one experiment in response to thapsigargin. Thus, in order to further investigate the changes in $[Ca^{2+}]_I$ transients in these cultures, cells were grouped according to their maximum Ca^{2+} response to thapsigargin when compared to baseline. These groups were, 0-50%, 50%-100%, 100%-150%, 150%-200% and >200% increase in $[Ca^{2+}]_i$. The average % increase for WT and *Cln3*$^{-/-}$ astrocytes in each of these groups is presented in Figure 4.5 B, a. Most of the WT and *Cln3*$^{-/-}$ astrocytes belonged to a group showing a 100%-150% increase in $[Ca^{2+}]_i$ upon thapsigargin treatment (47.4±1.8% of WT astrocyte population, and 25.9±12.9% of *Cln3*$^{-/-}$ astrocyte population). The second most common group for WT astrocytes was the group with a 50%-100% increase in $[Ca^{2+}]_i$ upon thapsigargin treatment (33.7±8.2% of WT astrocyte population). In contrast, the second most common group for *Cln3*$^{-/-}$ astrocytes was the group with a >200% increase in $[Ca^{2+}]_i$ upon thapsigargin treatment (21.4±5.7% of *Cln3*$^{-/-}$ astrocyte population). No such grouping existed for WT astrocytes (Figure 4.5 B, a). Similar differences in response to thapsigarding were confirmed using

frequency distribution analysis (Figure 4.5 B, b). *Cln3*$^{-/-}$ astrocytes displayd a larger variation in their response to thapsigargin compared to WT astrocytes (Figure 4.5 B, b). This difference was statistically significant based on the Kolmogorov-Smirnov test (D=0.35 and P=0.000). The maximum increase in $[Ca^{2+}]_i$ in response to thapsigargin within each group was also compared for WT and *Cln3*$^{-/-}$ astrocytes (Figure 4.5 C). For WT astrocytes these were 9.4±9.4% (0-50%), 75.8±2.4% (50%-100%), 125.2±3.1% (100%-150%) and 169.8±1.8% (150%-200%); and for *Cln3*$^{-/-}$ astrocytes were 18.1±10.9% (0-50%), 59.8±20.4% (50%-100%), 103.7±31.6% (100%-150%), 171.0±1.2% (150%-200%) and 244.7±17.5% (>200%). No significant differences were observed, except for the presence of the distinct population of *Cln3*$^{-/-}$ astrocytes, which displayed a very high increase in $[Ca^{2+}]_i$ (244.7±17.5%) following thapsigargin treatment. Thus, both WT and *Cln3*$^{-/-}$ astrocytes showed a heterogeneous response to thapsigargin, possibly due to variability in their ER Ca^{2+} content. Interestingly, a small subpopulation of *Cln3*$^{-/-}$ astrocytes were identified that displayed a very high increase in $[Ca^{2+}]_I$ upon inhibition of SERCA-pumps, suggesting that these astrocytes have a high amount of stored intracellular Ca^{2+}.

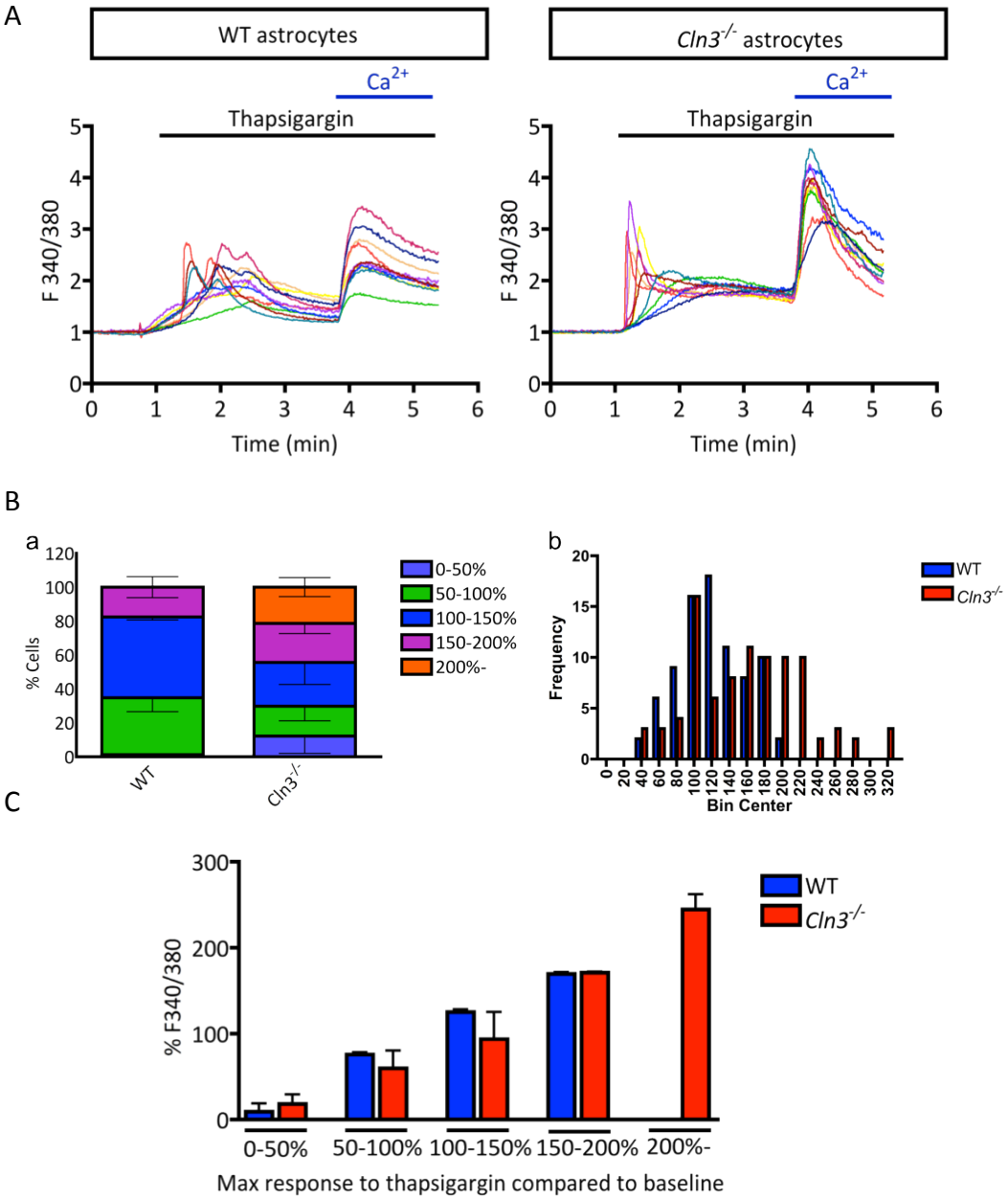

Figure 4.5. WT and *Cln3*$^{-/-}$ astrocytes display a variable response to thapsigargin. Fura-2 was used to measure the changes in $[Ca^{2+}]_i$ levels in both WT and *Cln3*$^{-/-}$ astrocytes upon thapsigargin application, and subsequent Ca^{2+} entry via SOCE upon externally applied Ca^{2+} (store operated calcium entry). (A) Examples of typical calcium traces in WT and *Cln3*$^{-/-}$ astrocytes upon thapsigargin application (1µM) (marked with black horizontal line, 10 randomly selected cells from one experiment in each case). Bath application of Ca^{2+} (100µM), which enabled SOCE, is marked with blue horizontal line. Thapsigargin induced heterogeneous Ca^{2+} transients in both WT and *Cln3*$^{-/-}$ astrocytes and SOCE was not altered in either genotype. (B) a Shows the average percentage of WT and *Cln3*$^{-/-}$ astrocytes from total cells measured grouped according to their maximum increase in $[Ca^{2+}]_i$ upon thapsigargin treatment. *Cln3*$^{-/-}$ astrocyte cultures contain a subpopulation of cells that exhibit a high increase in $[Ca^{2+}]_i$ upon thapsigargin treatment. b The frequency distribution is greater in *Cln3*$^{-/-}$ astrocyte population. (C) Average maximum increase in $[Ca^{2+}]_i$ within grouped WT and *Cln3*$^{-/-}$ astrocytes, showing no significant differences between WT and *Cln3*$^{-/-}$ astrocyte cultures, except for the subpopulation of *Cln3*$^{-/-}$ astrocytes with very high $[Ca^{2+}]_i$ levels induced by thapsigargin. In each experiment the intracellular calcium was measured from 20-50 cells and was repeated four times. The mean percentage±SEM are shown in (B) and (C).

Following thapsigargin-induced Ca^{2+} release from the ER, Ca^{2+} is cleared from the cytosol by being taken up by other intracellular stores, such as mitochondria or lysosomes, or by being transported into the extracellular space. In order to compare these types of Ca^{2+} clearance mechanisms in WT and *Cln3*$^{-/-}$ astrocytes, the difference between the maximum increase in $[Ca^{2+}]_I$ induced by thapsigargin and remaining levels of $[Ca^{2+}]_I$ after thapsigargin application (presented as Δ(Max $[Ca^{2+}]_I$ - Min $[Ca^{2+}]_I$)) were calculated (Figure 4.6 A, a and b). Due to the heterogeneous response to thapsigargin in both WT and *Cln3*$^{-/-}$ astrocyte cultures, as shown above, the recovery process was studied only between cells, which had a similar response to thapsigargin treatment (increase in $[Ca^{2+}]_I$ induced by thapsigargin >50% and <200% compared to baseline). WT astrocytes (Figure 4.6 A, a) showed a complete recovery after thapsigargin treatment, with $[Ca^{2+}]_I$ levels returning back to baseline. However, the recovery of *Cln3*$^{-/-}$ astrocytes appeared attenuated (Figure 4.6 A, b), with prolonged high $[Ca^{2+}]_I$ levels being observed following treatment. Indeed, there was a significant difference in Δ(Max $[Ca^{2+}]_I$ - Min $[Ca^{2+}]_I$) between WT and *Cln3*$^{-/-}$ astrocytes (26.0±5.6% decrease in Δ(Max $[Ca^{2+}]_I$ - Min $[Ca^{2+}]_I$) in *Cln3*$^{-/-}$ astrocytes compared to WT) (Figure 4.6 B). Thus, this attenuated recovery in *Cln3*$^{-/-}$ astrocytes following thapsigargin treatment may suggest that cytosolic Ca^{2+} clearance mechanisms are altered in *Cln3*$^{-/-}$ astrocytes.

A

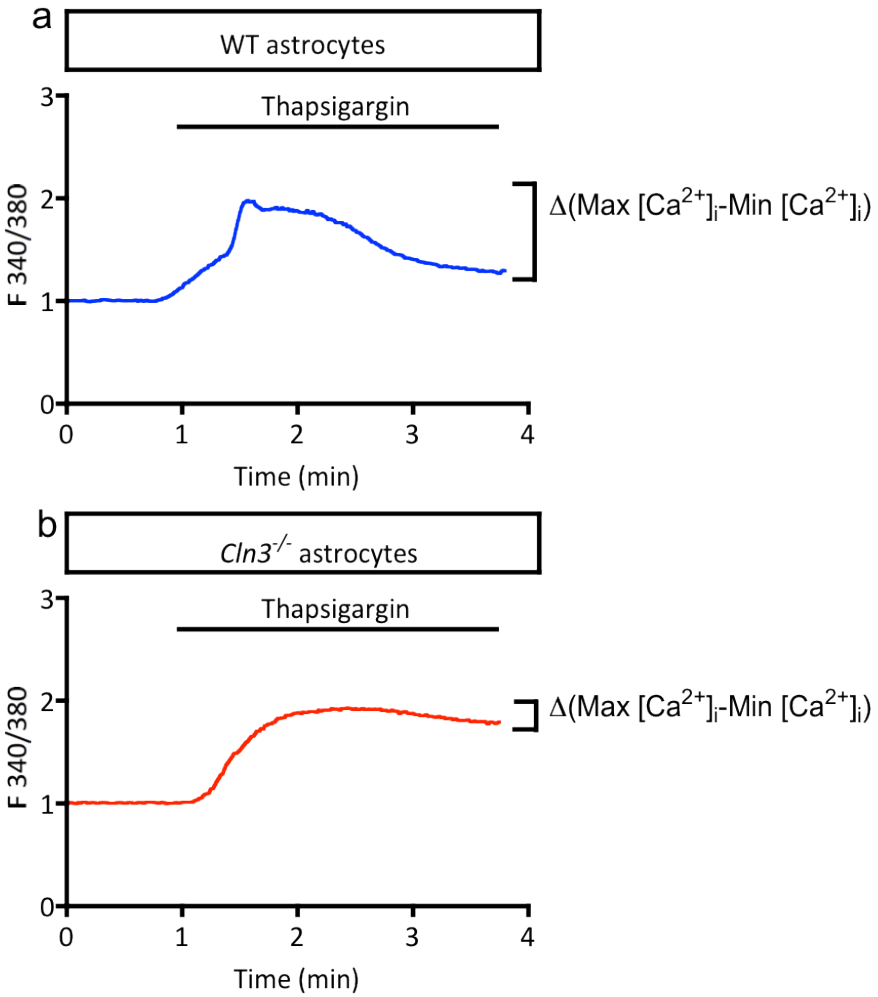

B

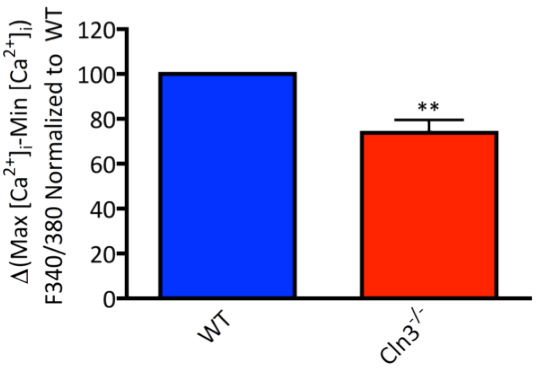

Figure 4.6. Cytosolic Ca^{2+} is not cleared properly in *Cln3*$^{-/-}$ astrocytes. (A) Typical Ca^{2+} traces (average of 15-30 cells per genotype per experiment) in WT (a) and *Cln3*$^{-/-}$ (b) astrocytes that have similar response to thapsigargin treatment (Max $[Ca^{2+}]_I$ induced by thapsigargin compared to baseline between 50% and 200%). The marked Δ(Max $[Ca^{2+}]_I$ - Min $[Ca^{2+}]_I$ illustrates the difference in cytosolic Ca^{2+} clearance between WT and *Cln3*$^{-/-}$ astrocytes. (B) Shows mean average±SEM of Δ(Max $[Ca^{2+}]_I$ - Min $[Ca^{2+}]_I$ values normalized to WT astrocyte values. The *Cln3*$^{-/-}$ astrocytes have a significantly smaller Δ(Max $[Ca^{2+}]_I$ - Min $[Ca^{2+}]_I$ value compared to WT astrocytes. In each experiment 10-40 cells were analyzed. Data is from 4 separate experiments.

Cln3$^{-/-}$ astrocytes show impaired protein secretion

Secretion of soluble factors is one of the key features of astrocytes under both physiological and pathological conditions (Ridet et al., 1997; Dong and Benveniste, 2001; Lucas et al., 2006; Farina et al., 2007; Bélanger and Magistretti, 2009; Sofroniew and Vinters, 2010). Astrocytes can secrete a wide range of neurotrophic factors, such as NGF and BDNF, that can support the survival of existing neurons, and potentially stimulate the growth and differentiation of new neurons and synapses (Miklic et al., 2004). Under pathological conditions, astrocytes may also enhance the secretion of a wide range of cytokines, chemokines and mitogens that are all important players in the inflammation process within the CNS (Ridet et al., 1997; Farina et al., 2007). These secreted soluble factors may have positive or negative effects within the brain (Ridet et al., 1997; Liberto et al., 2004; Cassina et al., 2005; Farina et al., 2007; Bélanger and Magistretti, 2009; Sofroniew and Vinters, 2010), and this response is compounded by the complex interactions that can occur between astrocyte-secreted proteins and those secreted by microglia, the other 'immune' cell in the brain (Minagar et al., 2002; Wyss-Coray and Mucke, 2002). Neuroinflammation and the appearance of autoantibodies in the CNS of *Cln3* deficient mice, as well as JNCL patient derived *post mortem* material, have been shown to play a role in the pathogenesis of this disease (Mitchison et al., 1999; Lim et al., 2007; Cooper, 2010; Seehafer et al., 2011). To determine whether difference in the protein secretion profile of *Cln3*$^{-/-}$ astrocytes could play a role in JNCL, a quantitative immunoassay (conducted by *Rules Based Medicine Inc*.) was used to compare the protein secretion of WT and *Cln3*$^{-/-}$ astrocytes under basal and LPS/IFNγ treated conditions.

To compare the protein secretion profiles of WT and *Cln3*$^{-/-}$ astrocytes, tissue culture supernatants were collected from untreated cultures and those that had been treated with LPS/IFNγ for 6 hours, 24 hours or 72 hours. The quantitative immunoassay employed (RodentMAP, Myriad RBM) enabled the simultaneous analysis of 59 different proteins from each sample. Given that *Cln3*$^{-/-}$ astrocytes proliferate slower than WT astrocytes (see Chapter 3, Figure 3.9), the protein

expression levels obtained for each sample were normalized to the relative number of cells present in the culture. Some of the proteins analyzed in this assay were secreted below detectable levels, and thus were excluded from this assay. The proteins analyzed were divided into subgroups according to their function: chemokines, anti-and pro- inflammatory cytokines, mitogens, proteins with vascular/haematological functions, and finally pleiotropic factors. All the data from this analysis is presented in Tables 4.1 and 4.2 (abbreviations explained in the list of abbreviations). Table 4.1 illustrates the differences in secreted levels of each protein between *Cln3*$^{-/-}$ and WT astrocyte cultures under basal conditions, while Table 4.2 illustrates differences between LPS/IFNγ treated samples. The difference in secreted protein levels is presented as the %change calculated by comparing protein expression values in *Cln3*$^{-/-}$ astrocyte samples to those in the corresponding WT astrocyte samples.

In general, this analysis revealed small, but specific, changes in the levels of secreted proteins between WT and *Cln3*$^{-/-}$ astrocytes under untreated conditions (Table 4.1). However, the levels of secreted proteins were generally reduced in *Cln3*$^{-/-}$ astrocyte cultures compared to their corresponding WT cultures upon exposure to LPS/IFNγ (Table 4.2). This reduction was more dramatic with prolonged exposure to the activation stimulus (Table 4.2).

After 24h of stimulation, proteins that were secreted at significantly lower levels by *Cln3*$^{-/-}$ astrocytes could be observed in all categories studied. Out of the 59 screened factors none (at 6h), 19 (at 24h) and 42 (at 72h) were secreted at significantly lower levels by *Cln3*$^{-/-}$ astrocytes upon activation with LPS/IFNγ. These included the reduced secretion of several mitogens (M-CFS, IL-3, FGF2, GM-CSF, FGF-9, TPO and IL-5), chemokines (Eotaxin, MIP1a, MCP-3, MCP-1, KC/GROa, MIP-3b, MIP-2, IP-10, RANTES, MDC, MCP-5, MIP-1γ, GCP-2 and MIP-1b), anti- and pro-inflammatory cytokines (IL-17a, IL-6, IL-12p70, IL-1 α, TNF α, IL-1b, IL-10, IL-2). Importantly, these cells also showed an impaired ability to secrete a range of neuroprotective proteins (IL-6, IL-3, GM-CSF, IL-10, MCP-1,

RANTES, and LIF). This data suggests that stimulated *Cln3*$^{-/-}$ astrocytes exhibit a markedly altered protein secretion profile (see Figure 4.7 for specific examples).

There were however, notable exceptions to these rules. Two of the chemokines: macrophage inflammatory protein-1γ (MIP-1γ) and glutamate carboxypeptidase 2 (GCP-2) were both secreted at significantly lower levels by *Cln3*$^{-/-}$ astrocytes compared to WT astrocytes under basal conditions (an observed reduction of 83.0±0.2% and 95.5±16.7% respectively), as was one mitogen analyzed, macrophage colony-stimulating factor (M-CSF, 41.4±0.5% reduction compared to WT at 72h).

Only one protein, tissue factor (TF), was secreted at higher levels by *Cln3*$^{-/-}$ astrocytes that WT astrocytes under basal conditions (97.3±84.5% increase at 72h), which is the major initiator of the coagulation protease cascade. Indeed, it has been suggested that astrocytes function as the primary source of TF in the CNS, making astrocytes the main regulators of haemorrhage in the brain (Eddleston et al., 1993).

Three proteins were found to be secreted significantly more by *Cln3*$^{-/-}$ astrocytes upon stimulation. These factors were the mitogen CRP (82.3±47.9% increase at 24h), fibrinogen (80.1±31.7% increase at 24h) and the anti-inflammatory factor immunoglobulin A (IgG A) (130.2±70.5% increase at 24h). Interestingly, CRP is an acute-phase protein, whose level increases during inflammation, and is involved in the activation of the complement system via C1q complex (Thompson et al., 1999; Wight et al., 2012).

Mitogens	6h Untreated	24h Untreated	72h Untreated
CRP mouse	78.5%±27.3	14.2%±8.3	31.7%±4.1
M-CSF	18.5%±18.1	−32.2%±16.1	−41.5%±0.5 *
EGF	17.1%±6.7	26.5%±19.5	20.2%±11.8
IL-3	−5.3%±16.	14.0%±39.0	31.1%±29.1
FGF basic	−0.3%±24.9	0.4%±5.2	−25.5%±10.1
SCF	−20.6%±23.6	−64.3%±1.2	−57.3%±1.7
GM-CSF	−30.7%±14.2	−35.4%±2.1	27.9%±36.7
FGF-9	−21.4%±16.8	-	−31.5%±13.5
TPO	-	-	-
IL-5	-	-	-
Pro-inflammatory	**6h Untreated**	**24h Untreated**	**72h Untreated**
IFN γ	−13.9%±20.3	−40.7%±5.4	−22.8%±5.9
IL-17a	-	56.5.5%±0	−14.6%±13.4
Oncostatin M	−11.9%±17.1	−39.9%±12.2	−51.8%±0.9
IL-6	−57.4%±4.7	−72.9%±0.5	−68.6%±1.8
IL-12p70	-	−49.4%±7.9	-
IL-1 α	−29.6%±11.8	−48.6%±1.9	−45.3%±2.6
IL-18	152.9%±204.7	64.6%±69.0	-
TNF α	19.6%±16.8	−51.5%±5.0	−47.6%±6.3
CD40 ligand	-	-	-
IL-1 β	31.9%±33.9	−74.9%±25.1	0.7%±57.7
Vascular/haematological	**6h Untreated**	**24h Untreated**	**72h Untreated**
Tissue Factor	168.5%±76.4	237.6%±56.7	97.3%±84.5 *
Haptoglobin	3.2%±6.0	−15.3%±4.9	10.1%±14.8
VEGF	3.9%±26.7	1.2%±23.0	−0.3%±2.5
Endothelin	17.9%±25.0	4.8%±25.6	10.6%±72.2
Factor VII	4.9%±5.5	−8.2%±14.2	−8.9%±5.6
Fibrinogen	10.8%±7.4	7.6%±8.0	6.2%±1.0
MPO	-	-	-
SAP	-	-	-
vWF	-	-	-
Chemokines	**6h Untreated**	**24h Untreated**	**72h Untreated**
Eotaxin	39.2%±47.1	−44.7%±0	−55.9%±15.2
MIP-1 α	10.1%±2.8	−6.8%±11.8	−44.1%±3.6
MCP-3	−68.1%±5.3	−74.8%±6.7	−82.1%±0.5
MCP-1	−63.2%±5.8	−74.1%±7.4	−81.5%±0.5
KC/GRO α	-	-	−93.7%±0.2
Lymphotactin	8.9%±13.1	−40.2%±21.0	−41.9%±0.9
MIP-3 β	21.8%±8.5	−5.6%±11.2	−7.4%±5.7
MIP-2	−37.0%±6.1	−35.4%±2.1	−44.7%±3.2
IP-10	−58.8%±6.3	−77.3%±3.2	−62.7%±4.9
RANTES	−73.4%±5.3	−71.5%±3.4	−73.9%±1.7
MDC	45.2±39.4	−23.8±7.6	−45.5±7.5
MCP-5	−71.2%±2.6	−79.9%±1.5	−83.1%±1.5
MIP-1 γ	−78.3%±2.9	−84.5%±2.9	−83.0%±0.2 ***
GCP-2	-	−94.8%±1.0	−95.5%±16.7 ***
MIP-1 β	−45.9%±7.5	−66.4%±3.6	−80.7%±1.5
Anti-inflammatory	**6h Untreated**	**24h Untreated**	**72h Untreated**
IgG A	68.6%±50.8	16.6%±6.8	49.3%±16.0
IL-4	-	-	-
IL-10	-	-	-
IL-2	-	-	-
Pleiotropic /others	**6h Untreated**	**24h Untreated**	**72h Untreated**
LIF	−30.8%±4.7	−19.5%±11.7	−19.1%±3.9
TIMP1	10.1%±15.0	−62.5%±4.0	−61.8%±1.7 *
IL-11	−48.7%±3.8	−71.5%±0.1	−55.5%±1.6
IL-7	-	−23.9%±3.1	−34.4%±2.7
VCAM1	−54.4%±5.8	−47.3%±6.2	−46.0%±3.6
GST-α	-	-	-
CD40	-	-	-
MMP 9	-	-	-
Myoglobin	-	-	-
Apolipoprotein A-I	-	-	-
SGOT	-	-	-

Table 4.1. Differences in protein secretion under basal unstimulated conditions. This table presents differences between levels of secreted proteins, classified according to their function, in supernatants collected after 6h, 24h and 72h from *Cln3*$^{-/-}$ astrocyte cultures and WT astrocyte cultures grown under basal conditions. Data presented as %change (values from *Cln3*$^{-/-}$ astrocyte samples compared to corresponding WT astrocyte values)±SEM from three biological replicates. Data not shown (-) where protein levels were below quantifiable detection levels. Abbreviations explained in the list of abbreviations page 14.

Mitogens	6h LPS/IFNY	24h LPS/IFNY	72h LPS/IFNY
CRP mouse	62.8%±44.5	82.3%±47.9 *	11.0%±15.6
M-CSF	60.9%±3.2	−14.3%±37.7	−21.1%±4.0 *
EGF	35.2%±2.8	29.1%±33.8	−31.6%±6.8 ***
IL-3	29.2%±10.8	−22.6%±37.8	−49.8%±3.1***
FGF basic	5.6%±13.0	−30.5%±17.6	−57.8%±2.1 ***
SCF	−3.4%±1.5	32.0%±49.0	−4.7%±3.5
GM-CSF	−3.4%±35.6	−20.3%±39.0	−88.1%±1.2 ***
FGF-9	−8%±11.8	−29.1%±30.6	−57.3%±1.1 ***
TPO	-	−61.4%11.8 **	−72.0%±4.7 ***
IL-5	-	-	-
Pro-inflammatory	**6h LPS/IFNY**	**24h LPS/IFNY**	**72h LPS/IFNY**
IFN γ	101.8%±67	34.2%±62.9	−92.4%±0.1 ***
IL-17a	18.8%±8.6	−59.5%±17.6 **	−80.3%±0.5 ***
Oncostatin M	16.2%±3.1	47.5%±53.6	4.0%±3.0
IL-6	−6.4%±12.4	−77.8%±10.9 ***	−93.9%±0.5 ***
IL-12p70	−9.7%±4.0	−44.3%±25.8	−72.3%±1.9 ***
IL-1 α	−14.9%±3.2	−6.0%±40.4	−70.0%±2.2 ***
IL-18	−40.6%±18.6	15.6%±74.5	−90.2%±4.9 **
TNF α	−43.8%±1.9	−53.3%±18.9 **	−71.4%±1.8 ***
CD40 ligand	-	28.8%±76.4	21.0%±50.0
IL-1 β	-	−66.3%±18.3	−53.8%±3.5 **
Vascular/haematological	**6h LPS/IFNY**	**24h LPS/IFNY**	**72h LPS/IFNY**
Tissue Factor	215.4%±79	−69.1%±12.2 **	−72.6%±6.2 ***
Haptoglobin	53.2%±23.1	143.0%±19.4	74.3%±26.7
VEGF	30%±6.4	−44.8%±25.1	−76.0%±1.9 ***
Endothelin	23%±19.1	−43.3%±28.4	−68.2%±4.4 ***
Factor VII	8.5%±6.8	1.8%±28.7	−42.4%±3.5 ***
Fibrinogen	5.0%±0.6	80.1%±31.7 ***	5.6%±5.0
MPO	-	-	-
SAP	-	-	-
vWF	-	-	-
Chemokines	**6h LPS/IFNY**	**24h LPS/IFNY**	**72h LPS/IFNY**
Eotaxin	73.5%±48.0	−71.03%±12.3 ***	−71.7%±2.8 ***
MIP-1 α	61.0%±3.2	−81.5%±8.0 **	−70.5%±1.1 ***
MCP-3	46.7%±54.5	−26.7%±35.1	−63.9%±2.3 ***
MCP-1	46.7%±4.8	−40.9%±28.5	−73.5%±1.4 ***
KC/GRO α	29.7%±32.8	−27.5%±35.6	−74.4%±3.7 ***
Lymphotactin	28.6%±6.0	40.4%±46.7	−3.6%±4.0
MIP-3 β	19.4%±5.7	−67.2%±10.5 ***	−73.2%±0.9 ***
MIP-2	19.3%±41.3	−51.2%±23.7 *	−86.4%±2.1 ***
IP-10	15.4%±8.4	−22.8%±29.4	−48.7%±5.6 ***
RANTES	−9.9%±22.6	−29.8%±33.7	−66.5%±3.4 ***
MDC	−22.5±12.6	−90.4±4.2 ***	−86.4±3.2 ***
MCP-5	−27.8%±12.6	−62.5%±17.8	−67.7%±0.9 ***
MIP-1 γ	−52.4%±6.5	−75.2%±11.6 ***	−55.0%±5.7 ***
GCP-2	−57.8%±16.7	−87.9%±5.8 ***	−84.4%±0.8 ***
MIP-1 β	−70.1%±2.4	−88.9%±4.8 ***	−81.7%±1.4 ***
Anti-inflammatory	**6h LPS/IFNY**	**24h LPS/IFNY**	**72h LPS/IFNY**
IgG A	123.8%±46.4	130.2%±70.5 **	49.7%±11.8
IL-4	57.9%±32.2	1.3%±31.1	−45.0%±3.5 ***
IL-10	36.1%±14.9	−48.3%±23.6 *	−75.4%±0.9 ***
IL-2	5.2%±6.6	−49.4%±23.8 **	−77.3%±0.7 ***
Pleiotropic /others	**6h LPS/IFNY**	**24h LPS/IFNY**	**72h LPS/IFNY**
LIF	40.1%±15.0	−31.8%±30.3	−72.3%±1.5 ***
TIMP1	32.1%±32.8	−57.9%±20.8 *	−62.5%±2.0 ***
IL-11	27.0%±6.9	−37.0%±26.7	−72.4%±4.8 ***
IL-7	6.5%±2.7	20.6%±41.9	−13.9%±1.4
VCAM1	−2.0%±9.1	−48.3%±22.3 **	−51.5%±2.8 ***
GST-α	-	−27.0%±30.1	−47.2%±15.7
CD40	-	−52.0%±21.4	−84.8%±2.9 ***
MMP 9	-	−85.1%±8.6 ***	−82.2%±0.3 ***
Myoglobin	-	-	-
Apolipoprotein A-I	-	-	-
SGOT	-	-	-

Table 4.2. Stimulated *Cln3*$^{-/-}$ astrocytes show attenuated protein secretion. This table presents differences between levels of secreted proteins, classified according to their function, in supernatants collected from *Cln3*$^{-/-}$ astrocytes and WT astrocytes after LPS/IFNγ induced activation for 6h, 24h and 72h. Data presented as %change (*Cln3*$^{-/-}$ astrocyte sample values compared to corresponding WT astrocyte values)±SEM from three biological replicates. Data not shown (-) where protein levels were below quantifiable detection levels. Abbreviations explained in the list of abbreviations page 14.

To illustrate the change in the protein secretion between untreated and LPS/IFNγ treated WT and *Cln3*$^{-/-}$ astrocytes over the studied time course, the protein expression levels of some selected proteins are presented in Figure 4.7 A-C. Graphs showing the protein expression profile over 6 hours, 24 hours and 72 hours of three chemokines, MIP-2, MIP-1β and MIP-1α, are shown in Figure 4.7 A, in which it is apparent that neither WT (blue line) nor *Cln3*$^{-/-}$ (red line) astrocytes secrete high levels of any of these chemokines under basal conditions. However, upon stimulation, secretion of these proteins is dramatically increased from WT astrocytes (blue dotted line), whereas *Cln3*$^{-/-}$ astrocytes (red dotted line) do not show any elevated secretion of these proteins (Figure 4.7 A). Similar secretion profiles are illustrated for three proteins with neuroprotective properties (IL-6, TNF-alpha and VEGF, Figure 4.7 B). Under basal conditions WT and *Cln3*$^{-/-}$ astrocytes both secrete moderate amounts of these factors, whereas LPS/IFNγ induced activation only results in enhanced secretion of these factors by WT astrocytes. As mentioned above, not all the proteins screened were secreted at lower levels by *Cln3*$^{-/-}$ astrocytes upon stimulation, for example, CRP and IgG A were secreted at higher levels (Figure 4.7 C), thus it appears that *Cln3*$^{-/-}$ astrocytes do have the capacity to secrete increased levels of some proteins into their environment when they are stimulated.

Overall, a significant decrease in the ability of *Cln3*$^{-/-}$ astrocytes to secrete a range of proteins following stimulation was observed. One can speculate that under chronic pathological situations, like in JNCL, this may have a significant impact on disease progression.

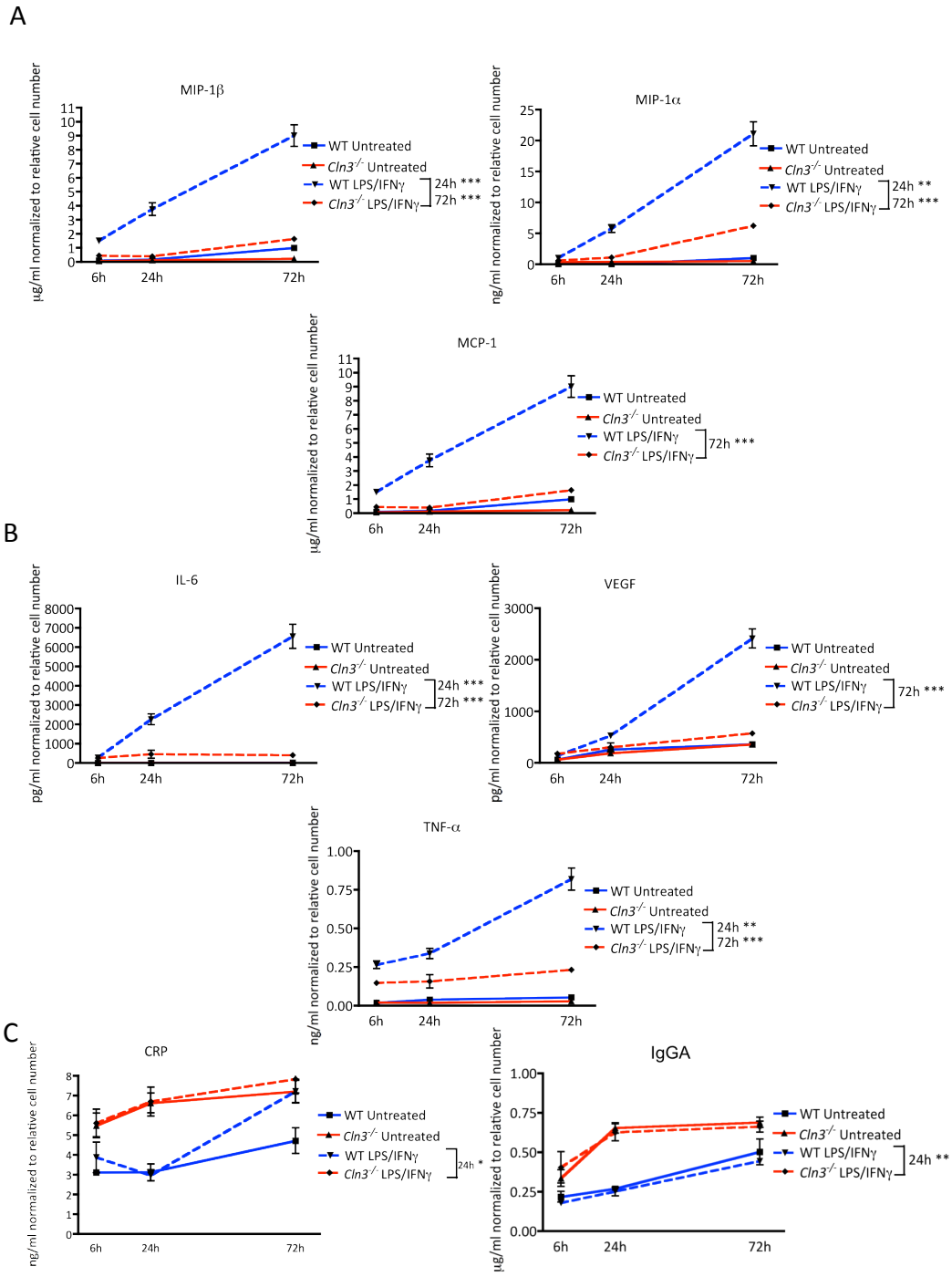

Figure 4.7. *Cln3*$^{-/-}$ astrocytes show alterations in their ability to secrete proteins. Secreted protein levels were quantified from supernatant derived from untreated and LPS/IFNγ treated WT and *Cln3*$^{-/-}$ astrocyte cultures. Examples of chemokines (A), neuroprotective factors (B) and proteins secreted at elevated levels by *Cln3*$^{-/-}$ astrocytes following activation (C), are provided. (A) *Cln3*$^{-/-}$ astrocytes secreted significantly less MIP-1ß, MIP-1α and MCP-1 when treated with LPS/IFNγ that do WT astrocytes. There was no significant difference between untreated WT and *Cln3*$^{-/-}$ samples. (B) *Cln3*$^{-/-}$ astrocytes secreted significantly less IL-6, TNF-α and VEGF upon activation than did *WT astrocytes*. There was no significant difference between untreated samples. (C) *Cln3*$^{-/-}$ astrocytes secreted significantly more CRP and IgG A after 24h exposure to LPS/IFNγ, no such change was observed in WT astrocytes. Data presented as mean expression values±SEM.

One possible explanation for the observed lack of protein secretion by *Cln3*$^{-/-}$ astrocytes, may be an inability to produce these proteins by these cells. This possibility was tested by quantifying the intracellular levels of two of these proteins, TNF-α and MIP-1γ, for which good antibodies were available by means of Western blotting.

To carry out these measurements, WT and *Cln3*$^{-/-}$ astrocytes were plated on 6-well plates (100,000 cells/well) and grown for 24h in the presence or absence of LPS/IFNγ before lysates were prepared for Western blotting (Chapter 2, Section 2.7). The intracellular expression levels of TNF-α and MIP1-γ were quantified and the protein expression levels in *Cln3*$^{-/-}$ astrocyte samples were normalized to matching WT samples. The intracellular TNF-α levels were higher in both untreated and LPS/IFNγ treated *Cln3*$^{-/-}$ astrocytes than in WT astrocytes (Figure 4.8 A). This increase was statistically significant in LPS/IFNγ treated samples, where *Cln3*$^{-/-}$ astrocytes contained 36.4±8.4% more intracellular TNF-α than WT astrocytes. The intracellular levels of MIP1-γ were very similar in untreated WT and *Cln3*$^{-/-}$ astrocytes (Figure 4.8 B), but upon LPS/IFNγ stimulation the intracellular level of MIP1-γ was increased in *Cln3*$^{-/-}$ astrocytes (a 26.2±40.1% increase), but due to the high variability between measured samples this increase was not statistically significant. Both of these proteins were observed to be secreted less by *Cln3*$^{-/-}$ astrocytes upon LPS/IFNγ stimulation (Table 4.2), suggesting that intracellular accumulation of these proteins occurs in *Cln3*$^{-/-}$ astrocytes. Thus, these observations support the view that *Cln3*$^{-/-}$ astrocytes are able to produce proteins, they just fail to secrete them.

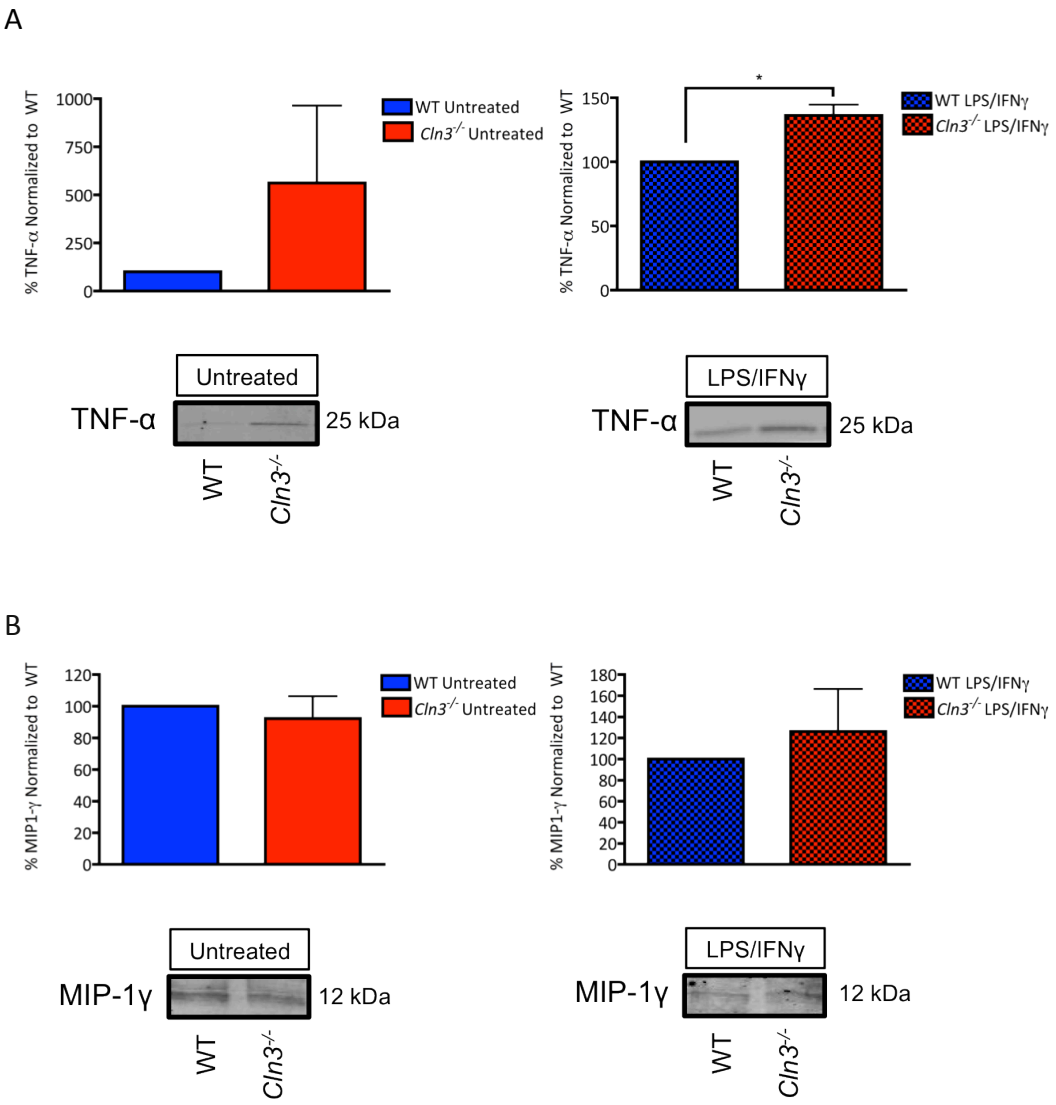

Figure 4.8. Protein synthesis is not reduced in *Cln3*$^{-/-}$ astrocytes. The intracellular expression levels of TNF-α and MIP1-γ were quantified in untreated and 24h LPS/IFNγ treated samples. The expression levels of each protein from WT astrocyte samples was compared to those from *Cln3*$^{-/-}$ astrocyte samples. (A) TNF-α expression was upregulated in LPS/IFNγ treated *Cln3*$^{-/-}$ samples compared to WT. No difference was observed in untreated conditions. (B) No difference in MIP1-α expression between untreated and LPS/IFNγ treated *Cln3*$^{-/-}$ and WT samples. Data presented as mean percentages ± SEM from n=3 experiments.

Cln3$^{-/-}$ astrocytes make, but fail to secrete, the antioxidant glutathione

Astrocytes protect neurons in many ways, including through metabolic and antioxidant support. One of the most important neuroprotective molecules is the antioxidant glutathione (GSH) (Schulz et al., 2000). Under oxidative stress conditions, the trafficking of GSH between astrocytes and neurons is particularly crucial (Dringen, 2000). By secreting GSH into the extracellular environment

astrocytes are able to increase neuronal GSH levels (Dringen et al., 1999). Glutathione levels have been shown to be lower in the JNCL brain, which may result in progressive oxidative damage in the CNS of *Cln3*$^{-/-}$ mice (Benedict et al., 2007; Chan et al., 2009; Tuxworth et al., 2011).

In order to study the role of astrocytes in defending the brain against oxidative stress in JNCL, the ability of *Cln3*$^{-/-}$ astrocytes to produce and secrete glutathione was examined. To do this, astrocytes were plated on 6-well plates at a density of 100,000 cells per well and, on the following day, the medium was replaced with fresh astrocyte medium containing LPS/IFNγ and incubated for either 24 or 48 hours. Control cultures of both genotypes were maintained for the same length of time, but without the addition of LPS/IFNγ. Subsequently, cells were washed, lysed and samples for the GSH assay were prepared as described in material and methods (Chapter 2, Section 2.9). A Lowry protein assay was used to determine the amount of total protein in each sample and the intracellular levels of the reduced form of GSH were measured by reverse-phase HPLC. In basal, untreated conditions, no significant differences in GSH levels were observed between WT and *Cln3*$^{-/-}$ astrocytes (Figure 4.9 A). However, upon LPS/IFNγ treatment the intracellular levels of the reduced form of GSH decreased significantly in the WT astrocytes, with a 56.3±12.0% reduction in GSH levels being observed after 24 hours exposure, and a 59.9±12.6% reduction after 48 hours (Figure 4.9 A). In contrast, intracellular levels of the reduced form of GSH increased in the *Cln3*$^{-/-}$ astrocytes after a 24 hours activation period, when compared to untreated samples (63±33.6% increase), before returning nearly back to baseline at 48 hours (28.1±19.3% increase) (Figure 4.9 A). These GSH levels were significantly lower in WT astrocytes after LPS/IFNγ treatment than in *Cln3*$^{-/-}$ astrocytes (59.6±12.2% decrease after 24h and a 51.9±14.3% decrease after 48h). However, since this experiment only measured the reduced form of glutathione, it is feasible that the results obtained could be explained by an opposing change in the level of oxidized glutathione (GSSG). This possibility was excluded by indirectly measuring intracellular GSSG levels in these same samples. This was carried out by incubating half of the sample volume with glutathione reductase

(GR), thus converting any GSSG present to GSH. HPLC analysis, as described above, was then used to measure the total glutathione and reduced GSH levels. No measurable difference between intracellular levels of GSH and total glutathione could be detected in any of these samples, suggesting that all the intracellular glutathione in both WT and *Cln3*$^{-/-}$ astrocytes is present in its reduced form (GSSG (total glutathione-GSH) levels: 0 nmol/mg protein (WT untreated), 0.42±0.28 nmol/mg protein (WT 24h LPS/IFNγ), 0 nmol/mg protein (WT 48h LPS/IFNγ), 1.31±0.51 nmol/mg protein (*Cln3*$^{-/-}$ untreated), 0 nmol/mg protein (*Cln3*$^{-/-}$ 24h LPS/IFNγ), 1.39±1.0 nmol/mg protein (*Cln3*$^{-/-}$ 48h LPS/IFNγ)). These total glutathione measurements were carried out on only one set of samples.

As mentioned above, astrocytes are able to secrete glutathione. Therefore an alternative explanation for the observed differences in the levels of intracellular GSH between astrocytes of different genotypes could be the lack of GSH secretion by *Cln3*$^{-/-}$ astrocytes, resulting in accumulation of intracellular GSH in LPS/IFNγ treated samples. Because many components of the astrocyte culture medium interfere with the electrochemical detection method used in HPLC analysis, the secreted levels of glutathione in the culture medium were analyzed by means of a luminescent GSH detection assay (Promega; Chapter 2, Section 2.9). The glutathione that accumulated in the medium over a period of 8 hours was quantified in samples collected from both WT and *Cln3*$^{-/-}$ astrocyte cultures that had either been treated with LPS/IFNγ, or maintained under basal conditions. Since GSH secreted into the medium is readily oxidized, the GSSG was converted to GSH using the strong reducing agent TCEP (12µM) prior to measuring the total GSH. These values were normalized to the relative amount of released LDH (%LDH from total LDH) in each sample to take into account any possible unspecific release of intracellular content into the medium under these experimental conditions. No significant difference in the total GSH levels between untreated WT (2.5±1.1 µM GSH/released %LDH) and *Cln3*$^{-/-}$ (0.28±0.1 µM GSH/released %LDH) samples was detected (Figure 4.9 B). This correlates well with the observation that intracellular levels of GSH do not differ between

untreated WT and *Cln3*$^{-/-}$ astrocytes (Figure 4.9 A). However, significantly increased GSH levels were observed in medium collected from LPS/IFNγ treated WT astrocyte cultures (4.3±1.1 µM GSH/released %LDH), when compared to medium collected from LPS/IFNγ treated *Cln3*$^{-/-}$ astrocyte cultures (0.4±0.2 µM GSH/released %LDH) (Figure 4.9 B). Based on these results it appears that *Cln3*$^{-/-}$ astrocytes are fully capable of making GSH, but fail to secrete this important antioxidant, particularly when activated with LPS/IFNγ.

A

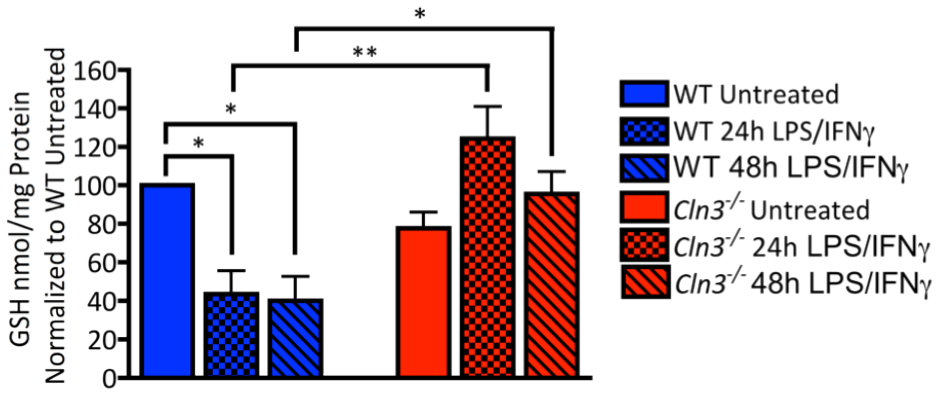

B

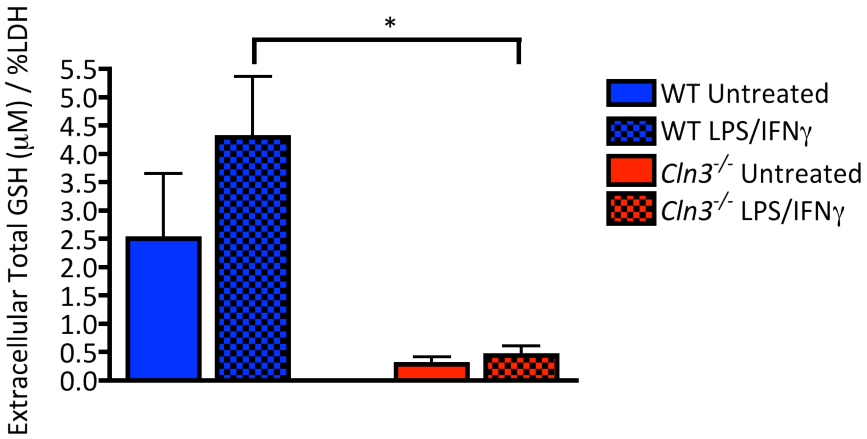

Figure 4.9. *Cln3*$^{-/-}$ astrocytes fail to secrete glutathione. Primary cortical WT and *Cln3*$^{-/-}$ astrocytes cultured on 6-well plates were analyzed for their ability to synthesize GSH (intracellular GSH, reduced form) and for their ability to secrete this protein (extracellular total GSH, reduced form). (A) Reverse phase HPLC was used to measure the intracellular levels of the reduced form of GSH in WT and *Cln3*$^{-/-}$ astrocytes treated with LPS/IFNγ for 24 or 48 hours, or from untreated samples. The GSH levels in each sample were normalized to the total amount of protein in that sample, thus results are presented in nmol/mg of protein. Additionally, these results were normalized to untreated WT astrocyte GSH levels in each experiment. LPS/IFNγ stimulation caused a significant decrease in the intracellular levels of GSH in WT astrocytes but not in *Cln3*$^{-/-}$ astrocytes. (B) The GSH-Glo kit was used to measure the total amount of GSH secreted into the medium over an 8 hours period by cultures of untreated and LPS/IFNγ treated WT and *Cln3*$^{-/-}$ astrocytes. TCEP (12uM) was used to convert of GSSH to GSH to measure the total amount of GSH in each sample. These results were normalized to released %LDH from total LDH. LPS/IFNγ treated *Cln3*$^{-/-}$ astrocytes secreted significantly reduced levels of GSH compared to LPS/IFNγ treated WT astrocytes. The results are presented as average mean±SEM. Three technical repeats were analyzed in each experiment, and the experiment was repeated four time for the results in (A) and six times for the results in (B).

An intact actin cytoskeleton is required for glutathione secretion

The actin cytoskeleton, among other cytoskeletal components, is important for exocytosis in astrocytes (Potokar et al., 2007), but our data revealed the actin

cytoskeleton to be abnormally organized in *Cln3*$^{-/-}$ astrocytes (Chapter 3, Figure 3.7). As such, the potential connection between the disrupted actin cytoskeleton and lack of glutathione secretion was examined by treating WT astrocyte cultures with cytochalasin D to inhibit the polymerization of actin. This resulted in a dramatic alteration in the actin cytoskeletal organization in these cells (Figure 4.10 A). Indeed, treatment with cytochalasin D (30 minutes pre-incubation before the 8 hour measurement period, 1µM) induced a significant reduction (50.1±12.7%) in the levels of extracellular glutathione in LPS/IFNγ treated WT astrocytes (Figure 4.10 B). Thus, an intact actin cytoskeletal is an essential element of the glutathione secretion machinery in astrocytes.

A

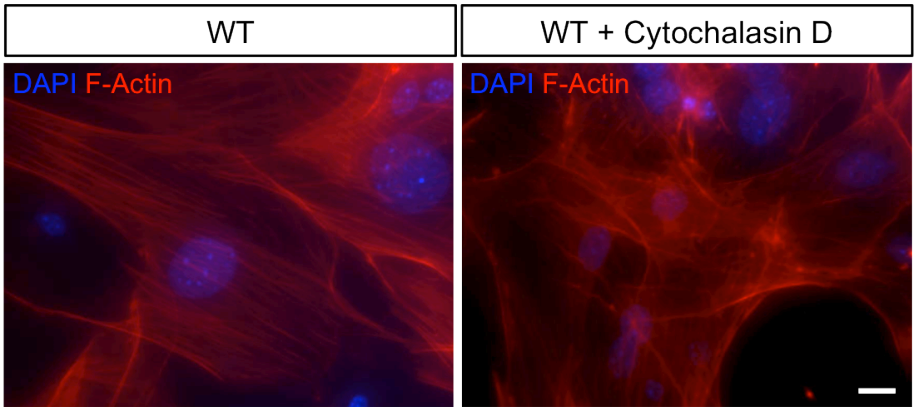

B

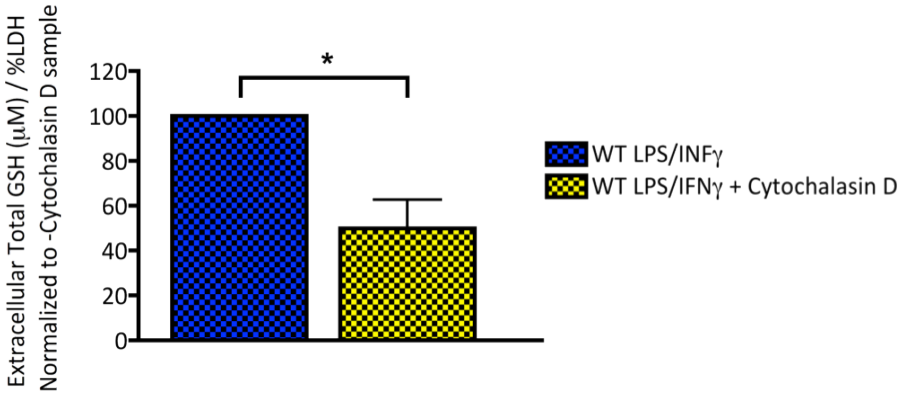

Figure 4.10. An intact actin cytoskeleton is essential for glutathione secretion. To study the importance of the actin cytoskeleton for GSH secretion in astrocytes, cytochalasin D was used. Cytochalasin D (1µM) was added to WT astrocytes for 30 minutes prior to the start of the 8 hours period over which the accumulation of secreted GSH in the medium was measured. Cells were then fixed and the actin cytoskeleton visualized with phalloidin. DAPI was used to visualize all nuclei. (A) Cytochalasin D clearly disturbed the F-actin filament organization in WT astrocytes. (B) Disturbing actin cytoskeletal polymerization significantly inhibited GSH secretion by WT astrocytes. Scale bar in (A) is 10µm.

Cln3$^{-/-}$ astrocytes secrete lactate normally, but show impaired glutamate scavenging

Neuronal activity is tightly coupled with regionally regulated blood flow and brain energy metabolism (Pellerin et al., 1998). It has become evident that highly regulated metabolic interactions take place between astrocytes and neurons (Tsacopoulos and Magistretti, 1996). A central player in these interactions is the glutamate released from neuronal cells during synaptic activity, and its subsequent reuptake into astrocytes that enwrap synapses via specific glutamate transporters such as GLT1 and GLAST expressed by these cells (EAAT1 and EAAT2 in humans) (Perego et al., 2000). This glutamate clearance by astrocytes has been shown to be a sodium-dependent process that triggers aerobic glycolysis (glucose uptake and utilization for lactate production by astrocytes). During this process, glutamate is co-transported into the cells with Na^+. This increased influx of Na^+ leads to an activation of the astrocyte Na^+/K^+-ATPase in an ATP-dependent manner resulting in enhanced glycolysis, which produces the energy substrates pyruvate and lactate (see Figure 1.5) (Parker and Hoffman, 1967; Lipton and Heimbach, 1978; Paul et al., 1979; Lynch and Balaban, 1987; Pellerin and Magistretti, 1994; Pellerin et al., 2007). Neurons can then take up the lactate released by astrocytes and utilize it as their energy substrate. A particular property of astrocytes that makes them an integral part of the energy supply system for neuronal cells is the fact that their end-feet, which are enriched in the glucose transporter Glut1, cover virtually all intraparenchymal capillaries (Kacem et al., 1998; Iadecola and Nedergaard, 2007), enabling direct glucose uptake by these cells from the blood supply. This forms the basis for the activity dependent lactate shuttle between astrocytes and neurons and supplies the energy for active synaptic transmission (Morgello et al., 1995; Pellerin et al., 1998; Pellerin and Magistretti, 2012).

Previous NMR-based studies on brain energy metabolism revealed a normal metabolic profile in JNCL patients (Brockmann et al., 1996). Some defects in energy metabolism, however, have been detected in different *Cln3* deficient mouse models, where a shift towards gluconeogenesis and down-regulation of

genes involved with energy production in the mitochondria have been reported (Brooks et al., 2003; Chattopadhyay et al., 2004). Despite this, no differences have been observed in blood lactate levels between *Cln3*$^{-/-}$ mice and WT control mice (Brooks et al., 2003; Chattopadhyay et al., 2004; Luiro et al., 2006). However, normal systemic lactate levels do not necessarily mean that the astrocyte-neuron lactate shuttling in the brain, which is required to meet neuronal energy demands, is also unaffected. Therefore, the lactate secretion of *Cln3*$^{-/-}$ astrocytes was studied.

Glutamate clearance by astrocytes has been shown to be essential in regulating extracellular glutamate concentrations, thereby preventing excitotoxic neuronal cell death and regulating synaptic transmission (Rothstein et al., 1996). Excitotoxicity may also play a potential role in JNCL pathogenesis. This is based on findings indicating that functional autoantibodies against GAD65, which reduced the activity of GAD and thus increased levels of glutamate, are present within the CNS of *Cln3* deficient mice, and in human JNCL (Chattopadhyay et al., 2002; Lim et al., 2006). Additionally, metabolic profiling in *Cln3*$^{-/-}$ mice has shown that altered glutamate/glutamine cycling, reduced levels of GABA and elevated glutamate can be detected at an early stage of disease progression (Pears et al., 2005). Thus, astrocyte dysfunction in JNCL could contribute towards the excess accumulation of glutamate at the synapse and hence to neuronal death.

To compare lactate secretion by WT and *Cln3*$^{-/-}$ astrocytes, cells were plated onto PDL coated 24-well plates at a density of 50,000 cells/well. 24 – 48 hours after plating, the medium was replaced with 500µl medium used for lactate measurements (Chapter 2, Section 2.12). After 4 hours incubation, this medium was collected for lactate measurements using a Lactate Colorimetric Kit (Abcam). Lactate levels in each sample were normalized to the total amount of protein present, as measured using a BCA protein quantification kit (Thermo Scientific). The secreted lactate values in *Cln3*$^{-/-}$ samples were additionally normalized to the corresponding WT values in order to compare the results between experiments. The medium collected from *Cln3*$^{-/-}$ astrocyte cultures exhibited a slight, but not

significant, increase in lactate levels compared to that collected from WT astrocytes (Figure 4.11 A). This result suggests that *Cln3*$^{-/-}$ astrocytes are able to secrete the lactate that they produce as a result of normal glycolysis.

To evaluate whether the uptake of glutamate was altered in *Cln3*$^{-/-}$ astrocytes, astrocytes of both genotypes were plated on 6-well, and then 24 - 48 hours later the culture medium in each well was replaced with 1.5ml of serum free HBSS that also contained 2mM glutamate. After incubation for 2 hours the medium was removed and the remaining glutamate in the medium was determined using a Glutamate Assay Kit (Abcam; Chapter 2, Section 2.13). Serum-free medium containing 2mM glutamate placed in wells that did not contain astrocytes was used as a control (100% remaining glutamate) for each experiment. The 'remaining' glutamate values obtained were normalized to the total amount of protein in each sample, and the values from *Cln3*$^{-/-}$ astrocyte cultures were normalized to the corresponding WT astrocyte values within each experiment. These measurements revealed that more glutamate remained in medium collected from *Cln3*$^{-/-}$ astrocytes cultures that in medium collected from WT astrocyte cultures. Indeed, the *Cln3*$^{-/-}$ astrocytes took up significantly less (48.0±14.0% reduction in glutamate clearance) glutamate when compared to WT astrocytes (Figure 4.11 B), suggesting that *Cln3*$^{-/-}$ astrocytes are not able to scavenge excess glutamate as effectively as WT astrocytes.

Based on these data, *Cln3*$^{-/-}$ astrocytes are able to produce and secrete the energy metabolite lactate when sufficient levels of glucose are available. However, *Cln3*$^{-/-}$ astrocytes did not take-up glutamate as efficiently as did their healthy counterparts, which may lead to excitotoxicity and thus contribute to neuronal death in the JNCL brain.

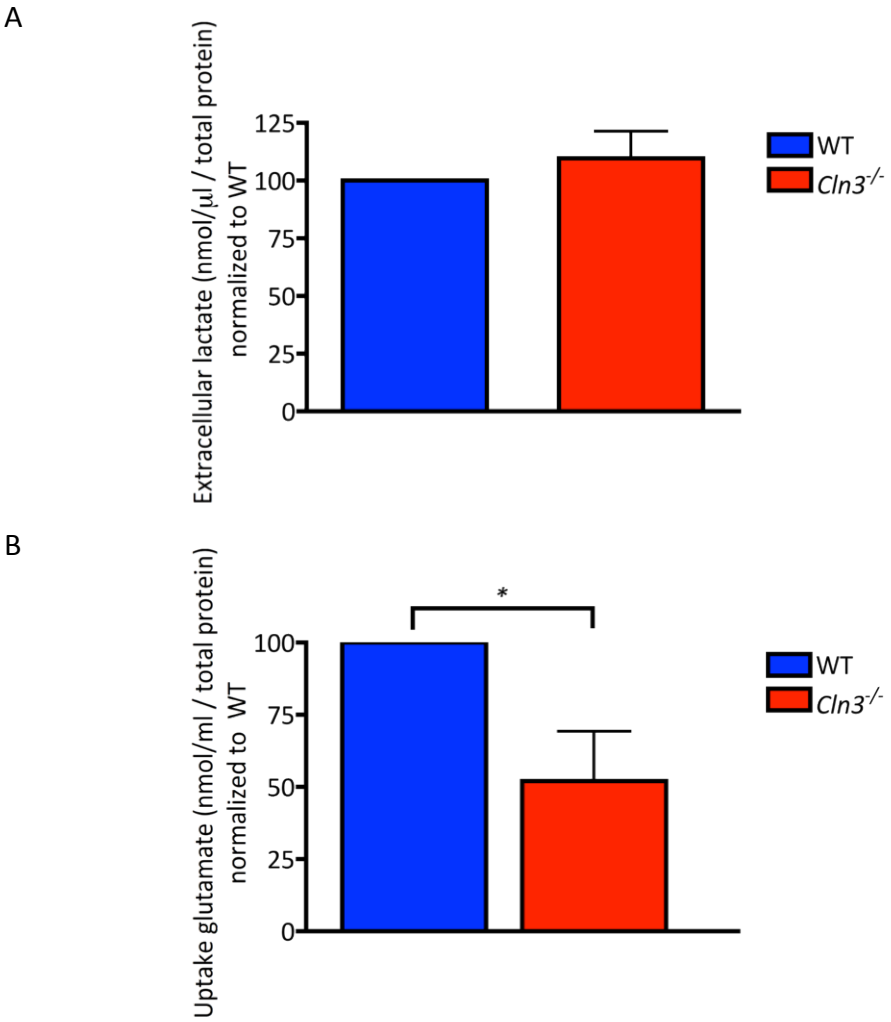

Figure 4.11. Lactate secretion is not altered in *Cln3*$^{-/-}$ astrocytes, but glutamate clearance is. WT and Cln3$^{-/-}$ astrocyte cultures plated on 6-well plates were used to measure the ability of these cells to secrete lactate and take up glutamate. (A) The amount of lactate secreted from WT and *Cln3*$^{-/-}$ astrocyte cultures over a 4 hours incubation period was measured using a lactate assay kit. These values were normalized to total amount of protein, and values from *Cln3*$^{-/-}$ astrocyte samples were normalized to WT astrocyte samples. There was no significant difference in the ability of WT and *Cln3*$^{-/-}$ astrocytes to secrete lactate. (B) The take-up of glutamate by WT and *Cln3*$^{-/-}$ astrocytes was assessed using a Glutamate Assay Kit. WT and *Cln3*$^{-/-}$ astrocytes were incubated with 2mM glutamate for 2 hours, and wells without astrocytes were used as controls. The glutamate remaining in the medium was quantified and normalized to total amount of protein, and the glutamate values of *Cln3*$^{-/-}$ astrocytes were normalized to those of WT astrocyte samples. *Cln3*$^{-/-}$ astrocytes took up significantly less glutamate than did WT astrocytes over the 2 hours period. Data is presented as average mean±SEM. This experiment was repeated five times and three technical repeats were analyzed for each condition in each experiment.

Migration of *Cln3*$^{-/-}$ astrocytes is attenuated

Generally astrocyte motility has been associated with various processes including embryonic development, wound healing and formation of a glial scar, local

inflammation processes and angiogenesis (Cayre et al., 2009). Thus, migration is an essential part of astrocyte biology and appropriate rearrangements of the cytoskeleton are pivotal for this process. Our data reveal that the actin and IF cytoskeleton is disorganized in *Cln3*$^{-/-}$ astrocytes, as was their ability to change morphologically in response to stimulation (Chapter 3, Figures 3.7 and 3.8). Moreover, recent reports suggest that CLN3 deficiency leads to impaired cellular motility in mouse embryonic fibroblasts via alterations in myosin-IIB activity (Getty et al., 2011). Thus, the possibility that the ability of *Cln3*$^{-/-}$ astrocytes to migrate may also be perturbed was investigated using live cell imaging of a 'scratch wound' assay.

Astrocytes were plated on Essen Image Lock 24-well plates at 50,000 cells (WT astrocytes) or 100,000 (*Cln3*$^{-/-}$ astrocytes) cells per well due to the observed differences in the proliferation of WT and *Cln3*$^{-/-}$ astrocytes (Chapter 3, Figure 3.9). After cells had formed a confluent monolayer and stopped dividing, an Essen Wound-maker was used to create a cell-free wound. Subsequently, fresh astrocyte culture medium with or without LPS/IFNγ, but containing Ara-C (to inhibit astrocyte proliferation during the experiment) was added to cultures and the migration of WT and *Cln3*$^{-/-}$ astrocytes was analyzed. Images from the cells were taken every 1 hour for 24 hours, and the width of the wound was measured. The rate of migration was calculated from the change in wound width over time, as previously described (Etienne-Manneville and Hall, 2001).

Following mechanical disruption of the confluent monolayer, untreated and LPS/IFNγ treated WT astrocytes migrated into the cell free area rapidly and nearly closed the gap within 24 hours (Figure 4.12 A and B). The migration distance of WT astrocytes did not significantly differ between treated and untreated cultures (Figure 4.12 A and B). For example, the average distance untreated WT astrocytes migrated during the first 4h after the scratch had been made was 22.9±3.1µm, whereas LPS/IFNγ treated WT astrocytes migrated 24.1±4.9µm (Figure 4.12 B). The distance *Cln3*$^{-/-}$ astrocytes migrated over this same time was significantly reduced in both untreated and LPS/IFNγ treated

conditions (Figure 4.12 A and B). This can be seen from the distance *Cln3*$^{-/-}$ astrocytes migrated during the first 4 hours of the experiment; 12.8±2.8μm in untreated conditions and 7.6±3.2μm in LPS/IFNγ treated conditions (Figure 4.12 B). Again activation with LPS/IFNγ did not significantly alter the distance *Cln3*$^{-/-}$ astrocytes migrated over time (Figure 4.12 B). Moreover, the rate of migration was significantly decreased in the absence of CLN3 in both treated and untreated conditions (Figure 4.12 C). The average migration rate for untreated WT astrocytes was approximately 5.3±0.6μm/h, and for LPS/IFNγ treated, approximately 5.3±0.4μm/h, while these numbers were 2.3±0.6μm/h for untreated and 1.5±0.3μm/h for LPS/IFNγ treated *Cln3*$^{-/-}$ astrocytes (Figure 4.12 C). Thus, the LPS/IFNγ treatment did not cause any significant changes in the migration speed in either WT or *Cln3*$^{-/-}$ astrocyte, indicating that this type of activation stimulus does not have any affect on the ability of astrocytes to migrate *in vitro*. However, in all conditions tested WT astrocytes migrated further and faster in the explored timescale than did *Cln3*$^{-/-}$ astrocytes. Thus, this attenuated migration of *Cln3*$^{-/-}$ astrocytes could alter their functioning during development and upon injury.

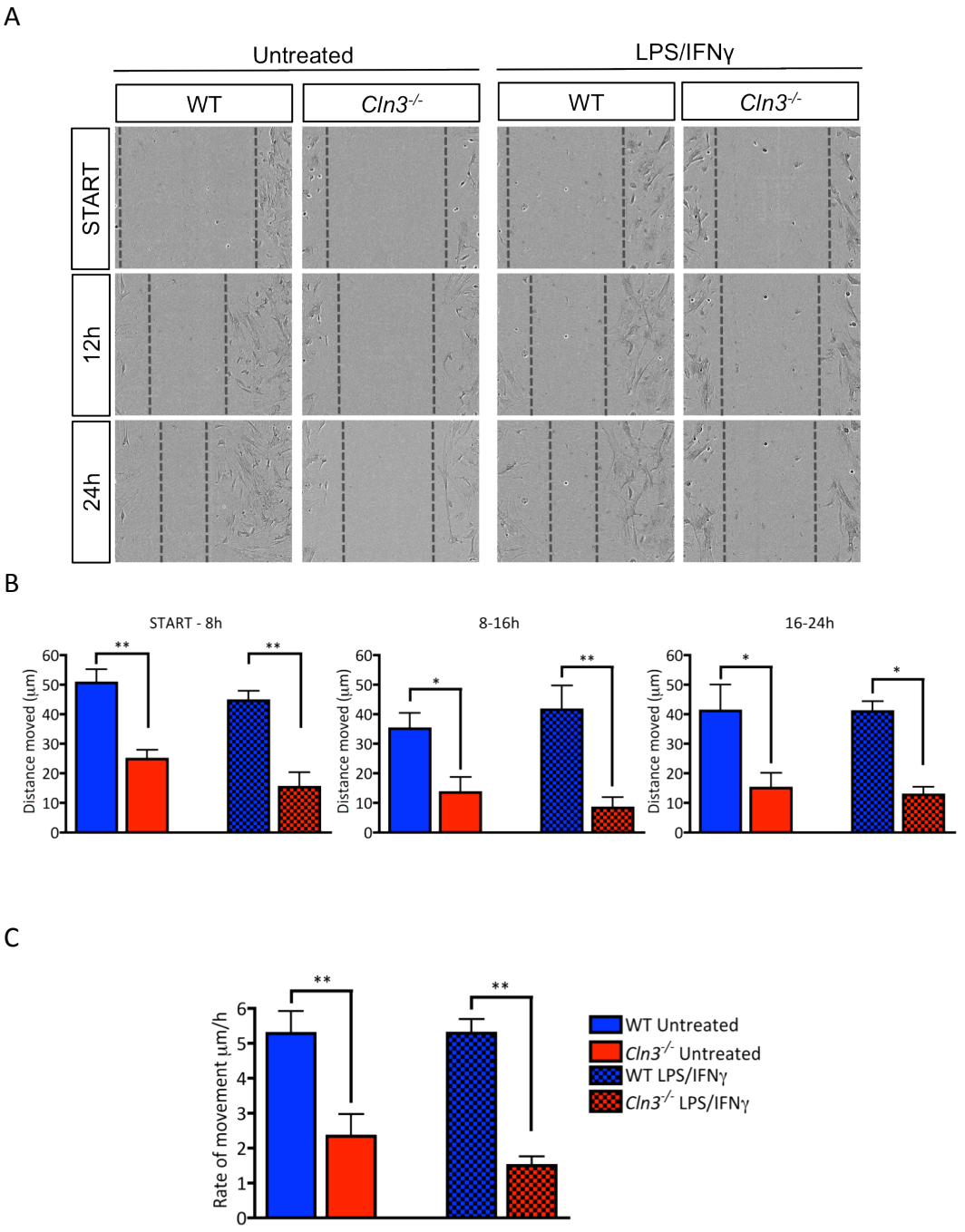

Figure 4.12. Scratch assay reveals a migration defect in *Cln3*$^{-/-}$ astrocytes. WT and *Cln3*$^{-/-}$ astrocytes were plated on Essen Image Lock 24-well plates, grown to confluence then scratched using an Essen wound maker. These cells were kept in astrocyte culture medium containing Ara-C, with or without LPS/IFNγ, as indicated. (A) Representative pictures of the wound at three time-points from untreated and LPS/IFNγ treated WT and *Cln3*$^{-/-}$ astrocytes. (B) The distance each edge of WT and *Cln3*$^{-/-}$ astrocytes traversed every 4 hours was calculated relative to the initial scratch distance. WT astrocytes migrated significantly further than did *Cln3*$^{-/-}$ astrocytes. (C) The Rate of migration was measured by calculating the distance migrated by these cells/h. *Cln3*$^{-/-}$ astrocytes migrated significantly slower than WT astrocytes. Data presented as mean±SEM. In each experiment three wound widths were measured per well, and three wells per experimental condition were quantified. This experiment was repeated four times.

4.3 Discussion

Any major alterations in the basic functions of astrocytes may have a significant impact on neuronal function and survival (Volterra and Meldolesi, 2005; Sidoryk-Wegrzynowicz et al., 2011). In this chapter we have shown that Ca^{2+} signaling, the basis for glial-glial and glial-neuronal cell communication in the brain (Fiacco and McCarthy, 2006; Zorec et al., 2012; Verkhratsky et al., 2012a), is abnormal in *Cln3*$^{-/-}$ astrocytes, with smaller and less frequent spontaneous oscillations and a lack of synchronized spontaneous calcium wave formation being observed, along with altered ER-calcium release and clearance. These cells were also shown to be impaired in their ability to secrete (although not synthesize) a range of chemokines, pro-and anti-inflammatory cytokines, neurotrophic factors and mitogens upon stimulation. This finding was extended to the major antioxidant of the brain, glutathione, that was synthesized but not secreted by these cells, suggesting that loss of CLN3 function in astrocytes could lead to oxidative stress-mediated neurodegeneration in JNCL (Dringen, 2000; Schulz et al., 2000; Benedict et al., 2007; Tuxworth et al., 2011). Furthermore, the observed failure of *Cln3*$^{-/-}$ astrocytes to take-up glutamate as effectively as WT astrocytes could contribute towards excitotoxic neuronal loss in this disease (Sattler and Rothstein, 2006). Finally, we show that CLN3 is important for the motility of astrocytes since lack of this protein causes astrocytes to migrate significantly slower than normal. Taken together these results indicate that many of the basic functional properties of *Cln3*$^{-/-}$ astrocytes are abnormal and could directly impact neuronal health, a hypothesis that will be tested in Chapter 6 of this thesis.

Specific alterations in *Cln3*$^{-/-}$ astrocytes calcium signaling

Ca^{2+} based signaling forms the basis for many functions of astrocytes (Zorec et al., 2012). An increase in $[Ca^{2+}]_I$ levels in astrocytes may result in gliotransmission (Halassa et al., 2007; Parpura and Zorec, 2010; Verkhratsky et al., 2012a). Upon being released into the extracellular space these gliotransmitters can exert their actions on neighboring neuronal cells modulating synaptic transmission and plasticity, or on other glial cells altering their neuroimmune responses (Agulhon

et al., 2012). Thus, Ca^{2+} based signaling is a crucial communication element exploited by astrocytes to connect them to other cells in the CNS. Our data revealed for the first time that the spontaneous $[Ca^{2+}]_I$ transients in *Cln3*$^{-/-}$ astrocytes were smaller and less frequent than in WT astrocytes (Chapter 4, Figure 4.1). Additionally, *Cln3*$^{-/-}$ astrocytes did not create a synchronized, propagating Ca^{2+} wave when grown as closely connected astrocyte sheets (Chapter 4, Figure 4.2). Both of these defects may be caused by abnormal ER-based Ca^{2+} signaling, as discussed below.

Many studies suggests that IP_3-dependent calcium-induced calcium release from the ER (CICR) is required for spontaneous Ca^{2+} oscillations in astrocytes (Aguado et al., 2002; Parri and Crunelli, 2003; Tanaka et al., 2007). Initially a small increase in $[Ca^{2+}]$ either via release from the ER or through voltage-gated Ca^{2+} channels (VGCC) is required for initiation of the CICR, and this subsequently leads to spontaneous Ca^{2+} oscillations (Latour et al., 2003; 2004; Wang et al., 2006). These spontaneous Ca^{2+} oscillations appeared to start moderately later in *Cln3*$^{-/-}$ astrocytes than in WT counterparts. These data suggest that the CICR mechanism is altered in these cells, or alternatively that the initial small increase in $[Ca^{2+}]$ required for the activation of CICR does not occur with the same velocity as in WT astrocytes. It may be that this small Ca^{2+} increase, generated either through voltage-gated Ca^{2+} channels (VGCC) expressed by cultured astrocytes (Latour et al., 2003; 2004), or from the ER via the activation of IP_3-receptors, is altered in *Cln3*$^{-/-}$ astrocytes leading to a delayed initiation of spontaneous Ca^{2+} oscillations. Any alterations in either one of these mechanisms would also explain the low frequency and smaller amplitude of the spontaneously induced increases in $[Ca^{2+}]_I$ in these Cln3 deficient cells. Some evidence suggests that spontaneous $[Ca^{2+}]_I$ transients are a common feature of resting astrocytes in numerous brain regions, but are absent in reactive astrocytes (Aguado et al., 2002). Given that the *Cln3*$^{-/-}$ astrocytes showed increased GFAP expression under resting conditions they may be more 'activated' than WT astrocytes, and thus show attenuated spontaneous $[Ca^{2+}]_I$ transients (Chapter 3, Figure 3.6). It would be interesting to study whether spontaneous $[Ca^{2+}]_I$ transients in WT and *Cln3*$^{-/-}$

astrocytes are altered after these cells have been activated with LPS/IFNγ. Spontaneous astrocytic $[Ca^{2+}]_I$ oscillations have been shown to trigger neuronal excitation in the thalamus (Parri et al., 2001). Thus, deregulated spontaneous astrocytic $[Ca^{2+}]_I$ oscillations could potentially lead to abnormal stimulation of neuronal networks in the *Cln3*$^{-/-}$ mouse brain (Pasti et al., 1997; Araque et al., 1998; Bezzi et al., 1998; Parri et al., 2001; Parpura et al., 2011).

Furthermore, spontaneously arising increases in $[Ca^{2+}]_I$, which are synchronized among a group of astrocytes to create a propagating calcium wave (Cornell-Bell et al., 1990a; Cotrina et al., 2000; Arcuino et al., 2002; Bowser and Khakh, 2007), was not observed in *Cln3*$^{-/-}$ astrocytes. Two routes have been established to enable calcium wave propagation between astrocytes: 1) via intercellular gap junctions, which allow diffusion of signaling molecules from one cell to another; or 2) via the extracellular space, which involves the release of signaling molecules that may then activate receptors on the membranes of adjacent cells (Scemes, 2000; Scemes and Giaume, 2006). The observed lack of synchronized Ca^{2+} wave propagation within cultured *Cln3*$^{-/-}$ astrocytes could be caused by alterations in one or both of these mechanisms. The role of gap junctions in Ca^{2+} wave propagation in astrocytes has remained controversial, which may be a reflection of the heterogeneous distribution of gap junctions in the CNS (Batter et al., 1992; Blomstrand et al., 1999; Scemes et al., 2000). The expression pattern of Cx43 protein, which is the main gap junction-forming connexin protein in astrocytes (Giaume et al., 1991; Scemes et al., 1998), was not found to be significantly altered in *Cln3*$^{-/-}$ astrocytes (Chapter 4, Figure 4.3). This observation would indicate that *Cln3*$^{-/-}$ astrocytes at least express and localize proteins involved in the formation of gap junctions correctly. However, based on this simple, qualitative observation, one cannot exclude the possibility that gap junction connectivity between *Cln3*$^{-/-}$ astrocytes is affected. As a next step it would be important to measure the connectivity of gap junctions within *Cln3*$^{-/-}$ astrocyte networks and compare this to their WT counterparts. This could be achieved by using an intercellular dye coupling method; loading of a low molecular weight fluorescent dye (such as Lucifer yellow CH) into astrocytes in

culture and monitor its transfer between connected astrocytes (el-Fouly et al., 1987; Naus et al., 1997). This would help to provide a better understanding of the trafficking of small molecules via gap junctions formed between *Cln3*$^{-/-}$ astrocytes.

ATP secretion by astrocytes and activation of P2Y1 receptors on neighboring cells has also been proposed to be important for astrocyte wave propagation (Scemes et al., 2000; Bowser and Khakh, 2007). Externally applied ATP produced normal $[Ca^{2+}]_i$ elevations in *Cln3*$^{-/-}$ astrocytes, and as such the ATP-induced Ca^{2+} release from the ER via the activation of IP_3-receptor channels does not appear to be affected in *Cln3*$^{-/-}$ astrocytes. However, perhaps the release of ATP required for wave propagation is abnormal in *Cln3*$^{-/-}$ astrocytes, thus explaining at least partly the poor propagation of their intercellular Ca^{2+} wave, an explanation worth considering since these cells fail to secretion a range of factors (Tables 4.1 and 4.2). One could test this possibility directly by measuring the release of ATP from *Cln3*$^{-/-}$ astrocyte cultures. Furthermore, analyzing the expression pattern of P2Y1 receptors on *Cln3*$^{-/-}$ astrocytes would broaden the understanding of the responsiveness of *Cln3*$^{-/-}$ astrocytes to purinergic based signaling, which is important for astrocyte-astrocyte and neuron-astrocyte communication (Fields and Burnstock, 2006). Finally, to ensure these deficits observed in cultured astrocytes truly reflect the situation in intact tissue, it is pivotal that Ca^{2+} wave propagation be studied in organotypic *Cln3*$^{-/-}$ cortical slices, and eventually also *in vivo* by means of two-photon microscopy, for example.

It has been previously demonstrated that an intact actin cytoskeleton is a key requirement for the generation of a long-distance calcium wave (Cotrina et al., 1998). Thus, the severely disrupted actin cytoskeleton observed in *Cln3*$^{-/-}$ astrocytes may be the reason behind the lack of synchronized calcium wave propagation by these cells, possibly due to its inability to serve as a scaffold for signaling molecules required for this process, such as PIP_2 and IP_3 and IP_3-R, all of which have been associated with actin in a number of systems (Feng and Kraus-Friedmann, 1993; Sastry and Horwitz, 1993; Miki et al., 1996; Cotrina et al., 1998;

Tojkander et al., 2012). Additionally, CLN3 has been suggested to be involved in the control of Na^+-K^+-ATPase turnover at the plasma membrane via fodrin, which is a cytoskeletal protein that is also associated with actin filaments (De Matteis and Morrow, 2000; Uusi-Rauva et al., 2008). Na^+-K^+-ATPase is involved in the regulation of ionic homeostasis and also participates in other intracellular signaling events, including Ca^{2+} signaling (Tian and Xie, 2008). It has been shown that ouabain, which is a ligand for Na^+-K^+-ATPase, can trigger calcium oscillations in cultured primary astrocytes (Liu et al., 2007). Thus, a lack of turnover of this protein at the plasma membrane, possibly due to a disrupted actin cytoskeleton, could also influence calcium oscillations in *Cln3*$^{-/-}$ astrocytes.

Cln3$^{-/-}$ astrocytes also displayed specific alterations in Ca^{2+} released from the ER in response to thapsigargin treatment (Chapter 4, Figure 4.5). A distinct subset of *Cln3*$^{-/-}$ astrocytes had a very large and fast release of Ca^{2+} from the ER, whereas Ca^{2+} release from the remaining *Cln3*$^{-/-}$ astrocytes was indistinguishable from that of WT astrocytes. This finding may indicate the existence of distinct group of *Cln3*$^{-/-}$ astrocytes with a very high $[Ca^{2+}]_{ER}$ content, or that the mechanisms behind the passive leakage of Ca^{2+} from ER are impaired in these particular cells. Moreover, the process of Ca^{2+} clearance from the cytosol to other intracellular stores or to the extracellular space was found to be attenuated in these cells, which was demonstrated by the prolonged high levels of $[Ca^{2+}]_I$ seen following thapsigargin treatment. Numerically this could have been verified by determining the TAU (decay) constant in WT and *Cln3*$^{-/-}$ astrocyte populations following thapsigargin treatment. However, in order to determine the TAU constant, Ca^{2+} current readouts from a specific channel are required. In this study, the Fura-2- Ca^{2+} indicator, which provides ratiometric Ca^{2+} readouts from two channels was used, thus, the determination of the Tau constant was not feasible and would require additional measurements. There are several possible explanations for this result, including the enhanced release of Ca^{2+} from other intracellular Ca^{2+}stores, or the impaired clearance of ER leaked Ca^{2+} into these stores; mainly mitochondria and lysosomes. Interestingly, dysregulated lysosome-based Ca^{2+} signaling has been described previously in other lysosomal

disorders (Lloyd-Evans and Platt, 2011). In fact, a number of acidic organelles, such as lysosomes, endosomes, and the Golgi complex have been recognized to function as intracellular Ca^{2+} stores, in which Ca^{2+} intake and release is mediated by a number of calcium pumps, exchangers and receptors (Patel and Docampo, 2010). For instance, defective lysosomal Ca^{2+} uptake and defective NAADP-mediated lysosomal Ca^{2+} release has been shown to lead to a disruption of endocytosis and lipid storage in Niemann-Pick type C (NPC) disease (Lloyd-Evans et al., 2008). Furthermore, neutrophil cells in Chediak-Higashi Syndrome exhibit enhanced lysosomal Ca^{2+} uptake (Styrt et al., 1988). Given that the primary location of CLN3 is thought to be in the lysosomal membrane, where the important players of lysosomal Ca^{2+} regulation are also located, altered lysosomal Ca^{2+} signaling may also play a role in the pathogenesis of JNCL. Furthermore, lysosomal location and maturation was found abnormal in *Cln3*$^{-/-}$ astrocytes (Chapter 3, Figure 3.11), which may alter lysosomal-mediated regulation of intracellular Ca^{2+} homeostasis in these cells. Indeed, the lack of cytosolic Ca^{2+} clearance may suggest that lysosomal Ca^{2+} regulation is disrupted in JNCL, something that certainly warrants further investigation.

Mitochondria are also essential for the regulation of cytosolic Ca^{2+} in astrocytes (Duchen, 2000; Reyes and Parpura, 2008). Thus, mitochondrial-mediated Ca^{2+} regulation may contribute towards the observed defects in *Cln3*$^{-/-}$ astrocyte Ca^{2+} signaling. Any impairments in mitochondrial Ca^{2+} uptake may also deregulate mitochondrial energy metabolism, since the mitochondrial Ca^{2+} uptake pathway provides a mechanism that couples energy demand to increased ATP production, via calcium-dependent up-regulation of mitochondrial enzyme activity (Duchen, 1999). Previously, CLN3 deficiency has been linked with abnormalities in the mitochondrial function in a variety of cellular models (Brooks et al., 2003; Chattopadhyay et al., 2004; Luiro et al., 2006). Thus, impaired Ca^{2+} uptake into mitochondria in *Cln3*$^{-/-}$ astrocytes may lead to a dysfunction in energy metabolism. It would be interesting to study if mitochondrial Ca^{2+} uptake, or release in *Cln3*$^{-/-}$ astrocytes, is impaired by directly measuring the mitochondrial Ca^{2+} content using mitochondrially localized Ca^{2+} indicators like rhod-2 (Boitier et

al., 1999). Moreover, similar investigations could be extended to lysosomes by using lysosome-specific Ca^{2+} indicators, such as genetically encoded Ca^{2+} indicator (GCaMP3) connected directly to TRPML1, which is one of the Ca^{2+} channels in the lysosomes (Shen et al., 2012). Alternatively, pharmacological agents like glycyl-L-phenylalanine-beta-naphthylamide (GPN) could be used to measure the lysosomal Ca^{2+} content in *Cln3*$^{-/-}$ astrocytes following ER-Ca^{2+} depletion with thapsigargin (Llyod-Evans et al., 2008).

It has been well established that astrocytes express a whole range of receptors that can be activated by many neurotransmitters, such as glutamate (Porter and McCarthy, 1996; Pasti et al., 1997), GABA (Kang et al., 1998) and ATP (Guthrie et al., 1999). Ultimately the activation of these receptors evokes elevated Ca^{2+} levels in astrocytes inducing gliotransmission, resulting in the release of other transmitters including glutamate, d-serine and ATP. These gliotransmitters are all neuroactive molecules that can modulate synaptic transmission, as well as facilitate inter-astrocytic Ca^{2+} signaling (Guthrie et al., 1999; Fellin et al., 2004). ATP evoked Ca^{2+} elevations were normal in *Cln3*$^{-/-}$ astrocytes, indicating that Ca^{2+} based mechanisms involved in gliotransmission would also be unaffected. One could measure the release of glutamate evoked by ATP stimulation in *Cln3*$^{-/-}$ astrocytes to confirm this. In addition, intracellular calcium elevations in astrocytes may be required for the secretion of other proteins, such as growth factors and cytokine (Agulhon et al., 2012). However, the ability of *Cln3*$^{-/-}$ astrocytes to secrete a range of proteins was studied and found to be severely impaired (Chapter, Tables 4.1 and 4.2), this may suggest that regardless of having a normal ATP response the subsequent Ca^{2+} triggered exocytosis may be affected in these cells, perhaps explaining at least partially the lack of protein secretion.

In cultured astrocytes, the addition of growth factors and cytokines were found to induce significant changes in the nature and propagation of intracellular Ca^{2+} signals (Morita et al., 2003). For instance, growth factors like EGF and FGF promoted Ca^{2+} oscillations, but these were inhibited by pro-inflammatory cytokines like IL-1β and TNF-α (Morita et al., 2003). Interestingly, these enhanced

calcium oscillations were found to be accompanied by an enlargement of the calcium store, cell proliferation and the development of hypertrophy (Carafoli, 2002; Morita et al., 2003). Growth factor and cytokine secretion by *Cln3*$^{-/-}$ astrocytes was revealed to be dramatically altered (Chapter 4, Tables 4.1 and 4.2) and this in turn may be linked to attenuated morphological transformation (Chapter 3, Figure 3.8) and proliferation (Chapter 3, Figure 3.9), which may both also be linked with abnormal calcium oscillations observed in these cells (Chapter 4, Figures 4.1 and 4.2) although this hypothesis awaits investigation.

Alterations in astrocyte calcium signaling have been linked to a number of CNS diseases. For example, in Alzheimer disease astrocytes display network-wide elevations in resting calcium levels, and enhanced network-level functional activity seen as more frequent propagation of intercellular calcium waves (Kuchibhotla et al., 2009). Indeed, the propagation of intercellular calcium waves has been postulated to function as a messenger to alert the rest of brain to a pathological insult (Fiacco and McCarthy, 2006; Scemes and Giaume, 2006; Agulhon et al., 2012). Cortical spreading depression (CSD) is a slowly propagating wave of neuronal depolarization (Leão, 1986; Gorji, 2001; Gorji et al., 2001) that has been shown clinically relevant in migraine, progression of cortical infarct volume after stroke and trauma (Lauritzen, 1994; Back et al., 1996; Hadjikhani et al., 2001; Smith et al., 2006). Based on a number of studies, CSD may be associated with calcium waves in astrocytes, with a currently unknown physiological purpose (Basarsky et al., 1998; Kunkler and Kraig, 1998; Martins-Ferreira et al., 2000; Strong et al., 2002; Peters et al., 2003; Fabricius et al., 2006; Chuquet et al., 2007; Luo and Chen, 2012). Nevertheless, these findings raise questions about the impact of the alterations observed in calcium signaling in *Cln3*$^{-/-}$ astrocytes, and whether these events are ultimately beneficial or detrimental towards disease progression in JNCL?

Epilepsy in one of the most prominent clinical features of JNCL (Mole et al., 2011). Such seizures often consist of a synchronous neuronal discharge that starts in a restricted brain area and then spreads to larger areas of the brain

(Avoli et al., 2002; Pinto et al., 2005; Trevelyan et al., 2006). Thus, epilepsy can be seen as a disorder of excess synchronization of neurons caused by an imbalance between excitatory and inhibitory mechanisms that generate neuronal hyperexcitability. In addition to the well-known contribution of voltage-gated Na^+, Ca^{2+} and K^+ channels to epileptogenesis (Lerche et al., 2001; Graves, 2006), astrocytic Ca^{2+} signaling has also been linked with this problem (de Lanerolle et al., 2010; Seifert and Steinhäuser, 2011). For instance, astrocytes can directly stimulate groups of neighboring neurons via Ca^{2+} dependent glutamate release (Parpura et al., 1994), and synchronize the activation of extrasynaptic NMDA-receptors (Fellin et al., 2004). These basic findings suggest that Ca^{2+} dependent gliotransmission by astrocytes may be involved in seizure generation. Moreover, it has been shown that the frequency of Ca^{2+} oscillations in astrocytes increases significantly during epileptic seizures (Tian et al., 2005; Fellin et al., 2006a). The ATP-mediated Ca^{2+} waves that propagate through astrocyte networks may also play a role in the control of the epileptic seizure propagation (Fellin et al., 2006a; Losi et al., 2012; Torres et al., 2012). ATP released from astrocytes through Cx43 hemichannels may enhance inhibitory transmission by acting upon the P2Y1 receptors expressed in a specific group of hippocampal interneurons (Torres et al., 2012). Thus, a lack of synchronized calcium wave formation, as well as attenuated spontaneous calcium oscillations in *Cln3*$^{-/-}$ astrocytes, may impact their ability to perform their inhibitory regulatory activities, leading to neuronal hyperexcitability in the JNCL brain and initiation of seizures. Moreover, autoantibodies against GAD65, which converts glutamic acid to GABA, have been discovered in the serum of *Cln3*$^{-/-}$ mice and individuals with JNCL (Chattopadhyay et al., 2002; Lim et al., 2006). The existence of these autoantibodies has been proposed to lead to higher levels of glutamate in the brain and may also contribute to the pronounced loss of GABAergic neurons typical in JNCL (Chattopadhyay et al., 2002). Additionally, *GAD65*$^{-/-}$ mice have been shown to develop spontaneous epileptic seizures, re-enforcing the role of the GABAergic inhibitory system in suppressing spontaneous epileptic seizures (Kash et al., 1997). Together with attenuated, non-synchronization of astrocytic calcium oscillations, the lack of GABA production due to GAD65 autoantibodies

may severely affect the neuronal inhibition in *Cln3*$^{-/-}$ mice. Such events may increase the susceptibility of these mice to epileptic seizures, and the same could be true in JNCL patients.

Given how important Ca^{2+} signaling is for the overall biology of astrocytes, any impairment of this process is bound to have significant consequences, not only on astrocyte function, but also on the activities of other glial cells, and importantly, neuronal cells. Thus, one may predict that the observed alterations in astrocytic Ca^{2+} signaling may be a key element in the pathological cascade that occurs in the *Cln3*$^{-/-}$ mouse brain.

Implications of impaired protein secretion in *Cln3*$^{-/-}$ astrocytes

Astrocytes secrete a wide array of soluble factors including chemokines, pro-and anti-inflammatory cytokines, mitogens and growth factors, in addition, astrocytes are highly responsive to virtually all of the factors they secrete (Ridet et al., 1997; Dong and Benveniste, 2001; John et al., 2003; Liberto et al., 2004; Miklic et al., 2004). In contrast to the marked morphological difference between *Cln3*$^{-/-}$ and WT astrocytes grown under basal conditions, their protein secretion profile did not differ greatly (Chapter 4, Table 4.1). This is not surprising since protein secretion by resting astrocytes is minimal, but is enhanced upon astrocyte activation (Ridet et al., 1997; Sofroniew and Vinters, 2010; Lee and Haydon, 2011). Nevertheless, *Cln3*$^{-/-}$ astrocytes did secrete significantly reduced amounts of M-CSF, MIP-1γ, GCP-2 and TIMP1 under resting conditions, whereas secretion of TF was increased. TF, which is mainly produced by astrocytes in the brain, is involved in the early stages of a cascade leading to blood coagulation, and also mediates pro-inflammatory responses (Eddleston et al., 1993; Chu, 2011). Indeed, several lines of evidence show that extracellular TF signaling via protease-activated receptors (PARs) is involved in angiogenesis, cell adhesion/migration, innate immunity and has been shown to mediate many pathophysiological mechanisms (Chu, 2011). Hence, if upregulation of TF expression by astrocytes also occurs in the *Cln3*$^{-/-}$ CNS, this could be one of key

mechanisms in the initiation of the neuroimmune responses observed in these mice.

Upon LPS/IFNγ activation the differences in protein secretion profiles between WT and *Cln3*$^{-/-}$ astrocytes become even more apparent, with the vast majority of these screened proteins being secreted at a significantly lower level by *Cln3*$^{-/-}$ astrocytes, although these cells appear to be still capable of synthesizing these proteins (Chapter 4, Figure 4.8). Interestingly, under these experimental conditions, a small subset of the screened proteins were secreted at a higher level by *Cln3*$^{-/-}$ astrocytes, or at similar levels to WT astrocytes (Chapter 4, Figure 4.7). This may suggest that astrocytes employ different mechanisms to secrete specific types of proteins, and only some of these mechanisms are affected by CLN3 deficiency. Most likely, the observed cytoskeletal abnormalities, together with atypical calcium signaling exhibited by *Cln3*$^{-/-}$ astrocytes may, at least partially, explain these secretion results.

One group of proteins secreted at significantly lower levels by *Cln3*$^{-/-}$ astrocytes were the chemokines. These proteins are involved in nearly all pathological conditions with an inflammatory component (Rostène et al., 2011). Indeed, over-expression of chemokines regulates recruitment of leukocytes to the site of inflammation, which may cause exacerbated monocyte/macrophage infiltration into the CNS (Ransohoff, 2009; Saederup et al., 2010; Semple et al., 2010). For instance, MCP-1, has been shown to control the migration of microglia, monocytes and lymphocytes to the site of inflammation within the injured CNS (Simpson et al., 1998; Deng et al., 2009). Additionally, the expression of chemokines by astrocytes has been shown to coincide with the presence of ramified microglial cells, making astrocytes key players in influencing microglial differentiation and activation (Rezaie et al., 2002). The dramatic reduction in chemokine secretion observed, particularly by activated *Cln3*$^{-/-}$ astrocytes, could therefore have a bearing on the attenuated microglial biology observed both *in vitro* and *in vivo* (Pontikis et al., 2004; 2005). Although, enhanced chemokine secretion associated with chronic inflammation may become damaging to the

brain, enhancing the destruction of axons, dendrites and synapses (Parpura et al., 2012), chemokines, such as RANTES, MCP-1 have been shown to be neuroprotective under certain *in vitro* conditions (Bruno et al., 2000; Eugenin et al., 2003). Thus, in the *Cln3*$^{-/-}$ CNS any neuroprotection afforded by these proteins would be severely reduced.

Chemokine expression has previously been compared in *Ppt1*$^{-/-}$ vs. *GFAP*$^{-/-}$*Vim*$^{-/-}$*Ppt1*$^{-/-}$ mice brains, in which a dramatic increase in expression of chemokines such as IP-10, MIP1-β, MIP-2, MCP-1, MCP3 and MCP-5 were reported in the latter (Macauley et al., 2011). This type of elevated chemokine expression was associated with enhanced neuroinflammation and accelerated disease progression in *GFAP*$^{-/-}$*Vim*$^{-/-}$*Ppt1*$^{-/-}$ mice. Based on these observations, it may be that endogenously impaired chemokine secretion, as well as attenuated astrocyte activation may actually play a beneficial role in the pathogenesis of JNCL. It would be extremely informative to study the expression levels of the proteins screened in this study *in vivo* to determine whether similar alterations are also evident in the intact *Cln3*$^{-/-}$ mouse brain.

Along with chemokines, many mitogens, pro-inflammatory, anti-inflammatory and haematological proteins were also secreted at a significantly lower level by *Cln3*$^{-/-}$ astrocytes (Chapter 4, Tables 4.1 and 4.2). The biological significance of these changes could be many fold due to these proteins having multiple effects on different cell types under both physiological and pathological situations (Allan and Rothwell, 2003; Farina et al., 2007; Singh et al., 2011; Ransohoff and Brown, 2012). To further complicate matters, many of these proteins have synergistic properties that can result in dramatic changes in both microglial and astrocyte function. For instance, IL-1β shows clear microglial immunoreactivity in *Cln3*$^{-/-}$ mice and in human JNCL and is secreted normally by *Cln3*$^{-/-}$ microglia cells (Dihanich, unpublished data, Lim and Cooper, unpublished data and Castaneda et al., 2008). In contrast, *Cln3*$^{-/-}$ astrocytes failed to secrete IL-1β. However, in the intact *Cln3*$^{-/-}$ mouse brain IL-1β secreted by microglia cells may induce IL-6

production in both glial cell-types, stimulating inducible nitric oxide synthase (iNOS) activity and thus leading to increased NO production by astrocytes (Rossi and Bianchini, 1996). Such increased production of NO due to the synergistic interactions between these two glial cell types may be neurotoxic in JNCL (Brown et al., 1995; Chao et al., 1995; Bolaños et al., 1997; Heales et al., 1997; Leist et al., 1997; Murphy, 2000; Wei et al., 2000). NO mediated signaling has been previously investigated in different models of JNCL (Kim et al., 2003; Ramirez-Montealegre and Pearce, 2005; Chan et al., 2009), and decreased arginine (substrate for NO production) availability was speculated to cause abnormal NO signaling in JNCL, which in addition to impacting neuronal viability could also impact other processes such as cell energetics, apoptosis, vasodilation and synaptic function (Garthwaite and Boulton, 1995; Prast and Philippu, 2001; Bronte and Zanovello, 2005).

Another interesting player that could mediate the interactions between astrocytes and microglia is TIMP-1 (Gardner and Ghorpade, 2003; Welser-Alves et al., 2011). TIMP-1 is an endogenous MMP inhibitor important for maintenance of proteolytic balance involved in cell migration, wound healing, angiogenesis and neuronal survival (Gardner and Ghorpade, 2003; Crocker et al., 2004; Ogier et al., 2006; Stetler-Stevenson, 2008). Indeed, TIMP-1 knock-out mice displayed increased levels of MMP-9 activity, resulting in BBB breakdown and increased lesion size in a focal cerebral ischemia model (Fujimoto et al., 2008). Moreover, adenoviral-mediated gene transfer of TIMP-1 and 2 resulted in reduced levels of neuronal death in a model of global cerebral ischemia (Magnoni et al., 2007). Importantly, TIMP proteins may also influence the growth and morphology of neuronal cells in a MMP-dependent manner (Qi et al., 2003). Thus, severely decreased TIMP-1 secretion by *Cln3*$^{-/-}$ astrocytes (observed in both untreated and LPS/IFNγ treated conditions, Tables 4.1 and 4.2) could have detrimental consequences that may result in a failure to establish proper neuronal morphology and astrocyte motility, and in increased neuronal cell death. Indeed, *Cln3*$^{-/-}$ astrocytes were found to negatively impact the morphology and survival of cortical neurons derived from both WT and

Cln3$^{-/-}$ deficient mice (Chapter 6, Figures 6.2-6.5). Additionally, the observed impaired migration of *Cln3*$^{-/-}$ astrocytes could plausibly be caused by reduced TIMP-1 secretion, since TIMP-1 mediated regulation of MMP-2 has been implicated in astrocyte motility (Ogier et al., 2006). Such hypotheses could be investigated directly in astrocyte cultures or co-culture systems by addition of the recombinant form of the particular protein under study (for example TIMP-1), followed by monitoring any improvements in pathological phenotype.

A wide range of proteins secreted by astrocytes have been shown to be important in tissue regeneration and promotion of neuron survival (Ridet et al., 1997; Meeuwsen et al., 2003; Farina et al., 2007). For instance, astrocytes secrete an enormous array of neurotrophic and neuroprotective factors: NGF, BDNF, CNTF, FGF-2, VEGF, IL-3, RANTES, LIF, IL-10, MCP-1 and IL-6 in response to CNS affecting injury or disease, and activation of the cytokine receptors they express (Schwartz and Nishiyama, 1994; Rudge et al., 1995; Uchida et al., 1998; Dietrich et al., 1999; Dreyfus et al., 1999; Bruno et al., 2000; Messersmith et al., 2000; Albrecht et al., 2002; Zambrano et al., 2007; Wang et al., 2009b; Moidunny et al., 2010). Some of these factors were included in our protein secretion analysis, and were found to be secreted at significantly lower levels by activated *Cln3*$^{-/-}$ astrocytes. A few examples of these neuroprotective factors: IL-6, TNF-α, VEGF, are discussed in more detail below.

The expression of IL-6 in the brain has been shown to become increased in a number of CNS disorders, including Alzheimer disease, Parkinson disease and stroke (Gruol and Nelson, 1997; Benveniste, 1998). IL-6 has been shown to function as a neurotrophic factor for forebrain neurons (Kushima et al., 1992), and to protect PC12 cells against hypoxia-reoxygenation (Maeda et al., 1994). Furthermore, glutamate-induced neuron death in hippocampal cultures has been shown to be reduced by IL-6, and *in vivo* this protein has been shown to protect against NMDA receptor mediated ischemic insult (Yamada and Hatanaka, 1994; Ali et al., 2000; Wang et al., 2009b). Hence, the lack of IL-6 secretion combined with the attenuated glutamate clearance by *Cln3*$^{-/-}$ astrocytes (Chapter 4, Figure

4.11) may make an extremely detrimental combination, and may stimulate neuron loss in JNCL. The mechanisms involved in IL-6 mediated neuroprotection, including promotion of production and secretion of neurotrophic factors (NGF, NT3 and NT4/5), may be altered in *Cln3*$^{-/-}$ astrocytes that display reduced IL-6 secretion. However, some authors have reported no beneficial effects of IL-6 against excitotoxicity in cortical neurons (Toulmond et al., 1992), or rather acceleration of NMDA induced neuronal death upon chronic exposure to IL-6 (Qiu et al., 1998). Moreover, mice overexpressing IL-6 display significant neurodegeneration, suggesting that chronic IL-6 over-expression has neurotoxic consequences (Campbell et al., 1993). Taken together, these data re-enforce the importance of appropriately regulating the concentration of IL-6 within the CNS. Perhaps it is important that astrocytes are able to respond to acute changes in the environment by increasing IL-6 secretion to guard against the initiation of signaling cascades leading to neuronal cell death. Hence, the lack of IL-6 secretion by activated *Cln3*$^{-/-}$ astrocytes over a relatively short period of time would most likely accelerate the neurodegeneration observed in *Cln3*$^{-/-}$ mice. On the other hand, reduced levels of IL-6 may equally have beneficial effects over a longer period of time.

Increasing evidence suggests that TNF-α can be neuroprotective against excitotoxicity in both *in vitro* and *in vivo* models (Bruce et al., 1996; Carlson et al., 1998; Wilde et al., 2000; Orellana et al., 2007; Rojo et al., 2008). In addition, mice deficient in TNF-α receptors showed enhanced sensitivity to ischemic stroke (Bruce et al., 1996). Under physiological conditions, TNF-α produced by glia may have the ability to enhance synaptic efficacy by increasing the surface expression of AMPA receptors, making TNF-α important for synaptic plasticity (Beattie et al., 2002). Hence, the ability of TNF-α to play its beneficial, neuroprotective role may be impaired in the *Cln3*$^{-/-}$ mouse brain due to lack of TNF-α secretion by astrocytes. On the other hand, excessive TNF-α secreted by activated astrocytes may exacerbate tissue damage by inhibiting neurite outgrowth and inducing oligodendrocyte cell death (D'Souza et al., 1996; Neumann et al., 2002). Moreover, TNF-α in combination with other cytokines, such as IL-1, can have

synergistic effects that may be neurotoxic (Chao et al., 1995; Hu et al., 1997). Indeed, mice overexpressing TNF-α only in astrocytes develop a neurological disorder that is characterized by ataxia, seizures and paralysis (Akassoglou et al., 1997). These conflicting data might reflect the complexity of actions of such cytokines upon neuronal function and neurodegeneration, which may vary greatly depending on the cell type, amount of cytokine secreted and type of insult in question. Overall, reduced secretion of TNF-α by reactive *Cln3*$^{-/-}$ astrocytes may affect synaptic plasticity and the survival of different types of neurons in JNCL.

VEGF is a trophic factor important for angiogenesis and endothelial cell proliferation (Neufeld et al., 1999). Increasing evidence has also suggested that VEGF, whose expression has been shown to increase upon CNS insults (Chodobski et al., 2003; Sköld et al., 2005), also has neurotrophic, neurogenic and neuroprotective functions (Pellerin and Magistretti, 1994; Thau-Zuchman et al., 2010; Zheng et al., 2010; Ma et al., 2011). For instance, VEGF was shown to be upregulated in both neurons and glial cells in various brain regions following pilocarpine-induced status epilepticus (Nicoletti et al., 2008). Furthermore, administration of exogenous VEGF in this same model induced a significant preservation of hippocampal neurons, suggesting a neuroprotective role for VEGF. During development, VEGF may also stimulate axonal outgrowth and promote the survival of dorsal root ganglion neurons and developing retinal cells. Under more chronic neurodegenerative conditions, such as in ALS, VEGF has been shown to function as a neuroprotective factor (Zheng et al., 2004; Storkebaum et al., 2005). Based on the results of our protein secretion screen, *Cln3*$^{-/-}$ astrocytes failed to secrete VEGF upon activation. This would severely reduce the potential neuroprotective and axonal growth stimulating activities of this protein over the course of disease progression.

In vivo studies of the expression of VEGF, TNF-α and Il-6 expression, or their receptors, have not yet been carried out in either murine or human JNCL. If their expression were found to be similarly altered *in vivo*, therapies based on

enhancing the expression or functions of these neuroprotective factors could be considered. Co-cultures composed of different combination of WT and *Cln3*$^{-/-}$ neurons and glia could be used as a starting point to test the potency of these factors. However, all of these factors may also provoke undesired effects *in vivo,* including altered blood brain barrier permeability, increased vessel density, and inflammation associated with VEGF based therapies (Vezzani and Granata, 2005; Ivens et al., 2007; Rigau et al., 2007; Tomkins et al., 2007; Vezzani and Baram, 2007). Thus, any therapy based on such neuroprotective factors should be designed in a way so that it only facilitates their regenerative activities.

Similar protein secretion profiling to that described here for WT and *Cln3*$^{-/-}$ astrocytes, has also been conducted on microglia cultures from these mice (S. Dihanich, unpublished data). Protein screening profiling of *Cln3*$^{-/-}$ microglia revealed reduced levels for a small but specific number of proteins; the chemokines, MIP-1γ, MIP-2 and RANTES, plus MMP9 and Von Willebrand Factor (VwF). Thus, changes in protein secretion appear to be a general property of glial cells in JNCL, although astrocytes appear to be more severely affected. This could lead to lack of communication between microglia and astrocytes in JNCL, since this is dependent on the controlled secretion of such soluble factors (Liu et al., 2011). Additionally, based on a small pilot study the protein secretion profile of *Ppt1*$^{-/-}$ astrocytes was also seen to be altered, however these changes were very different to those observed in *Cln3*$^{-/-}$ astrocytes. We observed an increased secretion of IL-4, MIP-1α, VEGF, IL-11, TIMP-1, and a decreased secretion of IL-6, TNF-α, MCP5, Lymphotactin, MIP-1β and FGF-9 (unpublished data). In this infantile form of NCL, glial activation is much more pronounced and disease progression is much more rapid than in JNCL (Bible et al., 2004; Pontikis et al., 2004; 2005; Cooper, 2010; Mole et al., 2011). Perhaps such dramatic differences in the secretion of soluble factors by astrocytes may play key roles in the different pathologies observed between different forms of NCLs.

As a next step, it will be important to determine whether the changes in the levels of proteins secreted by activated glial cells described above, are also

apparent *in vivo.* Interestingly, treatment of *Cln3*$^{-/-}$ mice with the immunosuppressant mycophenolate reduced the expression of GFAP and CD68, markers of activated astrocytes and microglia respectively, and markedly improved the motor performance of these mice (Seehafer et al., 2011). Based on this study a reduction in the immune-response mediated by glial cells appears to be beneficial to *Cln3*$^{-/-}$ mice. To coincide with this observation, mixed *Cln3*$^{-/-}$ glial cultures (containing both astrocytes and microglia) have a negative impact, where as WT glial cultures have a positive impact, on both the morphological complexity and survival of WT and *Cln3*$^{-/-}$ neurons (see data presented in Chapter 6). This negative impact of *Cln3*$^{-/-}$ glial cells could perhaps result from alterations in protein secretion as described above. However, further studies will be needed to confirm this hypothesis, possibly by attempting to reverse such negative affects by adding cocktails of these missing proteins. To overcome these secretion deficits, plausibly caused by a disrupted cytoskeleton in *Cln3*$^{-/-}$ astrocytes, neuron derived growth factors, such as FGF and EGF, that have the potential to facilitate re-arrangements in the astrocyte cytoskeleton in a Rho kinase signaling dependent manner, could also be tested (Kalman et al., 1999). Additionally, cell inserts upon which glial cells are grown, could be placed in wells containing cultured neurons to investigate directly the impact of glia-secreted proteins on neurons. Indeed, such studies may open up new avenues for therapeutic approaches designed to overcome the negative aspects of these secretion defects and to enhance any potential positive influences.

Undisrupted lactate secretion in *Cln3*$^{-/-}$ astrocytes

Astrocytes play a fundamental role as energy providers in the CNS (Tsacopoulos and Magistretti, 1996; Pellerin et al., 1998; Pellerin and Magistretti, 2012). The Na^+-dependent uptake of glutamate into astrocytes leads to a cascade of molecular events involving Na^+-K^+-ATPase, glycolytic processing of glucose and subsequent release of lactate from astrocytes (Pellerin and Magistretti, 1994; Takahashi et al., 1995). Some evidence suggests that lactate may be the preferred energy substrate for highly active neurons, directly coupling the energy

demand arising from synaptic activity with glucose utilization by astrocytes (Magistretti and Pellerin, 1999; Pellerin and Magistretti, 2012). Our data revealed that *Cln3*$^{-/-}$ astrocytes showed a normal ability to secrete lactate when glucose was provided as a fuel for lactate production (Figure 4.11). This result indicates that when *Cln3*$^{-/-}$ astrocytes are provided with an energy substrate, their ability to produce, and importantly secrete lactate, is not impaired. However, since the process of lactate shuttling between astrocytes and neurons is strongly driven by glutamate clearance, which we have shown to be impaired in *Cln3*$^{-/-}$ astrocytes (see below), this overall process may be compromised in the *Cln3*$^{-/-}$ mouse brain. Furthermore, CLN3 has been suggested to interact indirectly with the Na^+-K^+-ATPase, which is also a key player in the lactate shuttle process and the dynamic trafficking of Na^+-K^+-ATPase at the plasma membrane was found to be altered upon CLN3 deficiency (Uusi-Rauva et al., 2008). Therefore, despite the fact that *Cln3*$^{-/-}$ astrocytes do not show altered lactate secretion, the decreased glutamate clearance by these cells, taken together with potential alterations in the correct trafficking of Na^+-K^+-ATPase, may perturb the lactate shuttle system in the JNCL brain.

In the brain, blood glucose in a major energy substrate that may be taken up by both astrocytes and neurons via glucose transporters: GLUT1 in astrocytes and GLUT3 in neurons (Pellerin, 2003; Gladden, 2004). It is believed that blood glucose may be readily available to astrocytes since astrocyte end-feed tightly cover the surface of blood capillaries, providing a physical mechanism for efficient glucose uptake from the blood (Pellerin et al., 1998; Simard et al., 2003; Gladden, 2004). Due to the morphological abnormalities we have documented in *Cln3*$^{-/-}$ astrocytes, their capillary coverage via their end-feet may be compromised, which would alter their glucose uptake and energy metabolism in the *Cln3*$^{-/-}$ mouse brain. Indeed, in terms of energy metabolism in *Cln3*$^{-/-}$ mice, a shift towards gluconeogenesis and down-regulation of genes associated with energy production in mitochondria have been reported (Brooks et al., 2003; Chattopadhyay et al., 2004; Luiro et al., 2006). This may be an indication of enhanced energy demand arising from insufficient availability of energy

providers such as glucose in the CNS of *Cln3*$^{-/-}$ mice, potentially caused by alterations in astrocyte end-feet connectivity with blood vessels. Immunohistological investigation of interactions between astrocyte end-feet and blood vessels in the *Cln3*$^{-/-}$ mouse brain, and in brain sections from JNCL patients would provide further insights into this matter. Under conditions, such as during epileptic seizures, neuronal energy demand is extremely high (Cloix and Hévor, 2009), and demand for lactate produced via astrocyte glycogenolysis is increased. It would be interesting to investigate whether this mechanism could play a role in epileptogenesis in JNCL.

Excess glutamate is not cleared by *Cln3*$^{-/-}$ astrocytes

Glutamate is the major excitatory neurotransmitter in the mammalian CNS, and it may act as a potent neurotoxin and glutamate excitotoxicity has been implicated in a number of diseases, including epilepsy, stroke and ALS (Cendes et al., 1995; Pitt et al., 2000; Hazell, 2007). Glutamate transporters are expressed by many different cell types in the CNS, including neurons, microglia, oligodendrocytes, endothelial cells, and of course astrocytes. Indeed, astrocytes are recognized as key players in maintaining the appropriate extracellular levels of glutamate (Kanai and Hediger, 1992; Rothstein et al., 1994; Kondo et al., 1995; Domercq et al., 1999; O'Kane et al., 1999; Anderson and Swanson, 2000). Moreover, astrocyte-based regulation of glutamate concentration in the extracellular space is pivotal for the kinetics of glutamatergic synaptic activity (Danbolt, 2001; Minelli et al., 2001; Hertz and Zielke, 2004). As such, our finding of attenuated glutamate clearance by *Cln3*$^{-/-}$ astrocytes (Chapter 4, Figure 4.11) could not only impact synaptic activity, but also ultimately expose neurons in the JNCL brain to excitotoxicity.

Why do *Cln3*$^{-/-}$ astrocytes show an attenuated ability to uptake glutamate? The Na^+-dependent glutamate transporters: GLAST (EAAT1) and GLT-1 (EAAT2) are the key players in astrocyte glutamate clearance (Pines et al., 1992; Storck et al., 1992; Shashidharan and Plaitakis, 1993; Shashidharan et al., 1994). Immunohistological investigation of glutamate transporter expression in human

JNCL post-mortem tissue revealed reduced immunoreactivity particularly for the EAAT2 transporter (Hachiya et al., 2006). Such a reduced expression of a glutamate transporter could dramatically alter the ability of *Cln3*$^{-/-}$ astrocytes to take-up glutamate. Disrupted expression of glutamate transporters has been well established in epilepsy (Mathern et al., 1999; Proper et al., 2002), and the astrocyte-selective glutamate transporter EAAT2 has also been shown to be pivotal for maintaining extracellular glutamate below excitotoxic levels (Rothstein et al., 1996). In the healthy brain astrocytes are strategically located in close proximity to the synapse allowing the detection of, and reaction to, increased levels of extracellular glutamate (Volterra and Meldolesi, 2005). In the JNCL brain, these actions of astrocytes may be compromised accelerating the ongoing degenerative process and exposing the neurons to overstimulation typical for epileptogenesis (Rossi and Volterra, 2009). Studying the expression of glutamate transporters by astrocytes, both *in vitro* and *in vivo,* would provide important clues to mechanisms underlying glutamate metabolism in *Cln3*$^{-/-}$ mice.

Cytoskeletal components have been implied to be involved in a range of signal transduction pathways and in transporter trafficking (Apodaca, 2001; Tuvim et al., 2001; Najimi et al., 2002). For instance, inhibition of actin polymerization has been shown to attenuate glutamate clearance by astrocytes (Duan et al., 1999), whereas inhibition of microtubule formation had no effect on this process (Jordan and Wilson, 1998). Moreover, the actin cytoskeleton has been associated with transporter function, intracellular protein trafficking and signal transduction in many systems (Mills and Mandel, 1994; Tsakiridis et al., 1994; Lamaze et al., 1997; Wang et al., 1998). These findings suggest that the abnormal actin cytoskeleton in *Cln3*$^{-/-}$ astrocytes may be the key element in reduced glutamate clearance by these cells. Moreover, intermediate filament proteins, particularly, GFAP, have been shown to be involved in the modulation of astrocyte glutamate transporter trafficking and function (Hughes et al., 2004). Hence, abnormalities in both intermediate filaments and actin cytoskeleton (Chapter 3, Figure 3.7) could synergistically result in decreased glutamate clearance by *Cln3*$^{-/-}$ astrocytes.

Elevated levels of glutamate in the cerebellum and cortex of *Cln3*$^{-/-}$ mice have been reported previously, suggesting that glutamate neurotransmission may be altered in JNCL (Pears et al., 2005). The lack of astrocyte glutamate scavenging reported here (Chapter 4, Figure 4.11) may offer a realistic explanation for the increased levels of glutamate observed. Glutamate acts via its receptors (NMDA, AMPA, kainate and metabotropic receptors) that may all modulate synaptic transmission (Kew and Kemp, 2005). Intriguingly, cerebellar granule cells derived from *Cln3*$^{-/-}$ mice show a selectively increased sensitivity to AMPA-type glutamate receptor-mediated toxicity (Kovács et al., 2006), and treatment with specific AMPA antagonists resulted in a significant improvement in the motor skills of one-month-old *Cln3*$^{-/-}$ mice (Kovács and Pearce, 2008). Furthermore, the neuronal cells derived from *Cln3*$^{\Delta ex7/8}$ knock in mice are highly susceptible to both AMPA-and NMDA-type glutamate receptor over-activation (Finn et al., 2011). Based on these key findings one can speculate that abnormally enhanced glutamate receptor activity, which may well be down to the impaired regulation of glutamate concentration by *Cln3*$^{-/-}$ astrocytes, contributes significantly towards clinical manifestations and neuronal loss in JNCL. This suggests that regulation of glutamate metabolism by astrocytes could be considered as a potential therapeutic target in this disease.

What could be the implications of the disrupted glutathione secretion in JNCL?

Direct GSH-based connections between neurons and astrocytes have been well established. Astrocytes release GSH (Yudkoff et al., 1990; Sagara et al., 1996) via Mrp1 (Hirrlinger et al., 2002; Minich et al., 2006), which is cleaved by astrocyte and neuron-associated ectoenzymes to provide the rate limiting substrate, L-cystine, for neuronal GSH synthesis (Dringen et al., 1997; 1999b; 2001). This direct connection, enabling neuronal GSH production, may be altered in *Cln3*$^{-/-}$ astrocytes, since these cells fail to secrete the GSH they synthesize (Figure 4.9) Given that GSH is the most abundant mammalian thiol-containing antioxidant in

the CNS, lack of GSH secretion by *Cln3*$^{-/-}$ astrocytes may have significant consequences (Dringen, 2000).

The impaired glutathione secretion from *Cln3*$^{-/-}$ astrocytes could result from the failure of several cellular mechanisms. It is plausible that GSH trafficking and its secretion machinery could be impaired in *Cln3*$^{-/-}$ astrocytes, due to their cytoskeletal abnormalities (Potokar et al., 2005; Stenovec et al., 2007; Potokar et al., 2008). Indeed, disrupting the correct polymerization of actin cytoskeleton with cytochalasin D in WT astrocytes demonstrated the importance of actin cytoskeletal integrity for glutathione secretion by these cells (Chapter 4, Figure 4.10). One cannot exclude the possibility that an abnormal IF network organization may also play a role in this process. Alternatively, transport of GSH via MRP1 may be altered *Cln3*$^{-/-}$ astrocytes. Impaired MRP1-mediated export of products related to the GSH antioxidant system has been suggested to cause accumulation of glutathione-conjugated substrates in astrocytes, in a very similar fashion to that described here for *Cln3*$^{-/}$ astrocytes, subsequently leading to increased oxidative stress and cellular degeneration in Alzheimer disease (Sultana and Butterfield, 2004). This possibility could be explored directly by studying the expression, and by measuring the activity, of the MRP1 transporter in *Cln3*$^{-/-}$ astrocytes (Hipfner et al., 1999).

CLN3 has been proposed to play a protective role in managing the cellular response to oxidative stress in a *Drosophila* model of JNCL (Tuxworth et al., 2011). In this model, CLN3 deficiency caused accumulation of reactive oxygen species (ROS) leading to increased levels of oxidized cytosolic proteins, which may ultimately result in lysosomal dysfunction and cell death. In addition, increased oxidative stress has also been shown in a mouse model of JNCL (Benedict et al., 2007). Furthermore, multiple regions of the *Cln3*$^{-/-}$ mouse brain display a specific reduction of total glutathione, which could be caused by the lack of GSH secretion from astrocytes, as reported in this study (Chapter 4, Figure 4.9). Increased levels of manganese superoxide dismutase (MnSOD), which is another antioxidant enzyme, in *Cln3*$^{-/-}$ mice could be one of the mechanisms

employed to counteract such oxidative stress-mediated damage (Benedict et al., 2007). MnSOD is a mitochondrial antioxidant enzyme that is universally produced by all cells, and astrocytes do not play any significant role in MnSOD based antioxidant protection of neurons (Macmillan-Crow and Cruthirds, 2001). Hence, the lack of glutathione secretion by astrocytes might initiate a compensatory mechanism aimed to protect neurons against ongoing oxidative stress in *Cln3*$^{-/-}$ mice. In addition to dysfunctional GSH secretion from astrocytes, microarray studies on *Cln3*$^{-/-}$ mice have revealed an up-regulation of many proteins involved in oxidative stress responses (Brooks et al., 2003), further highlighting the potential role of oxidative stress as part of the pathogenesis of JNCL.

JNCL is certainly not the only neurological disease associated with oxidative stress. In fact oxidative stress has emerged as one of the key players in neurodegenerative mechanisms in numerous diseases, such as Alzheimer disease (Nunomura et al., 2006), Parkinson disease (Hald and Lotharius, 2005) and ALS (Boillée et al., 2006). Common changes caused by oxidative stress in these diseases include lipid, protein and DNA damage, and neurons appear to be especially susceptible to oxidative damage, possibly due to a combination of their longevity and high metabolic turnover (Halliwell, 2006). Thus, the lack of glutathione secretion from *Cln3*$^{-/-}$ astrocytes could make neurons highly susceptible to oxidative damage. This would suggest that one of the primary defects in JNCL pathogenesis could be the failure of astrocytes to respond appropriately to oxidative stress. To explore whether the impaired glutathione secretion by *Cln3*$^{-/-}$ astrocytes makes neurons more susceptible to cell death under oxidative stress conditions, induced by for example by using H_2O_2 (Desagher et al., 1996; Dringen et al., 1999a), co-cultures comprised of WT and *Cln3*$^{-/-}$ astrocytes and neurons could be used, and L-cysteine applied to rescue any defects arising from impaired glutathione secretion by *Cln3*$^{-/-}$ astrocytes.

The lysosomal dysfunction that is apparent in JNCL could additionally contribute to oxidative stress induced neurodegeneration, due to the unique ability of lysosomes to effectively degrade oxidatively damaged molecules and proteins

(Pivtoraiko et al., 2009). Indeed, lipofuscin accumulation, lysosomal dysfunction, impaired ER and mitochrondrial function, all of which are common features of pathogenesis of different forms of NCL, have all been shown to be consequences of oxidative damage (Wei et al., 2008; Pivtoraiko et al., 2009; Kim et al., 2010b; Mole et al., 2011). Indeed, oxidative damage has been reported in several other forms of NCL including *Ppt1*$^{-/-}$ (Kim et al., 2010b), *Cln6*$^{-/-}$ (Heine et al., 2003) and *Cln8*$^{-/-}$ (Guarneri et al., 2004). General mechanisms involved in neurodegeneration in the NCLs could include synergistic effects of reduced intracellular levels of GSH and reduced ATP production due to mitochondrial dysfunction, which have been shown to increase the susceptibility of dopaminergic neurons to both energy-stress-induced cell death and excitotoxicity both *in vitro* and *in vivo* (Zeevalk et al., 1997; 1998). Indeed, dramatic changes in the catabolism of dopamine, leading to elevation in reactive oxidative forms of dopamine have been proposed to be involved in the progressive dopaminergic neuronal loss in the striatum of *Cln3*$^{-/-}$ mice (Weimer et al., 2007). Attenuated activation of astrocytes (See Chapter 3 and Pontikis et al., 2004; 2005) and the lack of GSH secretion could also contribute to neuronal cell death in JNCL (Mytilineou et al., 1999). Various different forms of antioxidant based therapies have shown benefits regarding hindering the clinical progression in JNCL patients, although these results have not been clinically verified (Santavuori et al., 1988; 1989; Westermarck et al., 1997). Thus, antioxidant based therapies developed further, and in combination with other therapies, may help inhibit the earliest pathological events that accumulatively lead to progressive neuronal loss in JNCL.

Why do *Cln3*$^{-/-}$ astrocytes migrate so slowly and what could this mean?

Migration was severely attenuated in *Cln3*$^{-/-}$ astrocytes (Chapter 4, Figure 4.12). Such attenuated astrocyte migration may impact migration of reactive astrocytes towards sites of damaged (Fawcett and Asher, 1999; Saadoun et al., 2005), and localized immune responses (Merrill and Benveniste, 1996) in the JNCL brain, since all of these functions require correctly orchestrated movement of

astrocytes to particular locations within the CNS. The discovery of attenuated *Cln3*$^{-/-}$ astrocyte migration is in keeping with previous finding, which demonstrated a similar deficiency in the migration of *Cln3*$^{-/-}$ mouse embryonic fibroblasts (Getty et al., 2011). The disruption of the putative Myosin-IIβ-CLN3 interaction was speculated to be the cause of this improper cell migration (Lo et al., 2004; Vicente-Manzanares et al., 2007; 2009; Getty et al., 2011). Hence, it seems that CLN3 could indeed be involved in cell migration, via its proposed interactions with cytoskeletal components.

Additionally, several other mechanisms, including defects in metabolic status, proliferation, re-arrangement of cytoskeletal components, correct polarization, altered protein localization or deficient cell adhesion could each contribute towards inhibited migration (Etienne-Manneville and Hall, 2001; Etienne-Manneville, 2004). One can exclude the possible role of attenuated proliferation of *Cln3*$^{-/-}$ astrocytes in inhibited migration, since the scratch assay was performed on a confluent monolayer of astrocytes in the presence of Ara-C containing medium to block astrocyte proliferation. No detectable difference was observed in viability between WT and *Cln3*$^{-/-}$ astrocytes under these experimental conditions either. Thus, the attenuated migration of *Cln3*$^{-/-}$ astrocytes cannot be caused by poor survival of these cells under these experimental conditions. In this type of migration assay, primary astrocytes undergo a highly polarized migration in a direction perpendicular to the scratched area (Etienne-Manneville and Hall, 2001; Peng et al., 2008). Cell-adhesion proteins, N-cadherins and integrins, have been shown to direct such polarization and oriented migration in astrocytes (Camand et al., 2012). In embryonic CLN3 deficient fibroblasts the migration defect was not thought to be caused by cell adhesion defects, due to an evidently normal distribution of adherens junctions, which are formed by cadherin and catenin proteins, even in the absence of CLN3 (Getty et al., 2011). Thus, it is likely that the observed migration defects exhibited by *Cln3*$^{-/-}$ astrocytes are not caused by problems in cell adhesion. This, however, should be confirmed by examining the expression of N-cadherins and integrins in these astrocyte cultures. Intriguingly, inhibition of lysosome function by treating

embryonic CLN3 deficient fibroblasts with chloroquine exacerbated their migration defects, whereas WT fibroblasts were able to overcome this insult (Getty et al., 2011). Thus, alterations in lysosomes observed in *Cln3*$^{-/-}$ astrocytes (Chapter 3, Figures 3.11 and 3.13), could together with abnormal myosin-IIB-cytoskeleton dynamics decrease their ability to migrate.

Generally, depolymerization of actin filaments or microtubules, and lack of functional IFs impair the motility of astrocytes, and the correct interplay between each of these cytoskeletal components is crucial for astrocytic migration (Lepekhin et al., 2001; Etienne-Manneville, 2004). Thus, the abnormal cytoskeleton and possibly disrupted myosin-IIβ interaction may be the key factors explaining the migration defects in *Cln3*$^{-/-}$ astrocytes. To examine this further myosin-IIB distribution could be explored, and inhibition of myosin-IIB with, for example, blebbistatin in WT astrocytes could be tested to see if this resembles the migration defects seen in *Cln3*$^{-/-}$ astrocytes.

Astrocyte migration has been observed in many CNS diseases, for example it is necessary for Aβ clearance and the formation of a protective barrier between Aβ deposits and neurons in the Alzheimer brain (Wyss-Coray et al., 2003; Rossner et al., 2005). Interestingly, cultured adult mouse astrocytes have been shown to migrate in response to the MCP-1 chemokine that is present in Alzheimer disease lesions (Wyss-Coray et al., 2003). Our protein profiling analysis revealed that secretion of this chemokine by *Cln3*$^{-/-}$ astrocyte was significantly reduced (Chapter 4, Tables 4.1 and 4.2). MCP-1 mediated guidance of astrocyte migration along with the attenuated ability of *Cln3*$^{-/-}$ astrocytes to migrate could perhaps influence where reactive changes occur in the *Cln3*$^{-/-}$ mouse brain. Whether this has a positive or negative impact upon disease progression would depend on the exact role that these cells play in the pathogenesis of JNCL.

Indeed, astrocytes exert a wide range of crucial functions during CNS development and during post-natal stages, and many of them are dependent on astrocyte migration and motility. For example, astrocytes guide the migration of

developing axons and certain neuroblasts (Powell and Geller, 1999). Moreover, it was recently reported that migrating astrocytes are allocated to spatial domains in both the spinal cord and the brain, and that this is determined by their embryonic sites of origin in the ventricular zone (Tsai et al., 2012). These data reveal that region-restricted astrocyte migration is a general part of CNS development (Tsai et al., 2012). Based on this, the impaired migration ability of astrocytes due to CLN3 deficiency, could also alter the correct formation of region-specific astrocyte domains within the brain. Subsequently this could result in abnormal synaptogenesis and neuronal dysfunction within these domains (Molofsky et al., 2012; Tsai et al., 2012). More specific investigations are required to determine whether astrocyte migration is actually altered *in vivo* in the *Cln3*$^{-/-}$ mouse brain, and to determine the precise role of such impaired astrocyte migration in the development and local regulation of synaptogenesis.

Taken together these results imply that Cln3 deficiency has a direct impact upon astrocyte function. Our findings show a whole range of altered properties of *Cln3*$^{-/-}$ astrocytes, with the disrupted cytoskeletal organization observed in these cells potentially resulting in abnormal Ca^{2+} signaling and a severely impaired ability to secrete proteins, take-up transmitters and to migrate. Although the lack of a morphological response to stimulation that was observed *in vitro* does correlate well with the incomplete morphological transformation observed *in vivo*, we do not know whether any of the functional differences reported here also occur within the diseased CNS. Thus, future studies will be needed to determine how astrocyte functions are altered *in vivo* in *Cln3*$^{-/-}$ mice. Moreover, it will be important to determine the direct impact of these deficits on neuronal biology. This important question is the focus of experiments described in Chapter 6 of this thesis.

Chapter 5
The basic biology of *Cln3*$^{-/-}$ cortical neurons

5.1 Introduction

Although the precise function of CLN3 remains unknown, many studies have proposed that this protein may influence intracellular trafficking and the expression of various molecules involved in neurotransmission (Chapter 1, Section 1.2) (Järvelä et al., 1999; Haskell et al., 2000; Luiro et al., 2001; Fossale et al., 2004; Kyttälä et al., 2004; Storch et al., 2007; Uusi-Rauva et al., 2008; 2012). Given that the absence of CLN3 was observed to have a profound effect on astrocyte biology, at least *in vitro* (Chapters 3 and 4), an obvious next step was to use a similar approach to explore what influence the absence of this protein has on the biology of neurons. To this end, cortical neuronal cultures derived from P0 WT and *Cln3*$^{-/-}$ mice were generated and evaluated for a range of potential deficits based on the predicted function of CLN3 in neurons.

Many lines of evidence suggest that CLN3, via its proposed interaction partners fodrin, Rab7 and myosin IIB, may be involved in neurite growth and morphology (Tullio et al., 2001; Saxena et al., 2005a; Ryu et al., 2006; Weimer et al., 2009), which may alter synapse formation and neuronal connectivity in the JNCL brain. Therefore, the impact of CLN3 deficiency on neuronal size and neurite outgrowth and complexity was explored. In addition, spontaneous epileptic seizures are one of the most prominent clinical features of JNCL suggesting that the electrophysiological properties of Cln3 deficient neurons have been altered making them more susceptible to over-activation. It has recently been shown that neurons can fine-tune their excitability by activity-dependent relocation of the AIS along the axon (Grubb and Burrone, 2010b). Hence, the localization of AIS in neurons grown under basal conditions, and after chronic depolarization was investigated. Neurotransmission has been shown to be impaired in other forms of NCL (Kim et al., 2008; Koch et al., 2011), in particular the expression and localization of SNARE-complex proteins that are involved in synaptic vesicle fusion and neurotransmitter release at the synapse (Kavalali, 2002; Ungar and Hughson, 2003; Ramakrishnan et al., 2012) have been shown altered in different NCLs (Virmani et al., 2005; Kim et al., 2008; Partanen et al., 2008; Kielar et al., 2009). Given its synaptic localization (Järvelä et al., 1999; Haskell et al., 2000;

Luiro et al., 2001; Kyttälä et al., 2004; Phillips et al., 2005; Storch et al., 2007), the effect of CLN3 deficiency on the expression level of SNARE-complex proteins and their distribution along neuronal processes was analysed in primary cortical neuron cultures.

To date, no one has studied post-natal *Cln3*$^{-/-}$ cortical neurons in culture, a region, along with the thalamus and cerebellum, where neurons in the JNCL brain are profoundly affected. This approach will therefore not only provide novel insights into the consequences of CLN3 deficiency in cortical neurons, but will specifically focus on the intrinsic biological changes that occur within these cells rather than those resulting from interactions with other cell-types, like glial cells.

5. 2 Results

Generation of cortical neuron cell cultures

In order to compare the biology of *Cln3*$^{-/-}$ and wild type cortical neurons, cultures were generated from P0 wild type or *Cln3*$^{-/-}$ mice ((Tararuk et al., 2006; Semenova et al., 2007), also see Chapter 2, Section 2.3) and maintained in serum-free neurobasal medium supplemented with B27, to promote neuronal maturation, and Ara-C to inhibit glial proliferation. The purity of these neuronal cultures was assessed after 7 DIV by immunocytochemistry, using MAP2 and NeuN to identify neurons, O4 to identify oligodendrocytes, GFAP to identify astrocytes and CD68 to identify microglia (Figure 5.1 A, B and C). Most of the cells in these WT and *Cln3*$^{-/-}$ neuronal cultures were MAP2/NeuN expressing neurons (90.5±0.4% and 91.7±0.9% respectively, Figure 5.1 A and D); with 3.9±0.2% (WT) and 4.6±0.9% (*Cln3*$^{-/-}$) being GFAP^{+} astrocytes; 0.1±0% (WT) and 0.1±0.1% (*Cln3*$^{-/-}$) being CD68^{+} microglia; and 1.7±0.1% (WT) and 0.9±0.0% (*Cln3*$^{-/-}$) being O4^{+} oligodendrocytes (Figure 5.1 D). All the WT and *Cln3*$^{-/-}$ neuronal cultures used in this study were generated as described above, and had a similar composition.

A

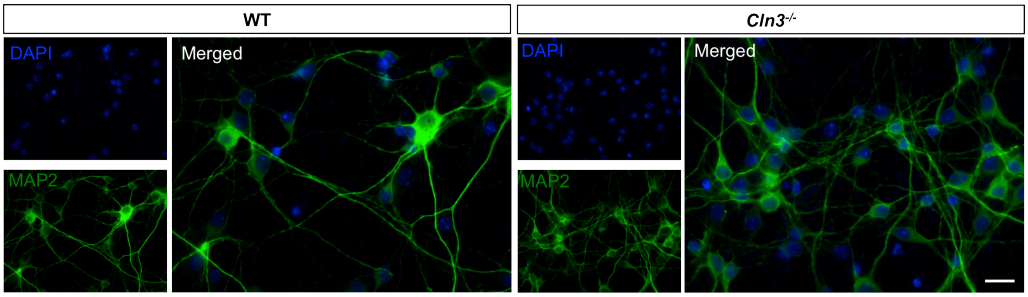

B

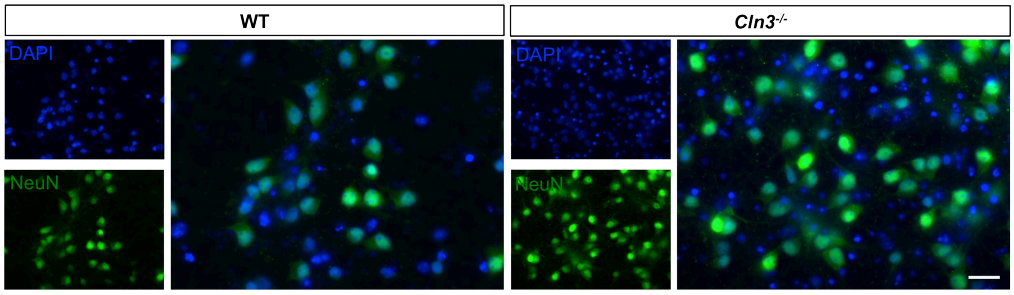

C

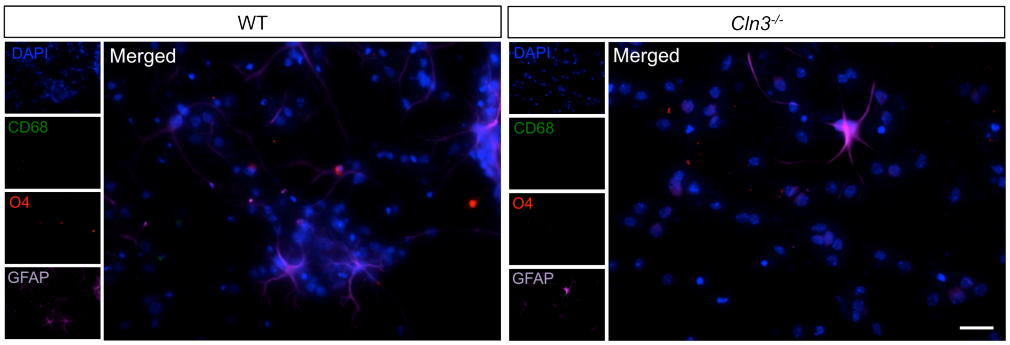

D

Mean percentage of each cell type ± SEM				
Sample	% Neuron ($MAP2^+$, $NeuN^+$)	% Astrocyte ($GFAP^+$)	% Microglia ($CD68^+$)	% Oligodendrocyte ($O4^+$)
WT	90.46±0.36	3.86±0.19	0.09±0.00	1.73±0.08
Cln3$^{-/-}$	91.74±0.92	4.55±0.87	0.10±0.05	0.90±0.04

Figure 5.1. Composition of P0 cortical neuron cultures. Primary cortical neuron cultures generated from P0 *Cln3*$^{-/-}$ or WT mice were stained with MAP2 and NeuN to identify neuronal cells, GFAP to identify astrocytes, CD68 to identify microglia and O4 to identify oligodendrocytes. DAPI was used to visualize all nuclei. Most of the cells were (A) MAP2 expressing, or (B) NeuN expressing neurons. (C) Glial contamination was mostly due to GFAP expressing astrocytes with CD68 expressing microglia and O4 expressing oligodendrocytes rarely being observed. The percentage of each cell type was determined by counting 5 random fields per coverslip and a minimum of two coverslips per experiment. The means ± SEM shown in (D) are from three separate experiments. Scale bar in (A) and (B) is 20µm, and in (C) 50µm.

No accumulation of autofluorescent storage material occurs within *Cln3*$^{-/-}$ cortical neuronal cultures

In JNCL, autofluorescent ceroid lipofuscin deposits enriched in subunit c of the mitochondrial ATP synthase complex accumulate within most nerve cells and, to a lesser extent, in numerous other cell types (Palmer et al., 1992; Seehafer and Pearce, 2006; Mole et al., 2011). We therefore explored whether there was any accumulation of such autofluorescent storage material within *Cln3*$^{-/-}$ neuronal cultures by viewing them at three different wavelengths, 488nm, 546nm and 633nm. Neither *Cln3*$^{-/-}$ nor WT neuronal cultures displayed any evidence for punctate autofluorescence (Figure 5.2), as was found in primary WT and *Cln3*$^{-/-}$ astrocyte cell cultures (Chapter 3, Figure 3.10). However, despite this lack of storage material accumulation, *Cln3*$^{-/-}$ neurons did have genotype-specific alterations in their basic biology, as presented below.

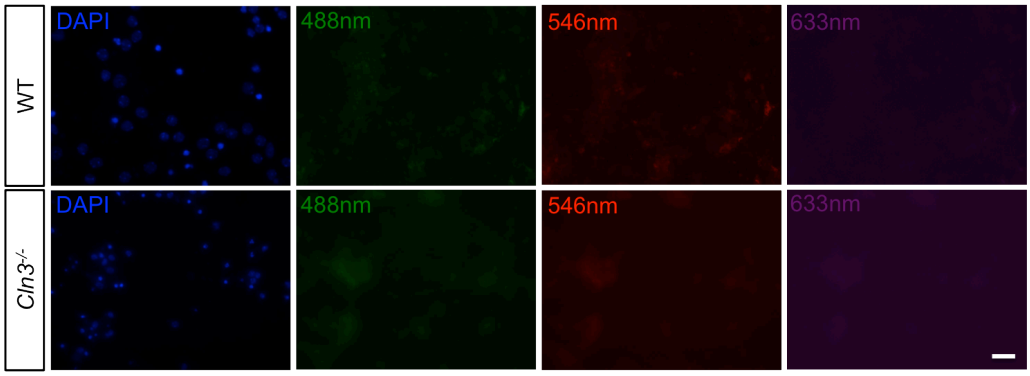

Figure 5.2. No accumulation of autofluorescent storage material within *Cln3*$^{-/-}$ neuron cultures. Cells were plated onto coverslips and fixed after 7 days in culture. DAPI was used to visualize all cell nuclei. Cells were exposed to three wavelengths: 488nm, 546nm and 633nm, to visualize any autofluorescent material within cells. Neither WT nor *Cln3*$^{-/-}$ neurons showed any apparent accumulation of autofluorescent storage material within their cell bodies. Scale bar is 50µm.

Cln3$^{-/-}$ cortical neurons are small and less complex

The ability of a neuron to correctly grow an axon and a complicated dendritic arbor, is vital for their connectivity and information processing (da Silva and Dotti, 2002; Goldberg, 2003). This process of neurite outgrowth has not been previously studied *in vitro* for any neurons lacking the CLN3 protein, but based

on *in vivo* evidence, dendritic arborization is altered in the cerebellum of *Cln3*$^{-/-}$ mice (Weimer et al., 2009).

Neuronal cultures established as described above were used to compare the neurite complexity of WT and *Cln3*$^{-/-}$ cultures. After 7DIV, cultures were fixed with 4% PFA and stained with MAP2, a neuron-specific microtubule associated protein, to visualize neurite morphology. When analyzing neurite complexity (See Figure 5.3 C), we determined: the number of primary neurites (1), secondary neurites (2), tertiary neurites (3), the total length of the primary neurites, and the length of the longest primary neurite. Additionally, the soma size of these neuronal cells was also measured (Chapter 2, Section 2.6).

A typical MAP2 expressing WT and *Cln3*$^{-/-}$ cortical neuron is shown in Figure 5.3, where it can be seen that the distribution of MAP2 immunoreactivity appears different in these two genotypes (Figure 5.3 A). In WT neurons MAP2 staining was relatively evenly distributed within both the cell soma and processes, whereas in *Cln3*$^{-/-}$ neurons MAP2 immunoreactivity appeared to be more intense within the cell soma. In addition, the soma size of *Cln3*$^{-/-}$ neurons was significantly smaller that that of WT cells (146.2±3.7 μm^2 compared to 187.2±9.9 μm^2, respectively, see Figure 5.3 B), and their neurite complexity was altered (Figure 5.3 C, b-f). As shown in Figures 5.3 C, b, c and d, the neurites of *Cln3*$^{-/-}$ neurons had slightly more branching points, seen as increased number of neurites (1 = 4.7±0.1, 2 = 1.4±0.2, 3 = 0.4±0.0), when compared to WT neurons (1 = 4.2±0.2, 2 = 1.2±0.1, 3 = 0.3±0.1), although these differences were not statistically significant. The length of the longest primary neurite, however, was significantly shorter in *Cln3*$^{-/-}$ neurons (104±6.1µm) than in WT neurons (149.3±12.7µm) (Figure 5.3 C, e), and WT neurons displayed a significantly longer network of primary neurites than did *Cln3*$^{-/-}$ neurons (279.8±27.9µm vs. 387.7±36.0µm, respectively, Figure 5.3 C, f). In conclusion, the *Cln3*$^{-/-}$ cortical neurons showed specific alterations in their morphological appearance; their cell soma size was smaller and the length of their primary neurites was significantly

decreased compered to WT cells, although the branching of these processes was not altered.

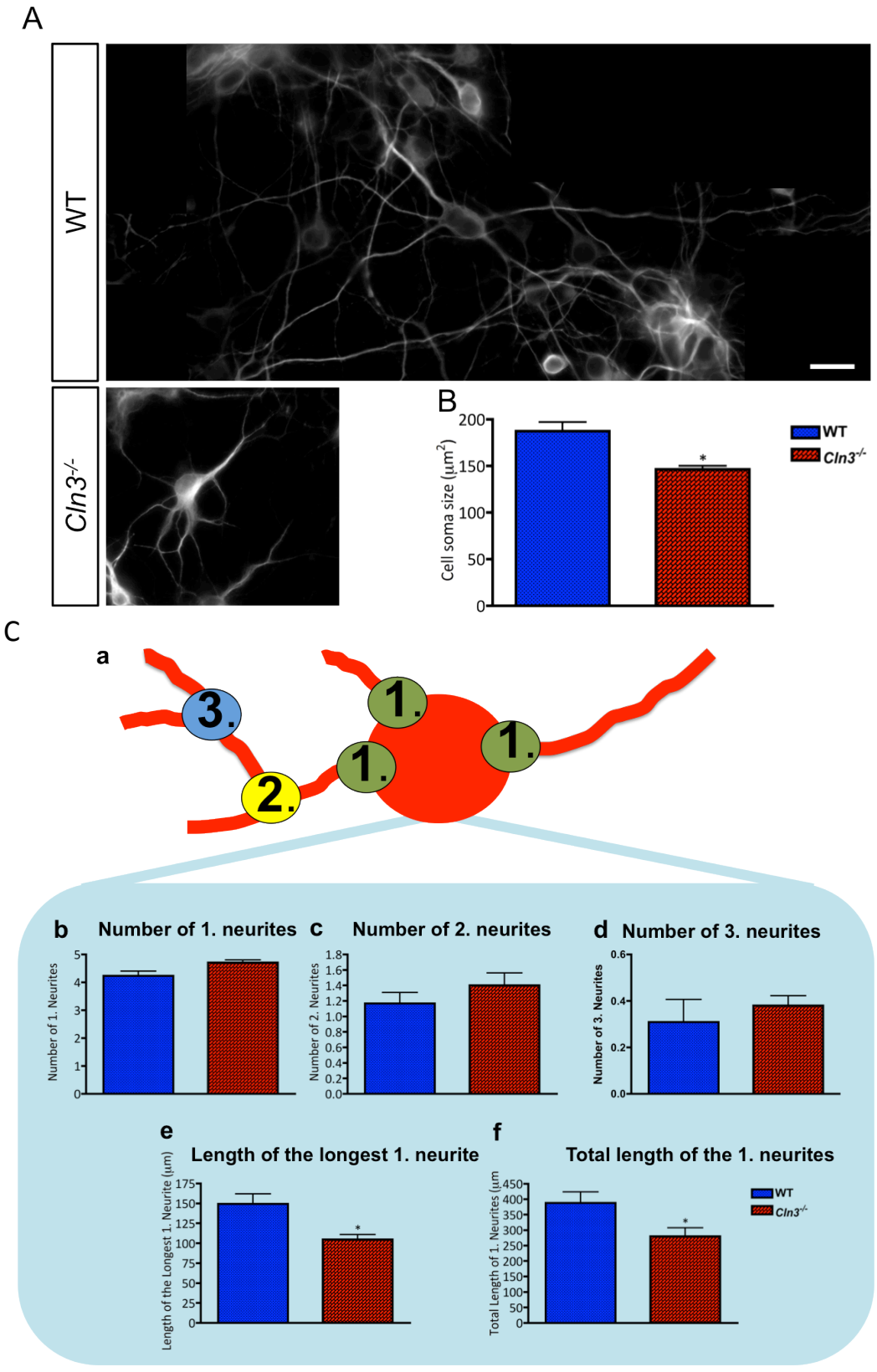

(Figure legend is on the following page)

Figure 5.3. *Cln3*$^{-/-}$ cortical neurons are small and have shortened processes. The morphology of primary cortical WT and *Cln3*$^{-/-}$ neurons was compared quantitatively using ImageJ after cultures were fixed and stained with MAP2. (A) MAP2 expressing WT and *Cln3*$^{-/-}$ cortical neurons showing that, unlike in WT cells, MAP2 immunoreactivity is not evenly distributed between the cell soma and processes in *Cln3*$^{-/-}$ neurons. (B) Quantification of cell soma size revealed that WT neurons have a significantly bigger cell soma than *Cln3*$^{-/-}$ neurons. (C) Quantitative assessment of neurite complexity, (a) schematic illustration of neurite branching, showing primary neurites (1) originating directly from the cell body, secondary neurites (2) originating from primary neurites, and tertiary neurites (3) originating from secondary neurites. The length of each of the primary neurites was analyzed, and the sum of the length of all of these neurites calculated. (b), (c) and (d) the number of each type of neurite did not differ between WT and *Cln3*$^{-/-}$ neurons. (e) WT neurons had a longer primary neurite, and (f) an increased total length of the primary neurites compared to *Cln3*$^{-/-}$ neurons. Data in (B) and (C) represent mean±SEM from approximately 40 individual cells analyzed in each experiment. This experiment was repeated three times. The scale bar in (A) is 20μm.

The AIS is located further from the cell soma in *Cln3*$^{-/-}$ neurons

Neurons contain multiple distinct membrane domains, one of which is the axon initial segment (AIS). This region, normally located at the start of axon, is highly enriched in ion channels, particularly Na_v, whose function is to integrate the input from synapses to produce an action potential (Palmer and Stuart, 2006; Atherton et al., 2008; Kole et al., 2008; Grubb and Burrone, 2010b; Popovic et al., 2011). Once the action potential is initiated in the AIS, it may propagate along the axon toward the axonal terminal where the neuronal output is mediated by the release of neurotransmitters. Importantly, changes in electrical activity can result in the movement of the AIS along the axon (Grubb and Burrone, 2010b). For example, chronic depolarization of hippocampal neurons *in vitro* caused a shift in the position of multiple components of the AIS, including the scaffolding protein ankyrin G (AnkG), BIV-spectrin, Na_v, Neurofascin and FGF14 (Figure 5.4 a) (Zhou et al., 1998; Ogawa and Rasband, 2008; Hu et al., 2009), away from the soma of excitatory neurons leading to alterations in current thresholds for action potential spiking (see Figure 5.4 b and (Grubb and Burrone, 2010b)). This endogenous mechanism enabling neurons to fine-tune their activation/firing can become vital during development and under pathological conditions (Grubb and Burrone, 2010b; Buffington and Rasband, 2011).

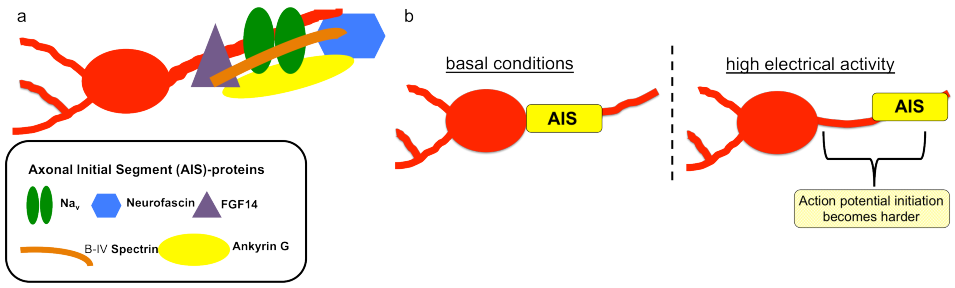

Figure 5.4. AIS components and movement. (a) The basic components of the AIS are Ankyrin G, which is the major scaffolding protein in the AIS, Nav-channels, Neurofascin, B-IV Spectrin and fibroblast growth factor-14 (FGF14). (b) Under resting conditions the AIS is located close to cell soma. High electrical activity induces chronic depolarization of the cell, which may cause a shift in the position of the AIS distally along the axon and away from the cell soma. This movement alters the current threshold for action potential spiking, making it harder for the initiation of an action potential to occur.

One of the most prominent clinical manifestations of JNCL is epileptic seizures, which may be caused by overstimulation of neurons (see Chapter 1, Section 1.2). Given that the AIS is essential for the integration of dendritic inputs to the neuron into an action potential output, as well as for fine-tuning neuronal excitability, the location of the AIS was compared in *Cln3*$^{-/-}$ and WT cortical neuronal cultures under basal conditions and upon chronic depolarization with K^+ (15mM) for a period of two days.

Cortical neuron cultures were grown on PDL coated coverslips for either 5 or 7 days, then fixed and stained with Ankyrin G to visualize the AIS (Chapter 2, Section 2.6). Images of neurons with an obvious AIS originating from their soma were acquired using a Zeiss LSM 710 confocal microscope. A Matlab based programme with custom-written functions was then used to quantify the location of the AIS in these cells (Chapter 2, Section 2.6, and see Grubb and Burrone, 2010b). The parameters used to define the AIS position along the axon in this study were the *START* position (relative to the cell soma), *MAX* position (maximum intensity of AnkG expression along the AIS), and *END* position (relative to the cell soma). Some WT and *Cln3*$^{-/-}$ cultures were exposed to chronic depolarization by treating them with 15mM extracellular potassium from either 5 to 7DIV to study the AIS localization in younger neurons, or 7 to 9DIV to study the AIS localization in older neurons. Corresponding control cells were exposed

to 15mM extracellular sodium to ensure isotonic experimental conditions between depolarized and control conditions.

In young WT neurons (5 to 7DIV) the AIS was located very close to the cell soma under control conditions (Figure 5.5 A, a). However, under chronic depolarization conditions, the AIS relocated distally away from the cell soma, with *START*, *MAX* and *END* measurements all being significantly changed (*START*: 9.0±0.8µm, *MAX*: 18.2±0.9µm, *END*: 30.3±1.0µm, Figure 5.5 A, b and B) compared to control unstimulated conditions (*START*: 5.5±0.7µm, *MAX*: 12.8±0.8µm, *END*: 22.1±0.9µm, Figure 5.5 A, a and B). In young *Cln3*$^{-/-}$ neurons the AIS was already located slightly further away from cell soma under unstimulated conditions (Figure 5.5 A, c). Global deloparization with high potassium again caused a significant shift in the location of *START* and *MAX* positions, whereas the *END* position remained unchanged (Compare c to d in figure 5.5 A) (AIS under High K^+; *START*: 9.5±1.1µm, *MAX*: 18.5±1.3µm, *END*: 29.5±1.4µm, and AIS in unstimulated conditions; *START*: 6.7±0.5µm, *MAX*: 15.6±0.7µm, *END*: 28.2±0.8µm) (Figure 5.5 B). By comparing the *START*, *MAX* and *END* positions of the AIS in young WT and *Cln3*$^{-/-}$ neurons under both unstimulated and high potassium conditions, a significant distal shift in the *MAX* and *END* positions of the AIS in *Cln3*$^{-/-}$ compared to WT neurons was detected under unstimulated conditions, whereas such significant differences could not be detected upon chronic depolarization with high potassium (Figure 5.5 D).

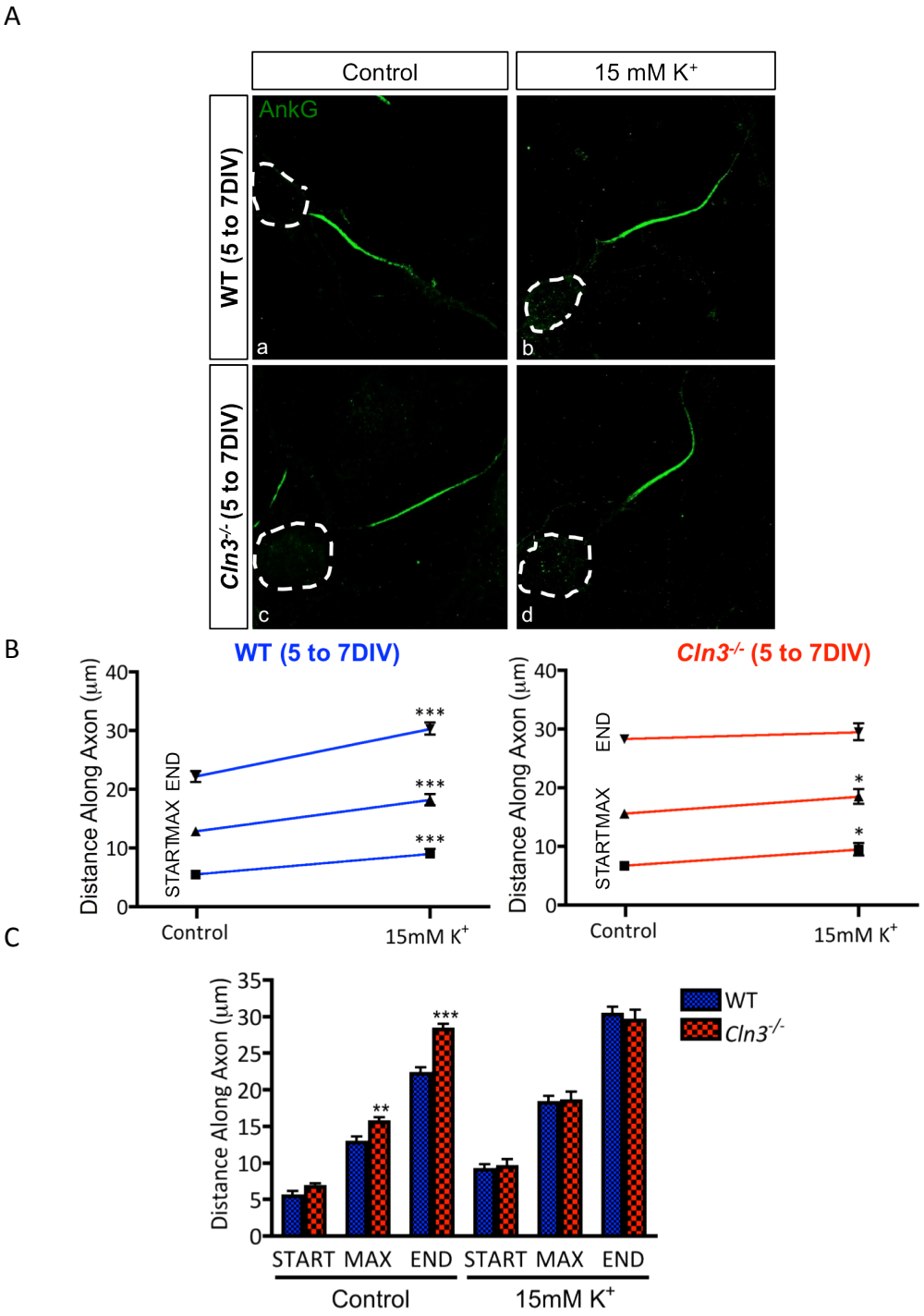

Figure 5.5. *Cln3*$^{-/-}$ neurons (5 to 7DIV) have a distally located AIS. Ankyrin G staining was used to compare the position of the AIS in WT and *Cln3*$^{-/-}$ cortical neuronal cultures under control conditions and when chronically depolarized with high potassium (15mM K^+) over period of two days (from 5 to 7DIV). The cell soma is denoted with dashed line. (A) The *START*, *MAX* and *END* positions of the AIS in WT and *Cln3*$^{-/-}$ cultures grown under control and depolarization conditions. (B) The AIS moved away from the cell soma in WT cultures treated with high K^+. The already displaced AIS moved even further away from cell soma in *Cln3*$^{-/-}$ cultures treated with high K^+. (C) The AIS is located further away from cell soma in *Cln3*$^{-/-}$ neurons than in WT neurons grown under control conditions. Data in B and C presented as mean±SEM derived from 40 cells, three different coverslips in one experiment. A T-test with Mann-Whitney U-test was used in (B), and A T-test was used in (C) for statistical analysis.

In more mature WT cortical neurons (7 to 9DIV) the AIS was again located in close proximity to the cell soma in unstimulated conditions (Figure 5.6 A, a and B, *START*: 6.4±0.6µm, *MAX*: 15.2±0.8µm, *END*: 27.1±1.2µm) and chronic depolarization caused a significant distal shift in the position of the AIS (Figure 5.6 A, b and B, *START*: 12.3±0.7µm, *MAX*: 20.4±0.8µm, *END*: 32.6±1.0µm). As observed in younger cultures, the AIS position had shifted distally away from the cell soma in older *Cln3*$^{-/-}$ neurons under unstimulated conditions (Figures 5.6 A, c and B, *START*: 10.3±0.9µm, *MAX*: 20.2±1.2µm, *END*: 34.4±1.6µm), but only one of the AIS position parameters, the *START* position, was significantly altered in chronically depolarized older *Cln3*$^{-/-}$ neurons (Figures 5.6 A, d and B, *START*: 14.3±1.0µm, *MAX*: 23.1±1.1µm, *END*: 36.7±1.3µm) compared to unstimulated controls (compare c to d in Figure 5.6 A). The observed distal shift displayed by these *Cln3*$^{-/-}$ neurons in *START*, *MAX* and *END* AIS positions in control conditions, as well as in *END* position upon chronic depolarization (Figure 5.6 C) was significantly different to WT neurons of the same age.

These analyses reveal that in *Cln3*$^{-/-}$ neurons the AIS is more distally located along the axon than in WT neurons and that this distal shift becomes greater with time in culture; reaching a distance from the cell body only seen in WT neurons when they are chronically depolarized. This may suggest that *Cln3*$^{-/-}$ neuronal cells are over-stimulated, for which they attempt to compensate by distally re-locating their AIS away from cell body, thus potentially increasing their threshold for initiation of action potential spiking.

A

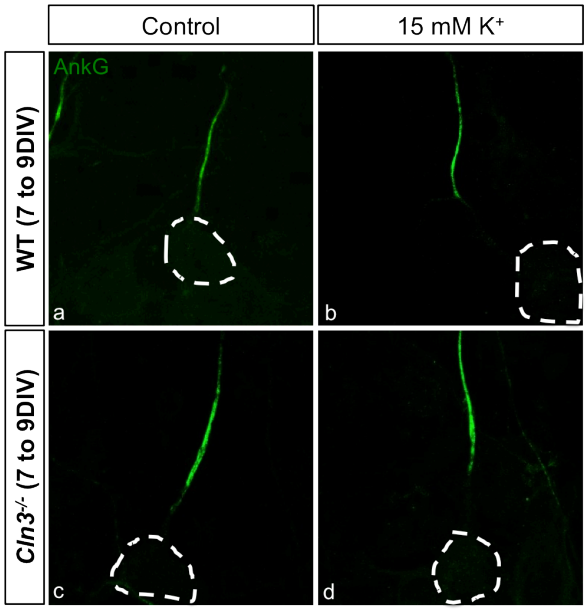

B

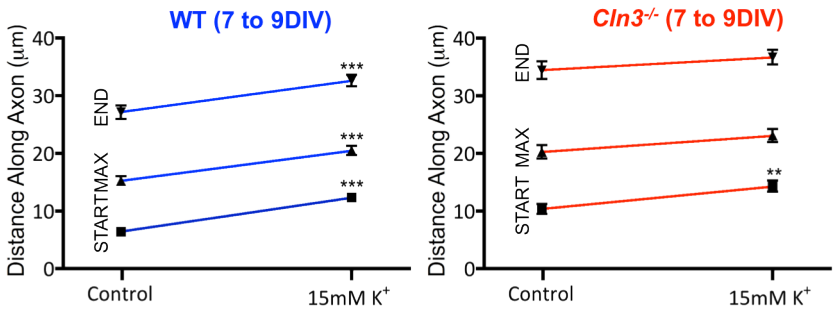

C

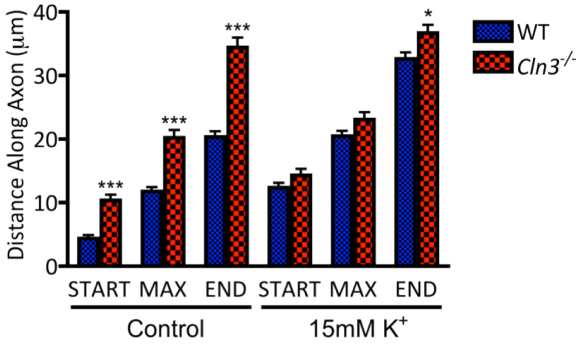

Figure 5.6. *Cln3*$^{-/-}$ neurons (7 to 9DIV) have a distally located AIS. Ankyrin G staining was used to compare the position of the AIS in WT and *Cln3*$^{-/-}$ cortical neuronal cultures under control unstimulated conditions and when chronically depolarized with high potassium (15mM K^+) over a period of two days (from 7 to 9DIV). The cell soma is denoted with a dashed line. (A) The *START*, *MAX* and *END* positions of AIS in WT and *Cln3*$^{-/-}$ cultures grown under unstimulated and depolarization conditions. (B) The AIS moved away from the cell soma in WT cultures treated with high K^+. Only the *START* position of the AIS moved further from cell soma in *Cln3*$^{-/-}$ cultures treated with high K^+. (C) The AIS is located further away from cell soma in *Cln3*$^{-/-}$ neurons than in WT neurons grown under unstimulated conditions. The *END* position of AIS in depolarized *Cln3*$^{-/-}$ was also further from the cell soma than in WT neurons. Data in B and C are presented as the mean±SEM derived from 40 cells, three different coverslips in one experiment. A T-test with Mann-Whitney U-test was used in (B), and A T-test was used in (C) for statistical analysis.

Distal movement of PanNa$_v$ expression is also evident in Cln3$^{-/-}$ neurons

We next investigated whether the distal shift in AIS position seen in *Cln3*$^{-/-}$ neuronal cells using AnKG as a marker, could also be seen by staining for other components of AIS. To do this WT and *Cln3*$^{-/-}$ cortical neurons were grown under unstimulated or depolarizing conditions (from 7 to 9DIV) and were fixed and co-labeled with AnkG and PanNa$_v$, which labels all isoforms of the voltage-gated sodium channels concentrated in the AIS (Figure 5.4, see Chapter 2, Section 2.6). This analysis revealed that PanNa$_v$ immunoreactivity was observed in approximately the same axonal region as the AnkG labeling in cultures of both genotypes under all experimental conditions tested (Figure 5.7, co-localization of PanNa$_v$ with AnkG marked with arrow heads in merged images). This indicated that other components of the AIS had undergone a similar distal shift in *Cln3*$^{-/-}$ neurons grown under basal conditions. Since the PanNa$_v$/AnkG co-localization was so evident, similar analyses to those described in Figures 5.5 and 5.6 were not carried out with PanNa$_v$.

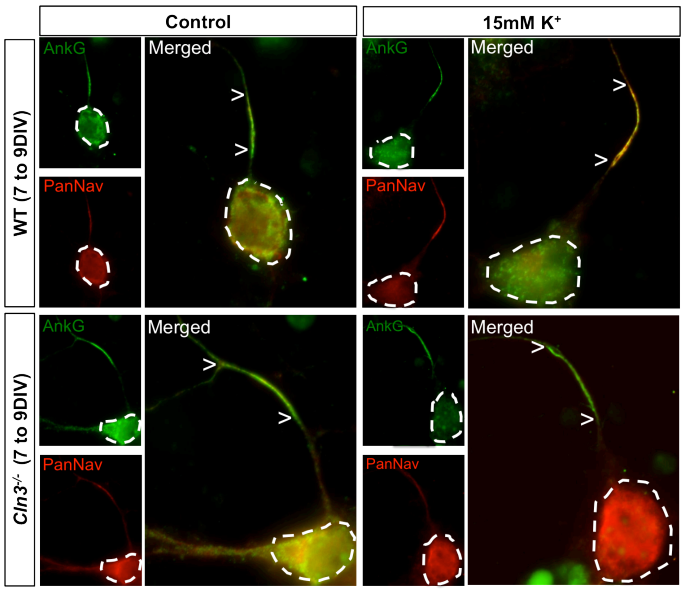

Figure 5.7. Na$_v$ relocation with AnkG in *Cln3*$^{-/-}$ neurons. WT and *Cln3*$^{-/-}$ neuron cultures grown under control or depolarization (15mM K$^+$) conditions (7 to 9DIV) were co-labeled with AnkG and PanNa$_v$. In both genotypes the PanNa$_v$ expressing voltage-gated sodium channels were localized to the same regions as AnkG under all experimental conditions tested. A distally re-located AIS was apparent with both AnkG and PanNa$_v$ labeling in *Cln3*$^{-/-}$ neurons under control conditions, and high K$^+$ induced a distal shift in WT neurons. This immunostaining was carried with cells from one neuronal culture.

AIS re-location occurs only in excitatory WT and Cln3$^{-/-}$ neurons

Previously it has been shown that, in primary hippocampal neuronal cell cultures, AIS plasticity occurs mostly in excitatory neurons (Grubb and Burrone, 2010b). In order to investigate whether AIS plasticity differs between excitatory and inhibitory neurons of the cortex, AIS positioning was studied in WT and *Cln3*$^{-/-}$ GABAergic inhibitory neurons. To identify GABAergic inhibitory neurons a cocktail of antibodies against parvalbumin, calbindin and calretinin was used instead of primary antibodies against GABA due to the poor quality of the latter (Figure 5.8). Only very few GABAergic inhibitory neuronal cells could be found in these cultures and the AIS position was not altered in these cells, but remained in close proximity to the cell soma. This was true for both WT and *Cln3*$^{-/-}$ GABAergic neurons grown under control conditions or after chronic depolarization with high K^+. This finding confirms that in primary cortical cultures AIS plasticity is predominantly a feature of excitatory neurons.

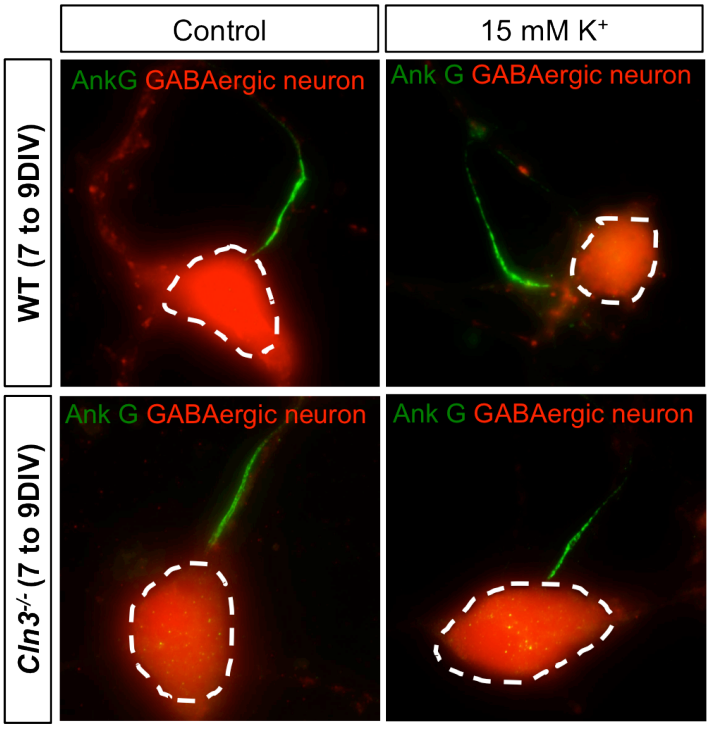

Figure 5.8. No AIS re-location in cortical GABAergic neurons. GABAergic inhibitory neurons within WT and *Cln3*$^{-/-}$ cortical cultures were identified using a cocktail of antibodies (parvalbumin, calretinin and calbindin). Ankyrin G was used to localize the AIS in these cells under control conditions and after chronic depolarization with 15mM K^+. The AIS was located close to the cell soma in WT and *Cln3*$^{-/-}$ GABAergic neurons under all conditions tested.

AIS movement is inhibited by blocking L-type calcium channels

The precise positioning of the AIS can be regulated by many intrinsic and extrinsic factors that are not yet fully understood (Goebel, 1995; Grubb and Burrone, 2010a; 2010b; Buffington and Rasband, 2011; Grubb et al., 2011). Generally, a high K^+ induced depolarization produces a chronic increase in neuronal $[Ca^{2+}]_I$. Specific blockers such as Nifedipine, which is an inhibitor of L-type calcium channels, may completely abolish AIS relocation upon chronic depolarization (Grubb and Burrone, 2010b). We hypothesized that the observed relocation of the AIS in cultured *Cln3*$^{-/-}$ neurons could be the result of overstimulation caused by extrinsic factors, which may be inhibited by blocking L-type calcium channels. To determine whether this was the case, AIS re-location was investigated in WT and *Cln3*$^{-/-}$ cultures grown under control unstimulated or in high potassium conditions in the presence or absence of Nifedipine (1µM) (Lee et al., 2006; Grubb and Burrone, 2010b). As with the investigation on AIS location described in Figures 5.5 and 5.6 above, treatments were carried out at two time points, from 5-7DIV and 7-9DIV.

In young WT neurons (5 to 7DIV) the nifedipine treatment inhibited the high potassium induced re-location of the AIS (Figure 5.9 A, b and B), as determined by a significant reduction in the *START*, *MAX*, but not in *END*, AIS position (*START*: 4.6±0.7µm, *MAX*: 15.4±0.5µm, *END*: 30.2±1.6µm) compared with non-treated cultures (*START*: 9.0±0.8µm, *MAX*: 18.2±0.9µm, *END*: 30.3±1.0µm, Figure 5.9 B). Nifedipine did not cause any significant alterations in the AIS position of WT neurons grown under control unstimulated conditions (Figure 5.9 A, a and B). In young *Cln3*$^{-/-}$ neurons nifedipine treatment inhibited the re-location of the AIS under control conditions, and after exposure to high potassium (Figure 5.9 A, c, d and B). This was indicated by a significant reduction in the *START*, *MAX* and *END* AIS positions in nifedipine treated control conditions (*START*: 4.3±0.4µm, *MAX*: 13.0±0.6µm, *END*: 25.3±0.7µm) compared to untreated, control conditions (*START*: 9.0±0.8µm, *MAX*: 18.2±0.9µm, *END*: 30.3±1.0µm), and in nifedipine treated, chronically depolarized conditions (*START*: 5.3±0.6µm, *MAX*: 12.6±0.8µm, *END*: 26.6±1.0µm) compared to non-treated, chronically

depolarized conditions (*START*: 9.5±1.1µm, *MAX*: 18.5±1.3µm, *END*: 29.5±1.4µm) (Figure 5.9 B). Indeed, no significant differences were observed in the AIS positions between corresponding WT and *Cln3*$^{-/-}$ neuronal cultures other than the *END* position of the AIS in Nifedipine treated, chronically depolarized *Cln3*$^{-/-}$ neuronal cells being significantly closer to the cell soma than in corresponding WT neurons (Figure 5.9 C). Similar effects with Nifedipine treatment were also seen in older WT and *Cln3*$^{-/-}$ cultures (See Figure 5.10). Thus, by blocking the activity of L-type calcium channels, AIS movement away from the cell soma was inhibited in both chronically depolarized WT neurons and in chronically depolarized and non-depolarized *Cln3*$^{-/-}$ neurons. This would suggest that *Cln3*$^{-/-}$ neurons are over-stimulated even when grown under basal conditions.

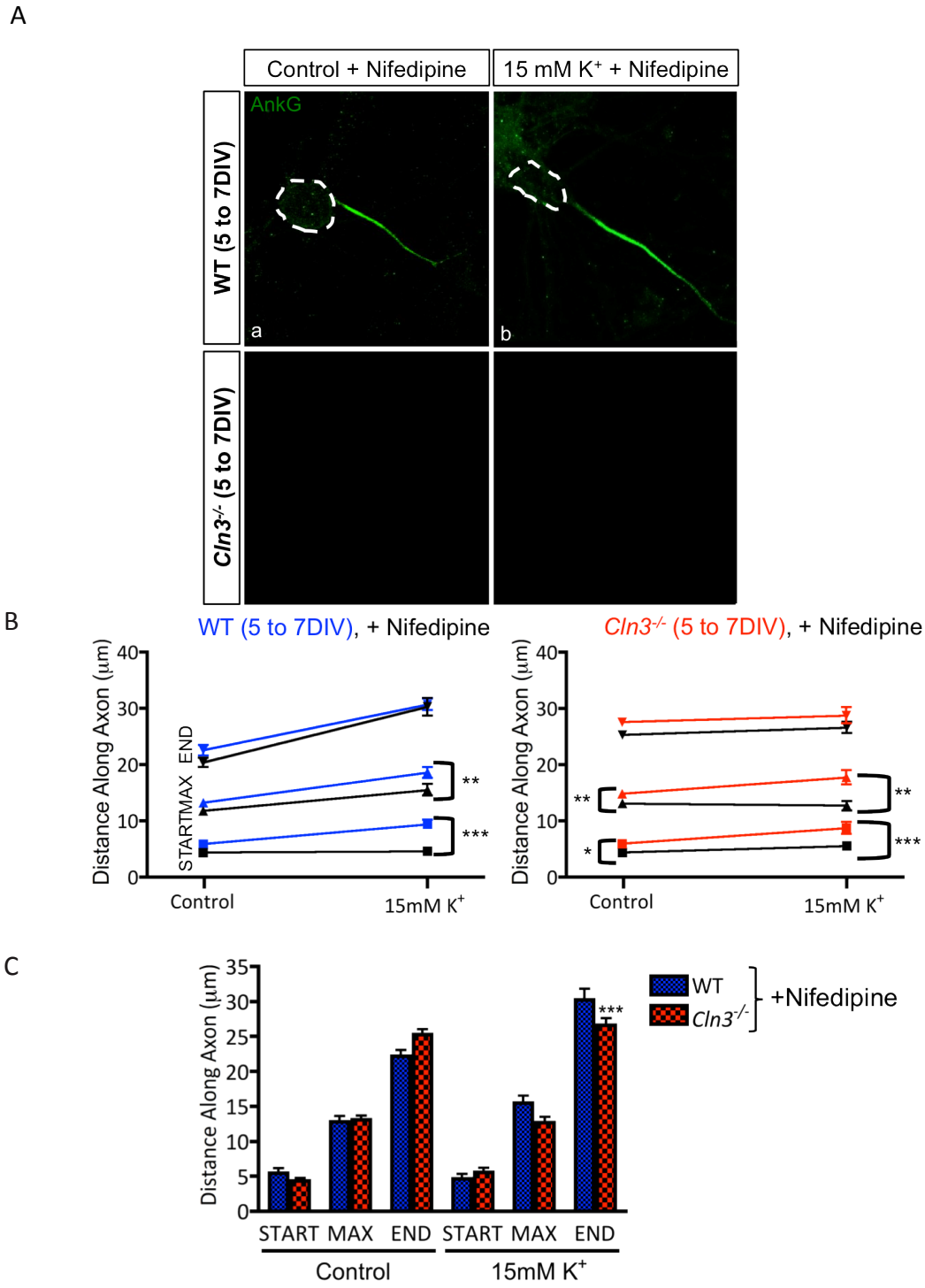

Figure 5.9. Nifedipine blocks AIS movement in young WT and *Cln3*$^{-/-}$ neurons. The location of the AIS was studied in nifedipine (1µM) treated WT and *Cln3*$^{-/-}$ cultures grown under control conditions and with chronic depolarization (5 to 7DIV), using AnKG to identify the AIS. (A) Representative cell images from all experimental conditions. (B) Nifedipine treatment inhibited AIS movement in chronically depolarized WT neurons, and in *Cln3*$^{-/-}$ neurons under control conditions and when chronically depolarized. (C) The *END* position of the AIS was closer to the cell soma in nifidepine treated, chronically depolarized *Cln3*$^{-/-}$ neurons than in WT neurons. Data in B and C represent the mean±SEM from 40 cells (three different coverslips from one experiment). Statistical analysis on the effect of nifedipine treatment was carried out using a 2-way ANOVA on ranked data (nifedipine x control/15mM K^+) with Bonferroni correction in B, and a T-test was used in C.

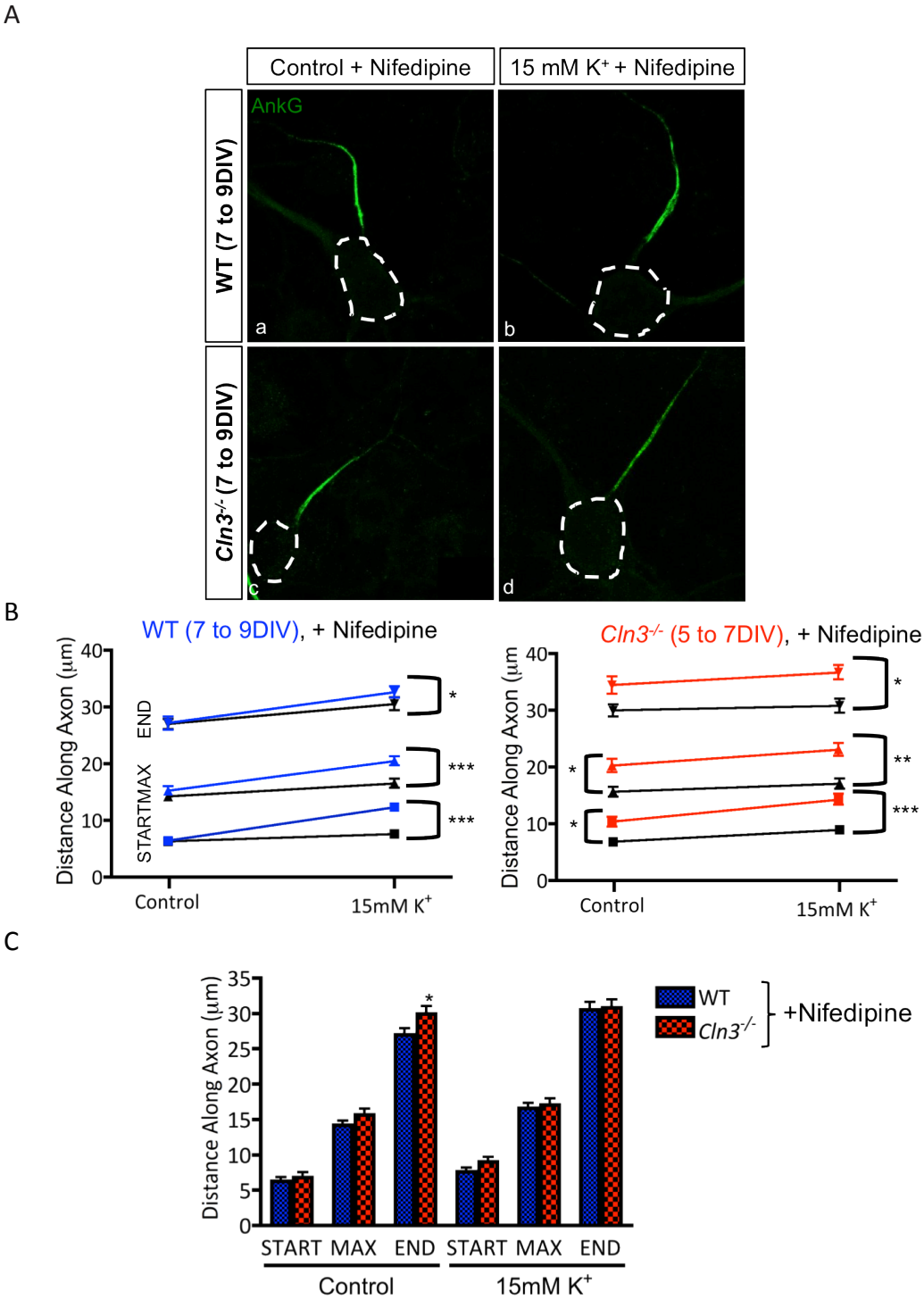

Figure 5.10. Nifedipine blocks AIS movements in old WT and *Cln3*$^{-/-}$ neurons. The location of the AIS was studied in nifedipine (1µM) treated WT and *Cln3*$^{-/-}$ cortical neuron cultures grown under control conditions and with chronic depolarization (7 to 9DIV), using AnkG to identify the AIS. (A) Representative cell images from all experimental conditions. (B) Nifedipine treatment inhibited AIS movement in chronically depolarized WT neurons, and in *Cln3*$^{-/-}$ neurons under control conditions and when chronically depolarized. (C) The *END* position of the AIS was further away to the cell soma in nifidepine treated *Cln3*$^{-/-}$ neurons compared to WT under control conditions. Data in B and C represent the mean±SEM from 40 cells (three different coverslips from one experiment). Statistical analysis on the effect of nifedipine treatment was carried out using 2-way ANOVA on ranked data (nifedipine x control/15mM K^+) with Bonferroni correction in B. T-test was used in C.

Cln3$^{-/-}$ cortical neurons distribute SNARE-complex proteins and EEA1 normally but show an increased expression of SNAP25

Neurotransmission is based on the fusion of synaptic vesicles with the plasma membrane to release the neurotransmitters they carry (Ramakrishnan et al., 2012). An essential step in this process is the interaction of the synaptic vesicle protein VAMP2, or its analogs, with syntaxin1 and SNAP25-like proteins in the plasma membrane, to form a fusion complex referred to as the SNARE-complex (Rothman, 1994; Jahn and Südhof, 1999; Bruns and Jahn, 2002; Kavalali, 2002). Prior to formation of the fusion complex, VAMP2 binds to the vesicle protein synaptophysin, which is thought to facilitate the subsequent SNARE-complex formation (Jahn and Südhof, 1999). Early synaptic pathology has been observed in mouse models of congenital NCL, INCL and vLINCL (Kim et al., 2008; Partanen et al., 2008; Kielar et al., 2009; Schantz et al., 2009), suggesting that neurotransmission may be perturbed in these diseases. Based on preliminary data synaptic pathology is also evident in *Cln3*$^{-/-}$ mice (M. O'Hare, unpublished data). Furthermore, endocytosis of neurotransmitter receptors, particularly excitatory glutamate receptors, plays an important role in modulating neurotransmission (Ehlers, 2000; Kittler et al., 2000; Lin et al., 2000; Man et al., 2000; Sheng and Kim, 2002), and EEA1, an early endosomal protein, has been shown to control vesicle fusion during endocytosis (Patki et al., 1997; Mills et al., 1998; Simonsen et al., 1998; Rubino et al., 2000). CLN3 has been linked with EEA1 expression and distribution of EEA1 expressing early endosomes (Fossale et al., 2004; Kyttälä et al., 2005; Uusi-Rauva et al., 2012), although no changes in these were observed in *Cln3*$^{-/-}$ astrocytes (Chapter 3, Figure 3.12). It has also been shown that the AIS controls protein transport into the axon (Winckler et al., 1999; Song et al., 2009; Al-Bassam et al., 2012), thus, altered AIS positioning in *Cln3*$^{-/-}$ neurons may also impact upon this process. Together, these observations led us to investigate the expression and distribution of EEA1, the SNARE-complex proteins SNAP25, VAMP2, and synaptophysin in WT and *Cln3*$^{-/-}$ cortical neurons.

Cln3$^{-/-}$ *neurons show increased expression of SNAP25*

The total expression of SNAP25, VAMP2, synaptophysin and EEA1 was quantified in 9 day old WT and *Cln3*$^{-/-}$ cortical neuron cultures by Western blot analysis (Chapter 2, Section 2.7), and the levels of these proteins were normalized against constitutively expressed β-actin. The expression of SNAP25 was significantly increased in *Cln3*$^{-/-}$ cultures (65.6±2.5% of B-actin expression) compared to WT cultures (46.7±1.2% of B-actin expression) (Figure 5.11 A), but no significant expression differences between genotypes were observed for VAMP2, Synaptophysin or EEA1 (Figure 5.11 B, C, D respectively). Hence, only very subtle differences exist in the expression of SNARE-complex proteins between healthy and *Cln3*$^{-/-}$ neurons.

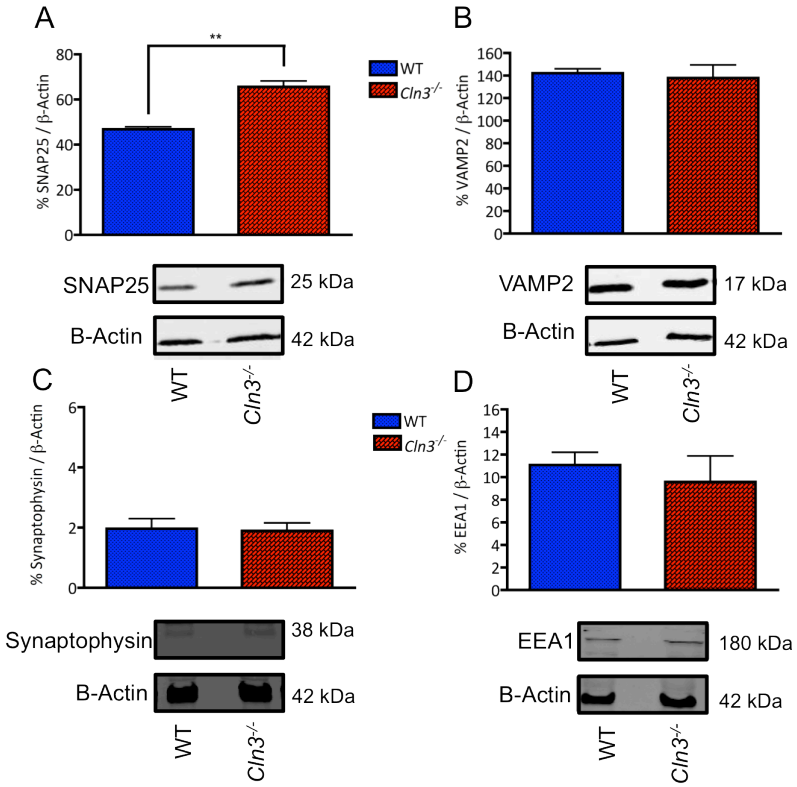

4

Figure 5.11. *Cln3*$^{-/-}$ neurons express more SNAP25 protein. Cell lysates obtained from cortical WT and *Cln3*$^{-/-}$ neuronal cultures were used to quantify the intracellular expression levels of SNAP25, VAMP2, Synaptophysin and EEA1 by Western blotting. β-Actin expression was used as an internal control of overall protein expression in each sample. (A) *Cln3*$^{-/-}$ neurons express significantly more SNAP25 protein than WT neurons. (B) Expression of VAMP2, (C) synaptophysin, and (D) EEA1 was not altered in *Cln3*$^{-/-}$ neurons. Date shown represents the percentage±SEM from three experiments.

Similar distribution of SNAP25, VAMP2, synaptophysin, and EEA1 along processes of WT and Cln3$^{-/-}$ neurons

To function properly, SNARE-complex proteins, and EEA1 must be transported along neuronal processes to where they are needed at synaptic sites. In order to investigate whether this trafficking is altered in *Cln3*$^{-/-}$ neurons, the distribution of these proteins along the processes of WT and *Cln3*$^{-/-}$ neurons was compared. For these experiments neurons were plated on PDL-coated coverslips at a density of 250,000 cells/coverslip and after 7 days in culture cells were fixed and labeled with markers for SNAP25, VAMP2, synaptophysin and EEA1 (Figure 5.12 a, b; Figure 5.13 A-C). Expression of these proteins was quantified along the processes in two regions, 0-25µm and 25-50µm away from the cell soma using ImageJ (Figure 5.12 c and d, for a high magnification image from the 0-25µm region of WT and *Cln3*$^{-/-}$ neuronal processes). In each experiment, the numbers of SNAP25, VAMP2, synaptophysin and EEA1 immunoreactive puncta in *Cln3*$^{-/-}$ neurons were compared to the corresponding numbers in WT neurons. All images within each experiment were analyzed using identical acquisition parameters, and immunopositive puncta were identified as regions of fluorescence in the neuronal processes above the background-subtracted threshold (See examples in Figure 5.12 c and d, marked with yellow circles). The quantification of these puncta was carried out manually.

Even though the total SNAP25 expression appeared higher in *Cln3*$^{-/-}$ neurons than in WT neurons (Figure 5.12, compare b to a), the number of SNAP25 immunopositive puncta along the two quantified regions, 0-25µm and 25-50µm along neuronal processes, did not differ between the two genotypes, suggesting that transportation of SNAP25 along the processes of *Cln3*$^{-/-}$ neurons is undisrupted (Figure 5.12, e). However, the increased total SNAP25 expression level observed above (Figure 5.11, A) may be explained by the marked accumulation of SNAP25 immunoreactivity in the soma of *Cln3*$^{-/-}$ neurons.

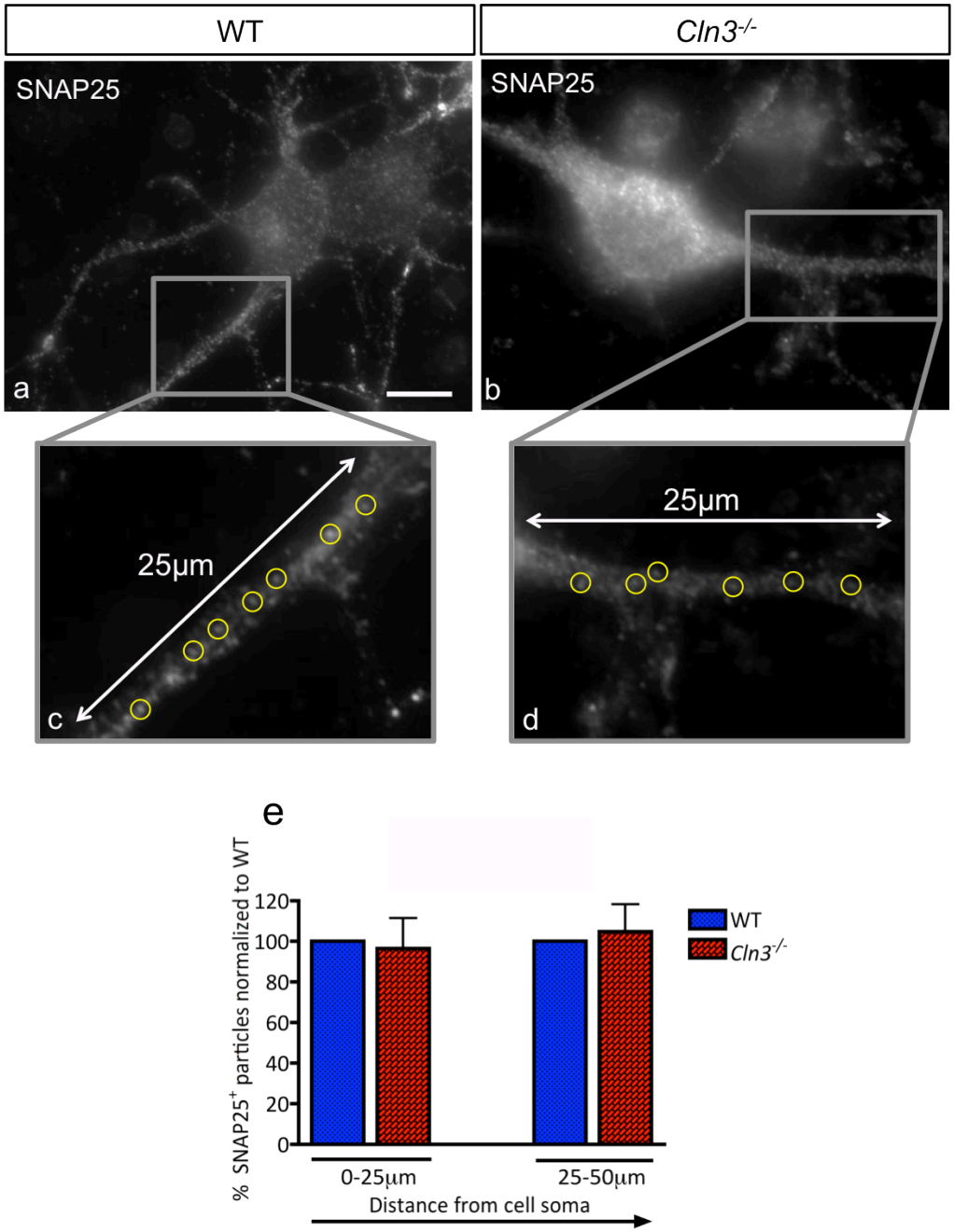

Figure 5.12. Altered distribution of SNAP25 in the soma, but not neurites of *Cln3*$^{-/-}$ neurons. The distribution of SNAP25 in the processes of WT and *Cln3*$^{-/-}$ neurons was examined (0-25µm and 25-50µm away from cell soma) by means of immunofluorescence staining. Manual quantification was performed with ImageJ from images acquired using a Zeiss AxioImager Z1 fluorescence microscope. The number SNAP25 immunopositive puncta (intensity above background) in *Cln3*$^{-/-}$ neurons were normalized to the corresponding WT values. *Cln3*$^{-/-}$ neurons (b) express more SNAP25 in their soma than do WT neurons (a). Higher magnifications shown in (c) and (d) represent the 0-25µm region along the processes away from the cell soma of these cells, with examples of SNAP25 immunopositive puncta marked with a yellow circle. (e) The distribution of SNAP25 along processes is not altered in *Cln3*$^{-/-}$ neurons. Scale bar in (a) is 10µm.

The somal expression of VAMP2 appeared to be very similar between WT (5.13 A, a) and *Cln3*$^{-/-}$ (5.13 A, b) neurons, and there was no significant difference in the number of VAMP2 immunopositive puncta along processes of WT and *Cln3*$^{-/-}$ neurons (Figure 5.13 A, c). The expression of both synaptophysin and EEA1 seemed higher in the soma of *Cln3*$^{-/-}$ neurons (Figure 5.13 B, b and C, b respectively) than in WT neurons (Figure 5.13 B, a, C, a respectively), but again no difference was found in the distribution of these proteins along processes (Figure 5.13 B, c and C, c). Thus, CLN3 does not appear to be involved in transport of SNARE-complex proteins or early endosomes along processes in primary cortical neuronal cells. Although there appeared to be pronounced changes in the distribution of these proteins within the soma of *Cln3*$^{-/-}$ neurons, these changes were not evident by Western blot analysis (Figure 5.11).

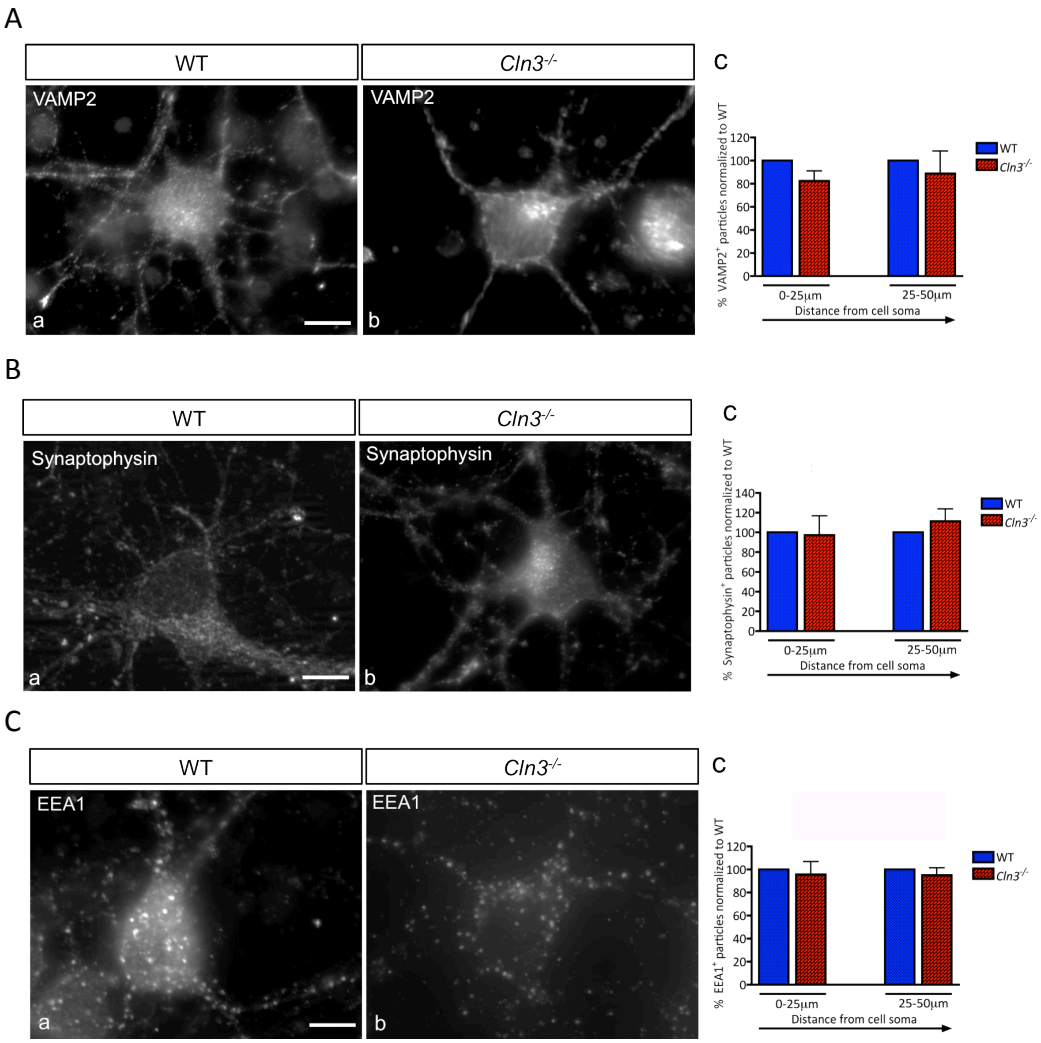

Figure 5.13. Distribution of VAMP2, Synaptophysin and EEA1 is not altered in *Cln3*$^{-/-}$ neurons. The distribution of VAMP2, synaptophysin and EEA1 in the processes of WT and *Cln3*$^{-/-}$ neurons was examined (0-25µm and 25-50µm away from cell soma). There was no difference in distribution of VAMP2 (A) synaptophysin (B) or EEA1 (C) immunopositive puncta along processes of WT (a) and *Cln3*$^{-/-}$ (b) processes, but there appeared to be more synaptophysin and EEA1 in the cell soma of *Cln3*$^{-/-}$ neurons (compare a, b in B and a, b in C). Scale bar in (A), (B) and (C) is 10µm.

5.3 Discussion

These studies revealed that *Cln3*$^{-/-}$ neurons were morphologically compromised, having smaller cell bodies and shorter primary neurites than WT neuronal cells. The AIS was found to have moved away from the cell body in excitatory *Cln3*$^{-/-}$ cortical neurons. This was possibly due to overstimulation caused by chronic depolarization, since blocking of L-type Ca^{2+} channel activity resulted in AIS localization being undistinguishable from that of WT neurons. Despite relocation of the AIS, *Cln3*$^{-/-}$ neurons displayed a normal distribution of SNARE-complex

proteins, and EEA1 along their processes, although total SNAP25 expression was up-regulated, predominantly in the cell soma. These results suggest that, in neurons, CLN3 plays a role in the regulation of neuronal morphology, neuronal excitability and the expression of specific synaptic proteins, but not in protein transport along neurites.

Why is the morphology of *Cln3*$^{-/-}$ neurons altered?

The maintenance of efficient neuronal circuits requires plasticity in the connectivity of neurons (Bienenstock et al., 1982; Yuste and Denk, 1995). Neurite morphology, which we have shown to be altered in *Cln3*$^{-/-}$ neuronal cells (Chapter 5, Figure 5.3), plays a pivotal role in this process (Tang, 2001; Kiryushko et al., 2004; Calabrese, 2008; Meldolesi, 2011). Neurite growth and complexity has never been studied in any model of JNCL. However, disrupted neurite outgrowth has been extensively reported in primary neuronal cultures from many other models of LSDs, including the *Ppt1*$^{-/-}$ mouse model of INCL, the *Cln8*$^{-/-}$ dog model of variant LINCL (Dunn et al., 1994; Virmani et al., 2005), Mucopolysaccharidosis type IIIA (MPS-IIIA, Sanfilippo syndrome) (Sutherland et al., 2008) and Sandhoff's disease (Sango et al., 2002; Pelled et al., 2003b; Sango et al., 2005). All of these studies reported similar impairments in neurite growth to those described here in *Cln3*$^{-/-}$ cortical neurons. In contrast, neurons isolated from the GBa mouse model of Gaucher's disease showed increased neurite length (Bodennec et al., 2002), and overgrowth of neurites was also reported in cortical neurons derived from the mouse model of mucopolysaccharidosis type IIIB (MPSIIIB, Sanfilippo syndrome type B) (Hocquemiller et al., 2010). In the case of MPSIIIB neurons, this neurite overgrowth was associated with an increased expression of growth associated protein 43 (GAP43), and by correcting the genetic defect in these cells both GAP43 expression and neurite outgrowth were normalized (Hocquemiller et al., 2010). GAP43 is an intrinsic potentiator of neurite outgrowth that interacts with PIP_2 in a calmodulin and PKC dependent manner by determining F-actin assembly and organization of microtubules (Benowitz and Routtenberg, 1997; Caroni, 2001). Interestingly, the CLN3 protein

has been suggested to co-localize with GAP43 in neurons (Luiro et al., 2001; Persaud-Sawin et al., 2004), thus, impaired neurite outgrowth in *Cln3*$^{-/-}$ neurons may be caused by altered GAP43 expression. One would need to explore the expression levels of GAP43 in *Cln3*$^{-/-}$ cortical neurons to confirm this.

Dynamic re-arrangement of cytoskeletal components is essential for the process of neurite outgrowth. The neural growth cone situated at the tip of the neurite is enriched in actin filaments together with adapter proteins and filament remodeling aiding proteins (Gordon-Weeks, 2004; Drees and Gertler, 2008; Mattila and Lappalainen, 2008). The dynamic re-modeling of the actin cytoskeleton at growth cones may be regulated via factors such as mitogen-activated protein kinase (MAPKs), in particular, extracellular signal-regulated kinase (ERK), c-Jun N-terminal kinase (JNK), Phosphatidylinositol 3-kinase/Protein Kinase B (PI3K/Akt), and small GTPases (Leppä et al., 1998; Higuchi et al., 2003; Ayala et al., 2007; Heasman and Ridley, 2008). Some evidence exists suggesting a role for MAPKs in neurite growth in *Cln3*$^{-/-}$ neurons, since CLN3 has been linked with a protein called Mekk1 (MAPKKK) (Tuxworth et al., 2011), which has been associated with NGF-induced neurite regrowth by balancing ERK1/2 and JNK2 signaling (Waetzig and Herdegen, 2005). Thus, it may be that abnormal MAPK signaling contributes to attenuated growth of *Cln3*$^{-/-}$ neurons. Additionally, up-regulation of the dual specificity protein phosphatase 2 (DUSP2) gene has been associated with mutation of the *CLN3* gene in JNCL patient samples, in cerebellar *Cln3*$^{\Delta ex7/8}$ precursor cells, and in acutely depleted CLN3 in HELA-cells (Lebrun et al., 2011). DUSP2 dephosphorylates both phosphotyrosine and phosphoserine/threonine residues simultaneously within ERK, p38 mitogen activated protein kinases and JNK, thus, inhibiting these MAPK signaling cascades associated with neurite outgrowth (Patterson et al., 2009). This becomes relevant since up-regulation of DUSP2 in *Cln3*$^{-/-}$ neurons may inhibit MAPK signaling and thereby decrease neurite outgrowth (Perron and Bixby, 1999; Shin et al., 2002; Liao et al., 2012; More et al., 2012). One could explore the activity of MAPK signaling pathways in *Cln3*$^{-/-}$neurons by using phospho-specific antibodies against the different components of MAPK signaling cascades. Then, for

example, if ERK activation is found altered, the impact on *Cln3*$^{-/-}$ neurons of ERK signaling promoters such as alpha-lipoic acid, lithium and curcuminoids, that have been shown to enhance neurite outgrowth (Wang et al., 2011a; 2011b; Liao et al., 2012), could be tested.

Moreover, CLN3 has been suggested to interact indirectly via Hook1 with the endosomal proteins Rab7, Rab9 and Rab11, and also directly with active GTP-bound Rab7 (Luiro et al., 2004; Uusi-Rauva et al., 2012). Rab proteins have also been shown to be involved in organelle trafficking, including the trafficking of signaling receptors to neuronal processes (Tang, 2001; Miaczynska et al., 2004; Gerges et al., 2005; Hutagalung and Novick, 2011). For example, Rab7 has been found to interact with TrkA, which is a receptor-tyrosine kinase for NGF shown to promote neuronal survival and neurite outgrowth (Snider, 1994; Zhang et al., 2000; Saxena et al., 2005a). Thus, perhaps the reduced neurite growth observed in *Cln3*$^{-/-}$ cortical neurons could be explained by mechanisms involving Rab7 mediated trafficking of receptors for neurotrophic factors to the tips of growing neurites. Indeed, evidence also exists that CLN3 can interact with motor components that drive microtubular trafficking, such as dynactin and dynein (Uusi-Rauva et al., 2012), and a lack of correct dynein-CLN3 interactions may interrupt the dynein-mediated vesicular transport of signaling receptors, like TrkA, along microtubules (Yano et al., 2001; Bananis et al., 2004; Heerssen et al., 2004). Further studies are required to confirm these hypotheses, for instance, one could study both anterograde and retrograde trafficking of TrkA internalized vesicles along the neurites of *Cln3*$^{-/-}$ cortical neurons by means of live-cell imaging (Ascaño et al., 2009). Additionally, investigation of the expression of receptors, such as TrkA, at the tips of *Cln3*$^{-/-}$ neurites, would reveal whether such receptors are present in similar numbers, or indeed at all in these cells.

Microtubules are also involved in the primary transport of plasmalemmal precursor vesicles (PPVs), required for the expansion of membrane at the tip of a growing neurites (Letourneau et al., 1987; Ferreira et al., 1992; Peretti et al., 2000; Pfenninger et al., 2003; Pfenninger, 2009). MAPs are thought to be

involved in microtubule-based transportation of cargo along neurites (Matus, 1988; Zakharenko and Popov, 1998; Liu et al., 1999; Buchstaller and Jay, 2000; Harada et al., 2002). Indeed, dendritic growth has been shown to be inhibited by knocking down MAP2 *in vivo*, and decreased expression of the MAP, tau, has been associated with reduced axon outgrowth, as well as with the size and motility of growth cones (Liu et al., 1999; Harada et al., 2002). When MAP2 was used to visualize the morphology of WT and *Cln3*$^{-/-}$ neurons, a difference was revealed in the distribution MAP2 in these cells (Chapter 5, Figure 5.3), with MAP2 appearing to accumulate in the cell body of *Cln3*$^{-/-}$ neurons and not spreading evenly along the processes as in WT cells. Such differences in localization of MAP2 may cause problems with protein kinase A (PKA) targeting to cellular compartments, since this protein uses MAP2 for attachment to microtubules. This in turn could lead to problems with PKA activation of CREB, a transcription factor that is involved in regulating neurite growth (Schmid et al., 1999; Cheng et al., 2002; Harada et al., 2002; Kao et al., 2002). Indeed, gene expression analysis in primary cortical *Cln3*$^{-/-}$ neurons (*E16.5*) revealed cytoskeleton related proteins as one of the most affected groups (Luiro et al., 2006). The most down-regulated gene was reported to be the dynactin motor protein of microtubules. Additionally, Clasp2, which is a microtubular plus-end tracking protein (TIP), was found to be up-regulated in *Cln3*$^{-/-}$ neurons. The Clasp2 protein is involved in stabilization of microtubules at neuronal growth cones and has been shown to function as one of the key regulators of axon and dendrite outgrowth, as well as synapse formation and activity (Galjart, 2005; Beffert et al., 2012). Thus, differential gene expression involving cytoskeletal players like dynactin and Clasp2, together with Rab7 and MAPK that mediate intracellular signaling cascades, may all contribute towards the attenuated neurite growth in *Cln3*$^{-/-}$ cortical neurons.

A great number of extracellular signaling factors, like the neurotrophins (NGF, BDNF, NT-3 and NT-4/5, (Bibel and Barde, 2000)), have been associated with promoting neurite outgrowth. The impact of these factors may vary greatly between different neuronal types and different neurotrophins may also act in

concert (Deister and Schmidt, 2006). For instance BDNF in combination with either NGF or CNTF has a greater positive impact on axonal growth than it would have alone (Lindsay et al., 1985; Goldberg et al., 2002). Trophic factors are produced by both neuronal and glial cells (Schwartz and Nishiyama, 1994; Rudge et al., 1995; Ridet et al., 1997; Huang and Reichardt, 2001; Albrecht et al., 2002; Chang et al., 2003; Liberto et al., 2004). Thus, neurons may respond to trophic factors produced and secreted by themselves, in a paracrine fashion, or to those secreted by other neurons or glial cells (Markus et al., 2002; Kiryushko et al., 2004; Deister and Schmidt, 2006). The proteins secreted by WT and *Cln3*$^{-/-}$ neurons were not compared in this study, so the possibility that *Cln3*$^{-/-}$ neurons fail to secrete neurotrophic factors involved in neurite outgrowth remains to be explored. Given that the protein secretion by *Cln3*$^{-/-}$ astrocytes was severely altered (Chapter 4, Tables 4.1 and 4.2), and *Cln3*$^{-/-}$ microglia also showed specific alterations in their protein secretion profile (S. Dihanich, unpublished data), it would not be surprising to discover similar defects in *Cln3*$^{-/-}$ neurons. However, one also needs to consider the fact that these neuronal cultures were not 100% pure, with 4-5% of cells being astrocytes. This small astrocyte contamination could play a significant role in promoting neurite outgrowth, at least in WT cultures (Wang et al., 1994; Powell et al., 1997b; Powell and Geller, 1999; Costa et al., 2002; Kanemaru et al., 2007). In contrast, the significant reduction in the level of neurotrophic factors such as BDNF and NGF secreted by *Cln3*$^{-/-}$ astrocytes could help explain the impaired neurite growth in these neuronal cultures. Indeed, the presence of *Cln3*$^{-/-}$ glial cells was found to negatively impact the neurite outgrowth of both WT and *Cln3*$^{-/-}$ neurons in co-culture experiments (see Chapter 6, Figures 6.4 and 6.5).

Numerous other important molecules are also essential for correct neurite growth. Surface-expressed cell adhesion molecules (CAMs), such as neural cell adhesion molecule (NCAM) and N-cadherin, interact with the surrounding environment via their extracellular domains, and use their intracellular domains to bind with the cytoskeleton (Maness and Schachner, 2007; Hansen et al., 2008). Thus, CAMs are important intermediaries between extracellular and

intracellular cues for promoting neurite growth (Maness and Schachner, 2007; Hansen et al., 2008). Various cell adhesion molecules, such as VLA-6 (alpha6beta1) integrin, which is the major receptor for interaction with laminin substrates (Hangan et al., 1997; Carloni et al., 2001), have been demonstrated to be differentially expressed at the gene level in different models of JNCL (Chattopadhyay et al., 2004; Lebrun et al., 2011), but no studies have ever been conducted to determine whether this translates into defects in neuronal cell biology. Thus, one cannot exclude the possibility that defects in the expression of cell adhesion molecules could help explain the observed neurite phenotype in *Cln3*$^{-/-}$ neurons.

To overcome this lack of neurite growth, various neurite outgrowth stimulating factors could be tested (Müller et al., 1995; More et al., 2012; Skaper, 2012). Indeed, by supporting the growth of various neuronal subtypes, BDNF-TrkB signaling has emerged as an important mediator of synaptic efficacy (via PLC and IP_3 dependent intracellular Ca^{2+}-release), neuronal connectivity (via ERK signaling) and survival (via PI-3 kinase/Akt) in other CNS affecting disorders (Barde, 1994; Lindvall et al., 1994; Patel and McNamara, 1995; Larsson et al., 1999; Lu and Chow, 1999; McAllister et al., 1999; Schinder and Poo, 2000; Sergeeva et al., 2000; Liu et al., 2002; Mattson et al., 2004; Nagahara and Tuszynski, 2011; Weishaupt et al., 2012). For example, fibroblasts engineered *ex vivo* to secrete BDNF have been shown to reduce cell loss and atrophy of neurons in a spinal cord injury model (Liu et al., 2002), and BDNF-TrkB-signaling has also been shown to protect certain neuronal populations against ischemic damage *in vivo* (Larsson et al., 1999). Primary cortical neuronal cell cultures, or perhaps neuron-glial co-culture systems, as described in Results Chapter 6, could be used to test the efficacy of such neurite outgrowth promoting factors on *Cln3*$^{-/-}$ neurons.

All in all, neurite outgrowth, encompassing both dendritic tree formation and axonal growth, is one of the most fundamental properties of any neuron, since these structures are required for synaptic transmission and neuronal circuit

formation (Hobert, 2009), and failure of neurons to connect and signal properly can lead to degeneration and cell death (Horner and Gage, 2000; Ciani and Salinas, 2005; Marmigère and Ernfors, 2007). Thus, impaired neurite outgrowth could result in problems with neuronal communication and this is turn could play a pivotal role in some of the clinical manifestations involving higher brain function observed in JNCL, such as mental retardation and other cognitive deficits, as demonstrated in other neurological disorders (Ramakers, 2002; Billuart and Chelly, 2003; Minshew and Williams, 2007).

Why do *Cln3*$^{-/-}$ neurons have a displaced AIS?

Neuronal cells are capable of activity-dependent plasticity, for instance, they are able to control their own excitability by altering the position of an entire subcellular compartment called the AIS, which is a specialized part of the axon enriched with ion channels required for initiation of an action potential (Ogawa and Rasband, 2008; Grubb and Burrone, 2010b). Under basal conditions the AIS is located close to the cell soma of a neuron, and overstimulation, involving chronic depolarization, causes a distal shift in the position of the AIS, subsequently altering the excitability of that neuron (Grubb and Burrone, 2010b). In *Cln3*$^{-/-}$ neurons the AIS was surprisingly found to be distally shifted under basal, unstimulated conditions, being at a similar position as the displaced AIS in WT neuronal cells that have been chronically depolarized (Chapter 5, Figures 5.5 and 5.6). In agreement with previous studies, such movement could not be detected in either WT or *Cln3*$^{-/-}$ GABAergic interneurons (Chapter 5, Figure 5.8), suggesting that AIS re-localization in an exclusive property of excitatory, cortical neurons (Grubb and Burrone, 2010b). Thus, it appears that neurons isolated from the *Cln3*$^{-/-}$ mouse cortex may have been overstimulated, and remain so even when grown in non-stimulating environment. We might assume that the observed movement of the AIS in *Cln3*$^{-/-}$ neurons is an attempt by these cells to become less excitable. Indeed, nifedipine treatment, which blocks L-type calcium channels (Lee et al., 2006; Grubb and Burrone, 2010b), resulted in AIS re-location back to the start of the axon in *Cln3*$^{-/-}$ neurons under

both basal conditions and when chronically depolarized with high potassium (Chapter 5, Figures 5.9 and 5.10). This would strongly suggest that *Cln3*$^{-/-}$ neurons are overstimulated due to the enhanced activity of L-type calcium channels resulting in increased calcium influx.

Several explanations for such overstimulation of *Cln3*$^{-/-}$ neuronal cells could be made based on the proposed functional roles of CLN3 (Getty and Pearce, 2011). CLN3 has been reported to interact with the cytoskeletal protein β-spectrin (β-fodrin) (Uusi-Rauva et al., 2008), one of the core-stabilizing proteins of the AIS, whose role is to anchor this whole subcellular structure to the actin cytoskeleton (Komada and Soriano, 2002; Lacas-Gervais et al., 2004; Yang et al., 2007; Grubb and Burrone, 2010b). Another potential interacting protein partner of CLN3 is Hook1, which is a microtubule binding protein involved in endocytosis (Krämer and Phistry, 1996; 1999; Walenta et al., 2001; Luiro et al., 2004), and Hook1 may interact with Ankyrin G, which is the main scaffolding protein of the AIS (Zhou et al., 1998; Atherton et al., 2008; Grubb and Burrone, 2010b; Grubb et al., 2011). Thus, the lack of interplay between CLN3 and β-spectrin and/or CLN3 and Hook1 could disrupt the correct assembly of AIS-related components and/or connection between the AIS and the actin cytoskeleton and could lead to the observed altered position of the AIS in *Cln3*$^{-/-}$ neuronal cells. However, this is an unlikely explanation for the observed AIS location in *Cln3*$^{-/-}$ neurons, since blocking of L-type calcium channels with nifedipine resulted in AIS movement back towards the cell soma. Thus, lack of CLN3 itself does not appear to prevent AIS movement.

CLN3 has also been reported to connect with the Na^+-K^+-ATPase complex via β-spectrin (Uusi-Rauva et al., 2008). The correct functioning of Na^+-K^+-ATPase is pivotal for neurons, since pumping Na^+ out and K^+ into the cell is crucial for maintaining and returning neurons back to their resting potential after depolarization (Kaplan, 2002). The ion pumping activity of Na^+-K^+-ATPase in embryonic *Cln3*$^{-/-}$ cortical neurons (*E16.5*) was found to function normally (Uusi-Rauva et al., 2008), but the dynamic trafficking of the Na^+-K^+-ATPase to the

plasma membrane was discovered to be significantly impaired in these cells (Uusi-Rauva et al., 2008). More specifically, it was shown that internalization of the Na^+-K^+-ATPase was decreased in *Cln3*$^{-/-}$ neurons, and that CLN3 may interact with the ER-resident chaperone protein CRP78/BiP that is vital for the intracellular maturation of Na^+-K^+-ATPase (Bertorello et al., 2003; Uusi-Rauva et al., 2008). Thus, defective transport and targeting of Na^+-K^+-ATPase to the plasma membrane of *Cln3*$^{-/-}$ neurons could alter their capacity to maintain and return to their resting potential. Investigation of the dynamic expression of Na^+-K^+-ATPase at the plasma membrane of *Cln3*$^{-/-}$ cortical neurons by means of FRAP-TIRF (fluorescence recovery after photobleaching (FRAP)-total internal reflection fluorescence (TIRF)) microscopy would enable this hypothesis to be tested.

Gene expression analysis performed in embryonic cortical *Cln3*$^{-/-}$ and WT neuronal cells revealed that the most up-regulated gene in *Cln3*$^{-/-}$ neuronal cells was Gnb1, which is a β1 subunit of the G protein complex involved in regulating the activity of different voltage-gated Ca^{2+} channels, and thus mediates synaptic transmission in neurons (De Waard et al., 1997; García et al., 1998; Luiro et al., 2006). It is known that T- and R-type voltage-gated Ca^{2+} channels are co-localized with Na^+ channels in the AIS, and that activation of these Ca^{2+} channels is important for the generation and timing of action potential bursts (Bender and Trussell, 2009). Also, the presence of N-type calcium channels, which are the determining factor in pyramidal cell excitability (Yu et al., 2010), has been reported in the AIS of cortical pyramidal neurons (Grubb et al., 2011). Thus, up-regulation of GnB1 expression in *Cln3*$^{-/-}$ neurons may alter the activity of different types of voltage gated Ca^{2+} channels, leading to an abnormal Ca^{2+} influx and thus explaining, at least partially, the state of overstimulation seen in *Cln3*$^{-/-}$ neurons as reflected in a distally displaced AIS. Basic calcium signaling has been studied in embryonic *Cln3*$^{-/-}$ cortical neurons (*E16.5*), in which the baseline Ca^{2+} concentration and response to depolarization did not differ from WT neurons (Luiro et al., 2006). However, upon selective blockade of N-type Ca^{2+} channels, the recovery from depolarization was found to be slower in embryonic *Cln3*$^{-/-}$ cortical neurons. This finding may be an indication of abnormally regulated Ca^{2+}

channels, which may lead to Ca^{2+} mediated overstimulation of *Cln3*$^{-/-}$ neurons. Critically, Ca^{2+} mediated, slow-onset excitatory-induced neurodegeneration may play a role in the neuron loss observed in JNCL, as it has been shown to do in many other neurodegenerative disorders, such as ALS, Alzheimer, Parkinson and Huntington diseases (Beal, 1992; 1995; Mattson et al., 2000a; Mattson, 2006). In order to test the impact of these Ca^{2+} channels on the excitability of *Cln3*$^{-/-}$ neurons, two-photon microscopy and whole-cell patch-clamp recordings could be used to examine the properties and role of these channels located in the AIS. If a dysregulation of Ca^{2+} signaling were found to be involved in the overstimulation of *Cln3*$^{-/-}$ neurons, this information could be used as a basis for novel therapies for JNCL. For example, a drug called MEM-1003 (Memory Pharmaceuticals, Montvale, New Jersey, USA), which is a L-type calcium channel inhibitor could be used to prevent the excessive calcium influx that can cause neurodegeneration (Bezprozvanny, 2009).

As mentioned above, the neuron cultures used in these experiments were not completely free from glial contamination. Thus, one cannot exclude the possibility that small, remaining populations of astrocytes, in particular, could play a significant part in the excitability and re-localization of the AIS in neurons via cell-cell interactions or via secreted of soluble factors (Debanne and Rama, 2011). It has been shown that astrocytes situated close to the axons of CA3 pyramidal neurons can cause the broadening of their action potentials by activation of AMPA-type glutamate receptors, leading to an intra-axonal increase in Ca^{2+} concentration and release of glutamate at presynaptic sites (Sasaki et al., 2011). The glutamate transporters situated on the surface of astrocytes may regulate this activity by controlling the diffusion and concentration of glutamate in the extracellular space (Rothstein et al., 1996; Bergles and Jahr, 1998). Keeping in mind the observation that glutamate clearance is attenuated in *Cln3*$^{-/-}$ astrocytes (Chapter 4, Figure 4.11), the resulting excess of glutamate in the extracellular space could induce overstimulation of *Cln3*$^{-/-}$ neurons, and hence explain the alteration in AIS position observed. Another essential function of astrocytes is their ability to act as a K^+ buffer, enabling neurons to cope with the

locally increased levels of external K^+ arising from high neuronal activity (Wallraff et al., 2006; Seifert and Steinhäuser, 2011; Parpura et al., 2012). Indeed, K^+ channels distributed in the AIS are important for both shaping action potentials and setting the resting membrane potential (Kole et al., 2007; Shu et al., 2007; Goldberg et al., 2008). Impairment in the K^+ buffering capacity of *Cln3*$^{-/-}$ astrocytes could cause overstimulation of *Cln3*$^{-/-}$ neurons within the same culture. It would be extremely useful to examine the AIS location in WT and *Cln3*$^{-/-}$ neurons co-cultured with either WT or *Cln3*$^{-/-}$ astrocytes to determine whether astrocytes do really influence the excitability of these neurons and whether this leads to altered AIS positioning.

Since the AIS acts as a central regulatory element for action potential modulation, it is particularly interesting, given the changes in AIS location observed in *Cln3*$^{-/-}$ neurons, that one of the most prominent clinical features of JNCL is epileptic seizures. A number of epilepsy-associated mutations have been found in AIS-related ion channels, including Na^+, K^+, and Ca^+ (Wimmer et al., 2010; Buffington and Rasband, 2011). For instance, loss of functional $Na_v1.1$ is associated with an early-onset form of epilepsy known as Dravet syndrome or severe myoclonic epilepsy in infancy, and missense mutations affecting the voltage sensing domain of $Na_v1.2$ also cause Dravet syndrome (Shi et al., 2009; Oakley et al., 2011). It has been proposed that the combined activities of multiple mutant ion channels, many of which can be associated with the AIS, are involved in the variability of epilepsy manifestations (Klassen et al., 2011). Moreover, many of the AIS-protein-encoding genes have been recognized as risk factors for a number of neurological disorders, including schizophrenia, autism spectrum disorders and autoimmune disorders (Buffington and Rasband, 2011). Thus, the altered AIS-positioning in *Cln3*$^{-/-}$ neurons may play a role in action potential firing in epileptogenesis, and possibly also in other abnormal higher brain functions in JNCL.

Finally, the function of the AIS is not only to determine action potential initiation, but also to control protein transport along the axon, thus, any alteration in its

organization may impact protein compartmentalization and neurite identity (Winckler et al., 1999; Song et al., 2009; Grubb and Burrone, 2010a). Indeed, recent findings confirm the role of the AIS as a vesicle filter that controls the differential trafficking of transport vesicles between dendrites and the axon (Al-Bassam et al., 2012). Hence, given that cultured *Cln3*$^{-/-}$ neurons display a distally located AIS possibly due to the environment encountered *in vitro* and the potential disruption of CLN3/AIS protein interactions, the trafficking of vesicle proteins into the processes of Cln3$^{-/-}$ neurons was also explored (Figures 5.12 and 5.13). However, this was found to be unaltered, at least for the proteins studied (discussed below).

In future experiments, electrophysiological recordings from *Cln3*$^{-/-}$ neurons should be carried out in order to determine whether the distally located AIS in these cells alters their electrophysiological properties. Also the examination of the location of the AIS in excitatory *Cln3*$^{-/-}$ neurons *in vivo,* as well as in brain sections from JNCL patients, will be essential to confirm if alterations in AIS localization also occur in intact tissue.

Overexpression of SNAP25 in *Cln3*$^{-/-}$ neurons

The importance of SNARE-complex proteins for synaptic transmission is unquestionable (Kavalali, 2002; Ungar and Hughson, 2003; Ramakrishnan et al., 2012). The most minimal machinery required for vesicle exocytosis is composed of SNAP25 and syntaxin 1A, both pre-synaptic plasma membrane proteins and VAMP2, a vesicle associated membrane protein (Wang and Tang, 2006). Synaptophysin plays a role in VAMP2 stabilization and synapse maturation, and EEA1 mediates vesicle fusion during endocytosis (Washbourne et al., 1995; Becher et al., 1999; Selak et al., 2004; 2006). Synaptic abnormalities have been shown in a number of other models of NCL, and this is thought to be one of the key, early neuropathological events in these diseases (Partanen et al., 2008; Benedict et al., 2009; Kielar et al., 2009). However, the only difference observed in the total expression of the synaptic proteins studied was that significantly

more SNAP25 was expressed by *Cln3*$^{-/-}$ neurons compared to WT neurons. Also, as stated above, the transport of these proteins along the processes of WT and *Cln3*$^{-/-}$ neuronal cells was not significantly altered (Chapter 5, Figures 5.12 and 5.13).

These results were surprising because *CLN3* has been reported to localize to the synaptic compartments of neurons, as well as to early endosomes (Järvelä et al., 1998; Luiro et al., 2001; Phillips et al., 2005). Therefore, one might have expected to detect more pronounced alterations in both the expression and distribution of these synaptic proteins in the absence of CLN3. Furthermore, early signs of synaptic dysfunction and degeneration have been shown to occur in other models of NCLs, (Virmani et al., 2005; Kim et al., 2008; Partanen et al., 2008; Kielar et al., 2009; Koch et al., 2011). For example, the expression of VAMP2, synaptophysin, and SNAP25 were all shown to be progressively downregulated in different brain regions of *Ppt1*$^{-/-}$ mice (model of INCL) over the course of the disease (Kielar et al., 2009). The general lack of altered synaptic proteins distribution we saw in our *Cln3*$^{-/-}$ cultures could be explained by the relatively short period of time these neurons were kept in culture prior to assessing protein expression and distribution. Perhaps with prolonged periods in culture, more pronounced alterations in expression of synaptic proteins would be observed. Moreover, the link between abnormal AIS location and transport of proteins to axons also requires additional investigation. This is because with the current analysis methods no discrimination between axonal and dendritic protein secretion was preformed. One could carry out co-labeling experiments with Ankyrin G and different SNARE-complex proteins to examine whether the transport of SNAREs is normal in axons of *Cln3*$^{-/-}$ neurons with a distal AIS. Also these results would need to be confirmed with immunohistological studies in *Cln3*$^{-/-}$ mice over the course of the disease.

Up- and down-regulation of SNAP25 expression has been associated with hippocampal long-term potentiation and passive avoidance learning, which is a model of memory-associated synaptic plasticity (Roberts et al., 1998; Hou et al.,

2004; 2006; O'Sullivan et al., 2007). Furthermore, substantial evidence associates altered SNAP25 gene expression with several cognitive impairments such as attention deficit hyperactivity (ADHD) and schizophrenia (Hess et al., 1996; Gabriel et al., 1997; Thompson et al., 1998; Young et al., 1998; Barr et al., 2000; Brophy et al., 2002; Mill et al., 2002; Lewis et al., 2003; Thompson et al., 2003; Wong et al., 2003; Mill et al., 2004; Jeans et al., 2007). In the case of schizophrenia, a reduction in SNAP25 expression in different brain regions has been associated with overall synaptic loss (Glantz and Lewis, 2000; Mukaetova-Ladinska et al., 2002; Thompson et al., 2003; Kolluri et al., 2005). In contrast, elevated levels of SNAP25 has also been detected in some brain regions (Gabriel et al., 1997; Thompson et al., 1998). Thus, decreased SNAP25 expression may be associated with depressed functionality or certain neural circuits, but also hyperactivity of other pathways may arise as a result of SNAP25 over-expression (Corradini et al., 2009). The functional consequences of altered SNAP25 expression has been previously studied by means of recombinant adenoassociated virus (AAV)-mediated gene delivery *into* the rat dorsal hippocampus (McKee et al., 2010). This chronic overexpression of SNAP25 caused a significant increase in the extracellular levels of glutamate, and a reduction in paired-pulse facilitation (a form of short-term synaptic plasticity) in the hippocampus, and produced cognitive deficits and impaired memory formation. Based on this study, the increased expression of SNAP25 may carry significant functional implications for *Cln3*$^{-/-}$ neurons, and may be involved in the cognitive deficits associated with JNCL. Furthermore, the SNARE-complex proteins such as VAMP2 and SNAP25A has been proposed to play roles in neurite elongation and sprouting (Shirasu et al., 2000; Kimura et al., 2003). Thus, altered SNAP25 expression may have implications in membrane expansion at the growth cones of *Cln3*$^{-/-}$ neurites, mediated by vesicles fusion, and may therefore help of explain the attenuated neurite growth observed in *Cln3*$^{-/-}$ neurons (Letourneau and Kater, 1991; Futerman and Banker, 1996). Studies are now underway to analyse the expression of SNAP25, along with other synaptic proteins, in different brain regions known to be relevant for JNCL pathogenesis in both *Cln3*$^{-/-}$ mice and brain sections from JNCL patients.

These findings provide novel insights into how loss of CLN3 impacts neuronal biology. In summary, neuronal morphology, in particular, neurite growth was found attenuated in *Cln3*$^{-/-}$ neurons. These neurons also appear be in a state of overstimulation, and over-express the synaptic protein SNAP25. Taken together, these results may imply that neuronal connectivity and signaling is compromised in *Cln3*$^{-/-}$ mice. Over time, these changes could lead to a disruption of neuronal circuits, epileptic seizures and cognitive defects, leading to wide spread neurodegeneration. This altered biology of *Cln3*$^{-/-}$ neurons may also be exacerbated by *Cln3*$^{-/-}$ glial cells, which our data reveal display many functional defects (Results Chapters 3. and 4, S. Dihanich, unpublished data). The impact that *Cln3*$^{-/-}$ glial cells have on neuronal health is investigated using co-culture experiments in Chapter 6.

Chapter 6
How do *Cln3*$^{-/-}$ glia impact neuronal heath?

6.1 Introduction

Studies using mouse models of JNCL have indicated that glial activation always precedes the loss of specific neuronal populations, particularly in the thalamus, cortex, hippocampus and cerebellum (Katz et al., 1999; Mitchison et al., 1999; Cotman et al., 2002; Pontikis et al., 2004; 2005; Eliason et al., 2007). These findings highlighted a potential connection between glial activation and neurodegeneration in JNCL. My research has pinpointed several defects in the biology of *Cln3*$^{-/-}$ astrocytes (Chapters 3 and 4) that could directly impact neuronal function and survival. These include, the failure of *Cln3*$^{-/-}$ astrocytes to secrete proteins that have a positive impact on neurons, such as FGF2 (Walicke et al., 1986; Alzheimer and Werner, 2002) and VEGF (Sun et al., 2003; Sköld et al., 2005; Ma et al., 2011), and their reduced ability to take up glutamate (Schousboe and Waagepetersen, 2005). Specific defects have also been identified in *Cln3*$^{-/-}$ microglia (S. Dihanich, unpublished data), which could also significantly impact neuronal heath, either directly or via influencing astrocyte biology (see Chapter 4, Discussion 4.3). For instance, attenuated microglial MIP-2 secretion could impact both astrocytes and neurons, since both of these cell types express MIP-2 receptor (CXCR2) (Hesselgesser and Horuk, 1999; De Paola et al., 2007), with the potential to exert either negative (De Paola et al., 2007; Rhodes et al., 2009) or positive (Kielian et al., 2004; Luo et al., 2005; Watson and Fan, 2005) effects upon neuronal survival. Indeed, the lack of chemokine-secretion, such as MIP-1γ, MIP-2 and RANTES, observed in both *Cln3*$^{-/-}$ microglia and astrocytes (Results Chapter 4, Tables 4.1 and 4.2), is likely to alter the communication between these two glia cell-types. This communication is pivotal for detecting and responding to alterations in the surrounding environment, as a part of their CNS's 'surveillance system', and this in turn could also impact on neuronal health (Hesselgesser and Horuk, 1999; Aloisi, 2001; Ransohoff, 2009; McKimmie and Graham, 2010; Semple et al., 2010; Rostène et al., 2011; Ransohoff and Brown, 2012).

This chapter will describe experiments designed to begin to understand the impact that JNCL glia may have on neuronal health. In these experiments WT and

Cln3$^{-/-}$ mixed glial and neurons were cultured together in different combinations and the health of the neurons in these co-cultures assessed. Such experiments not only allowed us to determine whether JNCL glia had a positive or negative role on JNCL neurons but, possibly more importantly, whether WT glia could improve some of the deficits observed in *Cln3*$^{-/-}$ neuronal cell biology (Chapter 5).

6.2 Results

Mixed glia cultures

Before setting up co-cultures with neurons, the cellular composition of our mixed glia cultures was determined. These cultures were derived from P2-P4 WT or *Cln3*$^{-/-}$ mice (see Chapter 2, Section 2.3) and grown for a minimum of three weeks to allow sufficient microglia to be generated along with the astrocytes. The cellular composition of these cultures was assessed by immunocytochemistry using CD68 to identify microglia, GFAP to identify astrocytes (Figure 6.1 A), and O4 to identify oligodendrocytes (Figure 6.1 B). MAP2 together with NeuN was used to confirm the lack of neuronal contamination in these cultures (Figure 6.1 C). The majority of cells present in WT and *Cln3*$^{-/-}$ mixed glia cultures were astrocytes (WT: 57.2±2.7%, *Cln3*$^{-/-}$: 63.8±1.9%) (Figure 6.1 A and D). Microglia made up 31.3±2.3% of WT and 24.5±6.3% of *Cln3*$^{-/-}$ mixed glia cultures (Figure 6.1 A and D), and less than 1% were oligodendrocytes (Figure 6.1 B and D). All the mixed glial cultures used in the following experiments have been generated as described here and had a similar cellular composition.

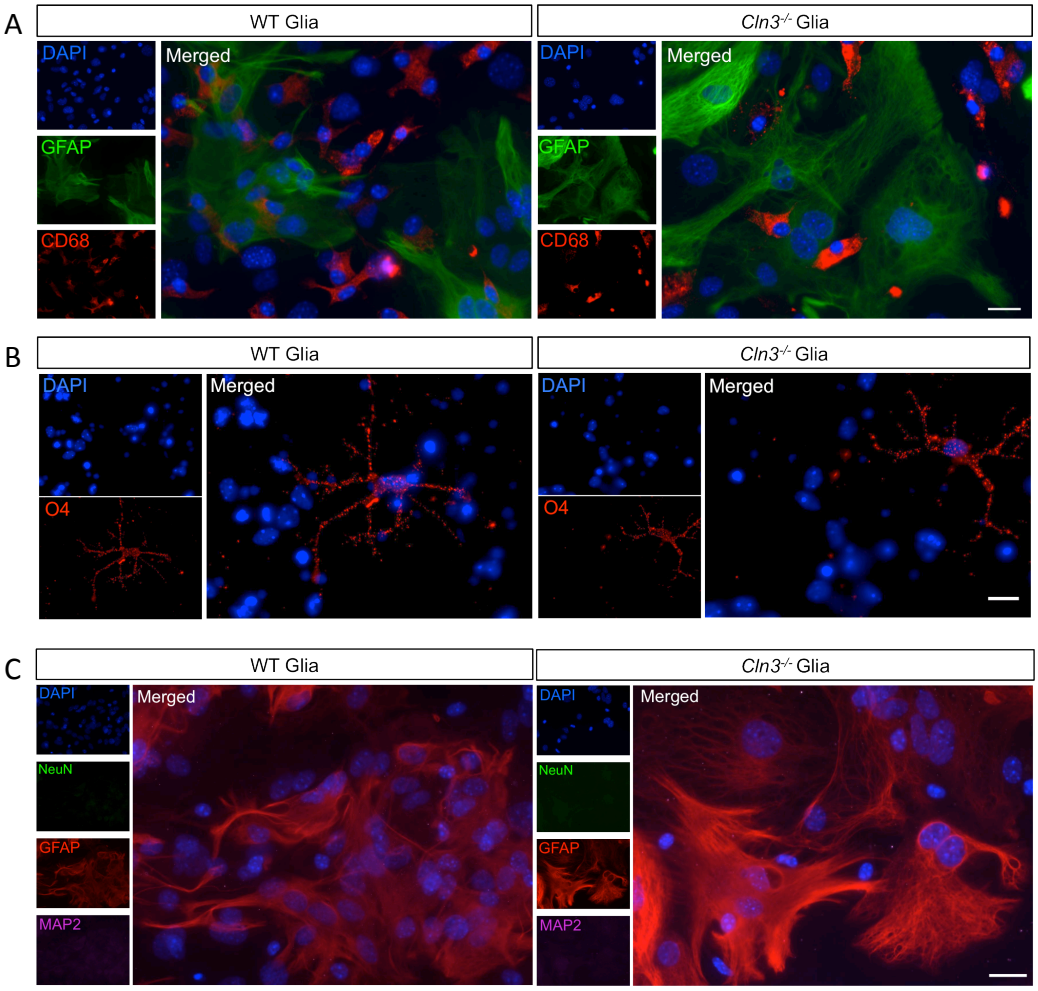

D

Mean percentage of each cell type ± SEM			
Sample	**% Astrocyte ($GFAP^+$, $CD68^-$, $O4^-$)**	**% Microglia ($CD68^+$)**	**% Oligodendrocyte ($O4^+$)**
WT	57.20±2.68	31.28±2.29	0.52±0.03
***Cln3*$^{-/-}$**	63.84±1.89	24.45±6.34	0.84±0.10

Figure 6.1. Composition of mixed glia cultures. Primary cortical mixed glia cultures generated from P2-P4 *Cln3*$^{-/-}$ or WT mouse cortex were stained with CD68 to identify microglia, GFAP to identify astrocytes, O4 to identify oligodendrocytes, MAP2 and NeuN to identify neuronal cells. DAPI was used to visualize all nuclei. (A) WT and *Cln3*$^{-/-}$ mixed glia cultures contained mostly astrocytes and microglia, (B) very few oligodendrocytes and (C) no neurons. (D) The overall composition of these cultures. The percentage of each cell type was determined by counting 5 random fields per coverslip and a minimum of three coverslips per experiment. The means ± SEM shown were calculated from three separate experiments. Scale bar in (A), (B) and (C) is 20µm.

Cln3$^{-/-}$ mixed glial cultures induce neuronal death

To determine whether or not *Cln3*$^{-/-}$ mixed glial influenced neuronal health, primary cortical WT or *Cln3*$^{-/-}$ neuronal cell cultures were plated on PDL-coated coverslips at a concentration of 250,000 cells/coverslip and grown for 7 days. At

this stage WT or *Cln3*$^{-/-}$ mixed glia cultures were seeded on top of them at a concentration of 50,000 cells per coverslip (see Chapter 2, Section 2.6). We considered that by using a co-culture system where glia cells and neurons were in direct connection, we would enhance the probability of seeing an effect since both cell-cell interactions and secreted factors would be brought into play (mimicking the *in vivo* situation). After 2 (2DIV) or an additional 5 days (7DIV), some co-cultures were used to assess total cell death in the cultures using an LDH assay, while other co-cultures were fixed to identify the types of cells that were dying by using a Live/dead fixable dead cell staining kit (Invitrogen) in combination with cell-type specific phenotypic markers for neurons (MAP2), astrocytes (GFAP) and microglia (CD68) (see Chapter 2, Section 2.6).

Cln3$^{-/-}$ *glia display a modest negative impact on neurons in co-cultures after 2 DIV*

After two days in co-culture hardly any dying cells (red nuclei indicates a dying cell, that when co-localized with a cell type specific marker (CD68/GFAP/MAP2) visualized with a green fluorophore can be seen as a 'yellowish' nucleus) could be detected in co-cultures of WT neurons grown together with WT mixed glia (WT Glia) (Figure 6.2 A, ai, aii, bi and bii). There appeared to be slightly more cell death in co-cultures of WT neurons and *Cln3*$^{-/-}$ glia, but these dying cells appear to be mostly astrocytes (Figure 6.2 A, ci, cii, **di** and dii, see arrowheads in di for examples of dying astrocytes). The greatest cell death, at this stage, was observed when *Cln3*$^{-/-}$ mixed glia were cultured with *Cln3*$^{-/-}$ neurons, and most of these dying cells expressed MAP2 (Figure 6.2 A, compare gii to cii, and hii to dii, arrows in gii show examples of dying neurons). In these studies two different MAP2 antibodies were used, a polyclonal for double labelling with CD68, and a monoclonal for double labelling with GFAP. Curiously, we noted that the monoclonal antibody, the one routinely used in this thesis, stained neuronal processes far more effectively that did the polyclonal antibody, which seemed to predominantly stain neuronal cell bodies (Figure 6.2 A, compare aii with bii, cii with dii, eii with fii and gii with hii). In the presence of *Cln3*$^{-/-}$ glia, *Cln3*$^{-/-}$ neurons displayed their typical morphology; a small cell body, less complex neurite

morphology and disrupted MAP2 staining (such as observed in *Cln3*$^{-/-}$ neuronal cultures, see Chapter 5, Figure 5.3). However, when cultured with WT glia, the morphology of the *Cln3*$^{-/-}$ neurons improved, looking more like that of a WT neurons (Figure 6.2 A, compare fii with hii, also see Figures 6.4 and 6.5 below), suggesting that WT glia have a positive impact on *Cln3*$^{-/-}$ neurons.

The amount of released LDH was also analyzed as an additional measurement of total cell death occurring in these co-cultures. However, at this time point no significant difference could be detected in the amount of released LDH under any condition tested (Figure 6.2 B). These results suggest that *Cln3*$^{-/-}$ glia have only a mild effect on neuronal survival after a short time in contact, but that WT glia can positively impact the morphology of *Cln3*$^{-/-}$ neurons during this time period.

A

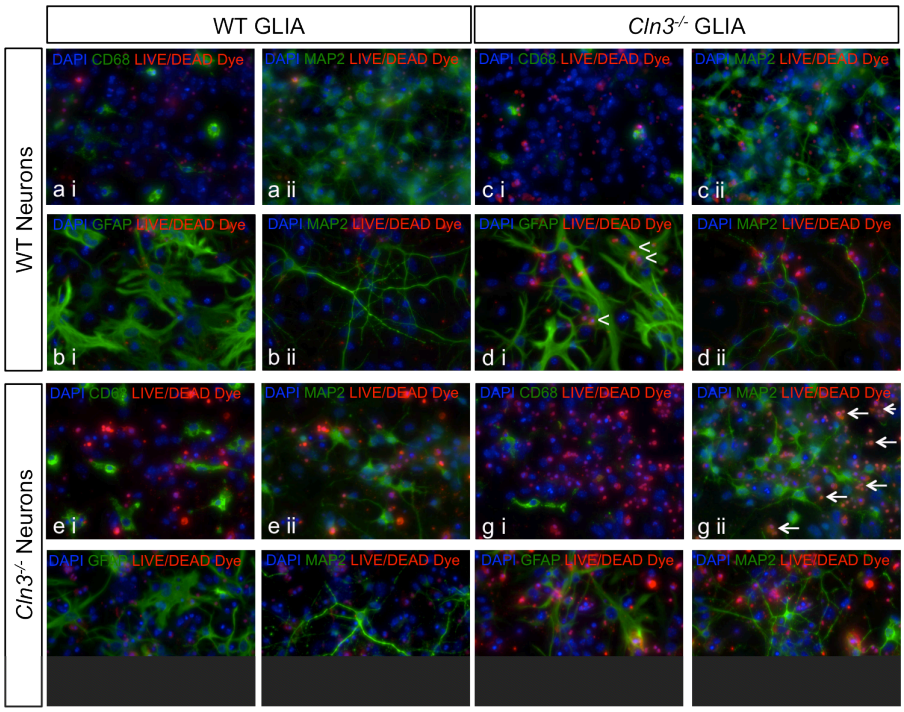

B

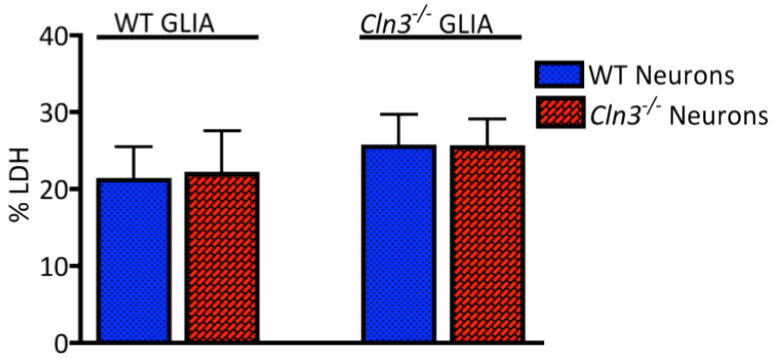

Figure 6.2. *Cln3*$^{-/-}$ glia have little influence upon neuronal survival after 2 DIV. P0 cortical WT or *Cln3*$^{-/-}$ neurons were combined with either WT or *Cln3*$^{-/-}$ mixed glial cultures to study the impact of these cells on neuronal survival. The level of cell death was investigated after co-culture by using a LIVE/DEAD Dye, where dead cells fluoresce red, together with staining for MAP2 (neurons), in combination with either CD68 (microglia) or GFAP (astrocytes). Analysis of the amount of LDH released from these co-culture combinations was used as an additional measurement of cell death. (A) WT mixed glia have a positive impact on both *Cln3*$^{-/-}$ and WT neurons seen as decreased amount of dead cells (red nuclei) compared to co-cultures containing *Cln3*$^{-/-}$ glia. A slight increase in neuron death is observed when *Cln3*$^{-/-}$ glia are co-cultured with WT or *Cln3*$^{-/-}$ neurons, with the latter being more sensitive to the presence of *Cln3*$^{-/-}$ mixed glia (more red nuclei). (B) There was no significant difference in the amount of LDH released among the different co-cultures after 2DIV. These immunofluoresecence studies were performed on three separate experiments. The data in (B) is presented as the mean±SEM derived form 6 separate co-culture experiments, in each experiment 3 technical replicates were measured. Scale bar is 20µm.

Cln3$^{-/-}$ *glia induce neuronal cell death in co-cultures after 7 DIV*

As might be expected, after 7 DIV co-cultures of WT mixed glia and WT neurons were still very healthy, with very few dying cells present (Figure 6.3 A and B). However, the MAP2 expressing processes of WT neurons grown with *Cln3*$^{-/-}$ glia appeared punctate, suggesting that neuronal health was compromised in this situation (Figure 6.3 A, compare cii to aii and dii to bii,). This was confirmed by the increased number of neurons with red nuclei observed in these co-cultures (examples marked with arrows in Figure 6.3 A, cii). Intriguingly, WT neurons seemed to induce the death of *Cln3*$^{-/-}$ glia, and of microglia in particular (example marked with dashed circle in Figure 6.3 A, ci). Such changes in neuronal morphology, or increases in neuron or glial death over time were not observed when these cell-types were grown individually (for neuronal cultures see Chapter 5, Figure 5.1, and for glia see Chapter 6, Figure 6.1). As observed after 2 DIV, WT glia had a positive influence on *Cln3*$^{-/-}$ neurons, with MAP2 expressing *Cln3*$^{-/-}$ neurons showing a more complex neurite structure (see Figure 6.3 A, fii, and Figures 6.4 and 6.5). Interestingly, after 7 days, *Cln3*$^{-/-}$ neurons clearly had a negative impact on WT astrocytes (Figure 6.3 A, compare fi to bi). Indeed, in these cultures many WT astrocyte nuclei were stained red with the live/dead dye (Figure 6.3 A, arrow heads in fi). Again, the co-culture combination of *Cln3*$^{-/-}$ neurons with *Cln3*$^{-/-}$ glia appeared the most detrimental for neuronal heath (Figure 6.3 A, gii and hii). An increased number of dying MAP2 expressing neurons (Figure 6.3 A, arrows in gii) could be seen in these co-cultures, compared to when WT glia were cultured with *Cln3*$^{-/-}$ neurons (Figure 6.3 A, compare gii to cii and hii to dii). Indeed, most of the *Cln3*$^{-/-}$ neurons in these co-cultures were either dead or appeared severely compromised, as judged by their morphology. It is worth noting that the morphology of *Cln3*$^{-/-}$ astrocytes also differed depending whether they had been co-cultured with WT or *Cln3*$^{-/-}$ neurons. In the presence of *Cln3*$^{-/-}$ neurons, *Cln3*$^{-/-}$ astrocytes had smaller cell bodies and longer more numerous processes (reminiscent of activated astrocytes in culture), when compared to *Cln3*$^{-/-}$ astrocytes grown with WT neurons (Figure 6.3 A, compare hi to di). The morphology of WT astrocytes was also influenced by *Cln3*$^{-/-}$ neurons (Figure 6.3 A, compare fi to bi), appearing smaller and having

thinner processes in these cultures, rather than a more rounded cell body with fewer processes, as was seen in co-cultures with WT neurons.

These findings using the Live/dead dye labeling of cells correlated well with the measurements of released LDH from the different co-cultures (Figure 6.3 B). The lowest LDH levels were observed when WT glia and neurons were co-cultured (%LDH: 13.0±2.2%). These LDH levels increased dramatically when *Cln3*$^{-/-}$ glia were co-cultured with WT or *Cln3*$^{-/-}$ neurons (%LDH in *Cln3*$^{-/-}$ glia/WT neuron co-cultures: 24.9±3.8%, and in *Cln3*$^{-/-}$ glia/*Cln3*$^{-/-}$ neuron co-cultures: 30.4±4.6%). When *Cln3*$^{-/-}$neurons were co-cultured with WT, rather than *Cln3*$^{-/-}$, glia a lower level of LDH release was observed (%LDH 20.8±3.7%), possibly due to the supportive influence of the WT cells. As might be expected, there was significantly more LDH released in *Cln3*$^{-/-}$ glia/*Cln3*$^{-/-}$ neuron co-cultures than in WT glia/WT neuron co-cultures (Figure 6.3 B).

These results suggest that *Cln3*$^{-/-}$ glia appear to be detrimental to the health of both WT and *Cln3*$^{-/-}$ neurons, with *Cln3*$^{-/-}$ neurons being the most vulnerable. In contrast, WT glia seem to have a positive influence on *Cln3*$^{-/-}$ neurons. A bi-directional interaction between neurons and glia is also evident in these co-cultures, as is apparent from the impact of *Cln3*$^{-/-}$ neurons upon WT astrocyte morphology, re-enforcing the importance of the interplay between neurons and glia within the CNS.

A

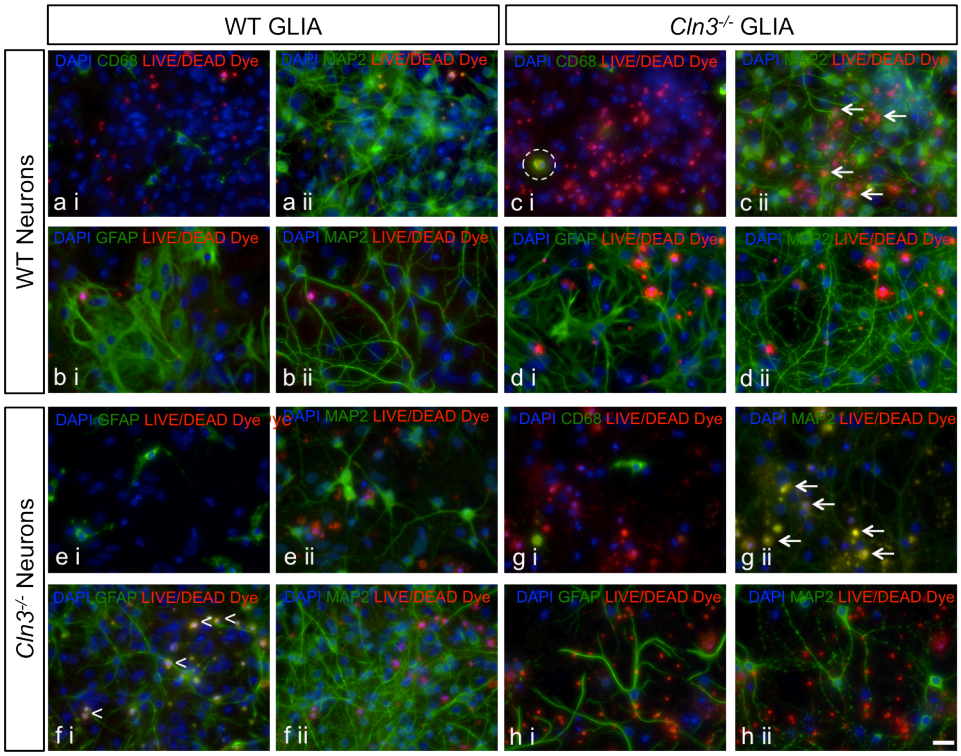

B

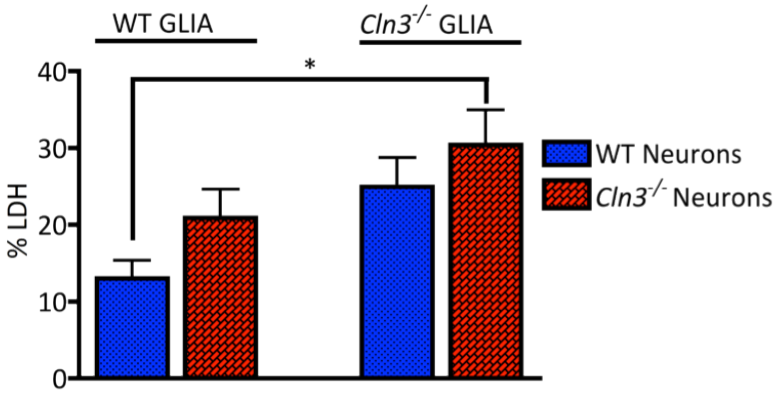

Figure 6.3. *Cln3*$^{-/-}$ cells negatively impact WT cells after 7 DIV. P0 cortical WT and *Cln3*$^{-/-}$ neurons were combined with either WT or *Cln3*$^{-/-}$ mixed glia cultures to study the impact of these cells on each other's survival. The levels of cell death were investigated after 7DIV in co-culture. (A) WT glia had a positive impact on both *Cln3*$^{-/-}$ and WT neurons. *Cln3*$^{-/-}$ glia accelerated cell death when cultured with either WT or *Cln3*$^{-/-}$ neurons, with mutant neurons being more sensitive (more red nuclei). (B) There was significantly more LDH released in WT neuron/WT glia co-cultures compared to *Cln3*$^{-/-}$ neuron/*Cln3*$^{-/-}$ glia co-cultures. These fluorescence studies were performed on three separate co-culture experiments. The data in (B) is presented as mean±SEM derived form 6 separate co-culture experiments each with three technical repeats. Scale bar in (A) is 20µm.

Reduced neurite complexity induced by *Cln3*$^{-/-}$ glia

In Chapter 5 (Figure 5.3) *Cln3*$^{-/-}$ neurons were shown have smaller cell bodies and shorter primary processes that WT neurons, suggesting that CLN3 deficiency impacts neuronal soma size and neurite length. In the intact brain, neurons are greatly influenced by glia, for instance, astrocytes may directly regulate neurite growth both by cell-contact and the proteins they secrete (Tomaselli et al., 1988; Powell et al., 1997b; Crone and Lee, 2002; Araújo and Tear, 2003). In contrast, in the damaged or diseased brain, reactive astrocytes may negatively impact neurite growth by over-expressing growth-inhibitory extracellular matrix (ECM) proteins, such as chondroitin and keratan sulphate proteoglycans, and by inhibiting the extension of regenerating axons (Silver and Miller, 2004). Moreover, microglia can also inhibit neurite outgrowth by acting as a source of inhibitory proteoglycans (Bovolenta et al., 1993). Indeed, as described above, WT astrocytes appeared to have a beneficial effect on *Cln3*$^{-/-}$ neurons, while *Cln3*$^{-/-}$ astrocytes had a detrimental effect on these cells. We therefore analysed these changes by using ImageJ to quantify the soma size of neurons and their neurite complexity (see Chapter 5, Figure 5.3) in the different co-culture combinations.

Figure 6.4 illustrates a typical MAP2 expressing WT neuron co-cultured with WT glia (a) or with *Cln3*$^{-/-}$ glia (b); and a typical MAP2 expressing *Cln3*$^{-/-}$ neuron co-cultured with WT glia (c) or with *Cln3*$^{-/-}$ glia (d). Neurons of both genotypes appeared very similar when grown with WT glia (Figure 6.4, see a and c). This is in contrast with the marked difference in the appearance of WT and *Cln3*$^{-/-}$ neurons grown without glia (see Chapter 5, Figure 5.3), with *Cln3*$^{-/-}$ neurons exhibiting significantly smaller cell soma and shorter primary processes than WT neurons. MAP2 expression was also more punctuate in WT neurons when they were co-cultured with *Cln3*$^{-/-}$ glia (see b, Figure 6.4), and this was even more evident when *Cln3*$^{-/-}$ neurons were co-cultured with *Cln3*$^{-/-}$ glia (Figure 6.4 d).

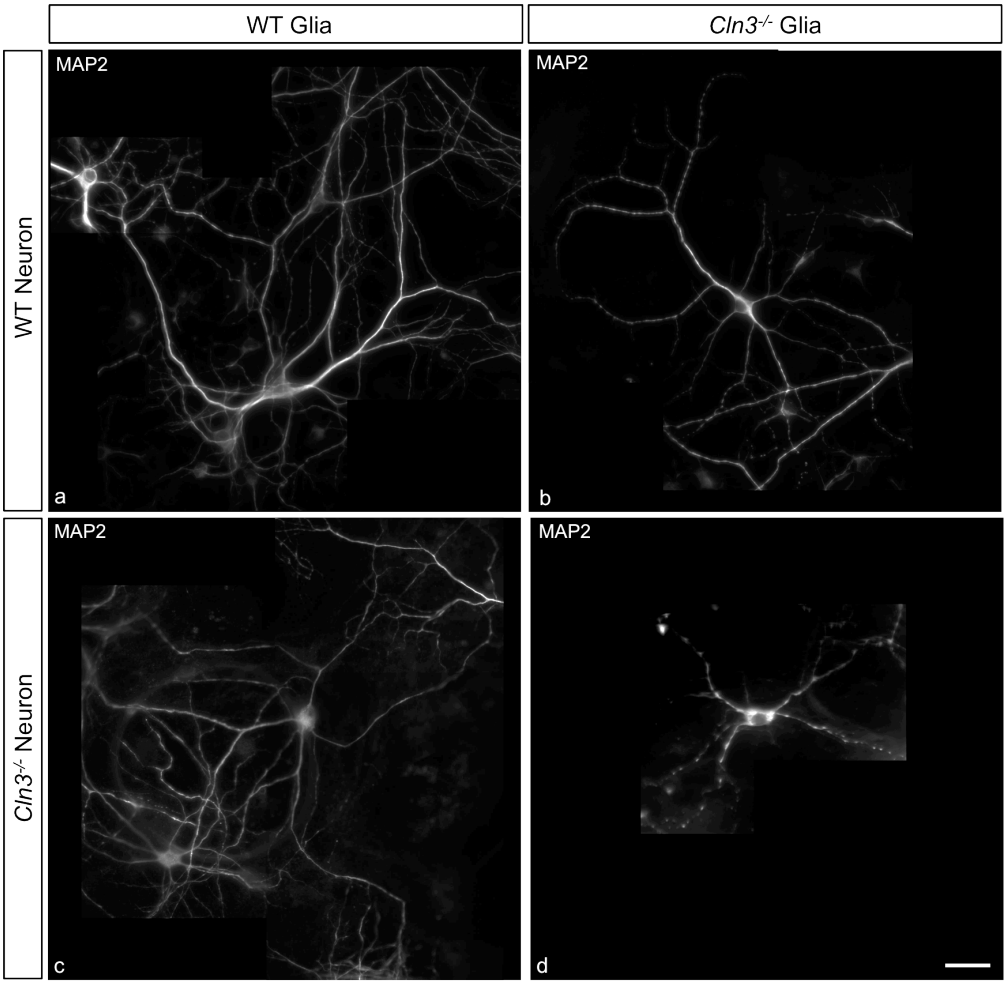

Figure 6.4. *Cln3*$^{-/-}$ glia negatively impact neuronal morphology. The influence of WT and *Cln3*$^{-/-}$ glia cells on the morphology of WT and Cln3$^{-/-}$ neurons was explored in 7 day old co-cultures, in which neuronal morphology was visualized with MAP2 and cell soma size and neurite complexity was analyzed. Representative images of WT and *Cln3*$^{-/-}$ neurons co-cultured either with WT or *Cln3*$^{-/-}$ glia are shown. *Cln3*$^{-/-}$ glia cause MAP2 staining in WT neuronal processes to appear punctate, and this is more evident in *Cln3*$^{-/-}$ neuronal processes. In contrast, WT glia have a positive impact on the morphology of *Cln3*$^{-/-}$ neurons. Scale bar is 20µm.

Analysis of neuronal soma sizes revealed that WT neurons co-cultured with WT glia had significantly bigger cell soma (180.6±5.6 (µm)^2) than *Cln3*$^{-/-}$ neurons co-cultured with *Cln3*$^{-/-}$ glia (151.4±3.2 (µm)^2) (Figure 6.5 A). *Cln3*$^{-/-}$ glia did not significantly alter the soma size of WT neurons (164.1±2.8 (µm)^2) when compared to those co-cultured with WT glia (180.6±5.6 (µm)^2). However, *Cln3*$^{-/-}$ glia significantly reduced the soma size of *Cln3*$^{-/-}$ neurons (151.4±3.2 (µm)^2), when compared to those co-cultured with WT glia (178.3±4.1 (µm)^2).

The number of primary neurites observed was not altered in these different co-culture systems (Figure 6.5 B, a). WT neurons had a significantly increased

number of secondary neurites when co-cultured with WT glia (2.8±0.3), compared to *Cln3*$^{-/-}$ neurons co-cultured with *Cln3*$^{-/-}$ glia (1.5±0.1) (Figure 6.5 B, b). The number of tertiary neurites was also significantly reduced in *Cln3*$^{-/-}$ neuron/ *Cln3*$^{-/-}$ glia co-cultures (0.4±0.1), compared to WT neuron/ WT glia co-cultures) (1.2±0.1) (Figure 6.5 B, c). *Cln3*$^{-/-}$ glia also caused a significant reduction in the number of tertiary neurites displayed by WT neurons (0.6±0.1), when compared to those co-cultured with WT glia (1.2±0.1) (Figure 6.5 B, c). Additionally, the total length of primary neurites was significantly reduced when *Cln3*$^{-/-}$ neurons were co-cultured with *Cln3*$^{-/-}$ glia (350.8±26.7µm), rather than WT glia (476.0±22.2µm) (Figure 6.5 C, a). While the total length of the primary neurites was found to be the greatest in WT neuron/ WT glia co-cultures (567.9±35.3.7µm) (Figure 6.5 C, a), this length was slightly decreased (423.7±59.6µm) when WT glia were replaced with *Cln3*$^{-/-}$ glia, although this change was not found to be significant. The longest primary neurite of either WT or *Cln3*$^{-/-}$ neurons was significantly longer when cultured with WT glia (218.1±12.9µm), than when grown with *Cln3*$^{-/-}$ glia (WT neurons: 165.7.8±13.9µm, *Cln3*$^{-/-}$ neurons: 119.8±6.3µm, Figure 6.5 C, b). Again, the longest primary neurite was significantly longer when WT neurons were co-cultured with WT glia than when *Cln3*$^{-/-}$ neurons co-cultured with *Cln3*$^{-/-}$ glia.

Taken together, these analyses of cell body size and neurite complexity revealed that *Cln3*$^{-/-}$ glia had a detrimental effect upon neuronal morphology, with *Cln3*$^{-/-}$ neurons being more susceptible than those from WT mice. Most importantly, WT glia appeared to exert a positive influence on *Cln3*$^{-/-}$ neurons.

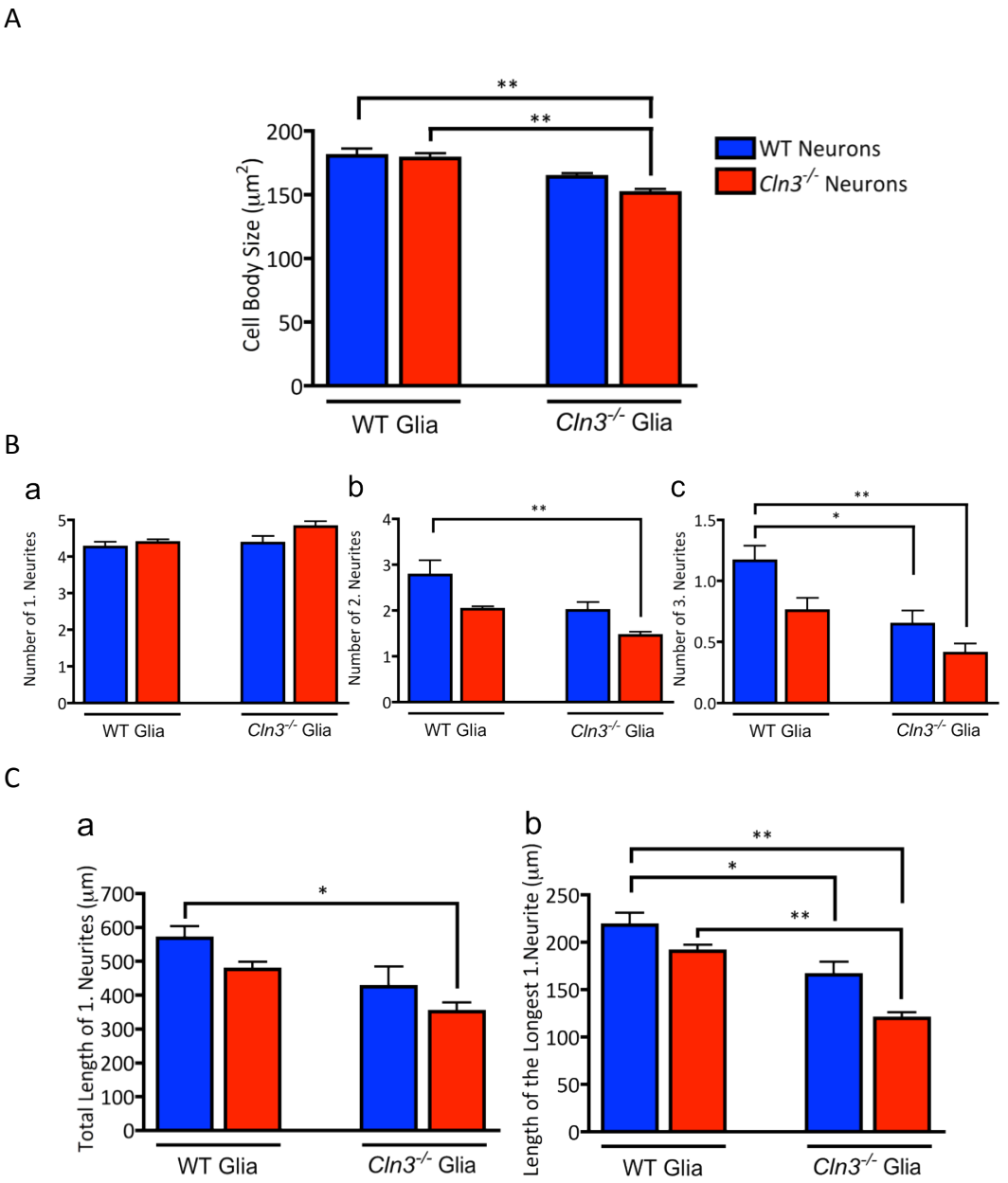

Figure 6.5. *Cln3*$^{-/-}$ glia induce a reduction in neuronal somal size and neurite complexity. (A) The soma size of MAP2 expressing WT and *Cln3*$^{-/-}$ neurons co-cultured with WT or *Cln3*$^{-/-}$ mixed glia was quantified using ImageJ. *Cln3*$^{-/-}$ neurons co-cultured with *Cln3*$^{-/-}$ glia had a significantly smaller cell soma that did WT neurons co-cultured with WT glia. The presence of WT glia significantly increased the soma size of *Cln3*$^{-/-}$ neurons compared to co-cultures with *Cln3*$^{-/-}$ glia. (B) (a) The number of primary neurites (1. neurites that are extended from cell bodies) did not differ between these co-cultures, (b) *Cln3*$^{-/-}$ glia significantly reduced the number of secondary neurites (2. neurites that branch off from primary neurites) in *Cln3*$^{-/-}$ neurons, (c) *Cln3*$^{-/-}$ glia significantly reduced the number of tertiary neurites (3. neurites that branch off from secondary neurites) in WT and *Cln3*$^{-/-}$ neurons. (C) (a) The total length of primary neurites was significantly reduced when *Cln3*$^{-/-}$ neurons were co-cultured with *Cln3*$^{-/-}$ glia compared to when WT neurons were co-cultured with WT glia, (b) *Cln3*$^{-/-}$ glia significantly reduced the length of the longest primary neurite in both WT and *Cln3*$^{-/-}$ neurons, and the length of the longest primary neurite was greater when WT neurons were co-cultured with WT glia than when *Cln3*$^{-/-}$ neurons were co-cultured with *Cln3*$^{-/-}$ glia. Data presented in (B), (C) and (D) are the mean±SEM from 40 cells in each experiment and the experiment was repeated three times.

Glial induced alterations in the expression of SNAREs in co-cultured WT and *Cln3*$^{-/-}$ neurons

It is well established that astrocytes can modulate the synaptic function of neurons by releasing a number of transmitters and factors such as glutamate, D-serine, ATP and BDNF (Volterra and Meldolesi, 2005; Parpura et al., 2010). This release may occur via Ca^{2+}-dependent exocytosis, which also forms the basis for astrocyte communication (Parpura et al., 2011; Zorec et al., 2012; Verkhratsky et al., 2012a). Both Ca^{2+} signaling and, in particular, protein secretion was found to be severely affected in *Cln3*$^{-/-}$ astrocytes (see Chapter 4, Tables 4.1 and 4.2). Specific alterations in protein secretion have also been identified in *Cln3*$^{-/-}$ microglia (S. Dihanich, unpublished data), which may impact upon neuronal synapses. Indeed, synaptic pathology has been recognized as one of the key early events in the NCLs (Virmani et al., 2005; Kim et al., 2008; Partanen et al., 2008; Kielar et al., 2009). We have already demonstrated that the distribution of SNARE-complex proteins and the early endosomal marker EEA1 are unaltered in *Cln3*$^{-/-}$ neuronal cultures (see Chapter 5, Figures 5.12 and 5.13). Now, in co-cultures, we investigated whether *Cln3*$^{-/-}$ (and WT) glia could influence the levels of expression and localization of these proteins and hence potentially influence synaptic function.

Which SNAREs are expressed by glia cells?

Astrocytes are known to express a variety of presynaptic proteins, including SNARE-complex proteins such as SNAP23 and VAMP2, both *in vivo* and *in vitro*. The expression of some of these proteins including SNAP25 and synaptophysin may be upregulated upon extended periods in culture (Wilhelm et al., 2004; Schubert et al., 2011). Therefore, the expression of SNAP25, VAMP2 and synaptophysin was first studied in both WT and *Cln3*$^{-/-}$ mixed glia cultures to determine whether any change in the level of expression of these proteins, as determined by Western blot analysis, could be considered neuron-specific (Figure 6.6 A-C). Mixed glial cultures from both genotypes were shown to express VAMP2 (Figure 6.6 A), but no expression of SNAP25 or synaptophysin could be detected (Figure 6.6 B and C). Thus, the expression of these latter two

markers was explored in co-cultures of WT and *Cln3*$^{-/-}$ neurons with either WT or *Cln3*$^{-/-}$ glia.

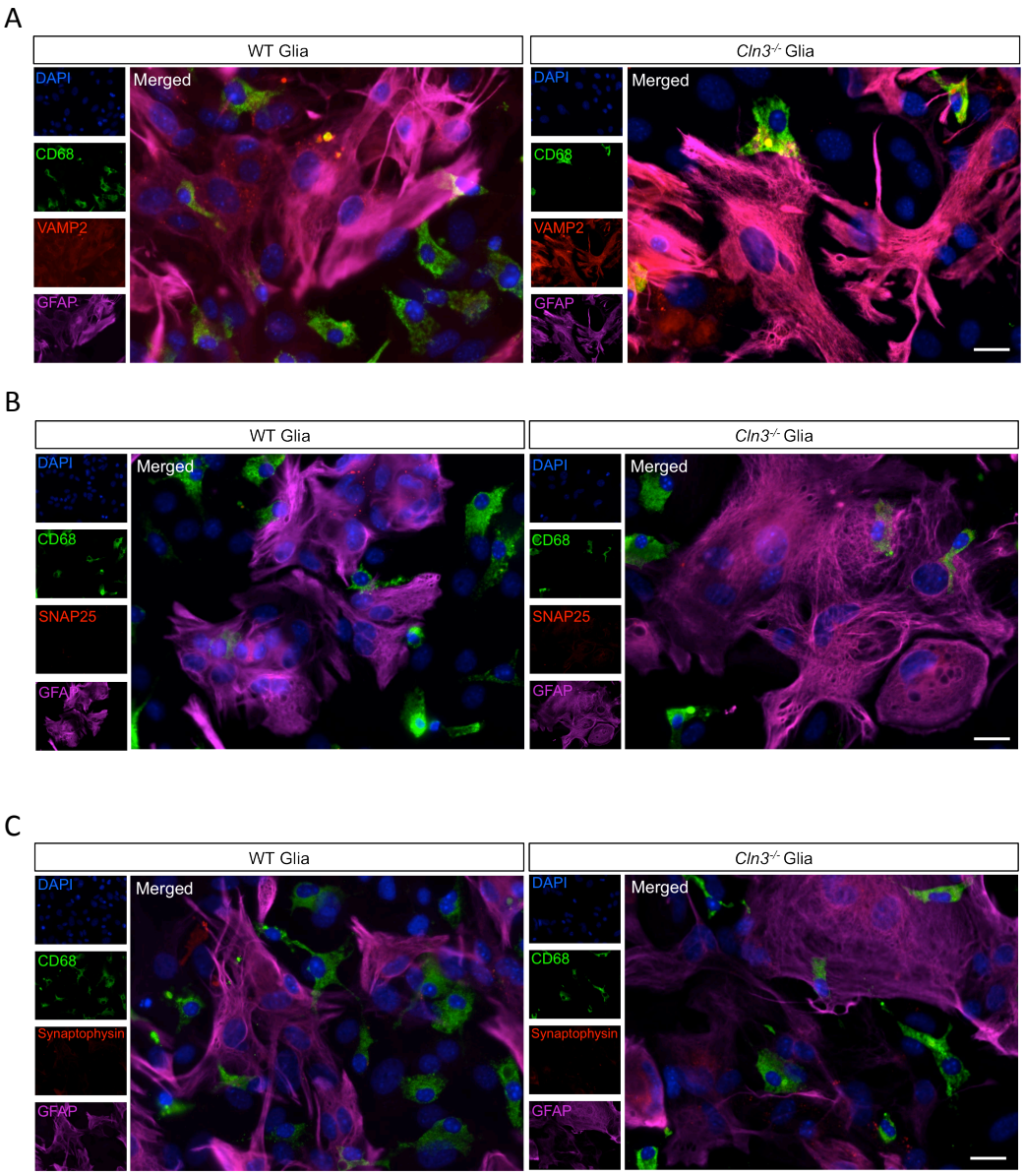

Figure 6.6. Mixed WT and *Cln3*$^{-/-}$ Glia do not express SNAP25 or synaptophysin. The expression of SNARE-complex proteins was studied in WT and *Cln3*$^{-/-}$ mixed glial cultures by immunostaining cells for VAMP2, SNAP25 or synaptophysin in association with GFAP and CD68. DAPI was used to visualize all nuclei. (A) VAMP2 was expressed by both WT and *Cln3*$^{-/-}$ astrocytes, but neither (B) SNAP25 nor (C) synaptophysin was expressed by WT or *Cln3*$^{-/-}$ glia. Scale bar in all images is 20µm.

Cln3$^{-/-}$ *glia alter the neuronal expression of synaptophysin, but not SNAP25*

To study the distribution of synaptic proteins, 7 day old co-cultures were fixed and stained with SNAP25 or synaptophysin in combination with MAP2 (Figures 6.7 A and 6.7 A). Additionally, Western blot analysis was carried out on cell

lysates derived from 7 day old co-cultures to quantify the total expression of SNAP25 and synatophysin (Figures 6.7 B and 6.7 B). Expression levels were normalized to the levels of β-actin in each sample.

SNAP25 staining was predominantly localized to the cell bodies of WT neurons co-cultured with WT glia, but some SNAP25 immunoreactivity was visible along their neurites (Figure 6.7 A, a). The expression in the cell soma was similar in co-cultures in which WT neurons were grown with *Cln3*$^{-/-}$ glia, but immunoreactivity for these proteins was markedly reduced in neurites in these co-cultures (Figure 6.7 A, b). SNAP25 immunoreactivity in *Cln3*$^{-/-}$ neurons co-cultured with WT glia appeared marginally fainter in the soma with fewer SNAP25 expressing puncta along the neurites, when compared to WT neurons co-cultured with WT glia (Figure 6.7 A c, and compare c to a). This reduction in staining intensity was more evident when *Cln3*$^{-/-}$ neurons were co-cultured with *Cln3*$^{-/-}$ glia (Figure 6.7 A d, compared d to a, b and c). When the total expression of SNAP25 in the cultures was quantified by Western blotting, the highest protein levels were observed in WT neurons under both co-culture combinations (Figure 6.7 B, WT neurons/WT glia: 23.4±1.1%, WT neurons/*Cln3*$^{-/-}$ glia: 26.1±2.8% when normalized to β-actin), with the presence of *Cln3*$^{-/-}$ glia not significantly altering SNAP25 protein levels in WT neurons. However, there was significantly less SNAP25 expressed in *Cln3*$^{-/-}$ neurons cultured with either WT or *Cln3*$^{-/-}$ glial cells (10.6±2.4% and 5.0±0.2% respectively when normalized to β-actin) (Figure 6.7 B). Moreover, WT neurons co-cultured with *Cln3*$^{-/-}$ glia had significantly more SNAP25 expression than *Cln3*$^{-/-}$ neurons co-cultured with either WT or *Cln3*$^{-/-}$ glia. However, the level of SNAP25 in *Cln3*$^{-/-}$ neurons was not significantly different when cultured with *Cln3*$^{-/-}$ or WT glia, suggesting that *Cln3*$^{-/-}$ glia did not have any further impact upon SNAP 25 levels in *Cln3*$^{-/-}$ neurons (Figure 6.7 B). Therefore, WT neurons appear to express more SNAP25 than *Cln3*$^{-/-}$ neurons, regardless of the presence of glial cells. On the contrary, *Cln3*$^{-/-}$ neurons expressed more SNAP25 when grown without glia (see Chapter 5, Figure 5.11).

A

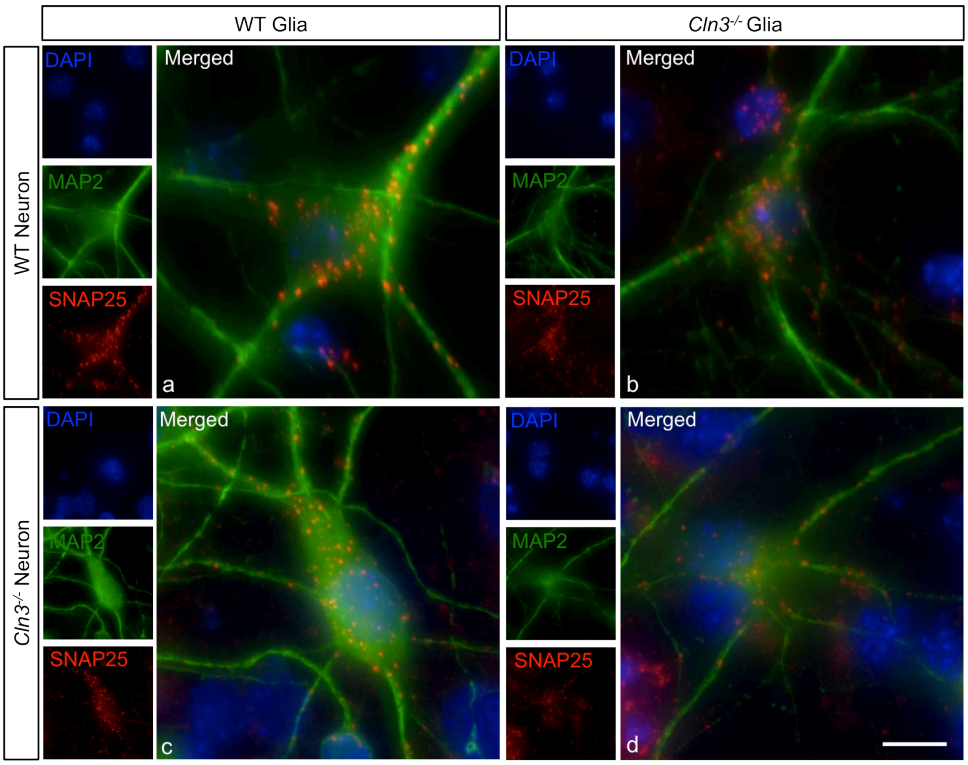

B

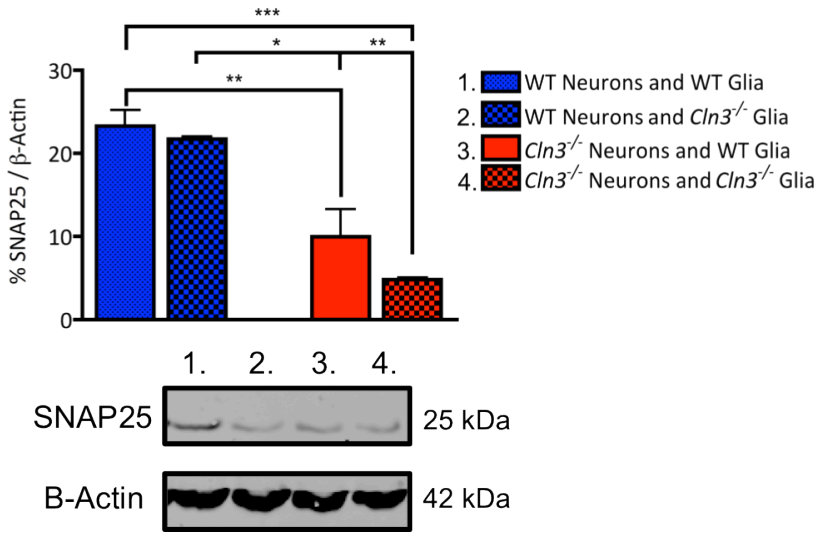

Figure 6.7. Glia do not alter neuronal SNAP25 expression. The distribution and total expression of SNAP25 was studied in WT and *Cln3*$^{-/-}$ neurons co-cultured with WT or *Cln3*$^{-/-}$ glia. Immunofluorescence staining for SNAP25 in combination with MAP2 was used to study protein distribution, and Western blotting was used to quantify total protein expression. (A) (a) SNAP25 was expressed in both the cell body and processes of WT neurons co-cultured with WT glia, (b) this expression was reduced in the soma and processes of WT neuronal cells co-cultured with *Cln3*$^{-/-}$ glia, (c) the expression of SNAP25 in *Cln3*$^{-/-}$ neurons cultured with WT glia was mainly in the soma with some expression in processes, (d) the expression of SNAP25 is reduced in the cell body and processes of *Cln3*$^{-/-}$ neurons co-cultured with *Cln3*$^{-/-}$ glia. (B) Total intracellular expression of SNAP25 (normalized to β-actin) is significantly reduced in *Cln3*$^{-/-}$ neurons grown with either WT or *Cln3*$^{-/-}$ glia when compared to WT neurons grown with WT or *Cln3*$^{-/-}$ glia. Data in (B) is presented as mean percentage±SEM from three separate biological samples. Scale bar in A is 20 µm.

As was the case with SNAP25, when co-cultured with WT glia, WT neurons expressed synaptophysin mainly in their cell bodies with some expression also evident in their neurites (Figure 6.8 A, a). This expression appeared to be reduced when WT neurons were co-cultured with *Cln3*$^{-/-}$ glia in both the cell body and processes (Figure 6.8 A, compare b to a). The *Cln3*$^{-/-}$ neurons in co-cultures with WT glia displayed very few synaptophysin immunoreactive puncta in their cell bodies and processes (Figure 6.8 A, c). However, the expression of synaptophysin seemed to be increased in both neurites and soma of *Cln3*$^{-/-}$ neurons when co-cultured with *Cln3*$^{-/-}$ glia (Figure 6.8 A, d). Indeed, *Cln3*$^{-/-}$ neurons co-cultured with *Cln3*$^{-/-}$ glia cells seemed to express more synaptophysin than WT neurons cells grown with WT glia cells (Figure 6.8 A, compare d to a).

These observations were confirmed by Western blotting, with total synaptophysin expression being reduced in WT neurons co-cultured with *Cln3*$^{-/-}$ glia rather than WT glia (1.1±0.1% and 3.3±1.3% respectively when normalized to β-actin), but this difference was not statistically significant (Figure 6.8 B). As suggested by immunostaining, *Cln3*$^{-/-}$ neurons expressed significantly more synaptophysin when co-cultured with *Cln3*$^{-/-}$ glia than when co-cultured with WT glia (4.5±0.5% versus 1.3±0.0% when normalized to β-actin) (Figure 6.8 B).

In summary, neither WT nor *Cln3*$^{-/-}$ glia appeared to have a significant impact on the neuronal expression of SNAP25, which overall, was higher in WT neurons than in *Cln3*$^{-/-}$ neurons. Interestingly the expression and distribution of synaptophysin, however, was upregulated in *Cln3*$^{-/-}$ neurons only in the presence of *Cln3*$^{-/-}$ glia. Thus, it appears that interactions between glia and neurons of different genotypes result in specific alterations in protein expression, detected here by studying the expression of two synaptic proteins

A

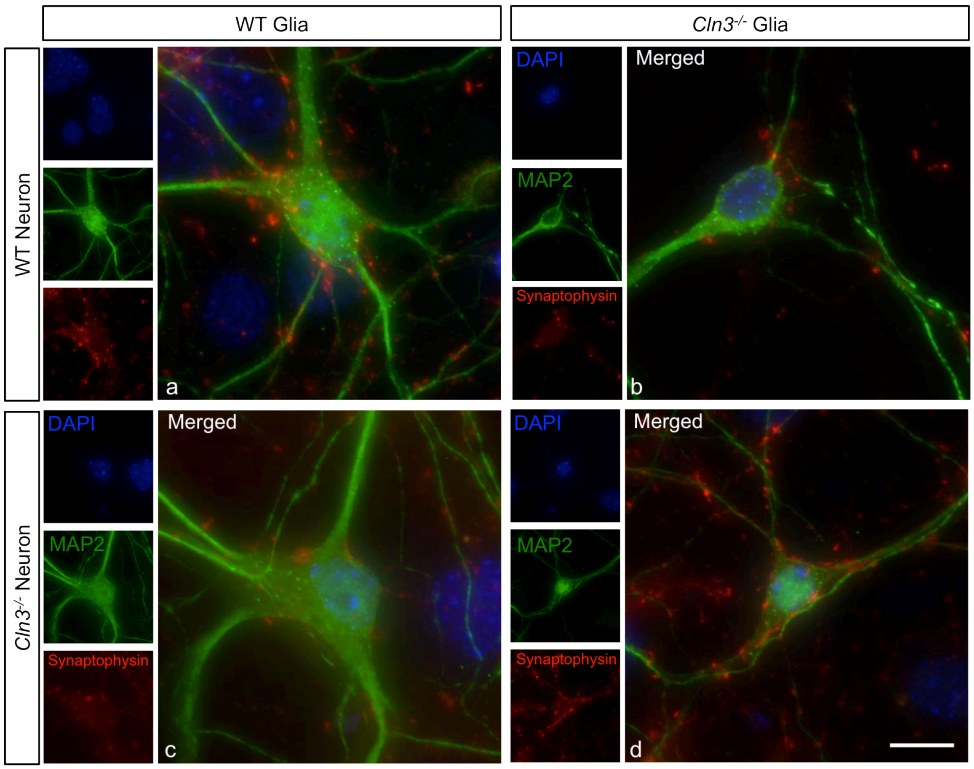

B

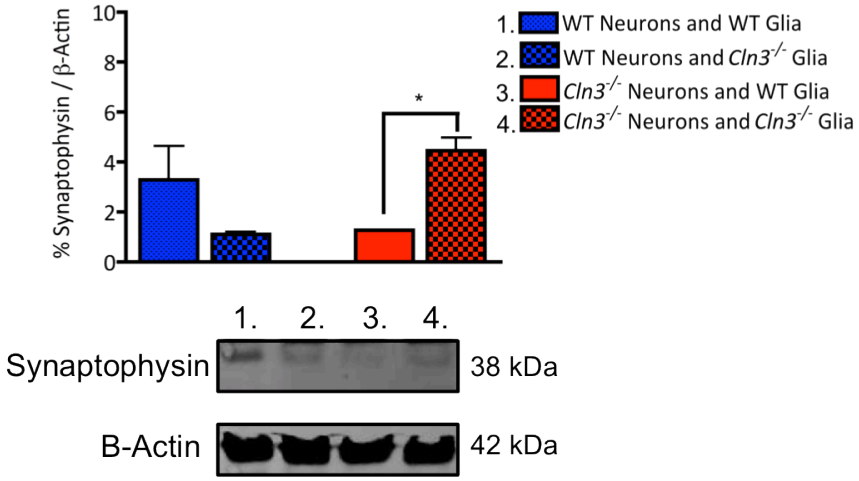

Figure 6.8 Synaptophysin expression is increased in *Cln3*$^{-/-}$ neurons by *Cln3*$^{-/-}$ glia. The distribution and total expression of synaptophysin was studied in WT and *Cln3*$^{-/-}$ neurons co-cultured with WT or *Cln3*$^{-/-}$ glia. Immunofluorescence staining for synaptophysin in combination with MAP2 was used to study protein distribution and Western blotting was used to quantify the total protein expression. (A) (a) Synaptophysin was expressed in the cell body and less so in the processes of WT neurons co-cultured with WT glia, (b) this expression was reduced in the soma and processes of WT neurons co-cultured with *Cln3*$^{-/-}$ glia, (c) *Cln3*$^{-/-}$ neurons cultured with WT glia express low levels of synaptophysin mainly in their soma, (d) the expression of SNAP25 was high in both the soma and processes in *Cln3*$^{-/-}$ neurons co-cultured with *Cln3*$^{-/-}$ glia. (B) Total expression of synaptophysin (normalized to β-actin) was significantly reduced in *Cln3*$^{-/-}$ neurons grown with WT glia compared to when grown with *Cln3*$^{-/-}$ glia. No other significant differences were found. Data in (B) is presented as mean±SEM from three separate biological samples. Scale bar in A is 20 µm.

6.3 Discussion

In this chapter, mixed glial-neuronal co-cultures were used to explore the impact of *Cln3*$^{-/-}$ glia (both astrocytes and microglia) upon neuronal survival, morphology and synaptic organization. *Cln3*$^{-/-}$ glia were observed to have a negative impact on the survival and morphology of both WT and *Cln3*$^{-/-}$ neurons, with *Cln3*$^{-/-}$ neurons being particularly vulnerable. In contrast, WT glia had a positive impact on *Cln3*$^{-/-}$ neuron survival and morphology; increasing cell soma size and overall neurite complexity. In addition, specific alterations in the expression of synaptic proteins were discovered. While SNAP25 expression was not influenced by the presence of glia of either genotype, *Cln3*$^{-/-}$ glia induced an increase in synaptophysin expression, but only in *Cln3*$^{-/-}$ neurons. These studies provide the first direct link between the compromised biology of *Cln3*$^{-/-}$ glia and neuron loss in JNCL, indicating that these cells are key players in the pathogenesis of JNCL. Such information may ultimately be used to design novel therapies for this disease, based on inhibiting the negative effects of altered glial biology.

Why are *Cln3*$^{-/-}$ glia harmful to other neural cell types?

Mixed cultures of *Cln3*$^{-/-}$ glia had a negative impact on neurons of both genotypes, and these became more apparent with increased time in co-culture (after 7 DIV), suggesting that the harmful effects of *Cln3*$^{-/-}$ glia are cumulative. This is consistent with *in vivo* findings in JNCL mouse models, where glial activation takes place early in the disease process and is followed by neurodegeneration in the same brain regions (Pontikis et al., 2004; 2005). In addition to the toxicity of *Cln3*$^{-/-}$ glia, *Cln3* deficient neurons also appeared to induce the death of WT astrocytes, suggesting that abnormal glial-neuron communication may exist in the *Cln3*$^{-/-}$ mouse brain. This astrocyte death was not apparent in co-cultures of *Cln3*$^{-/-}$ neurons and glia, possibly because the toxic effect of the *Cln3*$^{-/-}$ glia on *Cln3*$^{-/-}$ neurons was the more dominant, since in these co-cultures neuronal death was already apparent after 2 DIV but the effects of *Cln3*$^{-/-}$ neurons on astrocytes was not evident at this stage (see Chapter 6, Figure 6.2).

Healthy glial cells are known to support neuronal survival in many ways. For instance, they regulate extracellular potassium and thus regulate neuronal excitability, they sequester neurotrasmitters from the synaptic cleft to inhibit their toxic accumulation, they secrete bioactive factors like the energy substrate lactate and neurotrophic factors like NGF, FGFs and VEGF, and respond to neuron derived neuropeptides such as vasoactive intestinal peptide (VIP) by secreting neuroprotective factors including activity-dependent neuroprotective protein (ADNP) (Vernadakis, 1988; Vernadakis and Mangoura, 1988; Ang et al., 1992; Martin, 1992; Sass et al., 1993; Schmalenbach and Müller, 1993; Giulian et al., 1994; Wang et al., 1994; Gallo et al., 2000; Aloisi, 2001; Furman et al., 2004; Garden and Möller, 2006; Liu et al., 2011; Singh et al., 2011; Pascual et al., 2012). Given that glia carry out such a diverse range of functions to support neurons, it is not surprising that impaired glial biology has been found to contribute to neuronal dysfunction and loss in several CNS disorders, including MSD, NPC, ALS, Alzheimer, Parkinson, and Huntington diseases (Garden and Möller, 2006; Chen et al., 2007; Zhang et al., 2008; Rossi and Volterra, 2009; Möller, 2010; Zhang et al., 2010; Garwood et al., 2011; Kettenmann and Verkhratsky, 2011; Panaro and Cianciulli, 2012; Phani et al., 2012; Tufekci et al., 2012; Di Malta et al., 2012a; 2012b). From experiments described in this thesis, we have observed that under resting conditions *Cln3*$^{-/-}$ astrocytes displayed an impaired inability to take up glutamate (Chapter 4, Figure 4.11) and had abnormal Ca^{2+} signaling (Chapter 4, Figures 4.1-4.6). These deficits could directly impact neurons since impaired glutamate clearance could lead to the induction of excitotoxity and altered Ca^{2+} signaling could impair neuron-astrocyte and astrocyte-astrocyte communication (See discussion in Chapter 4, Section 4.3). Under basal conditions, *Cln3*$^{-/-}$ microglia did not display any overt functional deficits (S. Dihanich, unpublished data). Thus, neuronal loss caused by *Cln3*$^{-/-}$ glia in these co-cultures may initially be astrocyte-driven.

It has been suggested that glial-regulated neuronal survival *in vitro* is mediated at least partly by secreted soluble factors (Fishell and Hatten, 1991). Under basal conditions, *Cln3*$^{-/-}$ astrocytes secreted lower levels of the mitogen, M-CSF, the

chemokines, MIP-1γ, GCP-2 (glutamate carboxypeptidase -2 metalloproteinase) and TIMP-1, but increased levels of tissue factor (see Chapter 4, Tables 4.1 and 4.2). The implications of these secretion defects may be many fold since these factors may act on both glia and neurons, having both harmful and neuroprotective properties (Eddleston et al., 1993; Liu et al., 1994; Fujimoto et al., 2008; Semple et al., 2010; Rostène et al., 2011; Sidoryk-Wegrzynowicz et al., 2011). For instance, M-CSF is a hematopoietic cytokine that is secreted by both neurons and glia. This cytokine induces microglial activation, enhancing their proliferation, protein secretion and autophagy (Imai and Kohsaka, 2002; Hamill et al., 2005). Since, microglial activation has been associated with neuronal loss via production of potentially toxic cytokines, reactive oxygen and nitrogen species, and prostaglandins (McGeer and McGeer, 2002; Nau and Brück, 2002; Danton and Dietrich, 2003), M-CSF might be considered to be detrimental to neurons. However, this factor has also been shown to have neuroprotective properties both *in vivo* and *in vitro* (Berezovskaya et al., 1996; Fedoroff et al., 1997; Bruccoleri and Harry, 2000; Vincent et al., 2002a; 2002b). Additionally, increased microglial expression of the M-CSF receptor was found to be neuroprotective in a microglia-hippocampal organotypic co-culture system (Mitrasinovic et al., 2005). Thus, reduced M-SCF secretion in co-cultures with *Cln3*$^{-/-}$ astrocytes could lead to altered microglial-mediated neuroprotection. Furthermore, abnormal regulation of GCP-2, which is produced mainly by astrocytes in the adult CNS, has been associated with various neurological disorders, including ischemia, epilepsy and ALS (Tsai et al., 1991; Meyerhoff et al., 1992a; 1992b; Passani et al., 1997; Ghadge et al., 2003). GCP-2 is a key mediator of glutamate signaling since it may either cleave N-acetylaspartylglutamate (NAAG) to release glutamate and N-acetylaspartate (NAA), and/or be indirectly involved in NAAG-metabotropic glutamate signaling (Zhou et al., 2005). The importance of this proteinase in the CNS is highlighted by the fact that mice with an exon 9/10 deletion in the *Gcp-2 gene* are embryonic lethal (Bacich et al., 2002; Tsai et al., 2003). Perhaps, the attenuated GCP-2 secretion by *Cln3*$^{-/-}$ astrocytes, together with their reduced ability to take up glutamate, results in aberrant glutamate signaling within these co-cultures

leading to excitotoxicity. Recently, GCP-2 activity has also been linked with the degradation of Aß monomers and prevention of Aß-induced neurotoxicity (Kim et al., 2010a). Interestingly, altered processing of amyloid β-protein precursor, particularly in neurons, has also been reported in JNCL patient samples (Wisniewski et al., 1990; Golabek et al., 2000). Thus, lack of GCP-2 secretion by astrocytes *in vivo* could lead to accumulation of unprocessed Aß leading to neuronal loss in JNCL. This theory, however, needs to be subjected to further experimental verification. Furthermore, reduced TIMP-1 secretion could be involved in the attenuated neurite growth observed in co-cultures with *Cln3*$^{-/-}$ glia (discussed below). Thus, the observed changes in protein secretion by *Cln3*$^{-/-}$ astrocytes grown under basal conditions have the potential to adversely affect neurons. However, interpreting the impact of altered protein secretion upon neuronal health is difficult given that many of the factors secreted by glia display multiple, context-dependent functions, as discussed earlier (see discussion in Chapter 4, Section 4.3). Furthermore, the protein secretion profile of microglia and astrocytes may differ when these cell types are cultured alone, rather than as mixed glia cultures or in co-cultures with neurons (as in the protein profiling studies described in (Zietlow et al., 1999; Petegnief et al., 2001; Crocker et al., 2004; Jack et al., 2005; Saura, 2007; Welser-Alves et al., 2011). As such, it will be important in the future to study protein secretion in both mixed glia cultures, and in co-cultures. Ultimately, the secretion of these soluble factors within the CNS should also be investigated *in vivo*, even if this is a very challenging task, due to these factors being expressed at low levels and the difficulty in isolating tissue samples that are free from cytosolic contamination (Tracey and Cerami, 1993). However, overall quantification of soluble factor levels *in vivo* could be achieved by measuring specific proteins with immuno assays (such as ELISAs) from CNS homogenates derived from WT or *Cln3*$^{-/-}$ mice. Alternatively, secreted levels of proteins in the CNS could be measured via microdialysis probes that allow repeated sampling from freely moving mice, and permit the measurement of metabolites in the extracellular fluid (Woodroofe et al., 1991; Merali et al., 1997; Linthorst et al., 2000).

Upon activation, the differences in the secretion profiles of WT and *Cln3*$^{-/-}$ glia become more striking, with both *Cln3*$^{-/-}$ astrocytes and microglia failing to secrete a range of proteins, although astrocytes are the more severely affected (Chapter 4, S. Dihanich, unpublished data). As discussed in Chapter 4, these changes have the potential to be detrimental to neuronal health. This is relevant when it comes to hypothesizing why *Cln3*$^{-/-}$ glia might have a more pronounced effect on *Cln3*$^{-/-}$ neurons, since in this co-culture combination astrocytes appear morphologically activated, particularly after 7 day in culture (see Figure 6.3). The cell bodies of these *Cln3*$^{-/-}$ astrocytes are shrunken and they have extended processes resembling cultured astrocytes that are activated (Hu et al., 1998a; 1998b; Paradisi et al., 2004; Garwood et al., 2011). Therefore, this raises the possibility that *Cln3*$^{-/-}$ neurons secrete a cocktail of astrocyte-activating factors. Indeed, *in vitro* studies have shown that FGF-1 released by motor neurons exposed to oxidative stress, as could be caused by attenuated glutathione secretion (see Chapter 4, Figure 4.9), can activate astrocytes (Cassina et al., 2005). These activated astrocytes then initiated motor neuron apoptosis via activation of the p75 neurotrophin receptor (p75(NTR)) (Cassina et al., 2005), which is a member of tumor necrosis factor receptor superfamily (Dechant and Barde, 2002; Nykjaer et al., 2005), and is also known to be expressed by cultured mouse cortical neurons (Lemkuil et al., 2011; Ibáñez and Simi, 2012; Sun et al., 2012). Thus, *Cln3*$^{-/-}$ neurons may initiate activation of astrocytes and in doing so may aid their own death.

One feature common to both *Cln3*$^{-/-}$ microglia and astrocytes was that, upon isolation, both of these glial cell types appeared more activated than WT glia (Chapter 3, Figure 3.6 and S. Dihanich, unpublished data). *Cln3*$^{-/-}$ astrocytes displayed increased GFAP immunoreactivity, while more *Cln3*$^{-/-}$ microglia had a swollen cell body and had retracted their processes. Therefore, some signaling cascades involved in glia activation may have already been initiated *in vivo,* possibly due to the diseased environment. Equally, mutant glia may be more sensitive *to* the isolation procedure, or to being maintained in culture. Regardless, these changes could have an impact on the biology of the *Cln3*$^{-/-}$ glia

used in these co-cultures, even in the absence of further exogenous stimulation. Indeed, activated astrocytes have previously been shown to cause neuronal death, as well as increased neuronal susceptibility to 1-methyl-4-phenylpyridinium (MPP+) and 6-hydroxydopamine (6-OHDA) induced toxicity, in a co-culture system (McNaught and Jenner, 1999). This toxic effect was partially rescued either by addition of the NMDA/glutamate antagonist MK-801, by glutathione application or by inhibition of excess NO production. Moreover, it has been reported that increased NO and NOS production by activated microglia induced the death of co-cultured cerebellar granule neurons, and that this effect could be partially blocked by using an inhibitor of NO synthase (N^G-nitroarginine), deactivation of NO with oxyhemoglobin, NMDA-blockage with MK-801 and APV, or stabilization of NO with superoxide dismutase (Boje and Arora, 1992). Hence, if *Cln3*$^{-/-}$ glia cells are 'more activated' upon isolation they could cause neuron loss via mechanisms involving overstimulation of glutamate receptors, NO and NOS toxicity and/or collapse of the anti-oxidant defense system. Further support for this hypothesis comes from data linking CLN3 deficiency with abnormal NO signaling, as well as with enhanced oxidative stress (Ramirez-Montealegre and Pearce, 2005; Benedict et al., 2007; Chan et al., 2009; Tuxworth et al., 2011). Consistent with this, the lack of glutathione secretion by *Cln3*$^{-/-}$ astrocytes may lead to increased oxidative stress, and potentially change the neurotrophic effect of NO into a neurotoxic effect by compromising the neuronal mitochondrial electron transport chain (ETC) and thus energy production, triggering programmed cell death (Heales et al., 1996; Dringen, 2000; Canals et al., 2001; Gegg et al., 2005). Lack of CLN3 has already been associated with mitochondrial dysfunction, since the mitochondrial ATP synthase subunit c is the major component of the storage material in JNCL. In addition, the size and morphology of mitochondria is altered in different neuronal cell models derived from *Cln3*$^{-/-}$ or *Cln3*$^{\Delta ex7/8}$ mice (Fossale et al., 2004; Luiro et al., 2006), and mitochondrial enzymes, such as ATP synthase, have been suggested to be dysfunctional in patient fibroblasts and in the brains of *Cln3*$^{-/-}$ mice (Majander et al., 1995; Das and Kohlschütter, 1996; Dawson et al., 1996; Luiro et al., 2006). Altered levels of high-energy phosphate compounds are evident in patient

fibroblasts (50% reduction in ATP levels, 30% reduction in adenosine diphosphate (ADT) levels) and in cerebellar precursor cells derived from *Cln3*$^{\Delta ex7/8}$ mice (1.3 fold reduction in ATP compared to WT cells) (Das et al., 2001; Fossale et al., 2004). Thus, toxicity resulting from reactive oxygen/nitrogen species, together with reduced mitochondrial energy production could potentially also contribute to neuronal cell loss in these co-cultures, and should be investigated further. Accumulation of reactive oxygen and nitrogen species could be measured directly using commercially available fluorescent probes such as dichlorodihydrofluorescein diacetate (DCFH-DA), for measuring intracellular H_2O_2 and other oxidants, and dihydrorhodamine (DHR) for measuring nitrogen species (Uy et al., 2011; Kalyanaraman et al., 2012). Finally, inhibitors of NO synthesis or deactivation of NO, anti-oxidant treatments and glutamate receptor blockage could all be tested in these co-cultures to investigate whether these mechanisms contribute to the observed neuronal loss (Bolaños et al., 1997; Dringen et al., 1999b; Dringen, 2000; Dringen et al., 2001; Kemp and McKernan, 2002; Heales et al., 2004; Wu et al., 2004; Duncan and Heales, 2005; Gegg et al., 2005).

The impaired Ca^{2+}-based intercellular communication between *Cln3*$^{-/-}$ astrocytes that we have documented (see Chapter 4, Figures 4.1-4.6) could prevent their ability to synchronize any activities aimed to support neuronal survival. For example, increased spontaneous Ca^{2+} oscillations in astrocytes induced by Aß, whose accumulation is the hallmark of Alzheimer disease, was demonstrated to increase the death of co-cultured neurons (Abramov et al., 2003). This neuronal death was associated with Ca^{2+}-dependent glutathione depletion in both astrocytes and neurons. We have shown that spontaneous Ca^{2+}-oscillations were altered in *Cln3*$^{-/-}$astrocytes (see Chapter 4, Figures 4.1. and 4.2), which could help explain the observed accumulation of glutathione within these cells (Chapter 4, Figure 4.9). Subsequently, this could result in depletion of neuronal glutathione, whose production is dependent on substrates derived from the glutathione secreted by astrocytes, accelerating their death in co-cultures with *Cln3*$^{-/-}$ glia. Additionally, this abnormal Ca^{2+} signaling may be further impaired by the

mitochondrial dysfunction that has been suggested to be associated with *Cln3* deficiency, leading to reduced ATP (Majander et al., 1995; Das and Kohlschütter, 1996; Dawson et al., 1996; Das et al., 2001; Fossale et al., 2004; Luiro et al., 2006; Padilla-Lopez and Pearce, 2006). ATP released upon spontaneous Ca^{2+} oscillations in astrocytes has been shown to activate microglia, triggering the production and release of a number of pleotrophic cytokines such as IL-1β, or neuronal survival promoting trophic factors such as FGFs, NGF, NT-3 and CNTF (Verderio and Matteoli, 2001; Hansson and Rönnbäck, 2003; Bianco et al., 2005). Thus, impaired Ca^{2+} signaling observed in *Cln3*$^{-/-}$ astrocytes may not only cause problems for astrocyte function, but may also inhibit mechanisms involved in microglial-mediated neuronal survival.

In co-culture experiments, *Cln3*$^{-/-}$ neurons were observed to be far more vulnerable than WT neurons, when grown with *Cln3*$^{-/-}$ glia. While this may, in part, be due to *Cln3*$^{-/-}$ glia being activated when cultured with *Cln3*$^{-/-}$ neurons (as discussed above), it is also possible that *Cln3*$^{-/-}$ neurons have already been sensitized by loss of the CLN3 protein prior to isolation, or during the isolation and culturing procedure. *Cln3* mRNA levels have been shown to be highest during brain development and at early post-natal stages, suggesting that the protein is particularly required at these times (Mitchison et al., 1999; Pane et al., 1999). Furthermore, it has been suggested that CLN3 can interact with calsenilin (Chang et al., 2007), which is a Ca^{2+}-binding protein with apoptosis enhancing ability (Jo et al., 2001; Lilliehook et al., 2002). Indeed, CLN3 deficiency has been shown to accelerate neuronal cell death induced by high Ca^{2+} (Chang et al., 2007). This could suggest that CLN3 may have anti-apoptotic properties (Lane et al., 1996; Puranam et al., 1999; Narayan et al., 2006a), although there is no convincing evidence that this is the case. Nevertheless, *Cln3*$^{-/-}$ neurons would therefore be more susceptible to apoptosis than WT neurons. Additionally, the distally located AIS in *Cln3*$^{-/-}$ neurons (see Chapter 5, Figures 5.5 and 5.6) suggests that these cells are in a state of overstimulation (Grubb and Burrone, 2010b), which could also add to their vulnerability. One can image that the AIS was moved distally in an attempt to protect *Cln3*$^{-/-}$ neurons from increased

excitation due to a diseased environment, perhaps contributed to by dysfunctional glial cells (Schafer et al., 2009; Grubb and Burrone, 2010b). Indeed, neurons in different mouse models of JNCL display increased vulnerability towards AMPA and NMDA receptors-mediated excitotoxicity (Kovács et al., 2006; Finn et al., 2011), and attenuating AMPA-receptor activity resulted in improved motor performance and pathology in *Cln3*$^{-/-}$ mice (Kovács and Pearce, 2008; Kovács et al., 2012). Based on these observations, the neuroprotective power of selective AMPA- and NMDA-receptor antagonists could be explored in these co-culture systems to attempt to protect against neuronal cell death inflicted by *Cln3*$^{-/-}$ glia.

It is also possible that *Cln3*$^{-/-}$ neurons may be more susceptible to *Cln3*$^{-/-}$ glia due to differences in receptor expression, particularly receptors for survival factors such as TrkA and TrkB expressed by neurons within the cerebral cortex (McMillan et al., 1996; Lee et al., 1998; Miller and Pitts, 2000; Luiro et al., 2004; Makkerh et al., 2005; Bruns and Miller, 2007a; 2007b; Walkley, 2009). Diminished receptor expression and recycling via signaling endosomes in affected neuronal populations could accelerate neuronal dysfunction and drive neurodegeneration (Blesch, 2006; Twiss et al., 2006; Bronfman et al., 2007; Walkley, 2009). For instance, the expression levels of the TrkA receptor, which binds NGF, has been found to be significantly reduced in different brains regions of Alzheimer disease patients (Boissière et al., 1996; Hock et al., 1998; 2000; Counts and Mufson, 2005), and in Parkinson disease (Nagatsu et al., 2000; Tong et al., 2009). Furthermore, in embryonic striatal neurons derived from *Npc1*$^{-/-}$ mice (model for Niemann-Pick disease), TrkB signaling has been reported to be severely compromised causing unresponsiveness to neurotrophins, and was proposed to be one the neurodegenerative mechanisms in this disease (Henderson et al., 2000). It was also suggested that typical cholesterol accumulation in late endosomes/multivesicular bodies (MVBs) in *Npc1*$^{-/-}$ cells alters the ability of these organelles to traffic Trks via impacting Rab7 activity (Henderson et al., 2000; Saxena et al., 2005a; 2005b; Bronfman et al., 2007). Interestingly, the small GTPase Rab7, which is a potential interacting-partner of

CLN3 (Luiro et al., 2004; Uusi-Rauva et al., 2012), has been shown to control the endosomal trafficking of TrkA (Saxena et al., 2005a). Thus, lack of CLN3-Rab7 interaction together with attenuated receptor recycling observed upon CLN3 deficiency (Luiro et al., 2004) may lead to altered TrkA receptor expression on the cell membrane in *Cln3*$^{-/-}$ neurons. To determine whether this is indeed the case in *Cln3*$^{-/-}$ neurons, TIRF-microscopy could be used to investigate the expression of Trks on the cell membrane.

What could cause the death of WT astrocytes in co-cultures with *Cln3*$^{-/-}$ neurons? It is well-established that neuronal activity can depolarize glial cells (Orkand et al., 1966; Ransom and Goldring, 1973; Van Essen and Kelly, 1973; Schummers et al., 2008). Given that *Cln3*$^{-/-}$ neurons could be intrinsically in a state of over-stimulation (Chapter 5, Figure 5.5-5.10) this may also cause excessive glial depolarization, altering the membrane potential of astrocytes and inducing their death (Franco et al., 2006; Verkhratsky et al., 2012b). Altogether, these findings emphasize the importance of the interplay between glia and neurons in JNCL. However, gaining a better understanding of what kind of proteins *Cln3*$^{-/-}$ neurons secrete would help provide a more complete image of these interactions.

Cln3$^{-/-}$ glia influence neurite complexity

It is well-established that astrocytes promote neurite growth by providing a wide range of diffusible and contact-mediated factors (Tomaselli et al., 1988; Powell et al., 1997b; Crone and Lee, 2002; Araújo and Tear, 2003). Moreover, upon activation, astrocytes may overexpress growth-inhibitory extracellular matrix (ECM) proteins, like chondroitin and keratan sulphate proteoglycans, that may prevent the extension of regenerating axons (Silver and Miller, 2004). *Cln3*$^{-/-}$ glial cells severely affected the morphology of neurons (soma size, neurite length and number), with *Cln3*$^{-/-}$ neurons again being the most sensitive (see Figures 6.4 and 6.5). WT glia, on the other hand, seemed to ameliorate the morphological defects of *Cln3*$^{-/-}$ neurons. These observations are significant since maintaining their morphology, facilitated by undisrupted neurite growth, is pivotal for neuronal connectivity (see discussion in Chapter 5, Section 5.3).

Another way glial cells can impact neuronal growth is via Ca^{2+} signaling. Astrocytes display Ca^{2+} transients evoked by neurotransmitters, and they also exhibit spontaneous Ca^{2+} oscillations independent of neuronal influence (Verkhratsky et al., 1998; Parri et al., 2001; Aguado et al., 2002; Nett et al., 2002; Hirase et al., 2004). These spontaneous astrocytic Ca^{2+} oscillations, found to be attenuated in *Cln3*$^{-/-}$ astrocytes (Chapter 4, Figures 4.1 and 4.2), have been shown to facilitate neurite growth by inducing the expression of the cell-adhesion molecule, N-Cadherin (Kanemaru et al., 2007), that is involved in driving growth cone migration (Neugebauer et al., 1988; Tomaselli et al., 1988; Williams et al., 1994; Müller et al., 1995). Thus, the attenuated spontaneous Ca^{2+} oscillations we observed in *Cln3*$^{-/-}$ astrocytes could also play a part in the impaired neurite outgrowth we saw in co-cultures. To investigate this suggestion, the expression patterns of N-cadherin and other adhesion molecules could be investigated in neuron/*Cln3*$^{-/-}$ glia co-culture systems. Interestingly, the period when spontaneous Ca^{2+} oscillations occur most frequently has been shown to be the same stage of development when axons and dendrites actively develop to form thalamocortical circuits (Parri et al., 2001). Thus, if *Cln3*$^{-/-}$ glia have the same negative impact on neuronal growth *in vivo*, this could potentially alter thalamocortical circuit formation in the *Cln3*$^{-/-}$ brain. Indeed, thalamocortical neuron loss and localized reactive gliosis in the *Cln3* deficient mice has been well characterized (Pontikis et al., 2004; 2005; Weimer et al., 2006). Since the thalamus processes and relays sensory information to the cortex, the functional deficits documented in *Cln3*$^{\Delta ex7/8}$ mice may be caused by early dysfunction in the thalamocortical system (Pontikis et al., 2005; Staropoli et al., 2012). The evidence provided in this thesis (Chapter 5, Figure 5.5, Chapter 6, Figures 6.4 and 6.5) raises the possibility that this early dysfunction may be caused by reduced neurite growth, that would have a significant impact upon synaptic plasticity and connectivity, and that this may be caused by abnormal glial function. It would be interesting to test the functional integrity of the thalamocortical circuits in different mouse models of JNCL to confirm this hypothesis by using thalamocortical slice cultures to measure neuronal circuit activity via extracellular recordings of evoked field potentials (Song et al., 2012).

Additionally, JNCL mice where either astrocytes only or microglia only carry the most common *Cln3* mutation (in the process of being generated) could be used to investigate the specific roles that these glial cells play in the dysfunction of the thalamocortical system observed in this disease.

As discussed earlier, soluble factors secreted by glial cells could also significantly influence neurite growth in these co-culture systems (see discussion in Chapter 5, Section 5.3). We know that under basal conditions the secretion defect of *Cln3*$^{-/-}$ astrocytes is restricted to a small and specific set of proteins (TIMP1, MIP-1γ, GCP-2 and M-CFS), but this secretion defect becomes much more severe upon stimulation (Chapter 4, Tables 4.1 and 4.2 and Figure 4.7). Under basal conditions, *Cln3*$^{-/-}$ microglia secrete proteins normally, but also fail to secrete a subset of factors upon activation (MIP-2, RANTES, MIP-1γ, vW and MMP-9, S. Dihanich, unpublished data). At the moment we do not know precisely how protein secretion is changed in mixed glia-cultures, or how the presence of neurons may change this further, since all of these cell types are known to interact with one another via protein secretion (Aloisi, 2001; Bezzi et al., 2001; Sofroniew and Vinters, 2010; Kettenmann and Verkhratsky, 2011; Kettenmann et al., 2011; Parpura et al., 2011; Agulhon et al., 2012; Schafer et al., 2013). Nevertheless, the data presented in this thesis, and data from studies on *Cln3*$^{-/-}$ microglia (S. Dihanich, unpublished data), suggest that these cells do clearly have protein secretion defects. Previously, it has been shown that the reduced neurite extension ability of neurons cultured from the brains of newborn English setters with NCL (caused by a mutation in *Cln8*) could be overcome by addition of insulin-like growth factor I (IGF-I), EGF and PDGF to the cultures (Dunn et al., 1994). Additionally, BDNF has been shown to significantly improve the attenuated neurite outgrowth observed in retinas cultured from Sandhoff mice (Sango et al., 2005). Therefore, the observed reduction in neurite growth when neurons are co-cultured with *Cln3*$^{-/-}$ glia could be due to their failure to secrete the appropriate factors. For instance, attenuated secretion of VEGF (Chapter 4, Table 4.2 and Figure 4.7), which has been shown to increase the neurite outgrowth of cerebral cortical neurons by interacting with VEGFR2 and activating

Rho/ROK (Jin et al., 2006), could help explain the reduced neurite growth in co-cultures with *Cln3*$^{-/-}$ glia. Indeed, one could test whether providing a cocktail of neurite growth promoting factors, such as VEGF, IGF, EGF and PDGF, could reverse the negative impact of *Cln3*$^{-/-}$ glia upon neurite growth from WT and surviving *Cln3*$^{-/-}$neurons. However, it is worth remembering that in the cortical neuronal cultures described in Chapter 5, complex neurite extensions are observed, suggesting that factors from exogenous glial cells may not be needed for this process. This suggests that, the reduced neurite complexity observed in these co-cultures may be better explained by the inhibitory influence of *Cln3*$^{-/-}$ glia (as discussed above).

Altered cell-matrix within these co-culture combinations could also influence neurite growth. This includes laminin, whose production (Liesi et al., 1983; Costa et al., 2002; Tardy, 2002) could be attenuated in *Cln3*$^{-/-}$ astrocytes leading to a non-supportive cell-matrix for neurite growth in co-cultures that include these cells. Additionally, modulation of the ECM by proteinases such as MMPs, which are produced by both glial cell types, could also influence the composition of the ECM (Costa et al., 2002; Ould-yahoui et al., 2009; Welser-Alves et al., 2011). For example, the correct balance of MMP-2, and its inhibitor TIMP-2 together with laminin, have been shown to stabilize cell-matrix interactions and help regulate neurite outgrowth and migration (Costa et al., 2002). Both *Cln3*$^{-/-}$ astrocytes and microglia secrete less MMP-9, and *Cln3*$^{-/-}$ astrocytes also secrete less TIMP-1 both under basal conditions and after stimulation (S. Dihanich, unpublished data, Chapter 4, Tables 4.1 and 4.2), which could result in an environment that is unfavorable for neurite growth. One could test these possibilities by using laminin as a substrate for co-cultures (grown in this study on PDL, see Chapter 2, Section 2.3) and observing whether this restores neurite growth. Additionally, the impact of recombinant MMPs, MMP-neutralizing antibodies, or MMP-inhibitors, such as Ro 31-9790, on neurite growth could be investigated.

Emerging evidence also points towards the importance of microglia in the regulation of neuronal morphology (Trapp et al., 2007; Sisková et al., 2009;

Kettenmann and Verkhratsky, 2011; Kitayama et al., 2011; Schafer et al., 2013). The glial cultures used in these studies were mixed, being mainly composed of astrocytes and microglia. Therefore, any observed impact on neuronal health could be caused by just astrocytes, just microglia or both of these cell-types. Like astrocytes, microglia can also sense neuronal activity via their wide range of neurotransmitter receptors (Rock et al., 2004; Pocock and Kettenmann, 2007; Kettenmann et al., 2011). Based on *in vivo* evidence, microglia are constantly re-establishing connections with synaptic structures, indicating that dynamic interactions exist between microglia and neurons in the intact brain (Wake et al., 2009; Schafer et al., 2013). These interactions could be dictated by the levels of neurotransmitters present, which may be dramatically different in the different co-culture combinations, due to differences in the cellular homeostasis created by neuron-glia interactions and by the expression of different adhesion molecules. One way in which *Cln3*$^{-/-}$ microglia could exert a negative influence on neuronal morphology is via their ability to remove abnormally functioning synapses (Lindå et al., 2000; Trapp et al., 2007; Yamada et al., 2008). Moreover, microglia can also synthesize, release and respond to a distinct set of neurotrophins, including NGF, NT-3, GDNF and BDNF with neurite growth promoting ability (Elkabes et al., 1996; Heese et al., 1997; Morgan et al., 2004; Coull et al., 2005; Nakajima et al., 2007). Some evidence also exists that secretory proteases, particularly plasminogen-plasminogen activator (PGn-PA), released by microglia may regulate neuronal growth and function and thus could be involved in the regulation of neuronal circuits (Kohsaka et al., 1996; Nakanishi, 2003). Impaired secretion of neurotrophic factors and/or secretory proteases by *Cln3*$^{-/-}$microglia could partly explain the observed negative impact on neuronal growth observed in co-cultures of *Cln3*$^{-/-}$ glia with WT and *Cln3*$^{-/-}$ neurons. This would obviously need to be tested, but our observation that protein secretion is perturbed in these cells makes this a possibility worth considering. Furthermore, both *Cln3*$^{-/-}$ astrocytes (Chapter 3, Figure 3.6) and microglia (S. Dihanich, unpublished data) appear to be more activated than their WT counterparts when cultured under basal conditions (see above). This may help to explain their negative impact on neurite growth, an influence that

activated glia are known to have (Reier and Houle, 1988; McKeon et al., 1991; Laywell et al., 1992; Norton et al., 1992; Norenberg, 1994; Williams et al., 1994; Dayton and Major, 1996; Ridet et al., 1997; Raivich et al., 1999; Münch et al., 2003; Kitayama et al., 2011). More specifically, we demonstrated that activated *Cln3*$^{-/-}$ microglia secrete less MMP-9, which is an important regulator of NGF-induced neurite elongation (Costa et al., 2002; Shubayev and Myers, 2004; Ould-yahoui et al., 2009). Furthermore, the chemokine RANTES, another protein secreted at lower levels by these cells upon activation, has been shown to induce the neuronal expression of genes involved in promoting neurite outgrowth and synaptogenesis (Valerio et al., 2004). Additionally, activated astrocytes may produce and secrete arachidonic acid metabolites, TNF-α and NO that may have detrimental effects on neuronal biology and their ability to retain their morphological integrity (Williams et al., 1995; Dayton and Major, 1996; Neumann et al., 2002). However, microglia may produce significantly more of such cell damaging factors than astrocytes (Malipiero et al., 1990; Vincent et al., 1996; Münch et al., 2003; Kitayama et al., 2011). Thus, the most dramatic detrimental impact upon neurons may be mediated by microglia in the long run instead of astrocytes. Finally, activated microglia may inhibit neurite growth via increased expression of RGMa (repulsive guidance molecule), an effect that can be reversed by minocycline treatment that inhibits microglial activation (Kitayama et al., 2011). To investigate whether any of these hypotheses explain the diminished neurite growth seen when co-cultured with *Cln3*$^{-/-}$ glia, production of these factors and expression of membrane bound molecules should be investigated in these co-cultures, to determine how interaction between neurons and glia of different genotypes may influence the glial-based mechanisms that support neurite growth.

To conclude, both astrocytes and microglia have the potential to regulate the development of neurites in these co-culture systems. Both of these cell-types are capable of monitoring the status of neurite development and neuronal connectivity at synaptic sites. Indeed, both cell-types may remodel neuronal connectivity via alterations in neurite formation and synaptic pruning, and

therefore participate actively in the maintenance and plasticity of neural networks (Verkhratsky and Butt, 2007; Araque and Navarrete, 2010; Kettenmann et al., 2011; Liu et al., 2011). In the future, co-cultures in which only *Cln3*$^{-/-}$ astrocytes, or only *Cln3*$^{-/-}$ microglia, are co-cultured with neurons will shed light on the role that each of these cell-types play in this process.

Expression of SNAREs is altered by glial presence

In comparison to *Cln3*$^{-/-}$ neuronal cultures, in which only SNAP25 was found to be significantly upregulated (Chapter 5, Figure 5.11), more and different changes in SNARE-complex proteins were evident in our co-cultures, and particularly when *Cln3*$^{-/-}$ neurons were present (Chapter 6, Figures 6.6 and 6.7). The expression of SNAP25 was reduced when *Cln3*$^{-/-}$ neurons were co-cultured with either WT or *Cln3*$^{-/-}$ glia. In contrast, the expression of synaptophysin was enhanced, but only when grown with *Cln3*$^{-/-}$ glia. Indeed, the appropriate expression of synaptic proteins can be considered as a surrogate marker of normal synaptic function (discussed in Chapter 5, Section 5.3). It is well established that astrocytes increase the number of mature, functional synapses in the CNS via the factors they secrete, and are required for synaptic maintenance both *in vitro* and *in vivo* (Mauch et al., 2001; Ullian et al., 2001; 2004a; 2004b). Emerging evidence also highlights the importance of microglia in synaptic regulation (Kettenmann and Verkhratsky, 2011; Kettenmann et al., 2011; Stephan et al., 2012; Schafer et al., 2013).

Generally synaptic damage, seen here as altered SNAP25 and synaptophysin expression, is considered to be an early event in many neurodegenerative disorders, including different forms of NCLs (Kay et al., 2006; Weimer et al., 2007; Partanen et al., 2008; Kielar et al., 2009). Indeed, synaptic loss closely correlates with cognitive decline in JNCL (DeKosky and Scheff, 1990; Coleman et al., 2004; Scheff et al., 2006; Mandolesi et al., 2010; Milnerwood and Raymond, 2010; Stephan et al., 2012). While there are some situations in which synapse loss associated with neurodegeneration is considered to be a neuron-

autonomous event (Sisková et al., 2009; Perry and O'Connor, 2010), many studies suggest that glia are pivotal regulators of this process (Paradisi et al., 2004; Alexander et al., 2008; Rosen and Stevens, 2010; Schafer and Stevens, 2010; Garwood et al., 2011). In this study glia had an unexpected impact on synaptic protein expression. Even though WT glial cells were shown to have a positive impact on *Cln3*$^{-/-}$ neuronal survival and neurite growth (Results Chapter 6, Figures 6.2, 6.3, 6.5), this did not extend to rectifying their aberrant SNAP25 expression, nor did the negative impact of *Cln3*$^{-/-}$ glia on WT neuronal survival extend to a reduction in SNAP25 expression. Thus, some synaptic changes in *Cln3*$^{-/-}$ neurons could be intrinsic and caused by lack of functional synaptic CLN3 (Järvelä et al., 1998; Luiro et al., 2001; Kyttälä et al., 2005). Indeed, the observed over-expression of SNAP25 in *Cln3*$^{-/-}$ neuronal cultures suggests that this is the case (Chapter 5, Figure 5.11). The fact that SNA25 expression was reduced in *Cln3*$^{-/-}$neurons in all co-culture combinations with WT and *Cln3*$^{-/-}$ glia compared to WT neurons remains unexplained.

On the other hand, synaptophysin expression was increased in *Cln3*$^{-/-}$ neurons in the presence of *Cln3*$^{-/-}$ glia. Based on previous studies, altered synaptophysin expression has been associated with several neurodegenerative disease and psychiatric disorders, such as Alzheimer disease and schizophrenia (Masliah et al., 1994; Eastwood et al., 1995; Heinonen et al., 1995; Glantz and Lewis, 1997; 2000; Glantz et al., 2000). Glial activation has been linked with loss of synaptophysin expression, which is in contrast to findings in this study (Ojo et al., 2012). However, in some cases synaptophysin protein expression levels did not correlate with changes in mRNA levels. It was speculated that this could be caused by abnormal post-translational regulation of synaptophysin in the diseased brain (Glantz et al., 2000), which could also explain the over-expression of synaptophysin in *Cln3*$^{-/-}$ neurons co-cultured with *Cln3*$^{-/-}$ glia.

Both astrocytes and microglia are important regulators of a whole range of events involved in the maturation and maintenance of the synapse, including formation, modification and elimination of synaptic structures, as well as

synaptic plasticity (Allen and Barres, 2009; Ricci et al., 2009; Perry and O'Connor, 2010; Kettenmann and Verkhratsky, 2011; Tremblay and Majewska, 2011; Pascual et al., 2012; Schafer et al., 2013). For instance, cell death can be induced in hippocampal neuronal cultures exposed to Aß (Takashima et al., 1993; Goodman and Mattson, 1994; Paradisi et al., 2004). However, astrocyte conditioned medium can protect against this Aß-induced neurotoxicity, preventing neuritic dystrophy and synaptic damage, proposing a protective role for non-activated astrocytes (Paradisi et al., 2004). This protection was lost, however, when astrocytes were activated by treatment with Aß, suggesting that activated astrocytes can have a deleterious impact on neurons. The morphological appearance of *Cln3*$^{-/-}$ astrocytes co-cultured with *Cln3*$^{-/-}$ neurons suggested that these cells are at least partially activated (Chapter 6, Figures 6.4 and 6.5), which may alter their biology in a way that could damage synapses. Evaluating protein secretion within these co-cultures would enable us to investigate this hypothesis. Additionally, emerging evidence indicates that microglia send processes that dynamically survey synapses and may modify or eliminate them depending upon the levels of neuronal activity (Pocock and Kettenmann, 2007; Kettenmann and Verkhratsky, 2011; Seifert et al., 2011; Krabbe et al., 2012) (Wake et al., 2009; Tremblay et al., 2010; Schafer et al., 2013). Even when grown under resting conditions without glia, *Cln3*$^{-/-}$ neurons were apparently in a state of overstimulation, as judged by the displacement of their AIS (Chapter 5, Figures 5.5-5.10). Thus, different levels of basal neuronal activity evoked in co-cultured neurons (Hild and Tasaki, 1962; Lin et al., 2002), could perhaps explain some of these observations. Indeed, cultured P0 cortical neurons have the ability to exhibit spontaneous electrical activity (Choi et al., 1987; Li et al., 1998; Moody and Bosma, 2005). Thus, chronically more active *Cln3*$^{-/-}$ neurons could trigger stronger responses in glial cells, potentially explaining why we see more synaptic alterations in *Cln3*$^{-/-}$ neuron containing co-cultures. It would be interesting to investigate the localization of the AIS within these co-cultured neurons as a surrogate measurement of on-going levels of neuronal activity. However, it is not yet known whether this type of activity-dependent microglial function leads to elimination or strengthening of synapses

(Kettenmann et al., 2013). Nevertheless, activated microglia can physically contact injured neurons and remove synapses or dendrites (Rappert et al., 2004; de Jong et al., 2005; Stevens et al., 2007). For instance, both *in vivo* and *in vitro* evidence, suggest that glutamate excitotoxicity, may contribute to pathogenesis in *Cln3*$^{-/-}$ and *Cln3*$^{\Delta ex7/8}$ mice (Pears et al., 2005; Kovács et al., 2006; Kovács and Pearce, 2008; Finn et al., 2011). This may lead to induced expression and secretion of the chemokine CCL21 that has been linked to activation of microglia and subsequent dendritic degeneration of neurons (Rappert et al., 2004; de Jong et al., 2005). Thus, synaptic deficits may involve microglial activation orchestrated by a chemokine signaling cascade. Furthermore, such cascades may be used as a means of communication between microglia and astrocytes, which function together to either rescue or remove a synapse (Tran and Miller, 2003; Ransohoff, 2009; Stephan et al., 2012). Activated *Cln3*$^{-/-}$ microglia and astrocytes both showed impaired chemokine secretion (Chapter 4, Tables 4.1 and 4.2 and Figure 4.7, S. Dihanich, unpublished data,) suggesting that communication via chemokines could be interrupted in *Cln3*$^{-/-}$ mice. One important mediator of communication between neural cells is the chemokine stromal cell-derived factor-1 (SDF-1), secreted by astrocytes, which is the natural ligand of the CXCR4 receptor expressed by microglia, astrocytes and neurons (Tachibana et al., 1998; Bezzi et al., 2001; Lazarini et al., 2003; Calì and Bezzi, 2010; Wu et al., 2012). The importance of this chemokine is demonstrated by deletion of the SDF-1 or CXCR4 gene being embryonic lethal (Nagasawa et al., 1999). It is thought that SDF-1/CXCR4 is an integral part of the communication between glia and neurons. SDF-1 secreted by astrocytes may induce rapid Ca^{2+}-based signaling events in both these cell-types (Zheng et al., 1999a; 1999b), and also induce changes in electrophysiological and synaptic properties of neurons (Zheng et al., 1999a; Limatola et al., 2000). Additionally, SDF-1 may cause release of TNF-α, glutamate and PGE_2 from astrocytes leading to activating of microglial TNF-α production and release (Bezzi et al., 2001). Thus chemokine based signaling cascades link both microglia and astrocytes to neuronal function via synaptic changes (Bezzi et al., 2004; Rossi and Volterra, 2009). Hence, it would be interesting to investigate

whether SDF-1 based signaling has remained intact between *Cln3*$^{-/-}$ glia and neurons.

At present, however, there is no evidence that synapses are actually impaired in these co-cultures. To investigate this, co-localization of the presynaptic marker Bassoon and the postsynaptic protein called proline-rich synapse-associated protein 1 (ProSAP1)/Shank2 could be used as a measure of the number of synapses present (Pyka et al., 2011). Also, spontaneous synaptic activity could be measured to detect possible alterations in synapse function. Nevertheless, these results provide a link between synaptic alteration and glial cells in JNCL. Given that deficits in synaptic circuits are emerging as important underlying correlates of neurological disorders (Rubenstein and Merzenich, 2003; Belmonte et al., 2004; LeBlanc and Fagiolini, 2011; Melom and Littleton, 2011), and knowing that glia can mediate synaptic pruning via phagocytic immune pathways (Stevens et al., 2007; Schafer and Stevens, 2010; Schafer et al., 2013), it is highly likely that both astrocytes and microglia together contribute to JNCL symptoms, at least partly via aberrant neuronal-glial signaling at synapses.

A note on using mixed glial cultures

Various different types of co-culture systems have been used to examine glial-neuron interactions under physiological, as well as pathological, conditions (Sass et al., 1993; Giulian et al., 1994; Wang and Cynader, 1999; Gegg et al., 2005; Noble et al., 2009; Garwood et al., 2011; Shimizu et al., 2011; Jones et al., 2012; Skaper and Facci, 2012). To maximize the possibility of observing an effect in our co-culture experiments we chose to culture neurons with a mixed glial culture (composed of astrocyte, microglial cells and the rare oligodendrocyte), rather than with only astrocyte or only microglia cells. This approach had its benefits and limitations. Of benefit, is the fact that mixed glial cultures resemble more closely the environment in the brain, in which microglia and astrocytes are intimately connected. However, the limitations of this approach are that (1) the specific source of any negative or positive influence on neuronal health cannot

be determined, (2) the biology of *Cln3*$^{-/-}$ microglia and astrocytes have only been studied in >98% pure cultures (Chapter 3 and 4, S. Dihanich unpublished data), thus whether these biological changes will be exacerbated, ameliorated, or whether new problems will arise when astrocytes and microglia are grown as mixed cultures is unknown. For instance, it would be extremely informative to study protein secretion in WT and *Cln3*$^{-/-}$ mixed glial cultures under basal conditions and upon activation to explore whether the severely attenuated protein secretion observed in *Cln3*$^{-/-}$ astrocytes is affected by the presence of microglia. To take these co-culture studies further, one could use astrocyte/neurons or microglia/neuron co-cultures to investigate the role each of these glial cell types play in neuronal health. This would answer the question of whether the negative impact of *Cln3*$^{-/-}$ mixed glial on neurons is due to the presence of astrocytes or microglia, or whether both of these cell types work in concert to exert the observed effects. To further define the types of cell-cell interactions involved, one could use co-culture systems in which glia are not in physical connection with neurons, but are separated by a membrane that allows the free diffusion of soluble factors between the different cell types. This approach would help determine whether soluble factors alone are sufficient to recapitulate the observations, and such experiments are now ongoing in the laboratory. Nevertheless, using mixed glial cultures proved to be a very informative initial step in gaining a better understanding of the relationship between neurons and glia in JNCL.

Chapter 7
General discussion

The main objective of this thesis was to investigate how *Cln3* deficiency influenced the biology of astrocytes, and whether *Cln3* deficient glia had a detrimental influence on neuronal health.

Early glial activation that precedes neuronal loss is a well-characterized feature of many different forms of NCLs, including JNCL (Braak and Goebel, 1978; Chronister et al., 1995; Tyynelä et al., 1997; Herva et al., 2000; Nakanishi et al., 2001; Koike et al., 2003; Oswald et al., 2005; Pontikis et al., 2005; Kay et al., 2006; Luiro et al., 2006; Eliason et al., 2007; Partanen et al., 2008; Kuronen et al., 2012; Schmiedt et al., 2012). However, prior to the research described in this thesis very little was known about the biology of NCL glia, or whether these cells actually contribute to NCL pathogenesis. Using an *in vitro* approach we have identified a number of functional deficits in astrocytes isolated from the *Cln3* deficient mouse model of JNCL, most of which could be caused by the abnormal cytoskeletal organization displayed by these cells. For instance, *Cln3*$^{-/-}$ astrocytes exhibited an impaired ability to change morphologically in response to stimulation, to divide, to migrate, to secrete proteins and to take up glutamate. In addition, their Ca^{2+} signalling was abnormal and their endo/lysosomal pathway appeared disrupted (summarized in Figure 7.1 A). Using a similar approach, we also revealed that CLN3 deficiency also resulted in specific alterations to the biology of neurons, including compromised morphology, overexpression of the synaptic protein SNAP25 and a distally located AIS (summarized in Figure 7.1 B).

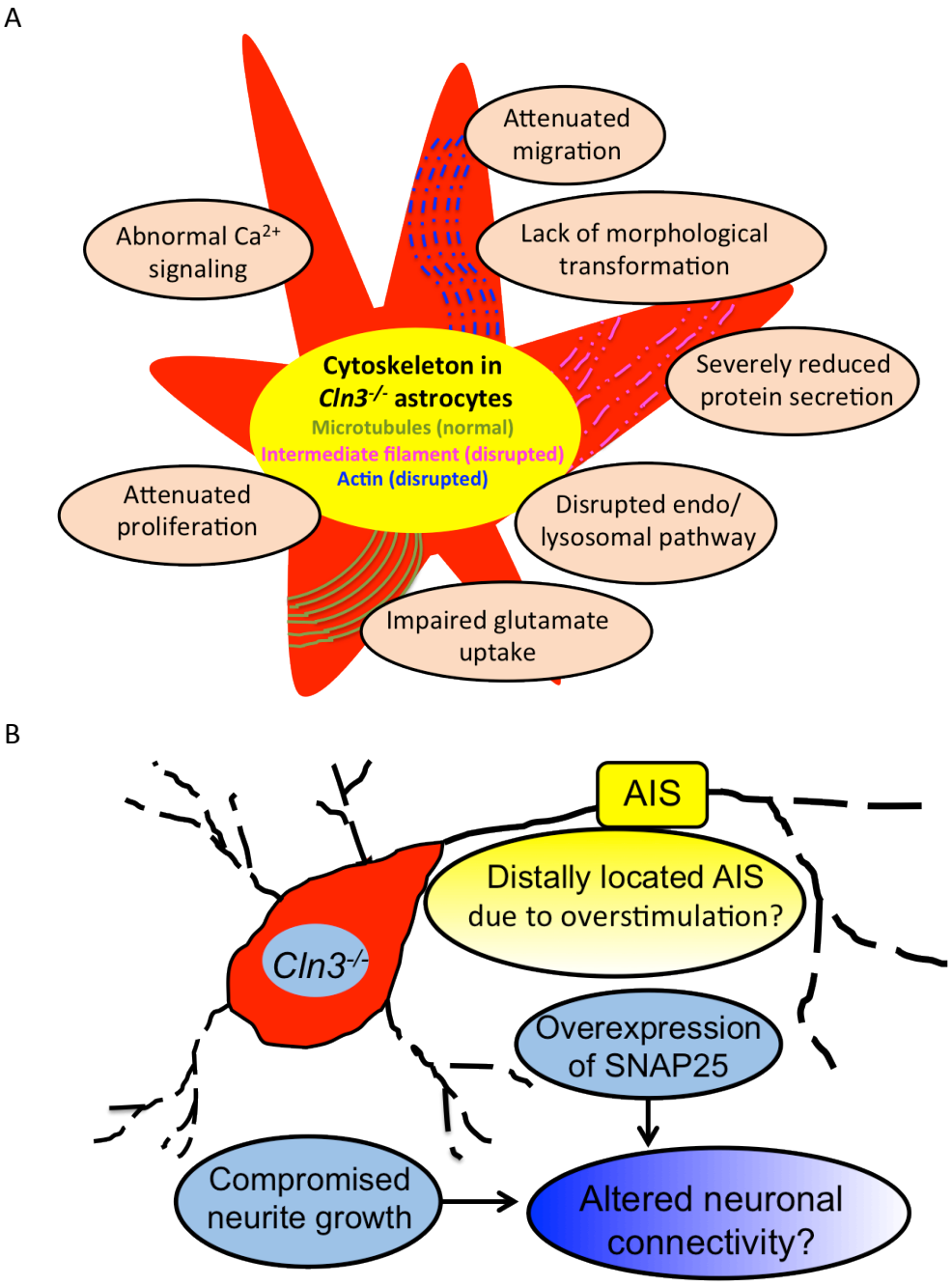

Figure 7.1. CLN3 deficiency causes impairments in the biology of astrocytes and neurons. (A) Studies on astrocyte cultures derived from the cortex of either *Cln3*$^{-/-}$ or WT mice (P1-P2) revealed a range of biological alterations. Many of these deficits can be linked to the cytoskeletal abnormalities observed in *Cln3*$^{-/-}$ astrocytes. (B) Studies on neuronal cultures derived from the cortex of either *Cln3*$^{-/-}$ or WT mice (P0) also revealed a range of specific alterations in neurons.

Most importantly, co-culture experiments carried out in this thesis have provided the first evidence that *Cln3*$^{-/-}$ glia can impact neuronal health. In fact, *Cln3*$^{-/-}$ glia had a negative impact on the survival and morphological integrity of both WT and *Cln3*$^{-/-}$ neurons. Synaptic protein expression was also altered, but

only in *Cln3*$^{-/-}$ neurons. In contrast, WT glia were able to ameliorate some of these defects by promoting both survival and neurite growth in *Cln3*$^{-/-}$ neurons (summarized in Figure 7.2).

The impact of *Cln3*$^{-/-}$ glia upon *Cln3*$^{-/-}$ neurons (summarized in Figure 7.2), could be explained, at least in part, by the attenuated protein secretion profile of these cells upon activation, that appears to be caused by the presence of *Cln3*$^{-/-}$ neurons (Chapter 6, Figures 6.2 and 6.3, discussion in Section 6.3). This could result in a lack of neuroprotective factors and the antioxidant glutathione in the medium, and this situation may be further exacerbated by the impaired glutamate clearance of the *Cln3*$^{-/-}$ astrocytes leading to excitotoxicity. Additionally, the evident impaired secretion of proteins from both *Cln3*$^{-/-}$ microglia and astrocytes may alter pivotal communication pathways, not only between these glial cell types, but also between glia and neurons. This may ultimately result in abnormal modulation of fundamental physiological processes such as neuronal development, synaptic transmission and plasticity, potentially leading to cell death (see discussion in Chapter 6, Section 6.3) (Hesselgesser and Horuk, 1999; Bezzi et al., 2001; John et al., 2003; Liberto et al., 2004; Ramírez et al., 2005; Röhl and Sievers, 2005; Röhl et al., 2008; Ransohoff, 2009; Sofroniew and Vinters, 2010; Lee and Haydon, 2011; Liu et al., 2011; Singh et al., 2011; Luo and Chen, 2012; Tian et al., 2012). Cellular communication between astrocytes and other glia cell-types as well as between astrocytes and neurons may also be affected by the failure of *Cln3*$^{-/-}$ astrocytes to form a propagating calcium wave, leading to insufficient activation of neighboring astrocytes as well as microglia (Verderio and Matteoli, 2001; Schipke et al., 2002; Davalos et al., 2005; Scemes and Giaume, 2006; Liu et al., 2011), further worsening their already attenuated secretion of cytokines (Hide et al., 2000; Bianco et al., 2005; Nedergaard and Dirnagl, 2005) and any associated protective functions (see discussion in Chapter 4, Section 4.3). Abnormal Ca^{2+} signaling may also alter the synchronization of any efforts within the astrocyte syncytium to maintain a favorable neuronal homeostasis, via K^+ buffering and scavenging of excitatory glutamate (Fiacco and McCarthy, 2006; Scemes and Giaume, 2006; Agulhon et al., 2012; Parpura et al.,

2012) (see Discussion 4.3). In summary, interrupted glia-neuronal interactions have the capability not only to underlie some of the disease symptoms, but also to contribute to disease progression in JNCL.

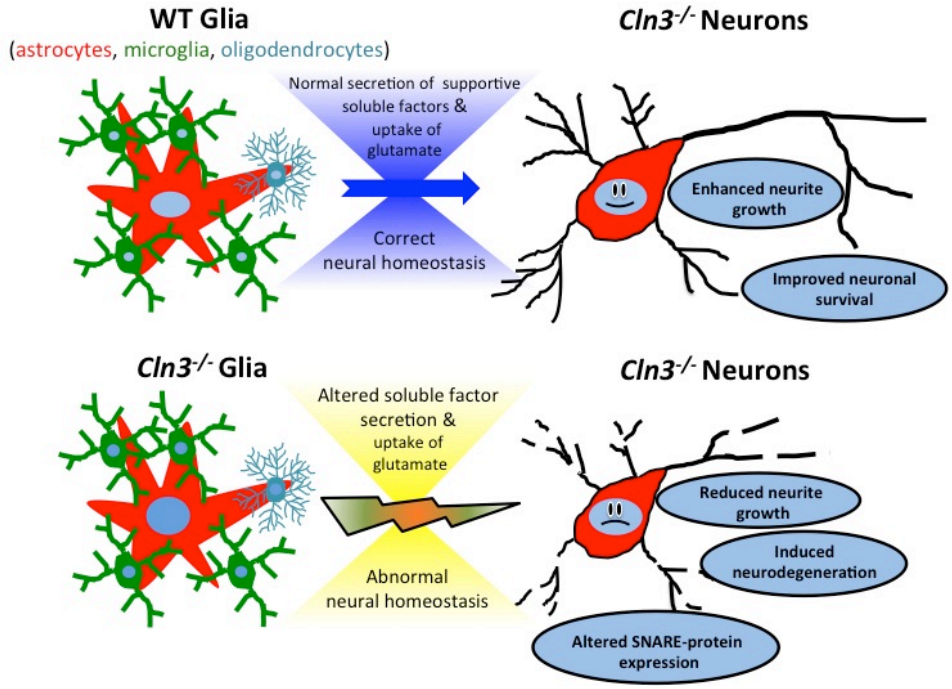

Figure 7.2. *Cln3*$^{-/-}$ glia negatively impact neurons. Co-culture experiments were carried out to determine the direct impact of *Cln3*$^{-/-}$ glia upon neurons. In comparison to WT glia, which had a positive impact on *Cln3*$^{-/-}$ neurons, *Cln3*$^{-/-}$ glia had a pronounced negative impact. Impaired protein secretion, as well as attenuated glutamate clearance by *Cln3*$^{-/-}$ glial may alter neuronal homeostasis and cause the observed effects.

Taken together our data provide the first evidence that astrocyte biology is compromised in JNCL, and reveals a direct link between glia and neurodegeneration in this disease. In addition, isolated *Cln3*$^{-/-}$ neurons also displayed biological defects (see Figure 7.1 B) that may alter their excitability and connectivity, making them more vulnerable to further stress, and may explain why these cells are more susceptible to *Cln3*$^{-/-}$ glia.

This research suggests that targeting glia could be a beneficial therapeutic approach for JNCL. Moreover, these results may offer clues to the role that glia may play in the pathogenesis of other forms of NCL. However, it is worth bearing in mind that this study provides information on cultured *Cln3*$^{-/-}$ astrocytes, and these may differ fundamentally from astrocytes *in vivo* (Barres, 2008; Cahoy et

al., 2008; Allen and Barres, 2009; Zhang and Barres, 2010). The functional properties of astrocytes *in vivo* are still not well understood, mainly because studying them is difficult since they are non-excitable cells that interact with multiple cell types in the CNS, including neurons, vascular cells, oligodendrocytes and microglia and they express a very similar range of receptors to neurons (Volterra and Meldolesi, 2005; Verkhratsky and Butt, 2007; Allen and Barres, 2009; Verkhratsky and Parpura, 2010). Additionally, human astrocytes are considered to be significantly more complex than rodent astrocytes (Oberheim et al., 2006; 2009; 2012). Studying human astrocytes derived from differentiated iPSCs from JNCL patients, together with *in situ* investigations of rodent astrocytes using organotypic slice cultures, would enable our results to be verified both in human cells and *in situ*.

Are glia really the bad guys in JNCL?

Because JNCL is a predominantly neurological disorder most attention has been focused upon the profound loss of neurons that occurs in this disease. However, an increasing number of studies have shown that glial activation can play a fundamental role in CNS disease progression and influence neurodegeneration (Liberto et al., 2004; Raivich, 2005; Garden and Möller, 2006; Sofroniew and Vinters, 2010; Tremblay et al., 2010; Verkhratsky and Parpura, 2010; Garwood et al., 2011; Macauley et al., 2011; Schafer et al., 2013). Indeed, there is evidence in several LSDs, including the NCLs, indicating that glia contribute to the pathogenesis of these diseases (German et al., 2002; Chen et al., 2007; Macauley et al., 2011; Di Malta et al., 2012a; 2012b). For instance, Niemann-Pick type C1 (Npc-1) deficient astrocytes have been shown to reduce neurite growth in WT neurons *in vitro* due to reduced estradiol secretion (Chen et al., 2007), and correction of the gene defect specifically in astrocytes of *Npc1*$^{-/-}$ mice enhanced their survival (Zhang et al., 2008). In parallel with this, decreased neuronal storage of cholesterol, neurodegeneration and astrocytosis, was observed, as well as improved myelination (Zhang et al., 2008). Furthermore, astrocyte-specific deletion of the Sumf1 gene (deficient in multiple sulfatase deficiency

(MSD), a severe lysosomal storage disorder) was sufficient to induce cell death in cortical neurons both *in vivo* and *in vitro* (Di Malta et al., 2012a). This toxic impact of astrocytes in MSD was attributed to dysfunctional lysosomes/autophagy (Di Malta et al., 2012b). These data indicate that a single gene mutation solely in glia is sufficient to cause serious problems for neurons. Thus, it is likely that, at least in some LSDs, non-cell autonomous mechanisms for neurodegeneration occur and these effects may be mediated by astrocytes alone or in combination with other glia. Conversely, impairing astrocytosis in *Ppt1*$^{-/-}$ mice resulted in an acceleration of disease progression (Macauley et al., 2011). Thus, in INCL astrocytes appear to protect neurons against pathogenic challenges. It is therefore evident that the role of astrocytes varies depending on the pathological situation and gene defect in question. Nevertheless, astrocytes appear to be integral components, not only in JNCL pathogenesis, but also in a range of other LSDs and this suggests that modulation of astrocyte activities may offer a valuable way to impact disease progression.

Experiments are at present underway to study the direct impact of glia upon disease progression in JNCL, by creating mice in which only astrocytes, only microglia, or both cell types carry the most common human mutation for this disease. Such studies will also provide evidence on the importance of each glial cell type to disease progression and this in turn may help inform future therapeutic strategies for JNCL.

Could glia based therapies be useful in JNCL?

Currently, there are no treatments available for JNCL, mainly due to the fact that CLN3 is a transmembrane protein whose normal function is unknown. Being a transmembrane protein, many therapies that have the potential to be successful in other forms of NCLs, such as enzyme replacement, gene transfer or even stem cell therapy (Griffey et al., 2006; Wong et al., 2010; Mole et al., 2011; Roberts et al., 2012), are not feasible options in JNCL (Cooper, 2008). These therapies are based on the principle of cross correction, where a soluble, diffusible protein can

be taken up by neighbouring cells to correct of their enzyme deficiency (Sands and Davidson, 2006; Wong et al., 2010). This approach is not feasible in the forms of NCL, like JNCL, that are caused by mutations in transmembrane proteins. However, with advances in gene transfer methodologies, it may be possible in the future to introduce a functional copy of the defective gene into a sufficient number of cells to have a therapeutic impact.

In infantile NCL storage material clearance with drugs such as cystagon may theoretically have beneficial impact (Mole et al., 2011), but this is yet to be realized in either *Ppt1*$^{-/-}$ mice or human patients. As yet there is no direct evidence that storage material is the primary pathogenic player that leads to neuron loss in the NCLs, and this includes JNCL. In cultured cells no accumulation of storage material was observed, suggesting that neither the phenotypes of *Cln3*$^{-/-}$ astrocytes or neurons described in this thesis, nor the negative effect of *Cln3*$^{-/-}$ glia upon neurons were caused by this. This study does however provide several possibilities for novel therapies for JNCL based on correcting the functional deficits observed in *Cln3*$^{-/-}$ astrocytes (see Figure 7.3).

Protein secretion: One of the most prominent features of *Cln3*$^{-/-}$ astrocytes was impaired protein secretion (chemokines, anti- and pro-inflammatoric cytokines, trophic factors, see Chapter 4, Discussion 4.3). As stated above, this could severely alter both glial/glial and glial/neuronal interactions within the JNCL brain (Saad et al., 1991; Eddleston and Mucke, 1993; Hewett et al., 1993; Ridet et al., 1997; Krieglstein et al., 1998; Hewett, 1999; John et al., 2003; Liberto et al., 2004; Miklic et al., 2004; Villoslada and Genain, 2004; Hamby et al., 2008; Mena and García de Yébenes, 2008; Hamby and Sofroniew, 2010; Singh et al., 2011), and may be a key element in the observed glial response and initiation of neurodegeneration in these mice. For example, activated *Cln3*$^{-/-}$ astrocytes failed to secrete anti-inflammatory cytokines, such as IL-4, IL-10 and IL-2, as well as neuroprotective factors, such as VEGF and FGF. Indeed, both genetic and pharmaceutical approaches to attenuate the adaptive immune response have been shown to resulted in a significant improvement in the pathology of *Cln3*$^{-/-}$

mice (Seehafer et al., 2011), and experiments are now underway to determine if targeting the innate immune response will offer further therapeutic benefit (JD Cooper & BP Williams, personal communication). There is a precedent for this approach, since non-steroidal anti-inflammatory drugs (NSAIDs) together with substrate reduction therapy (SRT) prolonged the lifespan and delayed the onset of clinical signs in NPC1 mice (Smith et al., 2009). Based on these findings we are now treating JNCL mice with a combination of anti-inflammatory drugs, neuroprotective drugs and immunosuppressants to determine if this will enhance the benefit seen when treating these mice with immunosuppressants alone (Seehafer et al., 2011). Another possibility might be to transplant genetically modified stem cells that would produce and secrete specific set of molecules, such as neuroprotective factors. This approach has been trialed in other neurodegenerative diseases, like ALS, where successful protection of dying motor neurons was achieved (Suzuki et al., 2007; Behrstock et al., 2008).

Glutamate clearance: Glutamate clearance by astrocytes has been shown to be impaired in various neurodegenerative conditions, such as spinocerebellar ataxia type 7 (SCA7), Huntington disease and ALS, and here we show that this is also the case with *Cln3*$^{-/-}$ astrocytes (Rothstein et al., 1992; 1996; Wang et al., 2003; Shin et al., 2005; Custer et al., 2006). Additionally, EAAT2 (glutamate receptor) expression has been shown to be reduced in JNCL patient tissue samples (Hachiya et al., 2006), and elevated glutamate levels have been detected at presynaptic sites in *Cln3*$^{-/-}$ mice (Chattopadhyay et al., 2004). Thus, manipulating glutamate clearance by astrocytes could be one way to help prevent neuronal overstimulation, as our data suggest to be the case by the presence of a distally located AIS in isolated cortical excitatory neurons. For instance, glutamate clearance by *Cln3*$^{-/-}$ astrocytes could theoretically be augmented using a drug called parawexin 1 that has been previously shown to use this mechanism to protect neurons against glutamate mediated excitotoxicity (Fontana et al., 2003; 2007). Additionally, certain ß-lactam antibiotics have been shown to potentiate astrocyte-mediated glutamate clearance through increased transcription of the Glt1 (glial glutamate transporter 1) gene (Rothstein et al., 2005). The ß-lactam

antibiotic, ceftriaxone, was shown to be neuroprotective in mouse models of ischaemic injury (Lipski, 2007), motor neuron disease (Rothstein et al., 2005) and Parkinson's disease (Rothstein et al., 2005; Leung et al., 2012). It would therefore be interesting and feasible to test the neuroprotective potential of this commercially available antibiotic in JNCL mouse models.

Another approach to combat the excess glutamate-induced excitotoxicity and particular vulnerability of neurons to AMPA and NMDA-receptor stimulation in *Cln3*$^{-/-}$ mice (Kovács et al., 2006; Kovács and Pearce, 2008; Finn et al., 2011; Kovács et al., 2011) could be to use glutamate receptor blockers. Indeed, previous studies have shown that acute attenuation of AMPA-receptor activity by the non-competitive AMPA antagonist, EGIS-8332, improved motor coordination and lifespan of these mice (Kovács and Pearce, 2008; Kovács et al., 2011). Moreover, memantine application, which results in the inhibition of NMDA-glutamate receptors, induced an improvement of motor skills (Kovács et al., 2012), although, this treatment did not impact overall microglial or astrocytes activation, or the survival of sensitive neuron populations. Treatment with EGIS-8332, however, did decrease astrocytosis in the somatosensory cortex of *Cln3*$^{-/-}$ mice (Kovács et al., 2012), which is consistent with another recent study revealing that chronic inhibition of AMPA receptors with a non-competitive blocker called talampanel prevents astrocyte activation (Greene et al., 2008). Thus, inhibition of glutamate-receptor over-activation may also lead to the attenuation of reactive astrocytosis, emphasizing the importance of balanced communication between neurons and glia, and therefore treating both of these events in *Cln3*$^{-/-}$ mice might be particularly beneficial.

Oxidative stress: Astrocytes are the major source of GSH in the CNS, an anti-oxidant that plays a crucial role in protecting neurons against oxidative stress (Dringen, 2000; Chen et al., 2001; Swanson et al., 2004; Duncan and Heales, 2005; Gegg et al., 2005; Benedict et al., 2007). *Cln3*$^{-/-}$ astrocytes can still make, but fail to secrete, glutathione, and therefore this protection may be lost. Modulating GSH secretion, or providing the essential rate limiting GSH substrates

for neuronal GSH production (such as cysteine), may help guard against oxidative stress (Shih et al., 2003; Darlington, 2005; Vargas et al., 2008; Chen et al., 2009; Fuller et al., 2009). Indeed, enhancing glutathione-based detoxification of oxidative factors has been shown to be neuroprotective in various models, such as Parkinson disease and ALS (Shih et al., 2003; Vargas et al., 2008; Chen et al., 2009), and this approach could feasibly also be trialed in JNCL (Schmidt and Dringen, 2010). For instance, fumaric acid esters (FAE) have been recognized as a promising therapy form for autoimmune-based neurological disorders, such as multiple sclerosis (Moharregh-Khiabani et al., 2009; Gold et al., 2012; Schmidt and Dringen 2010), based on their ability to deplete astrocyte GSH content (Mrowietz and Asadullah, 2005).

Calcium signaling: Spontaneous Ca^{2+} oscillations were attenuated in *Cln3*$^{-/-}$ astrocytes, and these cells failed to generate a synchronized calcium wave. Abnormal ER Ca^{2+} release followed by attenuated cytosolic Ca^{2+} clearance was also evident. Abnormal Ca^{2+} signaling has previously been reported in other LSD models (Pelled et al., 2003a; Ginzburg and Futerman, 2005; Pelled et al., 2005; Lloyd-Evans et al., 2008; Lloyd-Evans and Platt, 2011). For instance, abnormal Ca^{2+} storage in these acidic compartments is an important initiating factor in NPC1 disease pathogenesis (Lloyd-Evans et al., 2008). Cytosolic Ca^{2+} normalization with curcumin, which is an inhibitor of the histone acetyltransferase (HAT) p300 as well as a SERCA pump antagonist (Bilmen et al., 2001; Marcu et al., 2006), abolished typical NPC1 disease phenotypes in NCP1-mutant glia cells and slowed disease progression in NPC1 mice (Lloyd-Evans et al., 2008). Furthermore, curcumin is a promising therapeutic option in a number of neurological diseases based on its anti-inflammatory and antioxidant properties (Natarajan and Bright, 2002; Marcu et al., 2006; Laird et al., 2010; Lin et al., 2011). Curcumin has also been shown to increase epileptic seizure thresholds, via modulation of free radicals and NOS (DU et al., 2012), an approach which might also be beneficial in JNCL since these patients suffer from spontaneous epileptic seizures (Mole et al., 2011). Thus, it would be interesting to examine the impact of curcumin on Ca^{2+}-signaling in *Cln3*$^{-/-}$ astrocytes, and

whether activities dependent on correct Ca^{2+}-signaling, such as gliotransmission, are influenced by this treatment. In addition, the efficacy of curcumin to improve the anti-inflammatory response and to reduce seizure probability could also be tested in JNCL mouse models.

Cytoskeletal disruption: Both the actin and the intermediate filament cytoskeleton were found to be disrupted in *Cln3*$^{-/-}$ astrocytes. Ultimately many of the deficits we have discovered, including attenuated migration, division, secretion, glutamate clearance and Ca^{2+} wave propagation in these cells could plausibly be caused by this lack of proper cytoskeletal organization. The Rho subfamily of small GTPases (Rho and Rac) have been recognized as pivotal regulators of cytoskeletal organization (Van Aelst and D'Souza-Schorey, 1997; Hall, 1998; Kaibuchi et al., 1999; Ridley, 2001a; 2001b; Etienne-Manneville and Hall, 2002; Schmidt and Hall, 2002; Heasman and Ridley, 2008). Several studies have shown that growth factors, such as FGF and EGF, may stimulate Rho and Rac GTPase activities and induce cytoskeletal reorganization (Hou et al., 1995; Kalman et al., 1999; Maddala et al., 2003). Alternatively, the activation of Rho GTPases could be enhanced by guanine nucleotide exchange factors (GEFs), such as Tiam1, Net1 and Vav (Schmidt and Hall, 2002; Erickson and Cerione, 2004; Rossman et al., 2005; Buchsbaum, 2007). Thus, both growth factors and GEFs may offer a solution to help correct the disrupted cytoskeleton and dependent activities in *Cln3*$^{-/-}$ astrocytes, although the likely potential of many non-specific and negative impacts of growth factor administration would have to be carefully considered.

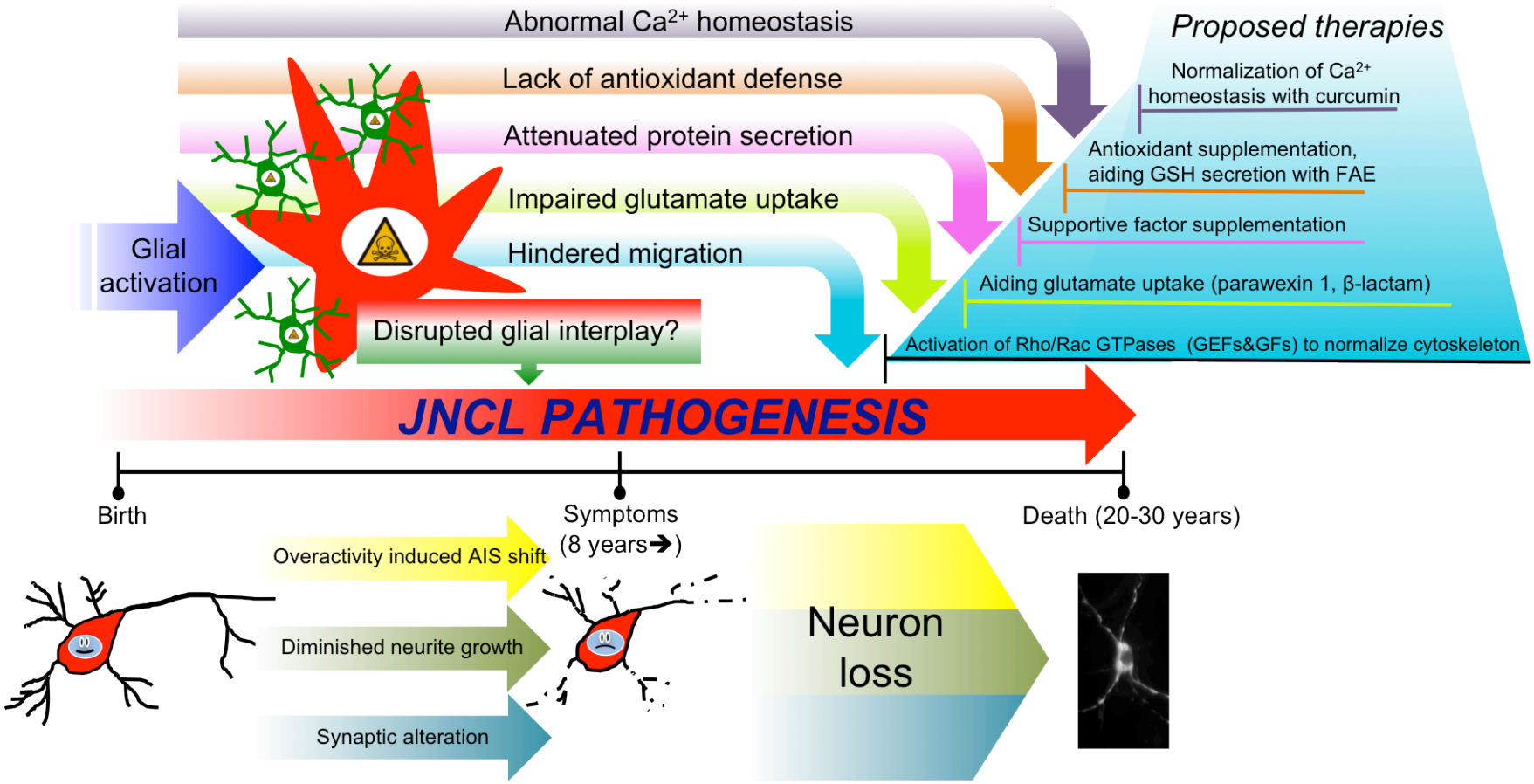

Figure 7.3. Roles of glia and neurons in the pathogenesis of JNCL and proposed glia based therapies. This figure summarises the deficits we have discovered in astrocytes and neurons, which may play a role in the pathogenesis of JNCL. Additionally, potential glial-based therapies are listed. Many of the astrocyte deficits caused by CLN3 deficiency may be caused by disrupted cytoskeleton. Thus, normalization of the cytoskeleton may also lead to improvements in the other observed functional impairments.

In summary, our analysis of astrocytes and neurons revealed that CLN3 deficiency caused newly identified alterations in the biology of both of these cell types. Importantly, glia were shown to directly impact the health of both WT and *Cln3*$^{-/-}$ neurons, with the latter being more sensitive possibly because of their intrinsic biological defects. Thus, it appears that glia could be key players in the pathogenesis of JNCL. In light of the recent findings demonstrating that other LSDs can be treated with therapeutic interventions that specifically target glia, it will be important to explore whether such approaches could also be beneficial in JNCL. Maybe it will prove most beneficial to use a combination of therapies to target glia, such as antioxidants, inhibitors of excitotoxicity, immunosuppressive drugs and supplementation of trophic factors, with treatment being initiated as early as possible to halt the progression of early pathological changes. Furthermore, since *CLN3* is expressed across the whole body, not only in the CNS (The International Batten Disease Consortium 1995; Pane et al., 1999; Chattopadhyay and Pearce, 2000; Mole et al., 2011), and has been proposed to serve 'housekeeping' functions in the cell (Mole et al., 2011), combination therapy approaches designed to treat the whole body together with the CNS may be necessary. The benefit of such an approach was demonstrated recently for INCL, in which CNS-directed AAV2/5-mediated gene therapy was combined with bone marrow transplant (BMT) in newborn *Ppt1*$^{-/-}$ mice (Macauley et al., 2012). This resulted in a two-fold increase in the lifespan of the mice, and prolonged improvements in motor function (Macauley et al., 2012).

From the work described here on JNCL, and published work on other LSDs, it is evident that glia play a pivotal role in these diseases. Based on these data we are beginning to use similar approaches to study glial biology in other forms of NCL and to determine whether such changes are beneficial or detrimental to neuronal health. Certainly, preliminary data from *Ppt1*$^{-/-}$ astrocytes suggests that these cells also have an altered protein secretion profile upon stimulation *in vitro*, in this case with enhanced secretion of many proteins, including neuroprotective factors. This correlates well with the *in vivo* findings indicating

that reactive astrocytosis protects neurons against cell death in *Ppt1*$^{-/-}$ mice (Macauley et al., 2011).

In conclusion, the research presented in this thesis not only expands our understanding of JNCL pathogenesis, highlighting the importance of astrocytes, but crucially these data also emphasize a whole range of potential targets for therapeutic intervention.

References

Abbott NJ, Rönnbäck L, Hansson E (2006) Astrocyte-endothelial interactions at the blood-brain barrier. Nat Rev Neurosci 7:41–53.

Aberg L, Lauronen L, Hämäläinen J, Mole SE, Autti T (2009) A 30-year follow-up of a neuronal ceroid lipofuscinosis patient with mutations in CLN3 and protracted disease course. Pediatr Neurol 40:134–137.

Aberg L, Liewendahl K, Nikkinen P, Autti T, Rinne JO, Santavuori P (2000) Decreased striatal dopamine transporter density in JNCL patients with parkinsonian symptoms. Neurology 54:1069–1074.

Abramov AY, Canevari L, Duchen MR (2003) Changes in intracellular calcium and glutathione in astrocytes as the primary mechanism of amyloid neurotoxicity. J Neurosci 23:5088–5095.

Adams H, de Blieck EA, Mink JW, Marshall FJ, Kwon J, Dure L, Rothberg PG, Ramirez-Montealegre D, Pearce DA (2006) Standardized assessment of behavior and adaptive living skills in juvenile neuronal ceroid lipofuscinosis. Dev Med Child Neurol 48:259–264.

Adams RH, Sato K, Shimada S, Tohyama M, Püschel AW, Betz H (1995) Gene structure and glial expression of the glycine transporter GlyT1 in embryonic and adult rodents. J Neurosci 15:2524–2532.

Aguado F, Espinosa-Parrilla JF, Carmona MA, Soriano E (2002) Neuronal activity regulates correlated network properties of spontaneous calcium transients in astrocytes in situ. J Neurosci 22:9430–9444.

Agulhon C, Sun M-Y, Murphy T, Myers T, Lauderdale K, Fiacco TA (2012) Calcium Signaling and Gliotransmission in Normal vs. Reactive Astrocytes. Front Pharmacol 3:139.

Ahtiainen L, van Diggelen OP, Jalanko A, Kopra O (2003) Palmitoyl protein thioesterase 1 is targeted to the axons in neurons. J Comp Neurol 455:368–377.

Akassoglou K, Probert L, Kontogeorgos G, Kollias G (1997) Astrocyte-specific but not neuron-specific transmembrane TNF triggers inflammation and degeneration in the central nervous system of transgenic mice. J Immunol 158:438–445.

Akhmanova A, Hammer JA (2010) Linking molecular motors to membrane cargo. Curr Opin Cell Biol 22:479–487.

Akira S, Takeda K (2004) Toll-like receptor signalling. Nat Rev Immunol 4:499–511.

Al-Bassam S, Xu M, Wandless TJ, Arnold DB (2012) Differential trafficking of transport vesicles contributes to the localization of dendritic proteins. Cell Rep 2:89–100.

Albrecht PJ, Dahl JP, Stoltzfus OK, Levenson R, Levison SW (2002) Ciliary neurotrophic factor activates spinal cord astrocytes, stimulating their production and release of fibroblast growth factor-2, to increase motor neuron survival. Exp Neurol 173:46–62.

Alexander JJ, Anderson AJ, Barnum SR, Stevens B, Tenner AJ (2008) The complement cascade: Yin-Yang in neuroinflammation--neuro-protection and -degeneration. J Neurochem 107:1169–1187.

Ali C, Nicole O, Docagne F, Lesne S, MacKenzie ET, Nouvelot A, Buisson A, Vivien D (2000) Ischemia-induced interleukin-6 as a potential endogenous neuroprotective cytokine against NMDA receptor-mediated excitotoxicity in the brain. J Cereb Blood Flow Metab 20:956–966.

Allaman I, Bélanger M, Magistretti PJ (2011) Astrocyte-neuron metabolic relationships: for better and for worse. Trends Neurosci 34:76–87.

Allan SM, Rothwell NJ (2001) Cytokines and acute neurodegeneration. Nat Rev Neurosci 2:734–744.

Allan SM, Rothwell NJ (2003) Inflammation in central nervous system injury. Philos Trans R Soc Lond, B, Biol Sci 358:1669–1677.

Allen NJ, Barres BA (2009) Neuroscience: Glia - more than just brain glue. Nature 457:675–677.

Aloisi F (2001) Immune function of microglia. Glia 36:165–179.

Alzheimer C, Werner S (2002) Fibroblast growth factors and neuroprotection. Adv Exp Med Biol 513:335–351.

Amos LA, Schlieper D (2005) Microtubules and maps. Adv Protein Chem 71:257–298.

An WF, Bowlby MR, Betty M, Cao J, Ling HP, Mendoza G, Hinson JW, Mattsson KI, Strassle BW, Trimmer JS, Rhodes KJ (2000) Modulation of A-type potassium channels by a family of

calcium sensors. Nature 403:553–556.
Ananthakrishnan R, Ehrlicher A (2007) The forces behind cell movement. Int J Biol Sci 3:303–317.
Anderson CM, Swanson RA (2000) Astrocyte glutamate transport: review of properties, regulation, and physiological functions. Glia 32:1–14.
Anderson GW, Goebel HH, Simonati A (2012) Human pathology in NCL. Biochim Biophys Acta.
Ang LC, Bhaumick B, Munoz DG, Sass J, Juurlink BH (1992) Effects of astrocytes, insulin and insulin-like growth factor I on the survival of motoneurons in vitro. J Neurol Sci 109:168–172.
Anon (1995) Isolation of a novel gene underlying Batten disease, CLN3. The International Batten Disease Consortium. Cell 82:949–957.
Aoyama K, Suh SW, Hamby AM, Liu J, Chan WY, Chen Y, Swanson RA (2006) Neuronal glutathione deficiency and age-dependent neurodegeneration in the EAAC1 deficient mouse. Nat Neurosci 9:119–126.
Aoyama K, Watabe M, Nakaki T (2008) Regulation of neuronal glutathione synthesis. J Pharmacol Sci 108:227–238.
Apodaca G (2001) Endocytic traffic in polarized epithelial cells: role of the actin and microtubule cytoskeleton. Traffic 2:149–159.
Araque A, Carmignoto G, Haydon PG (2001) Dynamic signaling between astrocytes and neurons. Annu Rev Physiol 63:795–813.
Araque A, Navarrete M (2010) Glial cells in neuronal network function. Philos Trans R Soc Lond, B, Biol Sci 365:2375–2381.
Araque A, Sanzgiri RP, Parpura V, Haydon PG (1998) Calcium elevation in astrocytes causes an NMDA receptor-dependent increase in the frequency of miniature synaptic currents in cultured hippocampal neurons. J Neurosci 18:6822–6829.
Araque A, Sanzgiri RP, Parpura V, Haydon PG (1999) Astrocyte-induced modulation of synaptic transmission. Can J Physiol Pharmacol 77:699–706.
Araújo SJ, Tear G (2003) Axon guidance mechanisms and molecules: lessons from invertebrates. Nat Rev Neurosci 4:910–922.
Arcuino G, Lin JH-C, Takano T, Liu C, Jiang L, Gao Q, Kang J, Nedergaard M (2002) Intercellular calcium signaling mediated by point-source burst release of ATP. Proc Natl Acad Sci USA 99:9840–9845.
Ascaño M, Richmond A, Borden P, Kuruvilla R (2009) Axonal targeting of Trk receptors via transcytosis regulates sensitivity to neurotrophin responses. J Neurosci 29:11674–11685.
Atherton JF, Wokosin DL, Ramanathan S, Bevan MD (2008) Autonomous initiation and propagation of action potentials in neurons of the subthalamic nucleus. J Physiol (Lond) 586:5679–5700.
Augestad LB, Flanders WD (2006) Occurrence of and mortality from childhood neuronal ceroid lipofuscinoses in norway. J Child Neurol 21:917–922.
Austin KM, Gupta ML, Coats SA, Tulpule A, Mostoslavsky G, Balazs AB, Mulligan RC, Daley G, Pellman D, Shimamura A (2008) Mitotic spindle destabilization and genomic instability in Shwachman-Diamond syndrome. J Clin Invest 118:1511–1518.
Autti T, Raininko R, Santavuori P, Vanhanen SL, Poutanen VP, Haltia M (1997) MRI of neuronal ceroid lipofuscinosis. II. Postmortem MRI and histopathological study of the brain in 16 cases of neuronal ceroid lipofuscinosis of juvenile or late infantile type. Neuroradiology 39:371–377.
Autti T, Raininko R, Vanhanen SL, Santavuori P (1996) MRI of neuronal ceroid lipofuscinosis. I. Cranial MRI of 30 patients with juvenile neuronal ceroid lipofuscinosis. Neuroradiology 38:476–482.
Avoli M, D'Antuono M, Louvel J, Köhling R, Biagini G, Pumain R, D'Arcangelo G, Tancredi V (2002) Network and pharmacological mechanisms leading to epileptiform synchronization in the limbic system in vitro. Prog Neurobiol 68:167–207.
Ayala R, Shu T, Tsai L-H (2007) Trekking across the brain: the journey of neuronal migration. Cell 128:29–43.
Bacich DJ, Ramadan E, O'Keefe DS, Bukhari N, Wegorzewska I, Ojeifo O, Olszewski R, Wrenn CC, Bzdega T, Wroblewska B, Heston WDW, Neale JH (2002) Deletion of the glutamate carboxypeptidase II gene in mice reveals a second enzyme activity that hydrolyzes N-acetylaspartylglutamate. J Neurochem 83:20–29.

Back T, Ginsberg MD, Dietrich WD, Watson BD (1996) Induction of spreading depression in the ischemic hemisphere following experimental middle cerebral artery occlusion: effect on infarct morphology. J Cereb Blood Flow Metab 16:202–213.
Baeuerle PA, Henkel T (1994) Function and activation of NF-kappa B in the immune system. Annu Rev Immunol 12:141–179.
Baldwin SA, Beal PR, Yao SYM, King AE, Cass CE, Young JD (2004) The equilibrative nucleoside transporter family, SLC29. Pflugers Arch 447:735–743.
Ball HL, Zhang B, Riches JJ, Gandhi R, Li J, Rommens JM, Myers JS (2009) Shwachman-Bodian Diamond syndrome is a multi-functional protein implicated in cellular stress responses. Hum Mol Genet 18:3684–3695.
Ballabio A, Gieselmann V (2009) Lysosomal disorders: from storage to cellular damage. Biochim Biophys Acta 1793:684–696.
Bampton ETW, Goemans CG, Niranjan D, Mizushima N, Tolkovsky AM (2005) The dynamics of autophagy visualized in live cells: from autophagosome formation to fusion with endo/lysosomes. Autophagy 1:23–36.
Bananis E, Nath S, Gordon K, Satir P, Stockert RJ, Murray JW, Wolkoff AW (2004) Microtubule-dependent movement of late endocytic vesicles in vitro: requirements for Dynein and Kinesin. Mol Biol Cell 15:3688–3697.
Banks WA (1999) Physiology and pathology of the blood-brain barrier: implications for microbial pathogenesis, drug delivery and neurodegenerative disorders. J Neurovirol 5:538–555.
Barde YA (1994) Neurotrophins: a family of proteins supporting the survival of neurons. Prog Clin Biol Res 390:45–56.
Barnett MW, Larkman PM (2007) The action potential. Pract Neurol 7:192–197.
Barr CL, Feng Y, Wigg K, Bloom S, Roberts W, Malone M, Schachar R, Tannock R, Kennedy JL (2000) Identification of DNA variants in the SNAP-25 gene and linkage study of these polymorphisms and attention-deficit hyperactivity disorder. Mol Psychiatry 5:405–409.
Barres BA (2008) The mystery and magic of glia: a perspective on their roles in health and disease. Neuron 60:430–440.
Basarsky TA, Duffy SN, Andrew RD, MacVicar BA (1998) Imaging spreading depression and associated intracellular calcium waves in brain slices. J Neurosci 18:7189–7199.
Batter DK, Corpina RA, Roy C, Spray DC, Hertzberg EL, Kessler JA (1992) Heterogeneity in gap junction expression in astrocytes cultured from different brain regions. Glia 6:213–221.
Bäckman ML, Santavuori PR, Aberg LE, Aronen ET (2005) Psychiatric symptoms of children and adolescents with juvenile neuronal ceroid lipofuscinosis. J Intellect Disabil Res 49:25–32.
Beal MF (1992) Does impairment of energy metabolism result in excitotoxic neuronal death in neurodegenerative illnesses? Ann Neurol 31:119–130.
Beal MF (1995) Aging, energy, and oxidative stress in neurodegenerative diseases. Ann Neurol 38:357–366.
Beattie EC, Carroll RC, Yu X, Morishita W, Yasuda H, Zastrow von M, Malenka RC (2000) Regulation of AMPA receptor endocytosis by a signaling mechanism shared with LTD. Nat Neurosci 3:1291–1300.
Beattie EC, Stellwagen D, Morishita W, Bresnahan JC, Ha BK, Zastrow Von M, Beattie MS, Malenka RC (2002) Control of synaptic strength by glial TNFalpha. Science 295:2282–2285.
Becher A, Drenckhahn A, Pahner I, Margittai M, Jahn R, Ahnert-Hilger G (1999) The synaptophysin-synaptobrevin complex: a hallmark of synaptic vesicle maturation. J Neurosci 19:1922–1931.
Beck A, Nieden RZ, Schneider H-P, Deitmer JW (2004) Calcium release from intracellular stores in rodent astrocytes and neurons in situ. Cell Calcium 35:47–58.
Beck KA, Nelson WJ (1996) The spectrin-based membrane skeleton as a membrane protein-sorting machine. Am J Physiol 270:C1263–C1270.
Beffert U, Dillon GM, Sullivan JM, Stuart CE, Gilbert JP, Kambouris JA, Ho A (2012) Microtubule Plus-End Tracking Protein CLASP2 Regulates Neuronal Polarity and Synaptic Function. J Neurosci 32:13906–13916.
Behrstock S, Ebert AD, Klein S, Schmitt M, Moore JM, Svendsen CN (2008) Lesion-induced increase in survival and migration of human neural progenitor cells releasing GDNF. Cell Transplant 17:753–762.
Bellettato CM, Scarpa M (2010) Pathophysiology of neuropathic lysosomal storage disorders. J

Inherit Metab Dis 33:347–362.
Belmonte MK, Allen G, Beckel-Mitchener A, Boulanger LM, Carper RA, Webb SJ (2004) Autism and abnormal development of brain connectivity. J Neurosci 24:9228–9231.
Bender KJ, Trussell LO (2009) Axon initial segment Ca2+ channels influence action potential generation and timing. Neuron 61:259–271.
Benedict JW, Getty AL, Wishart TM, Gillingwater TH, Pearce DA (2009) Protein product of CLN6 gene responsible for variant late-onset infantile neuronal ceroid lipofuscinosis interacts with CRMP-2. J Neurosci Res 87:2157–2166.
Benedict JW, Sommers CA, Pearce DA (2007) Progressive oxidative damage in the central nervous system of a murine model for juvenile Batten disease. J Neurosci Res 85:2882–2891.
Bennett V, Baines AJ (2001) Spectrin and ankyrin-based pathways: metazoan inventions for integrating cells into tissues. Physiol Rev 81:1353–1392.
Benowitz LI, Routtenberg A (1997) GAP-43: an intrinsic determinant of neuronal development and plasticity. Trends Neurosci 20:84–91.
Benveniste EN (1998) Cytokine actions in the central nervous system. Cytokine Growth Factor Rev 9:259–275.
Berezovskaya O, Maysinger D, Fedoroff S (1996) Colony stimulating factor-1 potentiates neuronal survival in cerebral cortex ischemic lesion. Acta Neuropathol 92:479–486.
Berggård T, Linse S, James P (2007) Methods for the detection and analysis of protein-protein interactions. Proteomics 7:2833–2842.
Bergles DE, Jahr CE (1998) Glial contribution to glutamate uptake at Schaffer collateral-commissural synapses in the hippocampus. J Neurosci 18:7709–7716.
Berridge MJ, Lipp P, Bootman MD (2000) The versatility and universality of calcium signalling. Nat Rev Mol Cell Biol 1:11–21.
Bertorello AM, Komarova Y, Smith K, Leibiger IB, Efendiev R, Pedemonte CH, Borisy G, Sznajder JI (2003) Analysis of Na+,K+-ATPase motion and incorporation into the plasma membrane in response to G protein-coupled receptor signals in living cells. Mol Biol Cell 14:1149–1157.
Bezprozvanny I (2005) The inositol 1,4,5-trisphosphate receptors. Cell Calcium 38:261–272.
Bezprozvanny I (2009) Calcium signaling and neurodegenerative diseases. Trends Mol Med 15:89–100.
Bezzi P, Carmignoto G, Pasti L, Vesce S, Rossi D, Rizzini BL, Pozzan T, Volterra A (1998) Prostaglandins stimulate calcium-dependent glutamate release in astrocytes. Nature 391:281–285.
Bezzi P, Domercq M, Brambilla L, Galli R, Schols D, De Clercq E, Vescovi A, Bagetta G, Kollias G, Meldolesi J, Volterra A (2001) CXCR4-activated astrocyte glutamate release via TNFalpha: amplification by microglia triggers neurotoxicity. Nat Neurosci 4:702–710.
Bezzi P, Gundersen V, Galbete JL, Seifert G, Steinhäuser C, Pilati E, Volterra A (2004) Astrocytes contain a vesicular compartment that is competent for regulated exocytosis of glutamate. Nat Neurosci 7:613–620.
Bélanger M, Magistretti PJ (2009) The role of astroglia in neuroprotection. Dialogues Clin Neurosci 11:281–295.
Bianco F, Pravettoni E, Colombo A, Schenk U, Möller T, Matteoli M, Verderio C (2005) Astrocyte-derived ATP induces vesicle shedding and IL-1 beta release from microglia. J Immunol 174:7268–7277.
Bibel M, Barde YA (2000) Neurotrophins: key regulators of cell fate and cell shape in the vertebrate nervous system. Genes Dev 14:2919–2937.
Bible E, Gupta P, Hofmann SL, Cooper JD (2004) Regional and cellular neuropathology in the palmitoyl protein thioesterase-1 null mutant mouse model of infantile neuronal ceroid lipofuscinosis. Neurobiol Dis 16:346–359.
Bienenstock EL, Cooper LN, Munro PW (1982) Theory for the development of neuron selectivity: orientation specificity and binocular interaction in visual cortex. J Neurosci 2:32–48.
Billiau A, Heremans H, Vermeire K, Matthys P (1998) Immunomodulatory properties of interferon-gamma. An update. Ann N Y Acad Sci 856:22–32.
Billuart P, Chelly J (2003) From fragile X mental retardation protein to Rac1 GTPase: new insights from Fly CYFIP. Neuron 38:843–845.
Bilmen JG, Khan SZ, Javed MH, Michelangeli F (2001) Inhibition of the SERCA Ca2+ pumps by curcumin. Curcumin putatively stabilizes the interaction between the nucleotide-binding

and phosphorylation domains in the absence of ATP. Eur J Biochem 268:6318–6327.
Bishop AL, Hall A (2000) Rho GTPases and their effector proteins. Biochem J 348 Pt 2:241–255.
Blesch A (2006) Neurotrophic factors in neurodegeneration. Brain Pathol 16:295–303.
Block ML, Zecca L, Hong J-S (2007) Microglia-mediated neurotoxicity: uncovering the molecular mechanisms. Nat Rev Neurosci 8:57–69.
Blomstrand F, Aberg ND, Eriksson PS, Hansson E, Rönnbäck L (1999) Extent of intercellular calcium wave propagation is related to gap junction permeability and level of connexin-43 expression in astrocytes in primary cultures from four brain regions. Neuroscience 92:255–265.
Bodennec J, Pelled D, Riebeling C, Trajkovic S, Futerman AH (2002) Phosphatidylcholine synthesis is elevated in neuronal models of Gaucher disease due to direct activation of CTP:phosphocholine cytidylyltransferase by glucosylceramide. FASEB J 16:1814–1816.
Boehm U, Klamp T, Groot M, Howard JC (1997) Cellular responses to interferon-gamma. Annu Rev Immunol 15:749–795.
Boillée S, Vande Velde C, Cleveland DW (2006) ALS: a disease of motor neurons and their nonneuronal neighbors. Neuron 52:39–59.
Boissière F, Lehéricy S, Strada O, Agid Y, Hirsch EC (1996) Neurotrophin receptors and selective loss of cholinergic neurons in Alzheimer disease. Mol Chem Neuropathol 28:219–223.
Boitano S, Dirksen ER, Sanderson MJ (1992) Intercellular propagation of calcium waves mediated by inositol trisphosphate. Science 258:292–295.
Boitier E, Rea R, Duchen MR (1999) Mitochondria exert a negative feedback on the propagation of intracellular Ca2+ waves in rat cortical astrocytes. J Cell Biol 145:795–808.
Boje KM, Arora PK (1992) Microglial-produced nitric oxide and reactive nitrogen oxides mediate neuronal cell death. Brain Res 587:250–256.
Bolaños JP, Almeida A, Stewart V, Peuchen S, Land JM, Clark JB, Heales SJ (1997) Nitric oxide-mediated mitochondrial damage in the brain: mechanisms and implications for neurodegenerative diseases. J Neurochem 68:2227–2240.
Bolaños JP, Heales SJ, Peuchen S, Barker JE, Land JM, Clark JB (1996) Nitric oxide-mediated mitochondrial damage: a potential neuroprotective role for glutathione. Free Radic Biol Med 21:995–1001.
Bolaños JP, Peuchen S, Heales SJ, Land JM, Clark JB (1994) Nitric oxide-mediated inhibition of the mitochondrial respiratory chain in cultured astrocytes. J Neurochem 63:910–916.
Bonifacino JS (2004) Insights into the biogenesis of lysosome-related organelles from the study of the Hermansky-Pudlak syndrome. Ann N Y Acad Sci 1038:103–114.
Bonifacino JS, Traub LM (2003) Signals for sorting of transmembrane proteins to endosomes and lysosomes. Annu Rev Biochem 72:395–447.
Boocock GRB, Morrison JA, Popovic M, Richards N, Ellis L, Durie PR, Rommens JM (2003) Mutations in SBDS are associated with Shwachman-Diamond syndrome. Nat Genet 33:97–101.
Borán MS, García A (2007) The cyclic GMP-protein kinase G pathway regulates cytoskeleton dynamics and motility in astrocytes. J Neurochem 102:216–230.
Boustany RM, Alroy J, Kolodny EH (1988) Clinical classification of neuronal ceroid-lipofuscinosis subtypes. Am J Med Genet Suppl 5:47–58.
Bovolenta P, Wandosell F, Nieto-Sampedro M (1993) Neurite outgrowth inhibitors associated with glial cells and glial cell lines. Neuroreport 5:345–348.
Bowman CC, Rasley A, Tranguch SL, Marriott I (2003) Cultured astrocytes express toll-like receptors for bacterial products. Glia 43:281–291.
Bowser DN, Khakh BS (2007) Vesicular ATP is the predominant cause of intercellular calcium waves in astrocytes. J Gen Physiol 129:485–491.
Boyes BE, Kim SU, Lee V, Sung SC (1986) Immunohistochemical co-localization of S-100b and the glial fibrillary acidic protein in rat brain. Neuroscience 17:857–865.
Bozorg S, Ramirez-Montealegre D, Chung M, Pearce DA (2009) Juvenile neuronal ceroid lipofuscinosis (JNCL) and the eye. Surv Ophthalmol 54:463–471.
Braak H, Braak E (1993) Pathoarchitectonic pattern of iso- and allocortical lesions in juvenile and adult neuronal ceroid-lipofuscinosis. J Inherit Metab Dis 16:259–262.
Braak H, Goebel HH (1978) Loss of pigment-laden stellate cells: a severe alteration of the isocortex in juvenile neuronal ceroid-lipofuscinosis. Acta Neuropathol 42:53–57.

Braak H, Goebel HH (1979) Pigmentoarchitectonic pathology of the isocortex in juvenile neuronal ceroid-lipofuscinosis: axonal enlargements in layer IIIab and cell loss in layer V. Acta Neuropathol 46:79–83.
Brangwynne CP, MacKintosh FC, Kumar S, Geisse NA, Talbot J, Mahadevan L, Parker KK, Ingber DE, Weitz DA (2006) Microtubules can bear enhanced compressive loads in living cells because of lateral reinforcement. J Cell Biol 173:733–741.
Braulke T, Bonifacino JS (2009) Sorting of lysosomal proteins. Biochim Biophys Acta 1793:605–614.
Bridgman PC, Dave S, Asnes CF, Tullio AN, Adelstein RS (2001) Myosin IIB is required for growth cone motility. J Neurosci 21:6159–6169.
Bridges R, Lutgen V, Lobner D, Baker DA (2012) Thinking outside the cleft to understand synaptic activity: contribution of the cystine-glutamate antiporter (system x_c^+) to normal and pathological glutamatergic signaling. PHARMACOLOGICAL REVIEWS 64:780-802, 2012.
Brix K, Jordans S (2005) Watching proteases in action. Nat Chem Biol 1:186–187.
Brockmann K, Pouwels PJ, Christen HJ, Frahm J, Hanefeld F (1996) Localized proton magnetic resonance spectroscopy of cerebral metabolic disturbances in children with neuronal ceroid lipofuscinosis. Neuropediatrics 27:242–248.
Bronfman FC, Escudero CA, Weis J, Kruttgen A (2007) Endosomal transport of neurotrophins: roles in signaling and neurodegenerative diseases. Dev Neurobiol 67:1183–1203.
Bronte V, Zanovello P (2005) Regulation of immune responses by L-arginine metabolism. Nat Rev Immunol 5:641–654.
Brooks AI, Chattopadhyay S, Mitchison HM, Nussbaum RL, Pearce DA (2003) Functional categorization of gene expression changes in the cerebellum of a Cln3-knockout mouse model for Batten disease. Mol Genet Metab 78:17–30.
Brophy K, Hawi Z, Kirley A, Fitzgerald M, Gill M (2002) Synaptosomal-associated protein 25 (SNAP-25) and attention deficit hyperactivity disorder (ADHD): evidence of linkage and association in the Irish population. Mol Psychiatry 7:913–917.
Brown GC, Bolaños JP, Heales SJ, Clark JB (1995) Nitric oxide produced by activated astrocytes rapidly and reversibly inhibits cellular respiration. Neurosci Lett 193:201–204.
Bruccoleri A, Harry GJ (2000) Chemical-induced hippocampal neurodegeneration and elevations in TNFalpha, TNFbeta, IL-1alpha, IP-10, and MCP-1 mRNA in osteopetrotic (op/op) mice. J Neurosci Res 62:146–155.
Bruce AJ, Boling W, Kindy MS, Peschon J, Kraemer PJ, Carpenter MK, Holtsberg FW, Mattson MP (1996) Altered neuronal and microglial responses to excitotoxic and ischemic brain injury in mice lacking TNF receptors. Nat Med 2:788–794.
Brunk UT, Terman A (2002) Lipofuscin: mechanisms of age-related accumulation and influence on cell function. Free Radic Biol Med 33:611–619.
Bruno V, Copani A, Besong G, Scoto G, Nicoletti F (2000) Neuroprotective activity of chemokines against N-methyl-D-aspartate or beta-amyloid-induced toxicity in culture. Eur J Pharmacol 399:117–121.
Bruns D, Jahn R (2002) Molecular determinants of exocytosis. Pflugers Arch 443:333–338.
Bruns MB, Miller MW (2007a) Functional nerve growth factor and trkA autocrine/paracrine circuits in adult rat cortex are revealed by episodic ethanol exposure and withdrawal. J Neurochem 100:1155–1168.
Bruns MB, Miller MW (2007b) Neurotrophin ligand-receptor systems in somatosensory cortex of adult rat are affected by repeated episodes of ethanol. Exp Neurol 204:680–692.
Bucci C, Thomsen P, Nicoziani P, McCarthy J, van Deurs B (2000) Rab7: a key to lysosome biogenesis. Mol Biol Cell 11:467–480.
Buchsbaum RJ (2007) Rho activation at a glance. J Cell Sci 120:1149–1152.
Buchstaller A, Jay DG (2000) Micro-scale chromophore-assisted laser inactivation of nerve growth cone proteins. Microsc Res Tech 48:97–106.
Buffington SA, Rasband MN (2011) The axon initial segment in nervous system disease and injury. Eur J Neurosci 34:1609–1619.
Buffo A, Rite I, Tripathi P, Lepier A, Colak D, Horn A-P, Mori T, Götz M (2008) Origin and progeny of reactive gliosis: A source of multipotent cells in the injured brain. Proc Natl Acad Sci USA 105:3581–3586.
Burgos M, Calvo S, Molina F, Vaquero CF, Samarel A, Llopis J, Tranque P (2007) PKCepsilon

induces astrocyte stellation by modulating multiple cytoskeletal proteins and interacting with Rho A signalling pathways: implications for neuroinflammation. Eur J Neurosci 25:1069–1078.
Burgoyne RD, O'Callaghan DW, Hasdemir B, Haynes LP, Tepikin AV (2004) Neuronal Ca2+-sensor proteins: multitalented regulators of neuronal function. Trends Neurosci 27:203–209.
Burroughs L, Woolfrey A, Shimamura A (2009) Shwachman-Diamond syndrome: a review of the clinical presentation, molecular pathogenesis, diagnosis, and treatment. Hematol Oncol Clin North Am 23:233–248.
Bush TG, Puvanachandra N, Horner CH, Polito A, Ostenfeld T, Svendsen CN, Mucke L, Johnson MH, Sofroniew MV (1999) Leukocyte infiltration, neuronal degeneration, and neurite outgrowth after ablation of scar-forming, reactive astrocytes in adult transgenic mice. Neuron 23:297–308.
Bushong EA, Martone ME, Jones YZ, Ellisman MH (2002) Protoplasmic astrocytes in CA1 stratum radiatum occupy separate anatomical domains. J Neurosci 22:183–192.
Butt AM, Duncan A, Berry M (1994) Astrocyte associations with nodes of Ranvier: ultrastructural analysis of HRP-filled astrocytes in the mouse optic nerve. J Neurocytol 23:486–499.
Butt AM, Duncan A, Hornby MF, Kirvell SL, Hunter A, Levine JM, Berry M (1999) Cells expressing the NG2 antigen contact nodes of Ranvier in adult CNS white matter. Glia 26:84–91.
Buxbaum JD, Choi EK, Luo Y, Lilliehook C, Crowley AC, Merriam DE, Wasco W (1998) Calsenilin: a calcium-binding protein that interacts with the presenilins and regulates the levels of a presenilin fragment. Nat Med 4:1177–1181.
Byrnes KR, Stoica BA, Fricke S, Di Giovanni S, Faden AI (2007) Cell cycle activation contributes to post-mitotic cell death and secondary damage after spinal cord injury. Brain 130:2977–2992.
Cahoy JD, Emery B, Kaushal A, Foo LC, Zamanian JL, Christopherson KS, Xing Y, Lubischer JL, Krieg PA, Krupenko SA, Thompson WJ, Barres BA (2008) A transcriptome database for astrocytes, neurons, and oligodendrocytes: a new resource for understanding brain development and function. J Neurosci 28:264–278.
Calabrese EJ (2008) Enhancing and regulating neurite outgrowth. Crit Rev Toxicol 38:391–418.
Calì C, Bezzi P (2010) CXCR4-mediated glutamate exocytosis from astrocytes. J Neuroimmunol 224:13–21.
Callahan JW, Bagshaw RD, Mahuran DJ (2009) The integral membrane of lysosomes: its proteins and their roles in disease. J Proteomics 72:23–33.
Camand E, Peglion F, Osmani N, Sanson M, Etienne-Manneville S (2012) N-cadherin expression level modulates integrin-mediated polarity and strongly impacts on the speed and directionality of glial cell migration. J Cell Sci 125:844–857.
Camello C, Lomax R, Petersen OH, Tepikin AV (2002) Calcium leak from intracellular stores--the enigma of calcium signalling. Cell Calcium 32:355–361.
Cameron RS, Rakic P (1991) Glial cell lineage in the cerebral cortex: a review and synthesis. Glia 4:124–137.
Campbell IL, Abraham CR, Masliah E, Kemper P, Inglis JD, Oldstone MB, Mucke L (1993) Neurologic disease induced in transgenic mice by cerebral overexpression of interleukin 6. Proc Natl Acad Sci USA 90:10061–10065.
Canals S, Casarejos MJ, de Bernardo S, Rodríguez-Martín E, Mena MA (2001) Glutathione depletion switches nitric oxide neurotrophic effects to cell death in midbrain cultures: implications for Parkinson's disease. J Neurochem 79:1183–1195.
Canuel M, Korkidakis A, Konnyu K, Morales CR (2008) Sortilin mediates the lysosomal targeting of cathepsins D and H. Biochem Biophys Res Commun 373:292–297.
Cao Y, Espinola JA, Fossale E, Massey AC, Cuervo AM, MacDonald ME, Cotman SL (2006) Autophagy is disrupted in a knock-in mouse model of juvenile neuronal ceroid lipofuscinosis. J Biol Chem 281:20483–20493.
Cao Y, Staropoli JF, Biswas S, Espinola JA, MacDonald ME, Lee J-M, Cotman SL (2011) Distinct early molecular responses to mutations causing vLINCL and JNCL presage ATP synthase subunit C accumulation in cerebellar cells. PLoS ONE 6:e17118.
Carafoli E (2002) Calcium signaling: a tale for all seasons. Proc Natl Acad Sci USA 99:1115–1122.
Carlén M, Meletis K, Göritz C, Darsalia V, Evergren E, Tanigaki K, Amendola M, Barnabé-Heider F, Yeung MSY, Naldini L, Honjo T, Kokaia Z, Shupliakov O, Cassidy RM, Lindvall O, Frisén J (2009) Forebrain ependymal cells are Notch-dependent and generate neuroblasts and

astrocytes after stroke. Nat Neurosci 12:259–267.
Carloni V, Mazzocca A, Pantaleo P, Cordella C, Laffi G, Gentilini P (2001) The integrin, alpha6beta1, is necessary for the matrix-dependent activation of FAK and MAP kinase and the migration of human hepatocarcinoma cells. Hepatology 34:42–49.
Carlson NG, Bacchi A, Rogers SW, Gahring LC (1998) Nicotine blocks TNF-alpha-mediated neuroprotection to NMDA by an alpha-bungarotoxin-sensitive pathway. J Neurobiol 35:29–36.
Carmona MA, Murai KK, Wang L, Roberts AJ, Pasquale EB (2009) Glial ephrin-A3 regulates hippocampal dendritic spine morphology and glutamate transport. Proc Natl Acad Sci USA 106:12524–12529.
Caroni P (2001) New EMBO members' review: actin cytoskeleton regulation through modulation of PI(4,5)P(2) rafts. EMBO J 20:4332–4336.
Carrión AM, Link WA, Ledo F, Mellström B, Naranjo JR (1999) DREAM is a Ca2+-regulated transcriptional repressor. Nature 398:80–84.
Carroll RC, Beattie EC, Zastrow von M, Malenka RC (2001) Role of AMPA receptor endocytosis in synaptic plasticity. Nat Rev Neurosci 2:315–324.
Case RM, Eisner D, Gurney A, Jones O, Muallem S, Verkhratsky A (2007) Evolution of calcium homeostasis: from birth of the first cell to an omnipresent signalling system. Cell Calcium 42:345–350.
Cassina P, Pehar M, Vargas MR, Castellanos R, Barbeito AG, Estévez AG, Thompson JA, Beckman JS, Barbeito L (2005) Astrocyte activation by fibroblast growth factor-1 and motor neuron apoptosis: implications for amyotrophic lateral sclerosis. J Neurochem 93:38–46.
Castaneda JA, Lim MJ, Cooper JD, Pearce DA (2008) Immune system irregularities in lysosomal storage disorders. Acta Neuropathol 115:159–174.
Cayre M, Canoll P, Goldman JE (2009) Cell migration in the normal and pathological postnatal mammalian brain. Prog Neurobiol 88:41–63.
Cendes F, Andermann F, Carpenter S, Zatorre RJ, Cashman NR (1995) Temporal lobe epilepsy caused by domoic acid intoxication: evidence for glutamate receptor-mediated excitotoxicity in humans. Ann Neurol 37:123–126.
Chan C-H, Ramirez-Montealegre D, Pearce DA (2009) Altered arginine metabolism in the central nervous system (CNS) of the Cln3-/- mouse model of juvenile Batten disease. Neuropathol Appl Neurobiol 35:189–207.
Chang J-W, Choi H, Cotman SL, Jung Y-K (2011) Lithium rescues the impaired autophagy process in CbCln3(Δex7/8/Δex7/8) cerebellar cells and reduces neuronal vulnerability to cell death via IMPase inhibition. J Neurochem 116:659–668.
Chang J-W, Choi H, Kim H-J, Jo D-G, Jeon Y-J, Noh J-Y, Park WJ, Jung Y-K (2007) Neuronal vulnerability of CLN3 deletion to calcium-induced cytotoxicity is mediated by calsenilin. Hum Mol Genet 16:317–326.
Chang M-Y, Son H, Lee Y-S, Lee S-H (2003) Neurons and astrocytes secrete factors that cause stem cells to differentiate into neurons and astrocytes, respectively. Mol Cell Neurosci 23:414–426.
Chao CC, Hu S, Ehrlich L, Peterson PK (1995) Interleukin-1 and tumor necrosis factor-alpha synergistically mediate neurotoxicity: involvement of nitric oxide and of N-methyl-D-aspartate receptors. Brain Behav Immun 9:355–365.
Charles AC, Merrill JE, Dirksen ER, Sanderson MJ (1991) Intercellular signaling in glial cells: calcium waves and oscillations in response to mechanical stimulation and glutamate. Neuron 6:983–992.
Chattopadhyay S, Ito M, Cooper JD, Brooks AI, Curran TM, Powers JM, Pearce DA (2002) An autoantibody inhibitory to glutamic acid decarboxylase in the neurodegenerative disorder Batten disease. Hum Mol Genet 11:1421–1431.
Chattopadhyay S, Kingsley E, Serour A, Curran TM, Brooks AI, Pearce DA (2004) Altered gene expression in the eye of a mouse model for batten disease. Invest Ophthalmol Vis Sci 45:2893–2905.
Chattopadhyay S, Pearce DA (2000) Neural and extraneural expression of the neuronal ceroid lipofuscinoses genes CLN1, CLN2, and CLN3: functional implications for CLN3. Mol Genet Metab 71:207–211.
Chen C-J, Ou Y-C, Lin S-Y, Liao S-L, Huang Y-S, Chiang A-N (2006) L-glutamate activates RhoA

GTPase leading to suppression of astrocyte stellation. Eur J Neurosci 23:1977–1987.
Chen G, Li H-M, Chen Y-R, Gu X-S, Duan S (2007) Decreased estradiol release from astrocytes contributes to the neurodegeneration in a mouse model of Niemann-Pick disease type C. Glia 55:1509–1518.
Chen JW, Murphy TL, Willingham MC, Pastan I, August JT (1985) Identification of two lysosomal membrane glycoproteins. J Cell Biol 101:85–95.
Chen P-C, Vargas MR, Pani AK, Smeyne RJ, Johnson DA, Kan YW, Johnson JA (2009) Nrf2-mediated neuroprotection in the MPTP mouse model of Parkinson's disease: Critical role for the astrocyte. Proc Natl Acad Sci USA 106:2933–2938.
Chen Y, Vartiainen NE, Ying W, Chan PH, Koistinaho J, Swanson RA (2001) Astrocytes protect neurons from nitric oxide toxicity by a glutathione-dependent mechanism. J Neurochem 77:1601–1610.
Cheng H-C, Shih H-M, Chern Y (2002) Essential role of cAMP-response element-binding protein activation by A2A adenosine receptors in rescuing the nerve growth factor-induced neurite outgrowth impaired by blockage of the MAPK cascade. J Biol Chem 277:33930–33942.
Cho K-S, Yang L, Lu B, Feng Ma H, Huang X, Pekny M, Chen DF (2005) Re-establishing the regenerative potential of central nervous system axons in postnatal mice. J Cell Sci 118:863–872.
Chodobski A, Chung I, Koźniewska E, Ivanenko T, Chang W, Harrington JF, Duncan JA, Szmydynger-Chodobska J (2003) Early neutrophilic expression of vascular endothelial growth factor after traumatic brain injury. Neuroscience 122:853–867.
Choi DW, Maulucci-Gedde M, Kriegstein AR (1987) Glutamate neurotoxicity in cortical cell culture. J Neurosci 7:357–368.
Chow JC, Young DW, Golenbock DT, Christ WJ, Gusovsky F (1999) Toll-like receptor-4 mediates lipopolysaccharide-induced signal transduction. J Biol Chem 274:10689–10692.
Christopherson KS, Ullian EM, Stokes CCA, Mullowney CE, Hell JW, Agah A, Lawler J, Mosher DF, Bornstein P, Barres BA (2005) Thrombospondins are astrocyte-secreted proteins that promote CNS synaptogenesis. Cell 120:421–433.
Chronister R, Dyken P, Fields PA, Maertens P (1995) Cellular distribution of lesions in Batten disease. Am J Med Genet 57:191–195.
Chu AJ (2011) Tissue factor, blood coagulation, and beyond: an overview. Int J Inflam 2011:367284.
Chung IY, Benveniste EN (1990) Tumor necrosis factor-alpha production by astrocytes. Induction by lipopolysaccharide, IFN-gamma, and IL-1 beta. J Immunol 144:2999–3007.
Chuquet J, Hollender L, Nimchinsky EA (2007) High-resolution in vivo imaging of the neurovascular unit during spreading depression. J Neurosci 27:4036–4044.
Ciani L, Salinas PC (2005) WNTs in the vertebrate nervous system: from patterning to neuronal connectivity. Nat Rev Neurosci 6:351–362.
Cloix J-F, Hévor T (2009) Epilepsy, regulation of brain energy metabolism and neurotransmission. Curr Med Chem 16:841–853.
Coco S, Calegari F, Pravettoni E, Pozzi D, Taverna E, Rosa P, Matteoli M, Verderio C (2003) Storage and release of ATP from astrocytes in culture. J Biol Chem 278:1354–1362.
Colangelo AM, Cirillo G, Lavitrano ML, Alberghina L, Papa M (2012) Targeting reactive astrogliosis by novel biotechnological strategies. Biotechnol Adv 30:261–271.
Coleman P, Federoff H, Kurlan R (2004) A focus on the synapse for neuroprotection in Alzheimer disease and other dementias. Neurology 63:1155–1162.
Colodner KJ, Montana RA, Anthony DC, Folkerth RD, De Girolami U, Feany MB (2005) Proliferative potential of human astrocytes. J Neuropathol Exp Neurol 64:163–169.
Colucci-Guyon E, Portier MM, Dunia I, Paulin D, Pournin S, Babinet C (1994) Mice lacking vimentin develop and reproduce without an obvious phenotype. Cell 79:679–694.
Conde C, Cáceres A (2009) Microtubule assembly, organization and dynamics in axons and dendrites. Nat Rev Neurosci 10:319–332.
Conti F, Minelli A, Melone M (2004) GABA transporters in the mammalian cerebral cortex: localization, development and pathological implications. Brain Res Brain Res Rev 45:196–212.
Conus S, Simon H-U (2008) Cathepsins: key modulators of cell death and inflammatory responses. Biochem Pharmacol 76:1374–1382.

Cooper JD (2003) Progress towards understanding the neurobiology of Batten disease or neuronal ceroid lipofuscinosis. Curr Opin Neurol 16:121–128.
Cooper JD (2008) Moving towards therapies for juvenile Batten disease? Exp Neurol 211:329–331.
Cooper JD (2010) The neuronal ceroid lipofuscinoses: the same, but different? Biochem Soc Trans 38:1448–1452.
Cooper JD, Russell C, Mitchison HM (2006) Progress towards understanding disease mechanisms in small vertebrate models of neuronal ceroid lipofuscinosis. Biochim Biophys Acta 1762:873–889.
Cornell-Bell AH, Finkbeiner SM, Cooper MS, Smith SJ (1990a) Glutamate induces calcium waves in cultured astrocytes: long-range glial signaling. Science 247:470–473.
Cornell-Bell AH, Thomas PG, Smith SJ (1990b) The excitatory neurotransmitter glutamate causes filopodia formation in cultured hippocampal astrocytes. Glia 3:322–334.
Corradini I, Verderio C, Sala M, Wilson MC, Matteoli M (2009) SNAP-25 in neuropsychiatric disorders. Ann N Y Acad Sci 1152:93–99.
Cortés-Vieyra R, Bravo-Patiño A, Valdez-Alarcón JJ, Cajero Juárez M, Finlay BB, Baizabal-Aguirre VM (2012) Role of glycogen synthase kinase-3 beta in the inflammatory response caused by bacterial pathogens. J Inflamm (Lond) 9:23.
Costa S, Planchenault T, Charriere-Bertrand C, Mouchel Y, Fages C, Juliano S, Lefrançois T, Barlovatz-Meimon G, Tardy M (2002) Astroglial permissivity for neuritic outgrowth in neuron-astrocyte cocultures depends on regulation of laminin bioavailability. Glia 37:105–113.
Cotman SL, Vrbanac V, Lebel L-A, Lee RL, Johnson KA, Donahue L-R, Teed AM, Antonellis K, Bronson RT, Lerner TJ, MacDonald ME (2002) Cln3(Deltaex7/8) knock-in mice with the common JNCL mutation exhibit progressive neurologic disease that begins before birth. Hum Mol Genet 11:2709–2721.
Cotrina ML, Lin JH, López-García JC, Naus CC, Nedergaard M (2000) ATP-mediated glia signaling. J Neurosci 20:2835–2844.
Cotrina ML, Lin JH, Nedergaard M (1998) Cytoskeletal assembly and ATP release regulate astrocytic calcium signaling. J Neurosci 18:8794–8804.
Couchie D, Fages C, Bridoux AM, Rolland B, Tardy M, Nunez J (1985) Microtubule-associated proteins and in vitro astrocyte differentiation. J Cell Biol 101:2095–2103.
Coull JAM, Beggs S, Boudreau D, Boivin D, Tsuda M, Inoue K, Gravel C, Salter MW, De Koninck Y (2005) BDNF from microglia causes the shift in neuronal anion gradient underlying neuropathic pain. Nature 438:1017–1021.
Coulter DA, Eid T (2012) Astrocytic regulation of glutamate homeostasis in epilepsy. Glia 60:1215–1226.
Counts SE, Mufson EJ (2005) The role of nerve growth factor receptors in cholinergic basal forebrain degeneration in prodromal Alzheimer disease. J Neuropathol Exp Neurol 64:263–272.
Cox TM, Cachón-González MB (2012) The cellular pathology of lysosomal diseases. J Pathol 226:241–254.
Cramer LP (1999) Organization and polarity of actin filament networks in cells: implications for the mechanism of myosin-based cell motility. Biochem Soc Symp 65:173–205.
Crippa D, Schenk U, Francolini M, Rosa P, Verderio C, Zonta M, Pozzan T, Matteoli M, Carmignoto G (2006) Synaptobrevin2-expressing vesicles in rat astrocytes: insights into molecular characterization, dynamics and exocytosis. J Physiol (Lond) 570:567–582.
Crocker SJ, Pagenstecher A, Campbell IL (2004) The TIMPs tango with MMPs and more in the central nervous system. J Neurosci Res 75:1–11.
Crone SA, Lee K-F (2002) The bound leading the bound: target-derived receptors act as guidance cues. Neuron 36:333–335.
Croopnick JB, Choi HC, Mueller DM (1998) The subcellular location of the yeast Saccharomyces cerevisiae homologue of the protein defective in the juvenile form of Batten disease. Biochem Biophys Res Commun 250:335–341.
Custer SK, Garden GA, Gill N, Rueb U, Libby RT, Schultz C, Guyenet SJ, Deller T, Westrum LE, Sopher BL, La Spada AR (2006) Bergmann glia expression of polyglutamine-expanded ataxin-7 produces neurodegeneration by impairing glutamate transport. Nat Neurosci 9:1302–

1311.
D'Souza SD, Alinauskas KA, Antel JP (1996) Ciliary neurotrophic factor selectively protects human oligodendrocytes from tumor necrosis factor-mediated injury. J Neurosci Res 43:289–298.
da Silva JS, Dotti CG (2002) Breaking the neuronal sphere: regulation of the actin cytoskeleton in neuritogenesis. Nat Rev Neurosci 3:694–704.
Danbolt NC (2001) Glutamate uptake. Prog Neurobiol 65:1–105.
Dani JW, Chernjavsky A, Smith SJ (1992) Neuronal activity triggers calcium waves in hippocampal astrocyte networks. Neuron 8:429–440.
Danton GH, Dietrich WD (2003) Inflammatory mechanisms after ischemia and stroke. J Neuropathol Exp Neurol 62:127–136.
Darlington CL (2005) Astrocytes as targets for neuroprotective drugs. Curr Opin Investig Drugs 6:700–703.
Das AM, Harlem von R, Feist M, Lücke T, Kohlschütter A (2001) Altered levels of high-energy phosphate compounds in fibroblasts from different forms of neuronal ceroid lipofuscinoses: further evidence for mitochondrial involvement. Eur J Paediatr Neurol 5 Suppl A:143–146.
Das AM, Kohlschütter A (1996) Decreased activity of the mitochondrial ATP-synthase in fibroblasts from children with late-infantile and juvenile neuronal ceroid lipofuscinosis. J Inherit Metab Dis 19:130–132.
Davalos D, Grutzendler J, Yang G, Kim JV, Zuo Y, Jung S, Littman DR, Dustin ML, Gan W-B (2005) ATP mediates rapid microglial response to local brain injury in vivo. Nat Neurosci 8:752–758.
Dawson G, Kilkus J, Siakotos AN, Singh I (1996) Mitochondrial abnormalities in CLN2 and CLN3 forms of Batten disease. Mol Chem Neuropathol 29:227–235.
Dayton ET, Major EO (1996) Recombinant human interleukin 1 beta induces production of prostaglandins in primary human fetal astrocytes and immortalized human fetal astrocyte cultures. J Neuroimmunol 71:11–18.
de Jong EK, Dijkstra IM, Hensens M, Brouwer N, van Amerongen M, Liem RSB, Boddeke HWGM, Biber K (2005) Vesicle-mediated transport and release of CCL21 in endangered neurons: a possible explanation for microglia activation remote from a primary lesion. J Neurosci 25:7548–7557.
De Keyser J, Mostert JP, Koch MW (2008) Dysfunctional astrocytes as key players in the pathogenesis of central nervous system disorders. J Neurol Sci 267:3–16.
de Lanerolle NC, Lee T-S, Spencer DD (2010) Astrocytes and epilepsy. Neurotherapeutics 7:424–438.
De Matteis MA, Morrow JS (2000) Spectrin tethers and mesh in the biosynthetic pathway. J Cell Sci 113 (Pt 13):2331–2343.
De Paola M, Buanne P, Biordi L, Bertini R, Ghezzi P, Mennini T (2007) Chemokine MIP-2/CXCL2, acting on CXCR2, induces motor neuron death in primary cultures. Neuroimmunomodulation 14:310–316.
De Waard M, Liu H, Walker D, Scott VE, Gurnett CA, Campbell KP (1997) Direct binding of G-protein betagamma complex to voltage-dependent calcium channels. Nature 385:446–450.
Debanne D, Campanac E, Bialowas A, Carlier E, Alcaraz G (2011) Axon physiology. Physiol Rev 91:555–602.
Debanne D, Rama S (2011) Astrocytes shape axonal signaling. Sci Signal 4:pe11.
Dechant G, Barde Y-A (2002) The neurotrophin receptor p75(NTR): novel functions and implications for diseases of the nervous system. Nat Neurosci 5:1131–1136.
Deister C, Schmidt CE (2006) Optimizing neurotrophic factor combinations for neurite outgrowth. J Neural Eng 3:172–179.
DeKosky ST, Scheff SW (1990) Synapse loss in frontal cortex biopsies in Alzheimer's disease: correlation with cognitive severity. Ann Neurol 27:457–464.
DeKosky ST, Styren SD, O'Malley ME, Goss JR, Kochanek P, Marion D, Evans CH, Robbins PD (1996) Interleukin-1 receptor antagonist suppresses neurotrophin response in injured rat brain. Ann Neurol 39:123–127.
Dell'Angelica EC (2004) The building BLOC(k)s of lysosomes and related organelles. Curr Opin Cell Biol 16:458–464.
Dell'Angelica EC, Mullins C, Caplan S, Bonifacino JS (2000) Lysosome-related organelles. FASEB J 14:1265–1278.
Deng YY, Lu J, Ling EA, Kaur C (2009) Monocyte chemoattractant protein-1 (MCP-1) produced via

NF-kappaB signaling pathway mediates migration of amoeboid microglia in the periventricular white matter in hypoxic neonatal rats. Glia 57:604–621.
Dermietzel R, Hertberg EL, Kessler JA, Spray DC (1991) Gap junctions between cultured astrocytes: immunocytochemical, molecular, and electrophysiological analysis. J Neurosci 11:1421–1432.
Derouiche A, Anlauf E, Aumann G, Mühlstädt B, Lavialle M (2002) Anatomical aspects of glia-synapse interaction: the perisynaptic glial sheath consists of a specialized astrocyte compartment. J Physiol Paris 96:177–182.
Desagher S, Glowinski J, Premont J (1996) Astrocytes protect neurons from hydrogen peroxide toxicity. J Neurosci 16:2553–2562.
Desai A, Mitchison TJ (1997) Microtubule polymerization dynamics. Annu Rev Cell Dev Biol 13:83–117.
Desnick RJ, Astrin KH, Bishop DF (1989) Fabry disease: molecular genetics of the inherited nephropathy. Adv Nephrol Necker Hosp 18:113–127.
Di Giovanni S, Movsesyan V, Ahmed F, Cernak I, Schinelli S, Stoica B, Faden AI (2005) Cell cycle inhibition provides neuroprotection and reduces glial proliferation and scar formation after traumatic brain injury. Proc Natl Acad Sci USA 102:8333–8338.
Di Malta C, Fryer JD, Settembre C, Ballabio A (2012a) Astrocyte dysfunction triggers neurodegeneration in a lysosomal storage disorder. Proc Natl Acad Sci USA 109:E2334–E2342.
Di Malta C, Fryer JD, Settembre C, Ballabio A (2012b) Autophagy in astrocytes: A novel culprit in lysosomal storage disorders. Autophagy 8:1871–1872.
Dietrich WD, Busto R, Bethea JR (1999) Postischemic hypothermia and IL-10 treatment provide long-lasting neuroprotection of CA1 hippocampus following transient global ischemia in rats. Exp Neurol 158:444–450.
Ding S-L, Tecedor L, Stein CS, Davidson BL (2011) A knock-in reporter mouse model for Batten disease reveals predominant expression of Cln3 in visual, limbic and subcortical motor structures. Neurobiol Dis 41:237–248.
Domercq M, Sánchez-Gómez MV, Areso P, Matute C (1999) Expression of glutamate transporters in rat optic nerve oligodendrocytes. Eur J Neurosci 11:2226–2236.
Dominguez R, Holmes KC (2011) Actin structure and function. Annu Rev Biophys 40:169–186.
Dong Y, Benveniste EN (2001) Immune function of astrocytes. Glia 36:180–190.
Drees F, Gertler FB (2008) Ena/VASP: proteins at the tip of the nervous system. Curr Opin Neurobiol 18:53–59.
Dreyfus CF, Dai X, Lercher LD, Racey BR, Friedman WJ, Black IB (1999) Expression of neurotrophins in the adult spinal cord in vivo. J Neurosci Res 56:1–7.
Dringen R (2000) Metabolism and functions of glutathione in brain. Prog Neurobiol 62:649–671.
Dringen R, Gutterer JM, Gros C, Hirrlinger J (2001) Aminopeptidase N mediates the utilization of the GSH precursor CysGly by cultured neurons. J Neurosci Res 66:1003–1008.
Dringen R, Kranich O, Hamprecht B (1997) The gamma-glutamyl transpeptidase inhibitor acivicin preserves glutathione released by astroglial cells in culture. Neurochem Res 22:727–733.
Dringen R, Kussmaul L, Gutterer JM, Hirrlinger J, Hamprecht B (1999a) The glutathione system of peroxide detoxification is less efficient in neurons than in astroglial cells. J Neurochem 72:2523–2530.
Dringen R, Pfeiffer B, Hamprecht B (1999b) Synthesis of the antioxidant glutathione in neurons: supply by astrocytes of CysGly as precursor for neuronal glutathione. J Neurosci 19:562–569.
Driskell OJ, Mironov A, Allan VJ, Woodman PG (2007) Dynein is required for receptor sorting and the morphogenesis of early endosomes. Nat Cell Biol 9:113–120.
DU P, Tang H-Y, Li X, Lin H-J, Peng W-F, Ma Y, Fan W, Wang X (2012) Anticonvulsive and antioxidant effects of curcumin on pilocarpine-induced seizures in rats. Chin Med J 125:1975–1979.
Duan S, Anderson CM, Stein BA, Swanson RA (1999) Glutamate induces rapid upregulation of astrocyte glutamate transport and cell-surface expression of GLAST. J Neurosci 19:10193–10200.
Duchen MR (1999) Contributions of mitochondria to animal physiology: from homeostatic sensor to calcium signalling and cell death. J Physiol (Lond) 516 (Pt 1):1–17.
Duchen MR (2000) Mitochondria and Ca(2+)in cell physiology and pathophysiology. Cell Calcium

28:339–348.
Duffy S, MacVicar BA (1994) Potassium-dependent calcium influx in acutely isolated hippocampal astrocytes. Neuroscience 61:51–61.
Duncan AJ, Heales SJR (2005) Nitric oxide and neurological disorders. Mol Aspects Med 26:67–96.
Dunn WA, Raizada MK, Vogt ES, Brown EA (1994) Growth factor-induced neurite growth in primary neuronal cultures of dogs with neuronal ceroid lipofuscinosis. Int J Dev Neurosci 12:185–196.
Duve C (1975) Exploring cells with a centrifuge. Science 189:186–194.
Eastwood SL, Burnet PW, Harrison PJ (1995) Altered synaptophysin expression as a marker of synaptic pathology in schizophrenia. Neuroscience 66:309–319.
Eddleston M, la Torre de JC, Oldstone MB, Loskutoff DJ, Edgington TS, Mackman N (1993) Astrocytes are the primary source of tissue factor in the murine central nervous system. A role for astrocytes in cerebral hemostasis. J Clin Invest 92:349–358.
Eddleston M, Mucke L (1993) Molecular profile of reactive astrocytes--implications for their role in neurologic disease. Neuroscience 54:15–36.
Efremov YM, Dzyubenko EV, Bagrov DV, Maksimov GV, Shram SI, Shaitan KV (2011) Atomic force microscopy study of the arrangement and mechanical properties of astrocytic cytoskeleton in growth medium. Acta Naturae 3:93–99.
Ehlers MD (2000) Reinsertion or degradation of AMPA receptors determined by activity-dependent endocytic sorting. Neuron 28:511–525.
el-Fouly MH, Trosko JE, Chang CC (1987) Scrape-loading and dye transfer. A rapid and simple technique to study gap junctional intercellular communication. Exp Cell Res 168:422–430.
Eliason SL, Stein CS, Mao Q, Tecedor L, Ding S-L, Gaines DM, Davidson BL (2007) A knock-in reporter model of Batten disease. J Neurosci 27:9826–9834.
Eliasson C, Sahlgren C, Berthold CH, Stakeberg J, Celis JE, Betsholtz C, Eriksson JE, Pekny M (1999) Intermediate filament protein partnership in astrocytes. J Biol Chem 274:23996–24006.
Elkabes S, DiCicco-Bloom EM, Black IB (1996) Brain microglia/macrophages express neurotrophins that selectively regulate microglial proliferation and function. J Neurosci 16:2508–2521.
Elobeid A, Bongcam-Rudloff E, Westermark B, Nistér M (2000) Effects of inducible glial fibrillary acidic protein on glioma cell motility and proliferation. J Neurosci Res 60:245–256.
Elshatory Y, Brooks AI, Chattopadhyay S, Curran TM, Gupta P, Ramalingam V, Hofmann SL, Pearce DA (2003) Early changes in gene expression in two models of Batten disease. FEBS Lett 538:207–212.
Emsley JG, Arlotta P, Macklis JD (2004) Star-cross'd neurons: astroglial effects on neural repair in the adult mammalian CNS. Trends Neurosci 27:238–240.
Erickson JW, Cerione RA (2004) Structural elements, mechanism, and evolutionary convergence of Rho protein-guanine nucleotide exchange factor complexes. Biochemistry 43:837–842.
Eskelinen E-L (2005) Maturation of autophagic vacuoles in Mammalian cells. Autophagy 1:1–10.
Eskelinen E-L (2006) Roles of LAMP-1 and LAMP-2 in lysosome biogenesis and autophagy. Mol Aspects Med 27:495–502.
Eskelinen E-L, Tanaka Y, Saftig P (2003) At the acidic edge: emerging functions for lysosomal membrane proteins. Trends Cell Biol 13:137–145.
Etienne-Manneville S (2004) Actin and microtubules in cell motility: which one is in control? Traffic 5:470–477.
Etienne-Manneville S, Hall A (2001) Integrin-mediated activation of Cdc42 controls cell polarity in migrating astrocytes through PKCzeta. Cell 106:489–498.
Etienne-Manneville S, Hall A (2002) Rho GTPases in cell biology. Nature 420:629–635.
Eugenin EA, D'Aversa TG, Lopez L, Calderon TM, Berman JW (2003) MCP-1 (CCL2) protects human neurons and astrocytes from NMDA or HIV-tat-induced apoptosis. J Neurochem 85:1299–1311.
Ezaki J, Takeda-Ezaki M, Koike M, Ohsawa Y, Taka H, Mineki R, Murayama K, Uchiyama Y, Ueno T, Kominami E (2003) Characterization of Cln3p, the gene product responsible for juvenile neuronal ceroid lipofuscinosis, as a lysosomal integral membrane glycoprotein. J Neurochem 87:1296–1308.
Fabricius M, Fuhr S, Bhatia R, Boutelle M, Hashemi P, Strong AJ, Lauritzen M (2006) Cortical spreading depression and peri-infarct depolarization in acutely injured human cerebral

cortex. Brain 129:778–790.
Fam SR, Gallagher CJ, Salter MW (2000) P2Y(1) purinoceptor-mediated Ca(2+) signaling and Ca(2+) wave propagation in dorsal spinal cord astrocytes. J Neurosci 20:2800–2808.
Farina C, Aloisi F, Meinl E (2007) Astrocytes are active players in cerebral innate immunity. Trends Immunol 28:138–145.
Faulkner JR, Herrmann JE, Woo MJ, Tansey KE, Doan NB, Sofroniew MV (2004) Reactive astrocytes protect tissue and preserve function after spinal cord injury. J Neurosci 24:2143–2155.
Fawcett JW, Asher RA (1999) The glial scar and central nervous system repair. Brain Res Bull 49:377–391.
Fedoroff S, Berezovskaya O, Maysinger D (1997) Role of colony stimulating factor-1 in brain damage caused by ischemia. Neurosci Biobehav Rev 21:187–191.
Fellin T, Gomez-Gonzalo M, Gobbo S, Carmignoto G, Haydon PG (2006a) Astrocytic glutamate is not necessary for the generation of epileptiform neuronal activity in hippocampal slices. J Neurosci 26:9312–9322.
Fellin T, Pascual O, Gobbo S, Pozzan T, Haydon PG, Carmignoto G (2004) Neuronal synchrony mediated by astrocytic glutamate through activation of extrasynaptic NMDA receptors. Neuron 43:729–743.
Fellin T, Sul J-Y, D'Ascenzo M, Takano H, Pascual O, Haydon PG (2006b) Bidirectional astrocyte-neuron communication: the many roles of glutamate and ATP. Novartis Found Symp 276:208–17–discussion217–21–233–7–275–81.
Feng L, Kraus-Friedmann N (1993) Association of the hepatic IP3 receptor with the plasma membrane: relevance to mode of action. Am J Physiol 265:C1588–C1596.
Ferreira A, Niclas J, Vale RD, Banker G, Kosik KS (1992) Suppression of kinesin expression in cultured hippocampal neurons using antisense oligonucleotides. J Cell Biol 117:595–606.
Fiacco TA, McCarthy KD (2006) Astrocyte calcium elevations: properties, propagation, and effects on brain signaling. Glia 54:676–690.
Fields RD, Burnstock G (2006) Purinergic signalling in neuron-glia interactions. Nat Rev Neurosci 7:423–436.
Fields RD, Stevens B (2000) ATP: an extracellular signaling molecule between neurons and glia. Trends Neurosci 23:625–633.
Filocamo M, Morrone A (2011) Lysosomal storage disorders: molecular basis and laboratory testing. Hum Genomics 5:156–169.
Filosa A, Paixão S, Honsek SD, Carmona MA, Becker L, Feddersen B, Gaitanos L, Rudhard Y, Schoepfer R, Klopstock T, Kullander K, Rose CR, Pasquale EB, Klein R (2009) Neuron-glia communication via EphA4/ephrin-A3 modulates LTP through glial glutamate transport. Nat Neurosci 12:1285–1292.
Finkbeiner SM (1993) Glial calcium. Glia 9:83–104.
Finn R, Kovács AD, Pearce DA (2011) Altered sensitivity of cerebellar granule cells to glutamate receptor overactivation in the Cln3(Δex7/8)-knock-in mouse model of juvenile neuronal ceroid lipofuscinosis. Neurochem Int 58:648–655.
Fishell G, Hatten ME (1991) Astrotactin provides a receptor system for CNS neuronal migration. Development 113:755–765.
Fletcher DA, Mullins RD (2010) Cell mechanics and the cytoskeleton. Nature 463:485–492.
Fok-Seang J, DiProspero NA, Meiners S, Muir E, Fawcett JW (1998) Cytokine-induced changes in the ability of astrocytes to support migration of oligodendrocyte precursors and axon growth. Eur J Neurosci 10:2400–2415.
Fontana ACK, de Oliveira Beleboni R, Wojewodzic MW, Ferreira Dos Santos W, Coutinho-Netto J, Grutle NJ, Watts SD, Danbolt NC, Amara SG (2007) Enhancing glutamate transport: mechanism of action of Parawixin1, a neuroprotective compound from Parawixia bistriata spider venom. Mol Pharmacol 72:1228–1237.
Fontana ACK, Guizzo R, de Oliveira Beleboni R, Meirelles E Silva AR, Coimbra NC, Amara SG, Santos dos WF, Coutinho-Netto J (2003) Purification of a neuroprotective component of Parawixia bistriata spider venom that enhances glutamate uptake. Br J Pharmacol 139:1297–1309.
Foo LC, Allen NJ, Bushong EA, Ventura PB, Chung W-S, Zhou L, Cahoy JD, Daneman R, Zong H, Ellisman MH, Barres BA (2011) Development of a method for the purification and culture of

rodent astrocytes. Neuron 71:799–811.
Fossale E, Wolf P, Espinola JA, Lubicz-Nawrocka T, Teed AM, Gao H, Rigamonti D, Cattaneo E, MacDonald ME, Cotman SL (2004) Membrane trafficking and mitochondrial abnormalities precede subunit c deposition in a cerebellar cell model of juvenile neuronal ceroid lipofuscinosis. BMC Neurosci 5:57.
Frade J, Pope S, Schmidt M, Dringen R, Barbosa R, Pocock J, Laranjinha J, Heales S (2008) Glutamate induces release of glutathione from cultured rat astrocytes--a possible neuroprotective mechanism? J Neurochem 105:1144–1152.
Franco R, Bortner CD, Cidlowski JA (2006) Potential roles of electrogenic ion transport and plasma membrane depolarization in apoptosis. J Membr Biol 209:43–58.
Frank-Cannon TC, Alto LT, McAlpine FE, Tansey MG (2009) Does neuroinflammation fan the flame in neurodegenerative diseases? Mol Neurodegener 4:47.
Franke H, Verkhratsky A, Burnstock G, Illes P (2012) Pathophysiology of astroglial purinergic signalling. Purinergic Signal 8:629–657.
Freeman MR (2010) Specification and morphogenesis of astrocytes. Science 330:774–778.
Fuchs E, Weber K (1994) Intermediate filaments: structure, dynamics, function, and disease. Annu Rev Biochem 63:345–382.
Fujimoto M, Takagi Y, Aoki T, Hayase M, Marumo T, Gomi M, Nishimura M, Kataoka H, Hashimoto N, Nozaki K (2008) Tissue inhibitor of metalloproteinases protect blood-brain barrier disruption in focal cerebral ischemia. J Cereb Blood Flow Metab 28:1674–1685.
Fukuda M (1991) Lysosomal membrane glycoproteins. Structure, biosynthesis, and intracellular trafficking. J Biol Chem 266:21327–21330.
Fuller S, Münch G, Steele M (2009) Activated astrocytes: a therapeutic target in Alzheimer's disease? Expert Rev Neurother 9:1585–1594.
Furman S, Steingart RA, Mandel S, Hauser JM, Brenneman DE, Gozes I (2004) Subcellular localization and secretion of activity-dependent neuroprotective protein in astrocytes. Neuron Glia Biol 1:193–199.
Futerman AH, Banker GA (1996) The economics of neurite outgrowth--the addition of new membrane to growing axons. Trends Neurosci 19:144–149.
Futerman AH, van Meer G (2004) The cell biology of lysosomal storage disorders. Nat Rev Mol Cell Biol 5:554–565.
Gabriel SM, Haroutunian V, Powchik P, Honer WG, Davidson M, Davies P, Davis KL (1997) Increased concentrations of presynaptic proteins in the cingulate cortex of subjects with schizophrenia. Arch Gen Psychiatry 54:559–566.
Gachet Y, Codlin S, Hyams JS, Mole SE (2005) btn1, the Schizosaccharomyces pombe homologue of the human Batten disease gene CLN3, regulates vacuole homeostasis. J Cell Sci 118:5525–5536.
Gadea A, Schinelli S, Gallo V (2008) Endothelin-1 regulates astrocyte proliferation and reactive gliosis via a JNK/c-Jun signaling pathway. J Neurosci 28:2394–2408.
Gadient RA, Cron KC, Otten U (1990) Interleukin-1 beta and tumor necrosis factor-alpha synergistically stimulate nerve growth factor (NGF) release from cultured rat astrocytes. Neurosci Lett 117:335–340.
Galjart N (2005) CLIPs and CLASPs and cellular dynamics. Nat Rev Mol Cell Biol 6:487–498.
Gallala HD, Sandhoff K (2011) Biological function of the cellular lipid BMP-BMP as a key activator for cholesterol sorting and membrane digestion. Neurochem Res 36:1594–1600.
Gallo F, Morale MC, Spina-Purrello V, Tirolo C, Testa N, Farinella Z, Avola R, Beaudet A, Marchetti B (2000) Basic fibroblast growth factor (bFGF) acts on both neurons and glia to mediate the neurotrophic effects of astrocytes on LHRH neurons in culture. Synapse 36:233–253.
Ganapathi KA, Austin KM, Lee C-S, Dias A, Malsch MM, Reed R, Shimamura A (2007) The human Shwachman-Diamond syndrome protein, SBDS, associates with ribosomal RNA. Blood 110:1458–1465.
García DE, Li B, García-Ferreiro RE, Hernández-Ochoa EO, Yan K, Gautam N, Catterall WA, Mackie K, Hille B (1998) G-protein beta-subunit specificity in the fast membrane-delimited inhibition of Ca2+ channels. J Neurosci 18:9163–9170.
Garden GA, Möller T (2006) Microglia biology in health and disease. J Neuroimmune Pharmacol 1:127–137.
Gardner J, Ghorpade A (2003) Tissue inhibitor of metalloproteinase (TIMP)-1: the TIMPed balance

of matrix metalloproteinases in the central nervous system. J Neurosci Res 74:801–806.
Garnham CP, Roll-Mecak A (2012) The chemical complexity of cellular microtubules: Tubulin post-translational modification enzymes and their roles in tuning microtubule functions. Cytoskeleton (Hoboken) 69:442–463.
Garrido JJ, Giraud P, Carlier E, Fernandes F, Moussif A, Fache M-P, Debanne D, Dargent B (2003) A targeting motif involved in sodium channel clustering at the axonal initial segment. Science 300:2091–2094.
Garthwaite J, Boulton CL (1995) Nitric oxide signaling in the central nervous system. Annu Rev Physiol 57:683–706.
Garwood CJ, Pooler AM, Atherton J, Hanger DP, Noble W (2011) Astrocytes are important mediators of Aβ-induced neurotoxicity and tau phosphorylation in primary culture. Cell Death Dis 2:e167.
Ge W-P, Miyawaki A, Gage FH, Jan YN, Jan LY (2012) Local generation of glia is a major astrocyte source in postnatal cortex. Nature 484:376–380.
Geering K (2005) Function of FXYD proteins, regulators of Na, K-ATPase. J Bioenerg Biomembr 37:387–392.
Geering K (2008) Functional roles of Na,K-ATPase subunits. Curr Opin Nephrol Hypertens 17:526–532.
Gegg ME, Clark JB, Heales SJR (2005) Co-culture of neurones with glutathione deficient astrocytes leads to increased neuronal susceptibility to nitric oxide and increased glutamate-cysteine ligase activity. Brain Res 1036:1–6.
Gennerich A, Vale RD (2009) Walking the walk: how kinesin and dynein coordinate their steps. Curr Opin Cell Biol 21:59–67.
Gerges NZ, Brown TC, Correia SS, Esteban JA (2005) Analysis of Rab protein function in neurotransmitter receptor trafficking at hippocampal synapses. Meth Enzymol 403:153–166.
German DC, Liang C-L, Song T, Yazdani U, Xie C, Dietschy JM (2002) Neurodegeneration in the Niemann-Pick C mouse: glial involvement. Neuroscience 109:437–450.
Getty AL, Benedict JW, Pearce DA (2011) A novel interaction of CLN3 with nonmuscle myosin-IIB and defects in cell motility of Cln3(-/-) cells. Exp Cell Res 317:51–69.
Getty AL, Pearce DA (2011) Interactions of the proteins of neuronal ceroid lipofuscinosis: clues to function. Cell Mol Life Sci 68:453–474.
Ghadge GD, Slusher BS, Bodner A, Canto MD, Wozniak K, Thomas AG, Rojas C, Tsukamoto T, Majer P, Miller RJ, Monti AL, Roos RP (2003) Glutamate carboxypeptidase II inhibition protects motor neurons from death in familial amyotrophic lateral sclerosis models. Proc Natl Acad Sci USA 100:9554–9559.
Giaume C, Fromaget C, Aoumari el A, Cordier J, Glowinski J, Gros D (1991) Gap junctions in cultured astrocytes: single-channel currents and characterization of channel-forming protein. Neuron 6:133–143.
Giaume C, Venance L (1998) Intercellular calcium signaling and gap junctional communication in astrocytes. Glia 24:50–64.
Ginzburg L, Futerman AH (2005) Defective calcium homeostasis in the cerebellum in a mouse model of Niemann-Pick A disease. J Neurochem 95:1619–1628.
Giulian D, Li J, Leara B, Keenen C (1994) Phagocytic microglia release cytokines and cytotoxins that regulate the survival of astrocytes and neurons in culture. Neurochem Int 25:227–233.
Gladden LB (2004) Lactate metabolism: a new paradigm for the third millennium. J Physiol (Lond) 558:5–30.
Glantz LA, Austin MC, Lewis DA (2000) Normal cellular levels of synaptophysin mRNA expression in the prefrontal cortex of subjects with schizophrenia. Biol Psychiatry 48:389–397.
Glantz LA, Lewis DA (1997) Reduction of synaptophysin immunoreactivity in the prefrontal cortex of subjects with schizophrenia. Regional and diagnostic specificity. Arch Gen Psychiatry 54:660–669.
Glantz LA, Lewis DA (2000) Decreased dendritic spine density on prefrontal cortical pyramidal neurons in schizophrenia. Arch Gen Psychiatry 57:65–73.
Goebel HH (1995) The neuronal ceroid-lipofuscinoses. J Child Neurol 10:424–437.
Goebel HH, Wisniewski KE (2004) Current state of clinical and morphological features in human NCL. Brain Pathol 14:61–69.

Golabek AA, Kaczmarski W, Kida E, Kaczmarski A, Michalewski MP, Wisniewski KE (1999) Expression studies of CLN3 protein (battenin) in fusion with the green fluorescent protein in mammalian cells in vitro. Mol Genet Metab 66:277–282.
Golabek AA, Kida E, Walus M, Kaczmarski W, Michalewski M, Wisniewski KE (2000) CLN3 protein regulates lysosomal pH and alters intracellular processing of Alzheimer's amyloid-beta protein precursor and cathepsin D in human cells. Mol Genet Metab 70:203–213.
Gold R, Linker RA, Stangel M (2012) Fumaric acid and its esters: an emerging treatment for multiple sclerosis with antioxidative mechanism of action. Clin Immunol 142:44–48.
Goldberg EM, Clark BD, Zagha E, Nahmani M, Erisir A, Rudy B (2008) K+ channels at the axon initial segment dampen near-threshold excitability of neocortical fast-spiking GABAergic interneurons. Neuron 58:387–400.
Goldberg JL (2003) How does an axon grow? Genes Dev 17:941–958.
Goldberg JL, Espinosa JS, Xu Y, Davidson N, Kovacs GTA, Barres BA (2002) Retinal ganglion cells do not extend axons by default: promotion by neurotrophic signaling and electrical activity. Neuron 33:689–702.
Goldstein LS, Yang Z (2000) Microtubule-based transport systems in neurons: the roles of kinesins and dyneins. Annu Rev Neurosci 23:39–71.
Gomi H, Yokoyama T, Fujimoto K, Ikeda T, Katoh A, Itoh T, Itohara S (1995) Mice devoid of the glial fibrillary acidic protein develop normally and are susceptible to scrapie prions. Neuron 14:29–41.
Goodman Y, Mattson MP (1994) Secreted forms of beta-amyloid precursor protein protect hippocampal neurons against amyloid beta-peptide-induced oxidative injury. Exp Neurol 128:1–12.
Gordon GRJ, Mulligan SJ, Macvicar BA (2007) Astrocyte control of the cerebrovasculature. Glia 55:1214–1221.
Gordon-Weeks PR (2004) Microtubules and growth cone function. J Neurobiol 58:70–83.
Gorina R, Font-Nieves M, Márquez-Kisinousky L, Santalucia T, Planas AM (2011) Astrocyte TLR4 activation induces a proinflammatory environment through the interplay between MyD88-dependent NFκB signaling, MAPK, and Jak1/Stat1 pathways. Glia 59:242–255.
Gorji A (2001) Spreading depression: a review of the clinical relevance. Brain Res Brain Res Rev 38:33–60.
Gorji A, Scheller D, Straub H, Tegtmeier F, Köhling R, Höhling JM, Tuxhorn I, Ebner A, Wolf P, Werner Panneck H, Oppel F, Speckmann EJ (2001) Spreading depression in human neocortical slices. Brain Res 906:74–83.
Goubard V, Fino E, Venance L (2011) Contribution of astrocytic glutamate and GABA uptake to corticostriatal information processing. J Physiol (Lond) 589:2301–2319.
Graves TD (2006) Ion channels and epilepsy. QJM 99:201–217.
Greene IP, Lee E-Y, Prow N, Ngwang B, Griffin DE (2008) Protection from fatal viral encephalomyelitis: AMPA receptor antagonists have a direct effect on the inflammatory response to infection. Proc Natl Acad Sci USA 105:3575–3580.
Griffey MA, Wozniak D, Wong M, Bible E, Johnson K, Rothman SM, Wentz AE, Cooper JD, Sands MS (2006) CNS-directed AAV2-mediated gene therapy ameliorates functional deficits in a murine model of infantile neuronal ceroid lipofuscinosis. Mol Ther 13:538–547.
Grover LM, Teyler TJ (1993) Role of adenosine in heterosynaptic, posttetanic depression in area CA1 of hippocampus. Neurosci Lett 154:39–42.
Grubb MS, Burrone J (2010a) Building and maintaining the axon initial segment. Curr Opin Neurobiol 20:481–488.
Grubb MS, Burrone J (2010b) Activity-dependent relocation of the axon initial segment fine-tunes neuronal excitability. Nature 465:1070–1074.
Grubb MS, Shu Y, Kuba H, Rasband MN, Wimmer VC, Bender KJ (2011) Short- and long-term plasticity at the axon initial segment. J Neurosci 31:16049–16055.
Gruol DL, Nelson TE (1997) Physiological and pathological roles of interleukin-6 in the central nervous system. Mol Neurobiol 15:307–339.
Grynkiewicz G, Poenie M, Tsien R (1985) A new generation of Ca^{2+} indicators with greatly improved fluorescence properties. JBC, Vol. 260, 3440-3450.
Gstraunthaler G (2003) Alternatives to the use of fetal bovine serum: serum-free cell culture. ALTEX 20:275–281.

Guarneri R, Russo D, Cascio C, D'Agostino S, Galizzi G, Bigini P, Mennini T, Guarneri P (2004) Retinal oxidation, apoptosis and age- and sex-differences in the mnd mutant mouse, a model of neuronal ceroid lipofuscinosis. Brain Res 1014:209–220.
Guasch RM, Tomas M, Miñambres R, Valles S, Renau-Piqueras J, Guerri C (2003) RhoA and lysophosphatidic acid are involved in the actin cytoskeleton reorganization of astrocytes exposed to ethanol. J Neurosci Res 72:487–502.
Guerini D, Coletto L, Carafoli E (2005) Exporting calcium from cells. Cell Calcium 38:281–289.
Guix FX, Uribesalgo I, Coma M, Muñoz FJ (2005) The physiology and pathophysiology of nitric oxide in the brain. Prog Neurobiol 76:126–152.
Gunteski-Hamblin AM, Greeb J, Shull GE (1988) A novel Ca2+ pump expressed in brain, kidney, and stomach is encoded by an alternative transcript of the slow-twitch muscle sarcoplasmic reticulum Ca-ATPase gene. Identification of cDNAs encoding Ca2+ and other cation-transporting ATPases using an oligonucleotide probe derived from the ATP-binding site. J Biol Chem 263:15032–15040.
Guthrie PB, Knappenberger J, Segal M, Bennett MV, Charles AC, Kater SB (1999) ATP released from astrocytes mediates glial calcium waves. J Neurosci 19:520–528.
Gutierrez MG, Munafó DB, Berón W, Colombo MI (2004) Rab7 is required for the normal progression of the autophagic pathway in mammalian cells. J Cell Sci 117:2687–2697.
Haber M, Zhou L, Murai KK (2006) Cooperative astrocyte and dendritic spine dynamics at hippocampal excitatory synapses. J Neurosci 26:8881–8891.
Hachiya Y, Hayashi M, Kumada S, Uchiyama A, Tsuchiya K, Kurata K (2006) Mechanisms of neurodegeneration in neuronal ceroid-lipofuscinoses. Acta Neuropathol 111:168–177.
Hadjikhani N, Sanchez Del Rio M, Wu O, Schwartz D, Bakker D, Fischl B, Kwong KK, Cutrer FM, Rosen BR, Tootell RB, Sorensen AG, Moskowitz MA (2001) Mechanisms of migraine aura revealed by functional MRI in human visual cortex. Proc Natl Acad Sci USA 98:4687–4692.
Hailer NP, Vogt C, Korf H-W, Dehghani F (2005) Interleukin-1beta exacerbates and interleukin-1 receptor antagonist attenuates neuronal injury and microglial activation after excitotoxic damage in organotypic hippocampal slice cultures. Eur J Neurosci 21:2347–2360.
Hailer NP, Wirjatijasa F, Roser N, Hischebeth GT, Korf HW, Dehghani F (2001) Astrocytic factors protect neuronal integrity and reduce microglial activation in an in vitro model of N-methyl-D-aspartate-induced excitotoxic injury in organotypic hippocampal slice cultures. Eur J Neurosci 14:315–326.
Halassa MM, Fellin T, Takano H, Dong J-H, Haydon PG (2007) Synaptic islands defined by the territory of a single astrocyte. J Neurosci 27:6473–6477.
Halassa MM, Haydon PG (2010) Integrated brain circuits: astrocytic networks modulate neuronal activity and behavior. Annu Rev Physiol 72:335–355.
Hald A, Lotharius J (2005) Oxidative stress and inflammation in Parkinson's disease: is there a causal link? Exp Neurol 193:279–290.
Hall A (1998) Rho GTPases and the actin cytoskeleton. Science 279:509–514.
Halliwell B (2006) Oxidative stress and neurodegeneration: where are we now? J Neurochem 97:1634–1658.
Haltia M (2003) The neuronal ceroid-lipofuscinoses. J Neuropathol Exp Neurol 62:1–13.
Haltia M (2006) The neuronal ceroid-lipofuscinoses: from past to present. Biochim Biophys Acta 1762:850–856.
Haltia M, Goebel HH (2012) The neuronal ceroid-lipofuscinoses: A historical introduction. Biochim Biophys Acta.
Haltia M, Herva R, Suopanki J, Baumann M, Tyynelä J (2001) Hippocampal lesions in the neuronal ceroid lipofuscinoses. Eur J Paediatr Neurol 5 Suppl A:209–211.
Hamby ME, Hewett JA, Hewett SJ (2008) TGF-beta1 reduces the heterogeneity of astrocytic cyclooxygenase-2 and nitric oxide synthase-2 gene expression in a stimulus-independent manner. Prostaglandins Other Lipid Mediat 85:115–124.
Hamby ME, Sofroniew MV (2010) Reactive astrocytes as therapeutic targets for CNS disorders. Neurotherapeutics 7:494–506.
Hamill CE, Goldshmidt A, Nicole O, McKeon RJ, Brat DJ, Traynelis SF (2005) Special lecture: glial reactivity after damage: implications for scar formation and neuronal recovery. Clin Neurosurg 52:29–44.
Hamilton N, Vayro S, Kirchhoff F, Verkhratsky A, Robbins J, Gorecki DC, Butt AM (2008)

Mechanisms of ATP- and glutamate-mediated calcium signaling in white matter astrocytes. Glia 56:734–749.
Hamilton SL (2005) Ryanodine receptors. Cell Calcium 38:253–260.
Hangan D, Morris VL, Boeters L, Ballestrem von C, Uniyal S, Chan BM (1997) An epitope on VLA-6 (alpha6beta1) integrin involved in migration but not adhesion is required for extravasation of murine melanoma B16F1 cells in liver. Cancer Res 57:3812–3817.
Hansen SM, Berezin V, Bock E (2008) Signaling mechanisms of neurite outgrowth induced by the cell adhesion molecules NCAM and N-cadherin. Cell Mol Life Sci 65:3809–3821.
Hansson E, Rönnbäck L (2003) Glial neuronal signaling in the central nervous system. FASEB J 17:341–348.
Harada A, Teng J, Takei Y, Oguchi K, Hirokawa N (2002) MAP2 is required for dendrite elongation, PKA anchoring in dendrites, and proper PKA signal transduction. J Cell Biol 158:541–549.
Haskell RE, Carr CJ, Pearce DA, Bennett MJ, Davidson BL (2000) Batten disease: evaluation of CLN3 mutations on protein localization and function. Hum Mol Genet 9:735–744.
Haspel RL, Salditt-Georgieff M, Darnell JE (1996) The rapid inactivation of nuclear tyrosine phosphorylated Stat1 depends upon a protein tyrosine phosphatase. EMBO J 15:6262–6268.
Hassinger TD, Atkinson PB, Strecker GJ, Whalen LR, Dudek FE, Kossel AH, Kater SB (1995) Evidence for glutamate-mediated activation of hippocampal neurons by glial calcium waves. J Neurobiol 28:159–170.
HAWKINS A, OLSZEWSKI J (1957) Glia/nerve cell index for cortex of the whale. Science 126:76–77.
Haydon PG (2001) GLIA: listening and talking to the synapse. Nat Rev Neurosci 2:185–193.
Haynes SE, Hollopeter G, Yang G, Kurpius D, Dailey ME, Gan W-B, Julius D (2006) The P2Y12 receptor regulates microglial activation by extracellular nucleotides. Nat Neurosci 9:1512–1519.
Hazell AS (2007) Excitotoxic mechanisms in stroke: an update of concepts and treatment strategies. Neurochem Int 50:941–953.
Häusser M (2007) Dendrites. Oxford University Press, USA.
Heales SJ, Barker JE, Stewart VC, Brand MP, Hargreaves IP, Foppa P, Land JM, Clark JB, Bolaños JP (1997) Nitric oxide, energy metabolism and neurological disease. Biochem Soc Trans 25:939–943.
Heales SJ, Bolaños JP, Clark JB (1996) Glutathione depletion is accompanied by increased neuronal nitric oxide synthase activity. Neurochem Res 21:35–39.
Heales SJR, Lam AAJ, Duncan AJ, Land JM (2004) Neurodegeneration or neuroprotection: the pivotal role of astrocytes. Neurochem Res 29:513–519.
Heasman SJ, Ridley AJ (2008) Mammalian Rho GTPases: new insights into their functions from in vivo studies. Nat Rev Mol Cell Biol 9:690–701.
Heerssen HM, Pazyra MF, Segal RA (2004) Dynein motors transport activated Trks to promote survival of target-dependent neurons. Nat Neurosci 7:596–604.
Heese K, Fiebich BL, Bauer J, Otten U (1997) Nerve growth factor (NGF) expression in rat microglia is induced by adenosine A2a-receptors. Neurosci Lett 231:83–86.
Heine C, Tyynelä J, Cooper JD, Palmer DN, Elleder M, Kohlschütter A, Braulke T (2003) Enhanced expression of manganese-dependent superoxide dismutase in human and sheep CLN6 tissues. Biochem J 376:369–376.
Heinonen O, Kyttälä A, Lehmus E, Paunio T, Peltonen L, Jalanko A (2000) Expression of palmitoyl protein thioesterase in neurons. Mol Genet Metab 69:123–129.
Heinonen O, Soininen H, Sorvari H, Kosunen O, Paljärvi L, Koivisto E, Riekkinen PJ (1995) Loss of synaptophysin-like immunoreactivity in the hippocampal formation is an early phenomenon in Alzheimer's disease. Neuroscience 64:375–384.
Henderson LP, Lin L, Prasad A, Paul CA, Chang TY, Maue RA (2000) Embryonic striatal neurons from niemann-pick type C mice exhibit defects in cholesterol metabolism and neurotrophin responsiveness. J Biol Chem 275:20179–20187.
Henneberger C, Papouin T, Oliet SHR, Rusakov DA (2010) Long-term potentiation depends on release of D-serine from astrocytes. Nature 463:232–236.
Henrich-Noack P, Prehn JH, Krieglstein J (1996) TGF-beta 1 protects hippocampal neurons against degeneration caused by transient global ischemia. Dose-response relationship and potential neuroprotective mechanisms. Stroke 27:1609–14–discussion1615.
Herrera-Molina R, Bernhardi von R (2005) Transforming growth factor-beta 1 produced by

hippocampal cells modulates microglial reactivity in culture. Neurobiol Dis 19:229–236.
Herrmann P, Druckrey-Fiskaaen C, Kouznetsova E, Heinitz K, Bigl M, Cotman SL, Schliebs R (2008) Developmental impairments of select neurotransmitter systems in brains of Cln3(Deltaex7/8) knock-in mice, an animal model of juvenile neuronal ceroid lipofuscinosis. J Neurosci Res 86:1857–1870.
HERS HG (1963) alpha-Glucosidase deficiency in generalized glycogenstorage disease (Pompe's disease). Biochem J 86:11–16.
HERS HG (1965) INBORN LYSOSOMAL DISEASES. Gastroenterology 48:625–633.
Hertz L, Zielke HR (2004) Astrocytic control of glutamatergic activity: astrocytes as stars of the show. Trends Neurosci 27:735–743.
Herva R, Tyynelä J, Hirvasniemi A, Syrjäkallio-Ylitalo M, Haltia M (2000) Northern epilepsy: a novel form of neuronal ceroid-lipofuscinosis. Brain Pathol 10:215–222.
Herx LM, Rivest S, Yong VW (2000) Central nervous system-initiated inflammation and neurotrophism in trauma: IL-1 beta is required for the production of ciliary neurotrophic factor. J Immunol 165:2232–2239.
Herx LM, Yong VW (2001) Interleukin-1 beta is required for the early evolution of reactive astrogliosis following CNS lesion. J Neuropathol Exp Neurol 60:961–971.
Hesling C, Oliveira CC, Castilho BA, Zanchin NIT (2007) The Shwachman-Bodian-Diamond syndrome associated protein interacts with HsNip7 and its down-regulation affects gene expression at the transcriptional and translational levels. Exp Cell Res 313:4180–4195.
Hess EJ, Collins KA, Wilson MC (1996) Mouse model of hyperkinesis implicates SNAP-25 in behavioral regulation. J Neurosci 16:3104–3111.
Hesse M, Magin TM, Weber K (2001) Genes for intermediate filament proteins and the draft sequence of the human genome: novel keratin genes and a surprisingly high number of pseudogenes related to keratin genes 8 and 18. J Cell Sci 114:2569–2575.
Hesselgesser J, Horuk R (1999) Chemokine and chemokine receptor expression in the central nervous system. J Neurovirol 5:13–26.
Hewett SJ (1999) Interferon-gamma reduces cyclooxygenase-2-mediated prostaglandin E2 production from primary mouse astrocytes independent of nitric oxide formation. J Neuroimmunol 94:134–143.
Hewett SJ, Corbett JA, McDaniel ML, Choi DW (1993) Interferon-gamma and interleukin-1 beta induce nitric oxide formation from primary mouse astrocytes. Neurosci Lett 164:229–232.
Hide I, Tanaka M, Inoue A, Nakajima K, Kohsaka S, Inoue K, Nakata Y (2000) Extracellular ATP triggers tumor necrosis factor-alpha release from rat microglia. J Neurochem 75:965–972.
Higuchi M, Onishi K, Masuyama N, Gotoh Y (2003) The phosphatidylinositol-3 kinase (PI3K)-Akt pathway suppresses neurite branch formation in NGF-treated PC12 cells. Genes Cells 8:657–669.
HILD W, TASAKI I (1962) Morphological and physiological properties of neurons and glial cells in tissue culture. J Neurophysiol 25:277–304.
Hipfner DR, Deeley RG, Cole SP (1999) Structural, mechanistic and clinical aspects of MRP1. Biochim Biophys Acta 1461:359–376.
Hirase H, Qian L, Barthó P, Buzsáki G (2004) Calcium dynamics of cortical astrocytic networks in vivo. PLoS Biol 2:E96.
Hirokawa N (2011) From electron microscopy to molecular cell biology, molecular genetics and structural biology: intracellular transport and kinesin superfamily proteins, KIFs: genes, structure, dynamics and functions. J Electron Microsc (Tokyo) 60 Suppl 1:S63–S92.
Hirrlinger J, Schulz JB, Dringen R (2002) Glutathione release from cultured brain cells: multidrug resistance protein 1 mediates the release of GSH from rat astroglial cells. J Neurosci Res 69:318–326.
Hirsch MR, Wietzerbin J, Pierres M, Goridis C (1983) Expression of Ia antigens by cultured astrocytes treated with gamma-interferon. Neurosci Lett 41:199–204.
Hobert JA, Dawson G (2007) A novel role of the Batten disease gene CLN3: association with BMP synthesis. Biochem Biophys Res Commun 358:111–116.
Hobert O (2009) Development of Neural Circuitry.
Hock C, Heese K, Müller-Spahn F, Hulette C, Rosenberg C, Otten U (1998) Decreased trkA neurotrophin receptor expression in the parietal cortex of patients with Alzheimer's disease. Neurosci Lett 241:151–154.

Hock CH, Heese K, Olivieri G, Hulette CH, Rosenberg C, Nitsch RM, Otten U (2000) Alterations in neurotrophins and neurotrophin receptors in Alzheimer's disease. J Neural Transm Suppl 59:171–174.
Hocquemiller M, Vitry S, Bigou S, Bruyère J, Ausseil J, Heard JM (2010) GAP43 overexpression and enhanced neurite outgrowth in mucopolysaccharidosis type IIIB cortical neuron cultures. J Neurosci Res 88:202–213.
Holán V, Krulová M, Zajícová A, Pindjáková J (2002) Nitric oxide as a regulatory and effector molecule in the immune system. Mol Immunol 38:989–995.
Holopainen JM, Saarikoski J, Kinnunen PK, Järvelä I (2001) Elevated lysosomal pH in neuronal ceroid lipofuscinoses (NCLs). Eur J Biochem 268:5851–5856.
Hopwood JJ, Bunge S, Morris CP, Wilson PJ, Steglich C, Beck M, Schwinger E, Gal A (1993) Molecular basis of mucopolysaccharidosis type II: mutations in the iduronate-2-sulphatase gene. Hum Mutat 2:435–442.
Horner PJ, Gage FH (2000) Regenerating the damaged central nervous system. Nature 407:963–970.
Horner PJ, Power AE, Kempermann G, Kuhn HG, Palmer TD, Winkler J, Thal LJ, Gage FH (2000) Proliferation and differentiation of progenitor cells throughout the intact adult rat spinal cord. J Neurosci 20:2218–2228.
Horvath CM (2004) The Jak-STAT pathway stimulated by interferon gamma. Sci STKE 2004:tr8.
Hou Q, Gao X, Zhang X, Kong L, Wang X, Bian W, Tu Y, Jin M, Zhao G, Li B, Jing N, Yu L (2004) SNAP-25 in hippocampal CA1 region is involved in memory consolidation. Eur J Neurosci 20:1593–1603.
Hou Q-L, Gao X, Lu Q, Zhang X-H, Tu Y-Y, Jin M-L, Zhao G-P, Yu L, Jing N-H, Li B-M (2006) SNAP-25 in hippocampal CA3 region is required for long-term memory formation. Biochem Biophys Res Commun 347:955–962.
Hou YJ, Yu AC, Garcia JM, Aotaki-Keen A, Lee YL, Eng LF, Hjelmeland LJ, Menon VK (1995) Astrogliosis in culture. IV. Effects of basic fibroblast growth factor. J Neurosci Res 40:359–370.
Hu J, Akama KT, Krafft GA, Chromy BA, Van Eldik LJ (1998a) Amyloid-beta peptide activates cultured astrocytes: morphological alterations, cytokine induction and nitric oxide release. Brain Res 785:195–206.
Hu J, LaDu MJ, Van Eldik LJ (1998b) Apolipoprotein E attenuates beta-amyloid-induced astrocyte activation. J Neurochem 71:1626–1634.
Hu S, Peterson PK, Chao CC (1997) Cytokine-mediated neuronal apoptosis. Neurochem Int 30:427–431.
Hu W, Tian C, Li T, Yang M, Hou H, Shu Y (2009) Distinct contributions of Na(v)1.6 and Na(v)1.2 in action potential initiation and backpropagation. Nat Neurosci 12:996–1002.
Huang EJ, Reichardt LF (2001) Neurotrophins: roles in neuronal development and function. Annu Rev Neurosci 24:677–736.
Huang EP (1997) Metal ions and synaptic transmission: think zinc. Proc Natl Acad Sci USA 94:13386–13387.
Huang YH, Bergles DE (2004) Glutamate transporters bring competition to the synapse. Curr Opin Neurobiol 14:346–352.
Hughes EG, Maguire JL, McMinn MT, Scholz RE, Sutherland ML (2004) Loss of glial fibrillary acidic protein results in decreased glutamate transport and inhibition of PKA-induced EAAT2 cell surface trafficking. Brain Res Mol Brain Res 124:114–123.
Hutagalung AH, Novick PJ (2011) Role of Rab GTPases in membrane traffic and cell physiology. Physiol Rev 91:119–149.
Iadecola C, Nedergaard M (2007) Glial regulation of the cerebral microvasculature. Nat Neurosci 10:1369–1376.
Ibáñez CF, Simi A (2012) p75 neurotrophin receptor signaling in nervous system injury and degeneration: paradox and opportunity. Trends Neurosci 35:431–440.
Iglesias R, Dahl G, Qiu F, Spray DC, Scemes E (2009) Pannexin 1: the molecular substrate of astrocyte "hemichannels". J Neurosci 29:7092–7097.
Illes P, Verkhratsky A, Burnstock G, Franke H (2012) P2X Receptors and Their Roles in Astroglia in the Central and Peripheral Nervous System. Neuroscientist 18:422–438.
Imai Y, Kohsaka S (2002) Intracellular signaling in M-CSF-induced microglia activation: role of

Iba1. Glia 40:164–174.
Inagaki M, Nakamura Y, Takeda M, Nishimura T, Inagaki N (1994) Glial fibrillary acidic protein: dynamic property and regulation by phosphorylation. Brain Pathol 4:239–243.
Isaac JTR, Ashby MC, McBain CJ (2007) The role of the GluR2 subunit in AMPA receptor function and synaptic plasticity. Neuron 54:859–871.
Isosomppi J, Heinonen O, Hiltunen JO, Greene ND, Vesa J, Uusitalo A, Mitchison HM, Saarma M, Jalanko A, Peltonen L (1999) Developmental expression of palmitoyl protein thioesterase in normal mice. Brain Res Dev Brain Res 118:1–11.
Israels SJ, Gerrard JM, Jacques YV, McNicol A, Cham B, Nishibori M, Bainton DF (1992) Platelet dense granule membranes contain both granulophysin and P-selectin (GMP-140). Blood 80:143–152.
Itoh TJ, Hotani H (2004) Microtubule dynamics and the regulation by microtubule-associated proteins (MAPs). Biol Sci Space 18:116–117.
Ivens S, Kaufer D, Flores LP, Bechmann I, Zumsteg D, Tomkins O, Seiffert E, Heinemann U, Friedman A (2007) TGF-beta receptor-mediated albumin uptake into astrocytes is involved in neocortical epileptogenesis. Brain 130:535–547.
Jack CS, Arbour N, Manusow J, Montgrain V, Blain M, McCrea E, Shapiro A, Antel JP (2005) TLR signaling tailors innate immune responses in human microglia and astrocytes. J Immunol 175:4320–4330.
Jackson IJ (1988) A cDNA encoding tyrosinase-related protein maps to the brown locus in mouse. Proc Natl Acad Sci USA 85:4392–4396.
Jahn R, Südhof TC (1999) Membrane fusion and exocytosis. Annu Rev Biochem 68:863–911.
Jaiswal JK (2001) Calcium - how and why? J Biosci 26:357–363.
Jalanko A, Braulke T (2009) Neuronal ceroid lipofuscinoses. Biochim Biophys Acta 1793:697–709.
Jalonen TO, Margraf RR, Wielt DB, Charniga CJ, Linne ML, Kimelberg HK (1997) Serotonin induces inward potassium and calcium currents in rat cortical astrocytes. Brain Res 758:69–82.
Jan YN, Jan LY (2001) Dendrites. Genes Dev 15:2627–2641.
Jäger S, Bucci C, Tanida I, Ueno T, Kominami E, Saftig P, Eskelinen E-L (2004) Role for Rab7 in maturation of late autophagic vacuoles. J Cell Sci 117:4837–4848.
Järvelä I, Autti T, Lamminranta S, Aberg L, Raininko R, Santavuori P (1997) Clinical and magnetic resonance imaging findings in Batten disease: analysis of the major mutation (1.02-kb deletion). Ann Neurol 42:799–802.
Järvelä I, Lehtovirta M, Tikkanen R, Kyttälä A, Jalanko A (1999) Defective intracellular transport of CLN3 is the molecular basis of Batten disease (JNCL). Hum Mol Genet 8:1091–1098.
Järvelä I, Sainio M, Rantamäki T, Olkkonen VM, Carpén O, Peltonen L, Jalanko A (1998) Biosynthesis and intracellular targeting of the CLN3 protein defective in Batten disease. Hum Mol Genet 7:85–90.
Jeans AF, Oliver PL, Johnson R, Capogna M, Vikman J, Molnár Z, Babbs A, Partridge CJ, Salehi A, Bengtsson M, Eliasson L, Rorsman P, Davies KE (2007) A dominant mutation in Snap25 causes impaired vesicle trafficking, sensorimotor gating, and ataxia in the blind-drunk mouse. Proc Natl Acad Sci USA 104:2431–2436.
Jenkins SM, Bennett V (2001) Ankyrin-G coordinates assembly of the spectrin-based membrane skeleton, voltage-gated sodium channels, and L1 CAMs at Purkinje neuron initial segments. J Cell Biol 155:739–746.
Jin K, Mao XO, Greenberg DA (2006) Vascular endothelial growth factor stimulates neurite outgrowth from cerebral cortical neurons via Rho kinase signaling. J Neurobiol 66:236–242.
Jo DG, Kim MJ, Choi YH, Kim IK, Song YH, Woo HN, Chung CW, Jung YK (2001) Pro-apoptotic function of calsenilin/DREAM/KChIP3. FASEB J 15:589–591.
Jochems CEA, van der Valk JBF, Stafleu FR, Baumans V (2002) The use of fetal bovine serum: ethical or scientific problem? Altern Lab Anim 30:219–227.
Johansson M, Rocha N, Zwart W, Jordens I, Janssen L, Kuijl C, Olkkonen VM, Neefjes J (2007) Activation of endosomal dynein motors by stepwise assembly of Rab7-RILP-p150Glued, ORP1L, and the receptor betalll spectrin. J Cell Biol 176:459–471.
John GR, Lee SC, Brosnan CF (2003) Cytokines: powerful regulators of glial cell activation. Neuroscientist 9:10–22.
John GR, Scemes E, Suadicani SO, Liu JS, Charles PC, Lee SC, Spray DC, Brosnan CF (1999) IL-1beta differentially regulates calcium wave propagation between primary human fetal astrocytes

via pathways involving P2 receptors and gap junction channels. Proc Natl Acad Sci USA 96:11613–11618.
Jones EV, Cook D, Murai KK (2012) A neuron-astrocyte co-culture system to investigate astrocyte-secreted factors in mouse neuronal development. Methods Mol Biol 814:341–352.
Jordan MA, Wilson L (1998) Use of drugs to study role of microtubule assembly dynamics in living cells. Meth Enzymol 298:252–276.
Jordens I, Fernandez-Borja M, Marsman M, Dusseljee S, Janssen L, Calafat J, Janssen H, Wubbolts R, Neefjes J (2001) The Rab7 effector protein RILP controls lysosomal transport by inducing the recruitment of dynein-dynactin motors. Curr Biol 11:1680–1685.
Junaid MA, Pullarkat RK (1999) Increased brain lysosomal pepstatin-insensitive proteinase activity in patients with neurodegenerative diseases. Neurosci Lett 264:157–160.
Juric DM, Carman-Krzan M (2001) Interleukin-1 beta, but not IL-1 alpha, mediates nerve growth factor secretion from rat astrocytes via type I IL-1 receptor. Int J Dev Neurosci 19:675–683.
Juurlink BH, Schültke E, Hertz L (1996) Glutathione release and catabolism during energy substrate restriction in astrocytes. Brain Res 710:229–233.
Kacem K, Lacombe P, Seylaz J, Bonvento G (1998) Structural organization of the perivascular astrocyte endfeet and their relationship with the endothelial glucose transporter: a confocal microscopy study. Glia 23:1–10.
Kaczmarski W, Wisniewski KE, Golabek A, Kaczmarski A, Kida E, Michalewski M (1999) Studies of membrane association of CLN3 protein. Mol Genet Metab 66:261–264.
Kaibuchi K, Kuroda S, Fukata M, Nakagawa M (1999) Regulation of cadherin-mediated cell-cell adhesion by the Rho family GTPases. Curr Opin Cell Biol 11:591–596.
Kalman D, Gomperts SN, Hardy S, Kitamura M, Bishop JM (1999) Ras family GTPases control growth of astrocyte processes. Mol Biol Cell 10:1665–1683.
Kalyanaraman B, Darley-Usmar V, Davies KJA, Dennery PA, Forman HJ, Grisham MB, Mann GE, Moore K, Roberts LJ, Ischiropoulos H (2012) Measuring reactive oxygen and nitrogen species with fluorescent probes: challenges and limitations. Free Radic Biol Med 52:1–6.
Kanai Y, Hediger MA (1992) Primary structure and functional characterization of a high-affinity glutamate transporter. Nature 360:467–471.
Kandel E, Schwartz J, Jessell T, Siegelbaum S, Hudspeth AJ (2012) Principles of Neural Science, Fifth Edition. McGraw-Hill Professional.
Kanemaru K, Okubo Y, Hirose K, Iino M (2007) Regulation of neurite growth by spontaneous Ca2+ oscillations in astrocytes. J Neurosci 27:8957–8966.
Kang J, Jiang L, Goldman SA, Nedergaard M (1998) Astrocyte-mediated potentiation of inhibitory synaptic transmission. Nat Neurosci 1:683–692.
Kao H-T, Song H-J, Porton B, Ming G-L, Hoh J, Abraham M, Czernik AJ, Pieribone VA, Poo M-M, Greengard P (2002) A protein kinase A-dependent molecular switch in synapsins regulates neurite outgrowth. Nat Neurosci 5:431–437.
Kaplan JH (2002) Biochemistry of Na,K-ATPase. Annu Rev Biochem 71:511–535.
Karcher RL, Deacon SW, Gelfand VI (2002) Motor-cargo interactions: the key to transport specificity. Trends Cell Biol 12:21–27.
Karlsson K, Carlsson SR (1998) Sorting of lysosomal membrane glycoproteins lamp-1 and lamp-2 into vesicles distinct from mannose 6-phosphate receptor/gamma-adaptin vesicles at the trans-Golgi network. J Biol Chem 273:18966–18973.
Kash SF, Johnson RS, Tecott LH, Noebels JL, Mayfield RD, Hanahan D, Baekkeskov S (1997) Epilepsy in mice deficient in the 65-kDa isoform of glutamic acid decarboxylase. Proc Natl Acad Sci USA 94:14060–14065.
Kastritsis CH, Salm AK, McCarthy K (1992) Stimulation of the P2Y purinergic receptor on type 1 astroglia results in inositol phosphate formation and calcium mobilization. J Neurochem 58:1277–1284.
Kato H, Takahashi A, Itoyama Y (2003) Cell cycle protein expression in proliferating microglia and astrocytes following transient global cerebral ischemia in the rat. Brain Res Bull 60:215–221.
Katz ML, Gao CL, Prabhakaram M, Shibuya H, Liu PC, Johnson GS (1997) Immunochemical localization of the Batten disease (CLN3) protein in retina. Invest Ophthalmol Vis Sci 38:2375–2386.
Katz ML, Johnson GS, Tullis GE, Lei B (2008) Phenotypic characterization of a mouse model of juvenile neuronal ceroid lipofuscinosis. Neurobiol Dis 29:242–253.

Katz ML, Shibuya H, Liu PC, Kaur S, Gao CL, Johnson GS (1999) A mouse gene knockout model for juvenile ceroid-lipofuscinosis (Batten disease). J Neurosci Res 57:551–556.
Kavalali ET (2002) SNARE interactions in membrane trafficking: a perspective from mammalian central synapses. Bioessays 24:926–936.
Kawajiri A, Yasui Y, Goto H, Tatsuka M, Takahashi M, Nagata K-I, Inagaki M (2003) Functional significance of the specific sites phosphorylated in desmin at cleavage furrow: Aurora-B may phosphorylate and regulate type III intermediate filaments during cytokinesis coordinatedly with Rho-kinase. Mol Biol Cell 14:1489–1500.
Kay GW, Palmer DN, Rezaie P, Cooper JD (2006) Activation of non-neuronal cells within the prenatal developing brain of sheep with neuronal ceroid lipofuscinosis. Brain Pathol 16:110–116.
Kemp JA, McKernan RM (2002) NMDA receptor pathways as drug targets. Nat Neurosci 5 Suppl:1039–1042.
Kettenmann H, Hanisch U-K, Noda M, Verkhratsky A (2011) Physiology of microglia. Physiol Rev 91:461–553.
Kettenmann H, Kirchhoff F, Verkhratsky A (2013) Microglia: new roles for the synaptic stripper. Neuron 77:10–18.
Kettenmann H, Verkhratsky A (2011) [Neuroglia--living nerve glue]. Fortschr Neurol Psychiatr 79:588–597.
Kew JNC, Kemp JA (2005) Ionotropic and metabotropic glutamate receptor structure and pharmacology. Psychopharmacology (Berl) 179:4–29.
Kielar C, Maddox L, Bible E, Pontikis CC, Macauley SL, Griffey MA, Wong M, Sands MS, Cooper JD (2007) Successive neuron loss in the thalamus and cortex in a mouse model of infantile neuronal ceroid lipofuscinosis. Neurobiol Dis 25:150–162.
Kielar C, Wishart TM, Palmer A, Dihanich S, Wong AM, Macauley SL, Chan C-H, Sands MS, Pearce DA, Cooper JD, Gillingwater TH (2009) Molecular correlates of axonal and synaptic pathology in mouse models of Batten disease. Hum Mol Genet 18:4066–4080.
Kielian T (2008) Glial connexins and gap junctions in CNS inflammation and disease. J Neurochem 106:1000–1016.
Kielian T, McMahon M, Bearden ED, Baldwin AC, Drew PD, Esen N (2004) S. aureus-dependent microglial activation is selectively attenuated by the cyclopentenone prostaglandin 15-deoxy-Delta12,14- prostaglandin J2 (15d-PGJ2). J Neurochem 90:1163–1172.
Kim K, Lee S-G, Kegelman TP, Su Z-Z, Das SK, Dash R, Dasgupta S, Barral PM, Hedvat M, Diaz P, Reed JC, Stebbins JL, Pellecchia M, Sarkar D, Fisher PB (2011) Role of excitatory amino acid transporter-2 (EAAT2) and glutamate in neurodegeneration: opportunities for developing novel therapeutics. J Cell Physiol 226:2484–2493.
Kim M-J, Chae SS, Koh YH, Lee SK, Jo SA (2010a) Glutamate carboxypeptidase II: an amyloid peptide-degrading enzyme with physiological function in the brain. FASEB J 24:4491–4502.
Kim S-J, Zhang Z, Saha A, Sarkar C, Zhao Z, Xu Y, Mukherjee AB (2010b) Omega-3 and omega-6 fatty acids suppress ER- and oxidative stress in cultured neurons and neuronal progenitor cells from mice lacking PPT1. Neurosci Lett 479:292–296.
Kim S-J, Zhang Z, Sarkar C, Tsai P-C, Lee Y-C, Dye L, Mukherjee AB (2008) Palmitoyl protein thioesterase-1 deficiency impairs synaptic vesicle recycling at nerve terminals, contributing to neuropathology in humans and mice. J Clin Invest 118:3075–3086.
Kim Y, Ramirez-Montealegre D, Pearce DA (2003) A role in vacuolar arginine transport for yeast Btn1p and for human CLN3, the protein defective in Batten disease. Proc Natl Acad Sci USA 100:15458–15462.
Kimelberg HK (2010) Functions of mature mammalian astrocytes: a current view. Neuroscientist 16:79–106.
Kimelberg HK, Nedergaard M (2010) Functions of astrocytes and their potential as therapeutic targets. Neurotherapeutics 7:338–353.
Kimura K, Mizoguchi A, Ide C (2003) Regulation of growth cone extension by SNARE proteins. J Histochem Cytochem 51:429–433.
Kingwell K (2012) Neurodegenerative disease: Microglia in early disease stages. Nat Rev Neurol 8:475.
Kirischuk S, Tuschick S, Verkhratsky A, Kettenmann H (1996) Calcium signalling in mouse Bergmann glial cells mediated by alpha1-adrenoreceptors and H1 histamine receptors. Eur J

Neurosci 8:1198–1208.
Kiryushko D, Berezin V, Bock E (2004) Regulators of neurite outgrowth: role of cell adhesion molecules. Ann N Y Acad Sci 1014:140–154.
Kiselyov K, Jennigs JJ, Rbaibi Y, Chu CT (2007) Autophagy, mitochondria and cell death in lysosomal storage diseases. Autophagy 3:259–262.
Kitayama M, Ueno M, Itakura T, Yamashita T (2011) Activated microglia inhibit axonal growth through RGMa. PLoS ONE 6:e25234.
Kittler JT, Delmas P, Jovanovic JN, Brown DA, Smart TG, Moss SJ (2000) Constitutive endocytosis of GABAA receptors by an association with the adaptin AP2 complex modulates inhibitory synaptic currents in hippocampal neurons. J Neurosci 20:7972–7977.
Kitzmüller C, Haines RL, Codlin S, Cutler DF, Mole SE (2008) A function retained by the common mutant CLN3 protein is responsible for the late onset of juvenile neuronal ceroid lipofuscinosis. Hum Mol Genet 17:303–312.
Kizhatil K, Sandhu NK, Peachey NS, Bennett V (2009) Ankyrin-B is required for coordinated expression of beta-2-spectrin, the Na/K-ATPase and the Na/Ca exchanger in the inner segment of rod photoreceptors. Exp Eye Res 88:57–64.
Klassen T, Davis C, Goldman A, Burgess D, Chen T, Wheeler D, McPherson J, Bourquin T, Lewis L, Villasana D, Morgan M, Muzny D, Gibbs R, Noebels J (2011) Exome sequencing of ion channel genes reveals complex profiles confounding personal risk assessment in epilepsy. Cell 145:1036–1048.
Koch G, Smith M, Macer D, Webster P, Mortara R (1986) Endoplasmic reticulum contains a common, abundant calcium-binding glycoprotein, endoplasmin. J Cell Sci 86:217–232.
Koch S, Molchanova SM, Wright AK, Edwards A, Cooper JD, Taira T, Gillingwater TH, Tyynelä J (2011) Morphologic and functional correlates of synaptic pathology in the cathepsin D knockout mouse model of congenital neuronal ceroid lipofuscinosis. J Neuropathol Exp Neurol 70:1089–1096.
Kohsaka S, Hamanoue M, Nakajima K (1996) Functional implication of secretory proteases derived from microglia in the central nervous system. Keio J Med 45:263–269.
Koike M, Shibata M, Ohsawa Y, Nakanishi H, Koga T, Kametaka S, Waguri S, Momoi T, Kominami E, Peters C, Figura KV, Saftig P, Uchiyama Y (2003) Involvement of two different cell death pathways in retinal atrophy of cathepsin D-deficient mice. Mol Cell Neurosci 22:146–161.
Kole MHP, Ilschner SU, Kampa BM, Williams SR, Ruben PC, Stuart GJ (2008) Action potential generation requires a high sodium channel density in the axon initial segment. Nat Neurosci 11:178–186.
Kole MHP, Letzkus JJ, Stuart GJ (2007) Axon initial segment Kv1 channels control axonal action potential waveform and synaptic efficacy. Neuron 55:633–647.
Kolluri N, Sun Z, Sampson AR, Lewis DA (2005) Lamina-specific reductions in dendritic spine density in the prefrontal cortex of subjects with schizophrenia. Am J Psychiatry 162:1200–1202.
Komada M, Soriano P (2002) [Beta]IV-spectrin regulates sodium channel clustering through ankyrin-G at axon initial segments and nodes of Ranvier. J Cell Biol 156:337–348.
Komuro H, Rakic P (1993) Modulation of neuronal migration by NMDA receptors. Science 260:95–97.
Komuro H, Rakic P (1998) Orchestration of neuronal migration by activity of ion channels, neurotransmitter receptors, and intracellular Ca2+ fluctuations. J Neurobiol 37:110–130.
Kondo K, Hashimoto H, Kitanaka J, Sawada M, Suzumura A, Marunouchi T, Baba A (1995) Expression of glutamate transporters in cultured glial cells. Neurosci Lett 188:140–142.
Kopra O, Vesa J, Schantz von C, Manninen T, Minye H, Fabritius A-L, Rapola J, van Diggelen OP, Saarela J, Jalanko A, Peltonen L (2004) A mouse model for Finnish variant late infantile neuronal ceroid lipofuscinosis, CLN5, reveals neuropathology associated with early aging. Hum Mol Genet 13:2893–2906.
Kornfeld S, Mellman I (1989) The biogenesis of lysosomes. Annu Rev Cell Biol 5:483–525.
Korolchuk VI, Rubinsztein DC (2011) Regulation of autophagy by lysosomal positioning. Autophagy 7:927–928.
Korolchuk VI, Saiki S, Lichtenberg M, Siddiqi FH, Roberts EA, Imarisio S, Jahreiss L, Sarkar S, Futter M, Menzies FM, O'Kane CJ, Deretic V, Rubinsztein DC (2011) Lysosomal positioning coordinates cellular nutrient responses. Nat Cell Biol 13:453–460.

Kousi M, Lehesjoki A-E, Mole SE (2012) Update of the mutation spectrum and clinical correlations of over 360 mutations in eight genes that underlie the neuronal ceroid lipofuscinoses. Hum Mutat 33:42–63.
Kovács AD, Pearce DA (2008) Attenuation of AMPA receptor activity improves motor skills in a mouse model of juvenile Batten disease. Exp Neurol 209:288–291.
Kovács AD, Saje A, Wong A, Ramji S, Cooper JD, Pearce DA (2012) Age-dependent therapeutic effect of memantine in a mouse model of juvenile Batten disease. Neuropharmacology 63:769–775.
Kovács AD, Saje A, Wong A, Szénási G, Kiricsi P, Szabó E, Cooper JD, Pearce DA (2011) Temporary inhibition of AMPA receptors induces a prolonged improvement of motor performance in a mouse model of juvenile Batten disease. Neuropharmacology 60:405–409.
Kovács AD, Weimer JM, Pearce DA (2006) Selectively increased sensitivity of cerebellar granule cells to AMPA receptor-mediated excitotoxicity in a mouse model of Batten disease. Neurobiol Dis 22:575–585.
Kozlov AS, Angulo MC, Audinat E, Charpak S (2006) Target cell-specific modulation of neuronal activity by astrocytes. Proc Natl Acad Sci USA 103:10058–10063.
Krabbe G, Matyash V, Pannasch U, Mamer L, Boddeke HWGM, Kettenmann H (2012) Activation of serotonin receptors promotes microglial injury-induced motility but attenuates phagocytic activity. Brain Behav Immun 26:419–428.
Krämer H, Phistry M (1996) Mutations in the Drosophila hook gene inhibit endocytosis of the boss transmembrane ligand into multivesicular bodies. J Cell Biol 133:1205–1215.
Krämer H, Phistry M (1999) Genetic analysis of hook, a gene required for endocytic trafficking in drosophila. Genetics 151:675–684.
Kreft M, Potokar M, Stenovec M, Pangrsic T, Zorec R (2009) Regulated exocytosis and vesicle trafficking in astrocytes. Ann N Y Acad Sci 1152:30–42.
Kremmidiotis G, Lensink IL, Bilton RL, Woollatt E, Chataway TK, Sutherland GR, Callen DF (1999) The Batten disease gene product (CLN3p) is a Golgi integral membrane protein. Hum Mol Genet 8:523–531.
Krieglstein K, Reuss B, Maysinger D, Unsicker K (1998) Short communication: transforming growth factor-beta mediates the neurotrophic effect of fibroblast growth factor-2 on midbrain dopaminergic neurons. Eur J Neurosci 10:2746–2750.
Krieglstein K, Suter-Crazzolara C, Fischer WH, Unsicker K (1995) TGF-beta superfamily members promote survival of midbrain dopaminergic neurons and protect them against MPP+ toxicity. EMBO J 14:736–742.
Kriegstein A, Alvarez-Buylla A (2009) The glial nature of embryonic and adult neural stem cells. Annu Rev Neurosci 32:149–184.
Krohne TU, Herrmann P, Kopitz J, Rüther K, Holz FG (2010) [Juvenile neuronal ceroid lipofuscinosis. Ophthalmologic findings and differential diagnosis]. Ophthalmologe 107:606–611.
Kuchibhotla KV, Lattarulo CR, Hyman BT, Bacskai BJ (2009) Synchronous hyperactivity and intercellular calcium waves in astrocytes in Alzheimer mice. Science Vol. 323 no 5918 pp. 1211-1215.
Kuga N, Sasaki T, Takahara Y, Matsuki N, Ikegaya Y (2011) Large-scale calcium waves traveling through astrocytic networks in vivo. J Neurosci 31:2607–2614.
Kuhlman P, Moy VT, Lollo BA, Brian AA (1991) The accessory function of murine intercellular adhesion molecule-1 in T lymphocyte activation. Contributions of adhesion and co-activation. J Immunol 146:1773–1782.
Kunkler PE, Kraig RP (1998) Calcium waves precede electrophysiological changes of spreading depression in hippocampal organ cultures. J Neurosci 18:3416–3425.
Kuronen M, Lehesjoki A-E, Jalanko A, Cooper JD, Kopra O (2012) Selective spatiotemporal patterns of glial activation and neuron loss in the sensory thalamocortical pathways of neuronal ceroid lipofuscinosis 8 mice. Neurobiol Dis 47:444–457.
Kushima Y, Hama T, Hatanaka H (1992) Interleukin-6 as a neurotrophic factor for promoting the survival of cultured catecholaminergic neurons in a chemically defined medium from fetal and postnatal rat midbrains. Neurosci Res 13:267–280.
Kyttälä A, Ihrke G, Vesa J, Schell MJ, Luzio JP (2004) Two motifs target Batten disease protein CLN3 to lysosomes in transfected nonneuronal and neuronal cells. Mol Biol Cell 15:1313–

1323.
Kyttälä A, Yliannala K, Schu P, Jalanko A, Luzio JP (2005) AP-1 and AP-3 facilitate lysosomal targeting of Batten disease protein CLN3 via its dileucine motif. J Biol Chem 280:10277–10283.
Lacas-Gervais S, Guo J, Strenzke N, Scarfone E, Kolpe M, Jahkel M, De Camilli P, Moser T, Rasband MN, Solimena M (2004) BetaIVSigma1 spectrin stabilizes the nodes of Ranvier and axon initial segments. J Cell Biol 166:983–990.
Laird MD, Sukumari-Ramesh S, Swift AEB, Meiler SE, Vender JR, Dhandapani KM (2010) Curcumin attenuates cerebral edema following traumatic brain injury in mice: a possible role for aquaporin-4? J Neurochem 113:637–648.
Lalonde S, Ehrhardt DW, Loqué D, Chen J, Rhee SY, Frommer WB (2008) Molecular and cellular approaches for the detection of protein-protein interactions: latest techniques and current limitations. Plant J 53:610–635.
Lamaze C, Fujimoto LM, Yin HL, Schmid SL (1997) The actin cytoskeleton is required for receptor-mediated endocytosis in mammalian cells. J Biol Chem 272:20332–20335.
Lamminranta S, Aberg LE, Autti T, Moren R, Laine T, Kaukoranta J, Santavuori P (2001) Neuropsychological test battery in the follow-up of patients with juvenile neuronal ceroid lipofuscinosis. J Intellect Disabil Res 45:8–17.
Lane SC, Jolly RD, Schmechel DE, Alroy J, Boustany RM (1996) Apoptosis as the mechanism of neurodegeneration in Batten's disease. J Neurochem 67:677–683.
Lange SC, Bak LK, Waagepetersen HS, Schousboe A, Norenberg MD (2012) Primary Cultures of Astrocytes: Their Value in Understanding Astrocytes in Health and Disease. Neurochem Res.
Larsson A, Wilhelmsson U, Pekna M, Pekny M (2004) Increased cell proliferation and neurogenesis in the hippocampal dentate gyrus of old GFAP(-/-)Vim(-/-) mice. Neurochem Res 29:2069–2073.
Larsson E, Nanobashvili A, Kokaia Z, Lindvall O (1999) Evidence for neuroprotective effects of endogenous brain-derived neurotrophic factor after global forebrain ischemia in rats. J Cereb Blood Flow Metab 19:1220–1228.
Lascola CD, Nelson DJ, Kraig RP (1998) Cytoskeletal actin gates a Cl- channel in neocortical astrocytes. J Neurosci 18:1679–1692.
Latour I, Hamid J, Beedle AM, Zamponi GW, Macvicar BA (2003) Expression of voltage-gated Ca2+ channel subtypes in cultured astrocytes. Glia 41:347–353.
Latour I, Louw DF, Beedle AM, Hamid J, Sutherland GR, Zamponi GW (2004) Expression of T-type calcium channel splice variants in human glioma. Glia 48:112–119.
Lauritzen M (1994) Pathophysiology of the migraine aura. The spreading depression theory. Brain 117 (Pt 1):199–210.
Laywell ED, Dörries U, Bartsch U, Faissner A, Schachner M, Steindler DA (1992) Enhanced expression of the developmentally regulated extracellular matrix molecule tenascin following adult brain injury. Proc Natl Acad Sci USA 89:2634–2638.
Lazarini F, Tham TN, Casanova P, Arenzana-Seisdedos F, Dubois-Dalcq M (2003) Role of the alpha-chemokine stromal cell-derived factor (SDF-1) in the developing and mature central nervous system. Glia 42:139–148.
Leão AA (1986) Spreading depression. Funct Neurol 1:363–366.
LeBlanc JJ, Fagiolini M (2011) Autism: a “critical period” disorder? Neural Plast 2011:921680.
Lebrun A-H, Moll-Khosrawi P, Pohl S, Makrypidi G, Storch S, Kilian D, Streichert T, Otto B, Mole SE, Ullrich K, Cotman S, Kohlschütter A, Braulke T, Schulz A (2011) Analysis of potential biomarkers and modifier genes affecting the clinical course of CLN3 disease. Mol Med 17:1253–1261.
Lee HH, Nemecek D, Schindler C, Smith WJ, Ghirlando R, Steven AC, Bonifacino JS, Hurley JH (2012) Assembly and architecture of biogenesis of lysosome-related organelles complex-1 (BLOC-1). J Biol Chem 287:5882–5890.
Lee S-Y, Haydon PG (2011) A cytokine-dependent switch for glial-neuron interactions. Neuron 69:835–837.
Lee T-S, Kaku T, Takebayashi S, Uchino T, Miyamoto S, Hadama T, Perez-Reyes E, Ono K (2006) Actions of mibefradil, efonidipine and nifedipine block of recombinant T- and L-type Ca channels with distinct inhibitory mechanisms. Pharmacology 78:11–20.
Lee TH, Kato H, Chen ST, Kogure K, Itoyama Y (1998) Expression of nerve growth factor and trkA

after transient focal cerebral ischemia in rats. Stroke 29:1687–96–discussion1697.
Lefrancois S, Zeng J, Hassan AJ, Canuel M, Morales CR (2003) The lysosomal trafficking of sphingolipid activator proteins (SAPs) is mediated by sortilin. EMBO J 22:6430–6437.
Lehnardt S (2010) Innate immunity and neuroinflammation in the CNS: the role of microglia in Toll-like receptor-mediated neuronal injury. Glia 58:253–263.
Lehtovirta M, Kyttälä A, Eskelinen EL, Hess M, Heinonen O, Jalanko A (2001) Palmitoyl protein thioesterase (PPT) localizes into synaptosomes and synaptic vesicles in neurons: implications for infantile neuronal ceroid lipofuscinosis (INCL). Hum Mol Genet 10:69–75.
Leist M, Fava E, Montecucco C, Nicotera P (1997) Peroxynitrite and nitric oxide donors induce neuronal apoptosis by eliciting autocrine excitotoxicity. Eur J Neurosci 9:1488–1498.
Lemkuil BP, Head BP, Pearn ML, Patel HH, Drummond JC, Patel PM (2011) Isoflurane neurotoxicity is mediated by p75NTR-RhoA activation and actin depolymerization. Anesthesiology 114:49–57.
Lepekhin EA, Eliasson C, Berthold CH, Berezin V, Bock E, Pekny M (2001) Intermediate filaments regulate astrocyte motility. J Neurochem 79:617–625.
Leppä S, Saffrich R, Ansorge W, Bohmann D (1998) Differential regulation of c-Jun by ERK and JNK during PC12 cell differentiation. EMBO J 17:4404–4413.
Lerche H, Jurkat-Rott K, Lehmann-Horn F (2001) Ion channels and epilepsy. Am J Med Genet 106:146–159.
Letourneau PC, Kater SB (1991) The Nerve growth cone. Raven Pr.
Letourneau PC, Shattuck TA, Ressler AH (1987) "Pull" and “push” in neurite elongation: observations on the effects of different concentrations of cytochalasin B and taxol. Cell Motil Cytoskeleton 8:193–209.
Leung TCH, Lui CNP, Chen LW, Yung WH, Chan YS, Yung KKL (2012) Ceftriaxone ameliorates motor deficits and protects dopaminergic neurons in 6-hydroxydopamine-lesioned rats. ACS Chem Neurosci 3:22–30.
Levison SW, Goldman JE (1993) Both oligodendrocytes and astrocytes develop from progenitors in the subventricular zone of postnatal rat forebrain. Neuron 10:201–212.
Levison SW, Hudgins SN, Crawford JL (1998) Ciliary neurotrophic factor stimulates nuclear hypertrophy and increases the GFAP content of cultured astrocytes. Brain Res 803:189–193.
Lewis CM et al. (2003) Genome scan meta-analysis of schizophrenia and bipolar disorder, part II: Schizophrenia. Am J Hum Genet 73:34–48.
Li JH, Wang YH, Wolfe BB, Krueger KE, Corsi L, Stocca G, Vicini S (1998) Developmental changes in localization of NMDA receptor subunits in primary cultures of cortical neurons. Eur J Neurosci 10:1704–1715.
Li L et al. (2008) Protective role of reactive astrocytes in brain ischemia. J Cereb Blood Flow Metab 28:468–481.
Li W, Yang Q, Mao Z (2011) Chaperone-mediated autophagy: machinery, regulation and biological consequences. Cell Mol Life Sci 68:749–763.
Liao K-K, Wu M-J, Chen P-Y, Huang S-W, Chiu S-J, Ho C-T, Yen J-H (2012) Curcuminoids promote neurite outgrowth in PC12 cells through MAPK/ERK- and PKC-dependent pathways. J Agric Food Chem 60:433–443.
Liberto CM, Albrecht PJ, Herx LM, Yong VW, Levison SW (2004) Pro-regenerative properties of cytokine-activated astrocytes. J Neurochem 89:1092–1100.
Liedtke W, Edelmann W, Bieri PL, Chiu FC, Cowan NJ, Kucherlapati R, Raine CS (1996) GFAP is necessary for the integrity of CNS white matter architecture and long-term maintenance of myelination. Neuron 17:607–615.
Liesi P, Dahl D, Vaheri A (1983) Laminin is produced by early rat astrocytes in primary culture. J Cell Biol 96:920–924.
Lilliehook C, Chan S, Choi EK, Zaidi NF, Wasco W, Mattson MP, Buxbaum JD (2002) Calsenilin enhances apoptosis by altering endoplasmic reticulum calcium signaling. Mol Cell Neurosci 19:552–559.
Lim MJ, Alexander N, Benedict JW, Chattopadhyay S, Shemilt SJA, Guérin CJ, Cooper JD, Pearce DA (2007) IgG entry and deposition are components of the neuroimmune response in Batten disease. Neurobiol Dis 25:239–251.
Lim MJ, Beake J, Bible E, Curran TM, Ramirez-Montealegre D, Pearce DA, Cooper JD (2006) Distinct patterns of serum immunoreactivity as evidence for multiple brain-directed

autoantibodies in juvenile neuronal ceroid lipofuscinosis. Neuropathol Appl Neurobiol 32:469–482.
Limatola C, Giovannelli A, Maggi L, Ragozzino D, Castellani L, Ciotti MT, Vacca F, Mercanti D, Santoni A, Eusebi F (2000) SDF-1alpha-mediated modulation of synaptic transmission in rat cerebellum. Eur J Neurosci 12:2497–2504.
Lin JW, Ju W, Foster K, Lee SH, Ahmadian G, Wyszynski M, Wang YT, Sheng M (2000) Distinct molecular mechanisms and divergent endocytotic pathways of AMPA receptor internalization. Nat Neurosci 3:1282–1290.
Lin M-S, Lee Y-H, Chiu W-T, Hung K-S (2011) Curcumin provides neuroprotection after spinal cord injury. J Surg Res 166:280–289.
Lin Y-C, Huang Z-H, Jan I-S, Yeh C-C, Wu H-J, Chou Y-C, Chang Y-C (2002) Development of excitatory synapses in cultured neurons dissociated from the cortices of rat embryos and rat pups at birth. J Neurosci Res 67:484–493.
Lindå H, Shupliakov O, Ornung G, Ottersen OP, Storm-Mathisen J, Risling M, Cullheim S (2000) Ultrastructural evidence for a preferential elimination of glutamate-immunoreactive synaptic terminals from spinal motoneurons after intramedullary axotomy. J Comp Neurol 425:10–23.
Lindholm D, Castrén E, Kiefer R, Zafra F, Thoenen H (1992) Transforming growth factor-beta 1 in the rat brain: increase after injury and inhibition of astrocyte proliferation. J Cell Biol 117:395–400.
Lindsay RM, Barde YA, Davies AM, Rohrer H (1985) Differences and similarities in the neurotrophic growth factor requirements of sensory neurons derived from neural crest and neural placode. J Cell Sci Suppl 3:115–129.
Lindvall O, Kokaia Z, Bengzon J, Elmér E, Kokaia M (1994) Neurotrophins and brain insults. Trends Neurosci 17:490–496.
Linthorst AC, Flachskamm C, Barden N, Holsboer F, Reul JM (2000) Glucocorticoid receptor impairment alters CNS responses to a psychological stressor: an in vivo microdialysis study in transgenic mice. Eur J Neurosci 12:283–291.
Lippincott-Schwartz J, Fambrough DM (1986) Lysosomal membrane dynamics: structure and interorganellar movement of a major lysosomal membrane glycoprotein. J Cell Biol 102:1593–1605.
Lipski J, Wan CK, Bai JZ, Pi R, Li D, Donnelly D (2007) Neuroprotective potential of ceftriaxone in in vitro models of stroke. Neuroscience 146: 617-629.
Lipton P, Heimbach CJ (1978) Mechanism of extracellular potassium stimulation of protein synthesis in the in vitro hippocampus. J Neurochem 31:1299–1307.
Liu CW, Lee G, Jay DG (1999) Tau is required for neurite outgrowth and growth cone motility of chick sensory neurons. Cell Motil Cytoskeleton 43:232–242.
Liu W, Brosnan CF, Dickson DW, Lee SC (1994) Macrophage colony-stimulating factor mediates astrocyte-induced microglial ramification in human fetal central nervous system culture. Am J Pathol 145:48–53.
Liu W, Tang Y, Feng J (2011) Cross talk between activation of microglia and astrocytes in pathological conditions in the central nervous system. Life Sci 89:141–146.
Liu XL, Miyakawa A, Aperia A, Krieger P (2007) Na,K-ATPase generates calcium oscillations in hippocampal astrocytes. Neuroreport 18:597–600.
Liu Y, Himes BT, Murray M, Tessler A, Fischer I (2002) Grafts of BDNF-producing fibroblasts rescue axotomized rubrospinal neurons and prevent their atrophy. Exp Neurol 178:150–164.
Llinás R, McGuinness TL, Leonard CS, Sugimori M, Greengard P (1985) Intraterminal injection of synapsin I or calcium/calmodulin-dependent protein kinase II alters neurotransmitter release at the squid giant synapse. Proc Natl Acad Sci USA 82:3035–3039.
Llinás RR (1988) The intrinsic electrophysiological properties of mammalian neurons: insights into central nervous system function. Science 242:1654–1664.
Lloyd-Evans E, Morgan AJ, He X, Smith DA, Elliot-Smith E, Sillence DJ, Churchill GC, Schuchman EH, Galione A, Platt FM (2008) Niemann-Pick disease type C1 is a sphingosine storage disease that causes deregulation of lysosomal calcium. Nat Med 14:1247–1255.
Lloyd-Evans E, Platt FM (2011) Lysosomal Ca(2+) homeostasis: role in pathogenesis of lysosomal storage diseases. Cell Calcium 50:200–205.
Lo C-M, Buxton DB, Chua GCH, Dembo M, Adelstein RS, Wang Y-L (2004) Nonmuscle myosin IIb is

involved in the guidance of fibroblast migration. Mol Biol Cell 15:982–989.
Lo K-J, Luk H-N, Chin T-Y, Chueh S-H (2002) Store depletion-induced calcium influx in rat cerebellar astrocytes. Br J Pharmacol 135:1383–1392.
Lodish H, Berk A, Kaiser CA, Krieger M, Scott MP, Bretscher A, Ploegh H, Matsudaira P (2007) Molecular Cell Biology. W. H. Freeman.
Lonka L, Salonen T, Siintola E, Kopra O, Lehesjoki A-E, Jalanko A (2004) Localization of wild-type and mutant neuronal ceroid lipofuscinosis CLN8 proteins in non-neuronal and neuronal cells. J Neurosci Res 76:862–871.
Losi G, Cammarota M, Carmignoto G (2012) The role of astroglia in the epileptic brain. Front Pharmacol 3:132.
Lu B, Chow A (1999) Neurotrophins and hippocampal synaptic transmission and plasticity. J Neurosci Res 58:76–87.
Lucas S-M, Rothwell NJ, Gibson RM (2006) The role of inflammation in CNS injury and disease. Br J Pharmacol 147 Suppl 1:S232–S240.
Luiro K, Kopra O, Blom T, Gentile M, Mitchison HM, Hovatta I, Törnquist K, Jalanko A (2006) Batten disease (JNCL) is linked to disturbances in mitochondrial, cytoskeletal, and synaptic compartments. J Neurosci Res 84:1124–1138.
Luiro K, Kopra O, Lehtovirta M, Jalanko A (2001) CLN3 protein is targeted to neuronal synapses but excluded from synaptic vesicles: new clues to Batten disease. Hum Mol Genet 10:2123–2131.
Luiro K, Yliannala K, Ahtiainen L, Maunu H, Järvelä I, Kyttälä A, Jalanko A (2004) Interconnections of CLN3, Hook1 and Rab proteins link Batten disease to defects in the endocytic pathway. Hum Mol Genet 13:3017–3027.
Luo Q, Ding Y, Watson K, Zhang J, Fan G-H (2005) N-methyl-D-aspartate attenuates CXCR2-mediated neuroprotection through enhancing the receptor phosphorylation and blocking the receptor recycling. Mol Pharmacol 68:528–537.
Luo X-G, Chen S-D (2012) The changing phenotype of microglia from homeostasis to disease. Transl Neurodegener 1:9.
Luo Y, Batalao A, Zhou H, Zhu L (1997) Mammalian two-hybrid system: a complementary approach to the yeast two-hybrid system. BioTechniques 22:350–352.
Luo Y, Berman MA, Zhai Q, Fischer FR, Abromson-Leeman SR, Zhang Y, Kuziel WA, Gerard C, Dorf ME (2002) RANTES stimulates inflammatory cascades and receptor modulation in murine astrocytes. Glia 39:19–30.
Lushnikova I, Skibo G, Muller D, Nikonenko I (2009) Synaptic potentiation induces increased glial coverage of excitatory synapses in CA1 hippocampus. Hippocampus 19:753–762.
Lutz SE, Zhao Y, Gulinello M, Lee SC, Raine CS, Brosnan CF (2009) Deletion of astrocyte connexins 43 and 30 leads to a dysmyelinating phenotype and hippocampal CA1 vacuolation. J Neurosci 29:7743–7752.
Luzio JP, Pryor PR, Bright NA (2007) Lysosomes: fusion and function. Nat Rev Mol Cell Biol 8:622–632.
Lübke T, Lobel P, Sleat DE (2009) Proteomics of the lysosome. Biochim Biophys Acta 1793:625–635.
Lynch RM, Balaban RS (1987) Coupling of aerobic glycolysis and Na+-K+-ATPase in renal cell line MDCK. Am J Physiol 253:C269–C276.
Ma Y, Liu W, Wang Y, Chao X, Qu Y, Wang K, Fei Z (2011) VEGF protects rat cortical neurons from mechanical trauma injury induced apoptosis via the MEK/ERK pathway. Brain Res Bull 86:441–446.
Macauley SL, Pekny M, Sands MS (2011) The role of attenuated astrocyte activation in infantile neuronal ceroid lipofuscinosis. J Neurosci 31:15575–15585.
Macauley SL, Roberts MS, Wong AM, McSloy F, Reddy AS, Cooper JD, Sands MS (2012) Synergistic effects of central nervous system-directed gene therapy and bone marrow transplantation in the murine model of infantile neuronal ceroid lipofuscinosis. Ann Neurol 71:797–804.
Macauley SL, Wozniak DF, Kielar C, Tan Y, Cooper JD, Sands MS (2009) Cerebellar pathology and motor deficits in the palmitoyl protein thioesterase 1-deficient mouse. Exp Neurol 217:124–135.
Macmillan-Crow LA, Cruthirds DL (2001) Invited review: manganese superoxide dismutase in disease. Free Radic Res 34:325–336.

Maddala R, Reddy VN, Epstein DL, Rao V (2003) Growth factor induced activation of Rho and Rac GTPases and actin cytoskeletal reorganization in human lens epithelial cells. Mol Vis 9:329–336.
Maeda Y, Matsumoto M, Hori O, Kuwabara K, Ogawa S, Yan SD, Ohtsuki T, Kinoshita T, Kamada T, Stern DM (1994) Hypoxia/reoxygenation-mediated induction of astrocyte interleukin 6: a paracrine mechanism potentially enhancing neuron survival. J Exp Med 180:2297–2308.
Maekawa F, Tsuboi T, Fukuda M, Pellerin L (2009) Regulation of the intracellular distribution, cell surface expression, and protein levels of AMPA receptor GluR2 subunits by the monocarboxylate transporter MCT2 in neuronal cells. J Neurochem 109:1767–1778.
Magistretti PJ, Pellerin L (1999) Astrocytes Couple Synaptic Activity to Glucose Utilization in the Brain. News Physiol Sci 14:177–182.
Magnoni S, Baker A, Thomson S, Jordan G, George SJ, McColl BW, McCulloch J, Horsburgh K (2007) Neuroprotective effect of adenoviral-mediated gene transfer of TIMP-1 and -2 in ischemic brain injury. Gene Ther 14:621–625.
Mahmood F, Fu S, Cooke J, Wilson SW, Cooper JD, Russell C (2013) A zebrafish model of CLN2 disease is deficient in Tripeptidyl-peptidase I and displays progressive neurodegeneration accompanied by reduction in proliferation. Brain (In Press).
Majander A, Pihko H, Santavuori P (1995) Palmitate oxidation in muscle mitochondria of patients with the juvenile form of neuronal ceroid-lipofuscinosis. Am J Med Genet 57:298–300.
Majumder S, Zhou LZ, Ransohoff RM (1996) Transcriptional regulation of chemokine gene expression in astrocytes. J Neurosci Res 45:758–769.
Makkerh JPS, Ceni C, Auld DS, Vaillancourt F, Dorval G, Barker PA (2005) p75 neurotrophin receptor reduces ligand-induced Trk receptor ubiquitination and delays Trk receptor internalization and degradation. EMBO Rep 6:936–941.
Malipiero UV, Frei K, Fontana A (1990) Production of hemopoietic colony-stimulating factors by astrocytes. J Immunol 144:3816–3821.
Mallik R, Carter BC, Lex SA, King SJ, Gross SP (2004) Cytoplasmic dynein functions as a gear in response to load. Nature 427:649–652.
Mallik R, Gross SP (2004) Molecular motors: strategies to get along. Curr Biol 14:R971–R982.
Man HY, Ju W, Ahmadian G, Wang YT (2000) Intracellular trafficking of AMPA receptors in synaptic plasticity. Cell Mol Life Sci 57:1526–1534.
Mandelkow E, Mandelkow EM (1994) Microtubule structure. Current Opinion in Structural Biology.
Mandolesi G, Grasselli G, Musumeci G, Centonze D (2010) Cognitive deficits in experimental autoimmune encephalomyelitis: neuroinflammation and synaptic degeneration. Neurol Sci 31:S255–S259.
Maness PF, Schachner M (2007) Neural recognition molecules of the immunoglobulin superfamily: signaling transducers of axon guidance and neuronal migration. Nat Neurosci 10:19–26.
Mao Q, Foster BJ, Xia H, Davidson BL (2003) Membrane topology of CLN3, the protein underlying Batten disease. FEBS Lett 541:40–46.
Marcu MG, Jung Y-J, Lee S, Chung E-J, Lee M-J, Trepel J, Neckers L (2006) Curcumin is an inhibitor of p300 histone acetylatransferase. Med Chem 2:169–174.
Margraf LR, Boriack RL, Routheut AA, Cuppen I, Alhilali L, Bennett CJ, Bennett MJ (1999) Tissue expression and subcellular localization of CLN3, the Batten disease protein. Mol Genet Metab 66:283–289.
Markus A, Patel TD, Snider WD (2002) Neurotrophic factors and axonal growth. Curr Opin Neurobiol 12:523–531.
Marmigère F, Ernfors P (2007) Specification and connectivity of neuronal subtypes in the sensory lineage. Nat Rev Neurosci 8:114–127.
Marsh M, Schmid S, Kern H, Harms E, Male P, Mellman I, Helenius A (1987) Rapid analytical and preparative isolation of functional endosomes by free flow electrophoresis. J Cell Biol 104:875–886.
Marshall CAG, Suzuki SO, Goldman JE (2003) Gliogenic and neurogenic progenitors of the subventricular zone: who are they, where did they come from, and where are they going? Glia 43:52–61.
Martin DL (1992) Synthesis and release of neuroactive substances by glial cells. Glia 5:81–94.

Martins-Ferreira H, Nedergaard M, Nicholson C (2000) Perspectives on spreading depression. Brain Res Brain Res Rev 32:215–234.
Masliah E, Mallory M, Hansen L, DeTeresa R, Alford M, Terry R (1994) Synaptic and neuritic alterations during the progression of Alzheimer's disease. Neurosci Lett 174:67–72.
Mathern GW, Mendoza D, Lozada A, Pretorius JK, Dehnes Y, Danbolt NC, Nelson N, Leite JP, Chimelli L, Born DE, Sakamoto AC, Assirati JA, Fried I, Peacock WJ, Ojemann GA, Adelson PD (1999) Hippocampal GABA and glutamate transporter immunoreactivity in patients with temporal lobe epilepsy. Neurology 52:453–472.
Mattila PK, Lappalainen P (2008) Filopodia: molecular architecture and cellular functions. Nat Rev Mol Cell Biol 9:446–454.
Mattson MP (2006) Neuronal life-and-death signaling, apoptosis, and neurodegenerative disorders. Antioxid Redox Signal 8:1997–2006.
Mattson MP, Culmsee C, Yu ZF (2000a) Apoptotic and antiapoptotic mechanisms in stroke. Cell Tissue Res 301:173–187.
Mattson MP, LaFerla FM, Chan SL, Leissring MA, Shepel PN, Geiger JD (2000b) Calcium signaling in the ER: its role in neuronal plasticity and neurodegenerative disorders. Trends Neurosci 23:222–229.
Mattson MP, Maudsley S, Martin B (2004) BDNF and 5-HT: a dynamic duo in age-related neuronal plasticity and neurodegenerative disorders. Trends Neurosci 27:589–594.
Matus A (1988) Microtubule-associated proteins: their potential role in determining neuronal morphology. Annu Rev Neurosci 11:29–44.
Matyash V, Kettenmann H (2010) Heterogeneity in astrocyte morphology and physiology. Brain Res Rev 63:2–10.
Mauch DH, Nägler K, Schumacher S, Göritz C, Müller EC, Otto A, Pfrieger FW (2001) CNS synaptogenesis promoted by glia-derived cholesterol. Science 294:1354–1357.
McAllister AK, Katz LC, Lo DC (1999) Neurotrophins and synaptic plasticity. Annu Rev Neurosci 22:295–318.
McCall MA, Gregg RG, Behringer RR, Brenner M, Delaney CL, Galbreath EJ, Zhang CL, Pearce RA, Chiu SY, Messing A (1996) Targeted deletion in astrocyte intermediate filament (Gfap) alters neuronal physiology. Proc Natl Acad Sci USA 93:6361–6366.
McCarthy KD, de Vellis J (1980) Preparation of separate astroglial and oligodendroglial cell cultures from rat cerebral tissue. J Cell Biol 85:890–902.
McGeer PL, McGeer EG (2002) Local neuroinflammation and the progression of Alzheimer's disease. J Neurovirol 8:529–538.
McKee AG, Loscher JS, O'Sullivan NC, Chadderton N, Palfi A, Batti L, Sheridan GK, O'Shea S, Moran M, McCabe O, Fernández AB, Pangalos MN, O'Connor JJ, Regan CM, O'Connor WT, Humphries P, Farrar GJ, Murphy KJ (2010) AAV-mediated chronic over-expression of SNAP-25 in adult rat dorsal hippocampus impairs memory-associated synaptic plasticity. J Neurochem 112:991–1004.
McKenna MC (2012) Substrate competition studies demonstrate oxidative metabolism of glucose, glutamate, glutamine, lactate and 3-hydroxybutyrate in cortical astrocytes from rat brain. Neurochem Res 37:2613–2626.
McKeon RJ, Schreiber RC, Rudge JS, Silver J (1991) Reduction of neurite outgrowth in a model of glial scarring following CNS injury is correlated with the expression of inhibitory molecules on reactive astrocytes. J Neurosci 11:3398–3411.
McKimmie CS, Graham GJ (2010) Astrocytes modulate the chemokine network in a pathogen-specific manner. Biochem Biophys Res Commun 394:1006–1011.
McMillan PJ, Singer CA, Dorsa DM (1996) The effects of ovariectomy and estrogen replacement on trkA and choline acetyltransferase mRNA expression in the basal forebrain of the adult female Sprague-Dawley rat. J Neurosci 16:1860–1865.
McMurray CT (2000) Neurodegeneration: diseases of the cytoskeleton? Cell Death Differ 7:861–865.
McNaught KS, Jenner P (1999) Altered glial function causes neuronal death and increases neuronal susceptibility to 1-methyl-4-phenylpyridinium- and 6-hydroxydopamine-induced toxicity in astrocytic/ventral mesencephalic co-cultures. J Neurochem 73:2469–2476.
McNicol A, Israels SJ (1999) Platelet dense granules: structure, function and implications for haemostasis. Thromb Res 95:1–18.

Meeuwsen S, Persoon-Deen C, Bsibsi M, Ravid R, van Noort JM (2003) Cytokine, chemokine and growth factor gene profiling of cultured human astrocytes after exposure to proinflammatory stimuli. Glia 43:243–253.
Meikle PJ, Hopwood JJ, Clague AE, Carey WF (1999) Prevalence of lysosomal storage disorders. JAMA 281:249–254.
Meldolesi J (2011) Neurite outgrowth: this process, first discovered by Santiago Ramon y Cajal, is sustained by the exocytosis of two distinct types of vesicles.
Melom JE, Littleton JT (2011) Synapse development in health and disease. Curr Opin Genet Dev 21:256–261.
Mena MA, García de Yébenes J (2008) Glial cells as players in parkinsonism: the "good," the "bad," and the “mysterious” glia. Neuroscientist 14:544–560.
Menne TF, Goyenechea B, Sánchez-Puig N, Wong CC, Tonkin LM, Ancliff PJ, Brost RL, Costanzo M, Boone C, Warren AJ (2007) The Shwachman-Bodian-Diamond syndrome protein mediates translational activation of ribosomes in yeast. Nat Genet 39:486–495.
Merali Z, Lacosta S, Anisman H (1997) Effects of interleukin-1beta and mild stress on alterations of norepinephrine, dopamine and serotonin neurotransmission: a regional microdialysis study. Brain Res 761:225–235.
Merrill JE, Benveniste EN (1996) Cytokines in inflammatory brain lesions: helpful and harmful. Trends Neurosci 19:331–338.
Messersmith DJ, Murtie JC, Le TQ, Frost EE, Armstrong RC (2000) Fibroblast growth factor 2 (FGF2) and FGF receptor expression in an experimental demyelinating disease with extensive remyelination. J Neurosci Res 62:241–256.
Messing A, Head MW, Galles K, Galbreath EJ, Goldman JE, Brenner M (1998) Fatal encephalopathy with astrocyte inclusions in GFAP transgenic mice. Am J Pathol 152:391–398.
Metcalf DJ, Calvi AA, Seaman MN, Mitchison HM, Cutler DF (2008) Loss of the Batten disease gene CLN3 prevents exit from the TGN of the mannose 6-phosphate receptor. Traffic 9:1905–1914.
Meyerhoff JL, Carter RE, Yourick DL, Slusher BS, Coyle JT (1992a) Genetically epilepsy-prone rats have increased brain regional activity of an enzyme which liberates glutamate from N-acetyl-aspartyl-glutamate. Brain Res 593:140–143.
Meyerhoff JL, Robinson MB, Koller KJ, Bixler MA, Coyle JT (1992b) Kindling increases brain levels of NAAG and seizures reduce activity of a NAAG-hydrolyzing enzyme, NAALADase. Epilepsy Res Suppl 8:297–305.
Miaczynska M, Christoforidis S, Giner A, Shevchenko A, Uttenweiler-Joseph S, Habermann B, Wilm M, Parton RG, Zerial M (2004) APPL proteins link Rab5 to nuclear signal transduction via an endosomal compartment. Cell 116:445–456.
Michelangeli F, Ogunbayo OA, Wootton LL (2005) A plethora of interacting organellar Ca2+ stores. Curr Opin Cell Biol 17:135–140.
Middeldorp J, Hol EM (2011) GFAP in health and disease. Prog Neurobiol 93:421–443.
Miernyk JA, Thelen JJ (2008) Biochemical approaches for discovering protein-protein interactions. Plant J 53:597–609.
Miki H, Miura K, Takenawa T (1996) N-WASP, a novel actin-depolymerizing protein, regulates the cortical cytoskeletal rearrangement in a PIP2-dependent manner downstream of tyrosine kinases. EMBO J 15:5326–5335.
Miklic S, Juric DM, Carman-Krzan M, Caman-Krzan M (2004) Differences in the regulation of BDNF and NGF synthesis in cultured neonatal rat astrocytes. Int J Dev Neurosci 22:119–130.
Mill J, Curran S, Kent L, Gould A, Huckett L, Richards S, Taylor E, Asherson P (2002) Association study of a SNAP-25 microsatellite and attention deficit hyperactivity disorder. Am J Med Genet 114:269–271.
Mill J, Richards S, Knight J, Curran S, Taylor E, Asherson P (2004) Haplotype analysis of SNAP-25 suggests a role in the aetiology of ADHD. Mol Psychiatry 9:801–810.
Miller LM, Xiao H, Burd B, Horwitz SB, Angeletti RH, Verdier-Pinard P (2010) Methods in tubulin proteomics. Methods Cell Biol 95:105–126.
Miller MW, Pitts FA (2000) Neurotrophin receptors in the somatosensory cortex of the mature rat: co-localization of p75, trk, isoforms and c-neu. Brain Res 852:355–366.
Mills IG, Jones AT, Clague MJ (1998) Involvement of the endosomal autoantigen EEA1 in

homotypic fusion of early endosomes. Curr Biol 8:881–884.
Mills JW, Mandel LJ (1994) Cytoskeletal regulation of membrane transport events. FASEB J 8:1161–1165.
Milnerwood AJ, Raymond LA (2010) Early synaptic pathophysiology in neurodegeneration: insights from Huntington's disease. Trends Neurosci 33:513–523.
Min K-J, Yang M-S, Kim S-U, Jou I, Joe E-H (2006) Astrocytes induce hemeoxygenase-1 expression in microglia: a feasible mechanism for preventing excessive brain inflammation. J Neurosci 26:1880–1887.
Minagar A, Shapshak P, Fujimura R, Ownby R, Heyes M, Eisdorfer C (2002) The role of macrophage/microglia and astrocytes in the pathogenesis of three neurologic disorders: HIV-associated dementia, Alzheimer disease, and multiple sclerosis. J Neurol Sci 202:13–23.
Minelli A, Barbaresi P, Reimer RJ, Edwards RH, Conti F (2001) The glial glutamate transporter GLT-1 is localized both in the vicinity of and at distance from axon terminals in the rat cerebral cortex. Neuroscience 108:51–59.
Minich T, Riemer J, Schulz JB, Wielinga P, Wijnholds J, Dringen R (2006) The multidrug resistance protein 1 (Mrp1), but not Mrp5, mediates export of glutathione and glutathione disulfide from brain astrocytes. J Neurochem 97:373–384.
Minshew NJ, Williams DL (2007) The new neurobiology of autism: cortex, connectivity, and neuronal organization. Arch Neurol 64:945–950.
Mitchison HM, Bernard DJ, Greene ND, Cooper JD, Junaid MA, Pullarkat RK, de Vos N, Breuning MH, Owens JW, Mobley WC, Gardiner RM, Lake BD, Taschner PE, Nussbaum RL (1999) Targeted disruption of the Cln3 gene provides a mouse model for Batten disease. The Batten Mouse Model Consortium [corrected]. Neurobiol Dis 6:321–334.
Mitchison HM, Lim MJ, Cooper JD (2004) Selectivity and types of cell death in the neuronal ceroid lipofuscinoses. Brain Pathol 14:86–96.
Mitchison HM, Taschner PE, Kremmidiotis G, Callen DF, Doggett NA, Lerner TJ, Janes RB, Wallace BA, Munroe PB, O'Rawe AM, Gardiner RM, Mole SE (1997) Structure of the CLN3 gene and predicted structure, location and function of CLN3 protein. Neuropediatrics 28:12–14.
Mitchison T, Kirschner M (1984) Dynamic instability of microtubule growth. Nature 312:237–242.
Mitrasinovic OM, Grattan A, Robinson CC, Lapustea NB, Poon C, Ryan H, Phong C, Murphy GM (2005) Microglia overexpressing the macrophage colony-stimulating factor receptor are neuroprotective in a microglial-hippocampal organotypic coculture system. J Neurosci 25:4442–4451.
Moharregh-Khiabani D, Linker RA, Gold R, Stangel M (2009) Fumaric Acid and its esters: an emerging treatment for multiple sclerosis. Curr Neuropharmacol 7:60–64.
Moidunny S, Dias RB, Wesseling E, Sekino Y, Boddeke HWGM, Sebastião AM, Biber K (2010) Interleukin-6-type cytokines in neuroprotection and neuromodulation: oncostatin M, but not leukemia inhibitory factor, requires neuronal adenosine A1 receptor function. J Neurochem 114:1667–1677.
Mole SE, Williams R, Goebel H (2011) The Neuronal Ceroid Lipofuscinoses (Batten Disease). Oxford Univ Pr.
Molofsky AV, Krencik R, Krenick R, Ullian EM, Ullian E, Tsai H-H, Deneen B, Richardson WD, Barres BA, Rowitch DH (2012) Astrocytes and disease: a neurodevelopmental perspective. Genes Dev 26:891–907.
Montagnese C, Poulain DA, Vincent JD, Theodosis DT (1988) Synaptic and neuronal-glial plasticity in the adult oxytocinergic system in response to physiological stimuli. Brain Res Bull 20:681–692.
Moody WJ, Bosma MM (2005) Ion channel development, spontaneous activity, and activity-dependent development in nerve and muscle cells. Physiol Rev 85:883–941.
Moore SJ, Buckley DJ, MacMillan A, Marshall HD, Steele L, Ray PN, Nawaz Z, Baskin B, Frecker M, Carr SM, Ives E, Parfrey PS (2008) The clinical and genetic epidemiology of neuronal ceroid lipofuscinosis in Newfoundland. Clin Genet 74:213–222.
More SV, Koppula S, Kim I-S, Kumar H, Kim B-W, Choi D-K (2012) The role of bioactive compounds on the promotion of neurite outgrowth. Molecules 17:6728–6753.
Morgan AJ, Jacob R (1994) Ionomycin enhances Ca2+ influx by stimulating store-regulated cation entry and not by a direct action at the plasma membrane. Biochem J 300 (Pt 3):665–672.
Morgan SC, Taylor DL, Pocock JM (2004) Microglia release activators of neuronal proliferation

mediated by activation of mitogen-activated protein kinase, phosphatidylinositol-3-kinase/Akt and delta-Notch signalling cascades. J Neurochem 90:89–101.
Morgello S, Uson RR, Schwartz EJ, Haber RS (1995) The human blood-brain barrier glucose transporter (GLUT1) is a glucose transporter of gray matter astrocytes. Glia 14:43–54.
Morita M, Higuchi C, Moto T, Kozuka N, Susuki J, Itofusa R, Yamashita J, Kudo Y (2003) Dual regulation of calcium oscillation in astrocytes by growth factors and pro-inflammatory cytokines via the mitogen-activated protein kinase cascade. J Neurosci 23:10944–10952.
Moreno C, Sampieri A, Vivas O, Pena-Segura C, Vaca L (2012) STIM1 and Orai1 mediate thrombin-induced Ca^{2+} influx in rat cortical astrocytes. Cell Calcium Volume 52, Issue 6, Pages 457-467.
Mothet J-P, Pollegioni L, Ouanounou G, Martineau M, Fossier P, Baux G (2005) Glutamate receptor activation triggers a calcium-dependent and SNARE protein-dependent release of the gliotransmitter D-serine. Proc Natl Acad Sci USA 102:5606–5611.
Möller T (2010) Neuroinflammation in Huntington's disease. J Neural Transm 117:1001–1008.
Mrowietz U, Asadullah K (2005) Dimethylfumarate for psoriasis: more than a dietary curiosity. Trends Mol Med 11:43–48.
Mucke L, Eddleston M (1993) Astrocytes in infectious and immune-mediated diseases of the central nervous system. FASEB J 7:1226–1232.
Mukaetova-Ladinska EB, Hurt J, Honer WG, Harrington CR, Wischik CM (2002) Loss of synaptic but not cytoskeletal proteins in the cerebellum of chronic schizophrenics. Neurosci Lett 317:161–165.
Mullins C, Bonifacino JS (2001) The molecular machinery for lysosome biogenesis. Bioessays 23:333–343.
Munroe PB, Mitchison HM, O'Rawe AM, Anderson JW, Boustany RM, Lerner TJ, Taschner PE, de Vos N, Breuning MH, Gardiner RM, Mole SE (1997) Spectrum of mutations in the Batten disease gene, CLN3. Am J Hum Genet 61:310–316.
Murai KK, Nguyen LN, Irie F, Yamaguchi Y, Pasquale EB (2003) Control of hippocampal dendritic spine morphology through ephrin-A3/EphA4 signaling. Nat Neurosci 6:153–160.
Murphy S (2000) Production of nitric oxide by glial cells: regulation and potential roles in the CNS. Glia 29:1–13.
Muzaffar NE, Pearce DA (2008) Analysis of NCL Proteins from an Evolutionary Standpoint. Curr Genomics 9:115–136.
Müller CM, Best J (1989) Ocular dominance plasticity in adult cat visual cortex after transplantation of cultured astrocytes. Nature 342:427–430.
Müller HW, Junghans U, Kappler J (1995) Astroglial neurotrophic and neurite-promoting factors. Pharmacol Ther 65:1–18.
Münch G, Gasic-Milenkovic J, Dukic-Stefanovic S, Kuhla B, Heinrich K, Riederer P, Huttunen HJ, Founds H, Sajithlal G (2003) Microglial activation induces cell death, inhibits neurite outgrowth and causes neurite retraction of differentiated neuroblastoma cells. Exp Brain Res 150:1–8.
Myer DJ, Gurkoff GG, Lee SM, Hovda DA, Sofroniew MV (2006) Essential protective roles of reactive astrocytes in traumatic brain injury. Brain 129:2761–2772.
Mytilineou C, Kokotos Leonardi ET, Kramer BC, Jamindar T, Olanow CW (1999) Glial cells mediate toxicity in glutathione-depleted mesencephalic cultures. J Neurochem 73:112–119.
Nag S (2011) Morphology and properties of astrocytes. Methods Mol Biol 686:69–100.
Nagahara AH, Tuszynski MH (2011) Potential therapeutic uses of BDNF in neurological and psychiatric disorders. Nat Rev Drug Discov 10:209–219.
Nagasawa T, Tachibana K, Kawabata K (1999) A CXC chemokine SDF-1/PBSF: a ligand for a HIV coreceptor, CXCR4. Adv Immunol 71:211–228.
Nagatsu T, Mogi M, Ichinose H, Togari A (2000) Changes in cytokines and neurotrophins in Parkinson's disease. J Neural Transm Suppl:277–290.
Najimi M, Maloteaux JM, Hermans E (2002) Cytoskeleton-related trafficking of the EAAC1 glutamate transporter after activation of the G(q/11)-coupled neurotensin receptor NTS1. FEBS Lett 523:224–228.
Nakajima K, Tohyama Y, Maeda S, Kohsaka S, Kurihara T (2007) Neuronal regulation by which microglia enhance the production of neurotrophic factors for GABAergic, catecholaminergic, and cholinergic neurons. Neurochem Int 50:807–820.
Nakanishi H (2003) Microglial functions and proteases. Mol Neurobiol 27:163–176.

Nakanishi H, Zhang J, Koike M, Nishioku T, Okamoto Y, Kominami E, Figura von K, Peters C, Yamamoto K, Saftig P, Uchiyama Y (2001) Involvement of nitric oxide released from microglia-macrophages in pathological changes of cathepsin D-deficient mice. J Neurosci 21:7526–7533.
Narayan SB, Rakheja D, Pastor JV, Rosenblatt K, Greene SR, Yang J, Wolf BA, Bennett MJ (2006a) Over-expression of CLN3P, the Batten disease protein, inhibits PANDER-induced apoptosis in neuroblastoma cells: further evidence that CLN3P has anti-apoptotic properties. Mol Genet Metab 88:178–183.
Narayan SB, Rakheja D, Tan L, Pastor JV, Bennett MJ (2006b) CLN3P, the Batten's disease protein, is a novel palmitoyl-protein Delta-9 desaturase. Ann Neurol 60:570–577.
Narayan SB, Tan L, Bennett MJ (2008) Intermediate levels of neuronal palmitoyl-protein Delta-9 desaturase in heterozygotes for murine Batten disease. Mol Genet Metab 93:89–91.
Nardocci N, Verga ML, Binelli S, Zorzi G, Angelini L, Bugiani O (1995) Neuronal ceroid-lipofuscinosis: a clinical and morphological study of 19 patients. Am J Med Genet 57:137–141.
Natarajan C, Bright JJ (2002) Curcumin inhibits experimental allergic encephalomyelitis by blocking IL-12 signaling through Janus kinase-STAT pathway in T lymphocytes. J Immunol 168:6506–6513.
Nau R, Brück W (2002) Neuronal injury in bacterial meningitis: mechanisms and implications for therapy. Trends Neurosci 25:38–45.
Naus CC, Bechberger JF, Zhang Y, Venance L, Yamasaki H, Juneja SC, Kidder GM, Giaume C (1997) Altered gap junctional communication, intercellular signaling, and growth in cultured astrocytes deficient in connexin43. J Neurosci Res 49:528–540.
Nedergaard M (1994) Direct signaling from astrocytes to neurons in cultures of mammalian brain cells. Science 263:1768–1771.
Nedergaard M, Dirnagl U (2005) Role of glial cells in cerebral ischemia. Glia 50:281–286.
Nedergaard M, Ransom B, Goldman SA (2003) New roles for astrocytes: redefining the functional architecture of the brain. Trends Neurosci 26:523–530.
Nelson WJ, Hammerton RW (1989) A membrane-cytoskeletal complex containing Na+,K+-ATPase, ankyrin, and fodrin in Madin-Darby canine kidney (MDCK) cells: implications for the biogenesis of epithelial cell polarity. J Cell Biol 108:893–902.
Nett WJ, Oloff SH, McCarthy KD (2002) Hippocampal astrocytes in situ exhibit calcium oscillations that occur independent of neuronal activity. J Neurophysiol 87:528–537.
Neufeld G, Cohen T, Gengrinovitch S, Poltorak Z (1999) Vascular endothelial growth factor (VEGF) and its receptors. FASEB J 13:9–22.
Neugebauer KM, Tomaselli KJ, Lilien J, Reichardt LF (1988) N-cadherin, NCAM, and integrins promote retinal neurite outgrowth on astrocytes in vitro. J Cell Biol 107:1177–1187.
Neumann H, Schweigreiter R, Yamashita T, Rosenkranz K, Wekerle H, Barde Y-A (2002) Tumor necrosis factor inhibits neurite outgrowth and branching of hippocampal neurons by a rho-dependent mechanism. J Neurosci 22:854–862.
Newman EA, Zahs KR (1998) Modulation of neuronal activity by glial cells in the retina. J Neurosci 18:4022–4028.
Nicoletti JN, Shah SK, McCloskey DP, Goodman JH, Elkady A, Atassi H, Hylton D, Rudge JS, Scharfman HE, Croll SD (2008) Vascular endothelial growth factor is up-regulated after status epilepticus and protects against seizure-induced neuronal loss in hippocampus. Neuroscience 151:232–241.
Nielsen MG, Turner FR, Hutchens JA, Raff EC (2001) Axoneme-specific beta-tubulin specialization: a conserved C-terminal motif specifies the central pair. Curr Biol 11:529–533.
Nijssen PCG, Ceuterick C, van Diggelen OP, Elleder M, Martin J-J, Teepen JLJM, Tyynelä J, Roos RAC (2003) Autosomal dominant adult neuronal ceroid lipofuscinosis: a novel form of NCL with granular osmiophilic deposits without palmitoyl protein thioesterase 1 deficiency. Brain Pathol 13:574–581.
Nimmerjahn A, Kirchhoff F, Helmchen F (2005) Resting microglial cells are highly dynamic surveillants of brain parenchyma in vivo. Science 308:1314–1318.
Nishi T, Forgac M (2002) The vacuolar (H+)-ATPases--nature's most versatile proton pumps. Nat Rev Mol Cell Biol 3:94–103.
Noble W, Garwood CJ, Hanger DP (2009) Minocycline as a potential therapeutic agent in

neurodegenerative disorders characterised by protein misfolding. Prion 3:78–83.
Norenberg MD (1994) Astrocyte responses to CNS injury. J Neuropathol Exp Neurol 53:213–220.
North RA, Verkhratsky A (2006) Purinergic transmission in the central nervous system. Pflugers Arch 452:479–485.
Norton WT, Aquino DA, Hozumi I, Chiu FC, Brosnan CF (1992) Quantitative aspects of reactive gliosis: a review. Neurochem Res 17:877–885.
Nugent T, Mole SE, Jones DT (2008) The transmembrane topology of Batten disease protein CLN3 determined by consensus computational prediction constrained by experimental data. FEBS Lett 582:1019–1024.
Nunomura A, Castellani RJ, Zhu X, Moreira PI, Perry G, Smith MA (2006) Involvement of oxidative stress in Alzheimer disease. J Neuropathol Exp Neurol 65:631–641.
Nykjaer A, Willnow TE, Petersen CM (2005) p75NTR--live or let die. Curr Opin Neurobiol 15:49–57.
O'Kane RL, Martínez-López I, DeJoseph MR, Viña JR, Hawkins RA (1999) Na(+)-dependent glutamate transporters (EAAT1, EAAT2, and EAAT3) of the blood-brain barrier. A mechanism for glutamate removal. J Biol Chem 274:31891–31895.
O'Neill L (2000) The Toll/interleukin-1 receptor domain: a molecular switch for inflammation and host defence. Biochem Soc Trans 28:557–563.
O'Sullivan NC, McGettigan PA, Sheridan GK, Pickering M, Conboy L, O'Connor JJ, Moynagh PN, Higgins DG, Regan CM, Murphy KJ (2007) Temporal change in gene expression in the rat dentate gyrus following passive avoidance learning. J Neurochem 101:1085–1098.
Oakley JC, Kalume F, Catterall WA (2011) Insights into pathophysiology and therapy from a mouse model of Dravet syndrome. Epilepsia 52 Suppl 2:59–61.
Obara M, Szeliga M, Albrecht J (2008) Regulation of pH in the mammalian central nervous system under normal and pathological conditions: facts and hypotheses. Neurochem Int 52:905–919.
Oberheim NA, Goldman SA, Nedergaard M (2012) Heterogeneity of astrocytic form and function. Methods Mol Biol 814:23–45.
Oberheim NA, Takano T, Han X, He W, Lin JH-C, Wang F, Xu Q, Wyatt JD, Pilcher W, Ojemann JG, Ransom BR, Goldman SA, Nedergaard M (2009) Uniquely hominid features of adult human astrocytes. J Neurosci 29:3276–3287.
Oberheim NA, Wang X, Goldman S, Nedergaard M (2006) Astrocytic complexity distinguishes the human brain. Trends Neurosci 29:547–553.
Occhipinti R, Somersalo E, Calvetti D (2009) Astrocytes as the glucose shunt for glutamatergic neurons at high activity: an in silico study. J Neurophysiol 101:2528–2538.
Ogata K, Kosaka T (2002) Structural and quantitative analysis of astrocytes in the mouse hippocampus. Neuroscience 113:221–233.
Ogawa Y, Rasband MN (2008) The functional organization and assembly of the axon initial segment. Curr Opin Neurobiol 18:307–313.
Ogier C, Bernard A, Chollet A-M, LE Diguardher T, Hanessian S, Charton G, Khrestchatisky M, Rivera S (2006) Matrix metalloproteinase-2 (MMP-2) regulates astrocyte motility in connection with the actin cytoskeleton and integrins. Glia 54:272–284.
Ohtsuki T, Ruetzler CA, Tasaki K, Hallenbeck JM (1996) Interleukin-1 mediates induction of tolerance to global ischemia in gerbil hippocampal CA1 neurons. J Cereb Blood Flow Metab 16:1137–1142.
Ojo B, Rezaie P, Gabbott PL, Davies H, Colyer F, Cowley TR, Lynch M, Stewart MG (2012) Age-related changes in the hippocampus (loss of synaptophysin and glial-synaptic interaction) are modified by systemic treatment with an NCAM-derived peptide, FGL. Brain Behav Immun 26:778–788.
Oliet SH, Piet R, Poulain DA (2001) Control of glutamate clearance and synaptic efficacy by glial coverage of neurons. Science 292:923–926.
Orellana DI, Quintanilla RA, Maccioni RB (2007) Neuroprotective effect of TNFalpha against the beta-amyloid neurotoxicity mediated by CDK5 kinase. Biochim Biophys Acta 1773:254–263.
Orkand RK, Nicholls JG, Kuffler SW (1966) Effect of nerve impulses on the membrane potential of glial cells in the central nervous system of amphibia. J Neurophysiol 29:788–806.
Osório NS, Sampaio-Marques B, Chan C-H, Oliveira P, Pearce DA, Sousa N, Rodrigues F (2009) Neurodevelopmental delay in the Cln3Deltaex7/8 mouse model for Batten disease. Genes

Brain Behav 8:337–345.
Oswald MJ, Palmer DN, Kay GW, Shemilt SJA, Rezaie P, Cooper JD (2005) Glial activation spreads from specific cerebral foci and precedes neurodegeneration in presymptomatic ovine neuronal ceroid lipofuscinosis (CLN6). Neurobiol Dis 20:49–63.
Ould-yahoui A, Tremblay E, Sbai O, Ferhat L, Bernard A, Charrat E, Gueye Y, Lim NH, Brew K, Risso J-J, Dive V, Khrestchatisky M, Rivera S (2009) A new role for TIMP-1 in modulating neurite outgrowth and morphology of cortical neurons. PLoS ONE 4:e8289.
Padilla-Lopez S, Pearce DA (2006) Saccharomyces cerevisiae lacking Btn1p modulate vacuolar ATPase activity to regulate pH imbalance in the vacuole. J Biol Chem 281:10273–10280.
Padmanabhan J, Shelanski ML (1998) Process formation in astrocytes: modulation of cytoskeletal proteins. Neurochem Res 23:377–384.
Paglinawan R, Malipiero U, Schlapbach R, Frei K, Reith W, Fontana A (2003) TGFbeta directs gene expression of activated microglia to an anti-inflammatory phenotype strongly focusing on chemokine genes and cell migratory genes. Glia 44:219–231.
Palmer DN, Fearnley IM, Walker JE, Hall NA, Lake BD, Wolfe LS, Haltia M, Martinus RD, Jolly RD (1992) Mitochondrial ATP synthase subunit c storage in the ceroid-lipofuscinoses (Batten disease). Am J Med Genet 42:561–567.
Palmer LM, Stuart GJ (2006) Site of action potential initiation in layer 5 pyramidal neurons. J Neurosci 26:1854–1863.
Pan Z, Kao T, Horvath Z, Lemos J, Sul J-Y, Cranstoun SD, Bennett V, Scherer SS, Cooper EC (2006) A common ankyrin-G-based mechanism retains KCNQ and NaV channels at electrically active domains of the axon. J Neurosci 26:2599–2613.
Panaro MA, Cianciulli A (2012) Current opinions and perspectives on the role of immune system in the pathogenesis of Parkinson's disease. Curr Pharm Des 18:200–208.
Pane MA, Puranam KL, Boustany RM (1999) Expression of cln3 in human NT2 neuronal precursor cells and neonatal rat brain. Pediatr Res 46:367–374.
Paradisi S, Sacchetti B, Balduzzi M, Gaudi S, Malchiodi-Albedi F (2004) Astrocyte modulation of in vitro beta-amyloid neurotoxicity. Glia 46:252–260.
Parker JC, Hoffman JF (1967) The role of membrane phosphoglycerate kinase in the control of glycolytic rate by active cation transport in human red blood cells. J Gen Physiol 50:893–916.
Parkinson-Lawrence EJ, Shandala T, Prodoehl M, Plew R, Borlace GN, Brooks DA (2010) Lysosomal storage disease: revealing lysosomal function and physiology. Physiology (Bethesda) 25:102–115.
Parpura V, Baker BJ, Jeras M, Zorec R (2010) Regulated exocytosis in astrocytic signal integration. Neurochem Int 57:451–459.
Parpura V, Basarsky TA, Liu F, Jeftinija K, Jeftinija S, Haydon PG (1994) Glutamate-mediated astrocyte-neuron signalling. Nature 369:744–747.
Parpura V, Grubišić V, Verkhratsky A (2011) Ca(2+) sources for the exocytotic release of glutamate from astrocytes. Biochim Biophys Acta 1813:984–991.
Parpura V, Heneka MT, Montana V, Oliet SHR, Schousboe A, Haydon PG, Stout RF, Spray DC, Reichenbach A, Pannicke T, Pekny M, Pekna M, Zorec R, Verkhratsky A (2012) Glial cells in (patho)physiology. J Neurochem 121:4–27.
Parpura V, Zorec R (2010) Gliotransmission: Exocytotic release from astrocytes. Brain Res Rev 63:83–92.
Parri HR, Crunelli V (2003) The role of Ca2+ in the generation of spontaneous astrocytic Ca2+ oscillations. Neuroscience 120:979–992.
Parri HR, Gould TM, Crunelli V (2001) Spontaneous astrocytic Ca2+ oscillations in situ drive NMDAR-mediated neuronal excitation. Nat Neurosci 4:803–812.
Partanen S, Haapanen A, Kielar C, Pontikis C, Alexander N, Inkinen T, Saftig P, Gillingwater TH, Cooper JD, Tyynelä J (2008) Synaptic changes in the thalamocortical system of cathepsin D-deficient mice: a model of human congenital neuronal ceroid-lipofuscinosis. J Neuropathol Exp Neurol 67:16–29.
Pascual O, Ben Achour S, Rostaing P, Triller A, Bessis A (2012) Microglia activation triggers astrocyte-mediated modulation of excitatory neurotransmission. Proc Natl Acad Sci USA 109:E197–E205.
Pascual O, Casper KB, Kubera C, Zhang J, Revilla-Sanchez R, Sul J-Y, Takano H, Moss SJ, McCarthy K, Haydon PG (2005) Astrocytic purinergic signaling coordinates synaptic networks. Science

310:113–116.
Passani LA, Vonsattel JP, Carter RE, Coyle JT (1997) N-acetylaspartylglutamate, N-acetylaspartate, and N-acetylated alpha-linked acidic dipeptidase in human brain and their alterations in Huntington and Alzheimer's diseases. Mol Chem Neuropathol 31:97–118.
Pasti L, Volterra A, Pozzan T, Carmignoto G (1997) Intracellular calcium oscillations in astrocytes: a highly plastic, bidirectional form of communication between neurons and astrocytes in situ. J Neurosci 17:7817–7830.
Pasti L, Zonta M, Pozzan T, Vicini S, Carmignoto G (2001) Cytosolic calcium oscillations in astrocytes may regulate exocytotic release of glutamate. J Neurosci 21:477–484.
Patel MN, McNamara JO (1995) Selective enhancement of axonal branching of cultured dentate gyrus neurons by neurotrophic factors. Neuroscience 69:763–770.
Patel S, Docampo R (2010) Acidic calcium stores open for business: expanding the potential for intracellular Ca2+ signaling. Trends Cell Biol 20:277–286.
Patki V, Virbasius J, Lane WS, Toh BH, Shpetner HS, Corvera S (1997) Identification of an early endosomal protein regulated by phosphatidylinositol 3-kinase. Proc Natl Acad Sci USA 94:7326–7330.
Patterson KI, Brummer T, O'Brien PM, Daly RJ (2009) Dual-specificity phosphatases: critical regulators with diverse cellular targets. Biochem J 418:475–489.
Paul RJ, Bauer M, Pease W (1979) Vascular smooth muscle: aerobic glycolysis linked to sodium and potassium transport processes. Science 206:1414–1416.
Pearce DA, Ferea T, Nosel SA, Das B, Sherman F (1999a) Action of BTN1, the yeast orthologue of the gene mutated in Batten disease. Nat Genet 22:55–58.
Pearce DA, Nosel SA, Sherman F (1999b) Studies of pH regulation by Btn1p, the yeast homolog of human Cln3p. Mol Genet Metab 66:320–323.
Pearce DA, Sherman F (1998) A yeast model for the study of Batten disease. Proc Natl Acad Sci USA 95:6915–6918.
Pearce RK, Owen A, Daniel S, Jenner P, Marsden CD (1997) Alterations in the distribution of glutathione in the substantia nigra in Parkinson's disease. J Neural Transm 104:661–677.
Pears MR, Cooper JD, Mitchison HM, Mortishire-Smith RJ, Pearce DA, Griffin JL (2005) High resolution 1H NMR-based metabolomics indicates a neurotransmitter cycling deficit in cerebral tissue from a mouse model of Batten disease. J Biol Chem 280:42508–42514.
Pekny M (2001) Astrocytic intermediate filaments: lessons from GFAP and vimentin knock-out mice. Prog Brain Res 132:23–30.
Pekny M, Eliasson C, Chien CL, Kindblom LG, Liem R, Hamberger A, Betsholtz C (1998) GFAP-deficient astrocytes are capable of stellation in vitro when cocultured with neurons and exhibit a reduced amount of intermediate filaments and an increased cell saturation density. Exp Cell Res 239:332–343.
Pekny M, Eliasson C, Siushansian R, Ding M, Dixon SJ, Pekna M, Wilson JX, Hamberger A (1999) The impact of genetic removal of GFAP and/or vimentin on glutamine levels and transport of glucose and ascorbate in astrocytes. Neurochem Res 24:1357–1362.
Pekny M, Levéen P, Pekna M, Eliasson C, Berthold CH, Westermark B, Betsholtz C (1995) Mice lacking glial fibrillary acidic protein display astrocytes devoid of intermediate filaments but develop and reproduce normally. EMBO J 14:1590–1598.
Pekny M, Nilsson M (2005) Astrocyte activation and reactive gliosis. Glia 50:427–434.
Pekny M, Pekna M (2004) Astrocyte intermediate filaments in CNS pathologies and regeneration. J Pathol 204:428–437.
Pelled D, Lloyd-Evans E, Riebeling C, Jeyakumar M, Platt FM, Futerman AH (2003a) Inhibition of calcium uptake via the sarco/endoplasmic reticulum Ca2+-ATPase in a mouse model of Sandhoff disease and prevention by treatment with N-butyldeoxynojirimycin. J Biol Chem 278:29496–29501.
Pelled D, Riebeling C, van Echten-Deckert G, Sandhoff K, Futerman AH (2003b) Reduced rates of axonal and dendritic growth in embryonic hippocampal neurones cultured from a mouse model of Sandhoff disease. Neuropathol Appl Neurobiol 29:341–349.
Pelled D, Trajkovic-Bodennec S, Lloyd-Evans E, Sidransky E, Schiffmann R, Futerman AH (2005) Enhanced calcium release in the acute neuronopathic form of Gaucher disease. Neurobiol Dis 18:83–88.
Pellerin L (2003) Lactate as a pivotal element in neuron-glia metabolic cooperation. Neurochem

Int 43:331–338.
Pellerin L, Bergersen LH, Halestrap AP, Pierre K (2005) Cellular and subcellular distribution of monocarboxylate transporters in cultured brain cells and in the adult brain. J Neurosci Res 79:55–64.
Pellerin L, Bouzier-Sore A-K, Aubert A, Serres S, Merle M, Costalat R, Magistretti PJ (2007) Activity-dependent regulation of energy metabolism by astrocytes: an update. Glia 55:1251–1262.
Pellerin L, Magistretti PJ (1994) Glutamate uptake into astrocytes stimulates aerobic glycolysis: a mechanism coupling neuronal activity to glucose utilization. Proc Natl Acad Sci USA 91:10625–10629.
Pellerin L, Magistretti PJ (2012) Sweet sixteen for ANLS. J Cereb Blood Flow Metab 32:1152–1166.
Pellerin L, Pellegri G, Bittar PG, Charnay Y, Bouras C, Martin JL, Stella N, Magistretti PJ (1998) Evidence supporting the existence of an activity-dependent astrocyte-neuron lactate shuttle. Dev Neurosci 20:291–299.
Peng H, Shah W, Holland P, Carbonetto S (2008) Integrins and dystroglycan regulate astrocyte wound healing: the integrin beta1 subunit is necessary for process extension and orienting the microtubular network. Dev Neurobiol 68:559–574.
Perea G, Araque A (2010) GLIA modulates synaptic transmission. Brain Res Rev 63:93–102.
Perea G, Navarrete M, Araque A (2009) Tripartite synapses: astrocytes process and control synaptic information. Trends Neurosci 32:421–431.
Perego C, Vanoni C, Bossi M, Massari S, Basudev H, Longhi R, Pietrini G (2000) The GLT-1 and GLAST glutamate transporters are expressed on morphologically distinct astrocytes and regulated by neuronal activity in primary hippocampal cocultures. J Neurochem 75:1076–1084.
Peretti D, Peris L, Rosso S, Quiroga S, Cáceres A (2000) Evidence for the involvement of KIF4 in the anterograde transport of L1-containing vesicles. J Cell Biol 149:141–152.
Perron JC, Bixby JL (1999) Distinct neurite outgrowth signaling pathways converge on ERK activation. Mol Cell Neurosci 13:362–378.
Perry VH, O'Connor V (2010) The role of microglia in synaptic stripping and synaptic degeneration: a revised perspective. ASN Neuro 2:e00047.
Persaud-Sawin D-A, McNamara JO, Rylova S, VanDongen A, Boustany R-MN (2004) A galactosylceramide binding domain is involved in trafficking of CLN3 from Golgi to rafts via recycling endosomes. Pediatr Res 56:449–463.
Persaud-Sawin D-ANW, VanDongen A, Boustany R-MN (2002) Motifs within the CLN3 protein: modulation of cell growth rates and apoptosis. Hum Mol Genet 11:2129–2142.
Petegnief V, Saura J, de Gregorio-Rocasolano N, Paul SM (2001) Neuronal injury-induced expression and release of apolipoprotein E in mixed neuron/glia co-cultures: nuclear factor kappaB inhibitors reduce basal and lesion-induced secretion of apolipoprotein E. Neuroscience 104:223–234.
Peters A, Palay SL, Webster HD (1991) The fine structure of the nervous system. Oxford University Press, USA.
Peters O, Schipke CG, Hashimoto Y, Kettenmann H (2003) Different mechanisms promote astrocyte Ca2+ waves and spreading depression in the mouse neocortex. J Neurosci 23:9888–9896.
Petersen OH, Michalak M, Verkhratsky A (2005) Calcium signalling: past, present and future. Cell Calcium 38:161–169.
Pfenninger KH (2009) Plasma membrane expansion: a neuron's Herculean task. Nat Rev Neurosci 10:251–261.
Pfenninger KH, Laurino L, Peretti D, Wang X, Rosso S, Morfini G, Cáceres A, Quiroga S (2003) Regulation of membrane expansion at the nerve growth cone. J Cell Sci 116:1209–1217.
Pfrieger FW, Barres BA (1995) What the fly“s glia tell the fly”s brain. Cell 83:671–674.
Phani S, Re DB, Przedborski S (2012) The Role of the Innate Immune System in ALS. Front Pharmacol 3:150.
Philbert MA, Beiswanger CM, Waters DK, Reuhl KR, Lowndes HE (1991) Cellular and regional distribution of reduced glutathione in the nervous system of the rat: histochemical localization by mercury orange and o-phthaldialdehyde-induced histofluorescence. Toxicol Appl Pharmacol 107:215–227.

Phillips SN, Benedict JW, Weimer JM, Pearce DA (2005) CLN3, the protein associated with batten disease: structure, function and localization. J Neurosci Res 79:573–583.
Pierre K, Chatton J-Y, Parent A, Repond C, Gardoni F, Di Luca M, Pellerin L (2009) Linking supply to demand: the neuronal monocarboxylate transporter MCT2 and the alpha-amino-3-hydroxyl-5-methyl-4-isoxazole-propionic acid receptor GluR2/3 subunit are associated in a common trafficking process. Eur J Neurosci 29:1951–1963.
Pierre K, Pellerin L (2005) Monocarboxylate transporters in the central nervous system: distribution, regulation and function. J Neurochem 94:1–14.
Pines G, Danbolt NC, Bjørås M, Zhang Y, Bendahan A, Eide L, Koepsell H, Storm-Mathisen J, Seeberg E, Kanner BI (1992) Cloning and expression of a rat brain L-glutamate transporter. Nature 360:464–467.
Pinto DJ, Patrick SL, Huang WC, Connors BW (2005) Initiation, propagation, and termination of epileptiform activity in rodent neocortex in vitro involve distinct mechanisms. J Neurosci 25:8131–8140.
Pitt D, Werner P, Raine CS (2000) Glutamate excitotoxicity in a model of multiple sclerosis. Nat Med 6:67–70.
Pivtoraiko VN, Stone SL, Roth KA, Shacka JJ (2009) Oxidative stress and autophagy in the regulation of lysosome-dependent neuron death. Antioxid Redox Signal 11:481–496.
Pocock JM, Kettenmann H (2007) Neurotransmitter receptors on microglia. Trends Neurosci 30:527–535.
Pollard TD, Cooper JA (2009) Actin, a central player in cell shape and movement. Science 326:1208–1212.
Pontikis CC, Cella CV, Parihar N, Lim MJ, Chakrabarti S, Mitchison HM, Mobley WC, Rezaie P, Pearce DA, Cooper JD (2004) Late onset neurodegeneration in the Cln3-/- mouse model of juvenile neuronal ceroid lipofuscinosis is preceded by low level glial activation. Brain Res 1023:231–242.
Pontikis CC, Cotman SL, MacDonald ME, Cooper JD (2005) Thalamocortical neuron loss and localized astrocytosis in the Cln3Deltaex7/8 knock-in mouse model of Batten disease. Neurobiol Dis 20:823–836.
Popovic MA, Foust AJ, McCormick DA, Zecevic D (2011) The spatio-temporal characteristics of action potential initiation in layer 5 pyramidal neurons: a voltage imaging study. J Physiol (Lond) 589:4167–4187.
Porter JT, McCarthy KD (1995) Adenosine receptors modulate [Ca2+]i in hippocampal astrocytes in situ. J Neurochem 65:1515–1523.
Porter JT, McCarthy KD (1996) Hippocampal astrocytes in situ respond to glutamate released from synaptic terminals. J Neurosci 16:5073–5081.
Potokar M, Kreft M, Li L, Daniel Andersson J, Pangrsic T, Chowdhury HH, Pekny M, Zorec R (2007) Cytoskeleton and vesicle mobility in astrocytes. Traffic 8:12–20.
Potokar M, Kreft M, Pangrsic T, Zorec R (2005) Vesicle mobility studied in cultured astrocytes. Biochem Biophys Res Commun 329:678–683.
Potokar M, Stenovec M, Gabrijel M, Li L, Kreft M, Grilc S, Pekny M, Zorec R (2010) Intermediate filaments attenuate stimulation-dependent mobility of endosomes/lysosomes in astrocytes. Glia 58:1208–1219.
Potokar M, Stenovec M, Kreft M, Gabrijel M, Zorec R (2011) Physiopathologic dynamics of vesicle traffic in astrocytes. Histol Histopathol 26:277–284.
Potokar M, Stenovec M, Kreft M, Kreft ME, Zorec R (2008) Stimulation inhibits the mobility of recycling peptidergic vesicles in astrocytes. Glia 56:135–144.
Powell EM, Fawcett JW, Geller HM (1997a) Proteoglycans provide neurite guidance at an astrocyte boundary. Mol Cell Neurosci 10:27–42.
Powell EM, Geller HM (1999) Dissection of astrocyte-mediated cues in neuronal guidance and process extension. Glia 26:73–83.
Powell EM, Meiners S, DiProspero NA, Geller HM (1997b) Mechanisms of astrocyte-directed neurite guidance. Cell Tissue Res 290:385–393.
Prasad VV, Pullarkat RK (1996) Brain lysosomal hydrolases in neuronal ceroid-lipofuscinoses. Mol Chem Neuropathol 29:169–179.
Prast H, Philippu A (2001) Nitric oxide as modulator of neuronal function. Prog Neurobiol 64:51–68.

Prehn JH, Backhauss C, Krieglstein J (1993) Transforming growth factor-beta 1 prevents glutamate neurotoxicity in rat neocortical cultures and protects mouse neocortex from ischemic injury in vivo. J Cereb Blood Flow Metab 13:521–525.
Press B, Feng Y, Hoflack B, Wandinger-Ness A (1998) Mutant Rab7 causes the accumulation of cathepsin D and cation-independent mannose 6-phosphate receptor in an early endocytic compartment. J Cell Biol 140:1075–1089.
Pressey SNR, O'Donnell KJ, Stauber T, Fuhrmann JC, Tyynelä J, Jentsch TJ, Cooper JD (2010) Distinct neuropathologic phenotypes after disrupting the chloride transport proteins ClC-6 or ClC-7/Ostm1. J Neuropathol Exp Neurol 69:1228–1246.
Proper EA, Hoogland G, Kappen SM, Jansen GH, Rensen MGA, Schrama LH, van Veelen CWM, van Rijen PC, van Nieuwenhuizen O, Gispen WH, de Graan PNE (2002) Distribution of glutamate transporters in the hippocampus of patients with pharmaco-resistant temporal lobe epilepsy. Brain 125:32–43.
Pullarkat RK, Morris GN (1997) Farnesylation of Batten disease CLN3 protein. Neuropediatrics 28:42–44.
Puranam KL, Guo WX, Qian WH, Nikbakht K, Boustany RM (1999) CLN3 defines a novel antiapoptotic pathway operative in neurodegeneration and mediated by ceramide. Mol Genet Metab 66:294–308.
Purves D (2011) Neuroscience. Sinauer Associates Incorporated.
Putney JW (1990) Capacitative calcium entry revisited. Cell Calcium 11:611–624.
Putney JW (2007) Recent breakthroughs in the molecular mechanism of capacitative calcium entry (with thoughts on how we got here). Cell Calcium 42:103–110.
Pyka M, Busse C, Seidenbecher C, Gundelfinger ED, Faissner A (2011) Astrocytes are crucial for survival and maturation of embryonic hippocampal neurons in a neuron-glia cell-insert coculture assay. Synapse 65:41–53.
Qi JH, Ebrahem Q, Moore N, Murphy G, Claesson-Welsh L, Bond M, Baker A, Anand-Apte B (2003) A novel function for tissue inhibitor of metalloproteinases-3 (TIMP3): inhibition of angiogenesis by blockage of VEGF binding to VEGF receptor-2. Nat Med 9:407–415.
Qiu Z, Sweeney DD, Netzeband JG, Gruol DL (1998) Chronic interleukin-6 alters NMDA receptor-mediated membrane responses and enhances neurotoxicity in developing CNS neurons. J Neurosci 18:10445–10456.
Quinlan RA, Brenner M, Goldman JE, Messing A (2007) GFAP and its role in Alexander disease. Exp Cell Res 313:2077–2087.
Quintero CA, Valdez-Taubas J, Ferrari ML, Haedo SD, Maccioni HJF (2008) Calsenilin and CALP interact with the cytoplasmic tail of UDP-Gal:GA2/GM2/GD2 beta-1,3-galactosyltransferase. Biochem J 412:19–26.
Raininko R, Santavuori P, Heiskala H, Sainio K, Palo J (1990) CT findings in neuronal ceroid lipofuscinoses. Neuropediatrics 21:95–101.
Raivich G (2005) Like cops on the beat: the active role of resting microglia. Trends Neurosci 28:571–573.
Raivich G, Bohatschek M, Kloss CU, Werner A, Jones LL, Kreutzberg GW (1999) Neuroglial activation repertoire in the injured brain: graded response, molecular mechanisms and cues to physiological function. Brain Res Brain Res Rev 30:77–105.
Raivich G, Liu ZQ, Kloss CUA, Labow M, Bluethmann H, Bohatschek M (2002) Cytotoxic potential of proinflammatory cytokines: combined deletion of TNF receptors TNFR1 and TNFR2 prevents motoneuron cell death after facial axotomy in adult mouse. Exp Neurol 178:186–193.
Rakowski RF, Gadsby DC, De Weer P (1989) Stoichiometry and voltage dependence of the sodium pump in voltage-clamped, internally dialyzed squid giant axon. J Gen Physiol 93:903–941.
Ramakers GJA (2002) Rho proteins, mental retardation and the cellular basis of cognition. Trends Neurosci 25:191–199.
Ramakrishnan NA, Drescher MJ, Drescher DG (2012) The SNARE complex in neuronal and sensory cells. Mol Cell Neurosci 50:58–69.
Ramirez-Montealegre D, Pearce DA (2005) Defective lysosomal arginine transport in juvenile Batten disease. Hum Mol Genet 14:3759–3773.
Ramírez G, Toro R, Döbeli H, Bernhardi von R (2005) Protection of rat primary hippocampal cultures from A beta cytotoxicity by pro-inflammatory molecules is mediated by astrocytes.

Neurobiol Dis 19:243–254.
Ransohoff RM (2009) Chemokines and chemokine receptors: standing at the crossroads of immunobiology and neurobiology. Immunity 31:711–721.
Ransohoff RM, Brown MA (2012) Innate immunity in the central nervous system. J Clin Invest 122:1164–1171.
Ransom BR, Goldring S (1973) Slow depolarization in cells presumed to be glia in cerebral cortex of cat. J Neurophysiol 36:869–878.
Rappert A, Bechmann I, Pivneva T, Mahlo J, Biber K, Nolte C, Kovac AD, Gerard C, Boddeke HWGM, Nitsch R, Kettenmann H (2004) CXCR3-dependent microglial recruitment is essential for dendrite loss after brain lesion. J Neurosci 24:8500–8509.
Reggio H, Bainton D, Harms E, Coudrier E, Louvard D (1984) Antibodies against lysosomal membranes reveal a 100,000-mol-wt protein that cross-reacts with purified H+,K+ ATPase from gastric mucosa. J Cell Biol 99:1511–1526.
Reier PJ, Houle JD (1988) The glial scar: its bearing on axonal elongation and transplantation approaches to CNS repair. Adv Neurol 47:87–138.
Relton JK, Rothwell NJ (1992) Interleukin-1 receptor antagonist inhibits ischaemic and excitotoxic neuronal damage in the rat. Brain Res Bull 29:243–246.
Remedios dos CG, Chhabra D, Kekic M, Dedova IV, Tsubakihara M, Berry DA, Nosworthy NJ (2003) Actin binding proteins: regulation of cytoskeletal microfilaments. Physiol Rev 83:433–473.
Reyes RC, Parpura V (2008) Mitochondria modulate Ca2+-dependent glutamate release from rat cortical astrocytes. J Neurosci 28:9682–9691.
Rezaie P, Trillo-Pazos G, Everall IP, Male DK (2002) Expression of beta-chemokines and chemokine receptors in human fetal astrocyte and microglial co-cultures: potential role of chemokines in the developing CNS. Glia 37:64–75.
Rhodes JKJ, Sharkey J, Andrews PJD (2009) The temporal expression, cellular localization, and inhibition of the chemokines MIP-2 and MCP-1 after traumatic brain injury in the rat. J Neurotrauma 26:507–525.
Ricci G, Volpi L, Pasquali L, Petrozzi L, Siciliano G (2009) Astrocyte-neuron interactions in neurological disorders. J Biol Phys 35:317–336.
Richardson SCW, Winistorfer SC, Poupon V, Luzio JP, Piper RC (2004) Mammalian late vacuole protein sorting orthologues participate in early endosomal fusion and interact with the cytoskeleton. Mol Biol Cell 15:1197–1210.
Ridet JL, Malhotra SK, Privat A, Gage FH (1997) Reactive astrocytes: cellular and molecular cues to biological function. Trends Neurosci 20:570–577.
Ridley AJ (2001a) Rho family proteins: coordinating cell responses. Trends Cell Biol 11:471–477.
Ridley AJ (2001b) Rho proteins: linking signaling with membrane trafficking. Traffic 2:303–310.
Riederer P, Sofic E, Rausch WD, Schmidt B, Reynolds GP, Jellinger K, Youdim MB (1989) Transition metals, ferritin, glutathione, and ascorbic acid in parkinsonian brains. J Neurochem 52:515–520.
Rigau V, Morin M, Rousset M-C, de Bock F, Lebrun A, Coubes P, Picot M-C, Baldy-Moulinier M, Bockaert J, Crespel A, Lerner-Natoli M (2007) Angiogenesis is associated with blood-brain barrier permeability in temporal lobe epilepsy. Brain 130:1942–1956.
Rink J, Ghigo E, Kalaidzidis Y, Zerial M (2005) Rab conversion as a mechanism of progression from early to late endosomes. Cell 122:735–749.
Rinne JO, Ruottinen HM, Någren K, Aberg LE, Santavuori P (2002) Positron emission tomography shows reduced striatal dopamine D1 but not D2 receptors in juvenile neuronal ceroid lipofuscinosis. Neuropediatrics 33:138–141.
Rizo J, Chen X, Araç D (2006) Unraveling the mechanisms of synaptotagmin and SNARE function in neurotransmitter release. Trends Cell Biol 16:339–350.
Robel S, Berninger B, Götz M (2011) The stem cell potential of glia: lessons from reactive gliosis. Nat Rev Neurosci 12:88–104.
Roberts LA, Morris BJ, O'Shaughnessy CT (1998) Involvement of two isoforms of SNAP-25 in the expression of long-term potentiation in the rat hippocampus. Neuroreport 9:33–36.
Roberts MS, Macauley SL, Wong AM, Yilmas D, Hohm S, Cooper JD, Sands MS (2012) Combination small molecule PPT1 mimetic and CNS-directed gene therapy as a treatment for infantile neuronal ceroid lipofuscinosis. J Inherit Metab Dis 35:847–857.

Rochlin MW, Itoh K, Adelstein RS, Bridgman PC (1995) Localization of myosin II A and B isoforms in cultured neurons. J Cell Sci 108 (Pt 12):3661–3670.
Rock RB, Gekker G, Hu S, Sheng WS, Cheeran M, Lokensgard JR, Peterson PK (2004) Role of microglia in central nervous system infections. Clin Microbiol Rev 17:942–64–tableofcontents.
Rojo LE, Fernández JA, Maccioni AA, Jimenez JM, Maccioni RB (2008) Neuroinflammation: implications for the pathogenesis and molecular diagnosis of Alzheimer's disease. Arch Med Res 39:1–16.
Rosen AM, Stevens B (2010) The role of the classical complement cascade in synapse loss during development and glaucoma. Adv Exp Med Biol 703:75–93.
Rossi D, Volterra A (2009) Astrocytic dysfunction: insights on the role in neurodegeneration. Brain Res Bull 80:224–232.
Rossi F, Bianchini E (1996) Synergistic induction of nitric oxide by beta-amyloid and cytokines in astrocytes. Biochem Biophys Res Commun 225:474–478.
Rossman KL, Der CJ, Sondek J (2005) GEF means go: turning on RHO GTPases with guanine nucleotide-exchange factors. Nat Rev Mol Cell Biol 6:167–180.
Rossner S, Lange-Dohna C, Zeitschel U, Perez-Polo JR (2005) Alzheimer's disease beta-secretase BACE1 is not a neuron-specific enzyme. J Neurochem 92:226–234.
Rostène W, Dansereau M-A, Godefroy D, Van Steenwinckel J, Reaux-Le Goazigo A, Mélik-Parsadaniantz S, Apartis E, Hunot S, Beaudet N, Sarret P (2011) Neurochemokines: a menage a trois providing new insights on the functions of chemokines in the central nervous system. J Neurochem 118:680–694.
Rothman JE (1994) Mechanisms of intracellular protein transport. Nature 372:55–63.
Rothstein JD, Dykes-Hoberg M, Pardo CA, Bristol LA, Jin L, Kuncl RW, Kanai Y, Hediger MA, Wang Y, Schielke JP, Welty DF (1996) Knockout of glutamate transporters reveals a major role for astroglial transport in excitotoxicity and clearance of glutamate. Neuron 16:675–686.
Rothstein JD, Martin L, Levey AI, Dykes-Hoberg M, Jin L, Wu D, Nash N, Kuncl RW (1994) Localization of neuronal and glial glutamate transporters. Neuron 13:713–725.
Rothstein JD, Martin LJ, Kuncl RW (1992) Decreased glutamate transport by the brain and spinal cord in amyotrophic lateral sclerosis. N Engl J Med 326:1464–1468.
Rothstein JD, Patel S, Regan MR, Haenggeli C, Huang YH, Bergles DE, Jin L, Dykes Hoberg M, Vidensky S, Chung DS, Toan SV, Bruijn LI, Su Z-Z, Gupta P, Fisher PB (2005) Beta-lactam antibiotics offer neuroprotection by increasing glutamate transporter expression. Nature 433:73–77.
Röhl C, Armbrust E, Kolbe K, Lucius R, Maser E, Venz S, Gülden M (2008) Activated microglia modulate astroglial enzymes involved in oxidative and inflammatory stress and increase the resistance of astrocytes to oxidative stress in vitro. Glia 56:1114–1126.
Röhl C, Sievers J (2005) Microglia is activated by astrocytes in trimethyltin intoxication. Toxicol Appl Pharmacol 204:36–45.
Rubenstein JLR, Merzenich MM (2003) Model of autism: increased ratio of excitation/inhibition in key neural systems. Genes Brain Behav 2:255–267.
Rubino M, Miaczynska M, Lippé R, Zerial M (2000) Selective membrane recruitment of EEA1 suggests a role in directional transport of clathrin-coated vesicles to early endosomes. J Biol Chem 275:3745–3748.
Rubinsztein DC, DiFiglia M, Heintz N, Nixon RA, Qin Z-H, Ravikumar B, Stefanis L, Tolkovsky A (2005) Autophagy and its possible roles in nervous system diseases, damage and repair. Autophagy 1:11–22.
Rubio N, de Felipe C (1991) Demonstration of the presence of a specific interferon-gamma receptor on murine astrocyte cell surface. J Neuroimmunol 35:111–117.
Rudge JS, Pasnikowski EM, Holst P, Lindsay RM (1995) Changes in neurotrophic factor expression and receptor activation following exposure of hippocampal neuron/astrocyte cocultures to kainic acid. J Neurosci 15:6856–6867.
Ruivo R, Anne C, Sagné C, Gasnier B (2009) Molecular and cellular basis of lysosomal transmembrane protein dysfunction. Biochim Biophys Acta 1793:636–649.
Ruocco A, Nicole O, Docagne F, Ali C, Chazalviel L, Komesli S, Yablonsky F, Roussel S, MacKenzie ET, Vivien D, Buisson A (1999) A transforming growth factor-beta antagonist unmasks the neuroprotective role of this endogenous cytokine in excitotoxic and ischemic brain injury. J

Cereb Blood Flow Metab 19:1345–1353.
Ruottinen HM, Rinne JO, Haaparanta M, Solin O, Bergman J, Oikonen VJ, Järvelä I, Santavuori P (1997) [18F]fluorodopa PET shows striatal dopaminergic dysfunction in juvenile neuronal ceroid lipofuscinosis. J Neurol Neurosurg Psychiatr 62:622–625.
Rutka JT, Smith SL (1993) Transfection of human astrocytoma cells with glial fibrillary acidic protein complementary DNA: analysis of expression, proliferation, and tumorigenicity. Cancer Res 53:3624–3631.
Ryu J, Liu L, Wong TP, Wu DC, Burette A, Weinberg R, Wang YT, Sheng M (2006) A critical role for myosin IIb in dendritic spine morphology and synaptic function. Neuron 49:175–182.
Saad B, Constam DB, Ortmann R, Moos M, Fontana A, Schachner M (1991) Astrocyte-derived TGF-beta 2 and NGF differentially regulate neural recognition molecule expression by cultured astrocytes. J Cell Biol 115:473–484.
Saadoun S, Papadopoulos MC, Watanabe H, Yan D, Manley GT, Verkman AS (2005) Involvement of aquaporin-4 in astroglial cell migration and glial scar formation. J Cell Sci 118:5691–5698.
Sachse M, Ramm G, Strous G, Klumperman J (2002) Endosomes: multipurpose designs for integrating housekeeping and specialized tasks. Histochem Cell Biol 117:91–104.
Saederup N, Cardona AE, Croft K, Mizutani M, Cotleur AC, Tsou C-L, Ransohoff RM, Charo IF (2010) Selective chemokine receptor usage by central nervous system myeloid cells in CCR2-red fluorescent protein knock-in mice. PLoS ONE 5:e13693.
Saftig P, Klumperman J (2009) Lysosome biogenesis and lysosomal membrane proteins: trafficking meets function. Nat Rev Mol Cell Biol 10:623–635.
Sagara J, Makino N, Bannai S (1996) Glutathione efflux from cultured astrocytes. J Neurochem 66:1876–1881.
Saha A, Kim S-J, Zhang Z, Lee Y-C, Sarkar C, Tsai P-C, Mukherjee AB (2008) RAGE signaling contributes to neuroinflammation in infantile neuronal ceroid lipofuscinosis. FEBS Lett 582:3823–3831.
Sands MS, Davidson BL (2006) Gene therapy for lysosomal storage diseases. Mol Ther 13:839–849.
Sango K, Takano M, Ajiki K, Tokashiki A, Arai N, Kawano H, Horie H, Yamanaka S (2005) Impaired neurite outgrowth in the retina of a murine model of Sandhoff disease. Invest Ophthalmol Vis Sci 46:3420–3425.
Sango K, Yamanaka S, Ajiki K, Tokashiki A, Watabe K (2002) Lysosomal storage results in impaired survival but normal neurite outgrowth in dorsal root ganglion neurones from a mouse model of Sandhoff disease. Neuropathol Appl Neurobiol 28:23–34.
Sann S, Wang Z, Brown H, Jin Y (2009) Roles of endosomal trafficking in neurite outgrowth and guidance. Trends Cell Biol 19:317–324.
Santavuori P (1988) Neuronal ceroid-lipofuscinoses in childhood. Brain Dev 10:80–83.
Santavuori P, Heiskala H, Autti T, Johansson E, Westermarck T (1989) Comparison of the clinical courses in patients with juvenile neuronal ceroid lipofuscinosis receiving antioxidant treatment and those without antioxidant treatment. Adv Exp Med Biol 266:273–282.
Santavuori P, Heiskala H, Westermarck T, Sainio K, Moren R (1988) Experience over 17 years with antioxidant treatment in Spielmeyer-Sjögren disease. Am J Med Genet Suppl 5:265–274.
Santavuori P, Linnankivi T, Jaeken J, Vanhanen SL, Telakivi T, Heiskala H (1993) Psychological symptoms and sleep disturbances in neuronal ceroid-lipofuscinoses (NCL). J Inherit Metab Dis 16:245–248.
Santello M, Calì C, Bezzi P (2012) Gliotransmission and the tripartite synapse. Adv Exp Med Biol 970:307–331.
Sappington RM, Pearce DA, Calkins DJ (2003) Optic nerve degeneration in a murine model of juvenile ceroid lipofuscinosis. Invest Ophthalmol Vis Sci 44:3725–3731.
Sarkar S, Floto RA, Berger Z, Imarisio S, Cordenier A, Pasco M, Cook LJ, Rubinsztein DC (2005) Lithium induces autophagy by inhibiting inositol monophosphatase. J Cell Biol 170:1101–1111.
Sarpong A, Schottmann G, Rüther K, Stoltenburg G, Kohlschütter A, Hübner C, Schuelke M (2009) Protracted course of juvenile ceroid lipofuscinosis associated with a novel CLN3 mutation (p.Y199X). Clin Genet 76:38–45.
Sasaki T, Matsuki N, Ikegaya Y (2011) Action-potential modulation during axonal conduction. Science 331:599–601.

Sass JB, Ang LC, Juurlink BH (1993) A simple, yet versatile, co-culture method for examining neuron-glia interactions. J Neurosci Methods 47:115–121.
Sastry SK, Horwitz AF (1993) Integrin cytoplasmic domains: mediators of cytoskeletal linkages and extra- and intracellular initiated transmembrane signaling. Curr Opin Cell Biol 5:819–831.
Satoh J, Paty DW, Kim SU (1996) Counteracting effect of IFN-beta on IFN-gamma-induced proliferation of human astrocytes in culture. Mult Scler 1:279–287.
Sattler R, Rothstein JD (2006) Regulation and dysregulation of glutamate transporters. Handb Exp Pharmacol:277–303.
Saura J (2007) Microglial cells in astroglial cultures: a cautionary note. J Neuroinflammation 4:26.
Saxena S, Bucci C, Weis J, Kruttgen A (2005a) The small GTPase Rab7 controls the endosomal trafficking and neuritogenic signaling of the nerve growth factor receptor TrkA. J Neurosci 25:10930–10940.
Saxena S, Howe CL, Cosgaya JM, Steiner P, Hirling H, Chan JR, Weis J, Kruttgen A (2005b) Differential endocytic sorting of p75NTR and TrkA in response to NGF: a role for late endosomes in TrkA trafficking. Mol Cell Neurosci 28:571–587.
Scemes E (2000) Components of astrocytic intercellular calcium signaling. Mol Neurobiol 22:167–179.
Scemes E, Dermietzel R, Spray DC (1998) Calcium waves between astrocytes from Cx43 knockout mice. Glia 24:65–73.
Scemes E, Giaume C (2006) Astrocyte calcium waves: what they are and what they do. Glia 54:716–725.
Scemes E, Suadicani SO, Spray DC (2000) Intercellular communication in spinal cord astrocytes: fine tuning between gap junctions and P2 nucleotide receptors in calcium wave propagation. J Neurosci 20:1435–1445.
Schafer DP, Jha S, Liu F, Akella T, McCullough LD, Rasband MN (2009) Disruption of the axon initial segment cytoskeleton is a new mechanism for neuronal injury. J Neurosci 29:13242–13254.
Schafer DP, Lehrman EK, Stevens B (2013) The “quad-partite” synapse: Microglia-synapse interactions in the developing and mature CNS. Glia 61:24–36.
Schafer DP, Stevens B (2010) Synapse elimination during development and disease: immune molecules take centre stage. Biochem Soc Trans 38:476–481.
Schantz von C, Kielar C, Hansen SN, Pontikis CC, Alexander NA, Kopra O, Jalanko A, Cooper JD (2009) Progressive thalamocortical neuron loss in Cln5 deficient mice: Distinct effects in Finnish variant late infantile NCL. Neurobiol Dis 34:308–319.
Scheff SW, Price DA, Schmitt FA, Mufson EJ (2006) Hippocampal synaptic loss in early Alzheimer's disease and mild cognitive impairment. Neurobiol Aging 27:1372–1384.
Schell MJ, Molliver ME, Snyder SH (1995) D-serine, an endogenous synaptic modulator: localization to astrocytes and glutamate-stimulated release. Proc Natl Acad Sci USA 92:3948–3952.
Schilling T, Nitsch R, Heinemann U, Haas D, Eder C (2001) Astrocyte-released cytokines induce ramification and outward K+ channel expression in microglia via distinct signalling pathways. Eur J Neurosci 14:463–473.
Schinder AF, Poo M (2000) The neurotrophin hypothesis for synaptic plasticity. Trends Neurosci 23:639–645.
Schindler C, Brutsaert S (1999) Interferons as a paradigm for cytokine signal transduction. Cell Mol Life Sci 55:1509–1522.
Schipke CG, Boucsein C, Ohlemeyer C, Kirchhoff F, Kettenmann H (2002) Astrocyte Ca2+ waves trigger responses in microglial cells in brain slices. FASEB J 16:255–257.
Schmalenbach C, Müller HW (1993) Astroglia-neuron interactions that promote long-term neuronal survival. J Chem Neuroanat 6:229–237.
Schmid RS, Graff RD, Schaller MD, Chen S, Schachner M, Hemperly JJ, Maness PF (1999) NCAM stimulates the Ras-MAPK pathway and CREB phosphorylation in neuronal cells. J Neurobiol 38:542–558.
Schmidt A, Hall A (2002) Guanine nucleotide exchange factors for Rho GTPases: turning on the switch. Genes Dev 16:1587–1609.
Schmidt MM, Dringen R (2010) Fumaric acid diesters deprive cultured primary astrocytes rapidly of glutathione. Neurochem Int 57:460–467.

Schmiedt M-L, Blom T, Blom T, Kopra O, Wong A, Schantz-Fant von C, Ikonen E, Kuronen M, Jauhiainen M, Cooper JD, Jalanko A (2012) Cln5-deficiency in mice leads to microglial activation, defective myelination and changes in lipid metabolism. Neurobiol Dis 46:19–29.
Schousboe A, Waagepetersen HS (2005) Role of astrocytes in glutamate homeostasis: implications for excitotoxicity. Neurotox Res 8:221–225.
Schroder K, Hertzog PJ, Ravasi T, Hume DA (2004) Interferon-gamma: an overview of signals, mechanisms and functions. J Leukoc Biol 75:163–189.
Schröder B, Wrocklage C, Pan C, Jäger R, Kösters B, Schäfer H, Elsässer H-P, Mann M, Hasilik A (2007) Integral and associated lysosomal membrane proteins. Traffic 8:1676–1686.
Schröder BA, Wrocklage C, Hasilik A, Saftig P (2010) The proteome of lysosomes. Proteomics 10:4053–4076.
Schubert P, Ferroni S (2003) Pathological glial reactions in neurodegenerative disorders: prospects for future therapeutics. Expert Rev Neurother 3:279–287.
Schubert V, Bouvier D, Volterra A (2011) SNARE protein expression in synaptic terminals and astrocytes in the adult hippocampus: a comparative analysis. Glia 59:1472–1488.
Schultz ML, Tecedor L, Chang M, Davidson BL (2011) Clarifying lysosomal storage diseases. Trends Neurosci 34:401–410.
Schulz JB, Lindenau J, Seyfried J, Dichgans J (2000) Glutathione, oxidative stress and neurodegeneration. Eur J Biochem 267:4904–4911.
Schummers J, Yu H, Sur M (2008) Tuned responses of astrocytes and their influence on hemodynamic signals in the visual cortex. Science 320:1638–1643.
Schwartz JP, Nishiyama N (1994) Neurotrophic factor gene expression in astrocytes during development and following injury. Brain Res Bull 35:403–407.
Seehafer SS, Pearce DA (2006) You say lipofuscin, we say ceroid: defining autofluorescent storage material. Neurobiol Aging 27:576–588.
Seehafer SS, Ramirez-Montealegre D, Wong AM, Chan C-H, Castaneda J, Horak M, Ahmadi SM, Lim MJ, Cooper JD, Pearce DA (2011) Immunosuppression alters disease severity in juvenile Batten disease mice. J Neuroimmunol 230:169–172.
Seifert G, Schilling K, Steinhäuser C (2006) Astrocyte dysfunction in neurological disorders: a molecular perspective. Nat Rev Neurosci 7:194–206.
Seifert G, Steinhäuser C (2011) Neuron-astrocyte signaling and epilepsy. Exp Neurol.
Seifert S, Pannell M, Uckert W, Färber K, Kettenmann H (2011) Transmitter- and hormone-activated Ca(2+) responses in adult microglia/brain macrophages in situ recorded after viral transduction of a recombinant Ca(2+) sensor. Cell Calcium 49:365–375.
Seigel GM, Lotery A, Kummer A, Bernard DJ, Greene NDE, Turmaine M, Derksen T, Nussbaum RL, Davidson B, Wagner J, Mitchison HM (2002) Retinal pathology and function in a Cln3 knockout mouse model of juvenile Neuronal Ceroid Lipofuscinosis (batten disease). Mol Cell Neurosci 19:515–527.
Selak S, Braun JE, Fritzler MJ (2004) Characterization of early endosome antigen 1 in neural tissues. Biochem Biophys Res Commun 323:1334–1342.
Selak S, Paternain AV, Fritzler MJ, Lerma J (2006) Human autoantibodies against early endosome antigen-1 enhance excitatory synaptic transmission. Neuroscience 143:953–964.
Semenova MM, Mäki-Hokkonen AMJ, Cao J, Komarovski V, Forsberg KM, Koistinaho M, Coffey ET, Courtney MJ (2007) Rho mediates calcium-dependent activation of p38alpha and subsequent excitotoxic cell death. Nat Neurosci 10:436–443.
Semple BD, Kossmann T, Morganti-Kossmann MC (2010) Role of chemokines in CNS health and pathology: a focus on the CCL2/CCR2 and CXCL8/CXCR2 networks. J Cereb Blood Flow Metab 30:459–473.
Sergeeva M, Ubl JJ, Reiser G (2000) Disruption of actin cytoskeleton in cultured rat astrocytes suppresses ATP- and bradykinin-induced [Ca(2+)](i) oscillations by reducing the coupling efficiency between Ca(2+) release, capacitative Ca(2+) entry, and store refilling. Neuroscience 97:765–769.
Serrano A, Haddjeri N, Lacaille J-C, Robitaille R (2006) GABAergic network activation of glial cells underlies hippocampal heterosynaptic depression. J Neurosci 26:5370–5382.
Shashidharan P, Plaitakis A (1993) Cloning and characterization of a glutamate transporter cDNA from human cerebellum. Biochim Biophys Acta 1216:161–164.
Shashidharan P, Wittenberg I, Plaitakis A (1994) Molecular cloning of human brain

glutamate/aspartate transporter II. Biochim Biophys Acta 1191:393–396.
Shen D, Wang X, Li X, Zhang X, Yao Z, Dibble S, Dong X-P, Yu T, Lieberman AP, Showalter HD, Xu H (2012) Lipid storage disorders block lysosomal trafficking by inhibiting a TRP channel and lysosomal calcium release. Nat Commun 3:731.
Sheng M, Kim MJ (2002) Postsynaptic signaling and plasticity mechanisms. Science 298:776–780.
Sheng W, Zong Y, Mohammad A, Ajit D, Cui J, Han D, Hamilton JL, Simonyi A, Sun AY, Gu Z, Hong J-S, Weisman GA, Sun GY (2011) Pro-inflammatory cytokines and lipopolysaccharide induce changes in cell morphology, and upregulation of ERK1/2, iNOS and $sPLA_2$-IIA expression in astrocytes and microglia. J Neuroinflammation 8:121.
Sherr CJ (1996) Cancer cell cycles. Science 274:1672–1677.
Shi S, Hayashi Y, Esteban JA, Malinow R (2001) Subunit-specific rules governing AMPA receptor trafficking to synapses in hippocampal pyramidal neurons. Cell 105:331–343.
Shi X, Yasumoto S, Nakagawa E, Fukasawa T, Uchiya S, Hirose S (2009) Missense mutation of the sodium channel gene SCN2A causes Dravet syndrome. Brain Dev 31:758–762.
Shih AY, Johnson DA, Wong G, Kraft AD, Jiang L, Erb H, Johnson JA, Murphy TH (2003) Coordinate regulation of glutathione biosynthesis and release by Nrf2-expressing glia potently protects neurons from oxidative stress. J Neurosci 23:3394–3406.
Shimizu S, Abt A, Meucci O (2011) Bilaminar co-culture of primary rat cortical neurons and glia. J Vis Exp.
Shin E-Y, Shin K-S, Lee C-S, Woo K-N, Quan S-H, Soung N-K, Kim YG, Cha CI, Kim S-R, Park D, Bokoch GM, Kim E-G (2002) Phosphorylation of p85 beta PIX, a Rac/Cdc42-specific guanine nucleotide exchange factor, via the Ras/ERK/PAK2 pathway is required for basic fibroblast growth factor-induced neurite outgrowth. J Biol Chem 277:44417–44430.
Shin J-Y, Fang Z-H, Yu Z-X, Wang C-E, Li S-H, Li X-J (2005) Expression of mutant huntingtin in glial cells contributes to neuronal excitotoxicity. J Cell Biol 171:1001–1012.
Shirasu M, Kimura K, Kataoka M, Takahashi M, Okajima S, Kawaguchi S, Hirasawa Y, Ide C, Mizoguchi A (2000) VAMP-2 promotes neurite elongation and SNAP-25A increases neurite sprouting in PC12 cells. Neurosci Res 37:265–275.
Shrikant P, Benveniste EN (1996) The central nervous system as an immunocompetent organ: role of glial cells in antigen presentation. J Immunol 157:1819–1822.
Shu Y, Yu Y, Yang J, McCormick DA (2007) Selective control of cortical axonal spikes by a slowly inactivating K+ current. Proc Natl Acad Sci USA 104:11453–11458.
Shubayev VI, Myers RR (2004) Matrix metalloproteinase-9 promotes nerve growth factor-induced neurite elongation but not new sprout formation in vitro. J Neurosci Res 77:229–239.
Sidoryk-Wegrzynowicz M, Wegrzynowicz M, Lee E, Bowman AB, Aschner M (2011) Role of astrocytes in brain function and disease. Toxicol Pathol 39:115–123.
Siintola E, Partanen S, Strömme P, Haapanen A, Haltia M, Maehlen J, Lehesjoki A-E, Tyynelä J (2006) Cathepsin D deficiency underlies congenital human neuronal ceroid-lipofuscinosis. Brain 129:1438–1445.
Silberstein FC, De Simone R, Levi G, Aloisi F (1996) Cytokine-regulated expression of platelet-derived growth factor gene and protein in cultured human astrocytes. J Neurochem 66:1409–1417.
Silver J, Miller JH (2004) Regeneration beyond the glial scar. Nat Rev Neurosci 5:146–156.
Simard M, Arcuino G, Takano T, Liu QS, Nedergaard M (2003) Signaling at the gliovascular interface. J Neurosci 23:9254–9262.
Simard M, Nedergaard M (2004) The neurobiology of glia in the context of water and ion homeostasis. Neuroscience 129:877–896.
Simons M, Wang M, McBride OW, Kawamoto S, Yamakawa K, Gdula D, Adelstein RS, Weir L (1991) Human nonmuscle myosin heavy chains are encoded by two genes located on different chromosomes. Circ Res 69:530–539.
Simonsen A, Lippé R, Christoforidis S, Gaullier JM, Brech A, Callaghan J, Toh BH, Murphy C, Zerial M, Stenmark H (1998) EEA1 links PI(3)K function to Rab5 regulation of endosome fusion. Nature 394:494–498.
Simpson JE, Newcombe J, Cuzner ML, Woodroofe MN (1998) Expression of monocyte chemoattractant protein-1 and other beta-chemokines by resident glia and inflammatory cells in multiple sclerosis lesions. J Neuroimmunol 84:238–249.
Singh S, Swarnkar S, Goswami P, Nath C (2011) Astrocytes and microglia: responses to

neuropathological conditions. Int J Neurosci 121:589–597.
Sisková Z, Page A, O'Connor V, Perry VH (2009) Degenerating synaptic boutons in prion disease: microglia activation without synaptic stripping. Am J Pathol 175:1610–1621.
Siu G, Hedrick SM, Brian AA (1989) Isolation of the murine intercellular adhesion molecule 1 (ICAM-1) gene. ICAM-1 enhances antigen-specific T cell activation. J Immunol 143:3813–3820.
Skaper SD (2012) Neuronal growth-promoting and inhibitory cues in neuroprotection and neuroregeneration. Methods Mol Biol 846:13–22.
Skaper SD, Facci L (2012) Central nervous system neuron-glia co-culture models. Methods Mol Biol 846:79–89.
Skoff RP, Knapp PE (1991) Division of astroblasts and oligodendroblasts in postnatal rodent brain: evidence for separate astrocyte and oligodendrocyte lineages. Glia 4:165–174.
Sköld MK, Gertten von C, Sandberg-Nordqvist A-C, Mathiesen T, Holmin S (2005) VEGF and VEGF receptor expression after experimental brain contusion in rat. J Neurotrauma 22:353–367.
Sleat DE, Sohar I, Pullarkat PS, Lobel P, Pullarkat RK (1998) Specific alterations in levels of mannose 6-phosphorylated glycoproteins in different neuronal ceroid lipofuscinoses. Biochem J 334 (Pt 3):547–551.
Sleat DE, Wiseman JA, El-Banna M, Kim K-H, Mao Q, Price S, Macauley SL, Sidman RL, Shen MM, Zhao Q, Passini MA, Davidson BL, Stewart GR, Lobel P (2004) A mouse model of classical late-infantile neuronal ceroid lipofuscinosis based on targeted disruption of the CLN2 gene results in a loss of tripeptidyl-peptidase I activity and progressive neurodegeneration. J Neurosci 24:9117–9126.
Slivka A, Mytilineou C, Cohen G (1987) Histochemical evaluation of glutathione in brain. Brain Res 409:275–284.
Small JV, Kaverina I, Krylyshkina O, Rottner K (1999) Cytoskeleton cross-talk during cell motility. FEBS Lett 452:96–99.
Smith D, Wallom K-L, Williams IM, Jeyakumar M, Platt FM (2009) Beneficial effects of anti-inflammatory therapy in a mouse model of Niemann-Pick disease type C1. Neurobiol Dis 36:242–251.
Smith JM, Bradley DP, James MF, Huang CL-H (2006) Physiological studies of cortical spreading depression. Biol Rev Camb Philos Soc 81:457–481.
Snider WD (1994) Functions of the neurotrophins during nervous system development: what the knockouts are teaching us. Cell 77:627–638.
Sofroniew MV (2009) Molecular dissection of reactive astrogliosis and glial scar formation. Trends Neurosci 32:638–647.
Sofroniew MV, Vinters HV (2010) Astrocytes: biology and pathology. Acta Neuropathol 119:7–35.
Solà C, Casal C, Tusell JM, Serratosa J (2002) Astrocytes enhance lipopolysaccharide-induced nitric oxide production by microglial cells. Eur J Neurosci 16:1275–1283.
Song A-H, Wang D, Chen G, Li Y, Luo J, Duan S, Poo M-M (2009) A selective filter for cytoplasmic transport at the axon initial segment. Cell 136:1148–1160.
Song H, Stevens CF, Gage FH (2002) Astroglia induce neurogenesis from adult neural stem cells. Nature 417:39–44.
Song M, Mohamad O, Gu X, Wei L, Yu SP (2012) Restoration of Intracortical and Thalamocortical Circuits after Transplantation of Bone Marrow Mesenchymal Stem Cells into the Ischemic Brain of Mice. Cell Transplant.
Söllner T, Bennett MK, Whiteheart SW, Scheller RH, Rothman JE (1993a) A protein assembly-disassembly pathway in vitro that may correspond to sequential steps of synaptic vesicle docking, activation, and fusion. Cell 75:409–418.
Söllner T, Whiteheart SW, Brunner M, Erdjument-Bromage H, Geromanos S, Tempst P, Rothman JE (1993b) SNAP receptors implicated in vesicle targeting and fusion. Nature 362:318–324.
Stachelek SJ, Tuft RA, Lifschitz LM, Leonard DM, Farwell AP, Leonard JL (2001) Real-time visualization of processive myosin 5a-mediated vesicle movement in living astrocytes. J Biol Chem 276:35652–35659.
Staropoli JF et al. (2012) Large-scale phenotyping of an accurate genetic mouse model of JNCL identifies novel early pathology outside the central nervous system. PLoS ONE 7:e38310.
Stein CS, Yancey PH, Martins I, Sigmund RD, Stokes JB, Davidson BL (2010) Osmoregulation of ceroid neuronal lipofuscinosis type 3 in the renal medulla. Am J Physiol, Cell Physiol

298:C1388–C1400.
Steinert PM, Chou YH, Prahlad V, Parry DA, Marekov LN, Wu KC, Jang SI, Goldman RD (1999) A high molecular weight intermediate filament-associated protein in BHK-21 cells is nestin, a type VI intermediate filament protein. Limited co-assembly in vitro to form heteropolymers with type III vimentin and type IV alpha-internexin. J Biol Chem 274:9881–9890.
Stenovec M, Kreft M, Grilc S, Potokar M, Kreft ME, Pangrsic T, Zorec R (2007) Ca2+-dependent mobility of vesicles capturing anti-VGLUT1 antibodies. Exp Cell Res 313:3809–3818.
Stephan AH, Barres BA, Stevens B (2012) The complement system: an unexpected role in synaptic pruning during development and disease. Annu Rev Neurosci 35:369–389.
Stetler-Stevenson WG (2008) Tissue inhibitors of metalloproteinases in cell signaling: metalloproteinase-independent biological activities. Sci Signal 1:re6.
Stevens B, Allen NJ, Vazquez LE, Howell GR, Christopherson KS, Nouri N, Micheva KD, Mehalow AK, Huberman AD, Stafford B, Sher A, Litke AM, Lambris JD, Smith SJ, John SWM, Barres BA (2007) The classical complement cascade mediates CNS synapse elimination. Cell 131:1164–1178.
Stewart M (1993) Intermediate filament structure and assembly. Curr Opin Cell Biol 5:3–11.
Stewart VC, Stone R, Gegg ME, Sharpe MA, Hurst RD, Clark JB, Heales SJR (2002) Preservation of extracellular glutathione by an astrocyte derived factor with properties comparable to extracellular superoxide dismutase. J Neurochem 83:984–991.
Storch S, Pohl S, Braulke T (2004) A dileucine motif and a cluster of acidic amino acids in the second cytoplasmic domain of the batten disease-related CLN3 protein are required for efficient lysosomal targeting. J Biol Chem 279:53625–53634.
Storch S, Pohl S, Quitsch A, Falley K, Braulke T (2007) C-terminal prenylation of the CLN3 membrane glycoprotein is required for efficient endosomal sorting to lysosomes. Traffic 8:431–444.
Storck T, Schulte S, Hofmann K, Stoffel W (1992) Structure, expression, and functional analysis of a Na(+)-dependent glutamate/aspartate transporter from rat brain. Proc Natl Acad Sci USA 89:10955–10959.
Storkebaum E et al. (2005) Treatment of motoneuron degeneration by intracerebroventricular delivery of VEGF in a rat model of ALS. Nat Neurosci 8:85–92.
Stout CE, Costantin JL, Naus CCG, Charles AC (2002) Intercellular calcium signaling in astrocytes via ATP release through connexin hemichannels. J Biol Chem 277:10482–10488.
Strijbos PJ, Rothwell NJ (1995) Interleukin-1 beta attenuates excitatory amino acid-induced neurodegeneration in vitro: involvement of nerve growth factor. J Neurosci 15:3468–3474.
Strong AJ, Fabricius M, Boutelle MG, Hibbins SJ, Hopwood SE, Jones R, Parkin MC, Lauritzen M (2002) Spreading and synchronous depressions of cortical activity in acutely injured human brain. Stroke 33:2738–2743.
Styrt B, Pollack CR, Klempner MS (1988) An abnormal calcium uptake pump in Chediak-Higashi neutrophil lysosomes. J Leukoc Biol 44:130–135.
Sudhof TC (2004) The synaptic vesicle cycle. Annu Rev Neurosci 27:509–547.
Sullivan KF (1988) Structure and utilization of tubulin isotypes. Annu Rev Cell Biol 4:687–716.
Sultana R, Butterfield DA (2004) Oxidatively modified GST and MRP1 in Alzheimer's disease brain: implications for accumulation of reactive lipid peroxidation products. Neurochem Res 29:2215–2220.
Sun D, Jakobs TC (2011) Structural Remodeling of Astrocytes in the Injured CNS. Neuroscientist.
Sun Y, Jin K, Xie L, Childs J, Mao XO, Logvinova A, Greenberg DA (2003) VEGF-induced neuroprotection, neurogenesis, and angiogenesis after focal cerebral ischemia. J Clin Invest 111:1843–1851.
Sun Y, Lim Y, Li F, Liu S, Lu J-J, Haberberger R, Zhong J-H, Zhou X-F (2012) ProBDNF collapses neurite outgrowth of primary neurons by activating RhoA. PLoS ONE 7:e35883.
Sutherland LM, Hemsley KM, Hopwood JJ (2008) Primary culture of neural cells isolated from the cerebellum of newborn and adult mucopolysaccharidosis type IIIA mice. Cell Mol Neurobiol 28:949–959.
Suzuki A, Stern SA, Bozdagi O, Huntley GW, Walker RH, Magistretti PJ, Alberini CM (2011) Astrocyte-neuron lactate transport is required for long-term memory formation. Cell 144:810–823.
Suzuki M, McHugh J, Tork C, Shelley B, Klein SM, Aebischer P, Svendsen CN (2007) GDNF

secreting human neural progenitor cells protect dying motor neurons, but not their projection to muscle, in a rat model of familial ALS. PLoS ONE 2:e689.
Swanson RA, Ying W, Kauppinen TM (2004) Astrocyte influences on ischemic neuronal death. Curr Mol Med 4:193–205.
Szabó C (1996) Physiological and pathophysiological roles of nitric oxide in the central nervous system. Brain Res Bull 41:131–141.
Szatkowski M, Barbour B, Attwell D (1990) Non-vesicular release of glutamate from glial cells by reversed electrogenic glutamate uptake. Nature 348:443–446.
Tachibana K, Hirota S, Iizasa H, Yoshida H, Kawabata K, Kataoka Y, Kitamura Y, Matsushima K, Yoshida N, Nishikawa S, Kishimoto T, Nagasawa T (1998) The chemokine receptor CXCR4 is essential for vascularization of the gastrointestinal tract. Nature 393:591–594.
Takagishi Y, Futaki S, Itoh K, Espreafico EM, Murakami N, Murata Y, Mochida S (2005) Localization of myosin II and V isoforms in cultured rat sympathetic neurones and their potential involvement in presynaptic function. J Physiol (Lond) 569:195–208.
Takahashi S, Driscoll BF, Law MJ, Sokoloff L (1995) Role of sodium and potassium ions in regulation of glucose metabolism in cultured astroglia. Proc Natl Acad Sci USA 92:4616–4620.
Takano T, Oberheim N, Cotrina ML, Nedergaard M (2009) Astrocytes and ischemic injury. Stroke 40:S8–S12.
Takashima A, Noguchi K, Sato K, Hoshino T, Imahori K (1993) Tau protein kinase I is essential for amyloid beta-protein-induced neurotoxicity. Proc Natl Acad Sci USA 90:7789–7793.
Tanaka H, Katoh A, Oguro K, Shimazaki K, Gomi H, Itohara S, Masuzawa T, Kawai N (2002) Disturbance of hippocampal long-term potentiation after transient ischemia in GFAP deficient mice. J Neurosci Res 67:11–20.
Tanaka M, Kawahara K, Kosugi T, Yamada T, Mioka T (2007) Changes in the spontaneous calcium oscillations for the development of the preconditioning-induced ischemic tolerance in neuron/astrocyte co-culture. Neurochem Res 32:988–1001.
Tanaka S, Morishita T, Hashimoto Y, Hattori S, Nakamura S, Shibuya M, Matuoka K, Takenawa T, Kurata T, Nagashima K (1994) C3G, a guanine nucleotide-releasing protein expressed ubiquitously, binds to the Src homology 3 domains of CRK and GRB2/ASH proteins. Proc Natl Acad Sci USA 91:3443–3447.
Tang BL (2001) Protein trafficking mechanisms associated with neurite outgrowth and polarized sorting in neurons. J Neurochem 79:923–930.
Tararuk T, Ostman N, Li W, Björkblom B, Padzik A, Zdrojewska J, Hongisto V, Herdegen T, Konopka W, Courtney MJ, Coffey ET (2006) JNK1 phosphorylation of SCG10 determines microtubule dynamics and axodendritic length. J Cell Biol 173:265–277.
Tardy M (2002) Role of laminin bioavailability in the astroglial permissivity for neuritic outgrowth. An Acad Bras Cienc 74:683–690.
Taschner PE, de Vos N, Breuning MH (1997) Cross-species homology of the CLN3 gene. Neuropediatrics 28:18–20.
Teismann P, Schulz JB (2004) Cellular pathology of Parkinson's disease: astrocytes, microglia and inflammation. Cell Tissue Res 318:149–161.
Terman A, Brunk UT (2004) Lipofuscin. Int J Biochem Cell Biol 36:1400–1404.
Thau-Zuchman O, Shohami E, Alexandrovich AG, Leker RR (2010) Vascular endothelial growth factor increases neurogenesis after traumatic brain injury. J Cereb Blood Flow Metab 30:1008–1016.
Theodosis DT, Poulain DA, Oliet SHR (2008) Activity-dependent structural and functional plasticity of astrocyte-neuron interactions. Physiol Rev 88:983–1008.
Thompson D, Pepys MB, Wood SP (1999) The physiological structure of human C-reactive protein and its complex with phosphocholine. Structure 7:169–177.
Thompson PM, Egbufoama S, Vawter MP (2003) SNAP-25 reduction in the hippocampus of patients with schizophrenia. Prog Neuropsychopharmacol Biol Psychiatry 27:411–417.
Thompson PM, Sower AC, Perrone-Bizzozero NI (1998) Altered levels of the synaptosomal associated protein SNAP-25 in schizophrenia. Biol Psychiatry 43:239–243.
Tian G-F, Azmi H, Takano T, Xu Q, Peng W, Lin J, Oberheim N, Lou N, Wang X, Zielke HR, Kang J, Nedergaard M (2005) An astrocytic basis of epilepsy. Nat Med 11:973–981.
Tian J, Xie Z-J (2008) The Na-K-ATPase and calcium-signaling microdomains. Physiology

(Bethesda) 23:205–211.
Tian L, Ma L, Kaarela T, Li Z (2012) Neuroimmune crosstalk in the central nervous system and its significance for neurological diseases. J Neuroinflammation 9:155.
Toda M, Miura M, Asou H, Toya S, Uyemura K (1994) Cell growth suppression of astrocytoma C6 cells by glial fibrillary acidic protein cDNA transfection. J Neurochem 63:1975–1978.
Tojkander S, Gateva G, Lappalainen P (2012) Actin stress fibers--assembly, dynamics and biological roles. J Cell Sci 125:1855–1864.
Tomaselli KJ, Neugebauer KM, Bixby JL, Lilien J, Reichardt LF (1988) N-cadherin and integrins: two receptor systems that mediate neuronal process outgrowth on astrocyte surfaces. Neuron 1:33–43.
Tomkins O, Friedman O, Ivens S, Reiffurth C, Major S, Dreier JP, Heinemann U, Friedman A (2007) Blood-brain barrier disruption results in delayed functional and structural alterations in the rat neocortex. Neurobiol Dis 25:367–377.
Tong M, Dong M, la Monte de SM (2009) Brain insulin-like growth factor and neurotrophin resistance in Parkinson's disease and dementia with Lewy bodies: potential role of manganese neurotoxicity. J Alzheimers Dis 16:585–599.
Torres A, Wang F, Xu Q, Fujita T, Dobrowolski R, Willecke K, Takano T, Nedergaard M (2012) Extracellular Ca^{2+} acts as a mediator of communication from neurons to glia. Sci Signal 5:ra8.
Toulmond S, Vige X, Fage D, Benavides J (1992) Local infusion of interleukin-6 attenuates the neurotoxic effects of NMDA on rat striatal cholinergic neurons. Neurosci Lett 144:49–52.
Tracey KJ, Cerami A (1993) Tumor necrosis factor, other cytokines and disease. Annu Rev Cell Biol 9:317–343.
Tran PB, Miller RJ (2003) Chemokine receptors: signposts to brain development and disease. Nat Rev Neurosci 4:444–455.
Trapp BD, Wujek JR, Criste GA, Jalabi W, Yin X, Kidd GJ, Stohlman S, Ransohoff R (2007) Evidence for synaptic stripping by cortical microglia. Glia 55:360–368.
Tremblay M-È, Lowery RL, Majewska AK (2010) Microglial interactions with synapses are modulated by visual experience. PLoS Biol 8:e1000527.
Tremblay M-È, Majewska AK (2011) A role for microglia in synaptic plasticity? Commun Integr Biol 4:220–222.
Trendelenburg G, Dirnagl U (2005) Neuroprotective role of astrocytes in cerebral ischemia: focus on ischemic preconditioning. Glia 50:307–320.
Trevelyan AJ, Sussillo D, Watson BO, Yuste R (2006) Modular propagation of epileptiform activity: evidence for an inhibitory veto in neocortex. J Neurosci 26:12447–12455.
Tsacopoulos M, Magistretti PJ (1996) Metabolic coupling between glia and neurons. J Neurosci 16:877–885.
Tsai G, Dunham KS, Drager U, Grier A, Anderson C, Collura J, Coyle JT (2003) Early embryonic death of glutamate carboxypeptidase II (NAALADase) homozygous mutants. Synapse 50:285–292.
Tsai GC, Stauch-Slusher B, Sim L, Hedreen JC, Rothstein JD, Kuncl R, Coyle JT (1991) Reductions in acidic amino acids and N-acetylaspartylglutamate in amyotrophic lateral sclerosis CNS. Brain Res 556:151–156.
Tsai H-H, Li H, Fuentealba LC, Molofsky AV, Taveira-Marques R, Zhuang H, Tenney A, Murnen AT, Fancy SPJ, Merkle F, Kessaris N, Alvarez-Buylla A, Richardson WD, Rowitch DH (2012) Regional astrocyte allocation regulates CNS synaptogenesis and repair. Science 337:358–362.
Tsakiridis T, Vranic M, Klip A (1994) Disassembly of the actin network inhibits insulin-dependent stimulation of glucose transport and prevents recruitment of glucose transporters to the plasma membrane. J Biol Chem 269:29934–29942.
Tufekci KU, Meuwissen R, Genc S, Genc K (2012) Inflammation in Parkinson's disease. Adv Protein Chem Struct Biol 88:69–132.
Tullio AN, Bridgman PC, Tresser NJ, Chan CC, Conti MA, Adelstein RS, Hara Y (2001) Structural abnormalities develop in the brain after ablation of the gene encoding nonmuscle myosin II-B heavy chain. J Comp Neurol 433:62–74.
Tuvim MJ, Adachi R, Hoffenberg S, Dickey BF (2001) Traffic control: Rab GTPases and the regulation of interorganellar transport. News Physiol Sci 16:56–61.
Tuxworth RI, Chen H, Vivancos V, Carvajal N, Huang X, Tear G (2011) The Batten disease gene

CLN3 is required for the response to oxidative stress. Hum Mol Genet 20:2037–2047.
Tuxworth RI, Vivancos V, O'Hare MB, Tear G (2009) Interactions between the juvenile Batten disease gene, CLN3, and the Notch and JNK signalling pathways. Hum Mol Genet 18:667–678.
Twiss JL, Chang JH, Schanen NC (2006) Pathophysiological mechanisms for actions of the neurotrophins. Brain Pathol 16:320–332.
Tyynelä J, Cooper JD, Khan MN, Shemilts SJA, Haltia M (2004) Hippocampal pathology in the human neuronal ceroid-lipofuscinoses: distinct patterns of storage deposition, neurodegeneration and glial activation. Brain Pathol 14:349–357.
Tyynelä J, Palmer DN, Baumann M, Haltia M (1993) Storage of saposins A and D in infantile neuronal ceroid-lipofuscinosis. FEBS Lett 330:8–12.
Tyynelä J, Suopanki J, Santavuori P, Baumann M, Haltia M (1997) Variant late infantile neuronal ceroid-lipofuscinosis: pathology and biochemistry. J Neuropathol Exp Neurol 56:369–375.
Uchida K, Baba H, Maezawa Y, Furukawa S, Furusawa N, Imura S (1998) Histological investigation of spinal cord lesions in the spinal hyperostotic mouse (twy/twy): morphological changes in anterior horn cells and immunoreactivity to neurotropic factors. J Neurol 245:781–793.
Ullian EM, Christopherson KS, Barres BA (2004a) Role for glia in synaptogenesis. Glia 47:209–216.
Ullian EM, Harris BT, Wu A, Chan JR, Barres BA (2004b) Schwann cells and astrocytes induce synapse formation by spinal motor neurons in culture. Mol Cell Neurosci 25:241–251.
Ullian EM, Sapperstein SK, Christopherson KS, Barres BA (2001) Control of synapse number by glia. Science 291:657–661.
Ungar D, Hughson FM (2003) SNARE protein structure and function. Annu Rev Cell Dev Biol 19:493–517.
Uusi-Rauva K, Kyttälä A, Kant R, Vesa J, Tanhuanpää K, Neefjes J, Olkkonen VM, Jalanko A (2012) Neuronal ceroid lipofuscinosis protein CLN3 interacts with motor proteins and modifies location of late endosomal compartments. Cell Mol Life Sci.
Uusi-Rauva K, Luiro K, Tanhuanpää K, Kopra O, Martín-Vasallo P, Kyttälä A, Jalanko A (2008) Novel interactions of CLN3 protein link Batten disease to dysregulation of fodrin-Na+, K+ ATPase complex. Exp Cell Res 314:2895–2905.
Uvebrant P, Hagberg B (1997) Neuronal ceroid lipofuscinoses in Scandinavia. Epidemiology and clinical pictures. Neuropediatrics 28:6–8.
Uy B, McGlashan SR, Shaikh SB (2011) Measurement of reactive oxygen species in the culture media using Acridan Lumigen PS-3 assay. J Biomol Tech 22:95–107.
Valerio A, Ferrario M, Martinez FO, Locati M, Ghisi V, Bresciani LG, Mantovani A, Spano P (2004) Gene expression profile activated by the chemokine CCL5/RANTES in human neuronal cells. J Neurosci Res 78:371–382.
Van Aelst L, D'Souza-Schorey C (1997) Rho GTPases and signaling networks. Genes Dev 11:2295–2322.
van der Vaart B, Akhmanova A, Straube A (2009) Regulation of microtubule dynamic instability. Biochem Soc Trans 37:1007–1013.
van der Valk J, Mellor D, Brands R, Fischer R, Gruber F, Gstraunthaler G, Hellebrekers L, Hyllner J, Jonker FH, Prieto P, Thalen M, Baumans V (2004) The humane collection of fetal bovine serum and possibilities for serum-free cell and tissue culture. Toxicol In Vitro 18:1–12.
Van Essen D, Kelly J (1973) Correlation of cell shape and function in the visual cortex of the cat. Nature 241:403–405.
van Meel E, Klumperman J (2008) Imaging and imagination: understanding the endo-lysosomal system. Histochem Cell Biol 129:253–266.
Van Seventer GA, Shimizu Y, Horgan KJ, Shaw S (1990) The LFA-1 ligand ICAM-1 provides an important costimulatory signal for T cell receptor-mediated activation of resting T cells. J Immunol 144:4579–4586.
Vangheluwe P, Raeymaekers L, Dode L, Wuytack F (2005) Modulating sarco(endo)plasmic reticulum Ca2+ ATPase 2 (SERCA2) activity: cell biological implications. Cell Calcium 38:291–302.
Vanlandingham PA, Ceresa BP (2009) Rab7 regulates late endocytic trafficking downstream of multivesicular body biogenesis and cargo sequestration. J Biol Chem 284:12110–12124.
Vardjan N, Gabrijel M, Potokar M, Svajger U, Kreft M, Jeras M, de Pablo Y, Faiz M, Pekny M, Zorec R (2012) IFN-γ-induced increase in the mobility of MHC class II compartments in astrocytes

depends on intermediate filaments. J Neuroinflammation 9:144.
Vargas MR, Johnson DA, Sirkis DW, Messing A, Johnson JA (2008) Nrf2 activation in astrocytes protects against neurodegeneration in mouse models of familial amyotrophic lateral sclerosis. J Neurosci 28:13574–13581.
Vellodi A (2005) Lysosomal storage disorders. Br J Haematol 128:413–431.
Verderio C, Matteoli M (2001) ATP mediates calcium signaling between astrocytes and microglial cells: modulation by IFN-gamma. J Immunol 166:6383–6391.
Verkhratsky A, Butt A (2007) Glial Neurobiology. Wiley.
Verkhratsky A, Kettenmann H (1996) Calcium signalling in glial cells. Trends Neurosci 19:346–352.
Verkhratsky A, Orkand RK, Kettenmann H (1998) Glial calcium: homeostasis and signaling function. Physiol Rev 78:99–141.
Verkhratsky A, Parpura V (2010) Recent advances in (patho)physiology of astroglia. Acta Pharmacol Sin 31:1044–1054.
Verkhratsky A, Rodríguez JJ, Parpura V (2012a) Calcium signalling in astroglia. Mol Cell Endocrinol 353:45–56.
Verkhratsky A, Sofroniew MV, Messing A, deLanerolle NC, Rempe D, Rodríguez JJ, Nedergaard M (2012b) Neurological diseases as primary gliopathies: a reassessment of neurocentrism. ASN Neuro 4.
Verkhratsky A, Verkhrasky A, Krishtal OA, Burnstock G (2009) Purinoceptors on neuroglia. Mol Neurobiol 39:190–208.
Vermeulen K, Van Bockstaele DR, Berneman ZN (2003) The cell cycle: a review of regulation, deregulation and therapeutic targets in cancer. Cell Prolif 36:131–149.
Vernadakis A (1988) Neuron-glia interrelations. Int Rev Neurobiol 30:149–224.
Vernadakis A, Mangoura DA (1988) Factors influencing glia growth in culture: nutrients and cell-secreted factors. Prog Clin Biol Res 259:57–79.
Vezzani A, Baram TZ (2007) New roles for interleukin-1 Beta in the mechanisms of epilepsy. Epilepsy Curr 7:45–50.
Vezzani A, Granata T (2005) Brain inflammation in epilepsy: experimental and clinical evidence. Epilepsia 46:1724–1743.
Vicente-Manzanares M, Ma X, Adelstein RS, Horwitz AR (2009) Non-muscle myosin II takes centre stage in cell adhesion and migration. Nat Rev Mol Cell Biol 10:778–790.
Vicente-Manzanares M, Zareno J, Whitmore L, Choi CK, Horwitz AF (2007) Regulation of protrusion, adhesion dynamics, and polarity by myosins IIA and IIB in migrating cells. J Cell Biol 176:573–580.
Villoslada P, Genain CP (2004) Role of nerve growth factor and other trophic factors in brain inflammation. Prog Brain Res 146:403–414.
Vincent VA, Tilders FJ, Van Dam AM (1997) Inhibition of endotoxin-induced nitric oxide synthase production in microglial cells by the presence of astroglial cells: a role for transforming growth factor beta. Glia 19:190–198.
Vincent VA, Van Dam AM, Persoons JH, Schotanus K, Steinbusch HW, Schoffelmeer AN, Berkenbosch F (1996) Gradual inhibition of inducible nitric oxide synthase but not of interleukin-1 beta production in rat microglial cells of endotoxin-treated mixed glial cell cultures. Glia 17:94–102.
Vincent VAM, Robinson CC, Simsek D, Murphy GM (2002a) Macrophage colony stimulating factor prevents NMDA-induced neuronal death in hippocampal organotypic cultures. J Neurochem 82:1388–1397.
Vincent VAM, Selwood SP, Murphy GM (2002b) Proinflammatory effects of M-CSF and A beta in hippocampal organotypic cultures. Neurobiol Aging 23:349–362.
Virmani T, Gupta P, Liu X, Kavalali ET, Hofmann SL (2005) Progressively reduced synaptic vesicle pool size in cultured neurons derived from neuronal ceroid lipofuscinosis-1 knockout mice. Neurobiol Dis 20:314–323.
Vitiello SP, Benedict JW, Padilla-Lopez S, Pearce DA (2010) Interaction between Sdo1p and Btn1p in the Saccharomyces cerevisiae model for Batten disease. Hum Mol Genet 19:931–942.
Vitner EB, Platt FM, Futerman AH (2010) Common and uncommon pathogenic cascades in lysosomal storage diseases. J Biol Chem 285:20423–20427.
Volterra A, Meldolesi J (2005) Astrocytes, from brain glue to communication elements: the revolution continues. Nat Rev Neurosci 6:626–640.

Voskuhl RR, Peterson RS, Song B, Ao Y, Morales LBJ, Tiwari-Woodruff S, Sofroniew MV (2009) Reactive astrocytes form scar-like perivascular barriers to leukocytes during adaptive immune inflammation of the CNS. J Neurosci 29:11511–11522.
Voss AK, Britto JM, Dixon MP, Sheikh BN, Collin C, Tan S-S, Thomas T (2008) C3G regulates cortical neuron migration, preplate splitting and radial glial cell attachment. Development 135:2139–2149.
Wade RH (2007) Microtubules: an overview. Methods Mol Med 137:1–16.
Waetzig V, Herdegen T (2005) MEKK1 controls neurite regrowth after experimental injury by balancing ERK1/2 and JNK2 signaling. Mol Cell Neurosci 30:67–78.
Wake H, Moorhouse AJ, Jinno S, Kohsaka S, Nabekura J (2009) Resting microglia directly monitor the functional state of synapses in vivo and determine the fate of ischemic terminals. J Neurosci 29:3974–3980.
Walenta JH, Didier AJ, Liu X, Krämer H (2001) The Golgi-associated hook3 protein is a member of a novel family of microtubule-binding proteins. J Cell Biol 152:923–934.
Walicke P, Cowan WM, Ueno N, Baird A, Guillemin R (1986) Fibroblast growth factor promotes survival of dissociated hippocampal neurons and enhances neurite extension. Proc Natl Acad Sci USA 83:3012–3016.
Walkley SU (2007) Pathogenic mechanisms in lysosomal disease: a reappraisal of the role of the lysosome. Acta Paediatr Suppl 96:26–32.
Walkley SU (2009) Pathogenic cascades in lysosomal disease-Why so complex? J Inherit Metab Dis 32:181–189.
Walkley SU, Sikora J, Micsenyi M, Davidson C, Dobrenis K (2010) Lysosomal compromise and brain dysfunction: examining the role of neuroaxonal dystrophy. Biochem Soc Trans 38:1436–1441.
Wallraff A, Köhling R, Heinemann U, Theis M, Willecke K, Steinhäuser C (2006) The impact of astrocytic gap junctional coupling on potassium buffering in the hippocampus. J Neurosci 26:5438–5447.
Wang D, Baldwin AS (1998) Activation of nuclear factor-kappaB-dependent transcription by tumor necrosis factor-alpha is mediated through phosphorylation of RelA/p65 on serine 529. J Biol Chem 273:29411–29416.
Wang L-Y, Fedchyshyn MJ, Yang Y-M (2009a) Action potential evoked transmitter release in central synapses: insights from the developing calyx of Held. Mol Brain 2:36.
Wang LC, Baird DH, Hatten ME, Mason CA (1994) Astroglial differentiation is required for support of neurite outgrowth. J Neurosci 14:3195–3207.
Wang Q, Bilan PJ, Tsakiridis T, Hinek A, Klip A (1998) Actin filaments participate in the relocalization of phosphatidylinositol3-kinase to glucose transporter-containing compartments and in the stimulation of glucose uptake in 3T3-L1 adipocytes. Biochem J 331 (Pt 3):917–928.
Wang T-F, Zhou C, Tang A-H, Wang S-Q, Chai Z (2006) Cellular mechanism for spontaneous calcium oscillations in astrocytes. Acta Pharmacol Sin 27:861–868.
Wang W, Redecker C, Yu Z-Y, Xie M-J, Tian D-S, Zhang L, Bu B-T, Witte OW (2008) Rat focal cerebral ischemia induced astrocyte proliferation and delayed neuronal death are attenuated by cyclin-dependent kinase inhibition. J Clin Neurosci 15:278–285.
Wang X, Wang Z, Yao Y, Li J, Zhang X, Li C, Cheng Y, Ding G, Liu L, Ding Z (2011a) Essential role of ERK activation in neurite outgrowth induced by α-lipoic acid. Biochim Biophys Acta 1813:827–838.
Wang X-Q, Peng Y-P, Lu J-H, Cao B-B, Qiu Y-H (2009b) Neuroprotection of interleukin-6 against NMDA attack and its signal transduction by JAK and MAPK. Neurosci Lett 450:122–126.
Wang XF, Cynader MS (1999) Effects of astrocytes on neuronal attachment and survival shown in a serum-free co-culture system. Brain Res Brain Res Protoc 4:209–216.
Wang Y, Tang BL (2006) SNAREs in neurons--beyond synaptic vesicle exocytosis (Review). Mol Membr Biol 23:377–384.
Wang Y, Zhou C-F (2005) Involvement of interferon-gamma and its receptor in the activation of astrocytes in the mouse hippocampus following entorhinal deafferentation. Glia 50:56–65.
Wang Z, Pekarskaya O, Bencheikh M, Chao W, Gelbard HA, Ghorpade A, Rothstein JD, Volsky DJ (2003) Reduced expression of glutamate transporter EAAT2 and impaired glutamate transport in human primary astrocytes exposed to HIV-1 or gp120. Virology 312:60–73.

Wang Z, Wang J, Li J, Wang X, Yao Y, Zhang X, Li C, Cheng Y, Ding G, Liu L, Ding Z (2011b) MEK/ERKs signaling is essential for lithium-induced neurite outgrowth in N2a cells. Int J Dev Neurosci 29:415–422.
Warr O, Takahashi M, Attwell D (1999) Modulation of extracellular glutamate concentration in rat brain slices by cystine-glutamate exchange. J Physiol (Lond) 514 (Pt 3):783–793.
Washbourne P, Schiavo G, Montecucco C (1995) Vesicle-associated membrane protein-2 (synaptobrevin-2) forms a complex with synaptophysin. Biochem J 305 (Pt 3):721–724.
Wasser CR, Ertunc M, Liu X, Kavalali ET (2007) Cholesterol-dependent balance between evoked and spontaneous synaptic vesicle recycling. J Physiol (Lond) 579:413–429.
Watanabe K-I, Ambekar C, Wang H, Ciccolini A, Schimmer AD, Dror Y (2009) SBDS-deficiency results in specific hypersensitivity to Fas stimulation and accumulation of Fas at the plasma membrane. Apoptosis 14:77–89.
Watson K, Fan G-H (2005) Macrophage inflammatory protein 2 inhibits beta-amyloid peptide (1-42)-mediated hippocampal neuronal apoptosis through activation of mitogen-activated protein kinase and phosphatidylinositol 3-kinase signaling pathways. Mol Pharmacol 67:757–765.
Wei H, Kim S-J, Zhang Z, Tsai P-C, Wisniewski KE, Mukherjee AB (2008) ER and oxidative stresses are common mediators of apoptosis in both neurodegenerative and non-neurodegenerative lysosomal storage disorders and are alleviated by chemical chaperones. Hum Mol Genet 17:469–477.
Wei T, Chen C, Hou J, Xin W, Mori A (2000) Nitric oxide induces oxidative stress and apoptosis in neuronal cells. Biochim Biophys Acta 1498:72–79.
Weimer JM, Benedict JW, Elshatory YM, Short DW, Ramirez-Montealegre D, Ryan DA, Alexander NA, Federoff HJ, Cooper JD, Pearce DA (2007) Alterations in striatal dopamine catabolism precede loss of substantia nigra neurons in a mouse model of juvenile neuronal ceroid lipofuscinosis. Brain Res 1162:98–112.
Weimer JM, Benedict JW, Getty AL, Pontikis CC, Lim MJ, Cooper JD, Pearce DA (2009) Cerebellar defects in a mouse model of juvenile neuronal ceroid lipofuscinosis. Brain Res 1266:93–107.
Weimer JM, Chattopadhyay S, Custer AW, Pearce DA (2005) Elevation of Hook1 in a disease model of Batten disease does not affect a novel interaction between Ankyrin G and Hook1. Biochem Biophys Res Commun 330:1176–1181.
Weimer JM, Custer AW, Benedict JW, Alexander NA, Kingsley E, Federoff HJ, Cooper JD, Pearce DA (2006) Visual deficits in a mouse model of Batten disease are the result of optic nerve degeneration and loss of dorsal lateral geniculate thalamic neurons. Neurobiol Dis 22:284–293.
Weisenberg RC, Deery WJ (1976) Role of nucleotide hydrolysis in microtubule assembly. Nature 263:792–793.
Weisenberg RC, Deery WJ, Dickinson PJ (1976) Tubulin-nucleotide interactions during the polymerization and depolymerization of microtubules. Biochemistry 15:4248–4254.
Weishaupt N, Blesch A, Fouad K (2012) BDNF: The career of a multifaceted neurotrophin in spinal cord injury. Exp Neurol 238:254–264.
Welser-Alves JV, Crocker SJ, Milner R (2011) A dual role for microglia in promoting tissue inhibitor of metalloproteinase (TIMP) expression in glial cells in response to neuroinflammatory stimuli. J Neuroinflammation 8:61.
Westergaard N, Sonnewald U, Schousboe A (1995) Metabolic trafficking between neurons and astrocytes: the glutamate/glutamine cycle revisited. Dev Neurosci 17:203–211.
Westermarck T, Aberg L, Santavuori P, Antila E, Edlund P, Atroshi F (1997) Evaluation of the possible role of coenzyme Q10 and vitamin E in juvenile neuronal ceroid-lipofuscinosis (JNCL). Mol Aspects Med 18 Suppl:S259–S262.
Wiche G (1998) Role of plectin in cytoskeleton organization and dynamics. J Cell Sci 111 (Pt 17):2477–2486.
Wiche G, Winter L (2011) Plectin isoforms as organizers of intermediate filament cytoarchitecture. Bioarchitecture 1:14–20.
Widestrand A, Faijerson J, Wilhelmsson U, Smith PLP, Li L, Sihlbom C, Eriksson PS, Pekny M (2007) Increased neurogenesis and astrogenesis from neural progenitor cells grafted in the hippocampus of GFAP-/- Vim-/- mice. Stem Cells 25:2619–2627.
Wight RD, Tull CA, Deel MW, Stroope BL, Eubanks AG, Chavis JA, Drew PD, Hensley LL (2012)

Resveratrol effects on astrocyte function: Relevance to neurodegenerative diseases. Biochem Biophys Res Commun 426:112–115.
Wilde GJ, Pringle AK, Sundstrom LE, Mann DA, Iannotti F (2000) Attenuation and augmentation of ischaemia-related neuronal death by tumour necrosis factor-alpha in vitro. Eur J Neurosci 12:3863–3870.
Wilhelm A, Volknandt W, Langer D, Nolte C, Kettenmann H, Zimmermann H (2004) Localization of SNARE proteins and secretory organelle proteins in astrocytes in vitro and in situ. Neurosci Res 48:249–257.
Wilhelmsson U, Bushong EA, Price DL, Smarr BL, Phung V, Terada M, Ellisman MH, Pekny M (2006) Redefining the concept of reactive astrocytes as cells that remain within their unique domains upon reaction to injury. Proc Natl Acad Sci USA 103:17513–17518.
Wilhelmsson U, Li L, Pekna M, Berthold C-H, Blom S, Eliasson C, Renner O, Bushong E, Ellisman M, Morgan TE, Pekny M (2004) Absence of glial fibrillary acidic protein and vimentin prevents hypertrophy of astrocytic processes and improves post-traumatic regeneration. J Neurosci 24:5016–5021.
Williams EJ, Furness J, Walsh FS, Doherty P (1994) Activation of the FGF receptor underlies neurite outgrowth stimulated by L1, N-CAM, and N-cadherin. Neuron 13:583–594.
Williams EJ, Mittal B, Walsh FS, Doherty P (1995) FGF inhibits neurite outgrowth over monolayers of astrocytes and fibroblasts expressing transfected cell adhesion molecules. J Cell Sci 108 (Pt 11):3523–3530.
Wimmer VC, Reid CA, So EY-W, Berkovic SF, Petrou S (2010) Axon initial segment dysfunction in epilepsy. J Physiol (Lond) 588:1829–1840.
Winckler B, Forscher P, Mellman I (1999) A diffusion barrier maintains distribution of membrane proteins in polarized neurons. Nature 397:698–701.
Wisniewski KE, Kida E, Gordon-Majszak W, Saitoh T (1990) Altered amyloid beta-protein precursor processing in brains of patients with neuronal ceroid lipofuscinosis. Neurosci Lett 120:94–96.
Wisniewski KE, Zhong N, Kaczmarski W, Kaczmarski A, Kida E, Brown WT, Schwarz KO, Lazzarini AM, Rubin AJ, Stenroos ES, Johnson WG, Wisniewski TM (1998) Compound heterozygous genotype is associated with protracted juvenile neuronal ceroid lipofuscinosis. Ann Neurol 43:106–110.
Wong AHC et al. (2003) Identification of candidate genes for psychosis in rat models, and possible association between schizophrenia and the 14-3-3eta gene. Mol Psychiatry 8:156–166.
Wong AMS, Rahim AA, Waddington SN, Cooper JD (2010) Current therapies for the soluble lysosomal forms of neuronal ceroid lipofuscinosis. Biochem Soc Trans 38:1484–1488.
Wong E, Cuervo AM (2010) Autophagy gone awry in neurodegenerative diseases. Nat Neurosci 13:805–811.
Woodroofe MN, Sarna GS, Wadhwa M, Hayes GM, Loughlin AJ, Tinker A, Cuzner ML (1991) Detection of interleukin-1 and interleukin-6 in adult rat brain, following mechanical injury, by in vivo microdialysis: evidence of a role for microglia in cytokine production. J Neuroimmunol 33:227–236.
Wraith JE (2004) The clinical presentation of lysosomal storage disorders. Acta Neurol Taiwan 13:101–106.
Wright SH (2004) Generation of resting membrane potential. Adv Physiol Educ 28:139–142.
Wu X, Zhu D, Jiang X, Okagaki P, Mearow K, Zhu G, McCall S, Banaudha K, Lipsky RH, Marini AM (2004) AMPA protects cultured neurons against glutamate excitotoxicity through a phosphatidylinositol 3-kinase-dependent activation in extracellular signal-regulated kinase to upregulate BDNF gene expression. J Neurochem 90:807–818.
Wu Y, Chen Q, Peng H, Dou H, Zhou Y, Huang Y, Zheng JC (2012) Directed migration of human neural progenitor cells to interleukin-1β is promoted by chemokines stromal cell-derived factor-1 and monocyte chemotactic factor-1 in mouse brains. Transl Neurodegener 1:15.
Wu Y-P, Proia RL (2004) Deletion of macrophage-inflammatory protein 1 alpha retards neurodegeneration in Sandhoff disease mice. Proc Natl Acad Sci USA 101:8425–8430.
Wyss-Coray T, Loike JD, Brionne TC, Lu E, Anankov R, Yan F, Silverstein SC, Husemann J (2003) Adult mouse astrocytes degrade amyloid-beta in vitro and in situ. Nat Med 9:453–457.
Wyss-Coray T, Mucke L (2002) Inflammation in neurodegenerative disease--a double-edged sword. Neuron 35:419–432.

Yamada J, Hayashi Y, Jinno S, Wu Z, Inoue K, Kohsaka S, Nakanishi H (2008) Reduced synaptic activity precedes synaptic stripping in vagal motoneurons after axotomy. Glia 56:1448–1462.
Yamada M, Hatanaka H (1994) Interleukin-6 protects cultured rat hippocampal neurons against glutamate-induced cell death. Brain Res 643:173–180.
Yang Y, Ogawa Y, Hedstrom KL, Rasband MN (2007) betaIV spectrin is recruited to axon initial segments and nodes of Ranvier by ankyrinG. J Cell Biol 176:509–519.
Yano H, Lee FS, Kong H, Chuang J, Arevalo J, Perez P, Sung C, Chao MV (2001) Association of Trk neurotrophin receptors with components of the cytoplasmic dynein motor. J Neurosci 21:RC125.
Yasui Y, Amano M, Nagata K, Inagaki N, Nakamura H, Saya H, Kaibuchi K, Inagaki M (1998) Roles of Rho-associated kinase in cytokinesis; mutations in Rho-associated kinase phosphorylation sites impair cytokinetic segregation of glial filaments. J Cell Biol 143:1249–1258.
Young CE, Arima K, Xie J, Hu L, Beach TG, Falkai P, Honer WG (1998) SNAP-25 deficit and hippocampal connectivity in schizophrenia. Cereb Cortex 8:261–268.
Yu Y, Maureira C, Liu X, McCormick D (2010) P/Q and N channels control baseline and spike-triggered calcium levels in neocortical axons and synaptic boutons. J Neurosci 30:11858–11869.
Yudkoff M, Pleasure D, Cregar L, Lin ZP, Nissim I, Stern J, Nissim I (1990) Glutathione turnover in cultured astrocytes: studies with [15N]glutamate. J Neurochem 55:137–145.
Yuste R, Denk W (1995) Dendritic spines as basic functional units of neuronal integration. Nature 375:682–684.
Zackroff RV, Goldman RD (1979) In vitro assembly of intermediate filaments from baby hamster kidney (BHK-21) cells. Proc Natl Acad Sci USA 76:6226–6230.
Zador Z, Stiver S, Wang V, Manley GT (2009) Role of aquaporin-4 in cerebral edema and stroke. Handb Exp Pharmacol:159–170.
Zakharenko S, Popov S (1998) Dynamics of axonal microtubules regulate the topology of new membrane insertion into the growing neurites. J Cell Biol 143:1077–1086.
Zamanian JL, Xu L, Foo LC, Nouri N, Zhou L, Giffard RG, Barres BA (2012) Genomic analysis of reactive astrogliosis. J Neurosci 32:6391–6410.
Zambrano A, Otth C, Mujica L, Concha II, Maccioni RB (2007) Interleukin-3 prevents neuronal death induced by amyloid peptide. BMC Neurosci 8:82.
Zeevalk GD, Bernard LP, Albers DS, Mirochnitchenko O, Nicklas WJ, Sonsalla PK (1997) Energy stress-induced dopamine loss in glutathione peroxidase-overexpressing transgenic mice and in glutathione-depleted mesencephalic cultures. J Neurochem 68:426–429.
Zeevalk GD, Bernard LP, Sinha C, Ehrhart J, Nicklas WJ (1998) Excitotoxicity and oxidative stress during inhibition of energy metabolism. Dev Neurosci 20:444–453.
Zeman W, Dyken P (1969) Neuronal ceroid-lipofuscinosis (Batten's disease): relationship to amaurotic family idiocy? Pediatrics 44:570–583.
Zhang D, Hu X, Qian L, O'Callaghan JP, Hong J-S (2010) Astrogliosis in CNS pathologies: is there a role for microglia? Mol Neurobiol 41:232–241.
Zhang L, Sheng R, Qin Z (2009a) The lysosome and neurodegenerative diseases. Acta Biochim Biophys Sin (Shanghai) 41:437–445.
Zhang M, Chen L, Wang S, Wang T (2009b) Rab7: roles in membrane trafficking and disease. Biosci Rep 29:193–209.
Zhang M, Strnatka D, Donohue C, Hallows JL, Vincent I, Erickson RP (2008) Astrocyte-only Npc1 reduces neuronal cholesterol and triples life span of Npc1-/- mice. J Neurosci Res 86:2848–2856.
Zhang Q, Pangrsic T, Kreft M, Krzan M, Li N, Sul J-Y, Halassa M, Van Bockstaele E, Zorec R, Haydon PG (2004) Fusion-related release of glutamate from astrocytes. J Biol Chem 279:12724–12733.
Zhang Y, Barres BA (2010) Astrocyte heterogeneity: an underappreciated topic in neurobiology. Curr Opin Neurobiol 20:588–594.
Zhang Y, Moheban DB, Conway BR, Bhattacharyya A, Segal RA (2000) Cell surface Trk receptors mediate NGF-induced survival while internalized receptors regulate NGF-induced differentiation. J Neurosci 20:5671–5678.
Zheng C, Nennesmo I, Fadeel B, Henter J-I (2004) Vascular endothelial growth factor prolongs

survival in a transgenic mouse model of ALS. Ann Neurol 56:564–567.
Zheng J, Ghorpade A, Niemann D, Cotter RL, Thylin MR, Epstein L, Swartz JM, Shepard RB, Liu X, Nukuna A, Gendelman HE (1999a) Lymphotropic virions affect chemokine receptor-mediated neural signaling and apoptosis: implications for human immunodeficiency virus type 1-associated dementia. J Virol 73:8256–8267.
Zheng J, Thylin MR, Ghorpade A, Xiong H, Persidsky Y, Cotter R, Niemann D, Che M, Zeng YC, Gelbard HA, Shepard RB, Swartz JM, Gendelman HE (1999b) Intracellular CXCR4 signaling, neuronal apoptosis and neuropathogenic mechanisms of HIV-1-associated dementia. J Neuroimmunol 98:185–200.
Zheng X-R, Zhang S-S, Yang Y-J, Yin F, Wang X, Zhong L, Yu X-H (2010) Adenoviral vector-mediated transduction of VEGF improves neural functional recovery after hypoxia-ischemic brain damage in neonatal rats. Brain Res Bull 81:372–377.
Zhou D, Lambert S, Malen PL, Carpenter S, Boland LM, Bennett V (1998) AnkyrinG is required for clustering of voltage-gated Na channels at axon initial segments and for normal action potential firing. J Cell Biol 143:1295–1304.
Zhou J, Neale JH, Pomper MG, Kozikowski AP (2005) NAAG peptidase inhibitors and their potential for diagnosis and therapy. Nat Rev Drug Discov 4:1015–1026.
Zietlow R, Dunnett SB, Fawcett JW (1999) The effect of microglia on embryonic dopaminergic neuronal survival in vitro: diffusible signals from neurons and glia change microglia from neurotoxic to neuroprotective. Eur J Neurosci 11:1657–1667.
Zigmond SH (1996) Signal transduction and actin filament organization. Curr Opin Cell Biol 8:66–73.
Zimek A, Stick R, Weber K (2003) Genes coding for intermediate filament proteins: common features and unexpected differences in the genomes of humans and the teleost fish Fugu rubripes. J Cell Sci 116:2295–2302.
Zimmer WE, Zhao Y, Sikorski AF, Critz SD, Sangerman J, Elferink LA, Xu XS, Goodman SR (2000) The domain of brain beta-spectrin responsible for synaptic vesicle association is essential for synaptic transmission. Brain Res 881:18–27.
Zorec R, Araque A, Carmignoto G, Haydon PG, Verkhratsky A, Parpura V (2012) Astroglial excitability and gliotransmission: an appraisal of Ca2+ as a signalling route. ASN Neuro 4.